Distributed optimal and predictive control methods for networks of dynamic systems

Eleftherios E. Vlahakis

Department of Electrical and Electronic Engineering
City, University of London

This dissertation is submitted for the degree of
Doctor of Philosophy

June 2020

to Aggela...

Declaration

I hereby declare that except where specific reference is made to the work of others, the contents of this dissertation are original and have not been submitted in whole or in part for consideration for any other degree or qualification in this, or any other university. This dissertation is my own work and contains nothing which is the outcome of work done in collaboration with others, except as specified in the text and Acknowledgements.

Eleftherios E. Vlahakis
June 2020

Acknowledgements

I greatly acknowledge the invaluable guidance and constant support of my supervisor, Professor George Halikias, whose knowledge, kindness, dedication and enthusiasm have helped me shape this thesis. He has been an incredible teacher and mentor constantly challenging me to improve as a researcher and engineer as well as a person.

I am greatly thankful to Professor Nicholas Karcanias who has changed the way I view science and engineering. I would also like to thank him for giving me the opportunity to start a research career.

I would also like to express my thanks to Dr Efstathios Milonidis, Professor George Papavassilopoulos and Professor Leonidas Dritsas for their support throughout my Ph.D. studies.

I want to thank especially my mother Vasoula, my father Evangelos, and my brothers Vassilis and Apostolos for their love and support throughout this research journey.

Above all, I want to thank my life partner Aggela for her love, patience, motivation and support throughout these years.

Abstract

Several recent approaches to distributed control design over networks of interconnected dynamic systems rely on certain assumptions, such as identical subsystem dynamics, absence of dynamical couplings, linear dynamics and undirected interaction schemes. In this thesis, we investigate systematic methods for relaxing a number of simplifying factors leading to a unifying approach for solving general distributed-control stabilization problems of networks of dynamic agents.

We show that the gain-margin property of LQR control holds for complex multiplicative input perturbations and a generic symmetric positive definite input weighting matrix. Proving also that the potentially non-simple structure of the Laplacian matrix can be neglected for stability analysis and control design, we extend two well-known distributed LQR-based control methods originally established for undirected networks of identical linear systems, to the directed case.

We then propose a distributed feedback method for tackling large-scale regulation problems of a general class of interconnected non-identical dynamic agents with undirected and directed topology. In particular, we assume that local agents share a minimal set of structural properties, such as input dimension, state dimension and controllability indices. Our approach relies on the solution of certain model-matching type problems using local linear state-feedback and input matrix transformations which map the agent dynamics to a target system, selected to minimize the joint control effort of the local feedback-control schemes. By adapting well-established distributed LQR control design methodologies to our framework, the stabilization problem of a network of non-identical dynamical agents is solved. We thereafter consider a networked scheme synthesized by multiple agents with nonlinear dynamics. Assuming that agents are feedback linearizable in a neighborhood near their equilibrium points, we propose a nonlinear model-matching control design for stabilizing networks of multiple heterogeneous nonlinear agents.

Motivated by the structure of a large-scale LQR optimal problem, we propose a stabilizing distributed state-feedback controller for networks of identical dynamically coupled linear agents. First, a fully centralized controller is designed which is subsequently substituted by a distributed state-feedback gain with sparse structure. The control scheme is obtained by

optimizing an LQR performance index with a tuning parameter utilized to emphasize/de-emphasize relative state difference between coupled systems. Sufficient conditions for stability of the proposed scheme are derived based on the inertia of a convex combination of two Hurwitz matrices. An extended simulation study involving distributed load frequency control design of a multi-area power network, illustrates the applicability of the proposed method.

Finally, we propose a fully distributed consensus-based model-matching scheme adapted to a model predictive control setting for tackling a structured receding horizon regulation problem.

Table of contents

List of figures

List of tables

Chapter 1

Introduction

DISTRIBUTED control is one of the most challenging research domains which deals with the study of how a global decision making task can be shared across several *local* controllers. The field is intrinsically connected to control of large dynamic systems, and its significance predominantly stems from the necessity or preference for control design in a decentralized manner. The concept of decentralization was initially introduced in socio-economic literature primarily devised to address the efficient capital allocation of competitive economic systems [88, 130, 136, 23]. Thereafter, the term *decentralized control* has been widely adopted by the control community in problems where typical centralized schemes result in prohibitive data handling and computational requirements. The interest in designing controllers in a non-classical decentralized fashion dates from the early 70s [82, 6, 111, 227], and has skyrocketed over the past few years due to the abundance of network applications demanding decentralized and distributed control schemes [233, 144, 181, 226].

Advances in information and computer science have revolutionized data and communication networks in recent years, leading to a global Internet that allows for information exchange among users worldwide. Data and communication networks usually consist of a modular architecture that allows for an anarchic proliferation of network nodes, despite their diversity in by-wire or wireless connections. This plug-and-play capacity of most information networks is established via network control protocols that tackle network caching, congestion, and routing problems in a decentralized fashion hence enabling nodes and links to be added to or removed from the overall scheme. For instance, the flow rate and path of data packets transmitted across the Internet obey the principles of the TCP/IP protocol, which provides peer-to-peer communication. While there is no ambiguity that data transmission among various computers and routers has been a tractable task over the past few years, further network interaction with the physical environment opens new opportunities and sets intense challenges for network control design. Sensor and actuation signals flowing in networks can

form elaborate aggregates of subsystems that tackle various tasks that do not admit a solution at the subsystem level. Progress along these lines, along with the digitalization of control systems, have enabled the development of highly sophisticated networked schemes, and have introduced new paradigms of large-scale complex systems. Intelligent highways and vehicle platoons, smart power grids, blockchain technologies, and smart supply and logistics chains are just a few instances of a growing array of network applications.

Networked systems are compositions of several entities that can exchange various types of information with each other over a network topology which has arisen naturally or designed for a specific purpose. From a control and systems perspective, such structures belong to the family of large-scale complex systems. In particular, each network building block represents a distinct dynamical system. In this regard, the network constitutes an aggregate of systems each defined by the interaction of local state and input variables. This network definition as a systems' aggregate allows us to decompose the network into simpler units and helps identify network problems both at global and local levels.

Further, recognising the network as an aggregate system often facilitates the introduction of a degree of local autonomy at the individual level, from which the notion of agent-based modeling emerges in a natural way. In this setup, the network becomes a multi-agent system, with each agent represented as an *intelligent* dynamical unit with fully independent actuation capacity. Agents can cooperate with some of their counterparts within the network towards a common objective or according to specific tasks despite their fully independent control operation. The advantages of introducing the notion of autonomous agents are especially clear in cases where network control strategies with distributed architecture are either imperative or desirable over policies imposed by a global coordinator of the network.

Most large-scale dynamic systems, networked systems inclusive, admit of architectures which group the various input and output variables of the total system into non-overlapping pairs [182]. Each pair representing a subsystem of the overall scheme, consists of two vectors of distinct input and output variables, respectively, and is designed either to operate completely independently or in a distributed fashion. Adopting this approach, the main difference of a decentralized control strategy over a distributed design is the absence of information exchange between control units of different subsystems. A simple example of a decentralized control pattern is illustrated in Fig. 1.1, where system S is decomposed into two state-dependent subsystems S_1, S_2, each represented by pair $(u_1,\ y_1)$, $(u_2,\ y_2)$, respectively. In this instance, the design of controllers u_1, u_2 is based on *local* information only, despite the mutual interaction between states x_1 and x_2 of each local subsystem. On the contrary, a distributed architecture allows for data transmissions between different control units, usually involving local information exchange. Fig. 1.2 highlights a simple example of this situation.

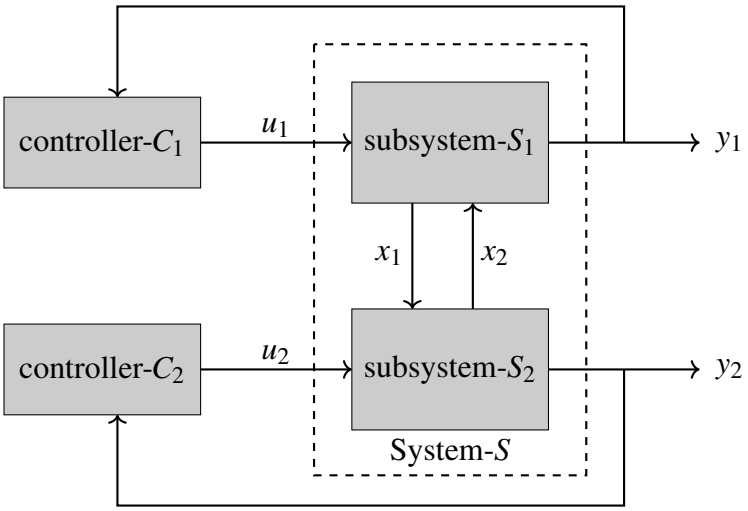

Fig. 1.1 Decentralized closed-loop configuration of a two input $(u_1,\ u_2)$ - two output $(y_1,\ y_2)$ system [182].

Despite the compelling reasons for devising decentralized and distributed control structures, it is worth noting that such schemes, either physically imposed or consciously conceived, may give rise to highly elaborate situations even if a centralized version of the problem admits a typically simple solution. The inherent intricacy of such complex control problems is further amplified by the presence of communication links in the overall system. Traditionally, control theory focuses on the study of interconnected dynamical systems linked via ideal channels. However, in practice, information exchange carried out over communication channels is usually limited by certain imperfections of the communication scheme, e.g. communication delays, distortion due to limited bandwidth, packet loss due to buffer overflows, channel multipath, thermal noise at receivers, etc. Overall, network control lies in the intersection of control and communication theories [80]. The combination of these two domains represents a substantial challenge for the efficient control design of networked systems in real applications.

Algebraic graph theory has proved powerful for network modeling and has been widely used in multi-agent network control. Essentially, each agent representing a dynamical system is denoted by a labeled node on a graph, while edges denote interactions/information exchange between two nodes. A typical assumption made in a variety of research works requires that the communication scheme (information exchange), and the interaction scheme (state/input dependence, control couplings) have identical topology. In these instances, the *information graph* and *interaction graph* coincide. Graph representation of multi-agent networks allows for 1) an algebraic interpretation of network's major attributes (complexity, connectivity, sparsity) and 2) a simpler view of the overall large-scale system. These are

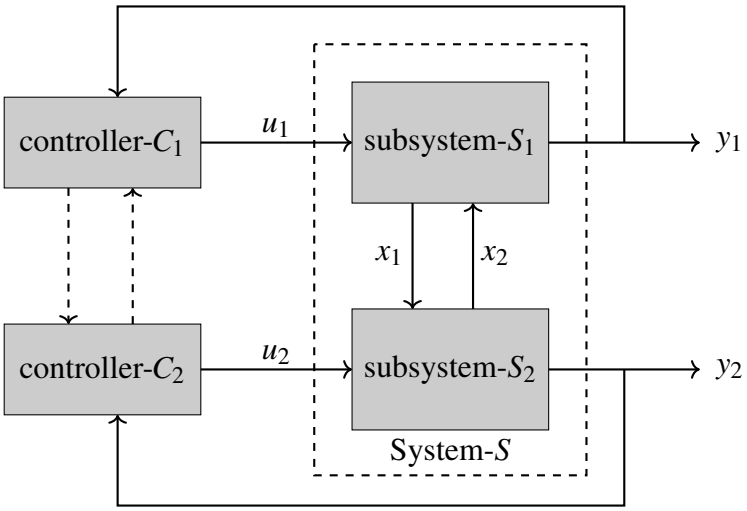

Fig. 1.2 Distributed closed-loop configuration of a two input $(u_1,\, u_2)$ - two output $(y_1,\, y_2)$ system [182].

highly beneficial for network control design and prove useful in a wide array of tasks associated with multi-agent networks.

Multi-vehicle formation problems, gossip algorithms, distributed estimation in networks, synchronization of multiple power units in smart power grids are typical application examples arising in multi-agent control. Various problems in networked systems often appear as state-agreement, synchronization, and consensus tasks [212, 42, 33, 180]. From a practical point of view, network stabilization is fundamental and one of the most challenging problems in multi-agent network control [153, 62]. Many significant results in this direction have made use of systems and control theory along with algebraic tools from graph theory. Frequently, the network stabilization task is considered as a large-scale regulation problem formulated as a structured optimal control problem. Despite the fact that optimal control theory is standard for centralized configurations, distributed optimal control design of large-scale structured systems is a definite challenge. Several contributions in this field are the result of simplifying assumptions such as homogeneous subsystem dynamics, bidirectional communication, dynamically decoupled subsystems, suboptimal control design.

Linear optimal control theory [85] has emerged as a tool of central importance in the development of solutions to problems of networked systems and multi-agent control. In general, the optimality of a control protocol often leads to desirable characteristics for network control design. For instance, the robust stability margins of the linear quadratic regulator (LQR), along with its appealingly simple feedback solution, constitute highly attractive features for distributed control design. In various cases, the task of network regulation is formulated as an infinite-time optimal control problem in the presence of constraints.

However, such problems are often hard to solve in an optimal sense. Network sparsity and absence of global information are two of the main limitations of optimal design and make suboptimal control approaches highly attractive [17, 46].

Model predictive control (MPC) techniques have also been considered for distributed design in multi-agent network control [182]. MPC relies on extensive computations carried out at run-time by solving sequentially several optimization problems in real-time. This concept can adapt straightforwardly to a distributed control setup by requiring that local MPC-based regulators predict their future control actions and the corresponding state trajectories and transmit them to neighboring control units. Recent results [176, 244, 129, 209, 16] in distributed optimization exemplify that MPC-based distributed control methods are very efficient for network control [184, 40, 64], although this is still an active area for research.

Various distributed design techniques for network control appearing in the literature conform to particular assumptions made on 1) the global network objective, 2) the type of interaction between distinct interconnected subsystems (dynamical couplings, information exchange), 3) the performance specifications of each subsystem (dynamics, constraints, objective), 4) the model of each subsystem (linear, nonlinear, continuous-time, discrete-time), 5) the structure of the information exchange scheme (connected, undirected, directed), and 6) the control design method to be utilized (optimal control, predictive control, nonlinear control).

This thesis deals with regulation problems of multi-agent networks. Our interpretation of networks as multi-agent configurations is inspired by the vast array of network applications involving multiple autonomously actuated systems. This inspiration is also enriched by the meteoric rise in popularity of multi-agent control design with distributed architecture. Our main focus is on the design of stabilizing distributed feedback controllers for three general setups:

1) networks of linear non-identical dynamically decoupled agents,

2) networks of nonlinear non-identical dynamically decoupled agents,

3) networks of linear dynamically coupled agents.

In the first two configurations, results are presented for both undirected and directed interconnection schemes, while in the third configuration, the dynamical couplings between interconnected agents are assumed to appear in a bidirectional manner.

The problem of distributed control for networks of decoupled systems, as defined in the first and second settings above, is formulated as follows. A network is composed of distinct dynamical subsystems that can be independently actuated. The subsystems have

joint objectives, which typically couple their dynamic behavior. Local interactions are represented by a connected graph, where the vertices denote subsystems, and the edges between vertices represent coupling terms in the controller associated with the respective vertices. It is assumed that the interaction graph also represents a communication scheme according to which subsystems exchange state-information with their neighboring peers. In the third setting above, we assume that dynamical couplings of the overall system are expressed in a state-space form, which is consistent with the associated interaction graph of the network. The distributed control scheme consists of local controllers, each corresponding to a subsystem where the inputs of each control unit are functions of local information only.

The aims and objectives of this thesis, along with the specific contributions and novelties of this work in the field of distributed network control, are summarized in the following two sections.

1.1 Aims and objectives

Many recent approaches of distributed control over networks of dynamical agents rely on the following simplifying assumptions:

1) bidirectional information exchange,

2) identical agent dynamics,

3) linear agent dynamics,

4) decoupled agent dynamics.

The main objective of this thesis is to propose systematic methods for relaxing these assumptions, thereby leading to enhanced applicability of distributed control techniques to the problem of stabilization of networks of dynamical agents.

Two complementary distributed LQR methods have been proposed in [17] and [46]. The first is a top-down approach, [17], in which the centralized optimal LQR controller is approximated by a distributed control scheme whose stability is guaranteed by the stability margins of LQR control. The second, [46], consists of a bottom-up approach in which optimal interactions between self-stabilizing agents are defined to minimize an upper bound of the global LQR criterion. Both methods require that 1) networks be composed of identical systems and 2) information exchange graph be undirected. Motivated by these two well-established distributed LQR-based control design methods, we attempt to remove the assumptions mentioned earlier, which may be unrealistic in practical applications. In

particular, in Chapter 4, we show that the strict limitation of bidirectional communication between interconnected agents, postulated in [17, 46], can be removed. In Chapter 5, we extend the two distributed LQR-based techniques [17, 46] to a more general agent-model setup. Therein, rather than assuming identical system dynamics, we consider that agent models belong to a class of systems that share the same structural properties (input and state dimensions, controllability indices). In this setting, the stabilization problem of networks of heterogeneous dynamically decoupled agents is tackled via a model-matching technique. In Chapter 6, motivated by the well-established feedback linearization method, we formulate and solve model-matching problems of a nonlinear type via feedback linearization control. Then, based on the results of Chapter 5, we generalize the regulation problem over networks of nonlinear dynamically decoupled agents.

Chapter 7 is devoted to the stabilization problem of networks of dynamically coupled agents. Focusing on linear dynamical agents, we assume that coupling terms between interconnected agents are expressed in a state-space form of a certain structure. We follow a top-down approach, which results in a distributed scheme whose stability is guaranteed via a stability test involving a convex combination of two Hurwitz matrices. In Chapter 8, a case study of load frequency control (LFC) problem over a six-area power network illustrates the applicability of the distributed control scheme proposed in Chapter 7. Finally, in Chapter 9, we consider the stabilization problem of networks in a model predictive control framework. Therein, we formulate the regulation problem of a network of dynamically decoupled linear agents as a large-scale receding horizon optimal control problem. Stability results and feasibility properties of the proposed distributed solution are presented. In the chapter, we also attempt to adapt the results of Chapter 5 to a model-predictive control setting, via a model-matching approach carried out in a fully distributed manner using a distributed gradient descent optimization algorithm.

1.2 Contributions and novelties

The main contributions and novelties of this thesis are summarized in this section. These are presented in detail as follows.

Chapter 3:

1) The gain-margin property of the LQR control holds for complex multiplicative input perturbations and a generic symmetric positive definite input weighting matrix R. The result is summarized in Theorem 3.2.8.

Chapter 4:

1) A new distributed control method for the regulator problem of networks with undirected topology is proposed. The control design is introduced via a two-stage optimization approach which combines techniques from the top-down [17] and bottom-up [46] methods presented in Chapter 3. Sufficient conditions for stability of the new distributed scheme are derived, minimizing an upper bound of the global LQR criterion.

2) The assumption of bidirectional communication between interconnected agents, postulated in [17, 46] is removed. This relaxation relies on the following useful results: (i) the gain-margin property of the LQR control holds for complex multiplicative perturbations (see Theorem 3.2.8), and (ii) the potentially non-simple structure of the Laplacian matrix can be neglected for stability analysis and control design. The distributed control design method for networks with directed topology adopting the top-down approach proposed in [17] is summarized in Theorem 4.3.4.

Chapter 5:

1) We propose a model-matching approach for distributed-control stabilization of networks with non-identical dynamics. Local agents are assumed to share a minimal set of structural properties, such as input dimension, state dimension, and controllability indices, which are generically satisfied for parametric families of systems. The method relies on the solution of certain model-matching type problems using local state-feedback and input matrix transformations, which map agents dynamics to a target system, selected to minimize the joint control effort of the local feedback-control schemes. By adapting two well-established distributed LQR control design methodologies to this setting, the stabilization problem of a network of non-identical dynamical agents is solved. The method is summarized in Theorem 5.4.1 and Theorem 5.4.2, for undirected and directed communication schemes, respectively. The results of this chapter have been published in [223, 221, 222].

2) In [223], we present a simulation study on a formation control problem of four non-identical low-speed experimental UAV's, illustrating the applicability of the method.

Chapter 6:

1) We propose a solution to the regulation problem of a network of heterogeneous nonlinear agents via a model-matching feedback linearization technique combined with a distributed LQR-based feedback control. The method is summarized in Theorem 6.5.5.

Chapter 7:

1) A distributed LQR method for solving regulator problems of networks of dynamically dependent agents is proposed. Dynamical couplings between state-dependent agents are expressed in a state-space form of a certain structure. This allows for approximating a centralized LQR optimal controller by a distributed scheme, the stability of which is guaranteed via a stability test applied to the convex combination of two Hurwitz matrices. The main results of the chapter are summarized in Theorem 7.1.3 and Theorem 7.2.1 and have been published in [220, 219].

Chapter 8:

1) A novel distributed-LQR control algorithm is proposed for solving the load frequency control problem of large-scale multi-area power systems.

2) The control scheme is obtained by optimizing an LQR performance index with a tuning parameter that can emphasize/de-emphasize relative state difference between interconnected areas. In effect, this parameter controls the magnitude of tie-line power exchange and frequency synchronization between interconnected areas.

3) Our approach enhances power system modularity and leads to a simple and verifiable stabilizability condition for a class of network topologies. Extensive simulations presented in this study support our conjecture that this stabilization criterion can be extended to more general LFC problems. The proposed method has been published in [217].

Chapter 9:

1) A novel distributed model-matching time-varying feedback technique is proposed. The matching protocol is combined with a distributed model predictive control scheme the stability of which is guaranteed subject to sufficient conditions. The main result is summarized in Theorem 9.2.14.

2) A distributed model-predictive solution is proposed for the load frequency control problem of multi-area power networks. The method relies on a novel decoupling approach, which allows for the formulation and solution of a model predictive control problem with a quadratic performance index and input saturating constraints along with an overall equality constraint to address the energy balance of the network. The MPC-based load frequency control method has been published in [218].

1.3 List of publications

1. Vlahakis, E. E., Dritsas, L. D., and Halikias, G. D. (2019c). Distributed LQR design for identical dynamically coupled systems : Application to Load Frequency Control of multi-area Power Grid . In *2019 IEEE Conf. Decis. Control*, pages 4471–4476

2. Vlahakis, E. E., Dritsas, L. D., and Halikias, G. D. (2019b). Distributed LQR based Suboptimal Control for Coupled Linear Systems. In *8th IFAC Work. Distrib. Estim. Control Networked Syst.*, volume 52, pages 109–114. Elsevier Ltd

3. Vlahakis, E. E., Dritsas, L. D., and Halikias, G. D. (2019d). Distributed Model Predictive Load Frequency Control of multi-area Power Grid: A Decoupling Approach. In *8th IFAC Work. Distrib. Estim. Control Networked Syst.*, volume 52, pages 205–210. Elsevier Ltd

4. Vlahakis, E., Dritsas, L., and Halikias, G. (2019a). Distributed LQR design for a class of large-scale multi-area power systems. *Energies*, 12(14)

5. Vlahakis, E. E. and Halikias, G. D. (2019). Distributed LQR Methods for Networks of Non-Identical Plants. In *Proc. IEEE Conf. Decis. Control*, volume 2018, pages 6145–6150. IEEE

6. Vlahakis, E. E. and Halikias, G. D. (2018). Model-Matching type-methods and Stability of Networks consisting of non-Identical Dynamic Agents. In *IFAC-PapersOnLine*, volume 51, pages 426–431. Elsevier B.V

7. Vlahakis, E. E., Milonidis, E., and Halikias, G. D. (2018). Cooperative Distributed LQR Control for Longitudinal Flight of a Formation of Non-Identical Low-Speed Experimental UAV's. In *2018 UKACC 12th International Conference on Control (CONTROL)*, pages 295–300

1.4 Structure of the thesis

In this section, we briefly discuss the breakdown of the thesis into chapters. There are ten chapters, listed below with brief comments.

Chapter 1 **- Introduction.** This is the introductory first chapter of the thesis.

Chapter 2 **- Literature survey.** This chapter is a thorough review of multi-agent and network control methods appearing in distributed control literature. We emphasize distributed control techniques that rely on optimal control theory, linear quadratic regulator, and model predictive control. Various significant results on consensus algorithms, formation control methods as well as distributed optimization techniques are also discussed in detail.

Chapter 3 **- Regulator Problem.** This chapter is a concise review of the linear quadratic regulator (LQR) problem, along with the basic mathematical results associated with it. The main scope of the chapter is to show how the LQR theory can be adapted to networks of interconnected systems. The concept of multi-agent networks and network control, as well as two well-established methods in the context of distributed LQR control, are introduced.

Chapter 4 **- Stabilization of multi-agent networks with undirected and directed topology.** In the first part of the chapter, we propose a new distributed control design method for stabilizing undirected networks of identical dynamic agents. The method combines techniques from two approaches discussed in Chapter 3. In the second part, we relax the assumption of undirected network topology, and we study the regulation problem of multiple identical agents over connected digraphs. The establishment of the proposed control schemes relies on the gain-margin property of LQR control and the non-simple structure of the Laplacian matrix of a connected digraph.

Chapter 5 **- Model-matching and regulation of interconnected heterogeneous linear agents.** In this chapter, we study the regulation problem of multiple heterogeneous dynamically decoupled agents over connected graphs and digraphs. Formulating the regulation problem as a large-scale structured optimal control problem, we propose a two-stage design procedure. In the first stage, we assume that agents constituting the network have the same structural properties, and we follow a model-matching approach to match agents' dynamics with a target model. Typically, we use local feedback controllers and input-matrix transformations to compensate for the dynamical mismatch among the models of the agents. We show that distributed control methods for networks formed of identical dynamically decoupled linear agents can adapt to the present setting, by merely constructing stabilizing distributed controllers depending on the target dynamics only. To exemplify our results, we employ two methods presented in Chapter 3.

Chapter 6 **- Feedback linearization and model-matching of nonlinear systems.** This chapter aims to extend the model-matching approach studied in Chapter 5 for linear systems,

to a particular class of nonlinear systems. We consider a model-matching problem of multiple nonlinear systems, which is solved by the feedback linearization technique. In effect, via feedback control and a coordinate transformation, the dynamics of each system are mapped to a linear model referred to as the target system. By establishing the notion of controllability indices for nonlinear systems, we adopt the proposed model-matching scheme to a network setup in which heterogeneous nonlinear self-linearizable agents are stabilized by a distributed LQR-based controller designed on target dynamics.

Chapter 7 **- Distributed LQR for coupled LTI systems.** This chapter is concerned with the regulation of a large-scale dynamical system that can be expressed as a network of multiple dynamically coupled linear agents. Typically, we assume that dynamical couplings among agents are expressed in a state-space form of a specific structure consistent with an undirected graph describing information exchange between coupled agents. We follow a top-down approach to approximate a centralized LQR optimal controller by a distributed control scheme. The stability of the proposed controller is guaranteed via a stability test applied to the convex combination of two Hurwitz matrices.

Chapter 8 **- Distributed LQR-based load frequency control of multi-area power system.** In this chapter, we present a simulation study of a six-area power network, highlighting the applicability of the results presented in the previous chapter. In particular, we consider a power system formed of six distinct control areas with identical dynamics that are interconnected via weak tie-lines. We then formulate the load frequency problem of the network as a disturbance rejection task of power-load step variations of unknown size. We approximate a centralized linear quadratic regulator (LQR) optimal controller by a distributed control scheme. Overall network stability is guaranteed via a stability test applied to a convex combination of Hurwitz matrices, the validity of which guarantees stable network operation for a class of network topologies. The efficiency of the proposed distributed load frequency controller is illustrated via various simulations. In the study, we also consider significant parametric variations in the parameters of each area.

Chapter 9 **- Distributed model predictive control design.** In this chapter, we start with a brief review of the deterministic model predictive control theory and then study the regulation problem over networks of dynamically decoupled linear systems from a model-predictive control (MPC) perspective. We propose a distributed MPC-based control scheme, the stability of which is proved via local Lyapunov functions. In the chapter, we also adapt the results of Chapter 5 to a model-predictive control setting, and propose a model-matching

control method carried out in a fully distributed manner using a distributed gradient descent optimization algorithm. Further, motivated by the structure of a multi-area power network, we consider a large-scale load frequency control problem of a power network composed of multiple interconnected areas. The task is formulated as a receding horizon optimal control problem with a quadratic performance index and input equality constraints that address the energy balance of the entire system.

Chapter 10 **- Conclusions and future work.** This is the final chapter of the thesis. It discusses the conclusions of the derived results and suggests various topics and directions for future work and research.

Chapter 2

Literature survey

Networked systems emerge in various disciplines and fields and are of particular interest to the control community due to their association with a broad spectrum of important applications. Many reasons, ranging from technological advances to economic benefits, have incentivized the development of large dynamic systems, often referred to as multi-agent networks, which are composed of several interacting subsystems and multiple control units. Due to various factors such as system complexity, robustness, and reliability problems as well as communication-related issues, distributed control techniques have experienced a considerable rise in popularity in multi-agent and network control domains.

The interest in dealing with large-scale control problems dates from the early 70s with the seminal works [82, 111, 227] establishing the decentralization concept in the distinct domain of control theory. Therein, a decentralized control scheme of a linear multivariable system is defined as a controller with several control units, each one having access only to local system outputs and controlling only local inputs. Adopting terminology from the economic literature and energy industry, [6] discusses the notion of local control agents acting on a large-scale dynamical system, the stability of which relies on the information exchange among agents. These early advances in control of large-scale systems, along with the ever-increasing integration of communication and control theories, have led to more sophisticated concepts such as distributed control and networked systems.

This chapter presents a comprehensive review of control methods appearing in the recent literature of distributed control. We focus on distributed control techniques that are based on optimal control theory, linear quadratic regulator, and model predictive control. Recent results on consensus algorithms, formation control methods as well as distributed optimization techniques, are also given attention.

Specifically, the chapter reviews recent research results in the following directions, which are not independent but actually overlap to some extent:

1) Distributed feedback design methods for stabilizing large-scale dynamic systems (distributed parameter systems, networked systems, multi-agent systems). Several references on this subject are reviewed in Section 2.1 and are associated with Chapter 3, Chapter 4, Chapter 5, Chapter 6, and Chapter 7.

2) Distributed control design protocols for agreement problems (consensus problems, formation control). Several references on this subject are reviewed in Section 2.2 and are associated with Chapter 4, Chapter 5, and Chapter 6.

3) Distributed model predictive control. A number of references on this subject are reviewed in Section 2.3 and are associated with Chapter 9.

4) Distributed gradient descent optimization methods. A number of references on this subject are reviewed in Section 2.4 and are associated with Chapter 9.

2.1 Distributed feedback control

Over the past few years, there has been a rapid rise in interest in large-scale control systems composed of several interconnected units with interactive and cooperative capacity [41, 24, 140, 63, 8, 9, 93, 56, 110, 75, 177, 99, 19, 100, 57, 74, 173, 18, 198]. Significant results in stability analysis of such schemes led to a deeper understanding of the relationship between algebraic properties of the interconnection graph and global stability of the overall system. Perhaps the most insightful contribution in this direction has been the significant work of [63], which establishes stability analysis tools for networks of identical linear dynamical systems over generic graph interconnection schemes. Therein, authors focusing on formation distributed control problems develop information exchange protocols that guarantee formation stability and performance and are robust to changes in the communication topology of the network.

Several studies are concerned with control problems of distributed parameter systems with spatially invariant dynamics and spatially distributed controls and measurements. The important work of [8] in this area discusses fully actuated distributed control problems involving quadratic criteria such as linear quadratic regulator (LQR), H_2, and H_∞. It is shown that for infinite-dimensional spatially invariant systems, optimal controllers have an inherent degree of decentralization, which helps decompose the problem exactly into a parameterized family of finite-dimensional optimal problems. Authors also establish a general result that applies to partially distributed control and a variety of performance criteria, proving that optimal controllers inherit the spatial invariance structure of the overall system. In [9],

another approach to distributed parameter system problems considers distributed control design in spatially invariant systems for which communication among subsystems is confined. In particular, authors assume that the controller is constrained so that information flow among sites is propagated with a delay that depends on the distance between subsystems. Authors term this structure as "funnel" causality, and show that the problem of optimal design can be cast as a convex problem as long as the overall system has a similar funnel-causality structure, and the propagation speeds in the controller are at least as fast as system dynamics.

Spatially invariant systems with special structure have also received attention. The study in [93] analyzes inverse optimality of localized distributed controllers for an infinite string of linear systems. Therein, a frequency domain criterion is established that separates controllers that are never optimal from controllers that are optimal (in the LQR sense). It is shown that this criterion can, in general, be expressed in terms of the reciprocal of sensitivity functions, and especially for single-input systems, it requires the return difference be at least equal to one at all spatial and temporal frequencies. Several results, however, pertain to spatio-temporal instability phenomena arising in the class of spatially invariant systems on lattices as a result of aggregate effects [95, 8, 203]. Authors in [94] and [185] have addressed some fundamental design limitations in the control design of systems on lattices focusing specifically on vehicle-platoon applications. In particular, [94] showed drawbacks of two widely cited papers [112, 137], which address the linear quadratic regulator problem for large-scale systems composed of moving vehicles. There, the authors employ spatially invariant theory to show analytically how these formulations lack stabilizability or detectability.

Further, the study of [185] proves that string stability of a finite platoon with linear dynamics cannot be achieved with any linear controller that uses only information on relative distance between two successive vehicles. An equivalent result was also exhibited earlier in [37], where string stability of a spatially invariant infinite string of moving vehicles was established with static feedback controllers of identical architecture. Interesting results with practical importance for automated highway systems are presented in [95]. Therein, the peaking phenomenon in the control of large-scale vehicular platoons is investigated, and it is shown that imposing a uniform rate of convergence for all vehicles towards their desired trajectories may generate unacceptable transient peaks in both velocity and control. Authors also derive explicit constraints on feedback gains that allow for desired position transients without peaking phenomena and excessive use of control effort.

A distinguished group of recent control strategies involves linear matrix inequality (LMI) relaxations to control problems of large-scale distributed systems. In [56], authors study networks of heterogeneous subsystems and derive sufficient conditions for the existence of distributed controllers that guarantee global stability. It is shown that under the proposed

distributed control scheme, a certain level of performance is guaranteed, with closed-loop systems being strictly contractive. The corresponding conditions are defined in general via an infinite-dimensional operator which becomes linear matrix inequalities when the state-space form of the overall system is either of finite extent or periodic in every variable. The work in [110] deals with the distributed control design of networks of finite and possibly nonidentical LTI systems over arbitrarily connected graphs. Authors assuming graphs with bidirectional edge orientation, formulate convex existence conditions for output-feedback controllers, which achieve a guaranteed H_∞ performance level. The resulting linear matrix inequalities grow redundant with the number of subsystems in the interconnection graph.

Computational complexity associated with the solution of a distributed optimal control problem is well elucidated in the study of [75]. Therein, the synthesis problem of a linear quadratic regulator (LQR) controller is studied when the matrix describing the control law is constrained to lie in a particular vector space. Authors consider the finite-horizon version of the problem and provide both a computationally intensive optimal solution and a sub-optimal solution that is computationally more tractable. There, the proposed method is applied to a decentralized vehicle formation control problem exemplifying the loss in performance due to the use of the suboptimal solution. A notable result in characterizing the complexity of large-scale optimal control design subject to constraints on the controller structure is proposed in [177]. Therein, authors formulate the task of constructing optimal decentralized controllers as a problem of minimizing the closed-loop norm of a feedback system subject to constraints on the controller structure. In particular, it is proved that quadratic invariance of the assumed controller structure implies that the corresponding minimum-norm problem may be solved efficiently via convex programming. The proposed results are developed in a very general framework and are shown to hold in both continuous and discrete-time, for both stable and unstable systems, and for any norm, thereby unifying many previous results in the class of convex decentralized control problems.

A powerful method for distributed LQR design for stabilizing networks of homogeneous dynamically decoupled LTI systems is presented in [17]. There, a distributed regulation task is formulated as a large-scale optimal control problem where the performance index couples the behavior of the systems. Authors propose a top-down approach in which the centralized optimal LQR controller is approximated by a distributed control scheme whose stability is guaranteed by the stability margins of LQR control. This elegant feature clarifies the connection of the stability of a large-scale system to the robustness of local controllers and the spectrum of a matrix representing the sparsity pattern of the corresponding interconnection graph. Although the assumptions of identical dynamics and suboptimality of the global controller may be restrictive in practice, however, they simplify the problem considerably.

The results can be used directly to improve stability margins and facilitate controller synthesis in the field of distributed receding horizon control [24, 99, 57].

A complementary method for designing distributed LQR controllers is presented in [46]. The proposed technique consists of a bottom-up approach in which optimal interactions between self-stabilizing agents are defined to minimize an upper bound of the aggregate LQR criterion. In the paper, an analysis of the proposed control law in the presence of delays in the relative communication scheme is carried out and a bound on the maximum delay accommodated by the proposed controller is established. A thorough procedure for designing distributed controllers for a class of identical dynamically coupled systems based on a decomposition approach has been presented in [132]. Therein, the validity of the proposed scheme relies on specific structural properties satisfied by the system matrices. Authors optimizing a multi-objective function subject to linear matrix inequality constraints derive explicit expressions for computing distributed feedback controllers with H_∞ and H_2 performance, respectively.

The synchronization problem of a set of identical independently actuated systems exchanging output-measurement information over a communication scheme is considered in [138]. Authors propose a distributed static output feedback controller with guaranteed H_2 performance, which is compared to a fully centralized scheme. Necessary conditions for network stability are expressed as convex linear matrix inequalities, the formulation of which allows for certain nonlinearities as well as uncertainties to be considered into the nominal systems' models. A "finite-section" approximation method for solving large-scale LQR optimal control problems of spatially distributed systems is introduced in [142]. The method involves the construction of a series of finite-dimensional LQR problems, such that their solutions converge to an infinite-dimensional LQR problem for large-scale systems. The authors study the limit behavior of the proposed approximation method and show that the solution of the approximate problems converges strongly to the solution of the large-scale problem. The proposed technique exemplifies the design of finite-dimensional local optimal controllers. The paper also proposes a spatial interpolation method which integrates all locally designed controllers to a parameterized family of stabilizing controllers for the spatially distributed system.

LQR control theory has also emerged as a critical tool for tackling consensus and state-agreement tasks over networked multi-agent systems. For instance, in [26], optimal algorithms are developed for mobile agents with single-integrator kinematics seeking consensus. Therein, authors focusing on continuous-time dynamical agents derive optimal linear consensus protocols from solving standard LQR control problems. Two different performance indices which couple the behavior of the agents are considered. In the first, the

weighting parameters are selected independently of the relative weighted graph, while in the second, the state weighting matrix is consistent with the entries of the associated weighted adjacency matrix. In the paper, a systematic procedure for deriving an optimal multiplicative feedback-gain shift of the Laplacian dynamics is also presented for a given interaction graph and a particular tuning of the LQR performance index. A similar LQR-based method for a formation control problem is presented in [87]. Therein, LQR design is employed for solving optimal formation control problems of multiple agents whose communication topology, as well as the interaction parameters, are tunable upon a global performance index defined as the summation of node-level LQR cost functions.

As mentioned earlier, networked control systems (NCS) lie in the intersection of control and communication theories. While this convergence effectively allows for control design with distributed architecture, robust control algorithms are needed to guarantee network stability and compensate for various communication imperfections and constraints. Typically, properties such as optimality and stability margins of networked control schemes vanish in the presence of delays leading often to instability phenomena under certain circumstances [38, 78]. Significant results on the effects of time-varying delays on the stability of NCS are presented in [38, 70, 96, 146, 243]. A Lyapunov-based stability criterion for discrete-time NCS models with bounded time-varying delays defined in terms of LMI's is proposed in [38]. In the study, delays assumed either greater or less in magnitude than the sampling interval, are expressed as a combination of uncertainty functions, an approach that allows for a model approximation that explicitly contains the bounds of the time-varying delays. An interesting work on NCS with uncertain delays is presented in [70]. Therein, authors based on polytopic inclusions for modeling systems with time-varying delays and using the Cayley–Hamilton theorem, propose a new technique for generating discrete-time models of linear systems with time-varying input delays. Effective stability criteria for continuous- and discrete-time systems with bounded time-varying delays are presented in [96]. It is shown that overall stability can be tested via a simple Bode diagram. Delay impulsive systems are investigated in [146]. Authors establish asymptotic and exponential stability theorems by employing Lyapunov functionals with discontinuities. Specifically, demonstrating that a NCS interconnected through imperfect communication channels can be modelled as a linear delay impulsive system, authors derive stability conditions for the closed-loop system in terms of LMI's. An iterative LMI-based approach for calculating stabilizing state-feedback gains for a class of networked control systems with random delays is proposed in [243]. In the study, stability conditions are established using Markov chain and switched systems theories.

2.2 Agreement control problems

Agreement control problems emerge in various domains ranging from physics and biology [107, 199] to robotics and computing [45, 211], and have been a subject of constant research over the past few years. Such problems typically arise in applications involving multi-agent networks where individual agents need to agree upon specific quantities related to a global objective. In essence, each agent resolves the agreement task via a distributed control protocol using local information. Next, we review some of the significant research results on distributed control of multi-agent networks for agreement problems classified into two categories. We list the following:

1) Consensus, synchronization, and rendezvous problems. These tasks pertain to the group behavior that all agents asymptotically reach a collective agreement through a local distributed protocol. We simply refer to this category as consensus problems.

2) Formation, flocking, and swarming problems. Such problems pertain to the group behavior that all agents form a pre-designed geometrical configuration through local interactions. We refer to this group of problems simply as formation control problems.

We emphasize that this distinction is not restrictive, in the sense that several problems arising in the two categories above may be interpreted from the same point of view.

2.2.1 Consensus problems

One of the most notable results in addressing consensus problems in their general form for networks of dynamic agents is presented in [155]. Therein, authors study convergence properties of consensus protocols for directed networks of multiple agents with single-integrator dynamics. Specifically, they establish a relationship between algebraic properties and the performance of reaching agreement of the network in the presence or absence of switching-topology and time-delay scenarios. It is shown that there is a connection between the performance of a linear consensus protocol on a directed network and the Fiedler eigenvalue of the disoriented version of the associated digraph modeling the information flow. Highlighting important properties of balanced graphs, authors derive necessary and sufficient conditions for a linear protocol to solve the average-consensus problem over a directed graph with fixed topology and in the absence of communication delays. Further, considering networks with switching topology, authors introduce a joint Lyapunov function that proves asymptotic convergence to a group decision value. In [155], using several tools from graph and control theories, a connection between the robustness margin to time-delays

and the maximum eigenvalue of a given network topology is established. Fundamental results of [155] are well exemplified in [154] via a more application-oriented study on consensus problems for networks of continuous-time as well as discrete-time agents with single-integrator dynamics. The study in [234] builds upon the results of [155, 154], and presents linear consensus control protocols for networks of multiple agents with more elaborate dynamics.

Simplicity in implementation as well as inherent robust characteristics are two of the main reasons that Proportional-Integral (PI) control is appealing for distributed control design especially in consensus applications. Stabilizing a system in the presence of unknown disturbances or compensating for model imperfections as well as nonlinearities are well-studied problems in the context of PI control. However, designing distributed PI controllers of networked systems is still a challenging problem mainly due to the difficulty in deriving stability conditions for generic system models [11]. Significant results on distributed PI control of networked systems with single- and double-integrator dynamics are proposed in [3]. Specifically, authors demonstrate that the proposed distributed PI control scheme enable systems to reach consensus while compensating for constant disturbances in the network. A tight upper bound on the integral gain is explicitly derived for both single- and double-integrator schemes. In this study, the proposed PI control design as well as necessary and sufficient conditions for consensus are derived for static interaction graphs. Similar works in designing distributed PI controllers in the presence of constant disturbances in networks can be found in [69, 83, 240].

Studying the effect of time-delays in consensus problems is an issue of fundamental importance since information exchange carried out over non-ideal communication channels is usually delivered with a delay. Research efforts in this area are manifested in several recent works [155, 186, 187, 161, 145, 86] addressing and evaluating the level of delays that can be accommodated in the exchange of information over multi-agent networks. Specifically, in [155], necessary and sufficient conditions are derived for average consensus problems of networks of single-integrator agents with fixed delays in the communication scheme. In [186, 187], authors consider double-integrator agents, each receiving its own output information instantaneously, and after a constant delay the information from its neighbors. The results are based on Lyapunov-Krasovskii techniques and are expressed in terms of LMI's. The effect of heterogeneous multiple delays on consensus in multi-agent systems is explored in [161], while robustness issues related to consensus of multi-agent systems subject to non-identical feedback delays are studied in [145]. In [86] a stability analysis of time-varying delays in consensus problems for multi-agent systems described by double-integrator dynamics are presented by employing Lyapunov–Razumikhin functions.

The problem of reaching consensus for multi-agent networks with varying topology is explored in [171]. There, authors consider a directional information exchange scheme subjected to variations and establish the minimum requirements for an update algorithm to converge, thereby generalizing the significant results presented in [91] on coordination rules for multi-agent networks with undirected topology. In particular, it is shown that information consensus under altering interaction topologies can be achieved asymptotically if the union of the directed interaction graphs has a spanning tree frequently enough as the system evolves.

Stationary consensus problems over multi-agent schemes are also studied in [10]. There, authors focusing on schemes with fixed topologies, define consensus as a group decision value, which is a function of the initial states of all agents. Enforcing this definition of consensus, authors establish sufficient conditions for a consensus value to be an attainable target and introduce a local nonlinear protocol allowing consensus on a general set of values. It is shown that these local protocols are solutions to individual optimization problems carried out entirely in a distributed fashion.

Agreement control protocols for leader-follower type consensus tasks over multi-vehicle schemes are proposed in [169]. In contrast to [155, 154, 171, 10], in [169], authors define consensus as a dynamic decision value which is expressed as a time-varying reference state. Specifically, they assume that a limited number of vehicles in the network have access to a reference state, which is either a time-varying exogenous signal or evolves according to a nonlinear model. For this setting, authors propose distributed consensus algorithms and derive necessary and sufficient conditions for a time-varying consensus achievement.

Optimal strategies for tackling consensus problems are presented in [43]. In particular, authors focus on directed networks of interconnected agents aiming to reach the average value of their initial positions and show that the optimal topology of the communication scheme among the agents is given by a de Bruijn graph. It is proved that for information exchange schemes designed as de Bruijn graphs with maximum out-degree bounded, the best consensus control policy among linear, nonlinear, and time-varying techniques, is a deadbeat strategy that converges in finite time. Authors also show that the proposed strategies can adapt to a more general consensus problem allowing for finite convergence even with quantized communication between agents.

Finite-time convergence in consensus problems is also explored in [225, 27, 67]. In particular, authors in [225] solve consensus problems of networks of agents with single-integrator dynamics in finite-time via continuous-time feedback control. On the contrary, the study in [67] focusing on directed topologies, proposes a discontinuous interaction rule which guarantees effective disturbance rejection and finite consensus-reaching time. Finite-time consensus problems are well reviewed in [27]. Therein, authors focusing on

networks with switching topology and a specific class of nonlinear agents, analyze the finite-time convergence of a continuous-time nonlinear consensus algorithm. It is proved that the proposed nonlinear consensus algorithm guarantees finite-time convergence when the switching interaction graph has a directed spanning tree at each time interval.

Another significant group of research results on consensus strategies involves multi-agent systems with high-order dynamics. Specifically, in [86], authors consider consensus problems for networks formed of interconnected double integrators representing planar mobile agents. In the study, it is assumed that communication among agents is corrupted by time-varying delays and topologies. Double-integrator dynamics are also considered in [238]. In particular, authors derive necessary and sufficient conditions for second-order consensus in a multi-agent network. In [238], it is pointed out that both the real and the imaginary parts of the eigenvalues of the associated Laplacian matrix play critical roles in consensus achievement. The proposed consensus algorithms guarantee consensus when communication delays are less than a specific value. In [245], the consensus problem is cast as a synchronization task over a network of multivariable dynamic systems. With this interpretation in force and assuming that communication topology remains invariant, authors in [245] propose a distributed observer-based consensus protocol expressed as a function of local states and relative output measurements. In the study, the notion of consensus region is also introduced and analyzed. Specifically, it is proved that local stabilizability and detectability are necessary and sufficient for the proposed distributed protocol to guarantee consensus yielding an unbounded consensus region.

Several works deal with the derivation of conditions that guarantee consensusability, a term which has been used by many researchers in the context of multi-agent control and refers to the existence of consensus protocols given the dynamic structure of each agent and the topology of the interaction scheme among agents. Existence conditions of a consensus protocol are derived in [122] for multi-agent networks of LTI systems with fixed topology. In [71], authors focusing on undirected graphs and single-input agents, derive a consensusability condition for a state-feedback controller. In the paper, it is also shown that introducing a properly designed dynamic filter into the local feedback protocols, the consensusability condition derived in [236] can be improved. Significant results on consensusability properties of multi-agent schemes interconnected over communication channels with time-varying delays are presented in [235, 230].

Most recent results involve the study of distributed feedback design of consensus protocols for networked systems of various setups. For instance, works [232, 3] study the design of distributed feedback protocols for consensus problems of undirected networks of multiple agents with general linear dynamics. Output and state feedback techniques are

proposed in [113] and [114], respectively, for multi-agent systems with directed topology. Feedback design for multi-agent schemes with both cooperative and competitive interactions is considered in [1]. Therein, the author introduces a suitable notion of consensus in the presence of antagonistic links and investigates conditions for which agents on signed graphs can achieve consensus via the proposed distributed feedback protocols.

Consensus problems of multi-agent systems with prescribed transient behavior has also been given attention by several authors. In particular, the study in [126], deals with a consensus problem of multiple double-integrator agents with transient constraints. Authors initially set time-dependent constraints on the transient response of the relative positions between neighboring agents and propose a distributed control law consisting of a proportional term of the transformed error and an additional damping term based on absolute velocities measurements. In the paper, an agreement protocol that can additionally achieve prescribed performance for a combined error of positions and velocities is also studied. Consensus algorithms for multi-agent schemes with nonlinear dynamics and transient constraints have also been explored. In [97] and [98], two prescribed performance consensus control schemes are designed for the first- and second-order nonlinear multi-agent systems, respectively. Authors in [228], propose a leader-follower consensus scheme for networked uncertain nonlinear strict-feedback systems with unknown control directions. The control methods proposed in [97, 98, 228] consider nonlinear dynamic agents described by differential equations linear in the control input. A general class of nonlinear dynamic agents is considered in [39]. Therein, authors study a prescribed performance distributed consensus problem of multiple nonlinear dynamic agents interconnected over a directed communication network.

Another critical group of recent results on consensus control problems deals with the design of resilient and secure control for multi-agent networks vulnerable to malicious activities. Distributed networked systems are prone to attacks and component failures, and therefore trustworthy control computation in the presence of misbehaving components is of fundamental importance. The characterization of the resilience properties of linear consensus strategies has been addressed in [163, 200, 201], where it is shown that the resilience to external attacks is limited by the connectivity of the network. In [163] the problem of detecting and identifying misbehaving agents in a linear consensus network is first introduced, and a solution is proposed for the single faulty agent case. Authors in [200] and [201], develop a distributed control strategy that enables all or a number of nodes to calculate any consensus task defined as a function of their initial states despite the presence of some malicious (or faulty) nodes. In [164], the effect of misbehaving inputs on the network performance is quantified from a system theoretic perspective. Therein, authors address the

problem of detection complexity and propose a computationally efficient detection method that is compatible with both discrete and continuous-time linear consensus networks.

2.2.2 Formation problems

Formation control deals with the coordination of interconnected vehicles and is important for many practical applications such as formation flying, cooperative transportation, and sensor networks. The main objective of distributed formation control is to enforce the desired motion pattern throughout a cooperative task of a multi-vehicle system. Excellent surveys of formation control of multi-agent systems are found in [154, 65, 28].

Existing approaches to vehicle formation control typically fall into two categories [63]. The "leader–follower" approach has the advantage of simplicity in that a reference trajectory is defined by the leader, and in that internal stability of the formation is implied by the stability of the individual vehicles' control laws. The second approach is the "virtual leader" approach [195, 59], in which mobile agents in the formation jointly synthesize a fictitious leader whose trajectory is cast as a leader for the group.

One of the most notable recent works on formation control is [63]. Therein, authors establish information exchange protocols that guarantee formation stability and performance and are robust to changes in the communication topology of the network. In the paper, the problem of cooperation among a collection of vehicles performing a shared task using inter-vehicle communication to coordinate their actions is considered. Authors prove a Nyquist criterion that uses the eigenvalues of the graph Laplacian matrix to determine the effect of the communication topology on formation stability. They also propose a method for decentralized information exchange between vehicles, which yields a dynamical system that supplies each vehicle with a common reference to be used for a cooperative motion.

The study in [170] presents a position-based control scheme considering mobile agents with double-integrator dynamics. Therein, agents are assumed to be able to measure their absolute positions and velocities, as well as relative positions of their neighbors. The authors propose a formation protocol that enables agents to move from their initial positions to the desired positions. The ending points of the formation, as well as the formation shape, are specified a priori. An equivalent method applied to multi-agent networks of nonholonomic systems is found in [52, 53]. There, authors propose a position-based control law that allows agents to track the desired trajectories. They also show that the proposed control scheme achieves satisfactory trajectory tracking for a static interaction graph. Similar problems for time-varying interaction graphs have been explored in [53, 179].

Collision avoidance is an important and rather difficult problem in multi-vehicle networks. Methods for distributed formation control with obstacle as well as inter-vehicle collision

avoidance capacity have been presented in [61, 197, 133, 193, 104, 77, 175]. The studies in [61, 193, 104, 77] propose receding horizon control techniques for tackling avoidance problems of nonholonomic vehicle formations. However, none of the works mentioned above addresses the feasibility and stability of the proposed control scheme explicitly. In [133], a switching control method that guarantees trajectory tracking with bounded tracking error and collision avoidance is proposed. The work of [175] presents a trajectory tracking method that enables obstacle and inter-vehicle collision avoidance and respects input saturation constraints. The method in [175] is only valid for formations of a limited number of vehicles. Communication preservation in multi-vehicle formation schemes is fundamental for collision avoidance purposes [7]. In [229], a multi-region control scheme is proposed for a formation of nonholonomic vehicles to track a reference trajectory while avoiding collisions and preserving network connectivity in unknown environments. Unfortunately, all the papers mentioned in this paragraph suffer from important drawbacks, namely, use of unbounded input forces, lack of scalability, irregular fragmentation and collapse. In contrast, the work in [29, 178], does not possess these undesirable properties. Collision and obstacle avoidance has been well-explored in research studies dealing with flocking problems of multi-agent systems.

Flocking is a term that refers to the collective behavior of a large number of agents that interact one another towards a common group objective. Swarming, schooling, and platooning are similar concepts, each pertaining to a particular family of applications. For instance, there are swarms/flocks of cooperative unmanned aerial vehicles (UAVs), vehicle platoons, and schooling schemes of multiple underwater vehicles. In the following, we adopt the flocking terminology. Stability is a fundamental qualitative property of flocking control since if it is not present, then it may be impossible for a multi-agent system to achieve any other global objective. Stability analysis of an M-dimensional mobile swarm with a fixed communication topology is considered in [121]. Therein, authors also derive conditions under which a mobile swarm can maintain cohesion during movements even in the presence of sensing delays and asynchronism. Authors in [206] propose a centralized algorithm for a particle system that leads to irregular collapse for generic initial states. They also suggest a distributed scheme that leads to irregular fragmentation. Fragmentation and collapse are two well-known pathological abnormalities arising in flocking schemes that are discussed in [153] in detail. In particular, [153] presents a theoretical framework for the design and analysis of distributed flocking algorithms. Author considers free-space flocking as well as flocking in the presence of multiple obstacles. The proposed distributed control algorithms, which lead to the emergence of collective behavior, are derived via a Lyapunov stability

approach. More recent results on flocking stability of distributed multi-agent systems can be found in [237, 73, 242, 213].

2.3 Optimization based control methods

Model predictive control (MPC) is an optimization-based control technique that uses a mathematical model to predict the system's behavior over a finite future horizon. A system's desirable behavior is manifested as the minimization of an objective function, possibly subjected to a set of constraints representing the acceptable range of state and input variables of the system. Typically, the input variables of a system are defined from the solution of an optimization problem carried out online at each time instant of a discretized time horizon. This iterative control calculation demands a control unit with intense computation capacity and represents the main drawback of model predictive control. However, its ability to handle explicitly complex phenomena, such as actuator constraints and multi-objective control problems, has been substantial, especially for tackling complex control problems of large-scale dynamic systems. Advances in communications, as well as the establishment of powerful computing resources, have led to an ever-increasing rise in popularity of MPC strategies for multi-agent problems and distributed network control. In the section, we review a limited number of papers on distributed MPC, identifying some of the most interesting works of this vast research area.

2.3.1 Distributed model predictive control methods

Recently, several approaches have been proposed for distributed MPC. Survey papers [182, 35, 152, 135] and textbook [128] provide comprehensive overviews of the relevant literature. An important group of results pertains to the study of large-scale systems that can be decomposed into a number of dynamic subsystems, possibly dynamically decoupled with state/input constraints and coupled objectives. Authors in [58], study a finite horizon optimal control problem of a set of interacting systems whose dynamic behavior is coupled via a given objective function. It is proved that a distributed receding horizon control implementation is stabilizing to a neighborhood of the objective states when subsystems and their constraints are open-loop separable. The proposed algorithm in [58], requires synchronous updates as well as exchange of the most recent optimal control trajectory between interconnected subsystems before each update. Similar approaches to optimal MPC control of open-loop decoupled systems are proposed in [99, 174].

Receding horizon optimal control problems of dynamically decoupled systems with coupled constraints have also been given attention. In such schemes, closed-loop performance is coupled even in the absence of coupling terms in the objective function. Finite horizon distributed control problems with coupled constraints are studied in [102] adopting a hybrid logic rule-based approach, in [168, 165] via a dual decomposition based method, as well as in [89, 196, 108] where excessive information exchange between coupled agents is required. The study in [100] proposes a decentralized scheme in which individual agents optimize a local performance index respecting objective functions of neighboring agents as well as coupling constraints with them.

Cooperative MPC, whereby each local controller optimizes a common objective function represented as a weighted sum of local cost functions, is initially introduced in [215] and also developed in [196]. Sequential [116–118] and iterative [119] approaches for cooperative MPC design are well exemplified in the review paper [35]. Therein, a cooperative MPC control problem with state and input constraints is tackled via a Lyapunov-based method. In particular, a stabilizing controller is designed in the absence of constraints by solving a typical infinite horizon linear quadratic regulator problem. Then, a distributed and a decentralized model predictive control strategies are employed to guarantee stability of the closed-loop agents in the presence of constraints. A complementary "almost decentralized" Lyapunov-based MPC method is described in [128]. A concise study of cooperative control problems of decoupled, nonlinear, discrete-time agents associated with objective functions composed of individual as well as cooperative terms, is considered in [68]. Therein, each agent is assumed to evolve in discrete-time, based on a locally computed control law, which is defined by exchanging delayed state-information with neighboring agents. A rigorous stability analysis considering the input-to-state stability properties of the receding-horizon local control laws is also carried out. Stability of the overall system is proved by utilizing small-gain theorem results. A similar multi-agent setup in which local control units have a limited access to global information as well as limited communication capacities is studied in [127]. In the proposed scheme, agents are assumed to communicate a limited number of times over a time interval in order to share information needed for making a cooperative decision. In the paper, authors propose an optimization procedure for designing a distributed controller, which guarantees stability of the overall system subject to a set of sufficient conditions.

Networked MPC methods deal with the development of distributed MPC-based control strategies of networked systems which are robust to network imperfections, such as time-varying transmission delays, topology variations, packet losses in data transmission [135]. Model predictive schemes have been effectively used to compensate for network delays oc-

curring on measurement channels [143], or in the presence of various measurements collected by distributed networked sensors. The study in [120] proposes a detailed stability analysis for designing distributed Lyapunov-based model predictive controllers that compensate for asynchronous and delayed measurements. Sufficient conditions for stability of the proposed distributed scheme are also derived. A robust control scheme combining model predictive control with a network delay compensation strategy is proposed in [166]. Therein, authors showing that the feasible region is invariant under the proposed networked closed-loop strategy, establish a feasibility property of the optimization problem associated with the proposed receding horizon control law. In this paper, robust stability of the closed-loop system is also established using a characterization of regional input-to-state stability and time-varying Lyapunov functions.

2.4 Distributed optimization

Control and optimization are two mathematical disciplines that are intrinsically connected. There are great advantages to formulating a control problem as an optimization problem. Perhaps the most essential is that the problem can then be solved efficiently and in a meaningful manner. Distributed optimization has emerged as a powerful paradigm for attacking large-scale control problems [12, 205] and, among others, has widely been adopted in the contexts of distributed feedback control [110, 115] and distributed model predictive control [182, 35, 152]. The development of distributed optimization algorithms and the study on their convergence properties help the implementation of computationally efficient control schemes. In this section, we review a number of recent distributed optimization methods which are important in solving complex control problems in networked and multi-agent systems. We focus on distributed (sub)-gradient descent (DGD) methods proposed for solving the following distributed optimization problem:

$$\underset{x \in \mathscr{X}}{\text{minimize}} \quad \sum_{i=1}^{m} f_i(x). \tag{2.1}$$

Several recent advances in distributed (sub)-gradient methods have built upon the seminal works [210, 211, 12], which have epitomized the analysis of optimization models for decision-making processes distributed across several decision-makers (agents). Inspired by this line of research, numerous recent results pertain to the study of distributed computation models for optimizing a global performance index expressed as a sum of multiple objective functions, each measuring a local performance controlled by a local agent. This particular problem,

which is also intensely related to the literature on reaching consensus and resource allocation in networks, is initially presented in the pioneering paper [151].

In [151], authors focus on the distributed control of a network consisting of several agents interacting over a time-varying topology. In contrast to the literature on consensus problems [91, 155, 21, 25, 156], the study in [151] assumes that the local cost functions depend on the entire decision vector. More specifically, the distributed algorithm proposed in [151] adapts to the following recursive setting: at each iteration, each agent estimates the optimal decision vector based on the subgradient of the local cost function evaluated at the previous estimated decision vector, plus a weighted average of neighboring estimates. Authors considering asynchronous time-varying connectivity prove that under some weak assumptions on the communication scheme among agents the proposed first-order distributed algorithm converges to an approximation of the global optimal solution. Authors also present a rate of convergence analysis showing that the trade-off between convergence speed and quality of an approximate optimal solution is controlled explicitly via the system and algorithm parameters.

First-order distributed algorithms for solving (2.1) have also been explored in [134, 239] focusing on (sub)-gradient descent methods, in [147, 148] and [92] establishing the (sub)gradient-push method and the fast (sub)-gradient method, respectively, and in [55] proposing the dual averaging method. Most of the aforementioned algorithms are studied given the assumption of bounded (sub)-gradients [192]. The work [134] considers convex functions with bounded Hessian matrices. These assumptions are relaxed in [239] for distributed gradient descent optimization. Projected first-order algorithms are proposed in [202, 246] for constrained problems in the form of (2.1) where $\mathscr{X} \subseteq \mathbb{R}^n$ is a bounded set, which also lead to bounded (sub)gradients and Hessian matrices.

All first-order methods mentioned above suffer from the possible failure to converge to an optimal solution of (2.1) when considering a fixed step-size in the algorithm updates. This inability to reach optimal consensus, which is irrespective of the differentiability of f_i's [239], is considered in [55, 92] proposing the use of specific diminishing step sizes that guarantee convergence to a minimizing point. A distributed first-order algorithm (abbreviated as EXTRA) with fixed step-size and exact convergence capacity is proposed in [192]. Therein, authors prove that each local variable controlled by a local agent converges uniformly and consensually to an exact minimizer of f in (2.1). In contrast to the well-known distributed gradient descent (DGD) algorithm [151], EXTRA uses the gradients of the last two iterates, unlike DGD, which uses just that of the last iterate.

A significant group of recent results on the distributed minimization of (2.1) involves the introduction of a gradient tracking technique, which allows for rapid convergence subject to

certain assumptions made on the communication scheme among the agents. For instance, the work in [150, 167] proposes a distributed scheme that enables each agent to estimate/track asymptotically the (sub-)gradient of the global function, thereby improving the computing efficiency of minimizing the global objective function. Recent advances in improving performance of DGD algorithms can be found in [51, 183, 176] and references therein, as well as the recent survey paper [149].

Some different variants of techniques for solving the distributed optimization problem (2.1) include the primal-dual methods proposed in [109], the alternating direction method of multipliers presented in [22, 231, 31, 30], and the distributed mirror descent/dual averaging methods found in [50]. The review of these significant works is beyond the scope of this thesis and is omitted.

2.5 Literature gaps - conclusions

As evidenced throughout this chapter, distributed control is a field of study that emerges in several domains and has many implications, problems and applications associated with it. The aim of this chapter is to review a non-exhaustive collection of notable works and significant results on this vast area of research. It also attempts to highlight particular gaps appearing in the relevant literature thereby emphasizing the scope of this thesis. In particular, we list a number of shortcomings in the literature identified primarily as the absence or presence of certain assumptions imposed on the structure or dynamic behaviour of a distributed control system.

I. Various results on distributed LQR-based control rely on the elegant properties of undirected graphs assuming bidirectional interaction schemes. Chapter 4 shows that the robust stability margins of LQR control can be used for distributed control design over connected digraphs.

II. Perhaps the most common assumption considered in the context of distributed control is the presence of multiple systems with identical dynamics. The relaxation of this assumption represents the main focus of this thesis and is addressed in Chapter 5, Chapter 6, and Chapter 9.

III. The majority of (if not all) papers on distributed LQR control postulate multi-agent systems with linear dynamics. Chapter 6 demonstrates a general method for distributed LQR design for a class of nonlinear systems.

IV. There is a specific gap in the literature of distributed LQR control associated with multi-agent systems with dynamical couplings between neighboring plants. In Chapter 7, we propose a top-down method for designing distributed LQR controllers for identical dynamically coupled systems.

V. Results on stability and convergence of distributed model predictive control systems interconnected over communication graphs rely on the assumption that individual systems are either identical or aware of the model parameters of their adjacent peers. Chapter 9 focusing on a particular family of linear systems sharing certain structural properties, proposes a hybrid method for relaxing this requirement based on a distributed optimization algorithm.

Chapter 3

Regulator Problem

3.1 Introduction

Regulator problem in systems and control theory involves the construction of a control law the application of which drives an arbitrary nonzero initial state of a system to the zero state, preferably as fast as possible. This is a fundamental problem since many tasks arising in control engineering can be cast in this setting. In modern control theory the regulator problem is formulated as an optimal control problem the objectives of which, apart from fast state-regulation, also include minimization of control effort required to effect the state transfer, during which certain measure of the state should be kept small. Quantities such as control and state energy can be denoted as quadratic functions of input-variables and state-variables, respectively. In effect, these quantities are included in a cost function referred to as performance index, the minimization of which leads to the derivation of the optimum controller. In other words, the regulator problem is translated to the task of finding a control law which ensures optimum performance index. In the special case where the state transition of the system is described by linear dynamics, the optimal regulator scheme results in a linear state-feedback control law. This is known in the literature as Linear Quadratic Regulator (LQR) [85] and the basic mathematical results associated with it are discussed in the following section. The stabilizing solution of an optimal regulator problem performed over infinite-time horizon is highlighted along with its robust stability margins. The main scope of the chapter is to show how the powerful solution of an LQR problem can be applied to stabilize networks of interconnected systems. This is discussed in Section 3.3, where the concept of multi-agent networks and networked control systems are introduced. Two well-established methods in literature [17, 46], for designing stabilizing LQR-based controllers with application to multi-agent networks with distributed architecture are presented. The first, [17], is referred to as top-down method and approximates a centralized LQR controller

by a distributed scheme the closed-loop stability of which is guaranteed by the infinite gain margin property of LQR controller. The second, [46], consists of a bottom-up approach in which optimal interactions between self-stabilizing agents are defined so as to minimize an upper bound of the global LQR criterion.

3.2 Linear quadratic regulator

The regulator problem of linear time-invariant (LTI) systems is formulated as an optimal control problem. First, the finite-time case is discussed and then the stabilizing solution of the infinite-time regulator problem is presented. The section attempts to summarize some of the main well-known results on the optimal control theory which will be utilized later in the chapter where distributed LQR control of multi-agent networks is discussed.

Throughout the chapter, we consider linear time-invariant (LTI) systems with dynamics represented by a state-space differential equation of the form:

$$\dot{x}(t) = Ax(t) + Bu(t),\ x(t_0) = x_0. \tag{3.1}$$

Here, $A \in \mathbb{R}^{n\times n}$, $B \in \mathbb{R}^{n\times m}$ are constant matrices, $x(t) \in \mathbb{R}^n$, $u(t) \in \mathbb{R}^m$ denote state and input vectors at time $t \in [0,\infty)$, respectively, and x_0 represents the initial state of the system. In the sequel, to avoid complicated notation the variable t may be omitted from vectors $x,\ u$. We assume that the state-vector x is continuously accessible to the controller and can be used for constructing the input signal u. An optimal regulator problem of finite-time horizon is defined next.

3.2.1 Finite-time optimal regulator problem

Consider performance index,

$$J(x(t_0),u(\cdot),t_0) = \int_{t_0}^{T} (x'(t)Qx(t) + u'(t)Ru(t))\ \mathrm{d}t + x'(T)Gx(T), \tag{3.2}$$

where $Q \in \mathbb{R}^{n\times n}$, $G \in \mathbb{R}^{n\times n}$ are symmetric non-negative definite matrices and $R \in \mathbb{R}^{m\times m}$ is symmetric positive definite matrix. The optimization problem is formulated as the task of finding an optimal control $u^*(t)$, $t \in [t_0,T]$, which minimizes J, and the associated optimum performance index $J^*(x(t_0),t_0)$. For the moment, T is assumed to be finite. Detailed derivation of the optimal solution can be found in [85]. Here we focus on the main results of the optimal solution which are summarized next.

I. The optimum performance index takes the quadratic form $x'(t)P(t)x(t)$, where $P(t)$ is a symmetric matrix.

II. Matrix $P(t)$ satisfies a nonlinear differential equation which is a matrix Riccati equation.

III. The optimal control is a linear function of the system state, i.e., $u^*(t) = K(t)x(t)$.

According to statement I., we consider optimal performance index with quadratic form which is given by:

$$J^*(x(t),t) = x'(t)P(t)x(t). \tag{3.3}$$

Let also the Hamilton-Jacobi equation associated with optimum performance index (3.3) be written as:

$$\frac{\partial J^*}{\partial t}(x(t),t) = -\min_{u(t)} \big\{x'(t)Qx(t) + u'(t)Ru(t) + \big[\frac{\partial J^*}{\partial x}(x(t),t)\big]'(Ax(t)+Bu(t))\big\}. \tag{3.4}$$

Substituting (3.3) into (3.4) leads to

$$x'\dot{P}x = -\min_{u(t)} \big\{x'Qx + u'Ru + 2x'PAx + 2x'PBu\big\}. \tag{3.5}$$

To find the minimum of the expression on the right-hand side of (3.5) we simply write the following identity which is obtained by completing the square:

$$\begin{aligned} x'Qx + u'Ru + 2x'PAx + 2x'PBu = (u + R^{-1}B'Px)'R(u + R^{-1}B'P) + \\ x'(Q - PBR^{-1}B'P + PA + A'P)x. \end{aligned} \tag{3.6}$$

Since $R > 0$ the left-hand side of (3.6) is minimized by setting:

$$\bar{u}(t) = -R^{-1}B'P(t)x(t). \tag{3.7}$$

Using now $\bar{u}(t)$ the Hamilton-Jacobi equation becomes:

$$x'(t)\dot{P}(t)x(t) = -x'(t)(Q - P(t)BR^{-1}B'P(t) + P(t)A + A'P(t))x(t), \tag{3.8}$$

which holds for all $x(t)$ and then we can write

$$-\dot{P}(t) = A'P(t) + P(t)A - P(t)BR^{-1}B'P(t) + Q, \tag{3.9}$$

since we have assumed that both sides are symmetric. Eq. (3.9) is a Riccati equation with a boundary condition following immediately from the Hamilton-Jacobi boundary condition. Recall that $J^*(x(T),T) = x'(T)Gx(T)$ which implies that $x'(T)P(T)x(T) = x'(T)Gx(T)$. Since $x(T)$ is arbitrary and both $P(T)$ and G are symmetric the boundary condition of (3.9) is:

$$P(T) = G. \tag{3.10}$$

Deriving the Riccati equation (3.9), it was shown that the minimizing control $u(t)$ is constructed as in (3.7). Thus the optimal control $u^*(t)$ is given by

$$u^*(t) = -R^{-1}B'P(t)x(t), \tag{3.11}$$

where $P(t)$ is the solution of (3.9) with boundary condition $P(T) = G$.

3.2.2 Infinite-time optimal regulator problem

Now we relax the restriction imposed earlier that the optimization interval be finite and we are interested in finding an optimal control $u(t)$ that minimizes the cost function $J(x(t_0),u(t),t)$ over infinite-time horizon. Thus, we let $T \to \infty$ in (3.2) and we also set the terminal cost $x'(T)Gx(T) = 0$. Then the optimal regulator problem is formulated as follows:

$$\min_{u(t)} J(x(t_0),u(t),t) \text{ subject to: } \dot{x} = Ax + Bu,\ x_0 = x(t_0), \tag{3.12}$$

where

$$J(x(t_0),u(t),t) = \int_{t_0}^{\infty} (x'Qx + u'Ru)\ \mathrm{dt}. \tag{3.13}$$

In view of (3.13) the minimization problem (3.12) does not always attain a finite optimal performance index as it is stated. To ensure that the regulator problem admits of a finite optimal solution the following assumption should be made.

Assumption 3.2.1. *System* (3.1) *is completely controllable. That is, given an arbitrary state $x(t_0)$ at time t_0, there exists a control depending on $x(t_0)$ and t_0, and a time t_1, depending on t_0, such that application of this control over the interval $[t_0,t_1]$ takes the state $x(t_0)$ to the zero state at time t_1.*

We note here that stabilizability of system (3.1) indicates a variant on Assumption 3.2.1 and suffices to ensure solvability of the infinite-time regulator problem. The solution to optimal regulator problem (3.12) is now stated under the Assumption 3.2.1.

Let $P(t,T)$ be solution to Riccati equation (3.9) with initial condition $P(T,T)=0$. Then $\lim_{T\to\infty} P(t,T) = \lim_{t\to-\infty} P(t,T) = \bar{P}$ exists and is constant. $\bar{P}$ satisfies

$$A'\bar{P} + \bar{P}A - \bar{P}BR^{-1}B'\bar{P} + Q = 0, \tag{3.14}$$

which is an Algebraic Riccati Equation (ARE) and $x'(t_0)\bar{P}x(t_0)$ is the optimal performance index when the initial state is $x(t_0)$ and the initial time is t_0. The optimal control law at time t is given by the constant control law

$$u^*(t) = -R^{-1}B'\bar{P}x(t), \tag{3.15}$$

which is independent of the initial time t_0. Due to infinite-time optimization interval the performance index (3.13) is not time dependent. This implies that the choice of the initial time can be arbitrary and thus all initial times give the same performance index, i.e., $\bar{P}$ is constant.

3.2.3 Stability of linear quadratic regulator (LQR)

We now focus on the closed-loop stability of the system under the application of the optimal state-feedback control $u^*(t)$ given in (3.15). Let the dynamics of the closed-loop system be given by

$$\dot{x} = (A - BR^{-1}B'\bar{P})x. \tag{3.16}$$

To guarantee asymptotic stability of the closed-loop system (3.16), it suffices to impose the following assumption.

Assumption 3.2.2. *The pair $(A,\ C)$ is completely observable, where C is any matrix such that $C'C = Q$.*

In view of Assumption 3.2.2, all trajectories $x(t)$ will show up in the $x'Qx$ part of the integrand of the performance index (3.13). Since the optimum performance index is known to have finite value, it turns out that all potentially unstable trajectories will be stabilized under the application of the optimal feedback control $u^*(t)$ given in (3.15). It is also worth noting that Assumption 3.2.2 is determined by Q itself and not by the particular factorization $C'C$. This means that if there exist C_1, C_2 such that $C_1'C_1 = C_2'C_2 = Q$ then both pairs (A,C_1), (A,C_2) are completely observable.

Before showing asymptotic stability of the closed-loop system we note the following results which are stated without proof.

Lemma 3.2.3. *Consider optimal regulator problem as defined in* (3.12)*. Let Assumption 3.2.1 holds. Then Assumption 3.2.2 is necessary and sufficient condition for $\bar{P}$ to be symmetric positive definite.*

Theorem 3.2.4. *Consider a time-invariant system $\dot{x} = f(x)$ with $f(0) = 0$ and $f(\cdot)$ continuous. Suppose that there is a scalar function $V(x)$ that is positive definite, approaches infinity as $\|x\|$ approaches infinity and is differentiable. Suppose also that the derivative of V along system trajectories, that is $\dot{V} = [\frac{\partial V}{\partial x}]' f(x)$, is negative definite. Then the system is globally asymptotically stable.*

Theorem 3.2.5. *Consider time-invariant system $\dot{x} = f(x)$ with $f(0) = 0$ and $f(\cdot)$ continuous. Suppose that there is a scalar function $V(x)$ that is positive definite, approaches infinity as $\|x\|$ approaches infinity and is differentiable. Suppose also that the derivative of V along system trajectories, that is $\dot{V} = [\frac{\partial V}{\partial x}]' f(x)$, is non-positive definite, and not identically zero on $[t_1, \infty)$ for any t_1, except for a trajectory starting from the zero state. Then the system is globally asymptotically stable.*

Proof of Lemma 3.2.3 can be found in [85]. Theorem 3.2.4 and Theorem 3.2.5 are well known results in the theory of Lyapunov stability. Their proof can be found in [103].

The asymptotic stability of the closed-loop system (3.16) is now established next. Adding $\bar{P}BR^{-1}B'\bar{P} - \bar{P}BR^{-1}B'\bar{P}$ in the left-hand side of (3.14) and rearranging the terms appropriately yields

$$\bar{P}(A - BR^{-1}B'\bar{P}) + (A' - \bar{P}BR^{-1}B')\bar{P} = -Q - \bar{P}BR^{-1}B'\bar{P}. \tag{3.17}$$

Let also $V(x) = x'\bar{P}x$ be a candidate Lyapunov function for the closed-loop system (3.16). Then Lemma 3.2.3 guarantees that $V(x)$ is positive definite. Since $\dot{V}(x) = \dot{x}'\bar{P}x + x'\bar{P}\dot{x}$, (3.17) implies that

$$\dot{V}(x) = -x'Qx - x'\bar{P}BR^{-1}B'\bar{P}x. \tag{3.18}$$

If Q is positive definite then it is intuitively clear that $\dot{V}$ is negative definite and therefore we can claim asymptotic stability from Theorem 3.2.4. Now, suppose that Q is non-negative definite, with Assumption 3.2.2 still holding. According to Theorem 3.2.5, to postulate asymptotic stability, it needs to be shown that $\dot{V}$ is not identically zero along system trajectories starting from nonzero initial states.

Let $\dot{V}$ be identically zero along a trajectory starting from a nonzero initial state $x_0 = x(t_0)$. Then both $x'Qx = 0$ and $x'\bar{P}BR^{-1}B'\bar{P}x = 0$. Also, $-R^{-1}B'\bar{P}x(t) = 0$ which is the optimal control for the open-loop system. Therefore, the trajectories of the open-loop and closed-loop system coincide and are given by $x(t) = e^{A(t-t_0)}x_0$. Since $x'Qx = 0$ and $Q = C'C$, then $x_0' e^{A'(t-t_0)}CC'e^{A(t-t_0)}x_0 = 0$ with x_0 being nonzero which contradicts Assumption 3.2.2. Thus,

it is impossible to have $\dot{V} = 0$ along a trajectory other than that starting from the zero state. Therefore, the asymptotic stability of (3.16) has been established.

In the analysis outlined above, the weighting matrices Q and R are assumed to be specified. The weights $(Q,\ R)$ are tuned to shift the design emphasis between penalty terms involving state and control variables, respectively. Since it is up to designer's discretion in adjusting system specifications, these matrices can be selected via a trial-and-error procedure which is usually guided by simulation results. Initial choice of the weights can be calculated by the Bryson's rule [79] which specifies that Q and R are diagonal with diagonal elements

$$Q_{ii} = \frac{1}{(x_{i,max})^2},\ R_{ii} = \frac{1}{(u_{i,max})^2}, \tag{3.19}$$

respectively. The terms $|x_{i,max}|$ and $|u_{i,max}|$ are the maximum required values of the state and control variables, respectively. Despite this rule of thumb, the closed-loop system is always stable, irrespective of the choice of Q and R given the definiteness properties mentioned earlier.

In the following paragraph, the hypotheses required for the infinite-time regulator problem along with the main results of its solution are summarized.

LQR problem and solution: Consider the system

$$\dot{x} = Ax + Bu,\ x(0) = x_0, \tag{3.20}$$

where the pair $(A,\ B)$ is completely controllable. Let $Q = Q' \geq 0$, $R = R' > 0$, $C'C = Q$, where $(A,\ C)$ is completely observable, and define the performance index

$$J(x_0, u(\cdot)) = \int_0^\infty (x'Qx + u'Ru)\ \mathrm{dt}. \tag{3.21}$$

The minimum value of $J(\cdot)$ is given by

$$J^*(x_0) = x_0' P x_0, \tag{3.22}$$

where P is the symmetric positive definite solution to the Algebraic Riccati Equation (ARE):

$$A'P + PA - PBR^{-1}B'P + Q = 0. \tag{3.23}$$

The associated optimal control is given by the linear feedback law

$$u^*(t) = Kx(t), \tag{3.24}$$

where $K = -R^{-1}B'P$, and the closed-loop matrix

$$A_{cl} = A + BK, \tag{3.25}$$

is Hurwitz. Matrix

$$\bar{A}_{cl} = A + \gamma BK, \tag{3.26}$$

is also Hurwitz for all $\gamma \in (\frac{1}{2}, \infty)$ which represents the infinite gain margin of the LQR controller [85]. This is explained in detail in the following section.

3.2.4 Stability margins of LQR controller

Before establishing robustness properties of the LQR controller, we state two preliminary results of the linear algebra and robust stability analysis, respectively. These can also be found in [85].

Lemma 3.2.6. *Let V, W be square complex matrices of the same dimensions such that*

$$(I+V^*)(I+V) \geq I, \tag{3.27}$$

$$W^* + W > I. \tag{3.28}$$

Then, $I+VW$ is nonsingular.

Proof. Consider $VWu = -u$ for some $u \neq 0$. Now, (3.27) gives:

$$I + V^* + V + V^*V \geq I, \tag{3.29}$$

which implies

$$W^*V^*W + W^*VW + W^*V^*VW \geq 0. \tag{3.30}$$

Premultiply and postmultiply the latter with u^* and u, respectively, yields:

$$-u^*Wu - u^*W^*u + u^*u \geq 0, \tag{3.31}$$

which can be written also as

$$u^*(W^* + W - I)u \leq 0, \tag{3.32}$$

which is clearly a contradiction due to (3.28). □

Lemma 3.2.7. *Consider the closed-loop system defined in Fig. 3.1 and assume there are no unstable pole-zero cancellations in product VW for all frequencies ω. Let also $V(j\omega)$,*

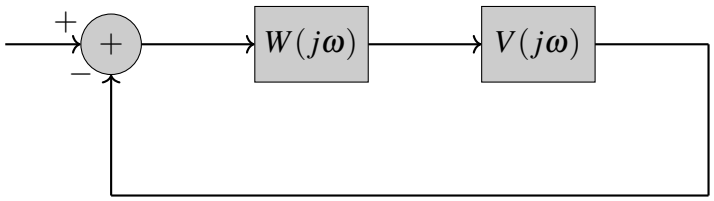

Fig. 3.1 Closed-loop system used for robustness result.

$W(j\omega)$ satisfy (3.27), (3.28) *of Lemma 3.2.6, respectively. Suppose also that substituting W for I, the closed-loop is stable. Then, the closed-loop configuration of Fig. 3.1 is stable.*

Proof. We substitute W for $\bar{W}_\varepsilon = (1-\varepsilon)I + \varepsilon W$, where $\varepsilon \in [0,1]$. Note that $\varepsilon = 0$ corresponds to a known stable situation by assumption, while $\varepsilon = 1$ to the situation of interest. We may also write

$$\bar{W}_\varepsilon^* + \bar{W}_\varepsilon = 2(1-\varepsilon)I + \varepsilon(W^* + W), \tag{3.33}$$

$$> 2(1-\varepsilon)I + \varepsilon I, \tag{3.34}$$

$$= (2-\varepsilon)I, \tag{3.35}$$

which implies

$$\bar{W}_\varepsilon^* + \bar{W}_\varepsilon > I. \tag{3.36}$$

Also, since $(I+V^*)(I+V) \geq I$, by assumption, from Lemma 3.2.6, $I + V(j\omega)\bar{W}_\varepsilon(j\omega)$ is a nonsingular matrix for all ω, $\varepsilon \in [0,1]$.

Now, with W replaced by $\bar{W}_\varepsilon$, the closed-loop transfer matrix is $V\bar{W}_\varepsilon(I+V\bar{W}_\varepsilon)^{-1}$. It can be easily verified that there is no unstable pole-zero cancellations in product $V\bar{W}_\varepsilon$. Then, as ε moves from 0 to 1, an instability can arise only if there is a closed-loop pole moving from the open left half-plane to the right half-plane, thereby crossing the imaginary axis. That is, $I + V(j\omega)\bar{W}_\varepsilon(j\omega)$ loses rank for some $\varepsilon \in [0,1]$ and some frequency ω, which is a contradiction. Thus, the presence of W does not violate closed-loop stability in Fig. 3.1. □

Let now matrix P be the symmetric positive definite solution to ARE:

$$A'P + PA - PBR^{-1}B'P + Q = 0, \tag{3.37}$$

associated with LQR problem with parameters $(A,\ B,\ Q,\ R)$. Let also $K = -R^{-1}B'P$ be the optimal state-feedback controller. Then, the following identity holds true:

$$R + \underbrace{B'(-j\omega I - A')^{-1}Q(j\omega I - A)^{-1}B}_{a} = (I - B'(-j\omega I - A')^{-1}K)R(I - K'(j\omega I - A)^{-1}B), \tag{3.38}$$

for all $\omega \in [0,\infty)$ and is referred to as the "return difference equation". Derivation of this can be found in [85]. Since a in (3.38) is a Hermitian positive definite matrix for $\omega \in [0,\infty)$, then

$$(I - B'(-j\omega I - A')^{-1}K)R(I - K'(j\omega I - A)^{-1}B) \geq R. \tag{3.39}$$

Pertaining to Fig. 3.1, let

$$V(j\omega) = -R^{1/2}K'(j\omega I - A)^{-1}BR^{-1/2}, \tag{3.40}$$

with (A,B,K,R) as defined above. In view of (3.38), we have that

$$(I + V^*)(I + V) \geq I, \tag{3.41}$$

which is in agreement with (3.27). Assume also that there is $W(j\omega) = R^{1/2}L(j\omega)R^{-1/2}$ satisfying (3.28). Then, with this setup in force, the closed-loop configuration in Fig. 3.1 is stable as long as

$$R^{-1/2}L^*R^{1/2} + R^{1/2}LR^{-1/2} > I, \tag{3.42}$$

or

$$L^*R + RL > R. \tag{3.43}$$

The following results are established for a diagonal choice of weight R. They also hold for single-input systems, since R is scalar in this setting. Let also $L = \mathrm{diag}(l_1,\ldots,l_m)$, m denoting the number of input channels. Then, (3.43) holds true if and only if

$$l_i^* + l_i > 1, \tag{3.44}$$

for $i = 1,\ldots,m$. If $l_i \in \mathbb{R}$ then, (3.44) is satisfied in the interval $(\frac{1}{2},\infty)$. This represents the gain margin of the LQR controller. If $l_i = e^{-j\phi_i}$, (3.44) is in force for all $|\phi_i| < \pi/3$ which implies that sixty degrees of phase margin can be tolerated in all input channels for a diagonal choice of matrix R.

We also remark that for a generic (not necessarily diagonal) weight $R = R' > 0$ and $L = \lambda I_m$, with $\lambda \in \mathbb{C}$, (3.43) may be written as

$$\lambda^* R + \lambda R > R, \tag{3.45}$$

or

$$\lambda^* + \lambda > 1, \tag{3.46}$$

which is equivalent to

$$\mathbf{Re}(\lambda) > \frac{1}{2}, \tag{3.47}$$

highlighting the one-half-gain-reduction and infinite-gain-amplification property of the LQR controller. Immediate implication of the latter is that for a multi-input system $(A,\ B)$ and LQR controller K, matrices

$$A_\gamma = A + \gamma BK \in \mathbb{C}^{n\times n}, \tag{3.48}$$

and A_γ^* are Hurwitz for all $\gamma \in \mathbb{C}$ with $\mathbf{Re}(\gamma) > \frac{1}{2}$. We summarize this result in the following theorem.

Theorem 3.2.8. *Consider system*

$$\dot{x} = Ax + Bu,\ x(0) = x_0, \tag{3.49}$$

where $(A,\ B)$ is controllable. Consider also optimal state-feedback controller K associated with LQR problem with parameters $(A,\ B,\ Q,\ R)$ where $Q = Q' \geq 0$ and $R = R' > 0$. Assume that $(A,\ C)$ is observable for any matrix C such that $C'C = Q$. Then, the complex matrix

$$A_\gamma = A + \gamma BK, \tag{3.50}$$

is Hurwitz for all $\gamma \in \mathbb{C}$ as long as $\mathbf{Re}(\gamma) > \frac{1}{2}$.

We omit the proof as it can readily be derived from the previous arguments. Later in the chapter (as well as in Chapter 4), it will be apparent that the robustness properties of LQR control are useful for designing stabilizing distributed LQR-based controllers of multi-agent networks with sparse structure. Specifically, it will be shown that condition $\mathbf{Re}(\gamma) > \frac{1}{2}$, which can be associated with a lower bound on the Fiedler value of a graph $\mathscr{G}$ (the second-smallest eigenvalue of the Laplacian matrix of $\mathscr{G}$), can be used to guarantee stability of a distributed LQR-based control system interconnected over a graph (cf. Theorem 3.3.14 and Theorem 4.3.4).

3.3 Regulator problems in multi-agent networks

We investigate the regulator problem in the context of multi-agent networks. The main focus of the section will be on network stability; two well-established methods for designing stabilizing distributed state-feedback control of multi-agent networks are presented. A multi-agent network is defined here as a large-scale dynamic system which can be decomposed into a finite number of identical subsystems each having a distinct control unit. In this regard, a subsystem (or just a system) representing an autonomous agent is assumed to be capable of: 1) producing actuation signals independently, and 2) exchanging state-information with a certain number of systems in the network referred to as neighboring agents (or just as neighbors). The state-information exchange established between neighboring systems determines network's topology and defines an interconnection and control scheme which is modelled as a graph. The nodes of the graph represent agents interacting dynamically (due to control applied) and exchanging information through links (edges) of the graph. The communication between neighboring agents is assumed to be bidirectional and thus the information exchange scheme is modelled as an undirected graph. Before proceeding to the networked regulator problem, we first introduce some interesting properties of a large-scale LQR problem of a certain structure. We also introduce the following notation and some useful concepts of graph theory.

3.3.1 Notation and preliminaries

The field of real and complex numbers are denoted by $\mathbb{R}$ and $\mathbb{C}$, respectively. $\mathbb{R}^n$ denotes the n-dimensional vector space over the field $\mathbb{R}$ and $\mathbb{R}^{n\times m}$ denotes the set of $n\times m$ real matrices. ξ' denotes the transpose of ξ. Matrix $\Xi\in\mathbb{R}^{n\times n}$ is called symmetric if $\Xi'=\Xi$. The identity matrix of dimension $m\times m$ is denoted by $I_m\in\mathbb{R}^{m\times m}$. The $n\times m$ zero matrix is denoted by $0_{n\times m}$ (subscript may be omitted when the dimensions are obvious). The set of complex numbers with negative and non-positive real part is denoted by $\mathbb{C}_{--}=\{s\in\mathbb{C}:\mathbf{Re}(s)<0\}$ and $\mathbb{C}_{-}=\{s\in\mathbb{C}:\mathbf{Re}(s)\leq 0\}$, respectively.

Definition 3.3.1. Let $A,B\in\mathbb{R}^{n\times n}$ be symmetric matrices. Then,

I. If $x'Ax>0$ $(x'Ax\geq 0)$ for all nonzero $x\in\mathbb{R}^n$, then A is positive (semi)definite. The positive (semi)definiteness of A is denoted by $A>0$ $(A\geq 0)$.

II. Matrix A is negative (semi)definite if $-A>0$ $(-A\geq 0)$.

III. $A<B$ $(A\leq B)$ means $A-B<0$ $(A-B\leq 0)$.

Let $A \in \mathbb{R}^{n\times m}$ and $B \in \mathbb{R}^{q\times p}$. Then the Kronecker product of A and B is denoted by $A \otimes B$ and defined as

$$A \otimes B = \begin{bmatrix} a_{11}B & \cdots & a_{1m}B \\ \vdots & \ddots & \vdots \\ a_{n1}B & \cdots & a_{nn}B \end{bmatrix} \in \mathbb{R}^{nq\times mp}, \tag{3.51}$$

where a_{ij} is the (i,j)-th entry of A, with $i = 1,\ldots,n$ and $j = 1,\ldots,m$.

Let $\lambda_i(\Xi)$ denote the i-th eigenvalue of $\Xi \in \mathbb{R}^{n\times n}$, $i = 1,\ldots,n$. Then, the spectrum of Ξ is denoted by $S(\Xi) = \{\lambda_1(\Xi),\ldots,\lambda_n(\Xi)\}$.

Definition 3.3.2. Matrix $\Xi \in \mathbb{R}^{n\times n}$ is called Hurwitz (or stable) if all its eigenvalues have negative real part, i.e., $\lambda_i(\Xi) \in \mathbb{C}_{--}$, $i = 1,\ldots,n$.

Proposition 3.3.1. *Let $A_1 = aI_m$ and $A_2 \in \mathbb{R}^{m\times m}$. Then $\lambda_i(A_1 + A_2) = a + \lambda_i(A_2)$, $i = 1,\ldots,m$.*

Proof. Let $\lambda_i(A_2)$ be any eigenvalue of A_2 with corresponding eigenvector $v_i \in \mathbb{C}^m$. Then $(A_1 + A_2)v_i = A_1v_i + A_2v_i = av_i + \lambda_i(A_2)v_i = (a + \lambda_i(A_2))v_i$. □

Proposition 3.3.2. *Consider matrices $A_1, A_2 \in \mathbb{R}^{m\times m}$ and $\Xi \in \mathbb{R}^{n\times n}$ and let $\bar{A}_1 = I_n \otimes A_1$ and $\bar{A}_2 = \Xi \otimes A_2$ with $\bar{A}_1, \bar{A}_2 \in \mathbb{R}^{nm\times nm}$. Then $S(\bar{A}_1 + \bar{A}_2) = \bigcup_{i=1}^{n} S(A_1 + \lambda_i(\Xi)A_2)$ where $\lambda_i(\Xi)$ represents the i-th eigenvalue of Ξ.*

Proof. Let $v \in \mathbb{C}^n$ be an eigenvector of Ξ associated with eigenvalue $\lambda(\Xi)$ and $u \in \mathbb{C}^m$ be an eigenvector of $M = A_1 + \lambda(\Xi)A_2$ associated with eigenvalue $\lambda(M)$. Define the vector $v \otimes u \in \mathbb{C}^{nm}$ and consider

$$\begin{aligned}(\bar{A}_1 + \bar{A}_2)(v \otimes u) &= v \otimes A_1u + \Xi u \otimes A_2u \\ &= v \otimes A_1u + \lambda(\Xi)v \otimes u \\ &= v \otimes (A_1u + \lambda(\Xi)A_2u).\end{aligned}$$

Since $(A_1 + \lambda(\Xi)A_2)u = \lambda(\Xi)u$, we get $(\bar{A}_1 + \bar{A}_2)(v \otimes u) = \lambda(\Xi)(v \otimes u)$. □

3.3.2 Graph theory preliminaries - Undirected graphs

An undirected graph (or just graph) $\mathscr{G}$ is defined as the ordered pair $\mathscr{G} = (\mathscr{V}, \mathscr{E})$, where $\mathscr{V}$ is the set of nodes (or vertices) $\mathscr{V} = \{1,\ldots,N\}$ and $\mathscr{E} \subseteq \mathscr{V} \times \mathscr{V}$ the set of edges (i,j) with $i \in \mathscr{V}$, $j \in \mathscr{V}$. The orientation of all edges is bidirectional. The degree d_j of vertex j is the number of edges that start from j. Let $d_{\max}(\mathscr{G})$ denote the maximum vertex degree of the graph $\mathscr{G}$. We denote by $\mathscr{A}(\mathscr{G})$ the $(0,1)$ adjacency matrix of the graph $\mathscr{G}$. In particular,

the (i,j)-th element of $\mathscr{A}$, $A_{ij} = 1$ if $(i,j) \in \mathscr{E}$ $\forall$ $i,j = 1,\ldots,N$, $i \neq j$ and zero otherwise. Let $j \in \mathscr{N}_i$ if $(i,j) \in \mathscr{E}$ and $i \neq j$. We call $\mathscr{N}_i$ the neighborhood of node i. The adjacency matrix $\mathscr{A}(\mathscr{G})$ of undirected graphs is symmetric. We define the Laplacian matrix as $\mathscr{L}(\mathscr{G}) = D(\mathscr{G}) - \mathscr{A}(\mathscr{G})$, where $D(\mathscr{G})$ is the diagonal matrix of vertex degrees d_i (also called the valence matrix). The Laplacian matrix of an undirected graph is a symmetric positive semidefinite matrix. Let $S(\mathscr{L}(\mathscr{G})) = \{\lambda_1(\mathscr{L}(\mathscr{G})),\ldots,\lambda_N(\mathscr{L}(\mathscr{G}))\}$ be the spectrum of the Laplacian matrix $\mathscr{L}$ associated with an undirected graph $\mathscr{G}$ arranged in a nondecreasing semi-order, with $\lambda_i(\mathscr{L}(\mathscr{G})) \geq 0$, $i = 1,\ldots,N$. The following Proposition is derived from Proposition 3.3.2 in a straightforward manner.

Proposition 3.3.3. *Let A, B be matrices of appropriate dimensions and $\mathscr{L}$ be the Laplacian matrix of graph $\mathscr{G}$ with spectrum $S(\mathscr{L}) = \{\lambda_1(\mathscr{L}),\ldots,\lambda_N(\mathscr{L})\}$. Then,*

$$S(I_N \otimes A + \mathscr{L} \otimes B) = \bigcup_{i \in [1:N]} S(A + \lambda_i(\mathscr{L})B),$$

with $\lambda_i(\mathscr{L}) \in S(\mathscr{L})$.

Next, we recall the Geršgoring disk theorem.

Theorem 3.3.4. *Let $M = (m_{ij})$ be an $n \times n$ real matrix. Then all eigenvalues of M are located in the union of the discs described by:*

$$\bigcup_i \Big\{ z \in \mathbb{C} \;\Big|\; |z - m_{ii}| \leq \sum_{\substack{j=1 \\ j \neq i}}^{n} |m_{ij}| \Big\}. \tag{3.52}$$

The location of the eigenvalues of a Laplacian matrix $\mathscr{L}$ may be determined via Theorem 3.3.4 as follows.

Proposition 3.3.5. *Let $\mathscr{G}$ be an undirected graph of N vertices with Laplacian matrix $\mathscr{L}$. Then, the spectrum of $\mathscr{L}$ lies on the line segment of the non-negative real axis defined by*

$$\{ z \in \mathbb{R} \mid |z - d_{\max}| \leq d_{\max} \}, \tag{3.53}$$

where $d_{\max}$ denotes the maximum vertex degree of $\mathscr{G}$. In other words, for every undirect graph $\mathscr{G}$, the eigenvalues of $\mathscr{L}$ are real and non-negative.

Proof. In view of Theorem 3.3.4, the eigenvalues of $\mathscr{L}$ lie in the complex region

$$\bigcup_i \{ z \in \mathbb{C} \;\big|\; |z - d_i| \leq d_i \}, \tag{3.54}$$

where d_i denotes the degree of the i-th vertex. However, $\mathscr{L}$ is a symmetric matrix and hence its spectrum is real, that is, z in (3.54) lies on the region defined by the intersection of the discs $|z-d_i| \leq d_i$ $i=1,\ldots,N$, and the non-negative real axis. Then, the line segment (3.53) readily follows since $d_i \leq d_{\max}$ $\forall i$. □

Proposition 3.3.5 defines the line segment in which all eigenvalues of a Laplacian matrix $\mathscr{L}$ are confined. To show explicitly the non-negativity of the Laplacian spectrum we argue the following. Let $\mathscr{G}=(\mathscr{V},\mathscr{E})$ be an undirected graph on N vertices with associated Laplacian matrix $\mathscr{L}$. For all $x \in \mathbb{R}^N$, x_i being the i-th entry of x, we may write

$$\begin{aligned}
\sum_{(i,j)\in\mathscr{E}} (x_i-x_j)^2 &= \frac{1}{2}\sum_{i\in\mathscr{V}} \sum_{j\in\mathscr{V}:(i,j)\in\mathscr{E}} (x_i-x_j)^2 \\
&= \frac{1}{2}\sum_{i\in\mathscr{V}} \sum_{j\in\mathscr{V}:(i,j)\in\mathscr{E}} (x_i^2+x_j^2-2x_ix_j) \\
&= \frac{1}{2}\sum_{i\in\mathscr{V}} x_i^2 d_i + \frac{1}{2}\sum_{j\in\mathscr{V}} x_j^2 d_j - \sum_{i,j\in\mathscr{V}} x_i a_{ij} x_j \\
&= \sum_{i\in\mathscr{V}} d_i x_i^2 - \sum_{i,j\in\mathscr{V}} a_{ij} x_i x_j \\
&= x'\mathscr{L}x, \qquad (3.55)
\end{aligned}$$

where d_i denotes the degree of the i-th vertex and a_{ij} is the (i,j)-th entry of the adjacency matrix of $\mathscr{G}$. Effectively, we have shown that $x'\mathscr{L}x$ is a (weighted) sum of squares and hence, it is non-negative for all $x \in \mathbb{R}^N$. This implies that $\mathscr{L}$ is a symmetric positive semi-definite matrix (Definition 3.3.1).

Consider now two graphs $\mathscr{G}=(\mathscr{V},\mathscr{E})$ and $\mathscr{G}'=(\mathscr{V}',\mathscr{E}')$ and let $\mathscr{V}' \subseteq \mathscr{V}$ and $\mathscr{E}' \subseteq \mathscr{E}$. We call $\mathscr{G}'$ a subgraph of $\mathscr{G}$. A tree is an undirected graph in which any two vertices are connected by exactly one edge. A spanning tree $\mathscr{T}$ of an undirected graph $\mathscr{G}$ is the subgraph $\mathscr{G}'$ that is a tree which includes all of the vertices of $\mathscr{G}$, with the minimum possible number of edges.

By definition the rows (columns) of a Laplacian matrix $\mathscr{L}$ sum to zero. This implies that $\mathscr{L}$ has at least one eigenvalue at the origin with associated eigenvector $q=[1\ 1\ \cdots\ 1]'$, i.e., $\mathscr{L}q=0$ and $q'\mathscr{L}=0$ (since $\mathscr{L}$ is symmetric). Consequently, the smallest eigenvalue of $\mathscr{L}$ is always equal to zero or $\lambda_1=0$. The second smallest eigenvalue, also referred to as Fiedler value, [141, 139], represents the algebraic connectivity of a graph. For instance, a graph which comprises two distinct weakly connected subgraphs is expected to have a Fiedler value close to zero.

An undirected graph is called connected if there is always a path (an edge or a sequence of edges) between every pair of its vertices. This implies that a connected graph contains at least a spanning tree. An algebraic property which links the connectivity of a graph with the spectrum of its associated Laplacian matrix is presented in the next theorem.

Theorem 3.3.6. *Let $\mathscr{G} = (\mathscr{V}, \mathscr{E})$ be an undirected graph of N vertices with associated Laplacian matrix $\mathscr{L}$. Let also $S(\mathscr{L}) = \{\lambda_1, \lambda_2, \ldots, \lambda_N\}$ represent the spectrum of $\mathscr{L}$ arranged in a nondecreasing semi-order with $\lambda_1 = 0$. Then, the graph $\mathscr{G}$ is connected if and only if $\lambda_2 > 0$.*

Proof. Let $q = [1\ 1\ \cdots\ 1]'$ be the eigenvector corresponding to the smallest eigenvalue $\lambda_1 = 0$. By the variational characterisation of eigenvalues, we may write

$$\lambda_2 = \min_{x \perp q} \frac{x' \mathscr{L} x}{x' x} = \min_{x \perp q,\ \|x\|=1} x' \mathscr{L} x. \tag{3.56}$$

If x is non-zero and orthogonal to q, it cannot be of the form $x = cq$ with $c \in \mathbb{R}$. Therefore, there must be some $(i, j) \in \mathscr{E}$ for which $x_i \neq x_j$, x_i being the i-th entry of x. The latter implies that $x' \mathscr{L} x = \sum_{(i,j)\in\mathscr{E}} (x_i - x_j)^2 > 0$ and this is true for all non-zero $x \perp q$. It follows straightforwardly that $\min_{x \perp q,\ \|x\|=1} x' \mathscr{L} x$ is strictly positive, i.e., $\lambda_2 > 0$. □

In the remaining of the chapter, we focus explicitly on undirected connected graphs. The next section studies a large-scale LQR problem of identical dynamically decoupled linear systems.

3.3.3 LQR properties of identical decoupled systems

Consider a set of N_L identical, dynamically decoupled linear time-invariant systems. The dynamics of the i-th system is described by the state-space equation

$$\dot{x}_i = A x_i + B u_i,\ x_i(0) = x_{i,0}, \tag{3.57}$$

where $x_i \in \mathbb{R}^n$, $u_i \in \mathbb{R}^m$ denote the state and input vectors of the i-th system, respectively, with $i = 1, \ldots, N_L$. Let now $\tilde{x} \in \mathbb{R}^{nN_L}$, $\tilde{u} \in \mathbb{R}^{mN_L}$ represent the aggregate state and input vectors, respectively, which are constructed by stacking the state and input vectors, respectively, of all N_L systems. The aggregate state-space equation, which collects the dynamics of all N_L systems, can be written as:

$$\dot{\tilde{x}} = \tilde{A}\tilde{x} + \tilde{B}\tilde{u},\ \tilde{x}_0 = [x_1'(0), \ldots, x_{N_L}'(0)]' \tag{3.58}$$

with

$$\tilde{A} = I_{N_L} \otimes A,\ \tilde{B} = I_{N_L} \otimes B. \tag{3.59}$$

We consider the following cost function pertinent to the set of N_L dynamically decoupled systems outlined above:

$$J(\tilde{u}, \tilde{x}_0) = \int_0^\infty \sum_{i=1}^{N_L} \left(x_i' Q_{ii} x_i + u_i' R_{ii} u_i + \frac{1}{2} \sum_{\substack{j=1 \\ j \neq i}}^{N_L} (x_i - x_j)' Q_{ij} (x_i - x_j) \right) \mathrm{dt} \tag{3.60}$$

with weights:

$$Q_{ii} = Q_{ii}' \geq 0,\ R_{ii} = R_{ii}' = R > 0,\ \text{for } i = 1, \ldots, N_L \tag{3.61a}$$

$$Q_{ij} = Q_{ij}' = Q_{ji} \geq 0,\ \text{for } i, j = 1, \ldots, N_L,\ j \neq i. \tag{3.61b}$$

In cost function (3.60) the terms associated with matrices Q_{ii} and R_{ii} weigh local states and inputs of the i-th system, respectively, while terms associated with matrices Q_{ij} penalize the relative state difference between system i and j. We will show that the control scheme obtained by optimizing an LQR performance index constructed as in (3.60) leads to a closed-loop performance that couples dynamically each individual system with its counterparts. A compact form of cost function (3.60) can be written as follows:

$$J(\tilde{u}, \tilde{x}_0) = \int_0^\infty (\tilde{x}' \tilde{Q} \tilde{x} + \tilde{u}' \tilde{R} \tilde{u})\ \mathrm{dt}, \tag{3.62}$$

where the structure of the weighting matrices $\tilde{Q}$ and $\tilde{R}$ is defined next. Matrices $\tilde{Q}$ and $\tilde{R}$ are partitioned into N_L^2 blocks of dimension $n \times n$ and $m \times m$, respectively:

$$\tilde{Q} = \begin{bmatrix} \tilde{Q}_{11} & \tilde{Q}_{12} & \cdots & \tilde{Q}_{1N_L} \\ \tilde{Q}_{21} & \tilde{Q}_{22} & \cdots & \vdots \\ \vdots & \ddots & \ddots & \vdots \\ \tilde{Q}_{N_L 1} & \cdots & \cdots & \tilde{Q}_{N_L N_L} \end{bmatrix},\ \tilde{R} = \begin{bmatrix} R & 0_{m\times m} & \cdots & 0_{m\times m} \\ 0_{m\times m} & R & \cdots & 0_{m\times m} \\ \vdots & \ddots & \ddots & \vdots \\ 0_{m\times m} & \cdots & \cdots & R \end{bmatrix} \tag{3.63}$$

with

$$\tilde{Q}_{ii} = Q_{ii} + \sum_{\substack{k=1 \\ k\neq i}}^{N_L} Q_{ik},\ i = 1,\ldots,N_L, \tag{3.64a}$$

$$\tilde{Q}_{ij} = -Q_{ij},\ i,j = 1,\ldots,N_L,\ j \neq i, \tag{3.64b}$$

$$\tilde{R} = I_{N_L} \otimes R. \tag{3.64c}$$

Remark 3.3.7. The performance index (3.60) can be used to describe several practical applications such as formation flight control, synchronization of multi-oscillator systems, frequency and power flow control of electric power systems [223, 222, 217, 17].

We consider now the following LQR problem:

$$\min_{\tilde{u}}\ J(\tilde{u},\tilde{x}_0) \text{ subject to: } \dot{\tilde{x}} = \tilde{A}\tilde{x} + \tilde{B}\tilde{u},\ \tilde{x}(0) = \tilde{x}_0, \tag{3.65}$$

where the performance index $J(\tilde{u},\tilde{x}_0)$ is constructed as in (3.62). As mentioned in Section 3.2.2 and 3.2.3, the LQR problem (3.65) has a unique optimal stabilizing solution $\tilde{u}^*$ resulting in a finite (optimum) performance index $J^*(\cdot)$ provided the following assumptions are in force.

Assumption 3.3.8. *The pair $(\tilde{A},\ \tilde{B})$ is stabilizable and the pair $(\tilde{A},\ \tilde{C})$ is observable, where $\tilde{C}$ is any matrix such that $\tilde{C}'\tilde{C} = \tilde{Q}$.*

We also enforce stabilizability and observability at individual system level:

Assumption 3.3.9. *The pair $(A,\ B)$ is stabilizable and the pairs $(A,\ C_{ii})$, $(A,\ C_{ij})$ are observable, where C_{ii} and C_{ij} are any matrices such that $C_{ii}'C_{ii} = Q_{ii}$ and $C_{ij}'C_{ij} = Q_{ij}$, respectively.*

We note here that the complete controllability of system $(A,\ B)$ enforced in Assumption 3.2.1 is relaxed with stabilizability of the pairs $(\tilde{A},\ \tilde{B})$ and $(A,\ B)$. This relaxation does not violate closed-loop stability since stable uncontrollable modes are guaranteed to exponentially decay to zero, irrespective of the control action $\tilde{u}$ (see [5, 85] and references therein).

Under Assumption 3.3.8 and 3.3.9, the minimizing solution $\tilde{u}^*$ to LQR problem (3.65) is a linear feedback law

$$\tilde{u}^* = \tilde{K}\tilde{x}, \tag{3.66}$$

with $\tilde{K} = -\tilde{R}^{-1}\tilde{B}'\tilde{P}$, and is associated with an optimal performance index $J^*(\tilde{x}_0) = \tilde{x}_0'\tilde{P}\tilde{x}_0$. Matrix $\tilde{P}$ is the symmetric positive definite solution to the algebraic Riccati equation (ARE)

$$\tilde{A}'\tilde{P} + \tilde{P}\tilde{A} - \tilde{P}\tilde{B}\tilde{R}^{-1}\tilde{B}'\tilde{P} + \tilde{Q} = 0. \tag{3.67}$$

We now partition matrices $\tilde{K}$ and $\tilde{P}$ into N_L^2 blocks of dimension $m \times n$ and $n \times n$, respectively. Let $K[(i-1)m+1 : im, (j-1)n+1 : jn]$ be the (i,j)-block of $\tilde{K}$ denoted as $\tilde{K}_{ij}$ and $P[(i-1)n+1 : in, (j-1)n+1 : jn]$ be the (i,j)-block of $\tilde{P}$ denoted as $\tilde{P}_{ij}$. The following two theorems show that $\tilde{K}_{ij}$ and $\tilde{P}_{ij}$ satisfy certain properties which stem from the special structure of the LQR problem (3.65). These will prove essential in Section 3.3.5 for designing stabilizing distributed controllers for the structured optimal control problem (3.81). In the following, we set $X = BR^{-1}B'$ for convenience. Theorem 3.3.10 and Theorem 3.3.11 have been established in [17] and are stated next without proof.

Theorem 3.3.10. *[17] Let $\tilde{K}$ and $\tilde{x}_0'\tilde{P}\tilde{x}_0$ be the optimal controller and the associated optimal performance index, respectively, of the LQR problem* (3.65)*. Let also $\tilde{K}_{ij}$ and $\tilde{P}_{ij}$ denote the (i,j)-block of $\tilde{K}$ and $\tilde{P}$, respectively. Then*

$$\sum_{i=1}^{N_L} \left(A'F_{ii} + F_{ii}A - F_{ii}XF_{ii} + Q_{ii}\right) = 0, \tag{3.68}$$

where $F_{ii} = \sum_{j=1}^{N_L} \tilde{P}_{ij}$.

In view of Theorem 3.3.10, we note that if all the weights $Q_{ii} = Q_1$, $i = 1, \ldots, N_L$, then eq. (3.68) becomes:

$$N_L \left(A'F_{ii} + F_{ii}A - F_{ii}XF_{ii} + Q_1\right) = 0, \tag{3.69}$$

which can be seen as a single-node algebraic Riccati equation with parameters $(A,\ B,\ Q_1,\ R)$. Additional properties of the solution of the LQR problem (3.65) with equal weights Q_{ii}, $i = 1, \ldots, N_L$ and equal Q_{ij}, $i, j = 1, \ldots, N_L$, $j \neq i$, are summarized in the following theorem.

Theorem 3.3.11. *[17] Let the weighting matrices* (3.61) *of the LQR problem* (3.65) *be chosen as*

$$Q_{ii} = Q_1,\ i = 1, \ldots, N_L \tag{3.70a}$$

$$Q_{ij} = Q_2,\ i, j = 1, \ldots, N_L,\ j \neq i. \tag{3.70b}$$

Let $\tilde{K}$ and $\tilde{x}_0'\tilde{P}\tilde{x}_0$ be the optimal controller and the associated optimal performance index, respectively, of the LQR problem (3.65) *with weights* (3.70)*. Let also $\tilde{K}_{ij}$ and $\tilde{P}_{ij}$ denote the (i,j)-block of $\tilde{K}$ and $\tilde{P}$, respectively. Then the following statements hold.*

I. $F_{ii} = \sum_{j=1}^{N_L} \tilde{P}_{ij} = P$ for all $i = 1, \ldots, N_L$, where P is the symmetric positive definite solution of the ARE associated with a single-node local problem:

$$A'P + PA - PBR^{-1}B'P + Q_1 = 0. \tag{3.71}$$

II. $\sum_{j=1}^{N_L} \tilde{K}_{ij} = K$ *for all* $i = 1,\ldots,N_L$, *where* $K = -R^{-1}B'P$.

III. $\tilde{P}_{ij} = \tilde{P}_{lm} = \tilde{P}_2$, $\forall\ i \neq j$ *and* $\forall\ l \neq m$, *is a symmetric negative semidefinite matrix associated with the node-level algebraic Riccati equation*

$$(A - XP)'(-N_L\tilde{P}_2) + (-N_L\tilde{P}_2)(A - XP) - (-N_L\tilde{P}_2)X(-N_L\tilde{P}_2) + N_LQ_2 = 0. \quad (3.72)$$

The hypothesis in (3.70) implies that the absolute local state x_i is equally penalized for all nodes $i = 1,\ldots,N_L$, via weighting matrix Q_1; similarly, the relative state-difference $x_i - x_j$ is identically weighed for all neighboring nodes $i, j = 1,\ldots,N_L$, $j \neq i$, via matrix Q_2. Under this assumption, Theorem 3.3.11 suggests that the solution $\tilde{P}$ of the large-scale ARE (3.67) has a repetitive pattern the building blocks $(\tilde{P}_{ij})$ of which can be obtained by solving two node-level algebraic Riccati equations, that is, (3.71) and (3.72). In particular, statements I and III imply that all (i,i) diagonal blocks $\tilde{P}_{ii}$, $i = 1,\ldots,N_L$, are equal to the symmetric positive definite matrix $P - (N_L - 1)\tilde{P}_2$ while all (i,j) off-diagonal blocks $\tilde{P}_{ij}$, $i, j = 1,\ldots,N_L$ and $j \neq i$, are equal to the symmetric negative semidefinite matrix $\tilde{P}_2$. The negative semidefiniteness of $\tilde{P}_2$ stems from the positive semidefiniteness of matrix $-N_L\tilde{P}_2 \geq 0$ which is a stabilizing solution to ARE (3.72). This particular structure of $\tilde{P}$ is shown below.

$$\tilde{P} = \begin{bmatrix} P - (N_L - 1)\tilde{P}_2 & \tilde{P}_2 & \cdots & \tilde{P}_2 \\ \tilde{P}_2 & P - (N_L - 1)\tilde{P}_2 & \cdots & \tilde{P}_2 \\ \vdots & \ddots & \ddots & \vdots \\ \tilde{P}_2 & \cdots & \cdots & P - (N_L - 1)\tilde{P}_2 \end{bmatrix}. \quad (3.73)$$

Since by assumption $\tilde{B} = I_{N_L} \otimes B$ and $\tilde{R} = I_{N_L} \otimes R$, the optimal state-feedback gain $\tilde{K} = -\tilde{R}^{-1}\tilde{B}'\tilde{P}$ in (3.66) retains the same structure with $\tilde{P}$. This implies that the optimal solution $\tilde{K}$ of LQR problem (3.65) with weighting matrices chosen as in (3.70) has the following structure:

$$\tilde{K} = \begin{bmatrix} K_1 & K_2 & \cdots & K_2 \\ K_2 & K_1 & \cdots & K_2 \\ \vdots & \ddots & \ddots & \vdots \\ K_2 & \cdots & \cdots & K_1 \end{bmatrix}, \quad (3.74)$$

with $K_1 = -R^{-1}B'P + (N_L - 1)R^{-1}B'\tilde{P}_2$ and $K_2 = -R^{-1}B'\tilde{P}_2$. Apart from the special structure of $\tilde{P}$ and $\tilde{K}$, shown in (3.73) and (3.74), respectively, Theorem (3.72) results in the following corollaries arising from properties of (3.72). In particular, (3.72), as already mentioned, can be seen as an ARE associated with an LQR problem with dynamics $(A - BR^{-1}B'P,\ B)$ and

weighting matrices $(N_L Q_2,\ R)$. Stability and robustness properties pertaining to an LQR problem with parameters $(A-XP,\ B,\ N_L Q_2,\ R)$ give rise to the following results.

Corollary 3.3.1. *Matrix $A-XP+N_L X\tilde{P}_2$ is Hurwitz.*

The following result is derived from the infinite gain margin of the LQR controller [85].

Corollary 3.3.2. *Matrix $A-XP+aN_L X\tilde{P}_2$ is Hurwitz for all $a\in(\frac{1}{2},\infty)$.*

This result is useful in the next section for designing stabilizing distributed LQR-based control. We also note that:

Remark 3.3.12. Matrix $A-XP=A+BK$ is Hurwitz since $K=-R^{-1}B'P$ is the optimal LQR state-feedback gain pertinent to LQR problem with parameters $(A,\ B,\ Q_1,\ R)$. Thus, the system in Corollary 3.3.2 is stable for $a=0$ as well.

In addition, we impose the following requirement.

Condition 3.3.13. *Matrix $A-XP+aN_L X\tilde{P}_2$ is Hurwitz for all $\alpha\in[0,1]$.*

Condition 3.3.13 states that all convex combinations of two Hurwitz matrices,

$$\mu\bar{A}_1+(1-\mu)\bar{A}_2 \text{ with } \mu\in[0,1], \tag{3.75}$$

are Hurwitz, where $\bar{A}_1=A-XP+N_L X\tilde{P}_2$ and $\bar{A}_2=A-XP$. Sufficient conditions for Hurwitz stability of a convex combination of Hurwitz matrices can be found in Theorem 2.2 in [14]. In essence, Condition 3.3.13 characterizes a class of LQR problems (3.65) where their solutions guarantee the validity of Condition 3.3.13. In the next section, we show that Condition 3.3.13 also extends the class of distributed controllers that can stabilize a multi-agent network of identical dynamically decoupled linear systems. For a given choice of weighting matrices $(Q_1,\ Q_2,\ R)$ in problem (3.65), the validity of Condition 3.3.13 can be verified by searching for a symmetric positive definite matrix $\bar{P}$ for which the following LMI,

$$\begin{bmatrix} -(\bar{A}_1'\bar{P}+\bar{P}\bar{A}_1) & 0_{n\times n} & 0_{n\times n} \\ 0_{n\times n} & -(\bar{A}_2'\bar{P}+\bar{P}\bar{A}_2) & 0_{n\times n} \\ 0_{n\times n} & 0_{n\times n} & \bar{P} \end{bmatrix} > 0, \tag{3.76}$$

is feasible. Obviously, if matrix $\bar{P}$ exists then premultiplying and postmultiplying (3.76) by $[\sqrt{\mu}I_n\ \sqrt{1-\mu}I_n\ 0_{n\times n}]$ and $[\sqrt{\mu}I_n\ \sqrt{1-\mu}I_n\ 0_{n\times n}]'$, respectively, with $\mu\in[0,1]$, leads to a Lyapunov inequality:

$$(\mu\bar{A}_1+(1-\mu)\bar{A}_2)'\bar{P}+\bar{P}(\mu\bar{A}_1+(1-\mu)\bar{A}_2)<0, \tag{3.77}$$

which admits solution $\bar{P} = \bar{P}' > 0$. This demonstrates that $\mu\bar{A}_1 + (1-\mu)\bar{A}_2$ is a Hurwitz matrix for all $\mu \in [0,1]$. Alternatively, the stability of $\mu\bar{A}_1 + (1-\mu)\bar{A}_2$ can be examined via a simple graphical test by plotting the eigenvalue with the maximum real part of the matrix $\mu\bar{A}_1 + (1-\mu)\bar{A}_2$ for $\mu \in [0,1]$.

In the subsequent sections we turn our attention to the networked regulator problem. This is formulated as a structured optimal control problem and is presented next.

3.3.4 Distributed LQR design of multi-agent networks

Let a network be composed of N identical, linear time-invariant, dynamically decoupled systems, referred to as agents. The dynamics of each agent are described by the state-space equation

$$\dot{x}_i = Ax_i + Bu_i,\ x_i(0) = x_{i,0}, \tag{3.78}$$

where $x_i \in \mathbb{R}^n$, $u_i \in \mathbb{R}^m$ denote state and input vectors, respectively, for $i = 1,\ldots,N$. A graph $\mathscr{G} = (\mathscr{V}, \mathscr{E})$ is employed to represent network's topology pertaining to the communication scheme among the N agents and the structure of the controls u_i, $i = 1,\ldots,N$. Specifically, node $i \in \mathscr{V}$ of $\mathscr{G}$ denotes agent-i, while edge $(i,j) \in \mathscr{E}$ implies that 1) agent-i has access to the state of agent-j and 2) control u_i minimizes (among other terms) a weighted norm of $x_i - x_j$. We also note that the communication between two nodes is assumed to be bidirectional, that is, $\mathscr{G} = (\mathscr{V}, \mathscr{E})$ is an undirected graph, i.e., $(i,j) \in \mathscr{E} \iff (j,i) \in \mathscr{E}$.

Construct now the aggregate state and input vectors, denoted here as $\hat{x} \in \mathbb{R}^{nN}$ and $\hat{u} \in \mathbb{R}^{mN}$, respectively, by stacking individual state and input vectors, respectively, of all N systems taken in an ascending order depending on their label in graph $\mathscr{G}$. The aggregate state-space form of the network becomes:

$$\dot{\hat{x}} = \hat{A}\hat{x} + \hat{B}\hat{u},\ \hat{x}(0) = \hat{x}_0, \tag{3.79}$$

with:

$$\hat{A} = I_N \otimes A,\ \hat{B} = I_N \otimes B. \tag{3.80}$$

Note that the aggregate state-space forms (3.79) and (3.58) differ only in number of subsystems. In particular, we denote an aggregate state-space form as in (3.58) when referring to a centralized control problem with N_L subsystems, while we use a notation as in (3.79) when pertaining to distributed control problems with N subsystems. Similarly, tilded matrices correspond to centralized problems while hatted matrices to distributed problems. Next, a class of matrices with a particular structure is highlighted.

Consider now matrix $\Xi \in \mathbb{R}^{mN\times nN}$ which is partitioned into N^2 blocks of dimension $m\times n$ each referred to as (i,j)-block of Ξ and denoted by $\Xi_{ij}\in\mathbb{R}^{m\times n}$ with $i,j=1,\ldots,N$. In particular, the (i,j)-block can be written as: $\Xi_{ij}=\Xi[(i-1)m+1:im,(j-1)n+1:jn]$. The class of structured matrices $\mathscr{K}^N_{n,m}(\mathscr{G})$ is now defined as follows:

Definition 3.3.3. $\mathscr{K}^N_{m,n}(\mathscr{G})=\{\Xi\in\mathbb{R}^{mN\times nN} \mid \Xi_{ij}=0_{m\times n} \text{ if } (i,j)\notin\mathscr{E},\ \Xi_{ij}=\Xi[(i-1)m+1:im,(j-1)n+1:jn],\ i,j=1,\ldots,N\}$.

A networked regulator problem of N agents formulated as a distributed optimal control problem is defined as follows:

$$\min_{\hat{u}}\ J(\hat{u},\hat{x}_0)=\int_0^\infty(\hat{x}'\hat{Q}\hat{x}+\hat{u}'\hat{R}\hat{u})\ \mathrm{dt} \tag{3.81a}$$

$$\text{subject to: } \dot{\hat{x}}=\hat{A}\hat{x}+\hat{B}\hat{u},\ \hat{x}(0)=\hat{x}_0, \tag{3.81b}$$

$$\hat{u}=\hat{K}\hat{x}, \tag{3.81c}$$

$$\hat{K}\in\mathscr{K}^N_{m,n}(\mathscr{G}), \tag{3.81d}$$

$$\hat{Q}\in\mathscr{K}^N_{n,n}(\mathscr{G}),\ \hat{R}=I_N\otimes R, \tag{3.81e}$$

where $\hat{Q}=\hat{Q}'\geq 0$ and $\hat{R}=\hat{R}'>0$. Controllability and observability assumptions are omitted here and will be identified clearly in the sequel. We note that in the absence of constraint (3.81d), the optimal control problem (3.81), if feasible, yields a centralized optimal control law $u^*=K^*\hat{x}$ with $K^*=-\hat{R}^{-1}\hat{B}'P^*$. Matrix P^* is the symmetric positive definite solution to:

$$\hat{A}'P^*+P^*\hat{A}-P^*\hat{B}\hat{R}^{-1}\hat{B}'P^*+\hat{Q}=0. \tag{3.82}$$

The networked regulator problem as stated in (3.81), is an NP-hard problem to solve due to the special structure of $\hat{K}$ imposed by (3.81d). Two complimentary methods for solving this problem approximately, have been established in [17] and [46]. Both approaches propose a suboptimal distributed state-feedback controller, $\hat{u}=\hat{K}\hat{x}$, with the following properties:

I. $\hat{K}\in\mathscr{K}^N_{m,n}(\mathscr{G})$.

II. The closed-loop matrix $\hat{A}+\hat{B}\hat{K}$ is Hurwitz.

III. A certain measure of suboptimality is introduced.

The first two properties will be proved and highlighted for each method separately in the subsequent sections, while a general rule for measuring the level of suboptimality of a distributed control scheme will be given in the last section of this chapter.

A schematic representation of the distributed state-feedback control scheme proposed in [17, 46] is illustrated in Fig. 3.2. Focusing on the individual system level, the figure indicates that agent-i, in order to construct its control signal u_i at time t, requires 1) local state $x_i(t)$, and 2) neighboring states $x_j(t),\dots,x_k(t)$, with $j,\dots,k \in \mathscr{N}_i$, be known signals at time t. In effect, the control protocol displayed in Fig. 3.2 suggests that agents are capable of communicating their state-information to their neighbors. These state transmissions among neighboring agents are assumed to be performed continuously over a communication network as highlighted in the figure.

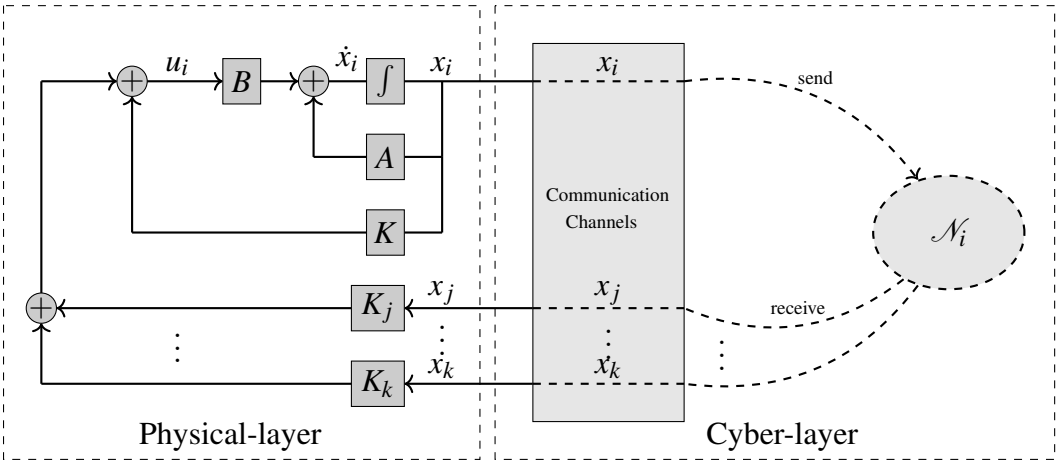

Fig. 3.2 Distributed closed-loop architecture of one agent in a multi-agent network.

In the following section, the distributed control design procedure, referred to as top-down method originally established in [17], is presented. It will be shown that the centralized solution of an LQR problem with weighting matrices as defined in Theorem 3.3.11 can be approximated by a distributed scheme, the closed-loop stability of which is guaranteed by the gain margin property of LQR control stated in Corollary 3.3.2.

3.3.5 Top-down method

A stabilizing distributed state-feedback controller, $\hat{u} = \hat{K}\hat{x}$, is proposed as a suboptimal solution to problem (3.81). The method is based on the centralized solution of an LQR problem as formulated in (3.65) and the selection of a symmetric $N \times N$ matrix with a certain spectral property. We note that the choice of this matrix is associated with the structure of graph $\mathscr{G}$. Pertaining to networked regulator problem (3.81), we recall that graph $\mathscr{G} = (\mathscr{V}, \mathscr{E})$ represents 1) coupling terms in the control objective, and 2) an interaction (communication) scheme among the N systems (agents), as outlined earlier in Section 3.3.4. We also denote

the maximum vertex degree of $\mathscr{G}$ as $d_{\max}$. The control design procedure is summarized in the following theorem.

Theorem 3.3.14. *[17] Consider LQR problem* (3.65) *with* $N_L = d_{\max} + 1$ *and weighting matrices chosen as in* (3.70)*. Define matrices* P *and* $\tilde{P}_2$ *from* (3.71) *and* (3.72)*, respectively. Let* $M \in \mathbb{R}^{N\times N}$ *be a symmetric matrix with the following property:*

$$\lambda_i(M) > \frac{N_L}{2},\ \forall \lambda_i(M) \in S(M)\backslash\{0\} \tag{3.83}$$

and construct the state-feedback gain:

$$\hat{K} = -I_N \otimes R^{-1}B'P + M \otimes R^{-1}B'\tilde{P}_2. \tag{3.84}$$

Then, the closed-loop system

$$A_{cl} = I_N \otimes A + (I_N \otimes B)\hat{K} \tag{3.85}$$

is asymptotically stable.

Proof. Consider the spectrum of the closed-loop system A_{cl}:

$$S(A_{cl}) = S\left(I_N \otimes (A - XP) + M \otimes (X\tilde{P}_2)\right) = \bigcup_{i=1}^{N} S\left(A - XP + \lambda_i(M)X\tilde{P}_2\right). \tag{3.86}$$

We will prove that $A - XP + \lambda_i(M)X\tilde{P}_2$ is a Hurwitz matrix $\forall\, i = 1,\ldots,N$. If $\lambda_i(M) = 0$, then matrix $A - XP$ is Hurwitz based on Remark 3.3.12. If $\lambda_i(M) \neq 0$, from Corollary 3.3.2 and hypothesis (3.83) we conclude that $A - XP + \lambda_i(M)X\tilde{P}_2$ is Hurwitz. □

Theorem 3.3.14 yields the following conclusions.

1) If $M \in \mathscr{K}_{1,1}^{N}(\mathscr{G})$ then $\hat{K}$ in (3.84) is a stabilizing distributed controller.

2) The spectrum of the large-scale closed-loop system A_{cl} can be computed through N (simple) eigenvalue computations as in (3.86).

3) The result is independent of the LQR tuning. Thus, matrices $Q_1,\ Q_2,\ R$ can be chosen such that the desired trade-off between various objectives in the global performance is achieved without affecting closed-loop stability.

4) Despite that it introduces additional suboptimality in the solution, selecting matrix M a posteriori the optimization enhances the modularity and scalability of the proposed distributed control algorithm.

Referring to the class of LQR problems for which Condition 3.3.13 is valid, the assumption (3.83) in Theorem 3.3.14 can be relaxed as follows:

Theorem 3.3.15. *[17] Consider LQR problem* (3.65) *with* $N_L = d_{\max} + 1$ *and weighting matrices chosen as in* (3.70)*. Define matrices P and* $\tilde{P}_2$ *from* (3.71) *and* (3.72)*, respectively. Let* $M \in \mathbb{R}^{N\times N}$ *be a symmetric matrix with the following property:*

$$\lambda_i(M) \geq 0,\ \forall \lambda_i(M) \in S(M)\backslash\{0\}. \tag{3.87}$$

Then the closed-loop system (3.85) *is asymptotically stable when* $\hat{K}$ *is constructed as in* (3.84)*.*

Detailed proof is omitted here since it follows similar arguments with proof of Theorem 3.3.14. In particular, closed-loop stability can be proved straightforwardly by replacing Corollary 3.3.2 with Condition 3.3.13 in proof of Theorem 3.3.14.

The construction of matrix M in Theorem 3.3.14 and Theorem 3.3.15 is now discussed. As already mentioned, in order for $\hat{K}$ to be a distributed controller, matrix M should be sparse reflecting the structure of graph $\mathscr{G}$ and satisfying either condition (3.83) or condition (3.87). In the following paragraph, a particular choice of M for arbitrary graph structures is highlighted.

Arbitrary graph structures: Consider a generic graph $\mathscr{G}$ of N nodes with a Laplacian matrix $\mathscr{L}$. Let $d_{\max}$ denote the maximum vertex degree of $\mathscr{G}$, $\lambda_i \in S(\mathscr{L})$ with $i = 1,\ldots,N$, and $0 = \lambda_1 < \lambda_2 \leq \ldots \leq \lambda_N$. The following corollary suggests a certain choice of M in (3.84) leading to a stabilizing state-feedback controller $\hat{K}$ with sparse structure.

Corollary 3.3.3. *Compute M in* (3.84) *as* $M = a\mathscr{L}$*. If* $a > \frac{N_L}{2\lambda_2(\mathscr{L})}$ *then the closed-loop matrix* A_{cl} *in* (3.85) *is Hurwitz when* $\hat{K}$ *is constructed as in* (3.84)*. In addition, if Condition 3.3.13 is valid, then* A_{cl} *in* (3.85) *is Hurwitz for all* $a \geq 0$*.*

In essence, Corollary 3.3.3 indicates that if $M = a\mathscr{L}$, with $\mathscr{L}$ being the Laplacian matrix of $\mathscr{G}$, then there is always an appropriate choice of the scaling factor a such that the distributed scheme (3.85) is asymptotically stable. Several choices for how to construct matrix M can be found in [17].

3.3.6 Bottom-up method

A bottom-up approach for solving problem (3.81) is proposed in [46]. In this method, which is carried out in two steps, N agents (represented as identical, dynamically decoupled, linear

time-invariant systems) are self-stabilized by a node-level LQR controller. Then an upper bound of the global LQR criterion is minimized by coordinating optimal interactions between neighboring agents. These interactions are manifested as coupling terms in the control objective as well as state-information transmissions between adjacent agents. Similarly to top-down method, the interconnection scheme (cf. Fig. 3.2) is represented by an undirected graph $\mathscr{G} = (\mathscr{V}, \mathscr{E})$ with a Laplacian matrix $\mathscr{L}$. Specifically, node $i \in \mathscr{V}$ denotes agent-i while edge $(i, j) \in \mathscr{E}$ indicates 1) state-information exchange between node i and j, and 2) that the control signal of node-i is partly constructed by the relative state-difference between node i and j. This relative information is defined next.

Let the state-space form

$$\dot{x}_i = Ax_i + Bu_i,\ x_i(0) = x_{i,0}, \tag{3.88}$$

describe the dynamics of the i-th agent, where $x_i \in \mathbb{R}^n$, $u_i \in \mathbb{R}^m$ denote state and input vectors, respectively, with $i = 1, \ldots, N$. The pair $(A,\ B)$ is assumed to be controllable. Let $\mathscr{N}_i \subset \mathscr{V}$ denote the neighborhood of the i-th node, that is, if $j \in \mathscr{N}_i$ then $(i, j) \in \mathscr{E}$. Considering $j \in \mathscr{N}_i$ implies that $x_i - x_j$ is a known signal to agent-i. Then, the signal representing the relative state-difference of agent-i with respect to its neighborhood is defined as

$$z_i = \sum_{j \in \mathscr{N}_i} \left(x_i - x_j\right). \tag{3.89}$$

Consider now performance index

$$J(\hat{u}, \hat{x}_0) = \int_0^\infty \left(\hat{x}'\hat{Q}\hat{x} + \hat{u}'\hat{R}\hat{u}\right) \mathrm{d}t, \tag{3.90}$$

where

$$\hat{Q} = I_N \otimes Q_1 + \mathscr{L} \otimes Q_2,\ \hat{R} = I_N \otimes R. \tag{3.91}$$

Here, $\hat{x} = [x_1', \ldots, x_N']' \in \mathbb{R}^{nN}$, $\hat{u} = [u_1', \ldots, u_N']' \in \mathbb{R}^{mN}$ and $\hat{x}_0 = [x_1(0)', \ldots, x_N(0)']' \in \mathbb{R}^{nN}$ denote the aggregate state, input and initial state vectors, respectively. Matrices $Q_1 = Q_1' \geq 0$ and $R = R' > 0$ penalize local states and inputs of each agent, respectively, while matrix $Q_2 = Q_2' \geq 0$ weighs state difference between two neighboring agents. Similarly to $\hat{x}$ and $\hat{u}$, the aggregate relative state-difference vector is defined as:

$$\hat{z} = (\mathscr{L} \otimes I_n)\hat{x}. \tag{3.92}$$

The method proposes a state-feedback control law which, at node level, takes the following form:

$$u_i = Kx_i + \Phi K z_i,\ i = 1,\ldots,N, \tag{3.93}$$

where $K \in \mathbb{R}^{m\times n}$ and $\Phi \in \mathbb{R}^{m\times m}$ are to be designed. At network level,

$$\hat{u} = \hat{K}\hat{x}, \tag{3.94}$$

is a distributed state-feedback controller, with

$$\hat{K} = I_N \otimes K + \mathscr{L} \otimes \Phi K. \tag{3.95}$$

The optimal control problem considered in [46] is shown below:

$$\min_{\hat{u}}\ J(\hat{u},\hat{x}_0) = \int_0^\infty \left(\hat{x}'(I_N \otimes Q_1 + \mathscr{L} \otimes Q_2)\hat{x} + \hat{u}'\hat{R}\hat{u}\right) \mathrm{dt}\ \text{ subject to:} \tag{3.96}$$

$$\dot{\hat{x}} = (I_N \otimes A)\hat{x} + (I_N \otimes B)\hat{u},\ \hat{x}(0) = \hat{x}_0, \tag{3.97}$$

$$\hat{u} = (I_N \otimes K + \mathscr{L} \otimes \Phi K)\hat{x}. \tag{3.98}$$

Note that the optimal control problem as stated in (3.96) is equivalent to (3.81). Note also that $I_N \otimes K + \mathscr{L} \otimes \Phi K \in \mathscr{K}^N_{m,n}(\mathscr{G})$ and $\hat{Q} \in \mathscr{K}^N_{m,n}(\mathscr{G})$. Thus, if matrices K, Φ are chosen such that $J(\hat{u}(\cdot),\hat{x}_0)$ is finite, then, $\hat{u}$ in (3.94) represents a (suboptimal) stabilizing distributed state-feedback controller. The problem of finding K and Φ will be tackled in a suboptimal way via a two-step optimization process which is outlined below.

At the first step, no interactions between agents are considered. Thus scaling matrix Φ in (3.93) and weight Q_2 in (3.90) are temporarily taken identical to zero. Then, setting $Q_2 = 0$, the performance index (3.90) is written as $J = \sum_{i=1}^N J_i$ where

$$J_i = \int_0^\infty \left(x_i' Q_1 x_i + u_i' R u_i\right) \mathrm{dt}. \tag{3.99}$$

At this stage, there is no coupling in the control objective, that is, K can designed as the optimal state-feedback gain derived from an LQR problem with parameters $(A,\ B,\ Q_1,\ R)$, i.e.,

$$K = -R^{-1}B'P, \tag{3.100}$$

where P is the symmetric positive definite solution to algebraic Riccati equation:

$$A'P + PA - PBR^{-1}B'P + Q_1 = 0. \tag{3.101}$$

This completes the first step of the design procedure. We now proceed with the design of matrix Φ in (3.93), lifting the temporary assumption that $Q_2 = 0$.

Letting $\mathscr{L} = V\Lambda V'$ be the spectral decomposition of the Laplacian matrix $\mathscr{L}$, where $V \in \mathbb{R}^{N\times N}$ is an orthogonal matrix composed of the eigenvectors of $\mathscr{L}$, and $\Lambda = \text{diag}(\lambda_1,\ldots,\lambda_N)$ with $\lambda_i \in S(\mathscr{L})$, $i = 1,\ldots,N$, define the following state-space transformation:

$$\hat{\xi} = (V \otimes I_n)\hat{x}. \tag{3.102}$$

Considering now that $\hat{u}$ is given as in (3.98), the closed-loop system in the original coordinates can be written as:

$$\dot{\hat{x}} = (I_N \otimes (A + BK) + \mathscr{L} \otimes (B\Phi K))\,\hat{x}, \tag{3.103}$$

while in the new coordinates, $\hat{\xi}$, we have

$$\dot{\hat{\xi}} = (I_N \otimes (A + BK) + \Lambda \otimes (B\Phi K))\,\hat{\xi}. \tag{3.104}$$

Note also that, in the new coordinates, the weighting matrix $I_N \otimes Q_1 + \mathscr{L} \otimes Q_2$ in (3.90) is mapped to:

$$(V \otimes I_n)(I_N \otimes Q_1 + \mathscr{L} \otimes Q_2)(V \otimes I_n)' = I_N \otimes Q_1 + \Lambda \otimes Q_2, \tag{3.105}$$

and thus, the performance index (3.90) can also be written as:

$$J(\cdot) = \int_0^\infty \left(\hat{\xi}'(I_N \otimes Q_1 + \Lambda \otimes Q_2)\hat{\xi} + \hat{u}'\hat{R}\hat{u}\right) \text{dt}. \tag{3.106}$$

Since matrix Λ is diagonal, letting $[\xi_1',\ldots,\xi_N']' \triangleq \hat{\xi}$, the closed-loop system (3.104) can be decomposed into N node-level state-space equations written as:

$$\dot{\xi}_i = (A + BK + \lambda_i B\Phi K)\xi_i,\ i = 1,\ldots,N. \tag{3.107}$$

Similarly, the performance index (3.106) can be reduced to:

$$J(\cdot) = \sum_{i=1}^{N} \int_0^\infty \left(\xi_i'(Q_1 + \lambda_i Q_2)\xi_i + u'Ru_i\right) \text{dt}. \tag{3.108}$$

For each decoupled node-level system in (3.107), consider a quadratic Lyapunov function $V_i = \xi_i' P_i \xi_i$ where P_i has the following structure:

$$P_i = \begin{bmatrix} P_{i,11} & 0 \\ 0 & \Pi_2 \end{bmatrix} > 0. \tag{3.109}$$

Here, $P_{i,11} \in \mathbb{R}^{(n-m)\times(n-m)}$, $\Pi_2 \in \mathbb{R}^{m\times m}$ are assumed to be symmetric positive definite matrices. Note that Π_2 is taken identical for all $i = 1,\ldots,N$. Finally, the second step of the design procedure attempts to tackle the following optimization problem.

$$\min \sum_{i=1}^{N} \text{trace}(P_i) \text{ subject to:} \tag{3.110a}$$

$$\begin{aligned} &P_i(A+BK+\lambda_i B\Phi K) + (A+BK+\lambda_i B\Phi K)' P_i + (Q_1+\lambda_i Q_2) \\ &\qquad + (K+\lambda_i \Phi K)' R (K+\lambda_i \Phi K) < 0,\ i = 1,\ldots,N, \end{aligned} \tag{3.110b}$$

$$P_i > 0,\ i = 1,\ldots,N. \tag{3.110c}$$

For an initial state $\hat{x}_0$ uniformly distributed on the surface of the n-dimensional unit sphere, the optimum performance index $J^*(\cdot)$ in (3.96) satisfies [20, 46]:

$$J^*(\cdot) \leq \sum_{i}^{N} \text{trace}(P_i), \tag{3.111}$$

with P_i as given in (3.109). Thus, the optimization problem (3.110) represents the minimization of an upper bound of the global LQR criterion. We also note the following:

1) The block diagonal structure of P_i in (3.109) introduces conservatism in the solution. This special structure is chosen to impose a convex representation of the optimization problem.

2) Setting $\Phi = 0$, then $P_i = P$ is a feasible solution to (3.110), where P is derived from (3.101). Thus the optimization problem is guaranteed to have a non-trivial solution.

3) $\hat{u}$ in (3.94) is a distributed state-feedback controller. It is also stabilizing if the optimization problem (3.110) is feasible.

Detailed description for how to solve the optimization problem (3.110) can be found in [46]. In Chapter 4, an attempt to combine the two distributed LQR-based control design methods (top-down, bottom-up) described in this chapter will be presented. Therein, all technical details for solving the optimization problem (3.110) will be clearly identified.

3.3.7 Measure of suboptimality

Two complementary techniques for designing stabilizing distributed state-feedback controllers were presented in Section 3.3.5 and Section 3.3.6, respectively. In both methods, approximate solutions to optimal control problem (3.81) were presented. Here, we wish to employ a suboptimality measure which can be cast as a performance loss index pertinent to a particular suboptimal distributed design. First, we define a performance reference index whereby a suboptimal distributed control scheme can be assessed. Such an index has been originally introduced in [17] and is also outlined here.

We consider optimal control problem (3.81) where constraint (3.81d) is not in force. In this case, (3.81) can be seen as a typical LQR problem with weights given as in (3.81e). In this respect, let K^* and P^* be the optimal LQR controller and the symmetric positive definite solution to the associated ARE, respectively. Therefore, $\hat{u}^* = K^*\hat{x}$ minimizes the LQR cost function for any $\hat{x}_0$:

$$J(\hat{u}^*, \hat{x}_0) = \hat{x}_0' P^* \hat{x}_0. \tag{3.112}$$

Note that, since constraint (3.81d) is ignored, K^* and P^* are centralized solutions, and thus, the value $\hat{x}_0' P^* \hat{x}_0$ is the minimum achievable performance index for a given $\hat{x}_0$.

Assume now that constraint (3.81d) is in force. Then a stabilizing distributed state-feedback controller $\hat{K}$ can be obtained either via the top-down or the bottom-up method described earlier. Assume that $\hat{K}$ is constructed as in (3.84) and the closed-loop system (3.85) is stable. Then, a performance index for this distributed scheme can be computed as

$$J(\hat{K}\hat{x}, \hat{x}_0) = \hat{x}_0' \hat{P} \hat{x}_0, \tag{3.113}$$

where $\hat{P}$ is the positive definite solution to the following Lyapunov equation:

$$(I_N \otimes A + (I_N \otimes B)\hat{K})'\hat{P} + \hat{P}(I_N \otimes A + (I_N \otimes B)\hat{K}) + (\hat{Q} + \hat{K}'\hat{R}\hat{K}) = 0. \tag{3.114}$$

Since P^* is optimal, $J(K^*\hat{x}, \hat{x}_0) \leq J(\hat{K}\hat{x}, \hat{x}_0)$ for all $\hat{x}_0$ and thus $\Delta P = \hat{P} - P^*$ is a positive semidefinite matrix which is equal to zero if $\hat{K} = K^*$. Any norm of ΔP can be considered as a measure of suboptimality of the distributed controller $\hat{K}$. In the sequel, we will use the Frobenius norm, $\|\Delta P\|_F$, in order to judge the suboptimality level of a distributed control scheme. The best linear state-feedback distributed controller could be constructed by solving:

$$J(\hat{x}_0) = \min_{\hat{K} \in \mathcal{K}_{m,n}^N} \|\Delta P\|_F, \tag{3.115}$$

which is an NP-hard problem to solve.

3.4 Conclusion

A concise review of the regulator problem is presented in the first part of this chapter. Structural assumptions for optimality and closed-loop stability of the infinite-time regulator problem are discussed and then properties of a large-scale LQR problem of decoupled linear systems are identified. In this setting, the concept of multi-agent networks and distributed control is developed for networked systems represented by undirected graphs. Two existing methods for designing stabilizing distributed state-feedback controllers are comprehensively described highlighting their properties. In the last section, a general rule, originally introduced in [17], for assessing the suboptimality level of a state-feedback controller with distributed structure is also presented. A distributed control design method which combines techniques from the top-down [17] and the bottom-up [46] approach is proposed in the following chapter. Therein, it also becomes evident that the distributed control methods originally presented here for tackling regulation problems of networks with undirected topology, can be extended to regulating networks with directed interconnection pattern.

Chapter 4

Stabilization of multi-agent networks with undirected and directed topology

4.1 Introduction

In the previous chapter the stabilization of multi-agent networks with sparse structure was considered. It was shown that this task can be formulated as a large-scale LQR problem augmented by control structure constraints. Two well-established methods (top-down [17], bottom-up [46]) for solving this problem approximately were discussed. Here, a new distributed control design method, which combines techniques from both aforementioned approaches, is presented. This hybrid method is initially exemplified in multi-agent networks with undirected topology, and then it is shown that it can successfully be extended also to directed networks. An illustrative numerical example attempts to show the applicability of the new distributed control algorithm. In the study, both cases of undirected and directed graphs are considered. The suboptimality measure discussed in Section 3.3.7 is used to evaluate the performance of the proposed distributed scheme with respect to a centralized optimal solution. Comparison with the suboptimality level achieved via the distributed solutions derived from both the top-down and bottom-up methods is also highlighted. Next, we start with the construction of the new stabilizing distributed controller for networks with undirected topology, while directed networks are studied in the last part of the chapter.

4.2 Distributed control for undirected networks

Consider a network of N identical, dynamically decoupled linear systems. Each system represents a dynamic agent with autonomous actuation capacity. Let the linear state-space

equation

$$\dot{x}_i = Ax_i + Bu_i,\ x_i(0) = x_{i,0}, \tag{4.1}$$

describe the dynamics of the i-th agent, where $x_i \in \mathbb{R}^n$ and $u_i \in \mathbb{R}^m$ denoting the i-th state- and input-vector, respectively, and $A \in \mathbb{R}^{n\times n}$, $B \in \mathbb{R}^{n\times m}$. Let also matrix $B \in \mathbb{R}^{n\times m}$ have the following structure:

$$B = \begin{bmatrix} 0 \\ B_2 \end{bmatrix}, \tag{4.2}$$

where matrix $B_2 \in \mathbb{R}^{m\times m}$ is nonsingular. The structure in (4.2) is called a regular form [36] and is a technical assumption postulated here for control design purposes. Note that this particular structure of B is considered without loss of generality since it can always be obtained via an appropriate change of coordinates in (4.1), provided matrix B has full-column rank. A linear map $B \to TB$ which ensures this form is constructed next:

Lemma 4.2.1. *Let matrix $B \in \mathbb{R}^{n\times m}$ have full-column rank. Then, there is always a nonsingular matrix $T \in \mathbb{R}^{n\times n}$ such that $TB = \begin{bmatrix} 0 & B_2' \end{bmatrix}'$ where $B_2 \in \mathbb{R}^{m\times m}$ is nonsingular.*

Proof. Let $U \begin{bmatrix} \Sigma \\ 0 \end{bmatrix} V'$ be singular value decomposition of B, i.e., $B = U \begin{bmatrix} \Sigma \\ 0 \end{bmatrix} V'$, where $U \in \mathbb{R}^{n\times n}$, $V \in \mathbb{R}^{m\times m}$ are unitary matrices and $\Sigma \in \mathbb{R}^{m\times m}$ is a diagonal nonsingular matrix. Let also $U = [U_1\ U_2]$, with $U_1 \in \mathbb{R}^{n\times m}$ and $U_2 \in \mathbb{R}^{n\times(n-m)}$. Then, we may write $[U_1\ U_2] \begin{bmatrix} \Sigma \\ 0 \end{bmatrix} = [U_2\ U_1] \begin{bmatrix} 0 \\ \Sigma \end{bmatrix}$, and $B = [U_2\ U_1] \begin{bmatrix} 0 \\ \Sigma V' \end{bmatrix}$. Let now a permutation matrix $\Pi = \begin{bmatrix} 0 & I_{n-m} \\ I_m & 0 \end{bmatrix}$ and define a non-singular matrix $T = (U\Pi)^{-1}$, where $\Pi^{-1} = \Pi$. Then, $TB = \begin{bmatrix} 0 \\ B_2 \end{bmatrix}$, with $B_2 = \Sigma V'$, and $\det B_2 \neq 0$, since matrices Σ, V are nonsingular by definition. □

The network is represented by an undirected graph $\mathcal{G} = (\mathcal{V}, \mathcal{E})$ with Laplacian matrix $\mathcal{L}$ and maximum vertex degree $d_{\max}$. We recall that node $i \in \mathcal{V}$ denotes agent-i while edge (i, j) represents coupling terms in the control objective as well as a state-information exchange between agent i and j. Let also $\mathcal{N}_i$ denote the set of neighbors of node-i, i.e., if $(i, j) \in \mathcal{E}$ then $j \in \mathcal{N}_i$. Constructing the aggregate state- and input-vector as $\hat{x} = [x_1', \ldots, x_N']'$ and $\hat{u} = [u_1', \ldots, u_N']'$, respectively, we represent the collective state-space form of the network as follows:

$$\dot{\hat{x}} = \hat{A}\hat{x} + \hat{B}\hat{u},\ \hat{x}(0) = \hat{x}_0, \tag{4.3}$$

where

$$\hat{A} = I_N \otimes A,\ \hat{B} = I_N \otimes B, \tag{4.4}$$

We wish to solve the following optimization problem:

$$\min_{\hat{u}} J(\hat{u},\hat{x}_0) \ \text{ subject to:} \tag{4.5a}$$

$$J(\hat{u},\hat{x}_0) = \int_0^\infty \left(\hat{x}'(I_N \otimes Q_1 + \mathscr{L} \otimes Q_2)\hat{x} + \hat{u}'(I_N \otimes R)\hat{u}\right) \mathrm{d}t, \tag{4.5b}$$

$$\dot{\hat{x}} = \hat{A}\hat{x} + \hat{B}\hat{u},\ \hat{x}(0) = \hat{x}_0, \tag{4.5c}$$

$$\hat{u} = (I_N \otimes K + M \otimes \Phi\tilde{K}_2)\hat{x}, \tag{4.5d}$$

$$M \in \mathscr{K}^N_{1,1}(\mathscr{G}), \tag{4.5e}$$

where K, M, Φ and $\tilde{K}_2$ are design parameters. In view of constraint (4.5e), matrix M determines the sparsity pattern of $\hat{u}$ in (4.5d) in line with the particular structure of graph $\mathscr{G}$. Here, we assume that matrix M is selected prior to problem (4.5) execution. A specific choice of M is defined later in the section.

In order for problem (4.5) to be feasible with a stabilizing solution $\hat{u}$ and finite performance index $J(\hat{x}_0)$, we require the following; $(A,\ B)$ is controllable, $(A,\ C_1)$ and $(A,\ C_2)$ are observable for any matrix C_1 and C_2, respectively, such that $C_1'C_1 = Q_1 = Q_1' \geq 0$ and $C_2'C_2 = Q_2 = Q_2' \geq 0$. We also assume that $R = R' > 0$.

We note that if we set $M = \mathscr{L}$ and $\tilde{K}_2 = K$, then problem (4.5) is identical to (3.96). Similarly, if $\Phi = I_m$, then the state-feedback gain $I_N \otimes K + M \otimes \Phi\tilde{K}_2$ in (4.5d) can be constructed as in (3.84) as shown in Theorem 3.3.14. Our interest here is to construct and propose a new stabilizing distributed solution to problem (4.5) borrowing techniques from both methods (top-down, bottom-up) presented in the previous chapter. Our approach follows a two-step optimization procedure which is outlined below.

In the first step of our method, we define the state-feedback gains K, $\tilde{K}_2$ by solving LQR problem (3.65) for $N_L = d_{\max} + 1$ systems with $\tilde{A} = I_{N_L} \otimes A$, $\tilde{B} = I_{N_L} \otimes B$, and weights $Q_{ii} = Q_1$ for $i = 1,\ldots,N_L$, $Q_{ij} = Q_2$ for $i,j = 1,\ldots,N_L$ with $j \neq i$, and $\tilde{R} = I_{N_L} \otimes R$. In view of Theorem 3.3.11, we compute P and $\tilde{P}_2$ from (3.71) and (3.72), respectively, and then we define $K = -R^{-1}B'P$ and $\tilde{K}_2 = R^{-1}B'\tilde{P}_2$. At this stage, a suboptimal distributed state-feedback controller may be constructed as in (3.84) of Theorem 3.3.14, that is,

$$\hat{u} = (I_N \otimes K + M \otimes \tilde{K}_2)\hat{x}, \tag{4.6}$$

provided the spectrum of the design matrix $M \in \mathbb{R}^{N\times N}$ satisfies property (3.83). Without loss of generality, let $M = a\mathscr{L}$ with $a > 0$. As mentioned in Section 3.3.5, we can always chose a scalar $a > 0$ such that $\hat{u}$ in (4.6) stabilizes the differential equation (4.5c). Since the choice of $M = a\mathscr{L}$ is either at the designer's discretion or imposed by the problem itself, it makes

sense to formulate a second-stage optimization problem that takes into account this particular choice of M. In essence, this second stage involves the procedure of finding matrix Φ in (4.5d). Before formulating the new optimization problem, some technical manipulations of the model need to be considered. These are outlined next.

Let $\tilde{P}_2$, defined earlier as solution to ARE (3.72), be partitioned as:

$$\tilde{P}_2 = \begin{bmatrix} \tilde{P}_{2,11} & \tilde{P}_{2,12} \\ \tilde{P}'_{2,12} & \tilde{P}_{2,22} \end{bmatrix}, \tag{4.7}$$

where $\tilde{P}_{2,11} \in \mathbb{R}^{(n-m)\times(n-m)}$, $\tilde{P}_{2,22} \in \mathbb{R}^{m\times m}$ with $\det \tilde{P}_{2,22} \neq 0$ since matrix $\tilde{P}_2$ is symmetric and nonsingular. Letting

$$T = \begin{bmatrix} I_{(n-m)} & 0 \\ \tilde{P}^{-1}_{2,22}\tilde{P}'_{2,12} & I_m \end{bmatrix}, \tag{4.8}$$

define matrices $(A,\ B,\ K,\ \tilde{K}_2,\ P,\ \tilde{P}_2,\ Q_1,\ Q_2)$ in the new coordinate system $(\bar{x} = Tx)$ as follows:

$$\bar{x} = Tx, \tag{4.9}$$
$$\bar{A} = TAT^{-1}, \tag{4.10}$$
$$\bar{B} = TB, \tag{4.11}$$
$$\bar{K} = KT^{-1}, \tag{4.12}$$
$$\bar{K}_2 = \tilde{K}_2 T^{-1}, \tag{4.13}$$
$$\bar{P} = (T^{-1})'PT^{-1}, \tag{4.14}$$
$$\bar{P}_2 = (T^{-1})'\tilde{P}_2 T^{-1}, \tag{4.15}$$
$$\bar{Q}_1 = (T^{-1})'Q_1 T^{-1}, \tag{4.16}$$
$$\bar{Q}_2 = (T^{-1})'Q_2 T^{-1}. \tag{4.17}$$

Computing

$$T^{-1} = \begin{bmatrix} I_{(n-m)} & 0 \\ -\tilde{P}^{-1}_{2,22}\tilde{P}'_{2,12} & I_m \end{bmatrix}, \tag{4.18}$$

in the new coordinates it can be easily verified that

$$\bar{P}_2 = \begin{bmatrix} \tilde{P}_{2,11} - \tilde{P}_{2,12}\tilde{P}^{-1}_{2,22}\tilde{P}'_{2,12} & 0 \\ 0 & \tilde{P}_{2,22} \end{bmatrix}, \tag{4.19}$$

and

$$\bar{K}_2 = \begin{bmatrix} 0 & K_2 \end{bmatrix}, \tag{4.20}$$

where $K_2 \in \mathbb{R}^{m\times m}$ and $\det K_2 \neq 0$. Note that, this special structure follows easily from $\bar{K}_2 = -R^{-1}B'\bar{P}_2$ since $\bar{P}_2$ is block-diagonal and $\bar{B} = TB = B$ is invariant in the new coordinates.

Let now the collective state-space form

$$\dot{Z} = (I_N \otimes \bar{A})Z + (I_N \otimes \bar{B})\hat{u},\ Z(0) = Z_0, \tag{4.21}$$

with $Z = (I_N \otimes T)\hat{x}$, describe the dynamics of the network in the transformed coordinates. In the new coordinate system the performance index in (4.5b) and the control law in (4.5d) can be written as

$$J(\cdot) = \int_0^\infty \left(Z'(I_N \otimes \bar{Q}_1 + \mathscr{L} \otimes \bar{Q}_2)Z + \hat{u}'\hat{R}\hat{u}\right) \mathrm{d}t, \tag{4.22}$$

$$\hat{u} = (I_N \otimes \bar{K} + a\mathscr{L} \otimes (\Phi\bar{K}_2))Z, \tag{4.23}$$

respectively. Note that we have made the choice of $M = a\mathscr{L}$. Since $a > 0$ is a scalar, it may be absorbed in the design matrix Φ. Finally, we may write

$$\hat{u} = (I_N \otimes \bar{K} + \mathscr{L} \otimes (\Phi\bar{K}_2))Z. \tag{4.24}$$

Substituting (4.24) into (4.21),the closed-loop system (in the new coordinates) at network level is written as

$$\dot{Z} = \left(I_N \otimes (\bar{A} + \bar{B}\bar{K}) + \mathscr{L} \otimes (\bar{B}\Phi\bar{K}_2)\right) Z,\ Z(0) = Z_0. \tag{4.25}$$

The subsequent analysis is concerned with the formulation of a convex optimization problem as stated in Section 3.3.6.

Let $\mathscr{L} = V\Lambda V'$ be the spectral decomposition of the Laplacian matrix $\mathscr{L}$ where $V \in \mathbb{R}^{N\times N}$ is an orthogonal matrix composed of the eigenvectors of $\mathscr{L}$, and $\Lambda = \mathrm{diag}(\lambda_1, \ldots, \lambda_N)$ where $\lambda_i \in S(\mathscr{L})$, $i = 1, \ldots, N$. Defining now a new state-space transformation as

$$\hat{\xi} = (V' \otimes I_n)Z, \tag{4.26}$$

the augmented state-space form (at network level) in these coordinates becomes

$$\dot{\hat{\xi}} = \left(I_N \otimes (\bar{A} + \bar{B}\bar{K}) + \Lambda \otimes (\bar{B}\Phi\bar{K}_2)\right) \hat{\xi},\ \hat{\xi}(0) = \hat{\xi}_0. \tag{4.27}$$

Clearly, the weighting matrix $I_N \otimes \bar{Q}_1 + \mathscr{L} \otimes \bar{Q}_2$ in (4.22) is mapped to

$$(V' \otimes I_n)(I_N \otimes \bar{Q}_1 + \mathscr{L} \otimes \bar{Q}_2)(V \otimes I_n) = I_N \otimes \bar{Q}_1 + \Lambda \otimes \bar{Q}_2, \tag{4.28}$$

while using (4.28), the performance index (4.22) can be written as

$$J(\cdot) = \int_0^\infty \left(\hat{\xi}'(I_N \otimes Q_1 + \Lambda \otimes Q_2)\hat{\xi} + \hat{u}'(I_N \otimes R)\hat{u} \right) \mathrm{d}t. \tag{4.29}$$

Letting $[\xi_1', \ldots, \xi_N']' \triangleq \hat{\xi}$, since matrix Λ is diagonal, the closed-loop (4.27) can be decomposed into N node-level state-space equations:

$$\dot{\xi}_i = (\bar{A} + \bar{B}\bar{K} + \lambda_i \bar{B}\Phi\bar{K}_2)\xi_i,\ \xi_{i,0} = \xi_i(0),\ i = 1, \ldots, N. \tag{4.30}$$

Similarly, the performance index (4.29) can be reduced to:

$$J(\cdot) = \sum_{i=1}^{N} \int_0^\infty \left(\xi_i'(Q_1 + \lambda_i Q_2)\xi_i + u_i' R u_i \right) \mathrm{d}t. \tag{4.31}$$

For each decoupled node-level system in (4.30), consider a quadratic Lyapunov function $V_i = \xi_i' P_i \xi_i$ where P_i has the following structure:

$$P_i = \begin{bmatrix} P_{i,1} & 0 \\ 0 & \Pi_2 \end{bmatrix} > 0. \tag{4.32}$$

Here, $P_{i,1} \in \mathbb{R}^{(n-m)\times(n-m)}$, $\Pi_2 \in \mathbb{R}^{m\times m}$ are assumed to be symmetric positive definite matrices. Note that Π_2 is taken identical for all $i = 1, \ldots, N$. Then, the second-stage optimization problem is formulated as follows.

$$\min \sum_{i=1}^{N} \mathrm{trace}(P_i) \text{ subject to:} \tag{4.33a}$$

$$\begin{aligned} &P_i(\bar{A} + \bar{B}\bar{K} + \lambda_i \bar{B}\Phi\bar{K}_2) + (\bar{A} + \bar{B}\bar{K} + \lambda_i \bar{B}\Phi\bar{K}_2)' P_i + (\bar{Q}_1 + \lambda_i \bar{Q}_2) \\ &\qquad + (\bar{K} + \lambda_i \Phi\bar{K}_2)' R (\bar{K} + \lambda_i \Phi\bar{K}_2) < 0,\ i = 1, \ldots, N, \end{aligned} \tag{4.33b}$$

$$P_i > 0,\ i = 1, \ldots, N. \tag{4.33c}$$

For an initial state $\hat{\xi}_0$ uniformly distributed on the surface of the n-dimensional unit sphere, the optimum performance index $J^*(\cdot)$ (4.5) satisfies [20, 46]:

$$J^*(\cdot) \leq \sum_i^N \text{trace}(P_i). \tag{4.34}$$

Consequently, the optimization problem (4.33) represents the minimization of an upper bound of the global LQR criterion. We remark that the problem (4.33) differs from (3.110) in the definition of $\tilde{K}_2$ as shown in (4.5d) only. In (3.110) this gain matrix was taken identical to K. However, in this new method, it has been shown that $\tilde{K}_2$ may also be constructed via the top-down technique (cf. Section 3.3.5) as $\tilde{K}_2 = R^{-1}B'\tilde{P}_2$, where the symmetric negative definite matrix $\tilde{P}_2$ is associated with ARE (3.72) while the latter is associated with LQR problem (3.65) of N_L systems as shown in Section 3.3.3 (cf. Theorem 3.3.11). Regarding problem (4.5) we also note the following:

1) The block diagonal structure of P_i in (4.32) introduces conservatism in the solution. This special structure is chosen to impose a convex representation of the optimization problem which is constructed in the following paragraph.

2) Setting $\Phi = 0$, $P_i = P$ is a feasible solution to (4.33), where P is derived from (3.71). Alternatively, setting $\Phi = aI_m$ for $a > 0$ such that $\hat{u}$ in (4.23) is stabilizing, a symmetric positive definite matrix P_i can be obtained by solving the Lyapunov equation:

$$\begin{aligned} P_i(\bar{A} + \bar{B}\bar{K} + a\lambda_i\bar{B}\bar{K}_2) + (\bar{A} + \bar{B}\bar{K} + a\lambda_i\bar{B}\bar{K}_2)'P_i + (\bar{Q}_1 + \lambda_i\bar{Q}_2) \\ + (\bar{K} + a\lambda_i\bar{K}_2)'R(\bar{K} + a\lambda_i\bar{K}_2) = 0, \end{aligned} \tag{4.35}$$

   for $i = 1, \ldots, N$. Thus, the optimization problem is guaranteed to have a non-trivial solution.

3) The state-space transformation (4.8) diagonalizes matrix $\tilde{P}_2$ and hence, in the transformed coordinates, gain matrix $\bar{K}_2$ in (4.5) has the particular structure (4.20). This will ensure a closed form for deriving matrix Φ as long as the optimization problem (4.5) is feasible.

4) $\hat{u}$ in (4.5d) is a distributed state-feedback controller since $M = a\mathscr{L} \in \mathscr{K}_{1,1}^N(\mathscr{G})$. It is also stabilizing if the optimization problem (4.33) is feasible.

5) The matrix inequality constraints in (4.33) grow in number with the number of subsystems constituting the network.

We now develop a convex formulation of the optimization problem (4.5) which has also been proposed in [46].

We define matrix

$$W_i \triangleq P_i^{-1} = \begin{bmatrix} W_{i,1} & 0 \\ 0 & \bar{W}_2 \end{bmatrix}. \tag{4.36}$$

From (4.32), clearly, $W_{i,1} = P_{i,1}^{-1}$ and $\bar{W}_2 = \Pi_2^{-1}$. Pre-multiplying and post-multiplying (4.33b) by W_i gives

$$\begin{aligned}(\bar{A}+\bar{B}\bar{K}+\lambda_i\bar{B}\Phi\bar{K}_2)W_i + W_i(\bar{A}+\bar{B}\bar{K}+\lambda_i\bar{B}\Phi\bar{K}_2)' + W_i(\bar{Q}_1+\lambda_i\bar{Q}_2)W_i \\ + W_i(\bar{K}+\lambda_i\Phi\bar{K}_2)'R(\bar{K}+\lambda_i\Phi\bar{K}_2)W_i < 0,\end{aligned} \tag{4.37}$$

for $i = 1,\ldots,N$. Clearly, since $W_i = W_i' > 0$, the negative definiteness of (4.33b) is consistent with (4.37). In view of the structure of $\bar{K}_2 = [0\ K_2]$ and $W_i = \mathrm{diag}(W_{i,1}, \bar{W}_2)$, the product

$$\Phi\bar{K}_2W_i = \begin{bmatrix} 0 & \Phi K_2\bar{W}_2 \end{bmatrix}, \tag{4.38}$$

in (4.37) may be written as a new variable defined as

$$\bar{Y} = \begin{bmatrix} 0 & Y_2 \end{bmatrix}, \tag{4.39}$$

with

$$Y_2 = \Phi K_2\bar{W}_2. \tag{4.40}$$

Provided that a particular value is assigned to matrix $\bar{Y}$, (4.40) represents a closed-form for Φ since, by definition, K_2 and $\bar{W}_2$ are nonsingular matrices.

Viewing (4.37), this is a quadratic matrix inequality in variable W_i, $i = 1,\ldots,N$, and hence convexity cannot clearly be concluded. In order to show that (4.37) is convex in W_i, we convert this representation into a linear matrix inequality (LMI) using the Schur complement condition [20] for positive definite matrices which is stated next.

Proposition 4.2.2. *Let $X = X' > 0$ be partitioned as*

$$X = \begin{bmatrix} X_{11} & X_{12} \\ X_{12}' & X_{22} \end{bmatrix} > 0. \tag{4.41}$$

Then, the Schur complement of block X_{22} of matrix X is defined as $X/X_{22} \triangleq X_{11} - X_{12}X_{22}^{-1}X_{12}'$ and is a positive definite matrix, i.e., $X_{11} - X_{12}X_{22}^{-1}X_{12}' > 0$.

Define now matrices

$$\Omega_i = \begin{bmatrix} -\Psi_i & W_i(\bar{Q}_1 + \lambda_i \bar{Q}_2)^{\frac{1}{2}} \\ (\bar{Q}_1 + \lambda_i \bar{Q}_2)^{\frac{1}{2}} W_i & I_n \end{bmatrix}, \tag{4.42}$$

$$H_i = \begin{bmatrix} (\lambda_i \bar{Y} + \bar{K} W_i)' \\ 0_{n\times m} \end{bmatrix}, \tag{4.43}$$

where $\Psi_i = (\bar{A} + \bar{B}\bar{K})W_i + \lambda_i \bar{B}\bar{Y} + W_i(\bar{A} + \bar{B}\bar{K})' + \lambda_i \bar{Y}'\bar{B}'$, $i = 1, \ldots, N$. Then, the quadratic matrix inequality (4.37) is expressed as Schur complement of the block $\mathrm{diag}(I_n, R^{-1}) > 0$ of the LMI

$$\begin{bmatrix} \Omega_i & H_i \\ H_i' & R^{-1} \end{bmatrix} > 0, \tag{4.44}$$

for $i = 1, \ldots, N$. Obviously, (4.44) is linear and convex in both variables W_i, $\bar{Y}$, and proves the convexity of (4.37) in W_i, $i = 1, \ldots, N$. After we have completed the convex representation of (4.33), we introduce the following symmetric positive definite matrices:

$$Z_i \triangleq \begin{bmatrix} Z_{i,1} & 0 \\ 0 & \bar{Z}_2 \end{bmatrix}, \tag{4.45}$$

with $Z_{i,1} \in \mathbb{R}^{(n-m)\times(n-m)}$ and $\bar{Z}_2 \in \mathbb{R}^{m\times m}$, for $i = 1, \ldots, N$. Then minimizing $\sum_{i=1}^{N} \mathrm{trace}(Z_i)$ subject to

$$\begin{bmatrix} Z_i & -I_n \\ -I_n & W_i \end{bmatrix} > 0, \tag{4.46}$$

and (4.44), for $i = 1, \ldots, N$, is equivalent to minimizing

$$\sum_{i=1}^{N} \mathrm{trace}(W_i^{-1}) = \sum_{i=1}^{N} \mathrm{trace}(P_i), \tag{4.47}$$

subject to (4.44), for $i = 1, \ldots, N$.

Finally, the optimization problem (4.33) can now be re-formulated as

$$\min_{W_i>0, \bar{Y}, Z_i>0} \sum_{i=1}^{N} \mathrm{trace}(Z_i) \text{ subject to } (4.44) - (4.46). \tag{4.48}$$

This is a convex optimization problem, linear in W_i, $\bar{Y}$ and Z_i, with linear matrix inequality constraints, and can be solved by a standard LMI solver. If (4.48) is feasible, then matrix Φ can be designed as $\Phi = Y_2 \bar{W}_2^{-1} K_2^{-1}$. This completes the second stage of the control design.

In this section, a new method for designing distributed state-feedback controllers for solving problem (4.5) has been proposed. In summary, the design approach is based on a two-stage optimization procedure where a centralized state-feedback controller is initially obtained from an LQR problem of $d_{\max}+1$ systems, $d_{\max}$ denoting the maximum vertex degree of the graph, and subsequently, a stabilizing distributed control scheme is constructed by minimizing an upper bound of the global LQR criterion. So far, only networks with undirected topology have been considered. In the following section, we remove the restrictive requirement of the two-way agent-to-agent interaction and attempt to generalize the top-down [17] and bottom-up [46] distributed control design techniques in this direction via a systematic approach.

4.3 Networks with directed topology

In this section, we focus on networks with directed topology. Our main objective is to show that the two powerful methods (top-down, bottom-up), presented in Chapter 3, can also be used for solving regulation problems of multi-agent networks with oriented interconnection topology. The relaxation of the two-way connectivity assumption considered in the original studies [17, 46], represents the main result of this chapter. Extension of the method proposed in Section 4.2, follows straightforwardly and is omitted. In the subsequent analysis, we use a graph representation to model coupling terms in local control actions and communication between neighboring agents. The special class of directed graphs is considered. In the sequel, these are referred to as digraphs. Redefining the notion of the adjacency, degree and Laplacian matrices of digraphs, we show that the stability of the distributed control scheme derived either from the top-down or the bottom-up technique, can effectively be identified by the spectrum of a block diagonal matrix. Next, we collect the main definitions and properties of digraphs.

4.3.1 Directed graphs, digraphs

Let $\mathscr{D}=(\mathscr{V},\mathscr{E})$ represent a digraph of N vertices with $i\in\mathscr{V}$, $i=1,\ldots,N$, denoting the index of each vertex, and $(i,j)\in\mathscr{E}$, $i,j=1,\ldots,N$ with $j\neq i$, denoting the edge between vertex i and j. In contrast to undirected graphs, every edge $(i,j)\in\mathscr{E}$ represents an ordered pair and can be seen as an arrow with i being its head and j its tail. This orientation assigns a direction to edges and can be described by a function in the following sense; let $f:\mathscr{E}\rightarrow\{-1,1\}$, with $f(i,j)=-f(j,i)$. Then, an edge (i,j) originates in j (tail) and terminates in i (head) if $f(i,j)=1$ otherwise $f(j,i)=-1$. It will be shown that this edge orientation choice will

facilitate the modelling of the information flow between agents. For instance, an edge (i, j) pointing from j to i implies that the i-th node is receiving information from node j. It also explains the semantics of the choice of the vertex in-degree instead of vertex degree. This is defined next.

For a digraph $\mathscr{D} = (\mathscr{V}, \mathscr{E})$ of N vertices we define the in-degree d_j of the j-th vertex as the number of edges terminating in j. Let $d_{\max}(\mathscr{D})$ denote the maximum vertex in-degree of $\mathscr{D}$. We denote by $\mathscr{A}(\mathscr{D})$ the $(0,1)$ adjacency matrix of the digraph $\mathscr{D}$. In particular, the (i, j)-th element of $\mathscr{A}$, $A_{ij} = 1$ if the ordered pair $(i, j) \in \mathscr{E}$ $\forall$ $i, j = 1, \ldots, N$, $i \neq j$ and zero otherwise. Clearly, the adjacency matrix $\mathscr{A}(\mathscr{D})$ of digraphs is not necessarily symmetric. Let $j \in \mathscr{N}_i$ if $(i, j) \in \mathscr{E}$ and $i \neq j$. Note here that (i, j) is an ordered pair and denotes an oriented edge starting from vertex j and terminating in vertex i. We call $\mathscr{N}_i$ the in-degree neighborhood (or just neighborhood) of vertex i. We define the in-degree Laplacian (or just Laplacian) matrix as $\mathscr{L}(\mathscr{D}) = D(\mathscr{D}) - \mathscr{A}(\mathscr{D})$, where $D(\mathscr{D})$ is the diagonal matrix of vertex in-degrees d_i. In contrast to undirected graphs, the Laplacian matrix of digraphs is generically non-symmetric.

We note here that our choice of in-degree to define the degree matrix $D(\mathscr{D})$ and the Laplacian matrix $\mathscr{L}(\mathscr{D})$ is primarily motivated by the way these matrices will be used in the network control design. As already seen from the previous analysis, carried out on undirected networks, the control action of each subsystem is a function of the local state as well as the states from adjacent subsystems. In other words, each agent, representing a distinct subsystem of the network, in order to construct its control signal, apart from its own state, requires also neighboring states be communicated to itself. Clearly, the choice of the out-degree version of the Laplacian matrix, which captures in essence how each node influences other nodes, would not accommodate the design of a distributed control scheme.

By construction, for every digraph $\mathscr{D}$ with associated in-degree Laplacian matrix $\mathscr{L}(\mathscr{D})$, it follows that

$$q \in \mathscr{N}(\mathscr{L}(\mathscr{D})), \tag{4.49}$$

where $q = [1\ 1\ \cdots\ 1]'$, and $\mathscr{N}(\cdot)$ denotes the null space of a matrix. This means that the Laplacian matrix $\mathscr{L}$ has at least one eigenvalue at the origin. Next, we indicate conditions which link the multiplicity of the zero eigenvalue of $\mathscr{L}$ with the structure of the corresponding digraph. We introduce now the following definitions.

Definition 4.3.1. A directed path in a digraph is a sequence of vertices in which there is a (directed) edge pointing from each vertex to its successor in the sequence, with no repeated edges.

Definition 4.3.2. A digraph is strongly connected if between every pair of distinct vertices there is a directed path.

A digraph $\mathscr{D}$ is said to have been disoriented if all of its directed edges have been replaced by undirected ones.

Definition 4.3.3. A digraph is weakly connected if its disoriented version is connected.

Obviously, all strongly connected digraphs are automatically weakly connected. A directed tree of a digraph $\mathscr{D} = (\mathscr{V}, \mathscr{E})$ is a subgraph $\mathscr{D}' = (\mathscr{V}', \mathscr{E}')$ of $\mathscr{D}$ which contains a vertex $r \in \mathscr{V}'$ such that for every other $j \in \mathscr{V}'$ with $j \neq r$ there is a directed path form r to j. If $\mathscr{V}' \equiv \mathscr{V}$ then the directed tree $\mathscr{D}'$ is spanning. In the sequel, we focus on the class of digraphs which are weakly connected and contain at least a directed spanning tree. We refer to this class of digraphs as connected digraphs. The rank of Laplacian matrix $\mathscr{L}$ of a connected digraph $\mathscr{D}$ is identified in the following proposition [139].

Proposition 4.3.1. *A weakly connected digraph $\mathscr{D} = (\mathscr{V}, \mathscr{E})$ of N vertices contains a directed spanning tree as a subgraph if and only if* $\operatorname{rank}(\mathscr{L}) = N - 1$. *In this case, $\mathscr{N}(\mathscr{L})$ is spanned by the vector $q = [1\ 1\ \cdots\ 1]'$.*

Proof. It is equivalent to show that zero as the root of the characteristic polynomial of $\mathscr{L}$ has algebraic multiplicity of one. Let

$$p(\lambda) = \lambda^N + a_{N-1}\lambda^{N-1} + \cdots + a_1\lambda + a_0, \tag{4.50}$$

be the characteristic polynomial of $\mathscr{L}$. Note that $a_0 = 0$ since zero is an eigenvalue of $\mathscr{L}$. Thus,

$$\operatorname{rank}(\mathscr{L}) = N - 1, \tag{4.51}$$

if and only if $a_1 \neq 0$. The coefficient a_1 satisfies:

$$a_1 = \sum_u \det(\mathscr{L}_u), \tag{4.52}$$

where $\mathscr{L}_u$ is the matrix obtained by deleting the u-th row and the u-th column of $\mathscr{L}$. From matrix-tree theorem (Theorem 2.12 of [139]) we have

$$\det(\mathscr{L}_u) \neq 0, \tag{4.53}$$

if and only if there is a directed spanning tree in $\mathscr{D}$ starting from vertex u. Hence, $a_1 \neq 0$ if and only if there is a directed spanning tree originated in some $u \in \mathscr{V}$ and therefore the zero

eigenvalue has algebraic multiplicity of one. Since an eigenvalue with algebraic multiplicity of one also has geometric multiplicity of one [84], for a weakly connected digraph $\mathscr{D}$, it follows that $\mathscr{L}p = 0$ if and only if $p \in \text{span}(q)$, i.e., $\text{rank}(\mathscr{L}) = N-1$. □

As shown in Proposition 4.3.1, the connectedness of N vertices over digraph $\mathscr{D}$ is established by the rank of the corresponding (in-degree) Laplacian matrix $\mathscr{L}$. We recall that for N vertices over a connected graph, the associated Laplacian matrix has also rank of $N-1$. So far, the differences between undirected and directed graphs have been identified mainly in the definition of the set of edges as well as the adjacency, degree and Laplacian matrices, respectively. Unfortunately, elegant properties, especially due to the symmetry of the adjacency and Laplacian matrices of undirected graphs, do not hold for the in-degree version of the corresponding matrices of digraphs. In particular, the in-degree Laplacian $\mathscr{L}$ is not necessarily symmetric and as a result its non-zero eigenvalues may be complex with algebraic and geometric multiplicities not necessarily coinciding. However, they are always located in the right half-plane. This is highlighted in the following proposition.

Proposition 4.3.2. *Let $\mathscr{D}$ be a digraph of N vertices with associated in-degree Laplacian matrix $\mathscr{L}$. Then the spectrum of $\mathscr{L}$ lies in the complex region denoted by*

$$\{z \in \mathbb{C} |\ |z - d_{\max}| \leq d_{\max}\}, \tag{4.54}$$

where $d_{\max}$ denotes the maximum vertex in-degree of $\mathscr{D}$. In other words, for every digraph $\mathscr{D}$, the eigenvalues of $\mathscr{L}$ have non-negative real parts.

The proof follows straightforwardly from Geršgorin disk Theorem 3.3.4 and is omitted.

Next, we consider the spectral decomposition of a Laplacian matrix $\mathscr{L}$ associated with a connected digraph $\mathscr{D}$ of N vertices. We recall that due to the directed orientation of $\mathscr{D}$, matrix $\mathscr{L}$ is not necessarily symmetric, and hence, may not be perfectly diagonalizable. Let $J(\Lambda)$ denote the Jordan canonical form of a Laplacian matrix $\mathscr{L}$. This is a block diagonal matrix where each diagonal block denoted as $J(\lambda_j)$, is also a block diagonal matrix, i.e., $J(\Lambda) = \text{diag}(J(\lambda_1), \ldots, J(\lambda_p))$ with $J(\lambda_j) = \text{diag}(J_1(\lambda_j), \ldots, J_{d_j}(\lambda_j))$, $j = 1, \ldots, p$. Note that the full dimension of $J(\lambda_j)$ represents the algebraic multiplicity of λ_j while the number of different blocks (d_j) pertinent to λ_j denotes the geometric multiplicity of λ_j. Clearly, if $\mathscr{L}$ is perfectly diagonalizable, $p = N$. Note also that $J(0) = 0$ since $\mathscr{D}$ is assumed to be

connected. Matrix $J_k(\lambda_j)$ has an upper-triangular form as shown below:

$$J_k(\lambda_j) = \begin{bmatrix} \lambda_j & 1 & 0 & 0 & 0 \\ 0 & \lambda_j & 1 & 0 & 0 \\ 0 & 0 & \ddots & \ddots & 0 \\ 0 & 0 & 0 & \ddots & 1 \\ 0 & 0 & 0 & \cdots & \lambda_j \end{bmatrix}. \tag{4.55}$$

Scalar λ_j appearing on the main diagonal of $J_k(\lambda_j)$, can be either real or complex. Let now

$$\mathscr{L} = PJ(\Lambda)P^{-1}, \tag{4.56}$$

be the Jordan decomposition of $\mathscr{L}$. Detailed description for how to construct matrix P can be found in [84]. Since $\mathscr{D}$ is connected, implying that $\text{rank}(\mathscr{L}) = N-1$, a nonsingular matrix P can be chosen such that

$$J(\Lambda) = \begin{bmatrix} 0 & 0 & \dots & 0 \\ 0 & J(\lambda_2) & \dots & 0 \\ \vdots & \ddots & \ddots & \vdots \\ 0 & \dots & 0 & J(\lambda_p) \end{bmatrix}, \tag{4.57}$$

where $\mathbf{Re}(\lambda_j) > 0 \; \forall \; j = 2, \dots, p$. We denote by

$$\bar{S}(\mathscr{L}) = \{0, \lambda_2, \dots, \lambda_p\}, \tag{4.58}$$

with $\lambda_j \in S(\mathscr{L})$, $j = 2, \dots, p$, the set of distinct modes of $\mathscr{L}$ without considering algebraic multiplicities. We also define a diagonal matrix Λ associated with the spectrum of $\mathscr{L}$ as follows:

$$\Lambda = \text{diag}(0, \lambda_2, \dots, \lambda_p). \tag{4.59}$$

Clearly, $S(\Lambda) \equiv \bar{S}(\mathscr{L})$. Later in the chapter, matrix Λ will prove useful for establishing closed-loop stability of networks with directed topology. Now, before proceeding to the regulator problem, we consider a simple consensus problem of networks with undirected and directed topology.

4.3.2 Agreement protocol for agents with single-integrator dynamics

To give insight to the subsequent analysis, we consider the following motivating example. Let

$$\dot{x}_i = u_i,\ x_i(0) = x_{i,0},\ i = 1,\dots,N, \tag{4.60}$$

be the state-space forms of N agents with single-integrator dynamics. For simplicity, let x_i, u_i be scalar, with $i = 1,\dots,N$. Here, we wish to solve the rendezvous problem of N agents via agreement protocol

$$\dot{x} = -\mathscr{L}x,\ x(0) = x_0, \tag{4.61}$$

where $x = [x_1,\dots,x_N]'$, and $\mathscr{L}$ is the Laplacian matrix of the graph associated with the interactions between agents. We consider two interconnection schemes, namely, 1) a connected undirected graph $\mathscr{G}$, and 2) a connected digraph $\mathscr{D}$.

Connected graph: We recall that the Laplacian matrix of an undirected graph is a symmetric positive semi-definite matrix with $\mathscr{L}\mathbf{1} = 0$, where $\mathbf{1} = [1\ 1\ \cdots\ 1]'$. The zero eigenvalue (with associated eigenvector $\mathbf{1}$) has algebraic multiplicity of one if and only if the undirected graph contains at least one spanning tree, i.e., it is connected. Hence, for a connected undirected graph the solution of (4.61), initialized from x_0, is

$$x(t) = e^{-\mathscr{L}t}x_0, \tag{4.62}$$

which can be decomposed into

$$x(t) = e^{-\lambda_1 t}(v_1'x_0)v_1 + e^{-\lambda_2 t}(v_2'x_0)v_2 + \cdots + e^{-\lambda_N t}(v_N'x_0)v_N, \tag{4.63}$$

where v_i is the i-th eigenvector of $\mathscr{L}$ associated with eigenvalue λ_i, $i = 1,\dots,N$, with $[v_1 \cdots v_N]$ forming a orthogonal matrix. Since $\lambda_i > 0$ for $i = 2,\dots,N$ and $\lambda_1 = 0$,

$$\lim_{t\to\infty} x(t) = (v_1'x_0)v_1 = \frac{\mathbf{1}'x_0}{N}\mathbf{1}, \tag{4.64}$$

where $v_1 \in \text{span}\{\mathbf{1}\}$ has been selected such that $v_1'v_1 = 1$. Therefore, the rendezvous problem of N agents interconnected over a connected undirected graph can be solved asymptotically under the Laplacian dynamics (4.61). The corresponding consensus value is the average of agents' initial states, i.e., $\frac{x_0'\mathbf{1}}{N}$.

Connected digraph: The (in-degree) Laplacian matrix of a digraph, is generically non-symmetric. Let $\mathscr{L} = PJ(\Lambda)P^{-1}$ be the Jordan decomposition of $\mathscr{L}$. Letting a digraph be

connected, a nonsingular matrix P can be chosen such that $J(\Lambda) = \text{diag}(0, J(\lambda_2), \ldots, J(\lambda_p))$, where $\mathbf{Re}(\lambda_j) > 0 \; \forall \; j = 2, \ldots, p$, and $J(\lambda_j)$ is a block-diagonal matrix formed of as many blocks as the geometric multiplicity of λ_j, i.e., $J(\lambda_i) = \text{diag}(J_1(\lambda_j), \ldots, J_{d_j}(\lambda_j))$ where d_j is the geometric multiplicity of λ_j. Now, from $\mathscr{L}P = PJ(\Lambda)$, we denote the first column of matrix P as p_1, which represents the right eigenvector associated with the zero eigenvalue of $\mathscr{L}$, that is, $\mathscr{L}p_1 = 0$. By definition of the in-degree Laplacian matrix, the latter implies that p_1 belongs to span$\{\mathbf{1}\}$. Similarly, from $P^{-1}\mathscr{L} = J(\Lambda)P^{-1}$, we denote the first row of P^{-1} as q_1', which represents the left eigenvector of $\mathscr{L}$ associated with the zero eigenvalue. Clearly, $p_1, \; q_1 \in \mathbb{R}^N$. Since, $PP^{-1} = I$, it follows that $p_1'q_1 = 1$. We may write

$$e^{-\mathscr{L}t} = P \begin{bmatrix} e^0 & 0 & \cdots & 0 \\ 0 & e^{J(-\lambda_2)t} & \cdots & 0 \\ \vdots & \vdots & \ddots & \vdots \\ 0 & 0 & \cdots & e^{J(-\lambda_p)t} \end{bmatrix} P^{-1}, \tag{4.65}$$

where $\lim_{t\to\infty} e^{-J(\lambda_j)t} = 0 \; \forall \; j = 2, \ldots, p$, since $\mathbf{Re}(\lambda_j) > 0$ for $j = 2, \ldots, p$. Thus, setting $p_1 = \mathbf{1}$ and letting $p_1'q_1 = 1$, the solution to (4.61), initialized from x_0, is:

$$\lim_{t\to\infty} x(t) = (q_1'x_0)\mathbf{1}. \tag{4.66}$$

From (4.66), it turns out that the consensus value obtained from the agreement protocol $-\mathscr{L}x$ does not necessarily converge to the average value of agents' initial states and generically differs from $\frac{\mathbf{1}'x_0}{N}\mathbf{1}$ for a directed topology.

In the following, the distributed control design method proposed in Section 4.2 is extended to networks with directed topology.

4.3.3 Regulator problem of directed networks

In this section, we turn our attention to a regulation problem pertaining to networked systems with directed interconnection topology. Specifically, focusing on the optimal control problem (4.5), we consider the following alterations.

Let

$$\dot{x}_i = Ax_i + Bu_i, \; x_i(0) = x_{i,0}, \; i = 1, \ldots, N, \tag{4.67}$$

be the state-space forms of N systems representing the dynamics of N autonomous agents which have the ability to exchange state-information with one another. Vectors $x_i \in \mathbb{R}^n$, $u_i \in \mathbb{R}^m$ represent the states and inputs of agent-i, respectively. Let also $\mathscr{D} = (\mathscr{V}, \mathscr{E})$ be a connected digraph of N nodes modelling the interaction scheme of the N agents. Clearly,

agent-i is associated with node-i. We denote by $\mathscr{L}$ the (in-degree) Laplacian matrix associated with $\mathscr{D}$. Constructing the aggregate state- and input-vector as $\hat{x} = \text{Col}(x_1, \ldots, x_N) \in \mathbb{R}^{nN}$ and $\hat{u} = \text{Col}(u_1, \ldots, u_N) \in \mathbb{R}^{mN}$, respectively, we write the collective state-space of the directed network as:

$$\dot{\hat{x}} = \hat{A}\hat{x} + \hat{B}\hat{u},\ \hat{x}(0) = \hat{x}_0, \tag{4.68}$$

where

$$\hat{A} = I_N \otimes A,\ \hat{B} = I_N \otimes B, \tag{4.69}$$

and we formulate the following optimization problem:

$$\min_{\hat{u}} J(\hat{u}, \hat{x}_0) \ \text{ subject to:} \tag{4.70a}$$

$$J(\hat{u}, \hat{x}_0) = \int_0^\infty \left(\hat{x}'(I_N \otimes Q_1 + \mathscr{L}_c \otimes Q_2)\hat{x} + \hat{u}'(I_N \otimes R)\hat{u}\right) \text{dt}, \tag{4.70b}$$

$$\dot{\hat{x}} = \hat{A}\hat{x} + \hat{B}\hat{u},\ \hat{x}(0) = \hat{x}_0, \tag{4.70c}$$

$$\hat{u} = (I_N \otimes K_1 + M \otimes K_2)\hat{x}, \tag{4.70d}$$

$$M \in \mathscr{K}^N_{1,1}(\mathscr{D}), \tag{4.70e}$$

with $Q_1 = Q_1' \geq 0$, $Q_2 = Q_2' \geq 0$ and $R = R' > 0$. Matrices $M \in \mathbb{R}^{N\times N}$, $K \in \mathbb{R}^{m\times n}$ and $K_2 \in \mathbb{R}^{m\times n}$ are design parameters. We note that $\mathscr{L}_c$ in (4.70b) is a symmetric matrix. The off-diagonal entries of $\mathscr{L}_c$ are constructed as follows:

$$\mathscr{L}_c(i,j) = \begin{cases} -1 & \text{if } \mathscr{L}(i,j) = -1 \text{ or } \mathscr{L}(j,i) = -1, \text{ for } i \neq j, \\ 0 & \text{if } \mathscr{L}(i,j) = \mathscr{L}(j,i) = 0, \text{ for } i \neq j, \end{cases} \tag{4.71}$$

while the diagonal entries of $\mathscr{L}_c$ are given by

$$\mathscr{L}_c(i,i) = -\sum_{\substack{p=1 \\ p\neq i}}^{N} \mathscr{L}_c(i,p),\ \text{for } i = 1, \ldots, N. \tag{4.72}$$

This choice of $\mathscr{L}_c$ guarantees that $\hat{Q} = I_N \otimes Q_1 + \mathscr{L}_c \otimes Q_2$ is a symmetric positive semidefinite matrix, and $J(\hat{u}, \hat{x}_0)$ in (4.70b) is well-defined.

Our objective is to design a stabilizing control law $\hat{u}$ with structure as in (4.70d). The two methods (top-down, bottom-up) presented in Chapter 3 are utilized here for constructing matrices K_1, M and K_2, indicating that these design techniques can effectively be used for regulating networks in the setting of problem 4.70.

Before presenting the first method, we consider the following closed-loop state-space form:

$$\dot{\hat{x}} = (I_N \otimes (A + BK_1) + M \otimes (BK_2))\hat{x}, \tag{4.73}$$

which arises by substituting $\hat{u}$ as given in (4.70d) into (4.68). We also write the closed-loop matrix:

$$A_{cl} = I_N \otimes (A + BK_1) + M \otimes (BK_2), \tag{4.74}$$

the inertia of which determines the stability of the closed-loop system. Without loss of generality let $M = \mathscr{L}$. Let also matrix $P \in \mathbb{R}^{N\times N}$ be an invertible matrix such that

$$\mathscr{L} = PJ(\Lambda)P^{-1}, \tag{4.75}$$

where $J(\Lambda)$ denotes a Jordan matrix with structure as shown in (4.57). Considering now a new coordinate system $\hat{\xi} = \hat{T}\hat{x}$ where $\hat{T} = P^{-1} \otimes I_n$, matrix

$$\hat{A}_{cl} = \hat{T}A_{cl}\hat{T}^{-1} = I_N \otimes (A + BK_1) + J(\Lambda) \otimes BK_2, \tag{4.76}$$

is clearly similar to matrix A_{cl}, thereby having identical eigenvalues. Note that $\hat{A}_{cl} \in \mathbb{C}^{nN\times nN}$ is a block diagonal matrix and hence its inertia is determined by the diagonal blocks. We denote as

$$\hat{A}_{cl,jj} = I_{k_j} \otimes (A + BK_1) + J(\lambda_j) \otimes BK_2, \tag{4.77}$$

the j-th diagonal block of $\hat{A}_{cl}$ associated with the j-th Laplacian mode $\lambda_j \in S(\mathscr{L})$ with algebraic multiplicity of k_j for $j = 1,\ldots,p$. Due to its block upper-triangular form, matrix $\hat{A}_{cl,jj}$ is Hurwitz if and only if matrix

$$\hat{A}_{cl,\lambda_j} = A + BK_1 + \lambda_j BK_2, \tag{4.78}$$

with $j = 1,\ldots,p$. In other words, closed-loop matrix A_{cl} in (4.74) is Hurwitz if and only if matrix

$$\hat{A}_{cl,\Lambda} = I_p \otimes (A + BK_1) + \Lambda \otimes BK_2, \tag{4.79}$$

is Hurwitz, where $\Lambda = \mathrm{diag}(0, \lambda_2, \ldots, \lambda_p)$. This result is stated in the following proposition.

Proposition 4.3.3. *Let matrix*

$$\tilde{A} = I_N \otimes A_1 + C \otimes A_2, \tag{4.80}$$

where $A_1 \in \mathbb{R}^{n\times n}$, $A_2 \in \mathbb{R}^{n\times n}$ and $C \in \mathbb{R}^{N\times N}$. Let also $(\lambda_1,\ldots,\lambda_p) \in S(C)$ be the distinct eigenvalues of matrix C without considering algebraic multiplicities. Then, matrix $\tilde{A}$ is

Hurwitz if and only if matrix

$$\tilde{A}_j = A_1 + \lambda_j A_2, \tag{4.81}$$

is Hurwitz $\forall\ j = 1, \ldots, p$.

The proof is omitted since it follows straightforwardly from the previous arguments. The main conclusions of this paragraph are now highlighted as follows.

1) The algebraic multiplicities of the eigenvalues of matrix M along with its potentially non-simple structure may be neglected for stability analysis of the closed-loop system (4.73).

2) Designing K_1, K_2 as suggested in the top-down method, closed-loop stability can be guaranteed via the robustness properties of LQR control.

3) Due to the structure of matrix $A_{cl,\Lambda}$ in (4.79), sufficient conditions for closed-loop stability can be formulated via Lyapunov inequalities as suggested in the bottom-up distributed control design approach.

Two different approaches to designing matrices K_1, K_2 and M are proposed in the following sections, illustrating the interesting implications mentioned above.

4.3.4 Top-down design for directed networks

As described in Section 3.3.5, for a multi-agent network with undirected topology, a distributed LQR-based controller can be constructed by solving a low dimension LQR problem (3.65) of $N_L = d_{\max} + 1$ subsystems, $d_{\max}$ denoting the maximum vertex degree of the corresponding graph. Then, stability of the overall distributed control system is established via the gain margin property of LQR control. Here, we build upon this method studying regulator problems of networked systems with directed topology. Our results primarily rely on two particular aspects, namely, 1) the simple structure of the low-dimension matrices (4.78), and 2) the complex-gain-margin property of LQR control stated in Theorem 3.2.8.

The method is generalized as follows. We solve an LQR problem (3.65) with weights $(Q_1,\ Q_2,\ R)$ for N_L systems. To avoid a trivial solution to (3.65), number N_L can be equal to $d_{\max} + 2$, $d_{\max}$ denoting the maximum vertex in-degree of the corresponding digraph. Then, the state-feedback gains K_1, K_2 are defined as follows:

$$K_1 = -R^{-1}B'P, \tag{4.82}$$

$$K_2 = R^{-1}B'\tilde{P}_2, \tag{4.83}$$

with P and $\tilde{P}_2$ being associated with ARE:

$$A'P + PA - PXP + Q_1 = 0, \tag{4.84}$$

$$(A - XP)'(-N_L\tilde{P}_2) + (-N_L\tilde{P}_2)(A - XP) - (-N_L\tilde{P}_2)X(-N_L\tilde{P}_2) + N_LQ_2 = 0, \tag{4.85}$$

respectively, where $X = BR^{-1}B'$. We recall that the expression (4.84) can be cast as an ARE associated with a node-level LQR problem with parameters $(A,\ B,\ Q_1,\ R)$, while the expression (4.85) can be seen as an ARE associated with an LQR problem with parameters $(A - BR^{-1}B'P,\ B,\ N_LQ_2,\ R)$. The following corollary follows from the stability of the two node-level LQR solutions pertinent to ARE (4.84) and ARE (4.85), respectively.

Corollary 4.3.1. *Matrix $A - BR^{-1}B'(P + \gamma N_L\tilde{P}_2)$ is Hurwitz for $\gamma = 0$ and $\gamma = 1$.*

From the robust stability property stated in Theorem 3.2.8, we also have the following result.

Corollary 4.3.2. *Matrix $A - BR^{-1}B'(P + \gamma N_L\tilde{P}_2)$ is Hurwitz $\forall \gamma \in \mathbb{C}$ such that $\boldsymbol{Re}(\gamma) > \frac{1}{2}$.*

The distributed control design (top-down) method for problem (4.70) is now summarized in the following theorem.

Theorem 4.3.4. *Consider LQR problem* (3.65) *with weights $(Q_1,\ Q_2,\ R)$ for $N_L = d_{\max} + 2$ systems. Define matrices P and $\tilde{P}_2$ from* (4.84) *and* (4.85)*, respectively. Define also $K_1 = -R^{-1}B'P$ and $K_2 = R^{-1}B'\tilde{P}_2$ and let $M \in \mathbb{R}^{N\times N}$ be a real matrix with the following property:*

$$\boldsymbol{Re}(\lambda_i) > \frac{N_L}{2},\ \forall\ \lambda_i \in S(M)\backslash\{0\}. \tag{4.86}$$

Then, constructing state-feedback gain:

$$\hat{K} = I_N \otimes K_1 + M \otimes K_2, \tag{4.87}$$

the closed-loop system

$$A_{cl} = I_N \otimes A + (I_N \otimes B)\hat{K}, \tag{4.88}$$

is asymptotically stable.

Proof. Consider closed-loop matrix A_{cl} which can be written as

$$A_{cl} = I_N \otimes (A + BK_1) + M \otimes BK_2. \tag{4.89}$$

From Proposition 4.3.3, matrix A_{cl} is Hurwitz if and only if

$$A_{cl,j} = A + BK_1 + \lambda_j BK_2, \tag{4.90}$$

is Hurwitz for all $\lambda_j \in S(M)$. If $\lambda_j = 0$, then, $A + BK_1$ is a Hurwitz matrix from Corollary 4.3.4. If $\lambda_j \neq 0$, then from Corollary 4.3.2 and condition (4.86) we conclude that matrix $A_{cl,j}$ is Hurwitz $\forall\ \lambda_j \in S(M)$. □

The main corollaries of Theorem 4.3.4 are listed below:

1) If $M \in \mathscr{K}^N_{m,n}(\mathscr{D})$, then $\hat{K}$ in (4.87) is a stabilizing distributed controller.

2) Closed-loop stability is irrespective of the LQR cost function tuning.

3) Stability can always be guaranteed with $M = a\mathscr{L}$ for

$$a > \frac{N_L}{2\mathbf{Re}(\lambda_2)}, \tag{4.91}$$

with $\lambda_2 \in S(\mathscr{L})$ denoting the non-zero eigenvalue of $\mathscr{L}$ with the smallest real part.

4.3.5 Bottom-up design for directed networks

Here, we propose a distributed control design for problem (4.70) using the bottom-up method presented in Section 3.3.6. The method requires input matrix

$$B = \begin{bmatrix} 0 \\ B_2 \end{bmatrix}, \tag{4.92}$$

where $\det B_2 \neq 0$. We recall that this structure of matrix B can always be attained considering a state-space transformation as suggested in Lemma 4.2.1. Setting, now,

$$K_1 = K, \tag{4.93}$$
$$K_2 = \Phi K, \tag{4.94}$$
$$M = \mathscr{L}, \tag{4.95}$$

in (4.70d), the distributed state-feedback control law $\hat{u}$ takes the following form:

$$\hat{u} = (I_N \otimes K + \mathscr{L} \otimes \Phi K)\hat{x}, \tag{4.96}$$

where $K = -R^{-1}B'P$ is derived from the solution of a node-level LQR problem with parameters $(A,\ B,\ Q_1,\ R)$, $\mathscr{L}$ is the (in-degree) Laplacian matrix of digraph $\mathscr{D}$, and Φ is the design matrix to be defined. We recall that in the original setup of the method, pertaining to networks with undirected topology, matrix Φ is computed by solving constrained optimization problem (3.110) the constraints of which represent sufficient conditions for closed-loop

stability. Therein, the formulation of these conditions relies on two simplifying factors: 1) the closed-loop system

$$\dot{\hat{x}} = (I_N \otimes (A+BK) + \mathscr{L} \otimes \Phi K)\hat{x}, \tag{4.97}$$

can be decomposed into N node-level differential equations (4.30) under a state-space transformation defined in (4.26), and 2) LQR cost function (4.70b), in the transformed coordinates, can be written as a sum of N node-level integrals (3.108). Unfortunately, these two elegant features vanish in the present setting and arise only if a network has an undirected topology.

In view of Proposition 4.3.3, closed-loop stability can be established by requiring the eigenvalues of

$$\hat{A}_{cl,j} = A + BK + \lambda_j B\Phi K, \text{ with } \lambda_j \in S(\mathscr{L}), \tag{4.98}$$

have negative real part $\forall\ j = 1, \ldots, p$. The derivation of sufficient conditions for closed-loop stability is outlined next.

First, we arrange the Laplacian modes into three groups:

1) The zero eigenvalue denoted as $\lambda_1 = 0$.

2) The purely real eigenvalues denoted as λ_ν where $\nu \in N_R$ with $N_R \subseteq \{2, \ldots, p\}$.

3) The complex eigenvalues denoted as λ_μ where $\mu \in N_C$ with

$$N_C \subseteq \{2, \ldots, p\} \backslash \bar{j} :\ \lambda_{\bar{j}} = \lambda_j^* \text{ and } j \in N_C. \tag{4.99}$$

Note that if $\lambda_j \in \mathbb{C}$ with $j \in N_C$ and $\lambda_{\bar{j}} = \lambda_j^*$ then $\bar{j} \not\subset N_C$.

Stability conditions for matrices $\hat{A}_{cl,j}$, $j = 1, \ldots, p$ in (4.98) are considered in the following three paragraphs, each one is associated with a certain type of Laplacian modes as listed above.

Zero eigenvalue: For $\lambda_1 = 0$, matrix

$$\hat{A}_{cl,1} = A + BK, \tag{4.100}$$

is clearly Hurwitz since K is the optimal gain obtained from LQR problem with parameters $(A,\ B,\ Q_1,\ R)$. This can be verified by checking the validity of the following LMI condition:

$$P_1(A+BK) + (A+BK)'P_1 < 0, \tag{4.101}$$

for $P_1 = P_1' > 0$.

Real eigenvalues: Let $\lambda_\nu \in S(\mathscr{L})$, with $\nu \in N_R$ as defined earlier, be a purely real non-zero Laplacian eigenvalue associated with matrix

$$\hat{A}_{cl,\nu} = A + BK + \lambda_\nu B\Phi K. \tag{4.102}$$

For a given matrix Φ, checking the inertia of $\hat{A}_{cl,\nu}$ can be seen as an LMI problem searching for matrix $P_\nu = P_\nu' > 0$ such that the following inequality:

$$P_\nu(A + BK + \lambda_\nu B\Phi K) + (A + BK + \lambda_\nu B\Phi K)' P_\nu < 0, \tag{4.103}$$

is satisfied.

Complex conjugate eigenvalues: Let $\lambda_\mu \in S(\mathscr{L})$, with $\mu \in N_C$ as defined earlier, be a complex Laplacian eigenvalue associated with matrix

$$\hat{A}_{cl,\mu} = A + BK + \lambda_\mu B\Phi K. \tag{4.104}$$

Before stating a stability condition of $\hat{A}_{cl,\mu}$ we consider the following proposition.

Proposition 4.3.5. *Let matrix $A \in \mathbb{C}^{n\times n}$ be written as $A = A_1 + \mathrm{i}A_2$ with $A_1 = \boldsymbol{Re}(A)$, $A_2 = \boldsymbol{Im}(A)$, and $\mathrm{i}^2 = -1$. Let also $\bar{A}$ denote its complex conjugate, i.e., $\bar{A} = A_1 - \mathrm{i}A_2$. Then matrix*

$$\tilde{A} = \begin{bmatrix} A & 0 \\ 0 & \bar{A} \end{bmatrix}, \tag{4.105}$$

is Hurwitz if and only if the real matrix

$$\hat{A} = \begin{bmatrix} A_1 & A_2 \\ -A_2 & A_1 \end{bmatrix}, \tag{4.106}$$

is Hurwitz with $\hat{A} \in \mathbb{R}^{2n\times 2n}$.

Proof. Let unitary matrix

$$T = \frac{1}{\sqrt{2}} \begin{bmatrix} I_n & \mathrm{i}I_n \\ \mathrm{i}I_n & I_n \end{bmatrix}. \tag{4.107}$$

It can easily be verified that $T\tilde{A}T^* = \hat{A}$. Since matrix T is unitary, matrices $\tilde{A}$ and $\hat{A}$ are similar and consequently they have equal eigenvalues. The latter proves the argument. □

For a given matrix Φ, suppose matrix $A+BK+\lambda_\mu B\Phi K \in \mathbb{C}^{n\times n}$ is Hurwitz and $\Gamma \in \mathbb{C}^{n\times n}$ is a Hermitian positive definite matrix such that

$$\Gamma(A+BK+\lambda_\mu B\Phi K)+(A+BK+\lambda_\mu B\Phi K)^*\Gamma<0. \tag{4.108}$$

Matrix Γ may be written as $\Gamma=\Gamma_1+\mathrm{i}\Gamma_2$, where $\Gamma_1=\mathbf{Re}(\Gamma)$ is a symmetric matrix, $\Gamma_2=\mathbf{Im}(\Gamma)$ is a skew-symmetric matrix, and $\mathrm{i}^2=-1$. Since $A+BK+\lambda_\mu B\Phi K$ is assumed to be Hurwitz, considering the conjugate expression of (4.108) leads to

$$\bar{\Gamma}(A+BK+\lambda_\mu^* B\Phi K)+(A+BK+\lambda_\mu^* B\Phi K)^*\bar{\Gamma}<0, \tag{4.109}$$

where $\bar{\Gamma}=\Gamma_1-\mathrm{i}\Gamma_2$ denotes the conjugate of Γ, and $\mathrm{i}^2=-1$. Clearly, matrix $A+BK+\lambda_\mu B\Phi K$ is also Hurwitz. Combining (4.108) and (4.109) results in a single inequality written as:

$$\begin{bmatrix}\Gamma & 0\\ 0 & \bar{\Gamma}\end{bmatrix}\begin{bmatrix}A+BK+\lambda_\mu B\Phi K & 0\\ 0 & A+BK+\lambda_\mu^* B\Phi K\end{bmatrix} + \begin{bmatrix}A+BK+\lambda_\mu B\Phi K & 0\\ 0 & A+BK+\lambda_\mu^* B\Phi K\end{bmatrix}^*\begin{bmatrix}\Gamma & 0\\ 0 & \bar{\Gamma}\end{bmatrix}<0. \tag{4.110}$$

Pre-multiplying and post-multiplying the former by T and T^*, respectively, T being unitary matrix constructed as in (4.107), does not violate the strict inequality condition and thus we may write:

$$T\begin{bmatrix}\Gamma & 0\\ 0 & \bar{\Gamma}\end{bmatrix}T^*T\begin{bmatrix}A+BK+\lambda_\mu B\Phi K & 0\\ 0 & A+BK+\lambda_\mu^* B\Phi K\end{bmatrix}T^* + T\begin{bmatrix}A+BK+\lambda_\mu B\Phi K & 0\\ 0 & A+BK+\lambda_\mu^* B\Phi K\end{bmatrix}^*T^*T\begin{bmatrix}\Gamma & 0\\ 0 & \bar{\Gamma}\end{bmatrix}T^*<0. \tag{4.111}$$

We use Proposition 4.3.5 to write

$$T\begin{bmatrix}\Gamma & 0\\ 0 & \bar{\Gamma}\end{bmatrix}T^*=\begin{bmatrix}\Gamma_1 & \Gamma_2\\ -\Gamma_2 & \Gamma_1\end{bmatrix} \tag{4.112}$$

and

$$T\begin{bmatrix} A+BK+\lambda_\mu B\Phi K & 0 \\ 0 & A+BK+\lambda_\mu^* B\Phi K \end{bmatrix} T^* = \begin{bmatrix} A+BK+a_\mu B\Phi K & b_\mu B\Phi K \\ -b_\mu B\Phi K & A+BK+a_\mu B\Phi K \end{bmatrix}, \quad (4.113)$$

where $a_\mu = \mathbf{Re}(\lambda_\mu)$ and $b_\mu = \mathbf{Im}(\lambda_\mu)$. Clearly, checking the inertia of $\hat{A}_{cl,\mu}$ can be imposed as an LMI problem searching for a symmetric positive definite matrix

$$P_\mu = \begin{bmatrix} P_{\mu,11} & P_{\mu,12} \\ -P_{\mu,12} & P_{\mu,11} \end{bmatrix}, \quad (4.114)$$

with $P_{\mu,11} = P'_{\mu,11}$ and $P_{\mu,12} = -P'_{\mu,12}$, such that the inequality

$$\begin{bmatrix} P_{\mu,11} & P_{\mu,12} \\ -P_{\mu,12} & P_{\mu,11} \end{bmatrix} \begin{bmatrix} A+BK+a_\mu B\Phi K & b_\mu B\Phi K \\ -b_\mu B\Phi K & A+BK+a_\mu B\Phi K \end{bmatrix} + \begin{bmatrix} A+BK+a_\mu B\Phi K & b_\mu B\Phi K \\ -b_\mu B\Phi K & A+BK+a_\mu B\Phi K \end{bmatrix}' \begin{bmatrix} P_{\mu,11} & P_{\mu,12} \\ -P_{\mu,12} & P_{\mu,11} \end{bmatrix} < 0, \quad (4.115)$$

is in force.

We collect now all stability conditions derived earlier for each Laplacian mode and write them in a compact form as follows:

$$P_1(\hat{A}_{cl,1}) + (\hat{A}_{cl,1})' P_1 < 0, \quad (4.116a)$$
$$P_1 > 0, \quad (4.116b)$$
$$P_\nu(\hat{A}_{cl,\nu}) + (\hat{A}_{cl,\nu})' P_\nu < 0, \quad (4.116c)$$
$$P_\nu > 0, \quad (4.116d)$$
$$P_\mu \hat{A}_\mu + \hat{A}'_\mu P_\mu < 0, \quad (4.116e)$$
$$P_\mu > 0, \quad (4.116f)$$

where matrices $\hat{A}_{cl,1}$, $\hat{A}_{cl,\nu}$ are as defined in (4.100), (4.102), respectively, $\lambda_\nu \in S(\mathscr{L})$ with $\nu \in N_R$, and

$$\hat{A}_\mu = \begin{bmatrix} A+BK+a_\mu B\Phi K & b_\mu B\Phi K \\ -b_\mu B\Phi K & A+BK+a_\mu B\Phi K \end{bmatrix}, \quad (4.117)$$

where $a_\mu = \mathbf{Re}(\lambda_\mu)$, $b_\mu = \mathbf{Im}(\lambda_\mu)$ and $\lambda_\mu \in S(\mathscr{L})$ with $\mu \in N_C$. Here, we have postulated that matrix Φ is known and hence LMI (4.116a)-(4.116e) can be seen as sufficient conditions for closed-loop stability. In the following, motivated by the systematic approach suggested in [46] for solving problem (3.110), we formulate a convex optimization problem and we propose a closed form expression for designing matrix Φ.

First, we consider a nonsingular matrix

$$\hat{T} = \begin{bmatrix} I_{(n-m)} & 0 \\ P_{22}^{-1} P_{12}' & I_m \end{bmatrix}, \tag{4.118}$$

where $P_{22} \in \mathbb{R}^{m \times m}$ and $P_{12} \in \mathbb{R}^{(n-m) \times m}$ are constructed by partitioning the unique symmetric positive definite solution P to ARE (4.84) as:

$$P = \begin{bmatrix} P_{11} & P_{12} \\ P_{12}' & P_{22} \end{bmatrix}. \tag{4.119}$$

We also define the following matrices:

$$\bar{A} = \hat{T} A \hat{T}^{-1}, \tag{4.120}$$
$$\bar{B} = \hat{T} B, \tag{4.121}$$
$$\bar{K} = K \hat{T}^{-1}, \tag{4.122}$$
$$\bar{P} = (\hat{T}^{-1})' P \hat{T}^{-1}, \tag{4.123}$$
$$\bar{Q}_1 = (\hat{T}^{-1})' Q_1 \hat{T}^{-1}, \tag{4.124}$$
$$\bar{Q}_2 = (\hat{T}^{-1})' Q_2 \hat{T}^{-1}. \tag{4.125}$$

Note that

$$\bar{B} = \begin{bmatrix} 0' & B_2' \end{bmatrix}', \tag{4.126}$$
$$\bar{K} = \begin{bmatrix} 0 & K_2 \end{bmatrix}. \tag{4.127}$$

Clearly, introducing a node-level state-space transformation $\bar{x}_i = \hat{T} x_i$, matrices (4.98) are similar to

$$\bar{A}_{cl,j} = \bar{A} + \bar{B}\bar{K} + \lambda_j \bar{B} \Phi \bar{K}, \text{ with } \lambda_j \in S(\mathscr{L}), \tag{4.128}$$

with $j = 1, \ldots, p$. We recall that p is the total number of the distinct eigenvalues of $\mathscr{L}$. Let now $j \in \{1, N_R, N_C\}$, and consider a symmetric positive definite matrix $P_j \; \forall \; j$. In particular,

for $j = 1$, define:

$$P_1 = \begin{bmatrix} P_{1,1} & 0 \\ 0 & \Pi_2 \end{bmatrix} > 0, \tag{4.129}$$

where $P_{1,1} \in \mathbb{R}^{(n-m)\times(n-m)}$ and $\Pi_2 \in \mathbb{R}^{m\times m}$ are assumed to be symmetric positive definite matrices. Similarly, for $j \in N_R$, set $j = \nu$ and define:

$$P_\nu = \begin{bmatrix} P_{\nu,1} & 0 \\ 0 & \Pi_2 \end{bmatrix} > 0, \tag{4.130}$$

where $P_{\nu,1} \in \mathbb{R}^{(n-m)\times(n-m)}$ is assumed to be a symmetric positive definite matrix. Finally, for $j \in N_C$, set $j = \mu$ and define:

$$P_\mu = \begin{bmatrix} P_{\mu,1} & 0 & P_{\mu,3} & 0 \\ 0 & \Pi_2 & 0 & 0 \\ -P_{\mu,3} & 0 & P_{\mu,1} & 0 \\ 0 & 0 & 0 & \Pi_2 \end{bmatrix} > 0, \tag{4.131}$$

where $P_{\mu,1} \in \mathbb{R}^{(n-m)\times(n-m)}$ is a symmetric positive definite matrix and $P_{\mu,3} \in \mathbb{R}^{(n-m)\times(n-m)}$ is a skew-symmetric matrix. We note that matrix Π_2 is assumed identical for all P_1, P_ν and P_μ, with $\nu \in N_R$ and $\mu \in N_C$, respectively. We now define $a_\mu = \mathbf{Re}(\lambda_\mu)$, $b_\mu = \mathbf{Im}(\lambda_\mu)$, and $\lambda_\nu, \lambda_\mu \in S(\mathscr{L})$ for $\nu \in N_R$ and $\mu \in N_C$, and introduce the following optimization problem:

$$\min \ \mathrm{trace}(P_1) + \sum_{\nu\in N_R} \mathrm{trace}(P_\nu) + \sum_{\mu\in N_C} \mathrm{trace}(P_\mu) \text{ subject to:} \tag{4.132a}$$

$$P_1(\bar{A} + \bar{B}\bar{K}) + (\bar{A} + \bar{B}\bar{K})' P_1 + \bar{Q}_1 + \bar{K}' R \bar{K} < 0, \tag{4.132b}$$

$$P_1 > 0, \tag{4.132c}$$

$$P_\nu(\bar{A} + \bar{B}\bar{K} + \lambda_\nu \bar{B}\Phi\bar{K}) + (\bar{A} + \bar{B}\bar{K} + \lambda_\nu \bar{B}\Phi\bar{K})' P_\nu + (\bar{Q}_1 + \lambda_\nu \bar{Q}_2) + (\bar{K} + \lambda_\nu \Phi\bar{K})' R (\bar{K} + \lambda_\nu \Phi\bar{K}) < 0, \tag{4.132d}$$

$$P_\nu > 0, \tag{4.132e}$$

$$P_\mu A_\mu + A_\mu' P_\mu + \begin{bmatrix} \bar{Q}_1 + a_\mu \bar{Q}_2 & 0 \\ 0 & \bar{Q}_1 + a_\mu \bar{Q}_2 \end{bmatrix} + \begin{bmatrix} \bar{K} + a_\mu \Phi\bar{K} & b_\mu \Phi\bar{K} \\ -b_\mu \Phi\bar{K} & \bar{K} + a_\mu \Phi\bar{K} \end{bmatrix}' \begin{bmatrix} R & 0 \\ 0 & R \end{bmatrix} \begin{bmatrix} \bar{K} + a_\mu \Phi\bar{K} & b_\mu \Phi\bar{K} \\ -b_\mu \Phi\bar{K} & \bar{K} + a_\mu \Phi\bar{K} \end{bmatrix} < 0, \tag{4.132f}$$

$$P_\mu > 0, \tag{4.132g}$$

where

$$A_\mu = \begin{bmatrix} \bar{A} + \bar{B}\bar{K} + a_\mu \bar{B}\Phi\bar{K} & b_\mu \bar{B}\Phi\bar{K} \\ -b_\mu \bar{B}\Phi\bar{K} & \bar{A} + \bar{B}\bar{K} + a_\mu \bar{B}\Phi\bar{K} \end{bmatrix}. \tag{4.133}$$

Pertaining to problem (4.132), we list the following remarks.

1) Constraints (4.132b)-(4.132g) can be cast as sufficient conditions for closed-loop stability for a given choice of design parameter Φ.

2) Problem (4.132) if feasible, admits of a conservative solution due to the special structure imposed on matrices P_1, P_ν and P_μ. This formulation will allow for a convex representation of the problem accommodating a closed-form expression for Φ.

3) Tuning LQR cost function with weight $Q_2 = 0$ (i.e., zero penalty on relative state-difference between neighboring agents), it can easily be seen that $\Phi = 0$ satisfies all constraints where optimal P_1, P_ν and P_μ can be obtained as

$$P_1 = P, \tag{4.134}$$
$$P_\nu = P, \tag{4.135}$$
$$P_\mu = \text{diag}(P, P), \tag{4.136}$$

for $\nu \in N_R$ and $\mu \in N_C$, respectively, where P is the optimal solution to ARE (4.84). Thus, we conclude that the optimization problem is guaranteed to have a meaningful solution.

4) The resulting matrix inequality constraints in (4.132) grow redundant with the number of subsystems constituting the network.

Constraints (4.132d) and (4.132f) are unambiguously nonlinear in variables P_ν, P_μ and Φ. Here, in order to define an equivalent optimization problem with linear constraints we introduce new variables as shown in the following.

Let matrices

$$W_1 = \begin{bmatrix} W_{1,1} & 0 \\ 0 & \bar{W}_2 \end{bmatrix} > 0, \tag{4.137}$$

$$W_\nu = \begin{bmatrix} W_{\nu,1} & 0 \\ 0 & \bar{W}_2 \end{bmatrix} > 0, \text{ for } \nu \in N_R, \tag{4.138}$$

$$W_\mu = \begin{bmatrix} W_{\mu,1} & 0 & W_{\mu,3} & 0 \\ 0 & \bar{W}_2 & 0 & 0 \\ -W_{\mu,3} & 0 & W_{\mu,1} & 0 \\ 0 & 0 & 0 & \bar{W}_2 \end{bmatrix} > 0, \text{ for } \mu \in N_C, \tag{4.139}$$

We require that

$$W_1 = P_1^{-1}, \tag{4.140}$$

$$W_\nu = P_\nu^{-1}, \text{ for } \nu \in N_R, \tag{4.141}$$

$$W_\mu = P_\mu^{-1}, \text{ for } \mu \in N_C. \tag{4.142}$$

It is easily verified that conditions (4.140), (4.141) and (4.142) hold true as long as

$$W_{1,1} = P_{1,1}^{-1}, \tag{4.143}$$

$$W_{\nu,1} = P_{\nu,1}^{-1}, \tag{4.144}$$

$$W_{\mu,1} = (P_{\mu,1} + P_{\mu,3}P_{\mu,1}^{-1}P_{\mu,3})^{-1}, \tag{4.145}$$

$$W_{\mu,3} = -P_{\mu,1}^{-1}P_{\mu,3}(P_{\mu,1} + P_{\mu,3}P_{\mu,1}^{-1}P_{\mu,3})^{-1}, \tag{4.146}$$

$$\bar{W}_2 = \Pi_2^{-1}, \tag{4.147}$$

for $\nu \in N_R$, $\mu \in N_C$. Clearly, $W_{1,1} = W_{1,1}' > 0$, $W_{\nu,1} = W_{\nu,1}' > 0$, $W_{\mu,1} = W_{\mu,1}' > 0$ and $\bar{W}_2 = \bar{W}_2' > 0$ are all symmetric positive definite matrices. We also note that $W_{\mu,3} = -W_{\mu,3}'$ is

a skew-symmetric matrix. This is shown next. From (4.146) we have:

$$\begin{aligned}
W'_{\mu,3} &= -(P_{\mu,1}^{-1}P_{\mu,3}(P_{\mu,1}+P_{\mu,3}P_{\mu,1}^{-1}P_{\mu,3})^{-1})' = ((P_{\mu,1}+P_{\mu,3}P_{\mu,1}P_{\mu,3})^{-1})'(-P_{\mu,1}^{-1}P_{\mu,3})' \\
&= -(P_{\mu,1}+P_{\mu,3}P_{\mu,1}^{-1}P_{\mu,3})^{-1}P'_{\mu,3}P_{\mu,1}^{-1} = -(P_{\mu,1}+P_{\mu,3}P_{\mu,1}^{-1}P_{\mu,3})^{-1}(-P_{\mu,3})P_{\mu,1}^{-1} \\
&= (P_{\mu,1}+P_{\mu,3}P_{\mu,1}^{-1}P_{\mu,3})^{-1}P_{\mu,3}P_{\mu,1}^{-1} = (P_{\mu,1}+P_{\mu,3}P_{\mu,1}^{-1}P_{\mu,3})^{-1}(P_{\mu,1}P_{\mu,3}^{-1})^{-1} \\
&= ((P_{\mu,1}P_{\mu,3}^{-1})(P_{\mu,1}+P_{\mu,3}P_{\mu,1}^{-1}P_{\mu,3}))^{-1} = (P_{\mu,1}P_{\mu,3}^{-1}P_{\mu,1}+P_{\mu,1}P_{\mu,1}^{-1}P_{\mu,3})^{-1} \\
&= (P_{\mu,3}+P_{\mu,1}P_{\mu,3}^{-1}P_{\mu,1})^{-1} = (P_{\mu,3}P_{\mu,1}^{-1}P_{\mu,1}+P_{\mu,1}P_{\mu,3}^{-1}P_{\mu,1})^{-1} \\
&= (P_{\mu,3}P_{\mu,1}^{-1}P_{\mu,3}P_{\mu,3}^{-1}P_{\mu,1}+P_{\mu,1}P_{\mu,3}^{-1}P_{\mu,1})^{-1} = ((P_{\mu,3}P_{\mu,1}^{-1}P_{\mu,3}+P_{\mu,1})(P_{\mu,3}^{-1}P_{\mu,1}))^{-1} \\
&= (P_{\mu,3}^{-1}P_{\mu,1})^{-1}(P_{\mu,3}P_{\mu,1}^{-1}P_{\mu,3}+P_{\mu,1})^{-1} = P_{\mu,1}^{-1}P_{\mu,3}(P_{\mu,3}P_{\mu,1}^{-1}P_{\mu,3}+P_{\mu,1})^{-1} \\
&= -W_{\mu,3}.
\end{aligned}$$

Now, pre-multiplying and post-multiplying (4.132b), (4.132d) and (4.132f) by W_1, W_ν, $\nu \in N_R$ and W_μ, $\mu \in N_C$, respectively, yields

$$(\bar{A}+\bar{B}\bar{K})W_1 + W_1(\bar{A}+\bar{B}\bar{K})' + W_1\bar{Q}_1W_1 + W_1\bar{K}'R\bar{K}W_\nu < 0, \tag{4.148}$$

$$\begin{aligned}
&(\bar{A}+\bar{B}\bar{K}+\lambda_\nu\bar{B}\Phi\bar{K})W_\nu + W_\nu(\bar{A}+\bar{B}\bar{K}+\lambda_\nu\bar{B}\Phi\bar{K})' + W_\nu(\bar{Q}_1+\lambda_\nu\bar{Q}_2)W_\nu \\
&\qquad + W_\nu(\bar{K}+\lambda_\nu\Phi\bar{K})'R(\bar{K}+\lambda_\nu\Phi\bar{K})W_\nu < 0,
\end{aligned} \tag{4.149}$$

$$\begin{aligned}
&A_\mu W_\mu + W_\mu A'_\mu + W_\mu \begin{bmatrix} \bar{Q}_1+a_\mu\bar{Q}_2 & 0 \\ 0 & \bar{Q}_1+a_\mu\bar{Q}_2 \end{bmatrix} W_\mu \\
&+ W_\mu \begin{bmatrix} \bar{K}+a_\mu\Phi\bar{K} & b_\mu\Phi\bar{K} \\ -b_\mu\Phi\bar{K} & \bar{K}+a_\mu\Phi\bar{K} \end{bmatrix}' \begin{bmatrix} R & 0 \\ 0 & R \end{bmatrix} \begin{bmatrix} \bar{K}+a_\mu\Phi\bar{K} & b_\mu\Phi\bar{K} \\ -b_\mu\Phi\bar{K} & \bar{K}+a_\mu\Phi\bar{K} \end{bmatrix} W_\mu < 0.
\end{aligned} \tag{4.150}$$

As seen in (4.127), due to the structure of $\bar{K} = [0\ K_2]$, the following products

$$\Phi\bar{K}W_\nu = \begin{bmatrix} 0 & \Phi K_2\bar{W}_2 \end{bmatrix}, \tag{4.151}$$

$$\Phi\bar{K}\begin{bmatrix} W_{\mu,1} & 0 \\ 0 & \bar{W}_2 \end{bmatrix} = \begin{bmatrix} 0 & \Phi K_2\bar{W}_2 \end{bmatrix}, \tag{4.152}$$

in (4.149) and (4.150), respectively, are all equal and can be represented as a separate variable defined as

$$\bar{Y} = \begin{bmatrix} 0 & Y_2 \end{bmatrix}, \tag{4.153}$$

with $Y_2 = \Phi K_2\bar{W}_2$. Next, we convert the quadratic matrix inequalities in (4.149) and (4.150) into linear matrix inequalities (LMI) using the Schur complement condition (see Proposition 4.2.2). Note that LMI's corresponding to (4.149) can be derived straightforwardly as shown

in Section 4.2. We define now the following matrices:

$$\Omega_1 = \begin{bmatrix} -\Psi_1 & W_1\bar{Q}_1^{\frac{1}{2}} \\ \bar{Q}_1^{\frac{1}{2}}W_1 & I_n \end{bmatrix}, \tag{4.154}$$

$$H_1 = \begin{bmatrix} (\bar{K}W_\nu)' \\ 0_{n\times m} \end{bmatrix}, \tag{4.155}$$

$$\Omega_\nu = \begin{bmatrix} -\Psi_\nu & W_\nu(\bar{Q}_1+\lambda_\nu\bar{Q}_2)^{\frac{1}{2}} \\ (\bar{Q}_1+\lambda_\nu\bar{Q}_2)^{\frac{1}{2}}W_\nu & I_n \end{bmatrix}, \tag{4.156}$$

$$H_\nu = \begin{bmatrix} (\lambda_\nu\bar{Y}+\bar{K}W_\nu)' \\ 0_{n\times m} \end{bmatrix}, \tag{4.157}$$

$$\Omega_\mu = \begin{bmatrix} -\Psi_\mu & W_\mu \begin{bmatrix} \bar{Q}_1+a_\mu\bar{Q}_2 & 0 \\ 0 & \bar{Q}_1+a_\mu\bar{Q}_2 \end{bmatrix}^{\frac{1}{2}} \\ \begin{bmatrix} \bar{Q}_1+a_\mu\bar{Q}_2 & 0 \\ 0 & \bar{Q}_1+a_\mu\bar{Q}_2 \end{bmatrix}^{\frac{1}{2}} W_\mu & I_{2n} \end{bmatrix}, \tag{4.158}$$

$$H_\mu = \begin{bmatrix} a_\mu\bar{Y}' + \begin{bmatrix} W_{\mu,1} & 0 \\ 0 & \bar{W}_2 \end{bmatrix}\bar{K}' & -b_\mu\bar{Y}' - \begin{bmatrix} W_3 & 0 \\ 0 & 0 \end{bmatrix}\bar{K}' \\ b_\mu\bar{Y}' + \begin{bmatrix} W_3 & 0 \\ 0 & 0 \end{bmatrix}\bar{K}' & a_\mu\bar{Y}' + \begin{bmatrix} W_{\mu,1} & 0 \\ 0 & \bar{W}_2 \end{bmatrix}\bar{K}' \\ 0_{n\times m} & 0_{n\times m} \\ 0_{n\times m} & 0_{n\times m} \end{bmatrix}, \tag{4.159}$$

where

$$\Psi_1 = (\bar{A}+\bar{B}\bar{K})W_1 + W_1(\bar{A}+\bar{B}\bar{K})', \tag{4.160}$$

$$\Psi_\nu = (\bar{A}+\bar{B}\bar{K})W_\nu + \lambda_\nu\bar{B}\bar{Y} + W_\nu(\bar{A}+\bar{B}\bar{K})' + \lambda_\nu\bar{Y}'\bar{B}', \tag{4.161}$$

$$\begin{aligned} \Psi_\mu = &\begin{bmatrix} (\bar{A}+\bar{B}\bar{K})\begin{bmatrix} W_{\mu,1} & 0 \\ 0 & \bar{W}_2 \end{bmatrix} + a_\mu\bar{B}\bar{Y} & (\bar{A}+\bar{B}\bar{K})\begin{bmatrix} W_{\mu,3} & 0 \\ 0 & 0 \end{bmatrix} + b_\mu\bar{B}\bar{Y} \\ (\bar{A}+\bar{B}\bar{K})\begin{bmatrix} -W_{\mu,3} & 0 \\ 0 & 0 \end{bmatrix} - b_\mu\bar{B}\bar{Y} & (\bar{A}+\bar{B}\bar{K})\begin{bmatrix} W_{\mu,1} & 0 \\ 0 & \bar{W}_2 \end{bmatrix} + a_\mu\bar{B}\bar{Y} \end{bmatrix} \\ &+ \begin{bmatrix} \begin{bmatrix} W_{\mu,1} & 0 \\ 0 & \bar{W}_2 \end{bmatrix}(\bar{A}+\bar{B}\bar{K})' + a_\mu\bar{Y}'\bar{B}' & \begin{bmatrix} W_{\mu,3} & 0 \\ 0 & 0 \end{bmatrix}(\bar{A}+\bar{B}\bar{K})' - b_\mu\bar{Y}'\bar{B}' \\ \begin{bmatrix} -W_{\mu,3} & 0 \\ 0 & 0 \end{bmatrix}(\bar{A}+\bar{B}\bar{K})' + b_\mu\bar{Y}'\bar{B}' & \begin{bmatrix} W_{\mu,1} & 0 \\ 0 & \bar{W}_2 \end{bmatrix}(\bar{A}+\bar{B}\bar{K})' + a_\mu\bar{Y}'\bar{B}' \end{bmatrix}, \end{aligned} \tag{4.162}$$

for $\nu \in N_R$ and $\mu \in N_C$, respectively. The quadratic matrix inequalities (4.148) and (4.149) can then be expressed as the Schur complement of the block $\begin{bmatrix} I_n & 0 \\ 0 & R^{-1} \end{bmatrix} > 0$ of the LMI

$$\begin{bmatrix} \Omega_1 & H_1 \\ H_1' & R^{-1} \end{bmatrix} > 0, \tag{4.163}$$

and

$$\begin{bmatrix} \Omega_\nu & H_\nu \\ H_\nu' & R^{-1} \end{bmatrix} > 0, \tag{4.164}$$

with $\nu \in N_R$, respectively. Similarly, the inequality condition (4.150) can be expressed as the Schur complement of the block $\begin{bmatrix} I_{2n} & 0 \\ 0 & I_2 \otimes R^{-1} \end{bmatrix} > 0$ of the LMI

$$\begin{bmatrix} \Omega_\mu & H_\mu \\ H_\mu' & I_2 \otimes R^{-1} \end{bmatrix} > 0, \tag{4.165}$$

with $\mu \in N_C$. We also define symmetric positive definite matrices Z_1, Z_ν and Z_μ which are assumed to have the same structure and properties with matrices P_1, P_ν and P_μ, for $\nu \in N_R$ and $\mu \in N_C$, respectively. Finally, we require that

$$\begin{bmatrix} Z_1 & -I_n \\ -I_n & W_1 \end{bmatrix} > 0, \tag{4.166}$$

$$\begin{bmatrix} Z_\nu & -I_n \\ -I_n & W_\nu \end{bmatrix} > 0, \tag{4.167}$$

$$\begin{bmatrix} Z_\mu & -I_{2n} \\ -I_{2n} & W_\mu \end{bmatrix} > 0. \tag{4.168}$$

Clearly, minimizing

$$\text{trace}(Z_1) + \sum_{\nu \in N_R} \text{trace}(Z_\nu) + \sum_{\mu \in N_C} \text{trace}(Z_\mu)$$

subject to (4.148), (4.149), (4.150), (4.166), (4.167) and (4.168) is equivalent to minimizing

$$\operatorname{trace}(W_1^{-1}) + \sum_{\nu \in N_R} \operatorname{trace}(W_\nu^{-1}) + \sum_{\mu \in N_C} \operatorname{trace}(W_\mu^{-1}) = \tag{4.169}$$

$$\operatorname{trace}(P_1) + \sum_{\nu \in N_R} \operatorname{trace}(P_\nu) + \sum_{\mu \in N_C} \operatorname{trace}(P_\mu), \tag{4.170}$$

subject to (4.163), (4.164) and (4.165). A convex representation of problem (4.132) with linear constraints can now be expressed as follows:

$$\min_{\substack{W_1, W_\nu, W_\mu > 0 \\ Z_1, Z_\nu, Z_\mu > 0 \\ \bar{Y}}} \operatorname{trace}(Z_1) + \sum_{\nu \in N_R} \operatorname{trace}(Z_\nu) + \sum_{\mu \in N_C} \operatorname{trace}(Z_\mu) \tag{4.171}$$

subject to (4.163) – (4.168).

If problem (4.171) is feasible, matrix Φ can be constructed via the closed-form expression:

$$\Phi = Y_2 \bar{W}_2^{-1} K_2^{-1}. \tag{4.172}$$

In the following paragraph, we slightly modify problem (4.171) and suggest a distributed controller as constructed in Section 4.2.

4.3.6 Hybrid method for directed networks

Let $\tilde{P}_2$, defined in Section 4.3.4 as solution to ARE (4.85), be partitioned as:

$$\tilde{P}_2 = \begin{bmatrix} \tilde{P}_{2,11} & \tilde{P}_{2,12} \\ \tilde{P}'_{2,12} & \tilde{P}_{2,22} \end{bmatrix}, \tag{4.173}$$

with $\tilde{P}_{2,11} \in \mathbb{R}^{(n-m)\times(n-m)}$ and $\tilde{P}_{2,22} \in \mathbb{R}^{m\times m}$, where $\tilde{P}_{2,22}$ is a symmetric nonsingular matrix since matrix $\tilde{P}_2$ is symmetric and nonsingular. Consider also a state-space transformation $\hat{T}$ as in (4.118) defined here as:

$$\hat{T} = \begin{bmatrix} I_{(n-m)} & 0 \\ \tilde{P}_{2,22}^{-1} \tilde{P}'_{2,12} & I_m \end{bmatrix}. \tag{4.174}$$

Defining $(\bar{A},\ \bar{B},\ \bar{K},\ \bar{P},\ \bar{Q}_1,\ \bar{Q}_2)$ as in (4.120)-(4.125) with $\hat{T}$ as in (4.174), and solving problem (4.171), matrix Φ can be designed as:

$$\Phi = Y_2 \bar{W}_2^{-1} \tilde{K}_2^{-1}, \tag{4.175}$$

where $\tilde{K}_2$ is obtained from:

$$R^{-1}B'\tilde{P}_2\hat{T}^{-1} = \begin{bmatrix} 0 & \tilde{K}_2 \end{bmatrix}. \tag{4.176}$$

Then, control law $\hat{u}$ in (4.70d) takes the following form:

$$\hat{u} = (-I_N \otimes (R^{-1}B'P) + \mathscr{L} \otimes \Phi(R^{-1}B'\tilde{P}_2))\hat{x}, \tag{4.177}$$

where P and $\tilde{P}_2$ are derived from (4.84) and (4.85), respectively.

Before illustrating the applicability of the control methods presented in this chapter via a numerical study, we investigate the regulation problem of a special class of directed networks. This is presented in the following section.

4.3.7 Cascaded networks

Let a network be composed of a single directed path of N nodes as depicted in Fig. 4.1. Such digraphs are clearly connected regardless the number of nodes are composed of, since a directed path of an arbitrary number of nodes represents a directed spanning tree itself. In the following, we denote the digraph of a directed path over N vertices as $\mathscr{D}_{P,N}$.

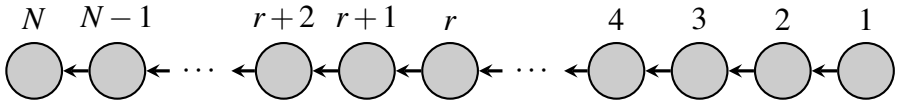

Fig. 4.1 Directed path of N nodes.

We will show that the adjacency matrix and the in-degree Laplacian matrix associated with digraphs representing directed paths retain certain properties irrespective of the number of vertices in the path. Let matrices $\mathscr{A}(\mathscr{D}_{P,N})$, $\mathscr{L}(\mathscr{D}_{P,N})$ denote the adjacency matrix and the in-degree Laplacian matrix, respectively, of digraph $\mathscr{D}_{P,N}$. These matrices are written as follows:

$$\mathscr{A}(\mathscr{D}_{P,N}) = \begin{bmatrix} 0 & 0 & \cdots & 0 & 0 \\ 1 & 0 & \cdots & 0 & 0 \\ 0 & 1 & \cdots & 0 & 0 \\ \vdots & \vdots & \ddots & \vdots & \vdots \\ 0 & 0 & \cdots & 1 & 0 \end{bmatrix}, \tag{4.178}$$

which is a nilpotent matrix, and

$$\mathscr{L}(\mathscr{D}_{P,N}) = \begin{bmatrix} 0 & 0 & 0 & \cdots & 0 \\ -1 & 1 & 0 & \cdots & 0 \\ 0 & -1 & 1 & \vdots & 0 \\ \vdots & \vdots & \ddots & \ddots & \vdots \\ 0 & 0 & \cdots & -1 & 1 \end{bmatrix}. \tag{4.179}$$

Next, we show that $S(\mathscr{L}(\mathscr{D}_{P,N})) = (0,1,\ldots,1)$. Let

$$T = \begin{bmatrix} 0 & 0 & \cdots & 0 & 1 \\ 0 & 0 & \cdots & 1 & 0 \\ \vdots & \vdots & \iddots & \vdots & 0 \\ 0 & 1 & \cdots & 0 & 0 \\ 1 & 0 & \cdots & 0 & 0 \end{bmatrix}, \tag{4.180}$$

be a permutation matrix with $T = T' = T^{-1}$. Then, matrix $\mathscr{L}(\mathscr{D}_{P,N})$ is similar to $\bar{\mathscr{L}} = T\mathscr{L}(\mathscr{D}_{P,N})T'$ with

$$\bar{\mathscr{L}} = \begin{bmatrix} 0 & -1 & 0 & \cdots & 0 \\ 0 & 1 & -1 & \cdots & 0 \\ \vdots & \vdots & \ddots & \ddots & \vdots \\ 0 & 0 & \cdots & 1 & -1 \\ 0 & 0 & \cdots & 0 & 1 \end{bmatrix}. \tag{4.181}$$

We consider the spectrum of matrix $-\bar{\mathscr{L}}$ with

$$\bar{\mathscr{L}} = -\begin{bmatrix} 0 & 1 & 0 & \cdots & 0 \\ 0 & -1 & 1 & \cdots & 0 \\ \vdots & \vdots & \ddots & \ddots & \vdots \\ 0 & 0 & \cdots & -1 & 1 \\ 0 & 0 & \cdots & 0 & -1 \end{bmatrix}. \tag{4.182}$$

Clearly,

$$S(-\bar{\mathscr{L}}) = (0,-1,\ldots,-1), \tag{4.183}$$

since $-\bar{\mathscr{L}} = \text{diag}(0, J_{N-1}(-1))$ where $J_{N-1}(-1)$ is the Jordan block associated with eigenvalue $\lambda = -1$ with algebraic multiplicity of $N-1$. From (4.183), we conclude

$$S(\mathscr{L}(\mathscr{D}_{P,N})) = (0, 1, \ldots, 1). \tag{4.184}$$

Now, we consider regulator problem (4.70) which is re-written here for convenience:

$$\min_{\hat{u}} J(\hat{u}, \hat{x}_0) \text{ subject to:} \tag{4.185a}$$

$$J(\hat{u}, \hat{x}_0) = \int_0^\infty \left(\hat{x}'(I_N \otimes Q_1 + \mathscr{L}_c \otimes Q_2)\hat{x} + \hat{u}'\hat{R}\hat{u}\right) \text{dt}, \tag{4.185b}$$

$$\dot{\hat{x}} = \hat{A}\hat{x} + \hat{B}\hat{u},\ \hat{x}(0) = \hat{x}_0, \tag{4.185c}$$

$$\hat{u} = (I_N \otimes K_1 + M \otimes K_2)\hat{x}. \tag{4.185d}$$

First, we wish to design matrices K_1, K_2 and M via the top-down method. For an arbitrary positive integer N_L, we solve LQR problem (3.65) with weights $(Q_1,\ Q_2,\ R)$ for N_L systems, and we define P and $\tilde{P}_2$ from (4.84) and (4.85), respectively. Then, from Corollary 4.3.2, matrix $A - BR^{-1}B'(P + \gamma N_L \tilde{P}_2)$ is Hurwitz for all $\gamma > \frac{1}{2}$.

From Proposition 4.3.3, the closed-loop matrix

$$A_{cl} = I_N \otimes (A + BK_1) + M \otimes BK_2, \tag{4.186}$$

is Hurwitz if and only if matrix

$$A_{cl,\lambda_j} = A + BK_1 + \lambda_j BK_2, \tag{4.187}$$

is Hurwitz $\forall\ \lambda_j \in S(M)$. Denoting the adjacency matrix (4.178) as $\mathscr{A}$, without loss of generality, we select $M = -\mathscr{A}$. Note that $\lambda_j = 0$ for $j = 1, \ldots, N$ and $\lambda_j \in S(\mathscr{A})$ since $\mathscr{A}$ is a nilpotent matrix as mentioned earlier. As a result of this particular option of M, we conclude that A_{cl} in (4.186) is Hurwitz irrespective of the choice of K_2 as long as matrix $A + BK_1$ is Hurwitz. Therefore, we may construct K_1 and K_2 in (4.185d) as

$$K_1 = -R^{-1}B'(P + \gamma_1 \tilde{P}_2), \tag{4.188}$$

$$K_2 = R^{-1}B'\tilde{P}_2, \tag{4.189}$$

respectively, where $\gamma_1 \in \mathbb{R}$. Finally, the closed-loop matrix A_{cl} becomes:

$$A_{cl} = I_N \otimes (A - BR^{-1}B'(P + \gamma_1 \tilde{P}_2)) - \mathscr{A} \otimes BR^{-1}B'\tilde{P}_2, \tag{4.190}$$

which is Hurwitz for all $\gamma_1 > \frac{N_L}{2}$.

Now, suppose $\hat{u}$ is constructed as in bottom-up method, i.e.,

$$\hat{u} = (-I_N \otimes R^{-1}B'P - \mathscr{L} \otimes \Phi R^{-1}B'P)\hat{x}, \tag{4.191}$$

with $\mathscr{L}$ denoting the Laplacian matrix (4.179). With this control law $\hat{u}$ in force, it follows that the closed-loop matrix

$$A_{cl} = I_N \otimes (A - BR^{-1}B'P) - \mathscr{L} \otimes B\Phi R^{-1}B'P, \tag{4.192}$$

is Hurwitz if and only if

$$A_1 = A - BR^{-1}B'P, \tag{4.193}$$

$$A_2 = A - B(I_m + \Phi)R^{-1}B'P, \tag{4.194}$$

are Hurwitz matrices. Clearly, matrix A_1 in (4.193) is Hurwitz, while matrix A_2 in (4.194) is Hurwitz for all $\Phi > -0.5I_m$. The latter stems from the gain-margin property of LQR control. Alternatively, matrix Φ can be derived from (4.172) solving optimization problem (4.171).

The stabilization of directed paths finalizes the study of the regulator problem of networks with directed topology. Next, a numerical example attempts to highlight the applicability of the control design methods proposed in this chapter.

4.3.8 Numerical example: regulation of interconnected agents

We consider eleven $(N = 11)$ identical, linear time-invariant systems, each representing an autonomous mobile agent. Specifically, agents are assumed to move in a plane with double integrator dynamics in both spatial directions (denoted as x-direction and y-direction, respectively, in simulations) described by the following state-space equations:

$$\dot{x}_i = Ax_i + Bu_i,\ x_i(0) = x_{i,0},\ i = 1, \ldots, 11, \tag{4.195}$$

with

$$A = \begin{bmatrix} 0 & I_2 \\ 0 & 0 \end{bmatrix},\ B = \begin{bmatrix} 0 \\ I_2 \end{bmatrix}. \tag{4.196}$$

Clearly, pair $(A,\ B)$ is controllable with input matrix B being in the regular form as in (4.2) and (4.92).

We examine two interconnection schemes, each specifying the communication scheme between agents as well as the structure of the entire distributed control system. The interaction

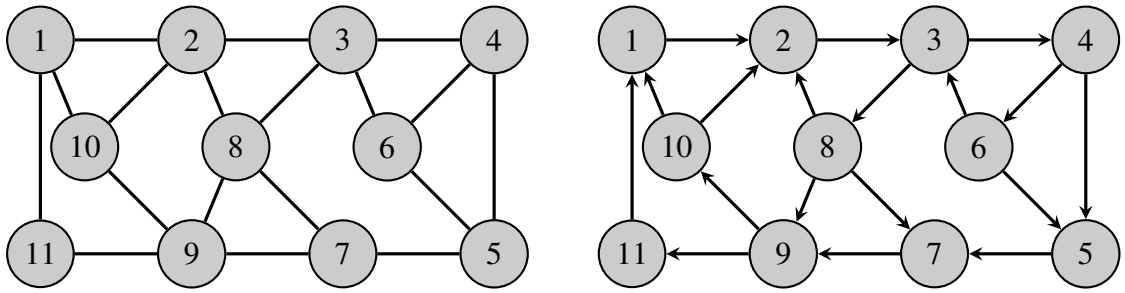

(a) Graph $\mathscr{G}_{11}$. (b) Digraph $\mathscr{D}_{11}$.

Fig. 4.2 Interconnection schemes of eleven agents.

graph of each scheme is depicted in Fig. 4.2. As can be seen, in the first scheme the interactions between agents are allowed to be bidirectional and thus are modelled by a connected graph shown in Fig. 4.2a. In the second, the information flow is restricted to be directed and is represented by a connected digraph shown in Fig. 4.2b.

In the following, we denote the Laplacian matrix associated with graph $\mathscr{G}$ (Fig. 4.2a) as $\mathscr{L}_{G,11}$, and the in-degree Laplacian matrix associated with digraph $\mathscr{D}$ (Fig. 4.2b) as $\mathscr{L}_{D,11}$. These are computed below:

$$\mathscr{L}_{G,11} = \begin{bmatrix} 3 & -1 & 0 & 0 & 0 & 0 & 0 & 0 & 0 & -1 & -1 \\ -1 & 4 & -1 & 0 & 0 & 0 & 0 & -1 & 0 & -1 & 0 \\ 0 & -1 & 4 & -1 & 0 & -1 & 0 & -1 & 0 & 0 & 0 \\ 0 & 0 & -1 & 3 & -1 & -1 & 0 & 0 & 0 & 0 & 0 \\ 0 & 0 & 0 & -1 & 3 & -1 & -1 & 0 & 0 & 0 & 0 \\ 0 & 0 & -1 & -1 & -1 & 3 & 0 & 0 & 0 & 0 & 0 \\ 0 & 0 & 0 & 0 & -1 & 0 & 3 & -1 & -1 & 0 & 0 \\ 0 & -1 & -1 & 0 & 0 & 0 & -1 & 4 & -1 & 0 & 0 \\ 0 & 0 & 0 & 0 & 0 & 0 & -1 & -1 & 4 & -1 & -1 \\ -1 & -1 & 0 & 0 & 0 & 0 & 0 & 0 & -1 & 3 & 0 \\ -1 & 0 & 0 & 0 & 0 & 0 & 0 & 0 & -1 & 0 & 2 \end{bmatrix}, \tag{4.197}$$

and

$$\mathscr{L}_{D,11} = \begin{bmatrix} 2 & 0 & 0 & 0 & 0 & 0 & 0 & 0 & 0 & -1 & -1 \\ -1 & 3 & 0 & 0 & 0 & 0 & 0 & -1 & 0 & -1 & 0 \\ 0 & -1 & 2 & 0 & 0 & -1 & 0 & 0 & 0 & 0 & 0 \\ 0 & 0 & -1 & 1 & 0 & 0 & 0 & 0 & 0 & 0 & 0 \\ 0 & 0 & 0 & -1 & 2 & -1 & 0 & 0 & 0 & 0 & 0 \\ 0 & 0 & 0 & -1 & 0 & 1 & 0 & 0 & 0 & 0 & 0 \\ 0 & 0 & 0 & 0 & -1 & 0 & 2 & -1 & 0 & 0 & 0 \\ 0 & 0 & -1 & 0 & 0 & 0 & 0 & 1 & 0 & 0 & 0 \\ 0 & 0 & 0 & 0 & 0 & 0 & -1 & -1 & 2 & 0 & 0 \\ 0 & 0 & 0 & 0 & 0 & 0 & 0 & 0 & -1 & 1 & 0 \\ 0 & 0 & 0 & 0 & 0 & 0 & 0 & 0 & -1 & 0 & 1 \end{bmatrix}. \tag{4.198}$$

For each interconnection scheme, the control objective is to regulate the state variables of each subsystem. In other words, we wish to move each agent to a desired position, here taken as the origin of the plane. This task can be formulated as the following regulation problem:

$$\min_{\hat{u}} J(\hat{u},\hat{x}_0) \text{ subject to:} \tag{4.199a}$$

$$J(\hat{u},\hat{x}_0) = \int_0^\infty \left(\hat{x}'(I_{11}\otimes Q_1 + \mathscr{L}_{G,11}\otimes Q_2)\hat{x} + \hat{u}'(I_{11}\otimes R)\hat{u}\right) \mathrm{dt}, \tag{4.199b}$$

$$\dot{\hat{x}} = \hat{A}\hat{x} + \hat{B}\hat{u},\ \hat{x}(0) = \hat{x}_0, \tag{4.199c}$$

$$\hat{u} = (I_{11}\otimes K_1 + M\otimes K_2)\hat{x}, \tag{4.199d}$$

where $\hat{A} = I_{11}\otimes A$, $\hat{B} = I_{11}\otimes B$. Note that depending on the topology of each interconnection scheme, matrix $M \in \mathscr{K}_{2,4}^{11}(\mathscr{G}_{11})$ or $M \in \mathscr{K}_{2,4}^{11}(\mathscr{D}_{11})$. In the study, we select matrix M as the Laplacian matrix of each particular structure, i.e., for the undirected topology $M = \mathscr{L}_{G,11}$, while for the directed topology $M = \mathscr{L}_{D,11}$. Note also that the Laplacian matrix $\mathscr{L}_{G,11}$ in the weighting matrix $\hat{Q} = I_{11}\otimes Q_1 + \mathscr{L}_{G,11}\otimes Q_2$ in (4.199b) has been chosen irrespective of the interconnection structure, in other words, the performance index (4.199b) is considered identical for both interconnection schemes. This is to guarantee that $J(\cdot)$ is well-defined and matrix $\hat{Q} = \hat{Q}' \geq 0$ for both schemes. We also note that matrix Q_1 is selected to penalize the local state of each agent while matrix Q_2 can be seen as a tuning parameter used to emphasize/de-emphasize relative state-difference between interconnected agents. For simulation purposes, we consider two different choices of the weights $(Q_1,\ Q_2)$, while we keep the input weighting matrix $R = I_2$ identical for both settings. In the first, we weigh local

and relative states equally:

$$Q_1 = Q_2 = \text{diag}(1,1,0,0), \tag{4.200}$$

while in the second setting we shift much more emphasis on the relative states $(x_i - x_j)$, by selecting $Q_2 = 10^6 Q_1$ with

$$Q_1 = \text{diag}(0.001, 0.001, 0, 0). \tag{4.201}$$

We remark that a control policy $\hat{u}$ tuned to minimize a heavily weighted norm of relative states among other terms, namely, a less weighted norm of absolute states, as well as a weighted norm of control effort, can be cast as a distributed state-agreement control protocol. This becomes apparent in the simulation results. Velocity states are not penalized in this numerical study. Design matrices K_1, K_2 in (4.199d) are constructed via the two methods (top-down, bottom-up) presented in Chapter 3. First, we present simulation results for the structure illustrated in Fig. 4.2a.

Undirected topology: We denote by

$$\hat{u}_t = (I_{11} \otimes \underbrace{(-R^{-1}B'P)}_{K_1} + \underbrace{\gamma \mathscr{L}_{G,11}}_{M} \otimes \underbrace{(R^{-1}B'\tilde{P}_2)}_{K_2})\hat{x}, \tag{4.202}$$

the control law derived from the top-down design. For each particular tuning of the cost function (4.199b), we solve an LQR problem (3.65), with tuning parameters $(Q_1,\ Q_2,\ R)$, for $N_L = d_{\max} + 1$ systems, $d_{\max} = 4$ denoting the maximum vertex degree of $\mathscr{G}_{11}$. We then define matrices P and $\tilde{P}_2$ in (4.202) by solving ARE (3.71) and (3.72), respectively. Scalar γ in (4.202) is independent of a particular LQR tuning. Any choice of

$$\gamma > \frac{N_L}{2\lambda_2(\mathscr{L}_{G,11})}, \tag{4.203}$$

where $\lambda_2(\mathscr{L}_{G,11})$ is the second smallest Laplacian eigenvalue, suffices for condition (3.83) to be in force. Since

$$S(\mathscr{L}_{G,11}) = (0,\ 0.629,\ 1.834,\ 1.937,\ 2.785,\ 3.554,\ 4,\ 4.528,\ 5.188,\ 5.645,\ 5.901), \tag{4.204}$$

we select

$$\gamma = 4, \tag{4.205}$$

with minimum value calculated at 3.9746.

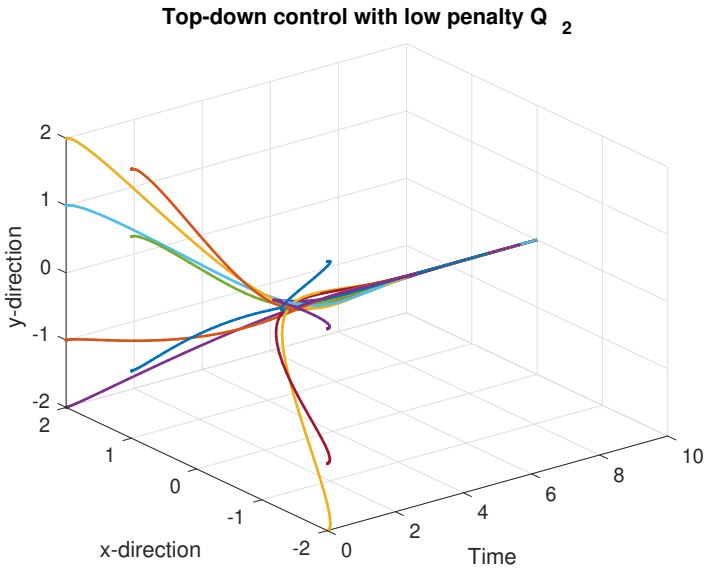

Fig. 4.3 Closed-loop behavior of the undirected distributed system under top-down control with low penalty Q_2.

Fig. 4.3 and Fig. 4.4 depict the closed-loop behavior of the large-scale distributed system under control action $\hat{u}_t$. Stable operation is maintained for both simulations where identical initial conditions are considered. It is evident that agents converge to the origin fairly faster in simulation shown in Fig. 4.3 than in simulation shown in Fig. 4.4. This is because, in the latter, the control action is tuned to minimize a heavily weighted state-distance $x_i - x_j$, thereby enforcing agents to synchronize with each other, reaching state-agreement first and converging subsequently to the origin.

Let now

$$\hat{u}_b = (I_{11} \otimes \underbrace{(-R^{-1}B'P)}_{K_1} + \underbrace{\mathscr{L}_{G,11}}_{M} \otimes \underbrace{\Phi(-R^{-1}B'P)}_{K_2})\hat{x}, \tag{4.206}$$

denote the control law obtained from the bottom-up approach, where matrix P is as defined in (4.202). Here, for each choice of tuning parameters $(Q_1,\ Q_2,\ R)$, we evaluate matrix Φ by solving optimization problem (3.110). In particular, for $Q_1 = Q_2$, we get

$$\Phi = 1.3058 I_2, \tag{4.207}$$

while for $Q_2 = 10000 Q_1$, we have, respectively,

$$\Phi = 1060.2 I_2. \tag{4.208}$$

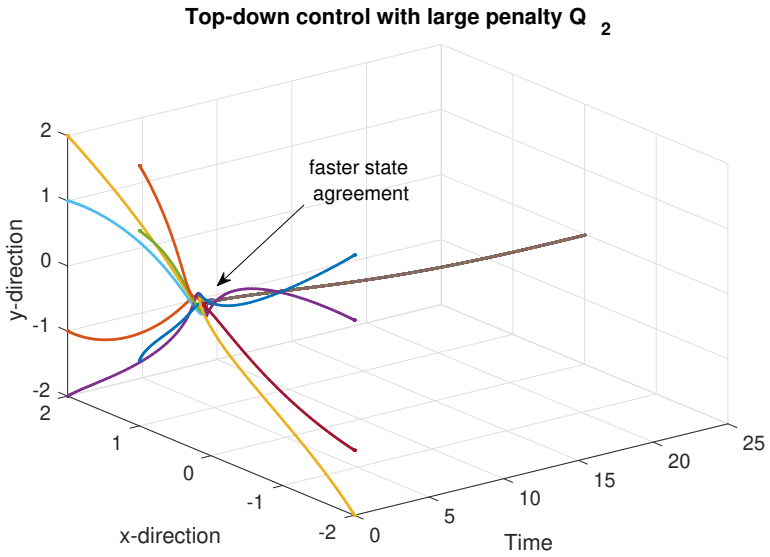

Fig. 4.4 Closed-loop behavior of the undirected distributed system under top-down control with large penalty Q_2.

The existence of matrix Φ such that problem (3.110) is feasible for both options of weighting parameters, guarantees network's closed-loop stability under control policy $\hat{u}_b$ as illustrated in Fig. 4.5 and Fig. 4.6. Viewing Fig. 4.3 and Fig. 4.5, it is obvious that both distributed control schemes regulate the network in a similar manner. On the contrary, despite agents reaching state-agreement under both distributed protocols, this objective is achieved relatively faster in simulation shown in Fig. 4.4 (with respect to the simulation shown in Fig. 4.6), with controller $\hat{u}_t$ outperforming control law $\hat{u}_b$. This is also evident from Table 4.1 where the top-down control $\hat{u}_t$ is approximately a thousand times less suboptimal than the bottom-up controller $\hat{u}_b$.

In order to compare the performance of the two control actions, we measure their suboptimality level with respect to an optimal centralized controller, as suggested in Section 3.3.7. Let $u^* = K^*\hat{x}$ be an optimal controller with $K^* = -\hat{R}^{-1}\hat{B}'P^*$. Matrix P^* is the symmetric positive definite solution to the large scale ARE with parameters $(\hat{A},\ \hat{B},\ \hat{Q},\ \hat{R})$, where $\hat{Q} = I_{11} \otimes Q_1 + \mathscr{L}_{G,11} \otimes Q_2$, and $\hat{R} = I_{11} \otimes R$. We denote by K_t and K_b the distributed state-feedback gain obtained from the top-down and bottom-up method, respectively.

As mentioned in Section 3.3.7, any norm of $\hat{P} - P^*$ can be cast as a measure of suboptimality of the corresponding distributed control scheme, where $\hat{P}$ is evaluated by the following Lyapunov equation:

$$(I_N \otimes A + (I_N \otimes B)\hat{K})'\hat{P} + \hat{P}(I_N \otimes A + (I_N \otimes B)\hat{K}) + (\hat{Q} + \hat{K}'\hat{R}\hat{K}) = 0, \tag{4.209}$$

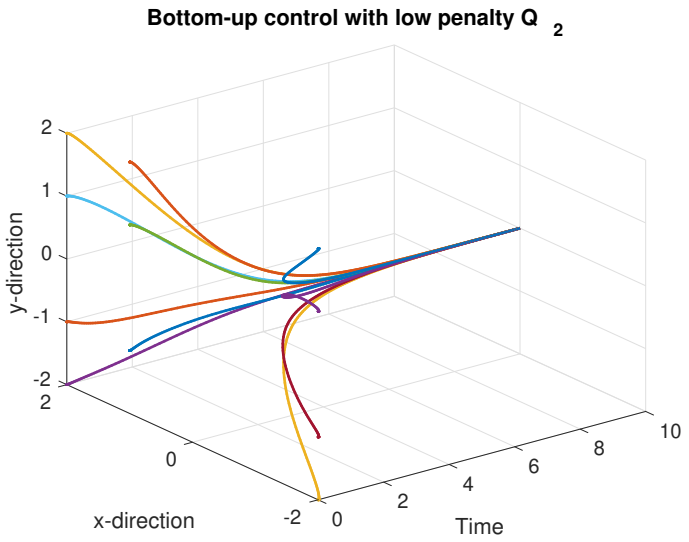

Fig. 4.5 Closed-loop behavior of the undirected distributed system under bottom-up control with low penalty Q_2.

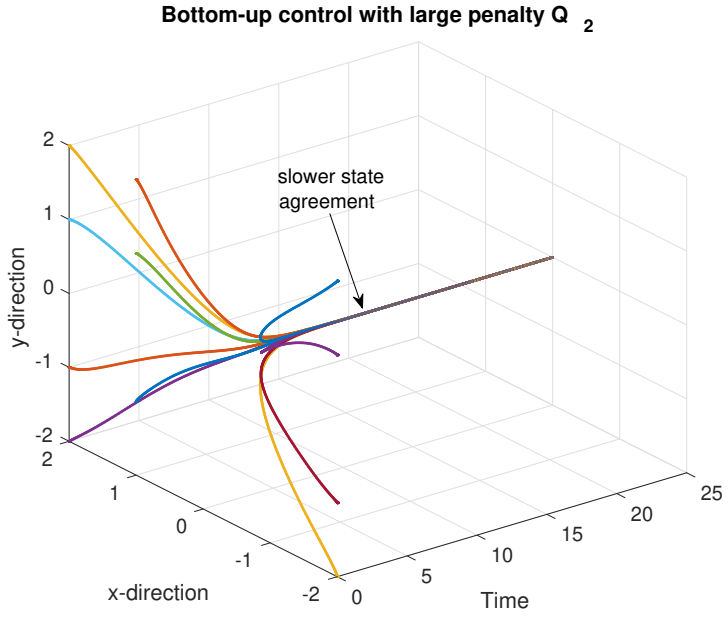

Fig. 4.6 Closed-loop behavior of the undirected distributed system under bottom-up control with large penalty Q_2.

$\lvert\hat{P}-P^*\rvert_F 10^{-8}$	$Q_2 = Q_1$	$Q_2 = 10^6 Q_1$
top-down	0.0016	0.058
bottom-up	1.0535	66.905

Table 4.1 Suboptimality measure of top-down and bottom-up schemes.

with $\hat{K}$ representing the distributed controllers K_t and K_b. The Frobenius norm of $\hat{P}-P^*$ for the various control settings is shown in Table 4.1.

While both distributed schemes are stabilizing, their performance differentiates considerably with respect to the optimal solution P^* as demonstrated in Table 4.1. Clearly, the top-down control strategy appears less expensive as well as less suboptimal in the Frobenius norm sense compared to the bottom-up setup.

Directed topology: Consider now the interconnection scheme shown in Fig. 4.2b. Here, we present simulations of the regulation problem (4.199) tuning the performance index in (4.199b) with $Q_2 = 10^6 Q_1$. The top-down control design is outlined next.

Matrices K_1, K_2 in (4.199d) are defined by solving an LQR problem (3.65), with weights $(Q_1,\ Q_2,\ R)$, for N_L systems. As mentioned in Section 4.3.4, N_L can be selected as $d_{\max}+2$, $d_{\max}$ denoting the maximum vertex in-degree of $\mathscr{D}_{11}$. Clearly, $d_{\max}=3$, then $N_L = d_{\max}+2 = 5$ suggesting that K_1 and K_2 may be selected as defined in (4.202). The distributed top-down controller is denoted by:

$$\bar{u}_t = (I_{11} \otimes \underbrace{(-R^{-1}B'P)}_{K_1} + \underbrace{\bar{\gamma}\mathscr{L}_{G,11}}_{M} \otimes \underbrace{(R^{-1}B'\tilde{P}_2)}_{K_2})\hat{x}, \tag{4.210}$$

where the selection of parameter $\bar{\gamma}$ guarantees stability of the directed network. In view of condition (4.91), we may choose any

$$\bar{\gamma} > \frac{N_L}{2\mathbf{Re}(\lambda_2)}, \tag{4.211}$$

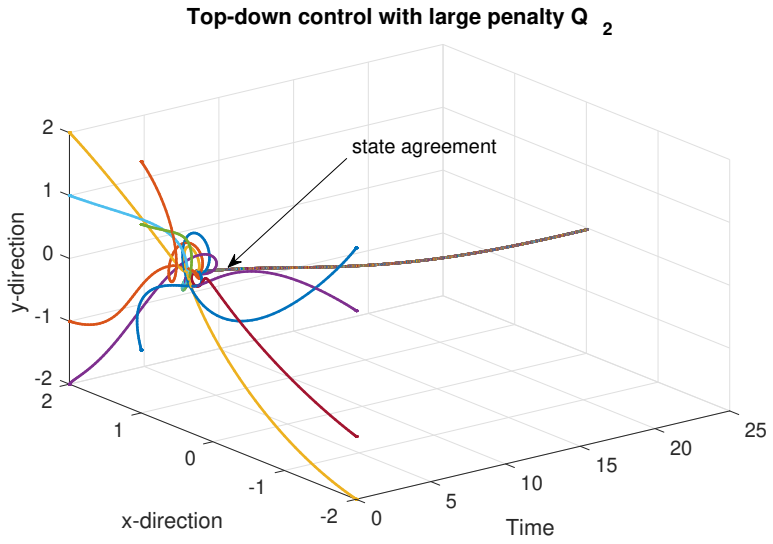

Fig. 4.7 Closed-loop behavior of the directed distributed system under top-down control with large penalty Q_2.

where λ_2 denotes the non-zero eigenvalue of $\mathscr{L}_{D,11}$ with the smallest real part. Calculating the Jordan matrix of $\mathscr{L}_{D,11}$:

$$J(\Lambda) = \begin{bmatrix} 0 & & & & & & & & & & & & & & \\ & 1 & 0 & & & & & & & & & & & & \\ & 0 & 1 & & & & & & & & & & & & \\ & & & 2 & 1 & 0 & & & & & & & & & \\ & & & 0 & 2 & 1 & & & & & & & & & \\ & & & 0 & 0 & 2 & & & & & & & & & \\ & & & & & & 2.76 & & & & & & & & \\ & & & & & & & 1.13+\mathrm{i}0.75 & & & & & & & \\ & & & & & & & & 1.13-\mathrm{i}0.75 & & & & & & \\ & & & & & & & & & 2.5+\mathrm{i}0.87 & & & & & \\ & & & & & & & & & & 2.5-\mathrm{i}0.87 & & & & \end{bmatrix}, \tag{4.212}$$

where $\mathrm{i}^2 = -1$, clearly, $\lambda_2 = 1$, and hence $\bar{\gamma} > 2.5$. The simulation shown in Fig. 4.7 illustrates the behavior of the directed network under the control law $\bar{u}_t$ with $\bar{\gamma} = 4$. Evidently, network's stability is maintained for $\bar{\gamma} = 4$, while any violation of condition (4.211) might result in instability phenomena as highlighted in Fig. 4.8.

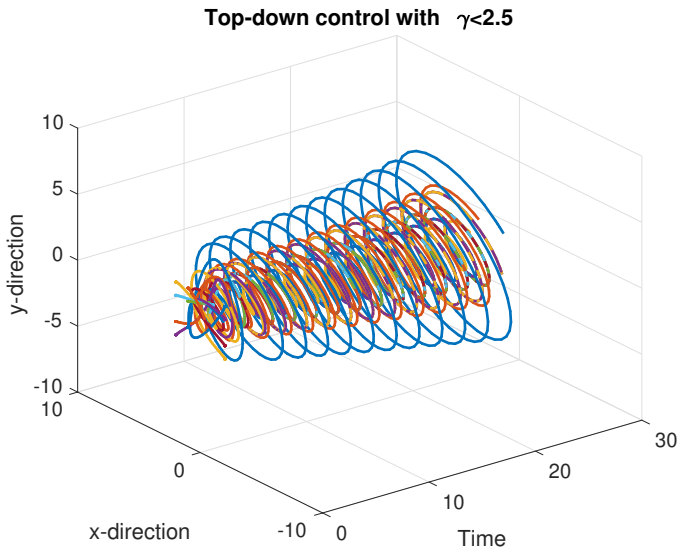

Fig. 4.8 Unstable behavior of the top-down directed distributed system for $\bar{\gamma} < 2.5$.

The design of distributed controller via the bottom-up method presented in Section 4.3.5 finalizes the numerical study. The control scheme, here, is denoted as

$$\bar{u}_b = (I_{11} \otimes \underbrace{(-R^{-1}B'P)}_{K_1} + \underbrace{\mathscr{L}_{G,11}}_{M} \otimes \Phi \underbrace{(-R^{-1}B'P)}_{K_2})\hat{x}, \tag{4.213}$$

where matrix P is defined as in (4.210). The design of matrix Φ depends on the feasible solution of problem (4.171) for a particular choice of weighting parameters. Optimization problem (4.171) is solved subject to $1+\nu+\mu$ constraints corresponding to $\nu+1$ real eigenvalues of $\mathscr{L}_{D,11}$ and μ complex Laplacian eigenvalues, (ν,μ) indicated in Table 4.2. Then, for weighting matrices $(Q_1,\ Q_2,\ R)$, as defined earlier with $Q_2 = 10^6 Q_1$, (4.171) is feasible and formula (4.172) yields:

$$\Phi = 9560.5 I_2. \tag{4.214}$$

The existence of Φ guarantees that $\bar{u}_b$ is a stabilizing distributed controller as illustrated in Fig. 4.9.

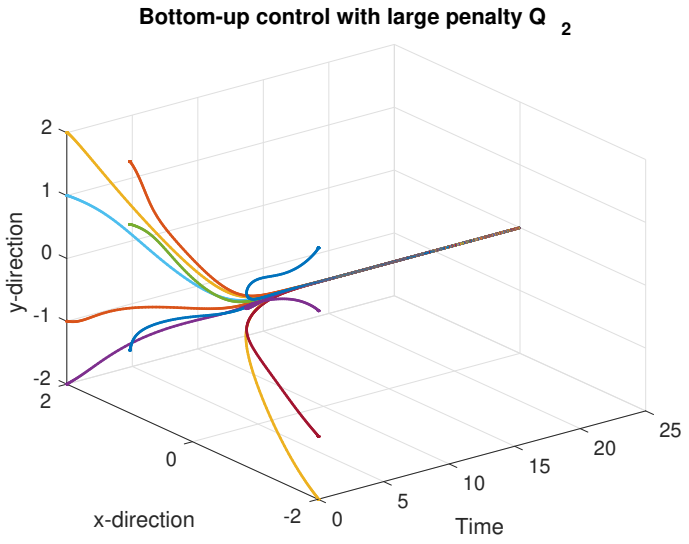

Fig. 4.9 Closed-loop behavior of the directed distributed system under bottom-up control with large penalty Q_2.

Eigenvalue	AM	GM	index ν	index μ
0	1	1	1	-
1	2	2	2	-
2	3	1	3	-
2.76	1	1	4	-
$1.13 \pm i0.75$	1	1	-	5
$2.5 \pm i0.87$	1	1	-	6

Table 4.2 Algebraic and geometric multiplicity (AM, GM) of the eigenvalues of $\mathscr{L}_{D,11}$.

4.4 Conclusion

In the first part of the chapter, a new distributed control method for solving a regulator problem of networked systems with undirected topology is proposed. The control design is introduced via a two-stage optimization approach which combines techniques from the top-down [17] and bottom-up [46] method presented in Chapter 3. Sufficient conditions for stability of the new distributed scheme are derived minimizing an upper bound of the global LQR criterion. Regulation problems over networks with directed topology are discussed in the second part of the chapter. Therein, we prove that the strict assumption of bidirectional communication between interconnected agents, postulated in the original version of the

aforementioned control techniques [17, 46] can be removed. We show that this relaxation relies on two elegant facts: 1) the gain-margin property of LQR control holds true for complex multiplicative perturbations, and 2) the potentially non-simple structure of the Laplacian matrix can be neglected for stability analysis and control design. These results highlight the main contributions of the chapter. A numerical study in the end of the chapter, attempts to illustrate these contributions. Having examined large-scale regulation problems of multi-agent networks of identical systems, we wish to tackle the stabilization problem of heterogeneous interconnected agents. This task is studied in the following chapter, where a general class of interconnected systems sharing common structural properties is introduced.

Chapter 5

Model-matching and regulation of interconnected heterogeneous linear agents

5.1 Introduction

The top-down [17] and bottom-up [46] control strategies presented in Chapter 3 have proved very powerful for designing distributed state-feedback controllers and tackling stabilization problems of multi-agent networks. Notable advantages of these two approaches are the results of two main simplifying assumptions compared to a general structured optimal design: 1) identical subsystem dynamics, and 2) undirected network topology. As shown in Chapter 4, the structural requirement of network's bidirectional connectivity can be relaxed for both methods via slight modifications. In this chapter, we wish to remove the strong assumption of agents' identical dynamics, which evidently might be unrealistic for certain applications. In essence, we replace this stringent limitation with a more natural requirement and consider a broader class of networked systems. In particular, we formulate a regulator problem of N interconnected heterogeneous agents as follows:

$$\min_{\hat{u}} J(\hat{u},\hat{x}_0) \;\text{ subject to:} \tag{5.1a}$$

$$J(\hat{u},\hat{x}_0) = \int_0^\infty \left(\hat{x}'\hat{Q}\hat{x} + \hat{u}'\hat{R}\hat{u}\right) \mathrm{dt}, \tag{5.1b}$$

$$\dot{\hat{x}} = \hat{A}\hat{x} + \hat{B}\hat{u},\ \hat{x}(0) = \hat{x}_0, \tag{5.1c}$$

$$\hat{u} = \mathscr{M}\hat{x}, \tag{5.1d}$$

where

$$\hat{A} = \text{diag}(A_1, \ldots, A_N), \tag{5.2}$$

$$\hat{B} = \text{diag}(B_1, \ldots, B_N), \tag{5.3}$$

and $\mathscr{M} \in \mathscr{K}^N_{m,n}(\mathscr{G})$ ($\mathscr{M} \in \mathscr{K}^N_{m,n}(\mathscr{D})$), with $\mathscr{G}$ ($\mathscr{D}$) denoting an undirected (directed) graph. The lack of homogeneity among the agents is clearly identified in (5.1c), with systems $(A_i,\ B_i)$, $i = 1, \ldots, N$ being generically non-identical. This represents the main difference of problem (5.1) with respect to regulator problems examined in Chapter 3 and Chapter 4.

Here, we attempt to solve problem (5.1) via a two-stage control strategy. In the first stage, we follow a model-matching approach to the network stabilization problem and assume that agents constituting the network have same structural properties. These are completely characterized by a set of integers referred to as controllability indices. Local state-feedback control and input-matrix transformations are used to solve model-matching type-problems and compensate for dynamical mismatch among the models of the agents. We emphasize that in our case, the definition of "model-matching" (in contrast to other "exact model-matching" problems defined in the literature) gives us considerable flexibility. In the present context, the output matrices of the mapped systems are required to be square and invertible but are otherwise arbitrary. In effect, the model of each agent matches the input-to-state part of a target system via state-feedback control and input matrix scaling. It is shown that the distributed control methods (top-down, bottom-up) presented earlier, can also be utilized in the present setting, simply by constructing stabilizing distributed controllers depending on the target dynamics only. This represents the second stage of the control design.

It is also shown, that the selection of the target model can be specified such that the perturbations in the agents' models produced by state-feedback controllers are minimal in a sense which is clearly defined. In this respect, the definition of target dynamics is achieved by minimizing a measure of the joint model-matching control effort. This allows closed-loop network performance to depend primarily on the LQR optimality criterion (5.1b), defined and optimized in the second stage of our approach.

In the chapter, a special case of multi-input systems is also considered in which agents are mapped to a single-input target system. This leads to the solution of the stabilization problem of networks composed of generic heterogeneous agent models of the same state dimension, of course at the expense of the number of independent input variables of each agent. Next, we formulate a general model-matching task and subsequently define a special class of systems for which the model-matching problem always admits of a solution.

5.2 Model-matching control

5.2.1 Problem definition

Throughout the chapter, we consider linear time-invariant systems referring to them as systems. Initially, we wish to identify a well-defined class of systems the state-space form of which can be mapped to a certain model (characterized in the sequel as target system, target model or target dynamics) via similarity transformations, state-feedback control, and input-matrix scaling. Next, we define the model-matching task of a set of systems as follows:

Problem 5.2.1. Consider $N+1$ controllable multi-input linear systems described by the state-space equation:

$$\dot{x}_i = A_i x_i + B_i u_i,\ x_i(0) = x_{i,0},\ i = 1,\ldots,N, \tag{5.4}$$

with $A_i \in \mathbb{R}^{n\times n}$, $B_i \in \mathbb{R}^{n\times m}$, and $\text{rank}(B_i) = m$. Let the pair $(A_{N+1},\ B_{N+1})$ pertain to the target dynamics. Then, we wish to find matrices P_i, F_i, and G_i of appropriate dimensions with $\det(P_i) \neq 0$ and $\det(G_i) \neq 0$ such that:

$$P_i(A_i + B_i F_i)P_i^{-1} = A_{N+1}, \tag{5.5}$$

$$P_i B_i G_i = B_{N+1}, \tag{5.6}$$

for $i = 1,\ldots,N$. □

Problem 5.2.1 involves the control design $u_i = F_i x_i + G_i v_i$, $v_i \in \mathbb{R}^m$, $i = 1,\ldots,N$, whereby N systems match their dynamics with a target model denoted as $(A_{N+1},\ B_{N+1})$. It also involves matrices P_i, $i = 1,\ldots,N$, which represent similarity transformations accommodating a change of local coordinates. In the following, the special class of systems with common controllability indices is defined. It will be shown that a solution to Problem 5.2.1 is always guaranteed for this family of systems. Some basic concepts of linear control theory, which are useful in our definitions and proofs, are introduced next.

5.2.2 Controllability indices of multi-input systems

In the following, we recall the notion of controllability indices of a controllable system $(A,\ B)$. Let

$$\dot{x} = Ax + Bu,\ x(0) = x_0, \tag{5.7}$$

be the state-space form of a controllable system $(A,\ B)$, where $A \in \mathbb{R}^{n\times n}$, $B \in \mathbb{R}^{n\times m}$, with $\text{rank}(B) = m$. Let also

$$\begin{aligned}\mathscr{C} &= [B,\ AB,\ \ldots,\ A^{n-1}B],\\ &= [b_1,\ \ldots,\ b_m,\ Ab_1,\ \ldots,\ Ab_m,\ \ldots,\ A^{n-1}b_1,\ \ldots,\ A^{n-1}b_m],\end{aligned} \tag{5.8}$$

be the controllability matrix of the pair $(A,\ B)$, where $b_1,\ldots,b_m$ represent the columns of B, and $\mathscr{C} \in \mathbb{R}^{n\times nm}$. Since $(A,\ B)$ is controllable, $\text{rank}(\mathscr{C}) = n$. Now, collect the first n linearly independent columns of $\mathscr{C}$ starting form the left and moving to the right; rearrange these columns to obtain

$$\bar{\mathscr{C}} = [b_1,\ Ab_1,\ \ldots,\ A^{\mu_1-1}b_1,\ \ldots,\ b_m,\ Ab_m,\ \ldots,\ A^{\mu_m-1}b_m], \tag{5.9}$$

where $\bar{\mathscr{C}} \in \mathbb{R}^{n\times n}$. The integer μ_j denotes the number of columns involving b_j in the set of the first n linearly independent columns of $\mathscr{C}$ while moving from left to right. The set of μ_j's is defined next.

Definition 5.2.1. The set of m integers $\{\mu_1,\ldots,\mu_m\}$, as defined in (5.9), with $\sum_{j=1}^{m}\mu_j = n$, represents the controllability indices of the controllable pair $(A,\ B)$ with $A \in \mathbb{R}^{n\times n}$, $B \in \mathbb{R}^{n\times m}$, and $\text{rank}(B) = m$.

The family of systems to be considered in this chapter is defined by the class of controllable systems with identical sets of controllability indices. In particular, we are interested in studying stabilizing (distributed) state-feedback solutions to the regulation problem (5.1) focusing on networks of non-identical agents with identical sets of controllability indices. The following lemma is standard and is included without proof, [5].

Lemma 5.2.2. *Given $(A,\ B)$ is controllable, then $(P(A+BF)P^{-1},\ PBG)$ has the same controllability indices (c.i.), up to reordering, for any P, F, and G ($\det(P) \neq 0$, $\det(G) \neq 0$) of appropriate dimensions.*

Lemma 5.2.2 states that the c.i. of a controllable pair $(A,\ B)$ is an invariant set under a state-space transformation P, a state-feedback control F, and an input scaling G. Pertaining to a set of systems $(A_i,\ B_i)$, $i = 1,\ldots,N$, characterized by identical sets of c.i., Lemma 5.2.2 also implies that pairs $(P_i(A_i+B_iF_i)P_i^{-1},\ P_iB_iG_i)$, $i = 1,\ldots,N$, coincide, for a certain choice of P_i, F_i, and G_i, $i = 1,\ldots,N$. This becomes evident in the following section.

5.2.3 Model-matching existence

We consider a set of N systems the dynamics of which are described by the state-space form rewritten here as:

$$\dot{x}_i = A_i x_i + B_i u_i,\ x_i(0) = x_{i,0},\ i = 1,\ldots,N, \tag{5.10}$$

where $x_i \in \mathbb{R}^n$, $u_i \in \mathbb{R}^m$ are the states and inputs of the i-th system, respectively. Let integers $\mu_1,\ldots,\mu_m$ be the controllability indices of the pairs $(A_i,\ B_i)$, $i = 1,\ldots,N$. Let also matrix P_i represent the similarity transformation that brings the i-th pair $(A_i,\ B_i)$ into controllable canonical form. We refer readers to [5] (Chapter 3, Section 3.4), for how to construct matrix P_i. Changing coordinates to $x_{c,i} = P_i x_i$, the i-th state-space form in the new coordinate system becomes

$$\dot{x}_{c,i} = A_{c,i} x_{c,i} + B_{c,i} u_i,\ x_{c,i}(0) = P_i x_{i,0}, \tag{5.11}$$

where $x_i = P_i^{-1} x_{c,i}$ represents the state vector x_i in the original coordinates. Matrices $A_{c,i}$, $B_{c,i}$ can be decomposed as follows:

$$A_{c,i} = \bar{A}_c + \bar{B}_c A_{m,i}, \tag{5.12a}$$

$$B_{c,i} = \bar{B}_c B_{m,i}, \tag{5.12b}$$

with $\bar{A}_c \in \mathbb{R}^{n\times n}$, $\bar{B}_c \in \mathbb{R}^{n\times m}$, $A_{m,i} \in \mathbb{R}^{m\times n}$ and $B_{m,i} \in \mathbb{R}^{m\times m}$. The pair $(\bar{A}_c,\ \bar{B}_c)$ is called the Brunovsky canonical form and is unique for all systems with identical sets of controllability indices. Detailed description of the Brunovsky form can be found in [5]. By definition, matrices $(A_{m,i},\ B_{m,i})$ are not fixed; Later, we show that the selection of a target model relies on these two matrices. The Brunovsky form $(\bar{A}_c,\ \bar{B}_c)$ has a block-diagonal structure as shown below:

$$\bar{A}_c = \mathrm{diag}(\bar{A}_{11},\ldots,\bar{A}_{mm}), \tag{5.13a}$$

$$\bar{B}_c = \mathrm{diag}(\bar{B}_{11},\ldots,\bar{B}_{mm}) \tag{5.13b}$$

where

$$\bar{A}_{jj} = \begin{bmatrix} 0 & \\ \vdots & I_{\mu_j-1} \\ 0 & \\ 0 & 0\cdots 0 \end{bmatrix} \in \mathbb{R}^{\mu_j \times \mu_j}, \tag{5.14a}$$

$$\bar{B}_{jj} = \begin{bmatrix} 0 \\ \vdots \\ 0 \\ 1 \end{bmatrix} \in \mathbb{R}^{\mu_j}, \tag{5.14b}$$

for $j = 1, \ldots, m$. We note here that the diagonal blocks in (5.14) are completely defined by the controllability indices $\mu_1, \ldots, \mu_m$. Consider now a target system denoted as $(A_{N+1},\ B_{N+1})$, and assume the pair $(A_{N+1},\ B_{N+1})$ has common c.i. with the remaining systems in the set. This implies identical Brunovsky forms for all $N+1$ systems. Without loss of generality, let $(A_{N+1},\ B_{N+1})$ be in canonical form. The state-space form of the target system is written as

$$\dot{x}_{N+1} = A_{N+1}x_{N+1} + B_{N+1}u_{N+1}, \tag{5.15}$$

where

$$A_{N+1} = \bar{A}_c + \bar{B}_c A_{m,N+1}, \tag{5.16a}$$

$$B_{N+1} = \bar{B}_c B_{m,N+1}. \tag{5.16b}$$

The pair $(\bar{A}_c,\ \bar{B}_c)$ represents the Brunovsky form with c.i. $\mu_1, \ldots, \mu_m$, while matrices $A_{m,N+1}$, $B_{m,N+1}$ are as defined earlier. Viewing (5.12) and (5.16), there is no ambiguity that matching $(A_{c,i},\ B_{c,i})$, $i = 1, \ldots, N$, with $(A_{N+1},\ B_{N+1})$ depends exclusively on matrices $A_{m,i}$, $B_{m,i}$, $i = 1, \ldots, N+1$. It is also clear that Problem 5.2.1 has a solution if and only if the $N+1$ systems have identical sets of controllability indices. This is expressed in the following theorem.

Theorem 5.2.3. *Consider N controllable systems $(A_i,\ B_i)$, with $A_i \in \mathbb{R}^{n\times n}$, $B_i \in \mathbb{R}^{n\times m}$,* $\operatorname{rank}(B_i) = m$, *$i = 1, \ldots, N$, and state-space form given in* (5.10)*. Let a target system be described by the state-space form:*

$$\dot{x}_{N+1} = A_{N+1}x_{N+1} + B_{N+1}u_{N+1}, \tag{5.17}$$

and assume that all pairs $(A_i,\ B_i)$, $i = 1,\ldots,N+1$ *have identical c.i.,* $\mu_1,\ldots,\mu_m$. *Then, there are always matrices* F_i, *and* G_i, *defined as*

$$\begin{aligned} F_i &= B_{m,i}^{-1}(A_{m,N+1} - A_{m,i})P_i, \\ G_i &= B_{m,i}^{-1}B_{m,N+1}, \end{aligned} \tag{5.18}$$

respectively, such that

$$\begin{aligned} \Phi_i^{-1}(A_i + B_iF_i)\Phi_i &= A_{N+1}, \\ \Phi_i^{-1}B_iG_i &= B_{N+1}, \end{aligned} \tag{5.19}$$

where $(A_{m,i},\ B_{m,i})$, $i = 1,\ldots,N$, *are defined in* (5.12), *pair* $(A_{m,N+1}, B_{m,N+1})$ *is defined in* (5.16), *and* $\Phi_i = P_i^{-1}P_{N+1}$, $i = 1,\ldots,N$, *with* $\det(\Phi_i) \neq 0$. *Matrices* P_i, $i = 1,\ldots,N+1$, *represent similarity transformations that bring the state-space form of the systems in a controllable canonical form.*

Proof. We denote by

$$\dot{x}_i = A_ix_i + B_iu_i, \tag{5.20}$$

the state-space form of the i-th system, with $i = 1,\ldots,N+1$, index $N+1$ referring to the target model, and we consider a change of coordinates $x_{c,i} = P_ix_i$, $i = 1,\ldots,N+1$. Applying

$$u_i = F_{c,i}x_{c,i} + G_iv_i, \tag{5.21}$$

for $i = 1,\ldots,N$, the closed-loop state-space form of the i-th system in the new coordinates is written as:

$$\dot{x}_{c,i} = (A_{c,i} + B_{c,i}F_{c,i})x_{c,i} + B_{c,i}G_iv_i, \tag{5.22a}$$

$$x_i = P_i^{-1}x_{c,i}. \tag{5.22b}$$

We require that

$$A_{c,i} + B_{c,i}F_{c,i} = A_{c,N+1} \tag{5.23a}$$

$$B_{c,i}G_i = B_{c,N+1}, \tag{5.23b}$$

for $i = 1,\ldots,N$. Since the pairs $(A_{c,i},\ B_{c,i})$, $i = 1,\ldots,N+1$, have identical c.i., thereby having identical Brunovsky form denoted as $(\bar{A}_c,\ \bar{B}_c)$, (5.23) leads to

$$F_{c,i} = B_{m,i}^{-1}(A_{m,N+1} - A_{m,i}), \tag{5.24a}$$

$$G_i = B_{m,i}^{-1}B_{m,N+1}, \tag{5.24b}$$

where $\det(B_{m,i}) \neq 0$ since, by assumption, $\text{rank}(B_i) = m$, $i = 1,\ldots,N$. From (5.23) we also write that

$$P_i(A_i + B_iF_i)P_i^{-1} = P_{N+1}A_{N+1}P_{N+1}^{-1} \tag{5.25a}$$

$$P_iB_iG_i = P_{N+1}B_{N+1}, \tag{5.25b}$$

or

$$A_i + B_iF_i = P_i^{-1}P_{N+1}A_{N+1}P_{N+1}^{-1}P_i \tag{5.26a}$$

$$B_iG_i = P_i^{-1}P_{N+1}B_{N+1}, \tag{5.26b}$$

where

$$F_i = B_{m,i}^{-1}(A_{m,N+1} - A_{m,i})P_i, \tag{5.27}$$

for $i = 1,\ldots,N$. Denoting $\Phi_i = P_i^{-1}P_{N+1}$ in (5.26) proves (5.19) while (5.24) along with (5.27) proves (5.18). □

For a family of N systems with identical sets of controllability indices, Theorem 5.2.3 essentially guarantees the existence of state-feedback gains F_i and input-matrix scaling transformations G_i such that:

$$\dot{x}_i = (A_i + B_iF_i)x_i + B_iG_iv_i, \tag{5.28}$$

$$\xi = \Phi_i^{-1}x_i, \tag{5.29}$$

for all $i = 1,\ldots,N$ where $\Phi_i = P_i^{-1}P_{N+1}$, with P_i, P_{N+1} as defined in the theorem. Since (5.29) represents a one-to-one linear map, Φ_i can be cast as a nonsingular output matrix of the i-th system. Note also that for identical initial conditions $x_{i,0}$, and controls v_i, $i = 1,\ldots,N$, the output trajectories of (5.28)-(5.29) coincide for all $i = 1,\ldots,N$, and are denoted as $\xi(t)$. Variable ξ can be seen as the state of the target model:

$$\dot{x}_{N+1} = A_{N+1}x_{N+1} + B_{N+1}u_{N+1}, \tag{5.30}$$

$$\xi = x_{N+1}. \tag{5.31}$$

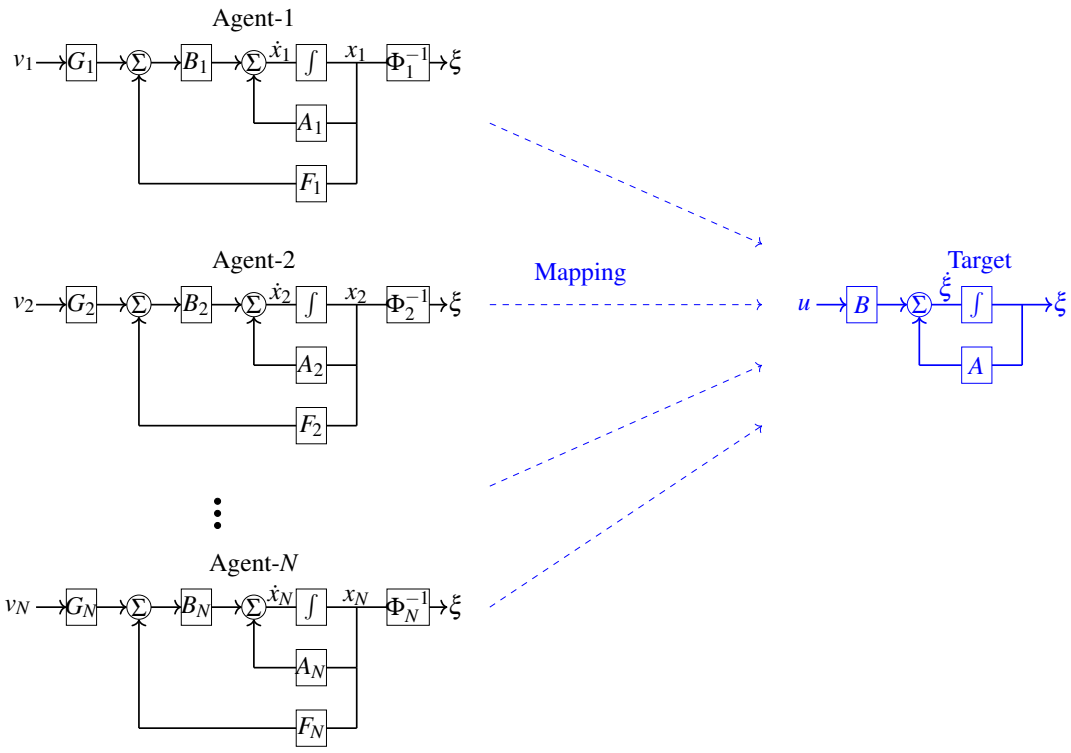

Fig. 5.1 Schematic representation of N agents matching the target dynamics.

This is also highlighted in Fig. 5.1 where the target system is denoted as $(A,\ B)$. We remark that the state-feedback and input-matrix operations defined in (5.18), represent the model-matching design of N systems with a target model specified a priori. In the following section, we introduce further existence conditions that are useful for the model-matching control synthesis.

5.2.4 Model-matching control synthesis

Consider a set of N controllable systems $(A_i,\ B_i)$ with

$$A_i = A_o + B_i Z_i, \tag{5.32a}$$

$$B_i = B_o G_i^{-1}, \tag{5.32b}$$

for $i = 1,\ldots,N$. Here $A_o \in \mathbb{R}^{n\times n}$ is assumed to be a fixed matrix, $Z_i \in \mathbb{R}^{m\times n}$ an arbitrary matrix, and $G_i \in \mathbb{R}^{m\times m}$ an arbitrary and nonsingular matrix for all $i = 1,\ldots,N$. Note that if all pairs $(A_i,\ B_i)$, $i = 1,\ldots,N$, have identical sets of controllability indices, their controllable canonical forms

$$(A_{c,i},\ B_{c,i}) = (P_i A_i P_i^{-1},\ P_i B_i),\ i = 1,\ldots,N, \tag{5.33}$$

satisfy condition (5.32). In this case, $(A_o,\ B_o) = (\bar{A}_c,\ \bar{B}_c)$ represents the Brunovsky form of all pairs $(A_i,\ B_i)$, $i = 1,\ldots,N$ with common controllability indices. Clearly, a possible target pair $(A_{N+1},\ B_{N+1})$ has to satisfy condition (5.32). The following lemma guarantees the existence of a input matrix transformation that maps B_i, $i = 1,\ldots,N$, matrices to a target (input) matrix denoted as B_{N+1}. In the following, let $\mathrm{Im}(\cdot)$ denote the subspace spanned by the columns of a matrix.

Lemma 5.2.4. *Let matrices $B_i \in \mathbb{R}^{n\times m}$, $i = 1,\ldots,N$, have full-column rank. Then, there are a matrix $B_o \in \mathbb{R}^{n\times m}$, and square and nonsingular matrices $G_i \in \mathbb{R}^{m\times m}$, $i = 1,\ldots,N$, such that $B_iG_i = B_o\ \forall i$, if and only if* $\mathrm{Im}(B_1) = \mathrm{Im}(B_2) = \cdots = \mathrm{Im}(B_N)$.

Proof. (i) Necessity: Let $\mathrm{Im}(B_i) = \mathscr{X} \subseteq \mathbb{R}^n$ with $\dim(\mathscr{X}) = m$. Then, B_i has a singular value decomposition:

$$B_i = U\Sigma_i V_i',\ i = 1,\ldots,N, \tag{5.34}$$

with $\mathrm{Im}(B_i) = \mathrm{Im}(U) = \mathscr{X}$ and $U'U = I_m$, $\det(\Sigma_i) \neq 0$, $V_i'V_i = V_iV_i' = I_m$. Define: $G_i = V_i\Sigma_i^{-1}$, $B_o = U$. Then, $B_iG_i = U\Sigma_iV_i'V_i\Sigma_i^{-1} = U = B_o$. (ii) Sufficiency is immediate. □

For simplicity, the matching problem 5.2.1 of N systems $(A_i,\ B_i)$, $i = 1,\ldots,N$, with structure as in (5.32), is first solved for $N = 2$ systems, and it is then generalized for an arbitrary number N. Consider the controllable pairs $(A_1,\ B_1)$, $(A_2,\ B_2)$ with $A_i \in \mathbb{R}^{n\times n}$, $B_i \in \mathbb{R}^{n\times m}$, $i = 1,2$. Assume that there are F_1, F_2 such that

$$A_1 + B_1F_1 = A_2 + B_2F_2, \tag{5.35}$$

and matrices B_1, B_2 satisfying Lemma 5.2.4. Let now $F_i = Y_iX_i^{-1}$, with $Y_i \in \mathbb{R}^{m\times n}$, and $X_i \in \mathbb{R}^{n\times n}$ being symmetric positive definite (s.p.d.), for $i = 1,2$. Then, (5.35) can be rewritten as:

$$A_1 + B_1Y_1X_1^{-1} = A_2 + B_2Y_2X_2^{-1}. \tag{5.36}$$

Assume there exists (s.p.d) $X \in \mathbb{R}^{n\times n}$ such that (5.35) gives

$$A_1 + B_1Y_1X^{-1} = A_2 + B_2Y_2X^{-1}, \tag{5.37}$$

which is then post-multiplied by X on both sides and results in

$$A_1X + B_1Y_1 = A_2X + B_2Y_2. \tag{5.38}$$

The following theorem generalizes the previous analysis to the case of N systems. First, we define a special class of systems.

Definition 5.2.2. Let $(A_o,\ B_o) \in \mathbb{R}^{n\times n} \times \mathbb{R}^{n\times m}$, with $\text{rank}(B_o) = m$. Define the set:

$$S(A_o,\ B_o) = \{(A_o + B_o Z,\ B_o G^{-1}) :\ Z \in \mathbb{R}^{m\times n},\ G \in \mathbb{R}^{m\times m} \text{ with } \det G \neq 0\}. \tag{5.39}$$

Theorem 5.2.5.

(*i*) *Let* $(A_i,\ B_i) \in S(A_o,\ B_o)$, $i = 1,\ldots,N$. *Then,* $\text{Im}(B_i) = \text{Im}(B_o)$, $\forall i = 1,\ldots,N$ *and there exist* $X \in \mathbb{R}^{n\times n}$, $X = X' > 0$, $Y_i \in \mathbb{R}^{m\times n}$ *such that*

$$A_i X + B_i Y_i - A_j X - B_j Y_j = 0, \tag{5.40}$$

for every pair $(i,j) \in \{1,2,\ldots,N\}^2$.

(*ii*) *Conversely, let* $\{(A_i,\ B_i)\}_{i=1}^N$ *be given with* $\text{Im}(B_i) = \mathscr{X} \subseteq \mathbb{R}^n$, $\forall i = 1,\ldots,N$, *and* $\dim(\mathscr{X}) = m$. *Suppose also that* (5.40) *is true for every pair* $(i,j) \in \{1,2,\ldots,N\}^2$ *for some* $X \in \mathbb{R}^{n\times n}$, $X = X' > 0$, *and* $\{Y_i\}_{i=1}^N$, $Y_i \in \mathbb{R}^{m\times n}$, $i = 1,\ldots,N$. *Then, there exist matrices* $A_o \in \mathbb{R}^{n\times n}$, *and* $B_o \in \mathbb{R}^{n\times m}$, *with* $\text{Im}(B_o) = \mathscr{X}$, *such that*

$$(A_i,\ B_i) = S(A_o,\ B_o), \tag{5.41}$$

for all $i \in \{1,\ldots,N\}$.

Note: If (5.40) *holds for* $X = X' > 0$ *and* $\{Y_i\}_{i=1}^N$, *then, for all* (5.40) $\exists \{F_i\}_{i=1}^N$, $F_i \in \mathbb{R}^{m\times n}$ *such that*

$$A_i + B_i F_i = A_j + B_j F_j, \tag{5.42}$$

for every pair $(i,j) \in \{1,2,\ldots,N\}^2$.

Proof. (*i*) If $(A_i,\ B_i) \in S(A_o,\ B_o)$, $i \in \{1,\ldots,N\}$, then

$$A_i = A_o + B_o Z_i \text{ and } B_i = B_o G_i^{-1}, \tag{5.43}$$

for $Z_i \in \mathbb{R}^{m\times n}$, $G_i \in \mathbb{R}^{m\times m}$, $\det(G_i) \neq 0$. Then, $B_i G_i = B_o$, $\forall i \in \{1,\ldots,N\}$, and hence, $\text{Im}(B_i) = \text{Im}(B_o)$, $\forall i \in \{1,\ldots,N\}$. Let $X = I_n$, $Y_i = -G_i Z_i$. Then, $\forall (i,j) \in \{1,\ldots,N\}^2$,

$$A_i X + B_i Y_i - A_j X - B_j Y_j = (A_o + B_o Z_i) I_n + B_o G_i^{-1}(-G_i Z_i) \tag{5.44}$$

$$- (A_o + B_o Z_j) I_n - B_o G_j^{-1}(-G_j Z_j) = 0, \tag{5.45}$$

as required. (ii) Conversely, let $\{(A_i,\, B_i)\}_{i=1}^{N}$ be given with $\mathrm{Im}(B_i) = \mathscr{X} \subseteq \mathbb{R}^n$, $\dim(\mathscr{X}) = m$. Then, let B_i have a singular value decomposition

$$B_i = \begin{bmatrix} U_1 & U_2 \end{bmatrix} \begin{bmatrix} \Sigma_i \\ 0 \end{bmatrix} V_i', \tag{5.46}$$

for $i = 1,\ldots,N$, with $U_1 \in \mathbb{R}^{n\times m}$, $\mathrm{Im}(U_1) = \mathrm{Im}(B_i) = \mathscr{X}$, $\mathrm{Im}(U_2) = \mathscr{X}^{\perp}$, $\det(\Sigma_i) \neq 0$ and $V_i'V_i = V_iV_i' = I_m$. Define $B_o = U_1$, $G_i = V_i\Sigma_i^{-1}$, for $i = 1,\ldots,N$. Then,

$$B_iG_i = U_1\Sigma_iV_i'V_i\Sigma_i^{-1} = U_1 = B_o, \tag{5.47}$$

which implies that $B_i = B_oG_i^{-1}$, $i = 1,\ldots,N$. Further, $\forall (i,j) \in \{1,\ldots,N\}^2$:

$$\begin{aligned}
&A_iX + B_iY_i - A_jX - B_jY_j = 0, && (5.48)\\
&\implies (A_i - A_j)X + B_oG_i^{-1}Y_i - B_oG_j^{-1}Y_j = 0, && (5.49)\\
&\implies A_i - A_j = B_o(G_j^{-1}Y_j - G_i^{-1}Y_i)X^{-1}, && (5.50)\\
&\implies U_2'(A_i - A_j) = U_2'U_1(G_j^{-1}Y_j - G_i^{-1}Y_i)X^{-1} = 0, && (5.51)\\
&\implies A_i - A_j = B_oZ_{ij}, && (5.52)
\end{aligned}$$

for some $Z_{ij} \in \mathbb{R}^{m\times n}$. Hence,

$$\begin{aligned}
A_1 - A_2 &= B_oZ_{12}, && (5.53)\\
A_2 - A_3 &= B_oZ_{23}, && (5.54)\\
&\vdots && (5.55)\\
A_{N-2} - A_{N-1} &= B_oZ_{N-2,N-1}, && (5.56)\\
A_{N-1} - A_N &= B_oZ_{N-1,N}. && (5.57)
\end{aligned}$$

Set now $A_o = A_N$, which implies $A_N = A_o + B_o0$. Then,

$$\begin{aligned}
A_{N-1} &= A_N + B_oZ_{N-1,N} = A_o + B_oZ_{N-1,N}, && (5.58)\\
A_{N-2} &= A_{N-1} + B_oZ_{N-2,N-1} = A_o + B_o(Z_{N-2,N-1} + Z_{N-1,N}), && (5.59)\\
&\vdots && (5.60)\\
A_1 &= A_2 + B_oZ_{12} = A_o + B_o(Z_{12} + Z_{23} + \cdots + Z_{N-1,N}), && (5.61)
\end{aligned}$$

and consequently,

$$(A_i,\ B_i) = S(A_o,\ B_o),\ \forall i = 1,\ldots,N. \tag{5.62}$$

□

For numerical reasons, we wish to relax the exact model-matching in (5.40) with approximate conditions. These are formulated in an LMI form [20] in the following paragraph.

5.2.5 Approximate model-matching

As shown in Theorem 5.2.5, the model-matching

$$A_i + B_i F_i = A_j + B_j F_j, \tag{5.63}$$

can be written as

$$A_i X + B_i Y_i = A_j X + B_j Y_j, \tag{5.64}$$

where $F_i = Y_i X^{-1}$, $F_j = Y_j X^{-1}$, for $i, j = 1,\ldots,N$, with $X = X' > 0$. For a sufficiently small tolerance $\gamma > 0$ we write

$$\|A_i X + B_i Y_i - (A_j X + B_j Y_j)\| < \gamma, \tag{5.65}$$

for $i, j = 1,\ldots,N$ and $i \neq j$. We also consider the following well-known fact.

Lemma 5.2.6. *Let $\Phi \in \mathbb{R}^{n\times n}$ be an arbitrary matrix. The following are equivalent.*

$$\|\Phi\| < \gamma \Leftrightarrow \Phi'\Phi < \gamma^2 I_n \Leftrightarrow \begin{bmatrix} I_n & \Phi \\ \Phi' & \gamma^2 I_n \end{bmatrix} > 0. \tag{5.66}$$

Using Lemma 5.2.6, conditions (5.65) can be formulated as linear matrix inequalities (LMI's):

$$\begin{gathered} X = X' > 0, \\ \begin{bmatrix} I & A_i X + B_i Y_i - A_j X - B_j Y_j \\ * & \gamma^2 I \end{bmatrix} \geq 0 \text{ for } i, j = 1,\ldots,N \text{ and } i \neq j, \end{gathered} \tag{5.67}$$

which can be seen as a standard LMI feasibility problem for a certain upper bound $\gamma > 0$. To construct the model-matching state-feedback gains $F_i = Y_i X^{-1}$, $i = 1,\ldots,N$, achieving minimum $\gamma > 0$, we may consider the following convex optimization problem:

$$\min_{\gamma>0} \gamma \text{ subject to (5.67)}, \tag{5.68}$$

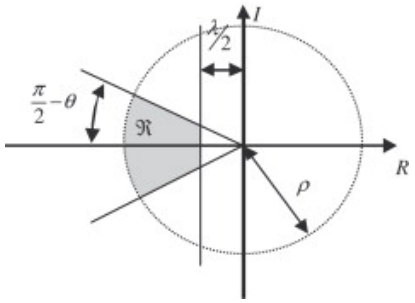

Fig. 5.2 LMI region $\mathfrak{R}$.

which can be used along with additional constraints (see next paragraph) to satisfy a numerical tolerance of the form $\|A_iX + B_iY_i - A_jX - B_jY_j\| \leq \gamma$. Finding optimal X, Y_i yields a target system, which can be specified by any of the pairs $(A_i + B_iF_i,\ B_i)$, $i = 1,\ldots,N$, with $F_i = Y_iX^{-1}$. We remark here that the inertia of $(A_i + B_iF_i)$ can not be controlled via constraints (5.67). Next, we impose certain stability specifications on the target dynamics by augmenting problem (5.68) by additional constraints.

5.2.6 Approximate model-matching with LMI stability constraints

As already mentioned, it might be desirable to solve a model-matching problem such that N systems be mapped to a stable target model. In a network setup, this will guarantee stability of the individual systems even in the presence of communication failure between agents. Pertaining to the approximate model-matching via LMI conditions shown above, it is possible to achieve stable target dynamics by adding extra LMI constraints to problem (5.68). In particular, we may allow the poles of the target system to lie in a confined region of the complex plane. If these regions are convex, then, they can be expressed as LMI constraints. For instance, such regions may be selected to ensure a minimum decay rate, a maximum undamped natural frequency, and a minimum damping ratio, each performance requirement specified by a parameter λ, ρ, and θ, respectively. An example of such a convex region of the complex plane is shown in Fig. 5.2. Comprehensive study of pole assignment via LMI constraints can be found in [34]. An approximate model-matching problem with additional pole clustering constraints is stated next.

We consider a set of N controllable pairs $(A_i,\ B_i)$, $i = 1,\ldots,N$, with structure as in (5.32), and $A_i \in \mathbb{R}^{n\times n}$, $B_i \in \mathbb{R}^{n\times m}$. We wish to construct state-feedback gains F_i, $i = 1,\ldots,N$, so that the eigenvalues of the i-th matrix $A_i + B_iF_i$ lie on a convex region of the complex plane

defined by performance parameters λ, ρ, and θ, as shown in Fig. 5.2. Let

$$X = X' > 0, \tag{5.69a}$$

$$\begin{bmatrix} I & A_iX + B_iY_i - A_jX - B_jY_j \\ * & \gamma^2 I \end{bmatrix} \geq 0 \text{ for } i, j = 1, \ldots, N \text{ and } i \neq j,$$

$$\lambda X + \Lambda_i + \Lambda_i' < 0,\ i \in \{1, \ldots, N\}, \tag{5.69b}$$

$$\begin{bmatrix} -\rho X & \Lambda_i' \\ * & -\rho X \end{bmatrix} < 0,\ i \in \{1, \ldots, N\}, \tag{5.69c}$$

$$\begin{bmatrix} \sin\theta[\Lambda_i + \Lambda_i'] & \cos\theta[-\Lambda_i + \Lambda_i'] \\ * & \sin\theta[\Lambda_i + \Lambda_i'] \end{bmatrix} < 0,\ i \in \{1, \ldots, N\}, \tag{5.69d}$$

where $\Lambda_i = A_iX + B_iY_i$, $i = 1, \ldots, N$, and $\gamma > 0$ is a small tolerance. Solving the following convex optimization problem:

$$\min_{\gamma > 0} \gamma \text{ subject to (5.69)}, \tag{5.70}$$

yields a target system with the desirable dynamics. The feasibility of problem (5.70) ensures that all eigenvalues of the closed-loop matrix $A_i + B_iF_i$ lie on a confined region of the complex plane specified by LMI conditions (5.69b), (5.69c), (5.69d). In the following section, we define particular performance indexes pertinent to a joint model-matching control effort and propose a systematic method for selecting target models the choice of which guarantees an optimal model-matching scheme.

5.3 Optimal selection of target system

So far in this chapter, we have shown that the model-matching problem of a family of systems, characterized by identical sets of controllability indices, can be solved via state-feedback control and input-matrix transformations. It has been shown that picking a target system with identical controllability indices, model-matching state-feedback compensators and input-matrix transformations can be obtained by (5.18). We have also shown that model-matching controllers incorporating additional objectives (stability, pole location) can be designed approximately via linear matrix inequalities. In this section, we shift our attention to the decision needed to be made on the choice of the target model for a particular set of dynamic agents, represented as N systems $(A_i,\ B_i)$, $i = 1, \ldots, N$, with identical sets of controllability indices. Defining the model-matching scheme as an aggregate of each local model-matching state-feedback controller, we attempt to minimize the joint model-matching control effort

associated with a particular target system. We impose this objective because we wish to use the "minimum amount of feedback" in the first stage of the control design of problem (5.1), so that the overall performance of the closed-loop network is effectively defined by the weighting matrices of the quadratic performance index (5.1b). For this purpose, we introduce the concept of a cost-function that indicates a specific measure of the joint model-matching energy loss. We also show that minimizing a model-matching cost-function results in a specific optimal target model. A worst-case control effort is examined first, defined as a discrete minimax problem the solution of which is achieved via an efficient steepest-descent algorithm. A quadratic cost-function involving a least-squares problem is also employed. It is shown that optimal target model in the least-squares sense can be derived from a closed form expression. Next, some preliminaries on minimax optimization are introduced.

5.3.1 Preliminaries on minimax theory

Consider N convex quadratic functions of $d \in \mathbb{R}^n$, denoted by $M_i(d)$, $i \in [1:N]$, and let

$$\phi(d) = \max_{i\in[1:N]} M_i(d), \tag{5.71}$$

be the maximum function $\phi(d)$. Finding d^* for which $\max_{i\in[1:N]} M_i(d^*)$ becomes minimum is formulated as the discrete minimax problem:

$$\min_{d\in\mathbb{R}^n} \phi(d) = \min_{d\in\mathbb{R}^n} \max_{i\in[1:N]} M_i(d). \tag{5.72}$$

Since $\phi(d)$ is a continuous and convex function, by the continuity and convexity of M_i's, $i = 1,\ldots,N$, and its sub-level sets are bounded, the minimizing solution d^* exists and is unique. An efficient ε-steepest decent algorithm is employed to approximate the optimal solution. We omit here detailed geometric interpretations of the problem (which can be found in [44]) and focus on basic definitions and concepts which are helpful for deriving the minimax algorithm.

Let

$$R_\varepsilon = \{i \mid 0 \le \phi(d) - M_i(d) \le \varepsilon\} \subseteq \{1,\ldots,N\}, \tag{5.73}$$

be the active set at point $d \in \mathbb{R}^n$. In essence, R_ε represents the set of indices i's for which $\phi(d) - M_i(d) \le \varepsilon$ is satisfied for a given $\varepsilon > 0$ and fixed d. Obviously, if $\varepsilon' \ge \varepsilon$ this implies $R_{\varepsilon'} \supset R_\varepsilon$. Let now

$$H_\varepsilon(d) = \Big\{Z \in \mathbb{R}^n \mid Z = \frac{\partial M_i(d)}{\partial d}, i \in R_\varepsilon\Big\}, \tag{5.74}$$

be the set of gradients of M_i for all $i \in R_\varepsilon$. Then,

$$L_\varepsilon(d) = \big\{ Z = \sum_{i \in R_\varepsilon(d)} \sigma_i \frac{\partial M_i(d)}{\partial d} \;\big|\; \sigma_i \geq 0 \text{ and } \sum_{i \in R_{\varepsilon(d)}} \sigma_i = 1 \big\}, \tag{5.75}$$

denotes the convex hull of $H_\varepsilon(d)$. Note that $L_\varepsilon(d)$ is a bounded, closed and convex set. The inclusion $\mathbf{0} \in L_\varepsilon(d^*)$ implies that d^* is ε-stationary point. This is a necessary condition for $\phi(d)$ to have a minimum on $\mathbb{R}^n$ at d^*. In our case, this condition is also sufficient (by assumption) due to convexity of $\phi(d)$ as a consequence of $M_i(d)$, $i = 1, \ldots, N$, being (quadratic) convex functions. This is stated next.

Proposition 5.3.1. *A point d^* is ε-stationary point of $\phi(d)$ if and only if the origin is a point of $L_\varepsilon(d^*)$, i.e., $\mathbf{0} \in L_\varepsilon(d^*)$.*

In effect, the solution to (5.72) relies on an approximation algorithm which searches for ε-stationary points of $\phi(d)$. The determination of ε-stationary points ($\varepsilon > 0$) can be accomplished by solving three auxiliary problems successively. The first involves the question whether the origin lies in the polyhedron $L_\varepsilon(d)$ and is equivalent to whether the system

$$\sum_{i=1}^{s} a_i Z_i = 0 \text{ subject to } \sum_{i}^{s} a_i = 1,\ a_i \geq 0,\ i \in [1:s], \tag{5.76}$$

is solvable, where $Z_1, \ldots, Z_s$ are points of $H_\varepsilon(d)$. This can be formulated as a linear programming problem. Proposition 5.3.1 implies that the inclusion of the origin in the Polyhedron $L_\varepsilon(d)$ is an equivalent necessary and sufficient condition for $\phi(d)$ to have minimum at d, and can be used as a termination condition for the approximation algorithm. If the origin fails to be included in $L_\varepsilon(d^*)$, then there is a unique ε-steepest descent direction along which the maximum function $\phi(d)$ decreases most rapidly. This direction is given in the following Proposition.

Proposition 5.3.2. *If d is not an ε-stationary point of $\phi(d)$, then $\phi(d)$ has a unique direction of ε-steepest descent $g_\varepsilon(d)$ at d: $g_\varepsilon(d) = -\frac{Z_\varepsilon^*}{\|Z_\varepsilon^*\|}$, where Z_ε^* is the point of $L_\varepsilon(d)$ nearest the origin.*

Let now $g_\varepsilon(d) = -\frac{Z_\varepsilon^*}{\|Z_\varepsilon^*\|}$, where Z_ε^* is the point of $L_\varepsilon(d)$ nearest the origin. Attaining Z_ε^* is the second auxiliary problem to be solved and is formulated here as the quadratic program:

$$\min_{a^s}\ (Z_i' a^s)'(Z_i' a^s), \text{ where} a^s = [a_1, \ldots, a_s]' \text{ subject to } \sum_{i}^{s} a_i = 1,\ a_i \geq 0,\ i \in [1:s], \tag{5.77}$$

where $Z_1,\ldots,Z_s$, are points of $H_\varepsilon(d)$. The minimizer vector a^s, obtained from (5.77), leads to $Z_\varepsilon^* = \sum_{i=1}^s a_i Z_i$. Assume now that d is not an ε-stationary point of $\phi(d)$, and g_ε is the ε-steepest descent direction of $\phi(d)$ at d. Consider the ray $d^+(a) = d + a g_\varepsilon$ with $a \geq 0$. The third auxiliary problem is to find optimal step-size $a^* \in [0,\infty)$ for which $\phi(d^+(a^*))$ attains its minimum along the ray d^+. We present here a pseudo-analytical procedure for obtaining this minimum.

Take $\gamma = \phi(d^+(0)) = \phi(d)$ and find the smallest $\bar{a} \geq 0$ for which $M_i(d^+(\bar{a})) \geq \gamma$ for all $i \in R_\varepsilon$. Then, the unique minimizer of $\phi(d^+(a))$ $a^* \in [0,\ \bar{a}]$. Let Π_s be the set comprising all the points a of the line segment $d^+(a)$, with $a \in [0,\ \bar{a}]$, for which $\frac{\partial M_s}{\partial a} = 0$ where $s \in R_\varepsilon$. Note that Π_s has the same cardinality with R_ε, say n_{R_ε}. Now with lexicographic order take all pairs (i,j) where $i,j \in R_\varepsilon$ and $i \neq j$ (e.g, if $R_\varepsilon = \{1,\ 2,\ 3\}$, then, consider the pairs $(1,2)$, $(1,3)$ and $(2,3)$) and find the two roots $(a_{i,j}^1,\ a_{i,j}^2)$ of each equation $M_i(a_{i,j}) = M_j(a_{i,j})$. Let set Ω_s consist of all the roots $a_{i,j} \in [0,\ \bar{a}]$ with cardinality at most $n_{R_\varepsilon}^2 - n_{R_\varepsilon}$. Clearly, the cardinality of the union $\Pi_s \cup \Omega_s$ is at most $n_{R_\varepsilon}^2$. The unique minimizer a^* is finally obtained by searching the minimum of $\phi(d)$ at distinct points which are at most $n_{R_\varepsilon}^2$, i.e.:

$$a^* = \arg \min_{a \in \Pi_s \cup \Omega_s} \phi(d^+(a)). \tag{5.78}$$

Now assume that the k^{th} approximation of the sequence $d_0,\ d_1,\ \ldots,\ d_k,\ \ldots$ has been obtained. A single iteration of the ε-steepest descent algorithm is presented in Algorithm 1. Performing the algorithm iteratively, an approximate solution d^* of (5.72) is attained given a desired level of convergence.

5.3.2 State-feedback design for optimal target system

We consider a set of N systems represented by controllable pairs $(A_i,\ B_i)$, $A_i \in \mathbb{R}^{n\times n}$, $B_i \in \mathbb{R}^{n\times m}$ with $\text{rank}(B_i) = m$ and state-space forms given as in (5.10). Let a target model be denoted by system matrices $(A_{N+1},\ B_{N+1})$ with $A_{N+1} \in \mathbb{R}^{n\times n}$, $B_{N+1} \in \mathbb{R}^{n\times m}$. We assume that systems $(A_i,\ B_i)$, $i = 1,\ldots,N+1$, are characterized by identical sets of controllability indices denoted as $\mu_1,\ldots,\mu_m$ with $\sum_{j=1}^m \mu_j = n$. Without loss of generality, let $(A_{N+1},\ B_{N+1})$ be written in canonical form given in (5.12), as

$$A_{N+1} = \bar{A}_c + \bar{B}_c A_{m,N+1}, \tag{5.79a}$$

$$B_{N+1} = \bar{B}_c B_{m,N+1}, \tag{5.79b}$$

where $A_m \in \mathbb{R}^{m\times n}$, $B_m \in \mathbb{R}^{m\times m}$ are defined in (5.12). The pair $(\bar{A}_c,\ \bar{B}_c)$ represents the Brunovsky form of all linear systems with controllability indices $\mu_1,\ldots,\mu_m$. To simplify the

Algorithm 1: ε-steepest descent algorithm.

input : $\varepsilon, d_k, a_k, \mu$
while $a_k > \mu$ **do**
  compute : $R_\varepsilon = \{i | \phi(d_k) - M_i(d_k) \leq \varepsilon\}$
    $H_\varepsilon(d_k) = \{\frac{\partial M_i(d_k)}{\partial d}, i \in R_\varepsilon\}$
    $L_\varepsilon(d_k)$
  if $\mathbf{0} \in L_\varepsilon(d_k)$ **then**
    $d_{k+1} = d_k$
    terminate
  else
    compute : $Z_k \in L_\varepsilon(d_k)$ nearest $\mathbf{0}$
      $g_\varepsilon^k = -\frac{Z_k}{\|Z_k\|}$
      $a_k = \texttt{OptimalStepSize}(d_k, g_\varepsilon^k, R_\varepsilon)$
      $d_{k+1} = d_k + a_k g_e^k$
  end
end
return d_{k+1}
Function: `OptimalStepSize`$(d, g_\varepsilon, R_\varepsilon)$
  set : $\gamma = \phi(d)$
  compute : smallest $\bar{a} > 0$: $M_i(d + \bar{a} g_\varepsilon) \geq \gamma \; \forall \; i \in R_\varepsilon$
  find : all $a_i \in [0 : \bar{a}]$ for which $\frac{\partial M_i}{\partial a} = 0$ with $i \in R_\varepsilon$
  set : $\Pi_s = \{a_i | i \in R_\varepsilon\}$
  find : $(a_{i,j}^{\rho_1}, a_{i,j}^{\rho_2})$ for all lexicographic pairs (i, j)
    with $i < j$ and $i, j \in R_\varepsilon$: $M_i(d + a g_\varepsilon) = M_j(d + a g_\varepsilon)$
  set : $\Omega_s = \{a_{i,j}^{\rho_{1,2}} \in [0, \bar{a}]\}$
  compute : $a^* = \arg \min_{a \in \Pi_s \cup \Omega_s} \phi(d + a g_\varepsilon)$
return

subsequent analysis, we consider $B_{m,N+1} = I_m$. Model-matching state-feedback gains and input-matrix transformations defined in (5.18) are written here as:

$$F_i = B_{m,i}^{-1}(A_{m,N+1} - A_{m,i})P_i, \tag{5.80a}$$

$$G_i = B_{m,i}^{-1}, \tag{5.80b}$$

where matrices $A_{m,i}$, $A_{m,N+1}$, $B_{m,i}$, P_i are as defined in Theorem 5.2.3. Letting now $u_i = F_i x_i + G_i v_i$, $i = 1 \cdots, N$, with $v_i \in \mathbb{R}^m$, the closed-loop state-space form of the i-th system

$$\dot{x}_i = (A_i + B_i F_i) x_i + B_i G_i v_i, \tag{5.81}$$

matches the target dynamics:

$$\dot{\xi} = A_{N+1}\xi + B_{N+1}u_{N+1}, \tag{5.82}$$

through the bijective mapping:

$$\xi = \Phi_i^{-1}x_i, \tag{5.83}$$

where $\Phi_i = P_i^{-1}$ is a nonsingular matrix. In view of (5.80), matrix $A_{m,N+1}$ is the only term that associates a specific target selection with the local model-matching control action. In this regard, we wish to identify an optimal matrix $A_{m,N+1}$ the selection of which minimizes a certain measure of the joint model-matching control-effort defined as a function of state-feedback gains F_i, $i = 1,\ldots,N$. In the following, two cost-functions are considered. These are referred to as model-matching performance indexes. Optimizing a performance index over the set of matrices $\bar{A}_m \in \mathbb{R}^{m\times n}$ results in a specific optimal target model. Before formulating the optimization problems, we state the following well-known fact which accommodates an isometric embedding of the Frobenius norm of a matrix in $\mathbb{R}^{m\times n}$ into the Euclidean norm of a vector in $\mathbb{R}^{mn}$.

Proposition 5.3.3. *Consider*

$$J(\Xi) = \|A\Xi B - C\|_F^2, \tag{5.84}$$

where $A \in \mathbb{R}^{p\times p}$, $B \in \mathbb{R}^{q\times q}$, C, $\Xi \in \mathbb{R}^{p\times q}$. Let $\mathrm{vec}(\cdot)$ *denote the vectorization operator (stacking columns of argument matrix). Then*

$$\mathrm{vec}(A\Xi B - C) = (B' \otimes A)\mathrm{vec}(\Xi) - \mathrm{vec}(C). \tag{5.85}$$

Let also $B' \otimes A = H$, $\mathrm{vec}(C) = c$, *and* $\mathrm{vec}(\Xi) = \xi$. *Since $\|\mathscr{M}\|_F = \|\mathrm{vec}(\mathscr{M})\|$, then*

$$J(\Xi) = \|H\xi - c\|^2, \tag{5.86}$$

where $\|\cdot\|$ is the Euclidean norm.

In the following, we define two performance indexes that penalize the joint control effort pertinent to the model-matching state-feedback scheme.

5.3.2.1 Minimum worst-case control

We denote the joint worst-case model-matching control action as the maximum function:

$$\phi(A_{m,N+1}) = \max_{i=[1:N]} M_i, \text{ where } M_i = \|F_i\|_F^2 = \|B_{m,i}^{-1}(A_{m,N+1} - A_{m,i})P_i\|_F^2, \tag{5.87}$$

and we wish to find matrix $A_{m,N+1} \in \mathbb{R}^{m\times n}$ for which $\phi(A_{m,N+1})$ attains its minimum. This is a discrete minimax problem formulated as

$$\min_{A_{m,N+1}\in\mathbb{R}^{m\times n}} \phi(A_{m,N+1}) = \min_{A_{m,N+1}\in\mathbb{R}^{m\times n}} \max_{i\in[1:N]} \|B_{m,i}^{-1}(A_{m,N+1} - A_{m,i})P_i\|_F^2. \tag{5.88}$$

To perform the optimization over the vector space $\mathbb{R}^{mn}$, we utilize the vectorization technique shown in Proposition 5.3.3. Let $M_i = \|H_i\xi - c_i\|^2$ where $\Xi = A_{m,N+1}$, $H_i = P_i' \otimes B_{m,i}^{-1}$, $C_i = B_{m,i}^{-1}A_{m,i}P_i$, $\xi = \mathrm{vec}(\Xi)$, $c_i = \mathrm{vec}(C_i)$, $i = 1,\ldots,N$. We recall that $\|\cdot\|$ stands for the Euclidean norm. The minimax problem (5.88) becomes

$$\min_{\xi\in\mathbb{R}^{m\cdot n}} \phi(\xi) = \min_{\xi\in\mathbb{R}^{m\cdot n}} \max_{i=[1:N]} M_i = \min_{\xi\in\mathbb{R}^{m\cdot n}} \max_{i=[1:N]} \xi'(H_i'H_i)\xi - 2\xi'(H_i'c_i) + c_i'c_i. \tag{5.89}$$

The maximum function $\phi(\xi)$ is continuous and convex by the continuity and convexity of M_i, $i = 1,\ldots,N$, and its sub-level sets are bounded. Thus, a minimizing solution ξ^* exists and is unique. The ε-steepest decent algorithm shown earlier can be employed here to approximate the optimal solution ξ^*. Letting ξ_0 be the initial choice of ξ and performing the algorithm iteratively, the optimal solution ξ^* is obtained approximately. Finally, the optimal solution to $\min\phi(A_{m,N+1})$ is derived from

$$A_{m,N+1}^* = \mathrm{vec}^{-1}(\xi^*). \tag{5.90}$$

Optimal model-matching state-feedback gains F_i, $i = 1,\ldots,N$, are constructed by substituting $\bar{A}_m^*$ into (5.80), while an optimal target system is defined as $(\bar{A}_c + \bar{B}_c A_{m,N+1}^*,\ \bar{B}_c)$.

5.3.2.2 Least-squares control

Another measure that penalizes the joint model-matching control effort is defined as

$$J(A_{m,N+1}) = \sum_{i=1}^{N} \|F_i\|_F^2 = \sum_{i=1}^{N} \|B_{m,i}^{-1}(A_{m,N+1} - A_{m,i})P_i\|_F^2. \tag{5.91}$$

Here, we are interested in finding a matrix $A_{m,N+1}$ for which J in (5.91) becomes minimum. Setting $\Xi = A_{m,N+1}$, $H_i = P_i' \otimes B_{m,i}^{-1}$, $C_i = B_{m,i}^{-1}A_{m,i}P_i$, $\xi = \mathrm{vec}(\Xi)$, $c_i = \mathrm{vec}(C_i)$, $i = 1,\ldots,N$, and embedding each matrix $B_{m,i}^{-1}(A_{m,N+1} - A_{m,i})P_i$ into $\mathbb{R}^{mn}$ as suggested in Proposition 5.3.3,

we can optimize J over $\xi \in \mathbb{R}^{mn}$. This is written as

$$J(\xi) = \sum_{i=1}^{N} \|H_i\xi - c_i\|^2 = \sum_{i=1}^{N} (\xi' H_i' - c_i')(H_i\xi - c_i)$$
$$= \xi'(\sum_{i=1}^{N} H_i' H_i)\xi - 2\xi'(\sum_{i=1}^{N} H_i' c_i) + \sum_{i=1}^{N} c_i' c_i, \tag{5.92}$$

which is a convex function of $\xi \in \mathbb{R}^{mn}$. Setting

$$\frac{\partial J}{\partial \xi} = 0, \tag{5.93}$$

leads to the least-squares solution, where the unique minimizer of $J(\xi)$ is attained by:

$$2(\sum_{i=1}^{N} H_i' H_i)\xi - 2(\sum_{i}^{N} H_i' c_i) = \underline{0}, \tag{5.94}$$

which gives

$$\xi^* = (\sum_{i}^{N} H_i' H_i)^{-1}(\sum_{i=1}^{N} H_i' c_i). \tag{5.95}$$

Then, the unique minimizer of $J(A_{m,N+1})$ is given by

$$A_{m,N+1}^* = \text{vec}^{-1}\left(\sum_{i=1}^{N}(H_i' H_i)^{-1}\sum_{i=1}^{N} H_i' c_i\right). \tag{5.96}$$

Optimal state-feedback gains F_i, $i = 1,\ldots,N$, in the least-squares sense are obtained by substituting $A_{m,N+1}^*$ into (5.80). The following section is devoted to the special model-matching problem of single-input linear systems.

5.3.3 Model-matching of single-input systems

The analysis presented earlier pertains to multi-input systems, thereby applying to single-input systems straightforwardly. Here, we study and build upon some interesting properties arising in model-matching problems with single-input target dynamics. In particular, focusing on a set of controllable systems $(A_i,\ b_i)$, $i = 1,\ldots,N$, that are mapped to a single-input target model $(A_d,\ b_d)$ via the model-matching operations defined in the previous sections, we remark the following:

1) Matrices A_i only need to have same dimensions.

2) Optimization problems defined in Section 5.3.2 may be augmented with stability constraints leading to an optimal single-input target model with certain stability and performance specifications.

3) The pair $(A_i,\ b_i)$ may represent a multi-input system $(A_i,\ B_i)$ that is converted to a controllable system $(A_i,\ B_i\xi_i)$, where $b_i = B_i\xi_i \in \mathbb{R}^{n\times 1}$.

Let

$$\dot{x}_i = A_i x_i + b_i u_i,\ x_i(0) = x_{i,0},\ i = 1,\ldots,N, \tag{5.97}$$

be the state-space forms of N single-input systems, where $A_i \in \mathbb{R}^{n\times n}$, $b_i \in \mathbb{R}^n$, $i = 1,\ldots,N$. We denote a single-input target system by pair $(A_d,\ b_d)$, with $A_d \in \mathbb{R}^{n\times n}$, $b_d \in \mathbb{R}^n$. We also note that there is always a similarity transformation that can be used to match the state-space forms of two controllable single-input systems with the same state dimensions, given that the two systems have identical poles. Clearly, this argument holds for multiple systems. In this respect, we show that a matching problem of N single-input systems reduces to a pole-placement task. Let now

$$a^i = \begin{bmatrix} a_0^i & a_1^i & \cdots & a_{n-1}^i \end{bmatrix}', \tag{5.98}$$

$$d = \begin{bmatrix} d_0 & d_1 & \cdots & d_{n-1} \end{bmatrix}', \tag{5.99}$$

denote the coefficients of the characteristic polynomials of system-i and the target model, respectively. We construct the following matrices: $T_i = (\Gamma_{c,i}H_{a,i})^{-1}$, $i = 1,\ldots,N$, where

$$\Gamma_{c,i} = \begin{bmatrix} b_i & A_i b_i & \ldots & A_i^{n-1} b_i \end{bmatrix}, \tag{5.100}$$

$$H_{a,i} = \begin{bmatrix} a_1^i & \cdots & a_{n-2}^i & a_{n-1}^i & 1 \\ \vdots & \iddots & a_{n-1}^i & 1 & 0 \\ a_{n-2}^i & \iddots & \iddots & \iddots & \vdots \\ a_{n-1}^i & 1 & \iddots & \iddots & 0 \\ 1 & 0 & \ldots & 0 & 0 \end{bmatrix}, \tag{5.101}$$

represent the controllability matrix and the Hankel matrix, respectively, of system-i. Similarly, we construct matrix $T_d = (\Gamma_{c,d}H_d)^{-1}$. We wish to represent systems in controllable canonical forms, i.e.,

$$(A_{c,i},\ e_n) = (T_i A_i T_i^{-1}, T_i b_i), \tag{5.102}$$

$$(A_{c,d},\ e_n) = (T_d A_d T_d^{-1}, T_d b_d), \tag{5.103}$$

where

$$e_n = \begin{bmatrix} 0 & \cdots & 0 & 1 \end{bmatrix}', \tag{5.104}$$

and letting state-feedback control $u_i = f_i' x_i$, we require that

$$T_i(A_i + b_i f_i')T_i^{-1} = T_d A_d T_d^{-1}. \tag{5.105}$$

In view of the special structure of the canonical forms $T_i A_i T_i^{-1}$, $i = 1,\ldots,N$, and $T_d A_d T_d^{-1}$, it is readily verified that the matching state-feedback gains f_i, $i = 1,\ldots,N$, can be obtained from

$$f_i = T_i'(a^i - d),\ i = 1,\ldots,N. \tag{5.106}$$

Clearly, defining a vector d (coefficients of the target characteristic polynomial) suffices in establishing a single-input target model. As suggested in the previous section, an optimal target system can be achieved by optimizing a specific model-matching performance index that penalizes the joint model-matching state-feedback control scheme. This is exemplified next.

5.3.3.1 Single-input optimal target system selection

In order to define an optimal (single-input) target model, we consider cost functions as introduced in the multi-input case earlier in the chapter. We recall that solving a discrete minimax problem formulated as

$$\min_{d\in\mathbb{R}^n} \phi(d) = \min_{d\in\mathbb{R}^n} \max_{i\in[1:N]} \|f_i\|^2, \tag{5.107}$$

leads to an optimal single-input target system (in the minimax sense) with characteristic polynomial $p(s,d^*)$, where d^* is the minimizing solution of (5.107). Then, a minimum worst-case model-matching control scheme can be achieved by designing state-feedback gains f_i, $i = 1,\ldots,N$, as in (5.106) with $d = d^*$.

Similarly, we consider the following quadratic function in $d \in \mathbb{R}^n$:

$$J(d) = \sum_{i=1}^{N} \|f_i\|^2. \tag{5.108}$$

Setting

$$\frac{\partial J}{\partial d} = 0, \tag{5.109}$$

yields the unique least-squares solution

$$d^* = (\sum_{i=1}^{N} T_i T_i')^{-1} (\sum_{i=1}^{N} T_i T_i' a^i). \tag{5.110}$$

Optimal state-feedback gains in the least-squares sense are obtained by substituting d^* to (5.106).

As was shown above, model-matching optimization problems adapted to the single-input case can be carried out straightforwardly over the coefficients of the target's characteristic polynomial denoted by vector $d \in \mathbb{R}^n$. This standard formulation facilitates the inclusion of constraints into the optimization problems representing stability specifications of target dynamics. In the single-input case, it makes sense that these extra constraints are derived from the Routh-Hurwitz stability criterion. This illustrated in the next simple numerical example.

Example 5.3.4. Let the state-space form of two unstable systems be given as

$$\dot{x}_i = A_i x_i + e_3 u_i, \tag{5.111}$$

with $i = 1,2$ where

$$A_1 = \begin{bmatrix} 0 & 1 & 0 \\ 0 & 0 & 1 \\ 1 & -3 & 1 \end{bmatrix}, A_2 = \begin{bmatrix} 0 & 1 & 0 \\ 0 & 0 & 1 \\ 1 & -2 & 1 \end{bmatrix}, e_3 = \begin{bmatrix} 0 \\ 0 \\ 1 \end{bmatrix}. \tag{5.112}$$

We wish to find the best Hurwitz characteristic polynomial that minimizes the joint state-feedback control effort denoted as $\sum_{i=1}^{2} \|a^i - d\|^2$. This is formulated as

$$\min_{d \in \mathbb{R}^3} \sum_{i=1}^{2} \|a^i - d\|^2 \text{ subject to } d_0 > 0,\ d_2 > 0, \text{ and } d_2 d_1 > d_0, \tag{5.113}$$

where a^i represents the coefficients of the characteristic polynomial of A_i, $i = 1,2$. The infimizing solution obtained in MatLab using the *fmincon* function, is

$$d^* = \begin{bmatrix} 0 & 2.5 & 0 \end{bmatrix}, \tag{5.114}$$

representing the coefficients of the best target polynomial. Note that two poles of the optimal solution lie on the imaginary axis which defines the boundary of the constrained set. This may be rectified, if desired, by redefining the stable region. □

Unfortunately, stability constraints derived from the Routh-Hurwitz criterion are highly nonlinear so they can be used effectively only for low-dimensional problems. An alternative approach is to enforce "local" stability conditions by calculating the maximum region in the coefficient space that the coefficients of a nominal Hurwitz polynomial, $p_o(s,d^o)$, can be perturbed so that the perturbed polynomial remains stable. This can be achieved by specifying the maximum stability radius $\rho(d^o)$ of a nominal Hurwitz polynomial,

$$p_o(s,d^o) = s^n + d^o_{n-1}s^{n-1} + \cdots + d^o_1 s + d^o_0, \tag{5.115}$$

defined either via the Euclidian or infinity norms of the coefficient vector. An explicit formula for calculating the distance ρ of a Hurwitz polynomial from the set of non-Hurwitz polynomials in the coefficient space is given in the following proposition.

Proposition 5.3.5. *If $p(s,d)$, $d \in \mathbb{R}^n$ is a Hurwitz polynomial,*

$$p(s,d) = p_1(-s^2) + sp_2(-s^2), \tag{5.116}$$

where $p_j(-s^2)$, $j = 1,2$ are real polynomials in $-s^2$, then

$$\rho(d) = \min\{d_0, [\max_{\omega^2 \in \mathbb{R}^+} f(\omega^2)]^{-1/2}\}, \tag{5.117}$$

where

$$f(\omega^2) = \begin{cases} \frac{1+\omega^4+\cdots+\omega^{2n-4}}{p_1^2(\omega^2)+p_2^2(\omega^2)}, & \text{for even } n, \\ \\ \frac{(1+\omega^4+\cdots+\omega^{2n-6})(1+\omega^4+\cdots+\omega^{2n-2})}{p_1^2(\omega^2)(1+\omega^4+\cdots+\omega^{2n-6})+p_2^2(\omega^2)(1+\omega^4+\cdots+\omega^{2n-2})}, & \text{for odd } n. \end{cases} \tag{5.118}$$

Proposition 5.3.5 can originally be found in [81]. For a Hurwitz polynomial $p(s,d)$ the distance ρ determines the largest radius of the open cube in $\mathbb{R}^n$ with center d and radius $\rho > 0$ for which the set

$$\{p(s,d) : \ |d_i - \delta_i| < \rho, \ i = 0,\ldots,n-1\}, \tag{5.119}$$

consists only of Hurwitz polynomials. In the following example, we show how to calculate the distance ρ of a Hurwitz polynomial.

Example 5.3.6. Consider polynomial:

$$p(s,d) = s^5 + 58.2s^4 + 1551s^3 + 2524s^2 + 2679s + 1767, \tag{5.120}$$

where

$$d = [d_0\ d_1\ \cdots\ d_4]' = [1767\ 2679\ 2524\ 1551\ 58.2]', \tag{5.121}$$

denotes the coefficient vector. The roots of $p(s,d)$ are:

$$\begin{aligned}
&-1.0548\\
&-28.2680+\mathrm{i}25.6135\\
&-28.2680-\mathrm{i}25.6135\\
&-0.3046+\mathrm{i}1.0288\\
&-0.3046-\mathrm{i}1.0288,
\end{aligned}$$

where $\mathrm{i}^2=-1$, illustrating that this is a Hurwitz polynomial. Defining a perturbation vector as

$$\delta = [\delta_0\ \delta_1\ \cdots\ \delta_4]', \tag{5.122}$$

we wish to find the maximum distance ρ with $|d_i-\delta_i|<\rho$, $i=0,1,\ldots,4$, for which any polynomial of fifth order $p(s,d-\delta)$ is Hurwitz. We write

$$p(s,d) = p_1(-s^2)+sp_2(-s^2), \tag{5.123}$$

where

$$p_1(-s^2) = 58.2(-s^2)^2-2524(-s^2)+1767, \tag{5.124}$$
$$p_2(-s^2) = (-s^2)^2-1551(-s^2)+2679. \tag{5.125}$$

Since $p(s,d)$ is of fifth order, we construct function

$$f(\omega^2) = \frac{(1+\omega^4)(1+\omega^4+\omega^8)}{p_1^2(\omega^2)(1+\omega^4)+p_2^2(\omega^2)(1+\omega^4+\omega^8)}, \tag{5.126}$$

and we solve the following minimization problem:

$$\min_{\omega^2\in\mathbb{R}^+} -f(\omega^2). \tag{5.127}$$

Using *fmincon* function in Matlab, the minimum of $-f(\omega^2)$ or equivalently, the maximum of $f(\omega^2)$ is found $3.1247e-04$ (at $\omega=1549.3$). This is also illustrated in Fig. 5.3 where $f(\omega^2)$ is plotted in logarithmic scale.

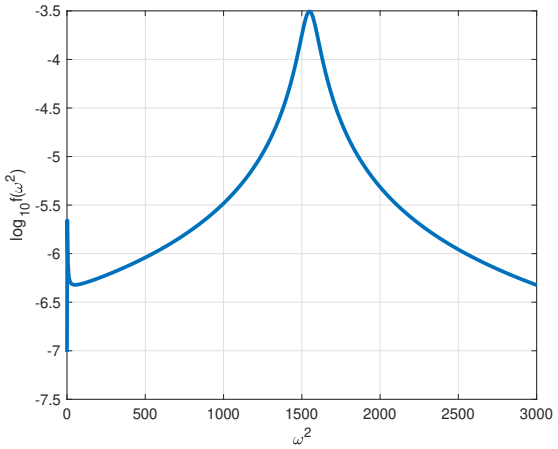

Fig. 5.3 Plot of $\log_{10} f(\omega^2)$

In view of Proposition 5.3.5, the maximum distance ρ is calculated as

$$\rho = \min(d_0, 3.1247e-04^{-1/2}) = \min(1767, 56.5715), \tag{5.128}$$

i.e., $\rho = 56.5715$. □

The constrained optimization problems are now outlined. Let $p_o(s, d^o)$ be a Hurwitz polynomial with a maximum stability radius ρ obtained as suggested in Proposition 5.3.5. Let also $\delta = [\delta_0, \ldots, \delta_{n-1}]'$, and $S \subseteq \mathbb{R}^n$ be such that

$$\delta \in S \text{ iff } |d_j^o - \delta_j| < \rho \ \forall \ j = 0, 1, \ldots, n-1. \tag{5.129}$$

Pertaining to a minimum worst-case model-matching control action, we solve

$$\inf_{d \in S} \max_{i \in [1:N]} \|T_i'(a^i - d)\|, \tag{5.130}$$

which involves the minimization of a continuous convex function over a compact set. Therefore, a unique minimum exists which can be calculated efficiently with the algorithms described in [44]. Similarly, solving optimization problem

$$\inf_{d \in S} \sum_{i=1}^{N} \|f_i\|^2 = \inf_{d \in S} \sum_{i=1}^{N} \|T_i'(a^i - d)\|^2, \tag{5.131}$$

results in a minimum model-matching control effort in the least-squares sense. Note that for nontrivial problems S is bounded, so constraining the problem on the closure of S guarantees a unique solution obtained via standard quadratic programming algorithms.

5.3.3.2 Single-input conversion of multi-input systems

Here we discuss briefly the model-matching problem of multi-input systems with non-identical sets of controllability indices. In particular, we consider a matching problem of systems $(A_i,\ B_i)$, $i = 1,\ldots,N$, with $A_i \in \mathbb{R}^{n\times n}$, $B_i \in \mathbb{R}^{n\times m_i}$, and assume that the requirement of common c.i. does not necessarily hold. A straightforward example arises when systems of identical state dimensions are controlled by different numbers of inputs. Our objective here is to highlight that the model-matching task of a family of controllable systems characterized by common state dimensions and arbitrary c.i., can be addressed by setting a single-input target model. In other words, we wish that each individual multi-input system is controlled by a single-input control scheme, say $u_i = \xi_i v$, with $v \in \mathbb{R}$. In effect, under this control action, systems are converted to single-input plants. As studied earlier in the section, the model-matching problem of a set of single-input systems has always a solution provided that systems are controllable. A solution to the model-matching problem of multi-input systems with non-identical sets of controllability indices is subject to the following result.

Theorem 5.3.7. *Let $(A_i,\ B_i)$, $i = 1,\ldots,N$, be controllable, with $A_i \in \mathbb{R}^{n\times n}$, $B_i \in \mathbb{R}^{n\times m_i}$, and* $\operatorname{rank}(B_i) = m_i$. *Then, there exist $\xi_i \in \mathbb{R}^{m_i}$, $i = 1,\ldots,N$, such that $(A_i,\ B_i\xi_i)$, $i = 1,\ldots,N$, are also controllable.*

Pertaining to Theorem 5.3.7, we note that a possible selection of ξ_i, $i = 1,\ldots,N$, may be almost any non-zero vector (i.e., that the set of vectors which do not give rise to this property has measure zero). We emphasize that this conjecture that systems $(A_i,\ B_i\xi_i)$, $i = 1,\ldots,N$, are controllable, is generically consistent. We also stress that this conversion to controllable single-input systems gives considerable flexibility to the model-matching design, naturally, at the expense of the degrees of freedom of each control input. Clearly, considering the controllability requirement is in force, model-matching state-feedback controllers of rank one can be designed as proposed in the previous section.

5.4 Distributed LQR-based control design

The section is devoted to the distributed LQR control which represents the second stage of the proposed design procedure. We recall that our main task throughout the chapter is to construct a distributed state-feedback controller which stabilizes a network of N heterogeneous agents. For convenience, the main assumptions of this problem are restated as follows.

We consider that the dynamics of N dynamic agents are described by N linear systems that belong to a family of systems sharing identical sets of controllability indices. Let the

state-space form of the i-th agent be written as

$$\dot{x}_i = A_i x_i + B_i u_i,\ x_i(0) = x_{i,0},\ i = 1,\ldots,N, \tag{5.132}$$

where $x_i \in \mathbb{R}^n$, $u_i \in \mathbb{R}^m$ denote state and input vectors, respectively. Let also $(A_i,\ B_i)$, $i = 1,\ldots,N$, be controllable pairs with identical c.i., denoted as $\mu_1,\ldots,\mu_m$, with $\sum_{j=1}^{m} \mu_j = n$. We use a graph (digraph) to represent interactions (couplings terms in controls, communication) between neighboring agents. Specifically, the i-th system is associated with the i-th vertex of a graph $\mathscr{G} = (\mathscr{V}, \mathscr{E})$ (digraph $\mathscr{D} = (\mathscr{V}, \mathscr{E})$). Matrix $\mathscr{L}$ represent the corresponding (in-degree) Laplacian matrix of $\mathscr{G}$ ($\mathscr{D}$). The presence of an edge $(i, j) \in \mathscr{E}$ connecting the i-th and j-th vertex implies the following:

1) The i-th system has full access to the state information of the j-th system.

2) The control action, u_i, is partly obtained by the solution of an LQR optimization problem which penalizes (among other terms) a weighted norm of the difference $x_i - x_j$.

We denote by $\mathscr{N}_i$ the set of adjacent vertices of the i-th vertex. We represent the aggregate state and input vectors of the network as $\hat{x} = \mathrm{Col}(x_1,\ldots,x_N)$ and $\hat{u} = \mathrm{Col}(u_1,\ldots,u_N)$, respectively. The regulation problem (5.1) is rewritten as follows:

$$\min_{\hat{u}} J(\hat{u}, \hat{x}_0) \ \text{ subject to:} \tag{5.133a}$$

$$J(\hat{u}, \hat{x}_0) = \int_0^\infty \left(\hat{x}'\hat{Q}\hat{x} + \hat{u}'\hat{R}\hat{u}\right) \mathrm{d}t, \tag{5.133b}$$

$$\dot{\hat{x}} = \hat{A}\hat{x} + \hat{B}\hat{u},\ \hat{x}(0) = \hat{x}_0, \tag{5.133c}$$

$$\hat{u} = \mathscr{M}\hat{x}, \tag{5.133d}$$

where

$$\hat{A} = \mathrm{diag}(A_1,\ldots,A_N), \tag{5.134}$$

$$\hat{B} = \mathrm{diag}(B_1,\ldots,B_N), \tag{5.135}$$

and

$$\hat{Q} = I_N \otimes Q_1 + \mathscr{L} \otimes Q_2, \tag{5.136}$$

$$\hat{R} = I_N \otimes R. \tag{5.137}$$

In order for problem (5.133) to be well-posed and have a stabilizing (sub)optimal solution (5.133d), we assume that there are matrices $C_1'C_1 = Q_1$ and $C_2'C_2 = Q_2$ such that $(A_i,\ C_1)$ and $(A_i,\ C_2)$ are observable for all $i = 1,\ldots,N$. Note that if matrix $\mathscr{M} \in \mathscr{K}^N_{m,n}(\mathscr{G})$ ($\mathscr{M} \in \mathscr{K}^N_{m,n}(\mathscr{D})$) in (5.133d), then the global control law $\hat{u} = \mathscr{M}\hat{x}$ represents a distributed state-feedback controller. For simplicity, we presently assume that the interconnection scheme of the network allows bidirectional connectivity between neighboring agents, thereby being represented by an undirected graph $\mathscr{G}$. At the end of the section, a directed network topology is also considered.

As mentioned above, our objective is to construct a stabilizing distributed solution to problem (5.133) following a two-step design method. In particular, we propose a state-feedback distributed control scheme which node-wise takes the following form:

$$u_i = (F_i + G_iK_1\Phi_i^{-1})x_i + aG_i \sum_{j\in\mathscr{N}_i} K_2(\Phi_i^{-1}x_i - \Phi_j^{-1}x_j), \tag{5.138}$$

with $a > 0$. At network level, the control law $\hat{u}$ may be written as:

$$\hat{u} = \big(\mathrm{diag}(F_1,\ldots,F_N) + \mathrm{diag}(G_1,\ldots,G_N)(I_N \otimes K_1 + M \otimes K_2)\mathrm{diag}(\Phi_1^{-1},\ldots,\Phi_N^{-1})\big)\,\hat{x}, \tag{5.139}$$

which is a distributed state-feedback controller. Matrix M in (5.139) reflects the structure of the interconnection scheme. For control scheme (5.139) to be consistent with the node-level controller in (5.138), matrix $M = a\mathscr{L}$ with $a > 0$. A schematic representation of the proposed control scheme at individual level is shown in Fig. 5.4.

In the first stage of the proposed design, we showed that solving a model-matching problem as suggested in Theorem 5.2.3, matrices F_i, G_i and Φ_i, $i = 1,\ldots,N$ can be constructed such that:

$$\dot{x}_i = (A_i + B_iF_i)x_i + B_iG_iv_i,\ x_i(0) = x_{i,0}, \tag{5.140}$$

$$\xi_i = \Phi_i^{-1}x_i, \tag{5.141}$$

where Φ_i, $i = 1,\ldots,N$, is a non-singular matrix, while the output variable $\xi_i \in \mathbb{R}^n$ can be cast as the state of a system described by target dynamics:

$$\dot{\xi} = A\xi + Bv. \tag{5.142}$$

Given that a target system $(A,\ B)$ has been specified, the next step of the method is to define matrices K_1, K_2, and M in (5.139), such that $\hat{u}$ stabilizes (5.133c), i.e., is a stabilizing

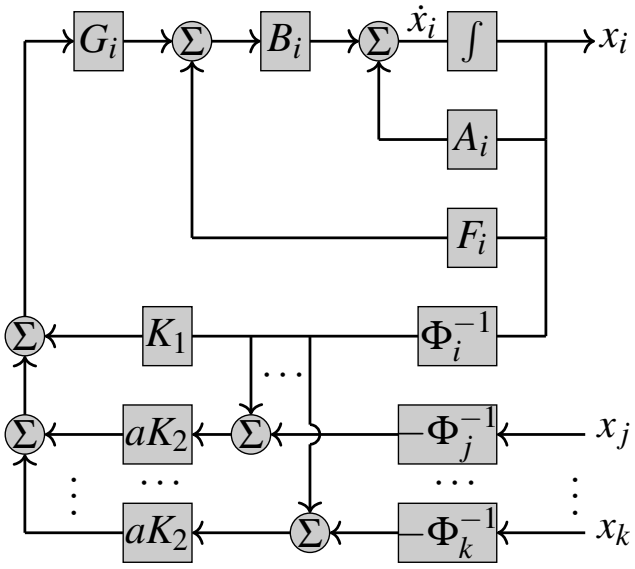

Fig. 5.4 Distributed node-level closed-loop architecture of interconnected heterogeneous linear agents.

distributed (suboptimal) solution of problem (5.133). This represents the main task of the second stage of our control design approach and is outlined as follows.

As can be seen from (5.141)-(5.142), the closed-loop state-space forms (5.140) match the dynamics of the target model $(A,\ B)$ through a bijective mapping represented by matrices Φ_i^{-1}, $i = 1,\ldots,N$. Therefore, matrices K_1, K_2 can be cast as functions of $(A,\ B,\ Q_1,\ Q_2,\ R)$, where pair $(A,\ B)$ denotes the model-matching dynamics, while matrices $(Q_1,\ Q_2,\ R)$ are tuning parameters of (5.133b). In this regard, the design matrices K_1 and K_2 can be derived from the methods studied in Chapters 3, 4. The top-down design procedure is formulated as follows. Solving LQR problem (3.65) with tuning parameters $(Q_1,\ Q_2,\ R)$ for $N_L = d_{\max} + 1$ systems $(A,\ B)$, $d_{\max}$ denoting the maximum vertex degree of graph $\mathscr{G}$, K_1, K_2 are defined from the following expressions:

$$K_1 = -R^{-1}B'P, \tag{5.143}$$

$$K_2 = R^{-1}B'\tilde{P}_2, \tag{5.144}$$

where P and $\tilde{P}_2$ are associated with ARE (3.71) and (3.72), respectively. We note that an alternative choice of K_1, K_2 may be obtained via the bottom-up method presented in Chapter

3. Then,

$$K_1 = -R^{-1}B'P, \tag{5.145}$$

$$K_2 = \Xi K_1, \tag{5.146}$$

where K_1 is as defined in top-down method above, while a matrix Ξ can obtained by solving a convex optimization problem as in (3.110). We remark that the option to select a distributed control method, originally established for networks of identical systems, for designing matrices K_1, K_2, simplifies considerably the design procedure and highlights the main advantage of the model-matching technique proposed in the first part of this chapter. The proposed control design as well as the closed-loop stability of the entire distributed control scheme with undirected topology are summarized in the following theorem.

Theorem 5.4.1. *Let N controllable pairs $(A_i,\ B_i)$, $i = 1,\ldots,N$, with $A_i \in \mathbb{R}^{n\times n}$, $B_i \in \mathbb{R}^{n\times m}$, have identical sets of controllability indices. Let also matrices A, B, F_i, G_i, and Φ_i be defined as in Theorem 5.2.3, such that*

$$(A,\ B) = (\Phi_i^{-1}(A_i + B_iF_i)\Phi_i,\ \Phi_i^{-1}B_iG_i),\ i = 1,\ldots,N, \tag{5.147}$$

where $(A,\ B)$ is a controllable pair. Consider LQR problem (3.65) *with tuning parameters $(Q_1,\ Q_2,\ R)$ for $N_L = d_{\max} + 1$ identical systems with dynamics described by the pair $(A,\ B)$, $d_{\max}$ denoting the maximum vertex degree of the associated graph. Define matrices P, $\tilde{P}_2$ as in* (3.71), (3.72)*, respectively, and let $K_1 = -R^{-1}B'P$, $K_2 = R^{-1}B'\tilde{P}_2$. Let also matrix $M \in \mathbb{R}^{N\times N}$ be a symmetric matrix with the following property:*

$$\lambda_i(M) > \frac{N_L}{2},\ \forall\ \lambda_i(M) \in S(M)\backslash\{0\}, \tag{5.148}$$

and construct a state-feedback controller as:

$$\hat{K} = (\mathrm{diag}(F_1,\ldots,F_N) + \mathrm{diag}(G_1,\ldots,G_N)(I_N \otimes K_1 + M \otimes K_2)\mathrm{diag}(\Phi_1^{-1},\ldots,\Phi_N^{-1}). \tag{5.149}$$

Then, the closed-loop matrix

$$A_{cl} = \mathrm{diag}(A_1,\ldots,A_N) + \mathrm{diag}(B_1,\ldots,B_N)\hat{K}, \tag{5.150}$$

is Hurwitz.

Proof. We define matrix $\bar{\Phi}$ as:

$$\bar{\Phi} = \text{diag}(\Phi_1, \ldots, \Phi_N). \tag{5.151}$$

From Theorem 5.2.3, matrices Φ_i, $i = 1, \ldots, N$, are nonsingular, hence $\bar{\Phi}$ is also nonsingular. Eq. (5.147) implies

$$I_N \otimes A = \bar{\Phi}^{-1}\text{diag}(A_1 + B_1F_1, \ldots, A_N + B_NF_N)\bar{\Phi}, \tag{5.152}$$
$$I_N \otimes B = \bar{\Phi}^{-1}\text{diag}(B_1G_1, \ldots, B_NG_N), \tag{5.153}$$

or

$$\bar{\Phi}(I_N \otimes A)\bar{\Phi}^{-1} = \text{diag}(A_1 + B_1F_1, \ldots, A_N + B_NF_N), \tag{5.154}$$
$$\bar{\Phi}(I_N \otimes B) = \text{diag}(B_1G_1, \ldots, B_NG_N). \tag{5.155}$$

Then, expanding A_{cl} as:

$$A_{cl} = \underbrace{\text{diag}(A_1 + B_1F_1, \ldots, A_N + B_NF_N)}_{a_1} + \underbrace{\text{diag}(B_1G_1, \ldots, B_NG_N)}_{b_1}(I_N \otimes K_1 + M \otimes K_2)\bar{\Phi}^{-1}, \tag{5.156}$$

and substituting a_1 and b_1 using (5.154) and (5.155), respectively, (5.156) becomes:

$$A_{cl} = \bar{\Phi}(I_N \otimes A)\bar{\Phi}^{-1} + \bar{\Phi}(I_N \otimes B)(I_N \otimes K_1 + M \otimes K_2)\bar{\Phi}^{-1}, \tag{5.157}$$

which can be written as:

$$A_{cl} = \bar{\Phi}\left(I_N \otimes A + (I_N \otimes B)(I_N \otimes K_1 + M \otimes K_2)\right)\bar{\Phi}^{-1}. \tag{5.158}$$

From (5.158), matrices A_{cl}, $I_N \otimes A + (I_N \otimes B)(I_N \otimes K_1 + M \otimes K_2)$ are similar. Also, from Theorem 3.3.14, $I_N \otimes A + (I_N \otimes B)(I_N \otimes K_1 + M \otimes K_2)$ is a Hurwitz matrix which implies that the closed-loop matrix A_{cl} is also Hurwitz. This proves the theorem. □

The main consequences of Theorem 5.4.1 are summarized as follows:

1) The state-feedback controller $\hat{K}$ in (5.149) has a distributed sparsity pattern provided that $M \in \mathscr{K}_{1,1}^N(\mathscr{G})$.

2) We can use any method for designing matrices K_1, K_2, and M that guarantees stability of the closed-loop system $I_N \otimes A + (I_N \otimes B)(I_N \otimes K_1 + M \otimes K_2)$.

3) The latter consequence implies that matrix M may be consistent with the topology of a connected digraph. This elegant feature stems from the specific structure of the model-matching problem defined in Section 5.2.

4) In the setting of Theorem 5.4.1, the closed-loop stability of the distributed scheme is irrespective of the particular tuning of the LQR performance index. Thus, selecting an optimal target model $(A,\ B)$ thereby minimizing the joint model-matching energy loss in a certain sense, network's performance can effectively be controlled via the tuning parameters Q_1, Q_2, R.

As concluded in the second and third consequence above, network's stability is guaranteed as long as matrix $I_N \otimes A + (I_N \otimes B)(I_N \otimes K_1 + M \otimes K_2)$ is Hurwitz. As shown in Chapter 4, since matrices K_1, K_2, M can also be defined for networks with directed interconnection topology via either the top-down or bottom-up method, the proposed model-matching distributed scheme can then be generalized towards this direction. This is summarized in the following theorem.

Theorem 5.4.2. *Let N controllable pairs $(A_i,\ B_i)$, $i = 1,\ldots,N$, with $A_i \in \mathbb{R}^{n\times n}$, $B_i \in \mathbb{R}^{n\times m}$, have identical sets of controllability indices. Let also matrices A, B, F_i, G_i, and Φ_i be defined as in Theorem 5.2.3, such that*

$$(A,\ B) = (\Phi_i^{-1}(A_i + B_i F_i)\Phi_i,\ \Phi_i^{-1} B_i G_i),\ i = 1,\ldots,N, \tag{5.159}$$

where $(A,\ B)$ is a controllable pair. Consider LQR problem (3.65) *with tuning parameters $(Q_1,\ Q_2,\ R)$ for $N_L = d_{\max} + 2$ identical systems with dynamics described by the pair $(A,\ B)$, $d_{\max}$ denoting the maximum vertex in-degree of the associated digraph. Define matrices P, $\tilde{P}_2$ as in* (3.71), (3.72)*, respectively, and let $K_1 = -R^{-1}B'P$, $K_2 = R^{-1}B'\tilde{P}_2$. Let also matrix $M \in \mathbb{R}^{N\times N}$ be a real matrix with the following property:*

$$\boldsymbol{Re}(\lambda_i(M)) > \frac{N_L}{2},\ \forall\ \lambda_i(M) \in S(M)\backslash\{0\}, \tag{5.160}$$

and construct a state-feedback controller as:

$$\hat{K} = (\mathrm{diag}(F_1,\ldots,F_N) + \mathrm{diag}(G_1,\ldots,G_N)(I_N \otimes K_1 + M \otimes K_2)\mathrm{diag}(\Phi_1^{-1},\ldots,\Phi_N^{-1}). \tag{5.161}$$

Then, the closed-loop matrix

$$A_{cl} = \text{diag}(A_1, \ldots, A_N) + \text{diag}(B_1, \ldots, B_N)\hat{K}, \tag{5.162}$$

is Hurwitz.

Proof. As shown in Theorem 5.4.1, matrix A_{cl} is similar to $I_N \otimes A + (I_N \otimes B)(I_N \otimes K_1 + M \otimes K_2)$ which is a Hurwitz matrix from Theorem 4.3.4. This proves the theorem. □

5.5 Numerical example: stabilization of network of non-identical oscillators

We consider a network of eleven harmonics oscillators, each one modelled by a two-mass-two-spring system depicted in Fig. 5.5. The i-th oscillator is composed of two masses, $m_{i,1}$

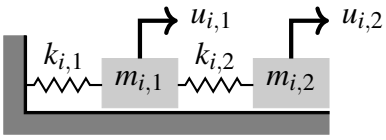

Fig. 5.5 Two-mass-two-spring harmonic oscillator.

and $m_{i,2}$, which are connected through a spring, with spring constant $k_{i,2}$, with the mass $m_{i,1}$ being attached to a rigid object through a spring with spring constant $k_{i,1}$. Two input forces $u_{i,1}$ and $u_{i,2}$ are applied on $m_{i,1}$ and $m_{i,2}$, respectively. The displacement of the two masses from their equilibrium position are represented by $x_{i,1}$ and $x_{i,2}$, respectively, with $i = 1, \ldots, 11$. The state-space forms of the eleven oscillators are written as follows:

$$\begin{bmatrix} \dot{x}_{i,1} \\ \ddot{x}_{i,1} \\ \dot{x}_{i,2} \\ \ddot{x}_{i,2} \end{bmatrix} = \underbrace{\begin{bmatrix} 0 & 1 & 0 & 0 \\ \frac{-k_{i,1}-k_{i,2}}{m_{i,1}} & 0 & \frac{k_{i,2}}{m_{i,1}} & 0 \\ 0 & 0 & 0 & 1 \\ \frac{k_{i,2}}{m_{i,2}} & 0 & \frac{-k_{i,2}}{m_{i,2}} & 0 \end{bmatrix}}_{A_i} \begin{bmatrix} x_{i,1} \\ x_{i,2} \\ \dot{x}_{i,1} \\ \dot{x}_{i,2} \end{bmatrix} + \underbrace{\begin{bmatrix} 0 & 0 \\ \frac{1}{m_{i,1}} & 0 \\ 0 & 0 \\ 0 & \frac{1}{m_{i,2}} \end{bmatrix}}_{B_i} \begin{bmatrix} u_{i,1} \\ u_{i,2} \end{bmatrix}, \; i = 1, \ldots, 11. \tag{5.163}$$

Parameters of all oscillators are summarized in Table 5.1. State-space forms (5.163) are

Table 5.1 Masses and spring constants

System	$k_{i,1}$	$k_{i,2}$	$m_{i,1}$	$m_{i,2}$
oscillator 1	1.50 N/m	1.00 N/m	1.10 kg	0.90 kg
oscillator 2	3.10 N/m	2.00 N/m	2.10 kg	1.50 kg
oscillator 3	0.50 N/m	1.10 N/m	1.50 kg	3.20 kg
oscillator 4	2.00 N/m	1.30 N/m	3.10 kg	2.10 kg
oscillator 5	1.70 N/m	3.10 N/m	4.10 kg	2.50 kg
oscillator 6	2.20 N/m	4.20 N/m	5.10 kg	4.20 kg
oscillator 7	4.10 N/m	2.50 N/m	1.20 kg	5.10 kg
oscillator 8	2.50 N/m	1.80 N/m	5.10 kg	2.30 kg
oscillator 9	10.5 N/m	30.3 N/m	1.30 kg	1.20 kg
oscillator 10	2.70 N/m	0.80 N/m	1.40 kg	5.20 kg
oscillator 11	5.20 N/m	2.20 N/m	3.50 kg	2.40 kg

clearly in controllable canonical form. Thus, matrices $(A_i,\ B_i)$ may be written as:

$$A_i = \underbrace{\begin{bmatrix} 0 & 1 & 0 & 0 \\ 0 & 0 & 0 & 0 \\ 0 & 0 & 0 & 1 \\ 0 & 0 & 0 & 0 \end{bmatrix}}_{\bar{A}_c} + \underbrace{\begin{bmatrix} 0 & 0 \\ 1 & 0 \\ 0 & 0 \\ 0 & 1 \end{bmatrix}}_{\bar{B}_c} \underbrace{\begin{bmatrix} \frac{-k_{i,1}-k_{i,2}}{m_{i,1}} & 0 & \frac{k_{i,2}}{m_{i,1}} & 0 \\ \frac{k_{i,2}}{m_{i,2}} & 0 & \frac{-k_{i,2}}{m_{i,2}} & 0 \end{bmatrix}}_{A_{m,i}},\ i = 1,\ldots,11, \tag{5.164a}$$

$$B_i = \underbrace{\begin{bmatrix} 0 & 0 \\ 1 & 0 \\ 0 & 0 \\ 0 & 1 \end{bmatrix}}_{\bar{B}_c} \underbrace{\begin{bmatrix} \frac{1}{m_{i,1}} & 0 \\ 0 & \frac{1}{m_{i,2}} \end{bmatrix}}_{B_{m,i}},\ i = 1,\ldots,11, \tag{5.164b}$$

respectively. The pair $(\bar{A}_c,\ \bar{B}_c)$ denotes the Brunovsky form which is clearly identical to all systems $(A_i,\ B_i)$, $i = 1,\ldots,11$. Obviously, systems $(A_i,\ B_i)$, $i = 1,\ldots,11$, have identical controllability indices which are identified here as $\mu_1 = 2$ and $\mu_2 = 2$.

We use a graph representation of the interaction between neighboring oscillators. Two interconnection schemes are assumed for simulation purposes, identical to those considered in the numerical study of Chapter 4. For convenience these are also shown in Fig. 5.6. Each graph indicates that if an edge (i, j), $i, j = 1,\ldots,11$, $i \neq j$ is present then the j-th oscillator has full information about the state of the i-th oscillator. We denote the Laplacian matrix of graph $\mathscr{G}_{11}$ shown in Fig. 5.6a by $\mathscr{L}_{G,11}$ and the in-degree Laplacian matrix of digraph $\mathscr{D}_{11}$ shown in Fig. 5.6b by $\mathscr{L}_{D,11}$. These have been defined in (4.197) and (4.198), respectively.

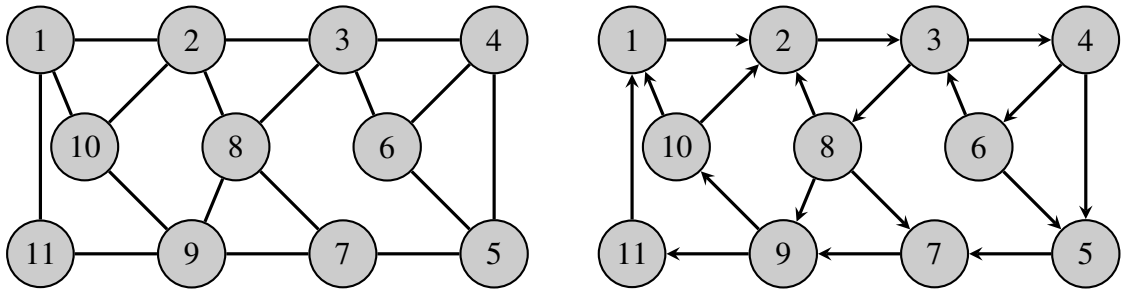

(a) Graph $\mathscr{G}_{11}$. (b) Digraph $\mathscr{D}_{11}$.

Fig. 5.6 Interconnection schemes of eleven oscillators.

For each topology scheme shown in Fig. 5.6, we wish to solve the following regulator problem:

$$\min_{\hat{u}} J(\hat{u},\hat{x}_0) \text{ subject to:} \tag{5.165a}$$

$$J(\hat{u},\hat{x}_0) = \int_0^\infty \left(\hat{x}'\hat{Q}\hat{x} + \hat{u}'\hat{R}\hat{u}\right) \mathrm{d}t \tag{5.165b}$$

$$\dot{\hat{x}} = \hat{A}\hat{x} + \hat{B}\hat{u},\ \hat{x}(0) = \hat{x}_0 \tag{5.165c}$$

$$\begin{aligned}\hat{u} = {} & (\mathrm{diag}(F_1,\ldots,F_N) \\ & + \mathrm{diag}(G_1,\ldots,G_N)(I_N \otimes K_1 + M \otimes K_2)\mathrm{diag}(\Phi_1^{-1},\ldots,\Phi_N^{-1}))\hat{x},,\end{aligned} \tag{5.165d}$$

where

$$\hat{A} = \mathrm{diag}(A_1,\ldots,A_N), \tag{5.166}$$

$$\hat{B} = \mathrm{diag}(B_1,\ldots,B_N), \tag{5.167}$$

and

$$\hat{Q} = I_N \otimes Q_1 + \mathscr{L}_{G,11} \otimes Q_2, \tag{5.168}$$

$$\hat{R} = I_N \otimes R. \tag{5.169}$$

Note that $\mathscr{L}_{G,11}$ in (5.168) is the Laplacian matrix of the graph $\mathscr{G}_{11}$. This symmetric selection of $\hat{Q}$ is in force for both interconnection schemes. We follow a two-stage control design as suggested earlier in the chapter. First, we construct the model-matching design parameters F_i, G_i, Φ_i, $i = 1,\ldots,11$. Since systems $(A_i,\ B_i)$, $i = 1,\ldots,11$, are in controllable canonical form, matrices Φ_i, $i = 1,\ldots,11$, can automatically be selected as the identity matrix. Setting $G_i = B_{m,i}^{-1}$, $i = 1,\ldots,11$, we design model-matching state-feedback gains F_i, $i = 1,\ldots,11$, in

the following fashion. We consider two model-matching performance indexes represented by

$$J_{aver}(A_m) = \sum_{i=1}^{N} \|F_i\|_F^2 = \sum_{i=1}^{N} \|B_{m,i}^{-1}(A_m - A_{m,i})\|_F^2, \tag{5.170}$$

and

$$J_{max}(A_m) = \max_{i\in[1:11]} \|F_i\|_F^2 = \max_{i\in[1:11]} \|B_{m,i}^{-1}(A_m - A_{m,i})\|_F^2, \tag{5.171}$$

respectively. Obviously, minimizing these two cost functions over matrices in $\mathbb{R}^{2\times 4}$ results in two different target models which are used later in the simulations. We denote by $A_{m,aver}^*$ the minimal solution of

$$\min\ J_{aver}(\cdot), \tag{5.172}$$

and by $A_{m,max}^*$ the approximate minimizer of the minimax problem:

$$\min\ J_{max}(\cdot), \tag{5.173}$$

derived from the efficient minimax algorithm discussed in Section 5.3.1. The least-squares solution results in

$$A_{m,aver}^* = \begin{bmatrix} -1.8534 & 0 & 1.0178 & 0 \\ 0.9168 & 0 & -0.9168 & 0 \end{bmatrix}, \tag{5.174}$$

while the minimax algorithm after 67 iterations converges to

$$A_{m,max}^* = \begin{bmatrix} -7.7488 & 0 & 5.6556 & 0 \\ 6.7050 & 0 & -6.7050 & 0 \end{bmatrix}, \tag{5.175}$$

with the convergence error set to 10^{-5}. Note the relatively large distance between matrices $A_{m,aver}^*$ and $A_{m,max}^*$. This stems from the extreme choice of high springs' stiffness of oscillator 9 as seen in Table 5.1. In essence, the least-squares solution $A_{m,aver}^*$ attempts to achieve the average of $\|F_i\|_F^2$, $i = 1,\ldots,11$, while the approximate minimizer $A_{m,max}^*$ is clearly attracted from the outlier matrix $A_{m,9}$. The optimal model of the target system arising from the minimization of the two performance indexes above, is obtained from $(\bar{A}_c + \bar{B}_c A_m^*,\ \bar{B}_c)$, A_m^* denoting each particular optimal solution (5.174), (5.175), respectively.

An alternative target model selection is outlined next. As mentioned in Section 5.2, it is possible to achieve a target model with certain performance specifications. As a third target choice, we require the eigenvalues of the target system lie in the cone represented by two line segments starting at the origin, each line segment forming an angle of $\pi/3$ with the negative

real axis. Requiring $\lambda = 0$, $\rho = 0$, $\theta = \pi/3$ and solving

$$\min_{\gamma>0} \gamma \text{ subject to: (5.69)}, \tag{5.176}$$

we get

$$A^*_{m,LMI} = \begin{bmatrix} -0.9259 & 0 & -2.2734 & 0 \\ 0 & -0.9257 & 0 & -2.2733 \end{bmatrix}. \tag{5.177}$$

Having obtained three different target models, the corresponding model-matching state-feedback gains for each choice are obtained from:

$$F_i = B^{-1}_{m,i}(A^*_m - A_{m,i}),\ i = 1,\ldots,11, \tag{5.178}$$

substituting $A^*_{m,aver}$, $A^*_{m,max}$, $A^*_{m,LMI}$ into A^*_m, respectively.

In the second stage of the control design, we define matrices K_1, K_2, M such that the control law in (5.165d) is stabilizing. The top-down approach is adopted next. The maximum vertex degree of $\mathscr{G}_{11}$ is $d_{\max,\mathscr{G}_{11}} = 4$ while the maximum vertex in-degree of $\mathscr{D}_{11}$ is $d_{\max,\mathscr{D}_{11}} = 3$, as seen in Fig. 5.6a, 5.6b, respectively. For each target system represented as $(A,\ B)$, we solve LQR problem (3.65) for $N_L = 5$ systems $(A,\ B)$ with tuning parameters $(Q_1,\ Q_2,\ R)$. This choice of N_L systems corresponds to either $d_{\max,\mathscr{G}_{11}} + 1$ or $d_{\max,\mathscr{D}_{11}} + 2$ which clearly coincide. This implies that matrices K_1, K_2 are chosen independently of the interconnection scheme. For a particular choice of $(Q_1,\ Q_2,\ R)$ matrices K_1, K_2 are defined as

$$K_1 = -R^{-1}B'P, \tag{5.179}$$

$$K_2 = R^{-1}B'\tilde{P}_2, \tag{5.180}$$

where P, $\tilde{P}_2$ are associated to ARE (3.71), (3.72), respectively.

The stability of each topology is guaranteed by appropriate selection of matrix M. Calculating the eigenvalues of matrices $\mathscr{L}_{G,11}$, $\mathscr{L}_{D,11}$ and choosing $M = \beta\mathscr{L}$, $\mathscr{L}$ denoting the Laplacian matrix of each topology, from Theorem 3.3.14 and 4.3.4, the closed matrix

$$A_{cl,11} = I_{11} \otimes A + (I_{11} \otimes B)(I_{11} \otimes K_1 + M \otimes K_2), \tag{5.181}$$

is guaranteed to be Hurwitz for all $\beta > 2.5$. Here, we choose $\beta = 2.6$ for both interconnection schemes.

The simulation results are presented for two different choices of the tuning parameters $(Q_1,\ Q_2,\ R)$. The first choice penalizes more heavily the local displacements $x_{i,1}$, $x_{i,2}$ than

Table 5.2 Dominant eigenvalues of the overall closed-loop distributed system with undirected topology for three selections of target model

Undirected	minimax	least-squares	LMI
$Q_1 = Q_2$	$-0.1369 \pm \mathrm{i}3.6642$	$-0.3129 \pm \mathrm{i}1.5991$	$-0.8446 \pm \mathrm{i}0.0000$
	$-0.1766 \pm \mathrm{i}3.6677$	$-0.3930 \pm \mathrm{i}1.6324$	$-1.1631 \pm \mathrm{i}0.0000$
	$-0.5092 \pm \mathrm{i}3.6794$	$-0.5467 \pm \mathrm{i}1.6839$	$-1.6134 \pm \mathrm{i}0.0000$
	$-0.4931 \pm \mathrm{i}3.6796$	$-0.6679 \pm \mathrm{i}1.7136$	$-1.3887 \pm \mathrm{i}0.0000$
$Q_1 = 0.0001 Q_2$	$-0.0137 \pm \mathrm{i}3.6616$	$-0.0319 \pm \mathrm{i}1.5683$	$-0.5348 \pm \mathrm{i}0.0000$
	$-0.0490 \pm \mathrm{i}1.0243$	$-0.0886 \pm \mathrm{i}0.5652$	$-1.7408 \pm \mathrm{i}0.0000$
	$-2.0748 \pm \mathrm{i}7.1738$	$-2.1406 \pm \mathrm{i}6.5086$	$-3.0436 \pm \mathrm{i}6.0379$
	$-2.1612 \pm \mathrm{i}6.4145$	$-2.1961 \pm \mathrm{i}6.3573$	$-3.0437 \pm \mathrm{i}6.0379$

the second and uses $Q_1 = \mathrm{diag}(1,1,0,0)$, $Q_2 = Q_1$, $R = I_2$. Velocities of mass displacements are not weighted in this simulation study. In the second choice, LQR cost function is tuned to place more emphasis on the relative state information $(x_i - x_j)$, by selecting $Q_1 = \mathrm{diag}(0.01, 0.01, 0, 0)$, $Q_2 = \mathrm{diag}(100, 100, 0, 0)$, $R = I_2$. Identical initial conditions are considered for all simulations.

Mass displacements of each oscillator with LQR performance index tuned to weigh equally local and relative state displacements are illustrated in Fig. 5.7-5.18 for both undirected and directed interconnection schemes. As indicated in these figures, the stable operation for both undirected and directed distributed schemes is irrespective of the target choice. However, the behavior of the network is fundamentally altered when a target model is selected to satisfy the performance specifications defined earlier. This difference in network's behavior is illustrated in Fig. 5.9, 5.12, 5.15 and 5.18 where systems depict an overdamped response complied with the specifications, in contrast to the oscillatory behavior demonstrated when an optimal target model is chosen. This drastic change in network's operation with respect to target selection is more amplified when LQR cost function penalizes heavily the relative state difference between neighboring oscillators. This is evident for both topologies as shown in Fig. 5.19-5.30. We emphasize here that the highly oscillatory behavior illustrated in these figures stems from the extremely low choice of matrix Q_1 in the local LQR problem $(A,\ B,\ Q_1,\ R)$ resulting in a closed-loop matrix $A - R^{-1}B'P$ with some eigenvalues lying near the imaginary axis (cf. Table 5.2). This may be rectified, if desired, by adjusting appropriately this tuning parameter. As a result, it is seen that the performance of the large-scale distributed control system is effectively controlled by tuning appropriately the LQR cost function. Clearly, this is more evident when the collective model-matching control effort is minimized, a fact that highlights a powerful feature of our model-matching

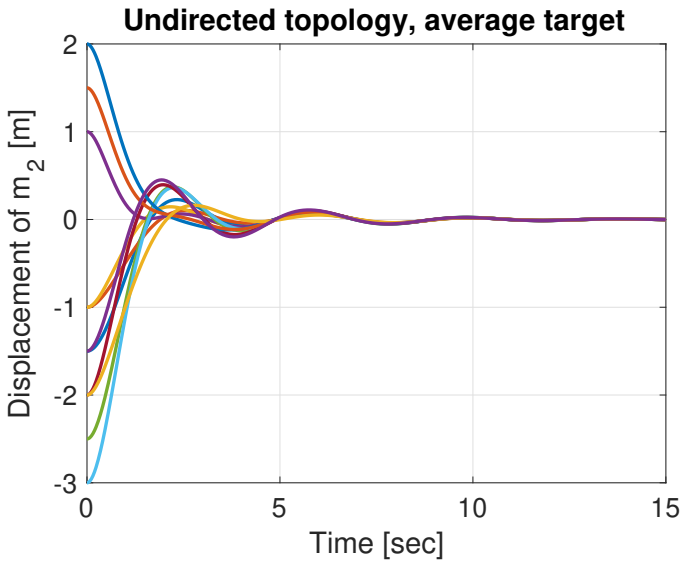

Fig. 5.7 Displacement of m_1 for tuning parameters $Q_1 = Q_2$, undirected topology and least-squares target selection.

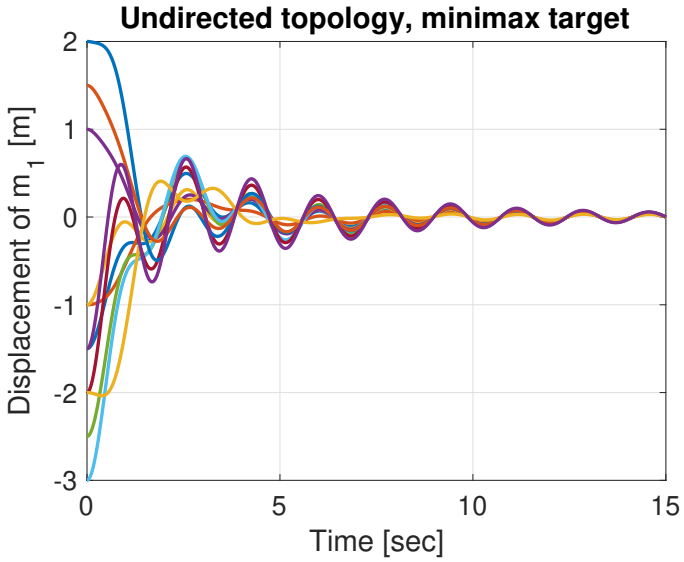

Fig. 5.8 Displacement of m_1 for tuning parameters $Q_1 = Q_2$, undirected topology and minimax target selection.

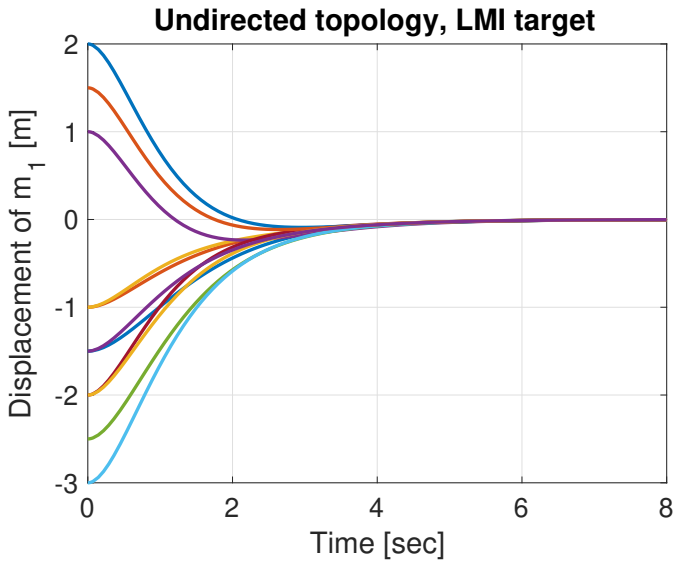

Fig. 5.9 Displacement of m_1 for tuning parameters $Q_1 = Q_2$, undirected topology and target system with performance specifications.

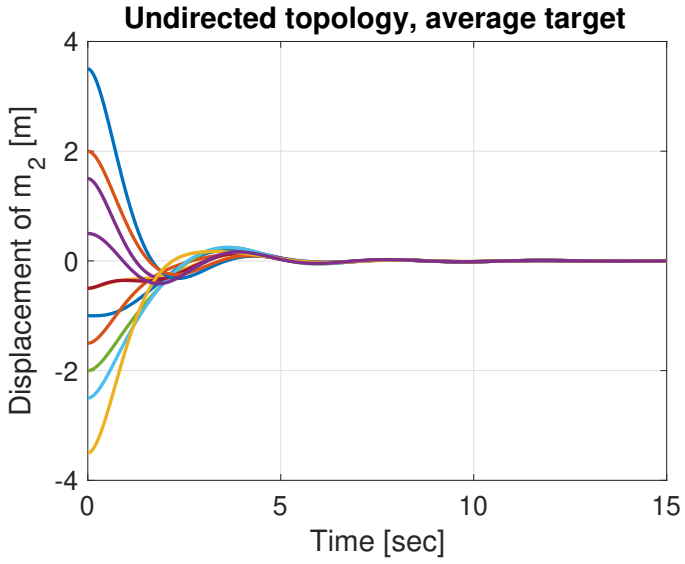

Fig. 5.10 Displacement of m_2 for tuning parameters $Q_1 = Q_2$, undirected topology and least-squares target selection.

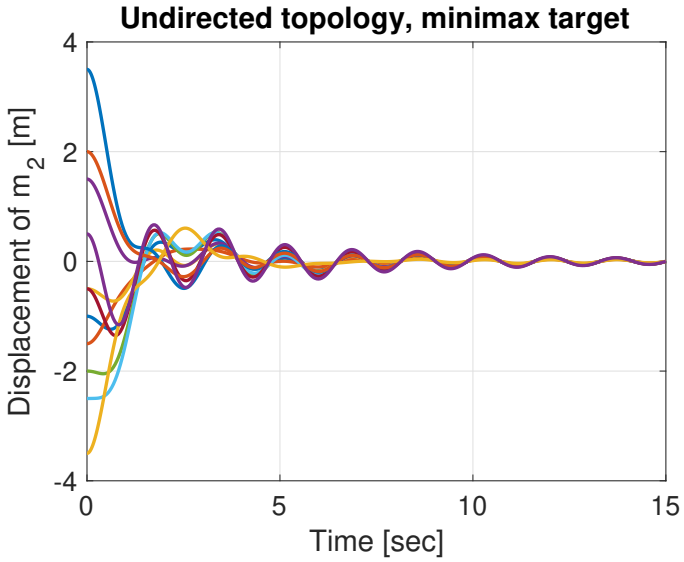

Fig. 5.11 Displacement of m_2 for tuning parameters $Q_1 = Q_2$, undirected topology and minimax target selection.

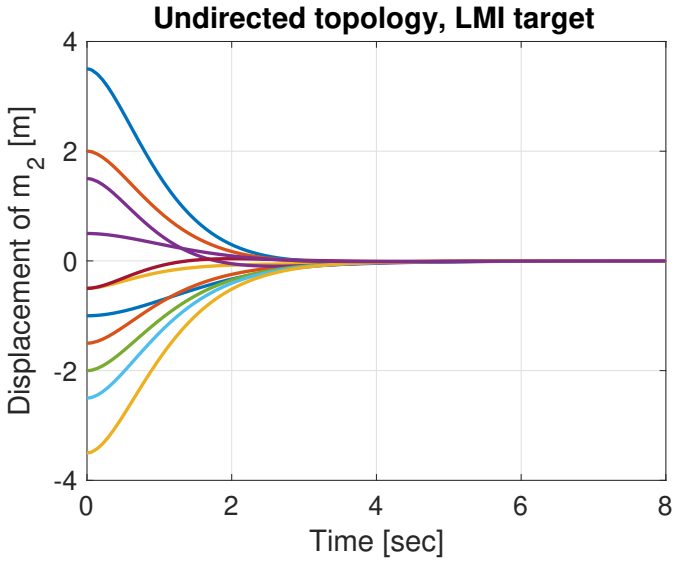

Fig. 5.12 Displacement of m_2 for tuning parameters $Q_1 = Q_2$, undirected topology and target system with performance specifications.

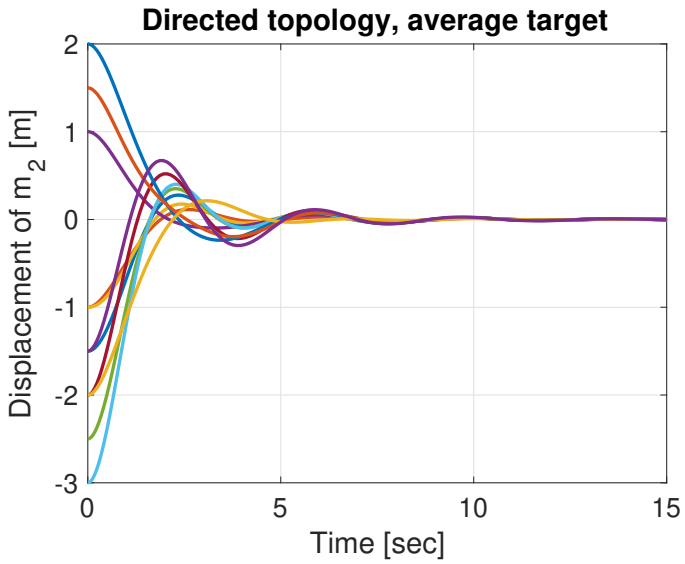

Fig. 5.13 Displacement of m_1 for tuning parameters $Q_1 = Q_2$, directed topology and least-squares target selection.

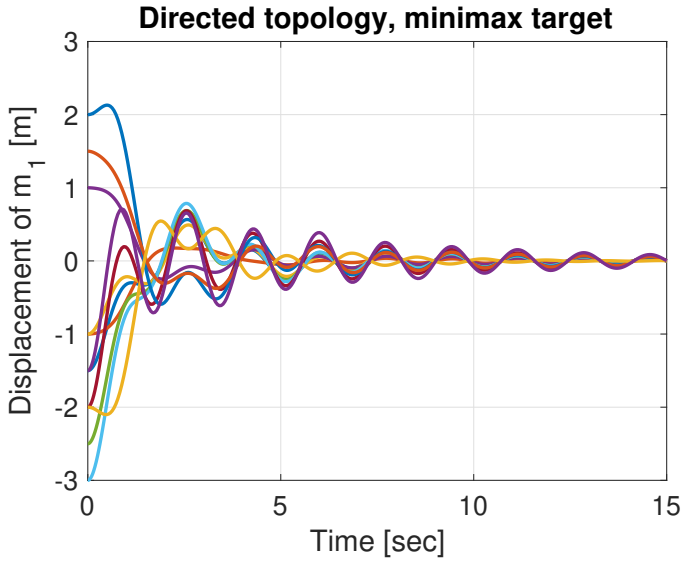

Fig. 5.14 Displacement of m_1 for tuning parameters $Q_1 = Q_2$, directed topology and minimax target selection.

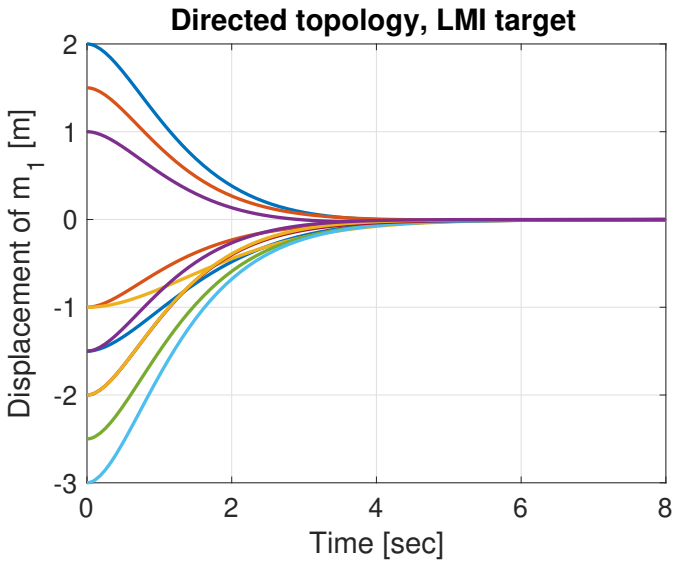

Fig. 5.15 Displacement of m_1 for tuning parameters $Q_1 = Q_2$, directed topology and target system with performance specifications.

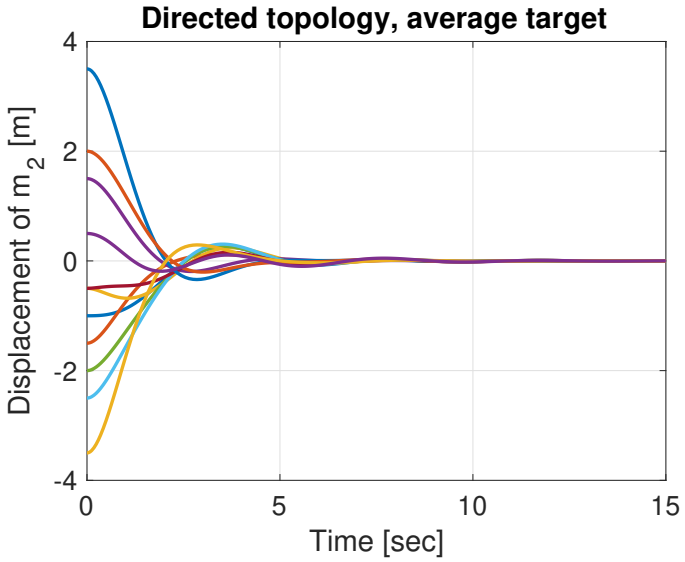

Fig. 5.16 Displacement of m_2 for tuning parameters $Q_1 = Q_2$, directed topology and least-squares target selection.

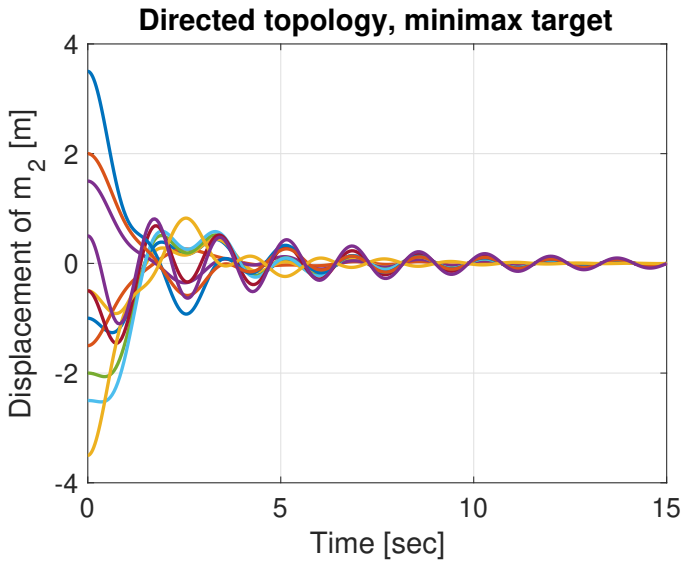

Fig. 5.17 Displacement of m_2 for tuning parameters $Q_1 = Q_2$, directed topology and minimax target selection.

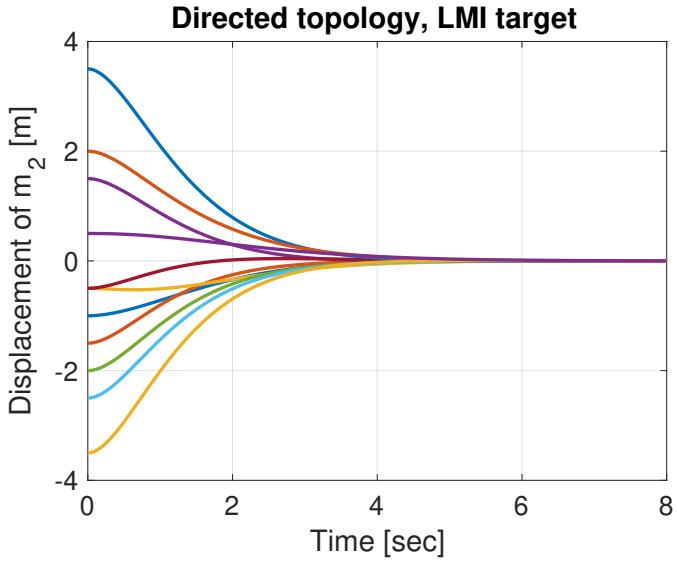

Fig. 5.18 Displacement of m_2 for tuning parameters $Q_1 = Q_2$, directed topology and target system with performance specifications.

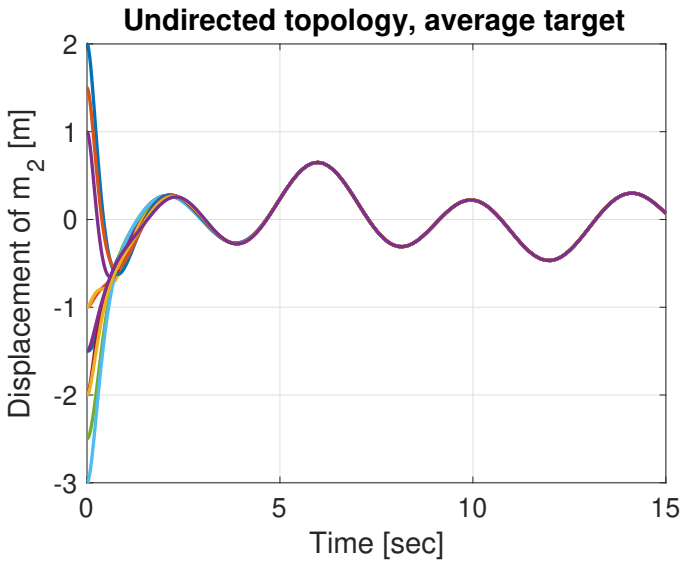

Fig. 5.19 Displacement of m_1 for tuning parameters $Q_2 = 10000Q_1$, undirected topology and least-squares target selection.

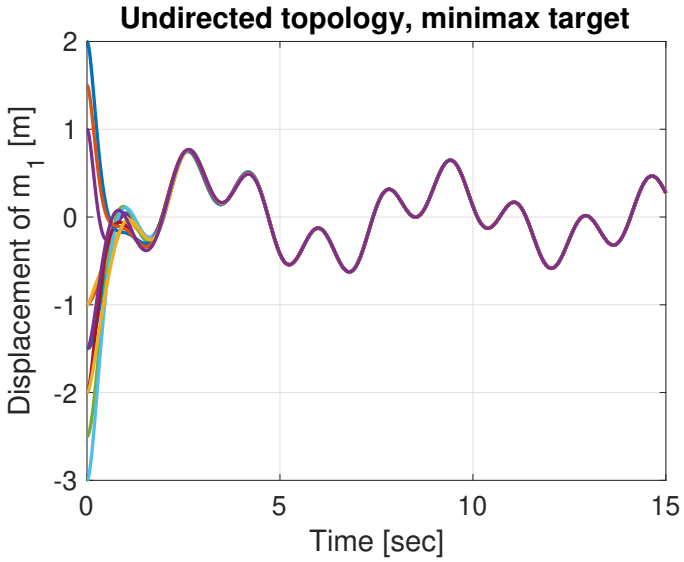

Fig. 5.20 Displacement of m_1 for tuning parameters $Q_2 = 10000Q_1$, undirected topology and minimax target selection.

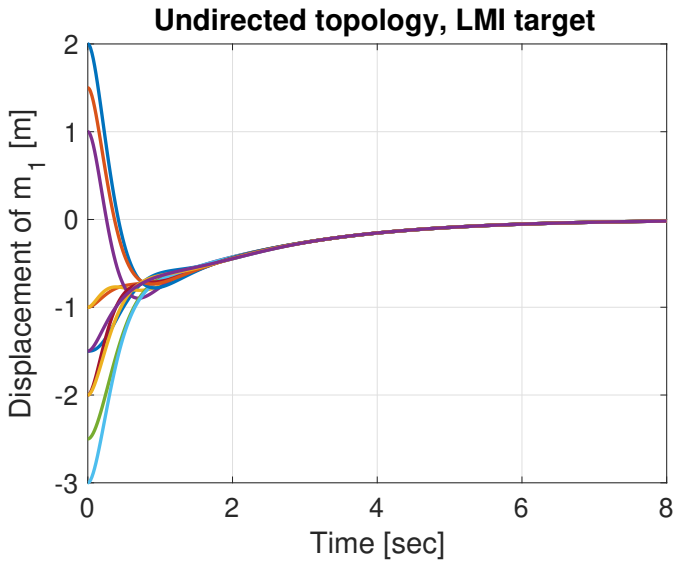

Fig. 5.21 Displacement of m_1 for tuning parameters $Q_2 = 10000Q_1$, undirected topology and target system with performance specifications.

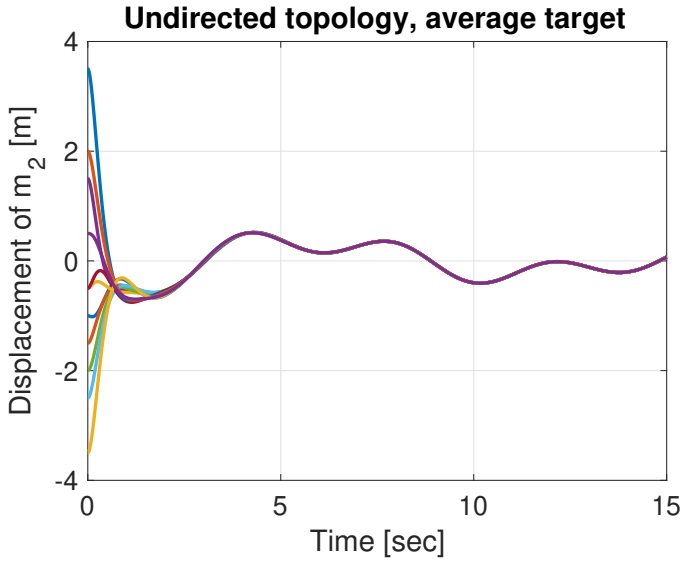

Fig. 5.22 Displacement of m_2 for tuning parameters $Q_2 = 10000Q_1$, undirected topology and least-squares target selection.

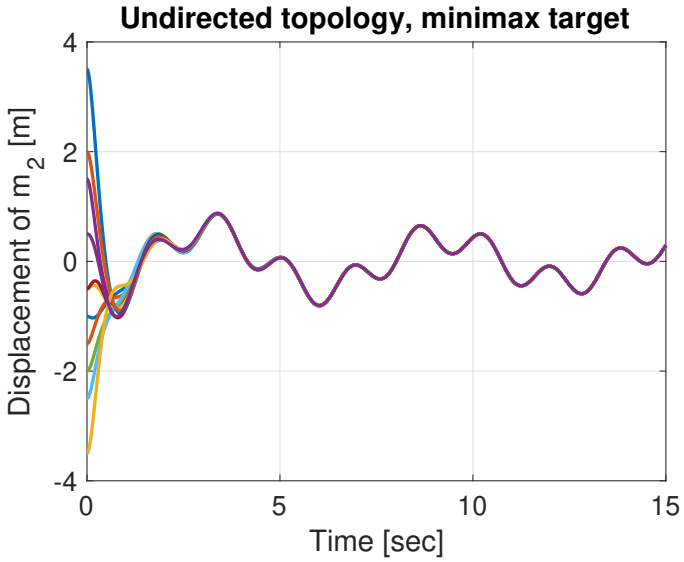

Fig. 5.23 Displacement of m_2 for tuning parameters $Q_2 = 10000Q_1$, undirected topology and minimax target selection.

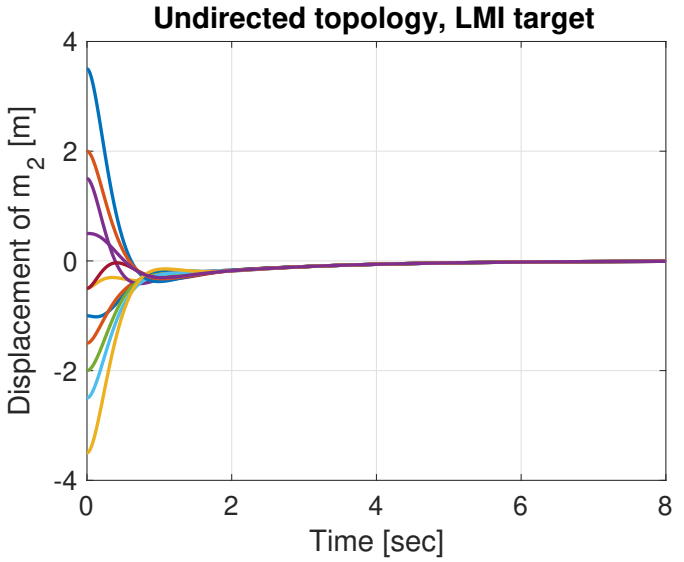

Fig. 5.24 Displacement of m_2 for tuning parameters $Q_2 = 10000Q_1$, undirected topology and target system with performance specifications.

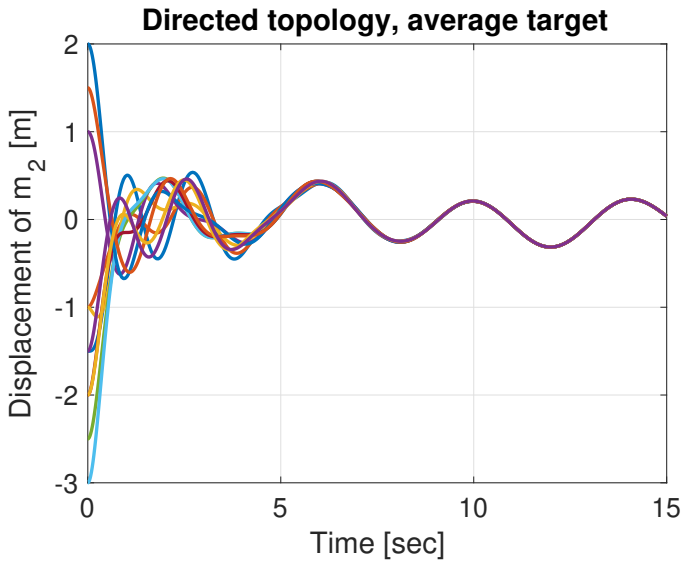

Fig. 5.25 Displacement of m_1 for tuning parameters $Q_2 = 10000Q_1$, directed topology and least-squares target selection.

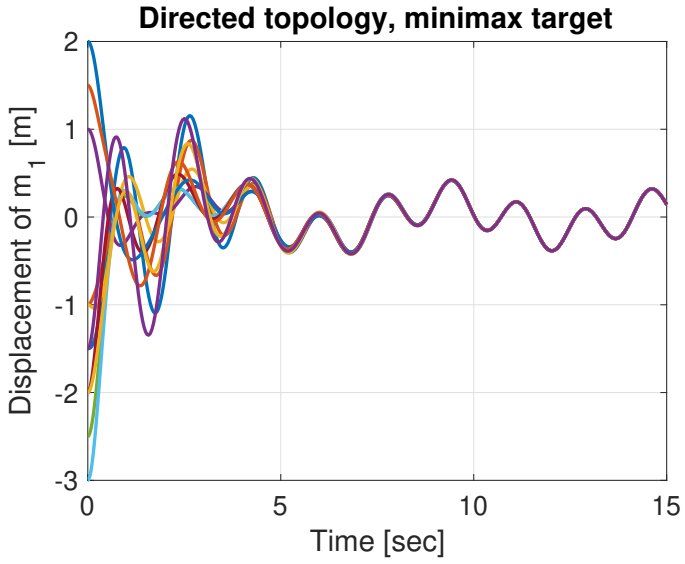

Fig. 5.26 Displacement of m_1 for tuning parameters $Q_2 = 10000Q_1$, directed topology and minimax target selection.

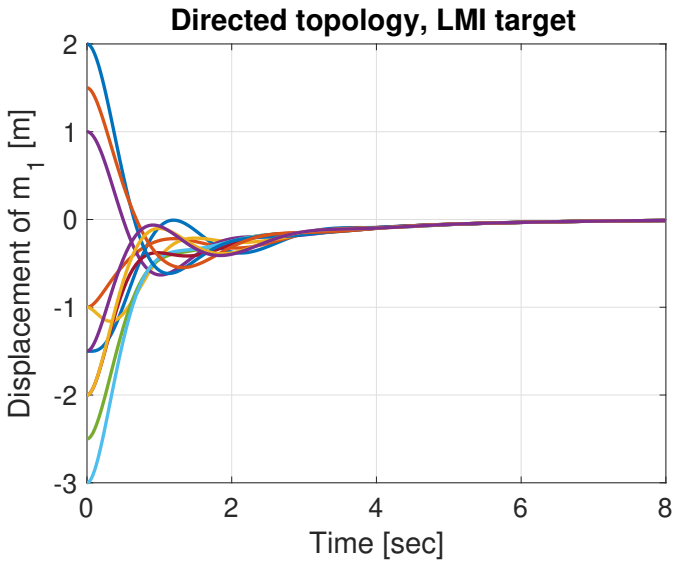

Fig. 5.27 Displacement of m_1 for tuning parameters $Q_2 = 10000Q_1$, directed topology and target system with performance specifications.

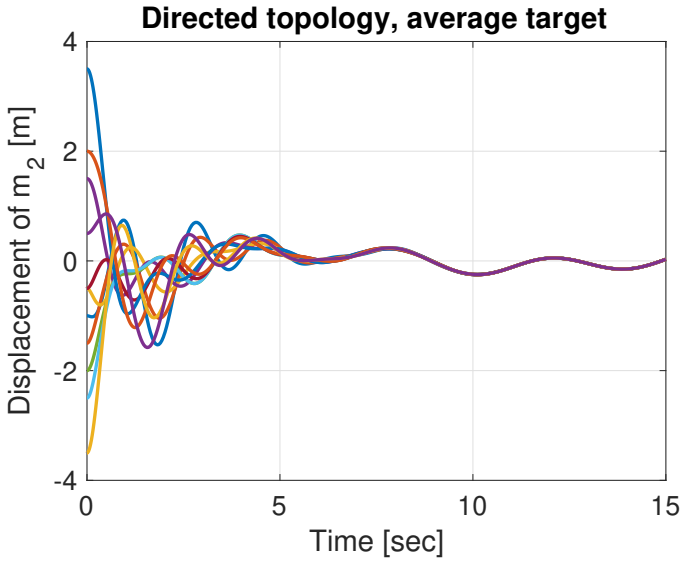

Fig. 5.28 Displacement of m_2 for tuning parameters $Q_2 = 10000Q_1$, directed topology and least-squares target selection.

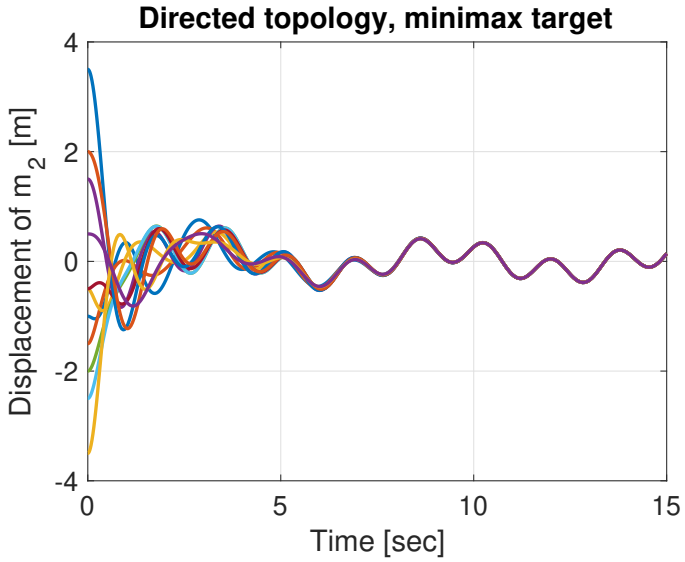

Fig. 5.29 Displacement of m_2 for tuning parameters $Q_2 = 10000Q_1$, directed topology and minimax target selection.

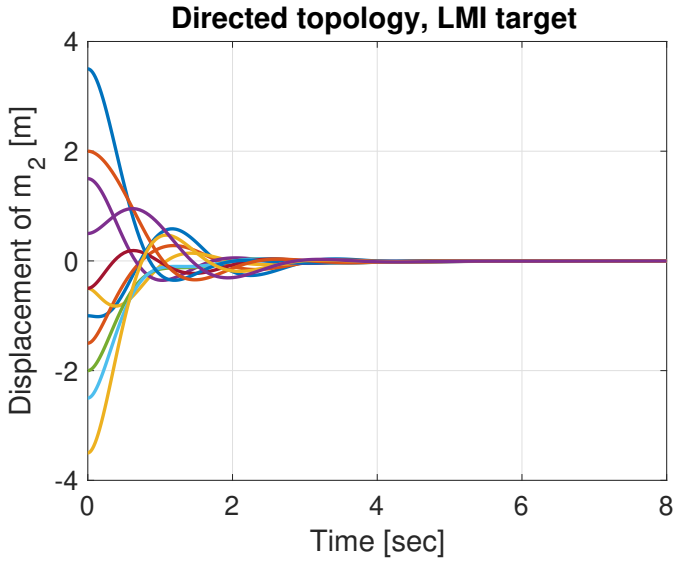

Fig. 5.30 Displacement of m_2 for tuning parameters $Q_2 = 10000Q_1$, directed topology and target system with performance specifications.

control approach. Similarly, enforcing a target model with certain dynamical requirements may be beneficial for the distributed control scheme for performance specifications which can not be imposed through the tuning parameters Q_1, Q_2, R, in a straightforward manner.

5.6 Conclusion

In this chapter, we have attempted to remove the restrictive assumption of identical system dynamics considered in two well-established distributed control methods. Via a two-stage control strategy, we have shown that this technical limitation can be relaxed with more natural requirements. In particular, we assume that agents constituting the network belong to the family of linear systems completely characterized by identical sets of controllability indices. The first stage of the method solves model-matching problems and synthesizes local state-feedback controllers defined such that the closed-loop agents are mapped to a target model. In the second stage of the method, the distributed control scheme is designed on the target dynamics via either the top-down or bottom-up method. Essentially, it is emphasized that any stabilizing distributed state-feedback scheme designed on the target dynamics, can be adopted in the present setting. This feature is indicative of the high flexibility of our approach. It has also been highlighted that the selection of the target model can be specified such that the perturbations in the systems' models produced by state-feedback controllers are minimal in a well-defined sense. The definition of the target model can then be attained by minimizing a certain measure of the joint model-matching control effort. In this respect, the closed-loop network performance depends primarily on the LQR optimality criterion. It will be shown that the model-matching approach to the distributed control design can be extended to a certain class of heterogeneous interconnected agents with nonlinear dynamics. This is studied in the following chapter.

Chapter 6

Feedback linearization and model-matching of nonlinear systems

6.1 Introduction

The chapter deals with a special family of nonlinear systems which are referred to as *feedback linearizable* systems. This characterization stems from the claim that certain nonlinear systems can be described by a set of linear equations by making an appropriate change of coordinates and applying a nonlinear state-feedback control law. Then, these linear equations can further be transformed to the Brunovsky canonical form completely characterized by the set of controllability indices as shown in Chapter 5. This method is called feedback linearization and has been broadly studied in the literature. Motivated by this well-established technique, our aim here is primarily to solve model-matching type problems over a set of nonlinear systems via feedback linearization control. In view of this objective and based on the results of the previous chapter, we show that, in a network setup with self-linearizable agents mapped to a specific linear target model via model-matching operations, the regulation problem can be solved via linear LQR-based control as evidenced in the previous chapter.

Reviewing first some useful results of differential geometry, we introduce necessary and sufficient conditions for feedback linearization of a class of nonlinear systems. Then, we define the model-matching problem over a set of systems as a linearization problem of multiple nonlinear models that are mapped to a certain linear system via nonlinear feedback control and a change of coordinates. The matching dynamics referred to as target model, can either be specified a priori or obtained by optimizing a model-matching performance index. The second selection strategy effectively suggests that a linear target system may be derived such that the perturbations in the agents' models produced by nonlinear feedback control

are minimal. In the linear case studied in Chapter 5, these perturbations were expressed as quadratic functions of some vector variable. However, in the present setting, defining a performance index of model-matching energy loss results in a highly nonlinear function the minimization of which can not be tackled straightforwardly. This is mainly due to nonlinear dependence of the cost function on state variables. This peculiarity is addressed by defining local cost functions expressed as weighted average model-matching energy measures over a specific range of the state-space in which state-vectors are distributed according to a joint density function. The latter may be utilized to emphasize/de-emphasize a specific region of the state-space and can be designed irrespective of the statistics of the state variables. It will be shown that the definition of weighted average cost functions simplifies the optimization problem significantly and allows for an optimal target solution independent of state variables.

The family of nonlinear systems studied in this chapter are described by a set of equations of the form:

$$\dot{x}(t) = \mathbf{f}[x(t)] + \sum_{j=1}^{m} u_j(t)\mathbf{g}_j[x(t)],\ x(0) = x_0, \tag{6.1}$$

where $x(t) \in \mathbb{R}^n$, $u_j \in \mathbb{R}$, $j = 1, \ldots, m$, and $\mathbf{f}, \mathbf{g}_1, \ldots, \mathbf{g}_m$ are vector fields on $\mathbb{R}^n$. In the sequel, $\mathbf{f}(x(t))$ and $\mathbf{g}_j(x(t))$ are denoted as $\mathbf{f}[x(t)]$ and $\mathbf{g}_j[x(t)]$, respectively, for clarity. Vector fields are defined precisely in Section 6.2 below. Here, we focus on nonlinear systems described by (6.1) which are assumed to be (locally) reachable at all points in some neighborhood of $x_0 \in \mathbb{R}^n$. The notion of local reachability is clearly defined in the next section along with some useful results of differential geometry. A thorough study of this subject can be found in [216]. We remark that differential geometric methods, utilized throughout the chapter, can also be applied to the general class of nonlinear systems with n states and m inputs described by

$$\dot{x}(t) = \mathbf{f}[x(t), u(t)]. \tag{6.2}$$

However, due to an enormous increase in complexity in this case, and in order to keep the subsequent technical analysis as simple as possible, we consider the less general, *linear in control* class of systems described by (6.1).

6.2 Basic results of differential geometry

First, we recall the well-known inverse function theorem and then we introduce the notions of a vector field, a form and various types of Lie derivatives.

Let $\mathbf{f}:\ \mathbb{R}^n \to \mathbb{R}^n$ and suppose each component of $\mathbf{f}$ is continuously differentiable with respect to each of its arguments. The latter can also be described by saying that $\mathbf{f}$ is $\mathscr{C}^1$. Then, the $m \times n$ matrix whose (i, j)-entry is $\partial f_i / \partial x_j$ is called the Jacobian matrix of $\mathbf{f}$ and is

denoted as $\partial \mathbf{f}/\partial x$. We say that $\mathbf{f}$ is smooth if every component of $\mathbf{f}$ has continuous derivatives of all orders with respect to all combinations of its arguments. Let now U, V be open subsets of $\mathbb{R}^n$ and $\mathbf{f}: U \to V$ be $\mathscr{C}^1$. It is said that $\mathbf{f}$ is a diffeomorphism of U onto V if:

(i) $\mathbf{f}(U) = V$.

(ii) $\mathbf{f}$ is one-to-one.

(iii) The inverse function $\mathbf{f}^{-1}: V \to U$ is also $\mathscr{C}^1$.

Then, $\mathbf{f}$ is called a smooth diffeomorphism if both $\mathbf{f}$ and $\mathbf{f}^{-1}$ are smooth functions. We now present the inverse function theorem as stated in [216].

Theorem 6.2.1 (Inverse Function Theorem, [216])**.** *Suppose $\boldsymbol{f}: \mathbb{R}^n \to \mathbb{R}^n$ is $\mathscr{C}^1$ at $x_0 \in \mathbb{R}^n$ and let $y_0 = \boldsymbol{f}(x_0)$. Let $[\partial \boldsymbol{f}/\partial x]_{x=x_0}$ be nonsingular. Then, there exist open sets $U \subseteq \mathbb{R}^n$ containing x_0 and $V \subseteq \mathbb{R}^n$ containing y_0 such that $\boldsymbol{f}$ is a diffeomorphism of U onto V. If, in addition, $\boldsymbol{f}$ is smooth, then $\boldsymbol{f}^{-1}$ is also smooth, i.e., $\boldsymbol{f}$ is a smooth diffeomorphism.*

We note that all diffeomorphisms considered throughout the chapter are assumed to be smooth, hence the term smooth is often omitted unless necessary.

In the sequel, an open set of $\mathbb{R}^n$ is denoted as $X \subseteq \mathbb{R}^n$, n representing the state-dimension of the system under study.

Definition 6.2.1. A vector field on X is a smooth function mapping X into $\mathbb{R}^n$. The set of all vector fields on X is denoted by $V(X)$.

Definition 6.2.2. The set of all smooth real-valued functions mapping X into $\mathbb{R}$ is denoted by $S(X)$.

For $a, b \in S(X)$ and $\mathbf{f}, \mathbf{g} \in V(X)$ the following hold true:

a(**f**+**g**)=a**f**+a**g**

(a+b)**f**=a**f**+b**f**

(ab)**f**=a(b**f**)

We also state the following definition.

Definition 6.2.3. A form on X is a smooth function mapping X into $(\mathbb{R}^n)^*$, which is the set of $1 \times n$ row vectors. The set of all forms on X is denoted by $F(X)$.

Clearly, from Definition 6.2.1 and 6.2.3, if $\mathbf{f} \in V(X)$ then $\mathbf{f}' \in F(X)$. Next, we define some basic operations involving vector fields, forms and smooth real-valued functions.

Suppose $x_0 \in X$ is given. A curve in X passing through x_0 is a smooth function c mapping some open interval $(-a,\ b)$ containing 0 into X, such that $c(0) = x_0$. Let now $\mathbf{f}$ be a vector field on X and that $x_0 \in X$ be given, and suppose that there exists a unique solution of the differential equation

$$\frac{d}{dt}x(t) = \mathbf{f}[x(t)],\ x(0) = x_0, \tag{6.3}$$

for sufficiently small values of t. Then, solution $x(\cdot)$ viewed as a function of t, defines a curve passing through x_0 which is called the integral curve of $\mathbf{f}$ and is denoted as $s_{\mathbf{f},t}(x_0)$.

Next, we define the transformation of a vector field under a change of coordinates. Let $\mathbf{f} \in V(X)$, $x_0 \in X$ be given and also T be a (smooth) diffeomorphism in some neighborhood of x_0. Defining change of coordinates $y = T(x)$, with $x(t)$ satisfying (6.3), then differentiating $y(t) = T[x(t)]$ yields

$$\dot{y}(t) = \mathbf{J}[x(t)]\mathbf{f}[x(t)] = [\mathbf{J}\mathbf{f}][T^{-1}y(t)], \tag{6.4}$$

where $\mathbf{J}$ denotes the Jacobian of T. Thus, in the new coordinates, vector field $\mathbf{f}$ becomes

$$\mathbf{f}_T(y) = \mathbf{J}[T^{-1}(y)]\mathbf{f}[T^{-1}(y)]. \tag{6.5}$$

6.2.1 Lie algebra

Suppose $a \in S(X)$, i.e., a is a smooth real-valued function on X (cf. Definition 6.2.2). Then, its gradient, denoted by ∇a or $\mathbf{d}a$, is defined as the row vector

$$\nabla a = \mathbf{d}a = \begin{bmatrix} \partial a/\partial x_1 & \cdots & \partial a/\partial x_n \end{bmatrix}. \tag{6.6}$$

Clearly, $\mathbf{d}a \in F(X)$, i.e., is a form on X. Next, we give the definition of a Lie derivative.

Definition 6.2.4. Let $a \in S(X)$ and $\mathbf{f} \in V(X)$. Then, the map

$$x \to \mathbf{d}a(x)\mathbf{f}(x) :\ X \to \mathbb{R}, \tag{6.7}$$

denoted by $L_{\mathbf{f}}a$, is smooth and is called Lie derivative of function a with respect to vector field $\mathbf{f}$.

Clearly, $L_{\mathbf{f}}a \in S(X)$. Interpreting $L_{\mathbf{f}}a$ as the derivative of a along integral curves of vector field $\mathbf{f}$, we note that

$$L_{\mathbf{f}}a(x) = \lim_{t\to 0}\frac{1}{t}\{a[s_{\mathbf{f},t}(x_0)] - a(x_0)\}. \tag{6.8}$$

Suppose, now, $\mathbf{h} \in F(X)$, i.e., $\mathbf{h}$ is a form on X. Then, the map

$$x \to \mathbf{h}(x)\mathbf{f}(x), \tag{6.9}$$

is smooth and real-valued and is denoted by **<h, f>**. The quantity **<h, f>** $\in S(X)$ and is called the inner product of the form $\mathbf{h}$ and the vector field $\mathbf{f}$.

A form $\mathbf{h}$ is called exact if there exists a smooth function $a \in S(X)$ such that $\mathbf{h} = \mathbf{d}a$. To determine whether a given form is exact or not we may perform the following procedure: Let X is an open ball in $\mathbb{R}^n$, i.e., a set of the form $\{x : \|x - x_0\| < \varepsilon\}$, for some x_0 and $\varepsilon > 0$ and construct $n \times n$ matrix J_h whose (i, j)-entry is $\partial h_j / \partial x_i$. Then $\mathbf{h}$ is exact if and only if J_h is a symmetric matrix for all $x \in X$.

We introduce now the definition of Lie bracket.

Definition 6.2.5. Suppose $\mathbf{f},\ \mathbf{g} \in V(X)$. Then, the Lie bracket of $\mathbf{f}$ and $\mathbf{g}$ is denoted by **[f, g]** and is the vector field defined by

$$\mathbf{[f,\ g]} = \frac{\partial \mathbf{g}}{\partial x}\mathbf{f} - \frac{\partial \mathbf{f}}{\partial x}\mathbf{g}. \tag{6.10}$$

Suppose $\mathbf{f}(x)$, $\mathbf{g}(x)$ are two given vector fields and consider a change of coordinates $y = T(x)$. Then, as seen in (6.5), $\mathbf{f}(x)$ and $\mathbf{g(x)}$ are transformed into $\mathbf{f}_T(y)$ and $\mathbf{g}_T(y)$, respectively. The Lie bracket of the vector fields after the coordinate change is computed as follows

$$\{\mathbf{J}(x)\mathbf{[f,\ g]}(x)\}_{x=T^{-1}(y)} = \frac{\partial \mathbf{g}_T(y)}{\partial y}\mathbf{f}_T(y) - \frac{\partial \mathbf{f}_T(y)}{\partial y}\mathbf{g}_T(y). \tag{6.11}$$

The next lemma relates repeated Lie derivatives to the Lie bracket. Its proof which is omitted can be found in [216].

Lemma 6.2.2. *Suppose $a \in S(X)$ and $\boldsymbol{f},\ \boldsymbol{g} \in V(X)$. Then,*

$$L_{[f,\ g]}a = L_f(L_g a) - L_g(L_f a). \tag{6.12}$$

Before proceeding to more properties of Lie derivatives, it is useful to define matrix $\nabla^2 a$, with $a \in S(X)$, to be the symmetric $n \times n$ matrix whose (i, j)-entry is $\partial^2 a / \partial x_i \partial x_j$. Matrix $\nabla^2 a$ is called the Hessian matrix of a.

Definition 6.2.6. let $\mathbf{f} \in V(X)$ and that $\mathbf{h} \in F(X)$. Then, the Lie derivative of $\mathbf{h}$ with respect to $\mathbf{f}$ is also a form and is defined as

$$L_{\mathbf{f}}\mathbf{h} = \mathbf{f}'\Big(\frac{\partial \mathbf{h}'}{\partial x}\Big)' + \mathbf{h}\frac{\partial \mathbf{f}}{\partial x}. \tag{6.13}$$

We summarize now the three types of Lie derivatives defined so far. Let $\mathbf{f},\ \mathbf{g} \in V(X)$, $a \in S(X)$ and $\mathbf{h} \in F(X)$. Then, the Lie derivative of the vector field $\mathbf{g}$ with respect to $\mathbf{f}$ is just the Lie bracket $\mathbf{[f,\ g]}$. The Lie derivative of the smooth function a with respect to $\mathbf{f}$ is the smooth real-valued function $\nabla a\mathbf{f}$. The Lie derivative of the form $\mathbf{h}$ with respect to $\mathbf{f}$ is given by (6.13). Note that the lie derivative of a vector field, a real-valued function and a form are again respectively a vector field, a real-valued function and a form. These derivatives can be related via a Leibniz type of product formula given in the following lemma.

Lemma 6.2.3. *Suppose* $\boldsymbol{f},\ \boldsymbol{g} \in V(X)$ *and* $\boldsymbol{h} \in F(X)$. *Then,*

$$L_f\boldsymbol{<h,\ g>} = \boldsymbol{<}L_f\boldsymbol{h,\ g>} + \boldsymbol{<h}L_f\boldsymbol{,\ g>}. \tag{6.14}$$

Some other properties of the Lie bracket which are ready consequences of the definition are listed in the following lemma.

Lemma 6.2.4. *Let* $\boldsymbol{f},\ \boldsymbol{g},\ \boldsymbol{h} \in V(X)$, $a \in S(X)$ *and* $\beta,\ \gamma \in \mathbb{R}$. *Then,*

$$\boldsymbol{[f,\ \beta g + \gamma h]} = \beta\boldsymbol{[f,\ g]} + \gamma\boldsymbol{[f,\ h]}, \tag{6.15}$$

$$\boldsymbol{[f,\ g]} = -\boldsymbol{[g,\ f]}, \tag{6.16}$$

$$\boldsymbol{[f,\ [g,\ h]]} + \boldsymbol{[g,\ [h,\ f]]} + \boldsymbol{[h,\ [f,\ g]]} = \boldsymbol{0}, \tag{6.17}$$

$$\boldsymbol{[f,\ \beta g]} = \beta\boldsymbol{[f,\ g]} + (L_f\beta)\boldsymbol{g}. \tag{6.18}$$

Suppose now $\mathbf{f}_1,\ldots,\mathbf{f}_k \in V(X)$ and $x_0 \in X$. Then, we say that vector fields $\mathbf{f}_1,\ldots,\mathbf{f}_k$ are linearly independent at x_0 if the column vectors $\mathbf{f}_1(x_0),\ldots,\mathbf{f}_k(x_0)$ are linearly independent. Linear independence of forms is defined in the same manner. Obviously, by virtue of continuity, if $\mathbf{f}_1,\ldots,\mathbf{f}_k$ are linearly independent at x_0, then, they are essentially linearly independent at all points in some neighborhood of x_0, i.e., in an open set containing x_0.

We conclude the section by denoting repeated Lie brackets of vector fields. For convenience, we introduce the "ad" symbol. For $\mathbf{f},\ \mathbf{g} \in V(X)$ and defining $\mathrm{ad}_{\mathbf{f}}^0\mathbf{g} = \mathbf{g}$, we may write

$$\mathrm{ad}_{\mathbf{f}}^{i+1}\mathbf{g} = \mathbf{[f,\ }\mathrm{ad}_{\mathbf{f}}^{i}\mathbf{g]}. \tag{6.19}$$

For instance,

$$\mathrm{ad}_{\mathbf{f}}^{1}\mathbf{g} = \mathbf{[f,\ g]}, \tag{6.20}$$

$$\mathrm{ad}_{\mathbf{f}}^{2}\mathbf{g} = \mathbf{[f,\ [f,\ g]]}, \tag{6.21}$$

$$\mathrm{ad}_{\mathbf{f}}^{3}\mathbf{g} = \mathbf{[f,\ [f,\ [f,\ g]]]}. \tag{6.22}$$

6.2.2 Distributions and the Frobenius theorem

The main result of differential geometry presented in this section is the Frobenius theorem. Before we state the theorem, we introduce some useful concepts such as submanifolds, distributions and involutivity.

Definition 6.2.7. A subset $M \subseteq X$ is a k-dimensional submanifold $(k < n)$ of X if it possesses the following property: For each $x_0 \in M$, there exists an open set $U \subseteq X$ containing x_0 and smooth functions $\phi_{k+1}, \ldots, \phi_n \in S(X)$ such that

(i) $\{\mathbf{d}\phi_i(x),\ i = k+1, \ldots, n\}$ is a linearly independent set of row vectors for all $x \in U$,

(ii) $U \cap M = \{x \in U : \phi_i(x) = 0 \text{ for } i = k+1, \ldots, n\}$.

In view of this definition, subset M may be interpreted locally as a k-dimensional surface in X defined by $n-k$ equations $\phi_i(x) = 0$, with $i = k+1, \ldots, n$. We remark here that, in general, these functions are not unique. We also present the following result.

Lemma 6.2.5 ([216])**.** *Suppose M is a k-dimensional submanifold of X. Suppose $x_0 \in M$, and that there exist open sets U, $V \in X$, each containing x_0, and smooth functions $\phi_{k+1}, \ldots, \phi_n \in S(X)$, $\psi_{k+1}, \ldots, \psi_n \in S(X)$, such that*

(i) the set $\{\boldsymbol{d}\phi_{k+1}(x), \ldots, \boldsymbol{d}\phi_n(x)\}$ is linearly independent for all $x \in V$,

(ii) the set $\{\boldsymbol{d}\phi_i(x),\ i = k+1, \ldots, n\}$ is linearly independent for all $x \in U$,

(iii) $U \cap M = \{x \in U : \phi_i(x) = 0 \text{ for } i = k+1, \ldots, n\}$,

(iv) $V \cap M = \{x \in V : \psi_i(x) = 0 \text{ for } i = k+1, \ldots, n\}$.

Under these conditions, the following statement is true for each $x \in U \cap V$: The $(n-k)$-dimensional subspace of $(\mathbb{R}^n)^*$ spanned by row vectors $\{\boldsymbol{d}\phi_{k+1}(x), \ldots, \boldsymbol{d}\phi_n(x)\}$ is identical to $(n-k)$-dimensional subspace of $(\mathbb{R}^n)^*$ spanned by row vectors $\{\boldsymbol{d}\psi_{k+1}(x), \ldots, \boldsymbol{d}\psi_n(x)\}$.

The tangent space of a k-dimensional submanifold is defined next.

Definition 6.2.8. Suppose M is a k-dimensional submanifold of X, and choose smooth functions $\phi_{k+1}, \ldots, \phi_n$ such that the conditions of Definition 6.2.7 are satisfied. Then, the tangent space of M at $x \in M$ is the k-dimensional subspace of $\mathbb{R}^n$ defined by

$$TM_x = \{v \in \mathbb{R}^n : \mathbf{<d}\phi_i(x),\ v\mathbf{>} = 0,\ \text{for } i = k+1, \ldots, n\}. \tag{6.23}$$

A vector field $\mathbf{f} \in V(X)$ is said to be tangent to M at x if $\mathbf{f}(x) \in TM_x$.

From Lemma 6.2.5, it follows straightforwardly that the above definition of TM_x does not depend on the particular choice of functions ϕ_i used to represent M in the vicinity of x. This indicates that TM_x is just the k-dimensional subspace of column vectors that are annihilated by the subspace spanned by the $n-k$ row vectors $\mathbf{d}\phi_{k+1}(x),\ldots,\mathbf{d}\phi_n(x)$.

Next, we show how to compute submanifolds using a change of coordinates. Let M be a k-dimensional submanifold of X and $x_0 \in M$. Then, in view of Definition 6.2.7, there is an open neighborhood $U \subseteq X$ of x_0 and smooth functions $\phi_{k+1},\ldots,\phi_n$ such that $\mathbf{d}\phi_{k+1}(x),\ldots,\mathbf{d}\phi_n(x)$ are linearly independent at all $x \in U$ and such that

$$U \cap M = \{x \in U : \phi_i(x) = 0 \text{ for } i = k+1,\ldots,n\}, \tag{6.24}$$

holds. Now select smooth functions $\phi_1,\ldots,\phi_k$ as $\phi_i = v_i(x-x_0)$ for $i = 1,\ldots,k$, where $v_1,\ldots,v_k$ is a set of constant row vectors chosen such that $\{\mathbf{d}\phi_i(x_0),\ i = 1,\ldots,n\}$ form a (row) basis for $\mathbb{R}^n$. Now define a map $T:\ \mathbb{R}^n \to \mathbb{R}^n$ as

$$y = T(x) = \begin{bmatrix} \phi_1 & \cdots & \phi_k & \phi_{k+1} & \cdots & \phi_n \end{bmatrix}', \tag{6.25}$$

with $y_i = \phi_i$, $i = 1,\ldots,n$ as defined above. By construction, the Jacobian $\partial J/\partial x$ evaluated at x_0 is a nonsingular matrix. Thus, from the inverse function theorem (Theorem 6.2.1), T is locally a diffeomorphism on some $U_0 \subseteq U$, with $x_0 \in U_0$. Viewing $y_1,\ldots,y_n$ as a new set of coordinates on U_0 and due to (6.24), we may write

$$M \cap U_0 = \left\{ \begin{bmatrix} z' & \mathbf{0}' \end{bmatrix}' :\ z \in N \subseteq \mathbb{R}^k \right\}, \tag{6.26}$$

where N is some neighborhood of $\mathbf{0}$ in $\mathbb{R}^k$.

We also consider the tangent space of M in the new coordinates. In terms of the y coordinates, it is clear that ϕ_i is the i-th coordinate of y. Hence, $\mathbf{d}\phi_i$ is a row vector with a 1 in the i-th position and zeros elsewhere. Note that a column vector v is annihilated by each of the elementary row vectors with a 1 in positions $k+1,\ldots,n$, respectively, if and only if the last $n-k$ components of v are zero. Thus, applying (6.23) we have

$$TM_{y_0} = \{v \in \mathbb{R}^n : v = \begin{bmatrix} v_1,\ldots,v_n \end{bmatrix}',\ v_i = 0 \text{ for } i = k+1,\ldots,n\}, \tag{6.27}$$

with $y_0 = T(x_0)$. Expression (6.27) implies that a vector field $\mathbf{f}$ is tangent to M at a point x_0 if and only if the transformed vector field $\mathbf{f}_T$ has the form:

$$\mathbf{f}_T(y) = \begin{bmatrix} \mathbf{f}_a \\ \mathbf{0}_{n-k} \end{bmatrix}. \tag{6.28}$$

Definition 6.2.9 ([216])**.** A k-dimensional distribution Δ on X is a map which assigns, to each $x \in X$, a k-dimensional subspace of $\mathbb{R}^n$ such that the following smoothness condition is satisfied: For each $x_0 \in X$ there exist an open set $U \subseteq X$ containing x_0 and k vector fields $\mathbf{f}_1, \ldots, \mathbf{f}_k$ such that (i) $\{\mathbf{f}_1(x), \ldots, \mathbf{f}_k(x)\}$ is a linearly independent set for each $x \in U$, and (ii)

$$\Delta(x) = \text{span}\{\mathbf{f}_1(x), \ldots, \mathbf{f}_k(x)\}, \ \forall x \in U. \tag{6.29}$$

In view of (6.29), a k-dimensional distribution may be defined as a map which assigns to each $x \in X$ a subspace of dimension no more than k, requiring that each open set U contain at least one point y such that $\dim(\Delta(y))$ exactly equals k. The latter leads to the following definition.

Definition 6.2.10. Point x is said to be a regular point of distribution Δ if there is a neighborhood U of x such that the dimension of $\Delta(y)$ is the same for all $y \in U$.

Now, if Δ is a given distribution and $\mathbf{f} \in V(X)$, then $\mathbf{f}$ belongs to Δ, denoted by $\mathbf{f} \in \Delta$, if $\mathbf{f}(x) \in \Delta(x)\ \forall x \in X$. A k-dimensional distribution Δ on X is said to be everywhere regular, if $\dim(\Delta(x)) = k\ \forall x \in X$.

Suppose Δ is a k-dimensional distribution, that $U \subseteq X$ is an open set, and $\mathbf{f}_1, \ldots, \mathbf{f}_k \in V(X)$, $m \geq k$, are vector fields that span Δ on U. Let also $\mathbf{f} \in \Delta$. Then, there exist smooth functions $a_1, \ldots, a_m \in S(X)$ such that

$$\mathbf{f} = \sum_{i=1}^{m} a_i \mathbf{f}_i, \ \forall x \in U. \tag{6.30}$$

Before stating the Frobenius theorem, we introduce the following definitions.

Definition 6.2.11. Let Δ be a given k-dimensional, everywhere regular, distribution on X. For each $x \in X$, suppose also that there exists a k-dimensional submanifold M_x of X containing x such that every vector field $\mathbf{f} \in \Delta$ is tangent to M_x at x, i.e., $TM_x = \Delta(x)$. Then, distribution Δ is said to be completely integrable, and M_x is said to be the integral manifold of Δ passing through x.

Definition 6.2.12. A distribution Δ is involutive if $[\mathbf{f},\ \mathbf{g}] \in \Delta$ whenever $\mathbf{f},\ \mathbf{g} \in \Delta$.

Immediate consequence of the latter definition is that a distribution is involutive if it closed under the Lie bracket. In view of Definition 6.2.11, a natural question which arises is when a distribution is completely integrable. The answer is provided by the Frobenius theorem stated below.

Theorem 6.2.6 (Frobenius, [216])**.** *A distribution is completely integrable if and only if it is involutive.*

From the Frobenius theorem, it turns out that a one-dimensional distribution Δ is automatically involutive, since $[a\mathbf{f},\ b\mathbf{f}] \in \text{span}\mathbf{f} = \Delta$, with $a,\ b \in S(X)$. Now, in order to check whether a k-dimensional distribution is involutive or not, with $k > 1$, it is only necessary to compute a finite number of Lie brackets. This is established in the following statement.

Proposition 6.2.7. *Let Δ denote a k-dimensional distribution on $U \subseteq X$ such that*

$$\Delta(x) = \text{span}\{\boldsymbol{f}_1(x), \ldots, \boldsymbol{f}_m(x)\},\ \forall x \in U. \tag{6.31}$$

Then, Δ is involutive if and only if $[\boldsymbol{f}_i, \boldsymbol{f}_j] \in \Delta \forall i, j$, i.e., there exist smooth functions $a_{ijl} \in S(U)$, $1 \leq i, j, l \leq m$, such that

$$[\boldsymbol{f}_i, \boldsymbol{f}_j] = \sum_{l=1}^{m} a_{ijl}(x)\boldsymbol{f}_l(x),\ \forall x \in U. \tag{6.32}$$

This leads to the following result which represents an alternate form of the Frobenius theorem stated earlier.

Theorem 6.2.8 (Alternate Frobenius, [216])**.** *Suppose $\boldsymbol{f}_1, \ldots, \boldsymbol{f}_m \in V(X)$, $N \subseteq X$ is an open set, $x_0 \in N$ and that the set $\boldsymbol{f}_1(x), \ldots, \boldsymbol{f}_m(x)$ contains k linearly independent vectors at each $x \in N$. Then, there exist functions $\phi_{k+1}, \ldots, \phi_n \in S(X)$ such that*

(i) $\boldsymbol{d}\phi_{k+1}(x_0), \ldots, \boldsymbol{d}\phi_n(x_0)$ are linearly independent,

(ii) there exists a neighborhood $V \subseteq N$ of x_0 such that

$$\langle \boldsymbol{d}\phi_i, \boldsymbol{f}_j \rangle(x) = 0,\ \forall x \in V,\ \text{for } k+1 \leq i \leq n,\ 1 \leq j \leq m, \tag{6.33}$$

if and only if the distribution spanned by $\boldsymbol{f}_1, \ldots, \boldsymbol{f}_m$ is involutive, i.e., there exist smooth functions a_{ijl} and a neighborhood $U \subseteq N$ of x_0 such that (6.32) *holds.*

Remark 6.2.9. Let vector fields $\mathbf{f}_1, \ldots, \mathbf{f}_k$ be given by

$$\mathbf{f}_1 = \begin{bmatrix} 1 \\ 0 \\ \vdots \\ 0 \end{bmatrix}, \ \cdots, \mathbf{f}_k = \begin{bmatrix} 0 \\ \vdots \\ 0 \\ 1 \\ 0 \\ \vdots \\ 0 \end{bmatrix}, \ \forall x \in X. \tag{6.34}$$

Clearly, $\mathbf{f}_i$ is a constant vector field with a 1 in the i-th position and zeros elsewhere. Define $\Delta = \text{span}\{\mathbf{f}_1, \ldots, \mathbf{f}_k\}$. Then, Δ is a k-dimensional distribution consisting of all vector fields of the form

$$\mathbf{f}(x) = \begin{bmatrix} \mathbf{f}_a(x) \\ \mathbf{0}_{n-k} \end{bmatrix}. \tag{6.35}$$

It is clear that Δ is completely integrable, thereby being involutive. Indeed, for $x_0 \in X$, the corresponding integral manifold M_{x_0} is the set

$$\{x \in \mathbb{R}^n : x_i = x_{0,i}, \ k+1 \leq i \leq n\}, \tag{6.36}$$

and functions $\phi_{k+1}, \ldots, \phi_n \in S(X)$ satisfying (6.33) are given by

$$\phi_i(x) = x_i, \ i = k+1, \ldots, n. \tag{6.37}$$

□

It is worth noting that all completely integrable k-dimensional distributions can be generated by vector fields $\mathbf{f}(x)$ as in (6.35) via a suitable change of coordinates. Naturally, the Frobenius theorem is not constructive in the sense that it does not show us how to construct the coordinate transformation, it only guarantees that such a suitable transformation exists.

6.2.3 Reachability of nonlinear systems

In this paragraph, we present the notion of reachability of nonlinear systems of the form:

$$\dot{x}(t) = \mathbf{f}[x(t)] + \sum_{j=1}^{m} u_j(t)\mathbf{g}_j[x(t)], \ x(0) = x_0, \tag{6.38}$$

where $\mathbf{f}$, $\mathbf{g}_1, \ldots, \mathbf{g}_m$ are vector fields in $V(X)$ and $X \subseteq \mathbb{R}^n$ is an open set. Given an initial state x_0, a system is said to be reachable in the sense that there is a control action that can steer the system to any state contained in a neighborhood of x_0. A more formal definition of reachability is given next.

Definition 6.2.13. System (6.38) is said to be (locally) reachable around a state $x_0 \in X$ if there exists a neighborhood U of x_0 such that, for each $x_f \in U$, there exist a time $\tau > 0$ and a set of control inputs $\{u_i(t),\ t \in [0,\ \tau],\ i = 1, \ldots, m\}$ such that, if the system starts in the state x_0 at time 0, then it reaches the state x_f at time τ.

We remark that the above definition is purely local and pertains to systems reachable nearby an initial state. All systems analysed in this chapter are assumed to be locally reachable. Before presenting conditions for local reachability of system (6.38), we introduce a few preliminary definitions along with some useful results.

Definition 6.2.14. Let Δ be a distribution on X and $\mathbf{f} \in V(X)$. Then Δ is said to be invariant under $\mathbf{f}$, or $\mathbf{f}$-invariant, if $[\mathbf{f},\ \mathbf{h}] \in \Delta\ \forall \mathbf{h} \in \Delta$.

Consider now system (6.38) and construct a sequence of distributions in the following manner.

Procedure 6.2.1 ([216])**.** *Step* 0*:* Set $i = 0$ and define

$$\Delta_0 = \text{span}\ \{\mathbf{g}_1, \ldots, \mathbf{g}_m\}. \tag{6.39}$$

Step 1*:* Let $\{\mathbf{h}_1^i, \ldots, \mathbf{h}_{k_i}^i\}$ be a set of vector fields that generate Δ_i. Clearly, for $i = 0$, this set spans distribution Δ_0, with $k_0 = m$. Check now if Δ_i is involutive in some neighborhood of x_0 by checking whether each Lie bracket $[\mathbf{h}_j^{(i)},\ \mathbf{h}_l^{(i)}]$ belongs to Δ_i for $j, l = 1, \ldots, k_i$. Check also if Δ_i is invariant under $\mathbf{f}$ by checking whether $[\mathbf{f},\ \mathbf{h}_l^{(i)}] \in \Delta_i$ for all j. If Δ_i is both involutive and invariant under $\mathbf{f}$, stop.

Step 2*:* If Δ_i is either not involutive or not invariant under $\mathbf{f}$, then set $i = i + 1$ and define Δ_{i+1} as

$$\Delta_{i+1} = \text{span}\ \{\mathbf{h}_j^{(i)},\ 1 \le j \le k_i\} \cup \{[\mathbf{h}_j^{(i)},\ \mathbf{h}_l^{(i)}],\ 1 \le j, l \le k_i\} \cup \{[\mathbf{f},\ \mathbf{h}_j^{(i)}],\ 1 \le j \le k_i\}, \tag{6.40}$$

and return to Step 1. Note that in order to construct Δ_{i+1}, it is only necessary to add Lie brackets $[\mathbf{h}_j^{(i)},\ \mathbf{h}_l^{(i)}]$ and $[\mathbf{f},\ \mathbf{h}_j^{(i)}]$ that are not contained in Δ_i. □

Procedure 6.2.1 generates a sequence of distributions $\{\Delta_i\}$ such that $\Delta_i(x) \subseteq \Delta_{i+1}(x)$ for all $x \in X$. If x_0 is a regular point of each Δ_i, then $\dim(\Delta_{i+1})$ is strictly larger than $\dim(\Delta_i)$.

Since $\dim(\Delta_i) \leq n \ \forall i$, the process cannot continue more than n times. Suppose that Δ_c denotes the distribution generated at the termination of the procedure. Then, this is both involutive as well as invariant under $\mathbf{f}$ and $\mathbf{g}_1, \ldots, \mathbf{g}_m$. Evidently, Δ_c is the smallest distribution with these two properties. If, now, $\dim(\Delta_c) = n$, with n denoting the state dimension, system (6.38) is locally reachable. This result is stated formally in the following theorem.

Theorem 6.2.10 ([216]). *For system* (6.38)*, the following statements are equivalent:*

(i) The system is locally reachable around $x_0 \in \mathbb{R}^n$ as defined in Definition 6.2.13.

(ii) There is a neighborhood U of x_0 such that distribution Δ_c constructed according to Procedure 6.2.1, has dimension n at all $x \in U$.

We also present the following result.

Corollary 6.2.1 ([216]). *Given system* (6.38)*, consider distribution*

$$\bar{\Delta}_{n-1} = \text{span}\,\{\text{ad}_{\boldsymbol{f}}^i \boldsymbol{g}_j,\ 1 \leq j \leq m,\ 0 \leq i \leq n-1\}. \tag{6.41}$$

If $\dim(\bar{\Delta}_{n-1}(x_0)) = n$, then the system is locally reachable around x_0.

We remark that the converse of Corollary 6.2.1 is not always true, i.e., $\dim(\bar{\Delta}_{n-1}) = n$ is not a necessary condition for local reachability. The next theorem states a sufficient condition for system (6.38) to be locally reachable around an equilibrium, that is, a vector $x_0 \in X$ such that $\mathbf{f}(x_0) = \mathbf{0}$.

Theorem 6.2.11 ([216]). *Consider system* (6.38)*, and suppose $x_0 \in X$ satisfies $\boldsymbol{f}(x_0) = \boldsymbol{0}$. Define matrix $A_0 \in \mathbb{R}^{n\times n}$ and vectors $b_{i,0} \in \mathbb{R}^n$, $i = 1, \ldots, m$, by*

$$A_0 = \left[\frac{\partial \boldsymbol{f}}{\partial x}\right]_{x=x_0},\ b_{i,0} = \boldsymbol{g}_i(x_0). \tag{6.42}$$

Consider linear system

$$\dot{z} = A_0 z + \sum_{i=1}^{m} b_{i,0} v_i. \tag{6.43}$$

Then, system (6.38) *is locally reachable if system* (6.43) *is reachable, i.e., if matrix*

$$W_0 = \begin{bmatrix} B_0 & A_0 B_0 & \cdots & A_0^{n-1} B_0 \end{bmatrix}, \tag{6.44}$$

has rank n, with

$$B_0 = \begin{bmatrix} b_{1,0} & \cdots & b_{m,0} \end{bmatrix} \tag{6.45}$$

6.3 Feedback linearization of nonlinear systems

In this section, we present an application of differential-geometric methods examined earlier, namely, the transformation of a given nonlinear system to a linear one via state-feedback control and a transformation of the state vector. This powerful method proves essential for solving model-matching type problems of a set of nonlinear systems. This will become evident later in the chapter. Next, we start our analysis with nonlinear systems controlled by a single input.

6.3.1 Single-input systems

Consider a system of the form

$$\dot{x} = \mathbf{f}(x) + u\mathbf{g}(x), \tag{6.46}$$

where $\mathbf{f}$ and $\mathbf{g}$ are smooth vector fields on some open set $X \subseteq \mathbb{R}^n$ containing $\mathbf{0}$, with $\mathbf{f}(\mathbf{0}) = \mathbf{0}$. We wish to examine if there exist smooth functions $q,\ s \in S(X)$, with $s(x) \neq 0$ for all x in some neighborhood $U \subseteq X$ nearby the origin, and a local diffeomorphism $T:\ U \to \mathbb{R}^n$ with $T(\mathbf{0}) = \mathbf{0}$, such that if we define

$$v = q(x) + s(x)u, \tag{6.47}$$

$$z = T(x), \tag{6.48}$$

then, variables z and v satisfy a linear differential equation of the form

$$\dot{z} = Az + bv, \tag{6.49}$$

where the pair $(A,\ b)$ is controllable. If this is possible, then system (6.46) is said to be feedback linearizable. Assuming now the latter is true and the pair $(A,\ b)$ is indeed controllable, consider a further state-space transformation

$$\bar{z} = Mz, \tag{6.50}$$

such that the resulting system is in controllable canonical form ([5, 32]), i.e.,

$$\dot{\bar{x}} = MAM^{-1}\bar{z} + Mbv, \tag{6.51}$$

with

$$MAM^{-1} = \begin{bmatrix} 0 & 1 & 0 & \dots & 0 \\ 0 & 0 & 1 & \dots & 0 \\ \vdots & \vdots & \vdots & \ddots & \vdots \\ 0 & 0 & 0 & \dots & 1 \\ -a_0 & -a_1 & -a_2 & \dots & -a_{n-1} \end{bmatrix}, \; Mb = \begin{bmatrix} 0 \\ 0 \\ \vdots \\ 0 \\ 1 \end{bmatrix}, \tag{6.52}$$

where a_i's denote the coefficients of the characteristic polynomial

$$|sI - A| = s^n + \sum_{i=0}^{n-1} a_i s^i. \tag{6.53}$$

Applying now linear state-feedback (with respect to $\bar{z}$ coordinates) of the form

$$v = \bar{v} + \begin{bmatrix} a_0 & a_1 & \cdots & a_{n-1} \end{bmatrix} \bar{z} \tag{6.54}$$

yields the closed-loop linear system

$$\dot{\bar{z}} = \bar{A}\bar{z} + \bar{b}\bar{v}, \tag{6.55}$$

with

$$\bar{A} = \begin{bmatrix} 0 & 1 & 0 & \dots & 0 \\ 0 & 0 & 1 & \dots & 0 \\ \vdots & \vdots & \vdots & \ddots & \vdots \\ 0 & 0 & 0 & \dots & 1 \\ 0 & 0 & 0 & \dots & 0 \end{bmatrix}, \; \bar{b} = \begin{bmatrix} 0 \\ 0 \\ \vdots \\ 0 \\ 1 \end{bmatrix}. \tag{6.56}$$

The problem of transforming a single-input nonlinear system described by (6.46) to a set of linear equations (6.55) via feedback control and state-space transformations is formally stated next.

Problem 6.3.1 (Feedback linearization problem (single-input case))**.** Given system (6.46), we wish to compute (i) a smooth function $q \in S(X)$, (ii) a smooth function $s \in S(X)$ with $s(x) \neq 0$ for all x in some neighborhood $U \subseteq \mathbb{R}^n$ of the origin $\mathbf{0}$, and (iii) a local diffeomorphism $T : U \to \mathbb{R}^n$ with $T(\mathbf{0}) = \mathbf{0}$, satisfying the following conditions: If new variables v and $z = \begin{bmatrix} z_1 & z_2 & \cdots & z_n \end{bmatrix}'$ are defined as in (6.47) and (6.48), respectively, then

$$\dot{z}_1 = z_2, \; \dot{z}_2 = z_3, \; \dots, \; \dot{z}_{n-1} = z_n, \; \dot{z}_n = v. \tag{6.57}$$

Note that representing (6.57) in a compact form results in (6.55). Necessary and sufficient conditions for a single-input nonlinear system (6.46) to be feedback linearizable are given in the following theorem.

Theorem 6.3.2 ([216]). *The feedback linearization problem for the single-input case has a solution if and only if the following two conditions are satisfied in some neighborhood of the origin:*

(i) The set of vector fields $\{\mathrm{ad}_{\boldsymbol{f}}^{i}\boldsymbol{g},\ 0 \le i \le n-1\}$ *is linearly independent.*

(ii) The set of vector fields $\{\mathrm{ad}_{\boldsymbol{f}}^{i}\boldsymbol{g},\ 0 \le i \le n-2\}$ *is involutive.*

Assuming the above conditions are satisfied for a given system (6.46), Theorem 6.3.2 [216] only guarantees Problem 6.3.1 has a solution but otherwise it does not provide a solution to this problem. In order to construct smooth functions $q(x)$, $s(x)$ as in (6.47) and a diffeomorphism $z = T(x)$ as in (6.48), we may perform the following constructive procedure.

Suppose a single-input system is described by (6.46), where $\mathbf{f}(\mathbf{0}) = \mathbf{0}$ and $x \in U$ with $U \in \mathbb{R}^n$ denoting a neighborhood of the origin $\mathbf{0}$. Then, a suitable non-constant smooth function $T_1(x)$ can be found such that

$$\mathbf{<d}T_1,\ \mathrm{ad}_{\mathbf{f}}^{i}\mathbf{g>} = 0,\ i = 0,1,\ldots,n-2,\ \forall x \in U, \tag{6.58}$$

and $T_1(\mathbf{0}) = 0$. Note that if $T_1(\mathbf{0}) \neq 0$, then, constant $T_1(\mathbf{0})$ can be subtracted from T_1 without affecting $\mathbf{d}T_1$ thereby the validity of (6.58). Next, we define $T_2,\ldots,T_n$ recursively by

$$T_{i+1} = \mathbf{<d}T_i,\ \mathbf{f>} = L_{\mathbf{f}}T_i,\ i = 1,\ldots,n-1. \tag{6.59}$$

Clearly, $T_i(\mathbf{0}) = 0$ for all i, since $\mathbf{f}(\mathbf{0}) = \mathbf{0}$. Finally, we define

$$q(x) = \mathbf{<d}T_n,\ \mathbf{f>}, \tag{6.60}$$

$$s(x) = \mathbf{<d}T_n,\ \mathbf{g>}. \tag{6.61}$$

Then, the feedback control is given by

$$u = -\frac{q(x)}{s(x)} + \frac{1}{s(x)}v, \tag{6.62}$$

where $s(x) \neq 0$ for all $x \in U$, and the transformation

$$z = \begin{bmatrix} T_1(x) & \cdots & T_n(x) \end{bmatrix}', \tag{6.63}$$

is a smooth diffeomorphism for all $x \in U$.

6.3.2 Multi-input case

In this section, the feedback linearization technique is extended to multi-input systems of the form

$$\dot{x} = \mathbf{f}(x) + \sum_{i=1}^{m} u_i \mathbf{g}_i(x),\ x(0) = x_0, \tag{6.64}$$

where $\mathbf{f}, \mathbf{g}_1, \ldots, \mathbf{g}_m$ are smooth vector fields on some neighborhood $X \subseteq \mathbb{R}^n$ near the origin containing x_0, with $\mathbf{f}(\mathbf{0}) = \mathbf{0}$. Clearly, it is reasonable to assume that vector fields $\mathbf{g}_1, \ldots, \mathbf{g}_m$ are linearly independent in some neighborhood of the origin, since, any input redundancy can be forestalled by redefining the inputs and reducing their number so that the linear independence assumption is satisfied. Before presenting conditions for feedback linearizability of system (6.64), some extra concepts need to be introduced.

The major difference between single-input and multi-input feedback linearizable systems is that, while there is a single canonical form which all controllable single-input linear systems of the same state dimension can be transformed to, for multi-input systems several canonical forms are possible. However, as shown in Chapter 5, if two multi-input systems have the same number of states and inputs, then they are said to be "feedback equivalent", in the sense that one system can be transformed into the other via state feedback and a state-space transformation, if and only if they have the same Brunovsky canonical form. We recall that the Brunovsky canonical form of a linear system is completely defined by a set of integers, namely, controllability indices. Thus it makes sense to derive a Brunovsky canonical form for nonlinear systems of the form (6.64) from a set of integers based on the structure of vector fields $\mathbf{f}, \mathbf{g}_1, \ldots, \mathbf{g}_m$ in (6.64). This set of integers is constructed via the following procedure.

Procedure 6.3.1 (Construction of controllability indices $\kappa_1, \ldots, \kappa_m$ of (6.64))**.** Given system (6.64), define the following distributions:

$$C_i = \{\mathrm{ad}_{\mathbf{f}}^k \mathbf{g}_j,\ 1 \le j \le m,\ 0 \le k \le i\}, \tag{6.65}$$

$$\Delta_i = \mathrm{span}\ C_i, \tag{6.66}$$

for $i = 0, 1, \ldots, n-1$. Assuming that x_0 is a regular point of the i-th distribution Δ_i, $i = 0, \ldots, n-1$, compute

$$\Delta_0 = \text{span}\{\mathbf{g}_1, \ldots, \mathbf{g}_m\}, \tag{6.67}$$

$$\Delta_1 = \text{span}\{\mathbf{g}_1, \ldots, \mathbf{g}_m, [\mathbf{f}, \mathbf{g}_1], \ldots, [\mathbf{f}, \mathbf{g}_1]\}, \tag{6.68}$$

$$\vdots$$

$$\Delta_{n-1} = \text{span}\{\mathbf{g}_1, \ldots, \mathbf{g}_m, [\mathbf{f}, \mathbf{g}_1], \ldots, [\mathbf{f}, \mathbf{g}_m], \ldots, \text{ad}_{\mathbf{f}}^{n-1}\mathbf{g}_1, \ldots, \text{ad}_{\mathbf{f}}^{n-1}\mathbf{g}_m\}. \tag{6.69}$$

Define also

$$r_0 = \dim(\Delta_0) = m, \tag{6.70a}$$

$$r_i = \dim(\Delta_i) - \dim(\Delta_{i-1}), \text{ for } i \geq 1. \tag{6.70b}$$

Then, the i-th integer κ_i, with $i = 1, \ldots, m$ is defined as the number of the integers r_i in (6.70) that are greater than or equal to i. □

We note here that the dimension of each distribution $\Delta_i(x)$ as defined in (6.66) may vary as x varies and thus, integers in (6.70) are not well-defined. To forestall this peculiarity a regularity assumption needs to be made. This is precisely the reason for requiring the origin be a regular point of Δ_i, $i = 0, \ldots, n-1$. With this assumption in force, $\dim(\Delta_i(x))$ is constant for all x in some neighborhood of $\mathbf{0}$ and hence the definition of integer r_i is irrespective of the state vector x.

Integers $\kappa_1, \ldots, \kappa_m$ as defined in Procedure 6.3.1 are called the controllability indices of system (6.64) (also referred to as Kronecker indices in [216]). Clearly,

$$\kappa_1 \geq \kappa_2 \geq \cdots \geq \kappa_m \geq 0, \text{ and } \sum_{i=1}^{m} \kappa_i = n. \tag{6.71}$$

Now the Brunovsky canonical form derived from the set of controllability indices $\kappa_1, \ldots, \kappa_m$ as defined above, is a linear system of the form

$$\dot{z} = \hat{A}z + \hat{B}v, \tag{6.72}$$

where $\hat{A}$ and $\hat{B}$ have the following special structures:

$$\hat{A} = \text{diag}(\hat{A}_1, \ldots, \hat{A}_m), \tag{6.73}$$

with $\hat{A}_i$ being the companion matrix corresponding to characteristic polynomial $|sI - \hat{A}_i| = s^{\kappa_i}$, i.e.,

$$\hat{A}_i = \begin{bmatrix} 0 & 1 & 0 & \dots & 0 \\ 0 & 0 & 1 & \dots & 0 \\ \vdots & \vdots & \vdots & \ddots & \vdots \\ 0 & 0 & 0 & \dots & 1 \\ 0 & 0 & 0 & \dots & 0 \end{bmatrix} \in \mathbb{R}^{\kappa_i \times \kappa_i}, \tag{6.74}$$

and

$$\hat{B} = \text{diag}(\hat{B}_1, \dots, \hat{B}_m), \tag{6.75}$$

with $\hat{B}_i$ being a column vector with a "1" in the last row and zeros elsewhere, i.e.,

$$\hat{B}_i = \begin{bmatrix} 0 \\ \vdots \\ 0 \\ 1 \end{bmatrix} \in \mathbb{R}^{\kappa_i}. \tag{6.76}$$

As evidently seen above, the set of controllability indices $\kappa_1, \dots, \kappa_m$ represent the sizes of the various blocks of the Brunovsky form. We also need to introduce one last set of integers. Let δ denote the largest value of i such that $r_i \neq 0$. Thus, $r_\delta > 0$ with $r_i = 0$ for all $i > \delta$. Finally, we define

$$m_\delta = r_\delta, \tag{6.77}$$

$$m_i = r_i - r_{i+1} \text{ for } i = 0, \dots, \delta - 1. \tag{6.78}$$

Integer δ is equal to the size of the largest block of the Brunovsky form minus one, i.e., $\delta = \kappa_1 - 1$. Integer m_i is the number of blocks of size $i+1$. Hence,

$$\sum_{i=0}^{\delta} m_i = m, \ \sum_{i=0}^{\delta} (i+1) m_i = n. \tag{6.79}$$

It is worth noting that integers $\kappa_1, \dots, \kappa_m$, as defined above, purely pertain to a nonlinear system (6.64) with given vector fields $\mathbf{f}, \mathbf{g}_1, \dots, \mathbf{g}_m$, in contrast to integers $\mu_1, \dots, \mu_m$ referred to as controllability indices of a linear system, as defined in Chapter 5. Yet, a Brunovsky canonical form (6.72) can purely constructed by integers $\kappa_1, \dots, \kappa_m$ as derived from the nonlinear model. In view of this connection between controllability indices of a nonlinear

system (6.64) and the corresponding Brunovsky form (6.72), the feedback linearization problem in the multi-input case is stated as follows.

Problem 6.3.3 (Feedback linearization problem (multi-input case))**.** Given system (6.64) with controllability indices $\kappa_1, \ldots, \kappa_m$ as constructed in Procedure 6.3.1, we wish to identify a neighborhood U of $\mathbf{0}$ and compute (i) a smooth function $\mathbf{q} : U \to \mathbb{R}^m$, (ii) a smooth function $\mathbf{S} : U \to \mathbb{R}^{m\times m}$ such that det $\mathbf{S}(\mathbf{0}) \neq 0$, and (iii) a local diffeomorphism $T : U \to \mathbb{R}^n$ such that $T(\mathbf{0}) = \mathbf{0}$, satisfying the following conditions: If new variables z and v are defined as

$$z = T(x), \tag{6.80}$$

and

$$v = \mathbf{q}(x) + \mathbf{S}(x)u, \tag{6.81}$$

respectively, where

$$u = \begin{bmatrix} u_1 & \cdots & u_m \end{bmatrix}', \tag{6.82}$$

then, the new variables z and v satisfy the set of linear differential equations:

$$\dot{z} = Az + Bv, \tag{6.83}$$

with $(A,\ B)$ being in Brunovsky canonical form corresponding to indices $\kappa_1, \ldots, \kappa_m$.

Necessary and sufficient conditions for this multi-input feedback linearization problem to have a solution are stated in the following theorem.

Theorem 6.3.4 ([216])**.** *Consider system* (6.64)*, and assume that the following are in force:*

(a) Vector fields $\boldsymbol{g}_1, \ldots, \boldsymbol{g}_m$ are linearly independent at x_0, so that $\dim(\Delta_0) = r_0 = m$*, with r_0 defined in* (6.70)*.*

(b) Initial condition x_0 is a regular point of the distribution Δ_i $\forall i \geq 0$.

Under these conditions, Problem 6.3.3 has a solution if and only if the following two conditions are satisfied:

(i) $\dim(\Delta_\delta) = n$*.*

(ii) Δ_{i-1} is involutive whenever $m_i \neq 0$.

Detailed proof of Theorem 6.3.4 can be found in [216]. Similarly to the single-input case, the theorem is not constructive in the sense that it only guarantees existence of a solution to

Problem 6.3.3 subject to conditions (i) and (ii), but otherwise, it does not show how to find it.

Suppose now the feedback linearization problem 6.3.3 has a solution, i.e., there exist a diffeomorphism $z = T(x)$ (6.80) on $U \in \mathbb{R}^n$ and smooth functions $\mathbf{q}(x)$, $\mathbf{S}(x)$ in (6.81) such that the linear differential equation

$$\dot{z} = Az + Bv, \tag{6.84}$$

is in Brunovsky canonical form corresponding to controllability indices $\kappa_1, \ldots, \kappa_m$. Writing

$$z = \begin{bmatrix} z_1 \\ z_2 \\ \vdots \\ z_m \end{bmatrix} \in \mathbb{R}^n, \tag{6.85}$$

where

$$z_i = \begin{bmatrix} z_{i,1} \\ z_{i,2} \\ \vdots \\ z_{i,\kappa_i} \end{bmatrix} \in \mathbb{R}^{\kappa_i}, \tag{6.86}$$

for $i = 1, \ldots, m$, and expanding (6.84) accordingly, the Brunovsky canonical form can be written as

$$\dot{z}_{i,l} = z_{i,l+1},\ l = 1, \ldots, \kappa_i - 1, \tag{6.87}$$

$$\dot{z}_{i,\kappa_i} = v_i, \tag{6.88}$$

for $i = 1, \ldots, m$.

Now the Brunovsky canonical form consists effectively of m decoupled single-input systems, with the number of states of the i-th system equaling κ_i. Defining m (non-constant) smooth functions $\phi_i, \ldots, \phi_m$ as

$$\phi_i(x) = z_{i,1},\ i = 1, \ldots, m, \tag{6.89}$$

such that

$$<\mathbf{d}\phi_i,\ \mathrm{ad}^l_{\mathbf{f}}\mathbf{g}_j> = 0,\ \text{for } l = 0, \ldots, \kappa_i - 2,\ \text{and } i, j = 1, \ldots, m, \tag{6.90}$$

and $\phi_i(\mathbf{0}) = 0$, and proceeding in a similar manner as in the single-input case, we may write

$$z_i(x) = \begin{bmatrix} \phi_i \\ L_{\mathbf{f}}\phi_i(x) \\ \vdots \\ L_{\mathbf{f}}^{\kappa_i - 1}\phi_i(x) \end{bmatrix} \in \mathbb{R}^{\kappa_i}. \tag{6.91}$$

Then, the map $T : U \to \mathbb{R}^n$ defined as

$$T(x) = \begin{bmatrix} z_1(x) \\ \vdots \\ z_m(x) \end{bmatrix}, \tag{6.92}$$

with $z_i(x)$, $i = 1, \ldots, m$ as in (6.91), is a smooth diffeomorphism on U.

Differentiating z_i, we write the last row of $\frac{d}{dt}z_i$ as

$$\frac{d}{dt}z_{i,\kappa_i} = L_{\mathbf{f}}^{\kappa_i}\phi_i + \sum_{j=1}^{m} u_j L_{\mathbf{g}_j} L_{\mathbf{f}}^{\kappa_i - 1}\phi_i. \tag{6.93}$$

Collecting now (6.93), as i varies from 1 to m, yields

$$\frac{d}{dt}\begin{bmatrix} z_{1,\kappa_1} \\ \vdots \\ z_{m,\kappa_m} \end{bmatrix} = \mathbf{q}(x) + \mathbf{S}(x)u, \tag{6.94}$$

where

$$\mathbf{q}(x) = \begin{bmatrix} L_{\mathbf{f}}^{\kappa_1}\phi_1 \\ \vdots \\ L_{\mathbf{f}}^{\kappa_m}\phi_m \end{bmatrix}, \tag{6.95}$$

and

$$\mathbf{S}(x) = \begin{bmatrix} L_{\mathbf{g}_1}L_{\mathbf{f}}^{\kappa_1 - 1}\phi_1 & \cdots & L_{\mathbf{g}_m}L_{\mathbf{f}}^{\kappa_1 - 1}\phi_1 \\ \vdots & \ddots & \vdots \\ L_{\mathbf{g}_1}L_{\mathbf{f}}^{\kappa_m - 1}\phi_m & \cdots & L_{\mathbf{g}_m}L_{\mathbf{f}}^{\kappa_m - 1}\phi_m \end{bmatrix}. \tag{6.96}$$

6.4 Model-matching problems

Motivated by the feedback linearization technique presented earlier, here, we wish to study the problem of mapping a set of nonlinear systems to a single linear target system. The task of mapping a given number of systems to a target model was thoroughly examined for linear systems in the previous chapter. Exploiting the feedback linearization technique, this section attempts to extend the matching approach to nonlinear systems. Later in the chapter, it becomes evident that this nonlinear model-matching control method simplifies the stabilization problem of networks formed of non-identical nonlinear agents allowing for a distributed control design based on LQR feedback techniques. In the present section, our objective is to identify the maximal set of nonlinear systems of a special form which, via nonlinear state-feedback control and a change of coordinates, can be mapped to the canonical form of a linear system with the same number of states and inputs. Existence conditions for the proposed model-matching scheme are identified. As an attempt to minimize the joint model-matching energy loss, we describe a systematic procedure for selecting target dynamics similar to the approach suggested in Chapter 5. We study first matching problems of single-input systems and then the model-matching scheme is extended to the multi-input case.

6.4.1 Model-matching of single-input nonlinear systems

We consider a set of N single-input nonlinear systems of the form

$$\dot{x}_i = \mathbf{f}_i(x_i) + u_i \mathbf{g}_i(x_i),\ x_i(0) = x_{i,0},\ i = 1,\ldots,N, \tag{6.97}$$

where $x_i \in \mathbb{R}^n$, $u_i \in \mathbb{R}$ denote the state and input vector, respectively, of the i-th system. Each $\mathbf{f}_i$ and $\mathbf{g}_i$ denotes a smooth vector field on some open set $X_i \subseteq \mathbb{R}^n$ around the origin containing $x_{i,0}$. We assume that $\mathbf{f}_i(\mathbf{0}) = \mathbf{0}$, $i = 1,\ldots,N$, i.e., $\mathbf{0}$ represents an equilibrium point of (6.97).

In order to proceed with formulating the model-matching problem, we suppose systems (6.97) are feedback linearizable in the sense that conditions (i) and (ii) of Theorem 6.3.2 are in force. Then, for each $i = 1,\ldots,N$, we can automatically assume that there exist smooth functions

$$q_i(x_i) \in S(X_i), \tag{6.98}$$

and

$$s_i(x_i) \in S(X_i),\ \text{with } s_i(x_i) \neq 0, \tag{6.99}$$

for all x_i in some neighborhood $U_i \subseteq X_i$ nearby $\mathbf{0}$, and a local diffeomorphism

$$T_i : U_i \to \mathbb{R}^n, \tag{6.100}$$

with

$$T_i(\mathbf{0}) = \mathbf{0}, \tag{6.101}$$

such that, if we define

$$v_i = q_i(x_i) + s_i(x_i)u_i, \tag{6.102}$$

$$z_i = T_i(x_i) = \begin{bmatrix} z_{i,1} & z_{i,2} & \cdots & z_{i,n-1} & z_{i,n} \end{bmatrix}, \tag{6.103}$$

then, all pairs $(z_i,\ v_i)$, $i = 1,\ldots,N$, satisfy the following set of linear equations:

$$\dot{z}_{i,1} = z_{i,2},\ \dot{z}_{i,2} = z_{i,3},\ \cdots,\ \dot{z}_{i,n-1} = z_{i,n},\ \dot{z}_{i,n} = v_i. \tag{6.104}$$

Suppose now a single-input linear system is described by

$$\dot{\xi} = A\xi + bv, \tag{6.105}$$

where $(A,\ b)$ is controllable. In the sequel, we refer to system (6.105) as target system. Then, due to controllability assumption, there exists a nonsingular matrix $M \in \mathbb{R}^{n\times n}$ such that

$$\dot{\hat{\xi}} = MAM^{-1}\hat{\xi} + Mbv, \tag{6.106}$$

is in controllable canonical form, with $\hat{\xi} = M\xi$. Let

$$\underline{a} = \begin{bmatrix} a_0 & a_1 & \cdots & a_{n-1} \end{bmatrix}', \tag{6.107}$$

with a_j, $j = 0,1,\ldots,n-1$, denoting the coefficients of characteristic polynomial

$$|sI - A| = s^n + \sum_{j=0}^{n-1} a_j s^j, \tag{6.108}$$

corresponding to the target model $(A,\ b)$. Setting now

$$v_i = -\underline{a}' z_i + \hat{v}_i, \tag{6.109}$$

in (6.102), and defining $\hat{z}_i = M^{-1} z_i$, with z_i as in (6.103), it is easy to verify that

$$\dot{\hat{z}}_i = A\hat{z}_i + b\hat{v}_i, \tag{6.110}$$

with $i = 1, \ldots, N$. Eq. (6.110) basically shows that the i-th nonlinear system

$$\dot{x}_i = \mathbf{f}_i(x_i) + \big(-\frac{q_i(x_i)}{s_i(x_i)} - \frac{1}{s_i(x_i)} \underline{a}' T_i(x_i) + \frac{1}{s_i(x_i)} \hat{v}_i \big) \mathbf{g}_i(x_i), \tag{6.111a}$$

$$\hat{z}_i = M^{-1} T_i(x_i), \tag{6.111b}$$

can precisely be described by the linear differential equation (6.105) representing a target model. In the sequel, system (6.111) is said to match with the model of linear system (6.105). This model-matching task of single-input systems described above, is formally stated as follows.

Problem 6.4.1 (Model-matching problem (single-input case))**.** Given N single-input nonlinear systems as in (6.97), and a single-input controllable system $(A,\ b)$, referred to as target, with characteristic polynomial $|sI - A| = s^n + \sum_{j=0}^{n-1} a_j s^j$, we wish to compute:

(a) a smooth function $q_i \in S(X_i)$ for each $i = 1, \ldots, N$,

(b) a smooth function $s_i \in S(X_i)$, with $s_i(x_i) \neq 0$ for all x_i in some neighborhood $U_i \subseteq \mathbb{R}^n$ around $\mathbf{0}$ containing $x_{i,0}$, for each $i = 1, \ldots, N$,

(c) a local smooth diffeomorphism $T_i : U_i \to \mathbb{R}^n$, with $T_i(\mathbf{0}) = \mathbf{0}$, for each $i = 1, \ldots, N$,

(d) a nonsingular matrix $M \in \mathbb{R}^{n \times n}$ such that pair $(MAM^{-1},\ Mb)$ is in controllable canonical form,

satisfying the following conditions: if we define feedback control

$$u_i = -\frac{q_i(x_i)}{s_i(x_i)} - \frac{1}{s_i(x_i)} \underline{a}' T_i(x_i) + \frac{1}{s_i(x_i)} \hat{v}_i, \tag{6.112}$$

with $\hat{v}_i \in \mathbb{R}$, $\underline{a} = \begin{bmatrix} a_0 & a_1 & \cdots & a_{n-1} \end{bmatrix}'$ and a change of coordinates as

$$\hat{z}_i = M^{-1} T_i(x_i), \tag{6.113}$$

then,

$$\dot{\hat{z}}_i = A\hat{z}_i + b\hat{v}_i,\ \hat{z}_{i,0} = M^{-1} T_i(x_{i,0}), \tag{6.114}$$

for $i = 1, \ldots, N$. □

We note that the initial conditions of systems in Problem 6.4.1, defined as $x_{i,0}$, $i = 1,\ldots,N$, need not coincide and, of course, generically differ to each other. The same holds true for neighborhoods U_i's each generated around the origin containing $x_{i,0}$. Yet, setting above $N = 1$ and selecting a target system with characteristic polynomial as s^n, Problem 6.4.1 is precisely identical to the feedback linearization problem 6.3.1. In this setting, model-matching problem 6.4.1 can be cast as N decoupled feedback linearization problems 6.3.1 carried out simultaneously. Clearly, Problem 6.4.1 has a solution as long as conditions (i) and (ii) of Theorem 6.3.2 are satisfied for each individual system. If these conditions are in force, then, a diffeomorphism $T_i(x_i)$ and smooth functions $q_i(x_i)$, $s_i(x_i)$ can be constructed for each $i = 1,\ldots,N$ as suggested in Section 6.3.1.

Suppose now N systems, defined as in (6.97), are feedback linearizable in the sense that conditions (i) and (ii) of Theorem 6.3.2 are satisfied. Suppose also functions T_i, q_i and s_i are known such that variables v_i, z_i as defined in (6.102), (6.103), respectively, satisfy (6.104) for $i = 1,\ldots,N$. A compact form of the latter is written below:

$$\dot{z}_i = \underbrace{\begin{bmatrix} 0 & 1 & 0 & \ldots & 0 \\ 0 & 0 & 1 & \ldots & 0 \\ \vdots & \vdots & \vdots & \ddots & \vdots \\ 0 & 0 & 0 & \ldots & 1 \\ 0 & 0 & 0 & \ldots & 0 \end{bmatrix}}_{A_o} z_i + \underbrace{\begin{bmatrix} 0 \\ 0 \\ \vdots \\ 0 \\ 1 \end{bmatrix}}_{b_t} v_i, \tag{6.115}$$

which can be seen as a target state-space form. Letting now

$$v_i = \hat{v}_i + f_i' z_i, \tag{6.116}$$

with $f_i = \begin{bmatrix} f_0 & f_1 & \cdots & f_{n-1} \end{bmatrix}'$ and $\hat{v}_i \in \mathbb{R}$, for each $i = 1,\ldots,N$, it is clear that a new target is attained, described by the canonical form $(A_t,\ b_t)$, where

$$A_t = A_o + \begin{bmatrix} 0 \\ \vdots \\ 0 \\ 1 \end{bmatrix} \begin{bmatrix} f_0 & f_1 & \cdots & f_{n-1} \end{bmatrix}. \tag{6.117}$$

Note that canonical form $(A_t,\ b_t)$ is completely defined by state-feedback gain f_i as selected in (6.116) where coefficients f_j, $j = 0,\ldots,n-1$, are associated with the characteristic polynomial $|sI - A_t|$. Evidently, any canonical form $(A_t,\ b_t)$, with $A_t \in \mathbb{R}^{n\times n}$ and $b_t \in \mathbb{R}^n$,

may be achieved with a suitable choice of f_i in (6.116). This implies that any controllable single-input linear system with n states may be selected as target model in this model-matching setting. This observation naturally begets the question of how one should select a target system in Problem 6.4.1. The following section attempts to address this task.

6.4.2 Target selection (single-input case)

We consider a set of N feedback linearizable systems defined as in (6.97), rewritten below as

$$\dot{x}_i = \mathbf{f}_i(x) + u_i \mathbf{g}_i(x),\ x_i(0) = x_{i,0},\ i = 1,\ldots,N. \tag{6.118}$$

Vectors $x_i \in \mathbb{R}^n$, $u_i \in \mathbb{R}$ and vector fields $\mathbf{f}_i$, $\mathbf{g}_i$, $i = 1,\ldots,N$, are as defined earlier. Suppose also that feedback functions q_i, s_i as well as a local diffeomorphism T_i exist and are known. Let pair $(A,\ b)$, with $A \in \mathbb{R}^{n\times n}$, $b \in \mathbb{R}$, representing a target system, denote any controllable single-input linear system. Let also nonsingular matrix $M \in \mathbb{R}^{n\times n}$ be such that pair $(MAM^{-1},\ Mb)$ is in controllable canonical form and vector

$$\underline{a} = \begin{bmatrix} a_0 & a_1 & \cdots & a_{n-1} \end{bmatrix}' \tag{6.119}$$

denote the coefficients of characteristic polynomial $|sI - A| = s^n + \sum_{j=1}^{n-1} a_j s^j$. Applying now feedback control

$$u_i = -\frac{q_i(x_i)}{s_i(x_i)} - \frac{1}{s_i(x_i)} \underline{a}' T_i(x_i) + \frac{1}{s_i(x_i)} \hat{v}_i,\ i = 1,\ldots,N, \tag{6.120}$$

where $\hat{v}_i \in \mathbb{R}$, and performing changes of coordinates defined as

$$\hat{z}_i = M^{-1} T_i(x_i),\ i = 1,\ldots,N, \tag{6.121}$$

it is readily verified that systems (6.118) match with the target model $(A,\ b)$ in the sense that variables $\hat{z}_i$, $\hat{v}_i$, $i = 1,\ldots,N$, satisfy the following linear equations:

$$\dot{\hat{z}}_i = A\hat{z}_i + b\hat{v}_i,\ i = 1,\ldots,N. \tag{6.122}$$

Clearly, a different target choice requires altering vector $\underline{a}$ in (6.120) resulting in different feedback control. Parameterizing each single-input target system by its characteristic polynomial and treating vector $\underline{a}$ as a design parameter, we wish to identify an optimal target model, such that a certain measure of the joint model-matching control effort expressed as a function of $u_1,\ldots,u_N$, is minimized. A metric of local model-matching energy loss is defined next.

For convenience, we write the control input of the i-th system as follows:

$$u_i = \underline{a}' \psi_i + \omega_i, \tag{6.123}$$

where

$$\psi_i(x_i) = -\frac{1}{s_i(x_i)} z_i, \tag{6.124}$$

$$\omega_i(x_i) = -\frac{q_i(x_i)}{s_i(x_i)}, \tag{6.125}$$

for $i = 1, \ldots, N$. Consider now the following function:

$$u_i^2 = (\psi_i' \underline{a} + \omega_i)(\psi_i' \underline{a} + \omega_i), \tag{6.126}$$

which can be written as

$$u_i^2 = \underline{a}' \psi_i \psi_i' \underline{a} + 2\underline{a}' \psi_i \omega_i + \omega_i^2, \tag{6.127}$$

for $i = 1, \ldots, N$. Note that ψ_i and ω_i, as defined above, are smooth functions of x_i in some neighborhood $U \subseteq \mathbb{R}^n$ containing all $x_{i,0}$'s. Yet, considering u_i^2 in (6.127) as a quadratic function in vector $\underline{a}$ does not simplify the formulation of an optimization problem since the nonlinear dependence of u_i^2 on x_i has no specific pattern. To forestall this difficulty, namely, the dependence of u_i^2 on x_i, we propose the following simplification.

Let $x_i \in \mathbb{R}^n$ representing the state-vector of i-th be written as

$$x_i = \begin{bmatrix} x_{i,1} & x_{i,2} & \cdots & x_{i,n}, \end{bmatrix}' \tag{6.128}$$

and suppose j-th state of i-th system denoted as $x_{i,j}$, with $i = 1, \ldots, N$, $j = 1, \ldots, n$, is a random variable with known probability density function (pdf) $f_{x_{i,j}}(x_{i,j})$. Let also $f_{x_i}(x_{i,1}, \ldots, x_{i,n})$ denote the joint pdf of random variables $x_{i,1}, \ldots, x_{i,n}$ corresponding to the states of i-th system. Then, treating $x_{i,j}$'s as random variables, function u_i as defined in (6.127) is also a random

variable with expected value computed as

$$\begin{aligned}\mathbb{E}[u_i^2] = \underline{a}'\Big(&\int_{-\infty}^{\infty}\cdots\int_{-\infty}^{\infty}\psi_i\psi_i' f_{x_i}(x_{i,1},\ldots,x_{i,n})\,\mathrm{d}x_{i,1}\cdots\mathrm{d}x_{i,n}\Big)\underline{a}\\ &+2\underline{a}'\int_{-\infty}^{\infty}\cdots\int_{-\infty}^{\infty}\psi_i\omega_i f_{x_i}(x_{i,1},\ldots,x_{i,n})\,\mathrm{d}x_{i,1}\cdots\mathrm{d}x_{i,n}\\ &+\int_{-\infty}^{\infty}\cdots\int_{-\infty}^{\infty}\omega_i^2 f_{x_i}(x_{i,1},\ldots,x_{i,n})\,\mathrm{d}x_{i,1}\cdots\mathrm{d}x_{i,n},\end{aligned}\tag{6.129}$$

which is clearly a quadratic function in vector $\underline{a}$.

We remark that treating states as random variables and defining the expected value of function u_i^2, gives considerable flexibility in the model-matching design. This is because function $f_{x_i}(x_{i,1},\ldots,x_{i,n})$ defined above as a joint probability density function, can also be seen as a weight function utilized to emphasize a particular range of x_i. A simple instance can be the following: suppose that x_i is a random variable uniformly distributed inside the volume of the n-dimensional hypercube with edge dimension equal to $\frac{\rho}{2}$ and center at the origin, defined as

$$V_i = \{x \in \mathbb{R}^n : \ -\frac{\rho}{2} \leq x_j \leq \frac{\rho}{2},\ \forall j = 1,\ldots,n\},\tag{6.130}$$

for $i = 1,\ldots,N$. Then, the corresponding probability density function

$$f_{x_i}(x_{i,1},\ldots,x_{i,n}) = \begin{cases}\frac{1}{\rho^n} & -\frac{\rho}{2} \leq x_j \leq \frac{\rho}{2},\ j = 1,\ldots,n,\\ 0 & \text{otherwise.}\end{cases}$$

Let now quadratic function $J_i(\underline{a})$ be defined as

$$J_i(\underline{a}) = \mathbb{E}[u_i^2],\tag{6.131}$$

for $i = 1,\ldots,N$. For convenience, define also

$$G_i = \int_{-\infty}^{\infty}\cdots\int_{-\infty}^{\infty}\psi_i\psi_i' f_{x_i}(x_{i,1},\ldots,x_{i,n})\,\mathrm{d}x_{i,1}\cdots\mathrm{d}x_{i,n},\tag{6.132}$$

and

$$\beta_i = \int_{-\infty}^{\infty} \cdots \int_{-\infty}^{\infty} \psi_i \omega_i f_{x_i}(x_{i,1}, \ldots, x_{i,n})\, \mathrm{d}x_{i,1} \cdots \mathrm{d}x_{i,n}, \tag{6.133}$$

for $i = 1, \ldots, N$, with all parameters as defined earlier. In the following, we suggest two types of performance indexes which measure joint model-matching energy loss inspired by the model-matching problem of linear systems studied in Chapter 5.

6.4.2.1 Minimum worst-case control

We express joint worst-case model-matching control action by the maximum function:

$$\phi(\underline{a}) = \max_{i=[1:N]} J_i \text{ with } J_i = \mathbb{E}[u_i^2], \tag{6.134}$$

and we wish to find vector $\underline{a} \in \mathbb{R}^n$ for which $\phi(\underline{a})$ attains its minimum. This is a discrete minimax problem formulated as

$$\min_{\underline{a} \in \mathbb{R}^n} \phi(\underline{a}) = \min_{\underline{a} \in \mathbb{R}^n} \max_{i \in [1:N]} \mathbb{E}[u_i^2]. \tag{6.135}$$

The maximum function $\phi(\underline{a})$ is continuous and convex by the continuity and convexity of J_i, $i = 1, \ldots, N$, and its sub-level sets are bounded. Thus, minimizing solution $\underline{a}^*$ exists and is unique. The ε-steepest decent algorithm presented in Chapter 5 can be employed here to approximate the optimal solution $\underline{a}^*$. The corresponding model-matching feedback control u_i is constructed by substituting $\underline{a}^*$ into (6.120).

6.4.2.2 Least-squares control

An index which measures joint model-matching control effort in a different manner is denoted by

$$J(\underline{a}) = \sum_{i=1}^{N} J_i(\underline{a}). \tag{6.136}$$

Here, we are interested in a vector $\underline{a}$ for which J in (6.136) becomes minimum. Requiring

$$\frac{\partial J}{\partial \underline{a}} = 0, \tag{6.137}$$

the least squares solution yields,

$$\underline{a}^* = -G^{-1}\beta, \tag{6.138}$$

where

$$G = \sum_{i=1}^{N} G_i, \tag{6.139}$$

and

$$\beta = \sum_{i=1}^{N} \beta_i, \tag{6.140}$$

with G_i, β_i as defined in (6.132), (6.133), respectively. Substituting $\underline{a}^*$ into (6.120) yields the corresponding model-matching feedback laws u_i, $i = 1,\ldots,N$.

The following numerical example illustrates a model-matching problem of N single-input systems with a target model, optimally selected in the least-squares sense suggested above.

Example 6.4.2. Consider N single-input systems, each representing a mass constrained by a nonlinear spring and a nonlinear viscous damper, and driven by an external force. The i-th system is described by

$$m_i\ddot{r}_i + d_i(\dot{r}_i) + k_i(r_i) = u_i,\ i = 1,\ldots,N, \tag{6.141}$$

where m_i, r_i, d_i and k_i denote mass, displacement, damping force and restoring force, respectively. Let $d_i = c_i\dot{r}_i^3$ and $k_i = h_i r_i^3$, where $c_i,\ h_i \in \mathbb{R}$, $i = 1,\ldots,N$, denote some positive constants. A natural choice of state-vectors is

$$x_i = \begin{bmatrix} x_{i,1} \\ x_{i,2} \end{bmatrix} = \begin{bmatrix} r_i \\ \dot{r}_i \end{bmatrix},\ i = 1,\ldots,N. \tag{6.142}$$

Then, the dynamics of the N systems are represented by

$$\dot{x}_i = \mathbf{f}_i + u_i\mathbf{g}_i,\ i = 1,\ldots,N, \tag{6.143}$$

where

$$\mathbf{f}_i = \begin{bmatrix} x_{i,2} \\ -\frac{c_i}{m_i}x_{i,2}^3 - \frac{h_i}{m_i}x_{i,1}^3 \end{bmatrix},\ \mathbf{g}_i = \begin{bmatrix} 0 \\ \frac{1}{m_i} \end{bmatrix},\ i = 1,\ldots,N. \tag{6.144}$$

The objective here is to match the i-th state-space form (6.143) with a linear target model described by a pair $(A_t,\ b_t)$ applying nonlinear feedback laws u_i, $i = 1,\ldots,N$, and performing changes of coordinates $z_i = T_i$, $i = 1,\ldots,N$. For simplicity, let system $(A_t,\ b_t)$ be in controllable canonical form and let also vector

$$\underline{a} = \begin{bmatrix} a_0 \\ a_1 \end{bmatrix}, \tag{6.145}$$

denote the coefficients of the characteristic polynomial $|sI - A_t| = s^2 + a_1 s + a_0$. Then, we wish to construct the following feedback control inputs:

$$u_i = \underline{a}' \psi_i + \omega_i,\ i = 1, \ldots, N, \tag{6.146}$$

where

$$\psi_i(x_i) = -\frac{1}{s_i(x_i)} z_i,\ i = 1, \ldots, N, \tag{6.147}$$

$$\omega_i(x_i) = -\frac{q_i(x_i)}{s_i(x_i)},\ i = 1, \ldots, N. \tag{6.148}$$

Since $\mathbf{f}(\mathbf{0}) = \mathbf{0}$, let $x_{i,0} = \mathbf{0}$, be an equilibrium of the i-th system. From Theorem 6.3.2, the i-th system can be transformed to (6.57) if and only if the following two conditions hold over some neighborhood of $x_{i,0}$: (i) the set $\{\mathbf{g}_i,\ \mathrm{ad}_{\mathbf{f}_i}\mathbf{g}_i\}$ is linearly independent, and (ii) the set $\{\mathbf{g}_i\}$ is involutive. Evaluating $\mathrm{ad}_{\mathbf{f}_i}\mathbf{g}_i = \mathbf{[f}_i,\ \mathbf{g}_i\mathbf{]}$ we have

$$[\mathbf{g}_i\ \mathrm{ad}_{\mathbf{f}_i}\mathbf{g}_i] = \begin{bmatrix} 0 & \frac{1}{m_i} \\ \frac{1}{m_i} & -\frac{3c_i}{m_i^2} x_{i,2}^2 \end{bmatrix}. \tag{6.149}$$

The determinant of this matrix is $-1/m_i^2$ which is obviously nonzero irrespective of the value of $x_{i,2}$. Hence, condition (i) is in force. Condition (ii) also holds since any distribution spanned by a constant vector is involutive. This is easily verified by letting function $\phi_{i,2} = x_{i,2}$. Then, clearly,

$$\mathbf{<d}\phi_i(x_i),\ \mathbf{g}_i\mathbf{>} = 0,\ \forall x_i \in \mathbb{R}^2, \tag{6.150}$$

which is precisely what Theorem 6.2.8 requires in (6.33). Hence, from Theorem 6.3.2, we conclude that i-th system is feedback linearizable.

To construct a linearizing transformation, we wish to find a non-constant function

$$T_i(x_i) = \begin{bmatrix} T_{i,1} \\ T_{i,2} \end{bmatrix}, \tag{6.151}$$

such that

$$\mathbf{<d}T_{i,1},\ \mathbf{g}_i\mathbf{>} = 0, \tag{6.152}$$

which implies

$$\frac{1}{m_i} \frac{\partial T_{i,1}}{\partial x_{i,2}} = 0. \tag{6.153}$$

An obvious choice is $T_{i,1} = x_{i,1} = r_i$. Of course this choice is not unique. Now,

$$T_{i,2} = \mathbf{<d}T_{i,1},\ \mathbf{f}_i\mathbf{>} = x_{i,2}. \tag{6.154}$$

This shows that the nonlinear state transformation, in the present case, is the linear map $T_i = I_2 x_i$. This further means that we can linearize i-th system without changing coordinates. We also compute

$$q_i = \mathbf{<d}T_{i,2},\ \mathbf{f}_i\mathbf{>} = -\frac{1}{m_i}(c_i x_{i,2}^3 + h_i x_{i,1}^3), \tag{6.155}$$

and

$$s_i = \mathbf{<d}T_{i,2},\ \mathbf{g}_i\mathbf{>} = \frac{1}{m_i}. \tag{6.156}$$

Note that q_i is a smooth function $\forall x_i \in \mathbb{R}^2$ and $s_i \neq 0\ \forall x_i \in \mathbb{R}^2$. Substituting, now, q_i and s_i into (6.147) and (6.148), we have

$$\psi_i = -m_i \begin{bmatrix} x_{i,1} \\ x_{i,2} \end{bmatrix}, \tag{6.157}$$

$$\omega_i = c_i x_{i,2}^3 + h_i x_{i,1}^3. \tag{6.158}$$

Defining a function $J = \sum_{i=1}^N u_i^2$ with

$$u_i = \underline{a}'\psi_i + \omega_i,\ i = 1,\ldots,N, \tag{6.159}$$

results in

$$J = \underline{a}' \sum_{i=1}^N \psi_i \psi_i' \underline{a} + 2\underline{a}' \sum_{i=1}^N \psi_i \omega_i + \sum_{i=1}^N \omega_i^2. \tag{6.160}$$

To construct vector $\underline{a}$ we proceed with the following hypothesis. Let x_i be a two-dimensional random variable, uniformly distributed inside the two-dimensional cube defined as

$$Q = \{x \in \mathbb{R}^2 : -1 \leq x_j \leq 1,\ \forall j = 1,2\}. \tag{6.161}$$

In this setting, function J is also a random variable with expected value given as

$$\mathbb{E}[J(\underline{a})] = \underline{a}'\Big(\sum_{i=1}^N \int_{-1}^{1}\int_{-1}^{1} \psi_i \psi_i' \mathrm{d}x_{i,1}\mathrm{d}x_{i,2}\Big)\underline{a} + 2\underline{a}' \sum_{i=1}^N \int_{-1}^{1}\int_{-1}^{1} \psi_i \omega_i \mathrm{d}x_{i,1}\mathrm{d}x_{i,2}$$
$$+ \sum_{i=1}^N \int_{-1}^{1}\int_{-1}^{1} \omega_i^2 \mathrm{d}x_{i,1}\mathrm{d}x_{i,2}. \tag{6.162}$$

Then, an optimal vector $\underline{a}$ can be computed as

$$\underline{a}^* = \text{argmin}\ \mathbb{E}[J(\underline{a})]. \tag{6.163}$$

Evaluating the following integrals:

$$G_i = \int_{-1}^{1}\int_{-1}^{1} \psi_i \psi_i' \mathrm{d}x_{i,1}\mathrm{d}x_{i,2} = \frac{m_i^2}{4}\int_{-1}^{1}\int_{-1}^{1} \begin{bmatrix} x_{i,1}^2 & x_{i,1}x_{i,2} \\ x_{i,2}x_{i,1} & x_{i,2}^2 \end{bmatrix} \mathrm{d}x_{i,1}\mathrm{d}x_{i,2} \tag{6.164}$$

$$= \frac{m_i^2}{4}\int_{-1}^{1} \begin{bmatrix} \frac{1}{3}x_{i,1}^3 & \frac{1}{2}x_{i,2}x_{i,1}^2 \\ \frac{1}{2}x_{i,2}x_{i,1}^2 & x_{i,2}^2 x_{i,1} \end{bmatrix}_{x_{i,1}=-1}^{x_{i,1}=1} \mathrm{d}x_{i,2} = \frac{m_i^2}{4}\int_{-1}^{1} \begin{bmatrix} \frac{2}{3} & 0 \\ 0 & 2x_{i,2}^2 \end{bmatrix} \mathrm{d}x_{i,2} \tag{6.165}$$

$$= \frac{m_i^2}{4}\begin{bmatrix} \frac{2}{3}x_{i,2} & 0 \\ 0 & \frac{2}{3}x_{i,2}^3 \end{bmatrix}_{x_{i,2}=-1}^{x_{i,2}=1} = \frac{m_i^2}{3}\begin{bmatrix} 1 & 0 \\ 0 & 1 \end{bmatrix}, \tag{6.166}$$

$$\beta_i = \int_{-1}^{1}\int_{-1}^{1} \psi_i \omega_i \mathrm{d}x_{i,1}\mathrm{d}x_{i,2} = -\frac{m_i}{4}\int_{-1}^{1}\int_{-1}^{1} \begin{bmatrix} x_{i,1} \\ x_{i,2} \end{bmatrix} (c_i x_{i,2}^3 + h_i x_{i,1}^3)\mathrm{d}x_{i,1}\mathrm{d}x_{i,2} \tag{6.167}$$

$$= -\frac{m_i}{4}\int_{-1}^{1}\int_{-1}^{1} \begin{bmatrix} c_i x_{i,2}^3 x_{i,1} + h_i x_{i,1}^4 \\ c_i x_{i,2}^4 + h_i x_{i,2} x_{i,1}^3 \end{bmatrix} \mathrm{d}x_{i,1}\mathrm{d}x_{i,2} = -\frac{m_i}{4}\int_{-1}^{1} \begin{bmatrix} \frac{c_i}{2}x_{i,2}^3 x_{i,1}^2 + \frac{h_i}{5}x_{i,1}^5 \\ c_i x_{i,2}^4 x_{i,1} + \frac{h_i}{4}x_{i,2}x_{i,1}^4 \end{bmatrix}_{x_{i,1}=-1}^{x_{i,1}=1} \mathrm{d}x_{i,2} \tag{6.168}$$

$$= -\frac{m_i}{4}\int_{-1}^{1} \begin{bmatrix} \frac{2h_i}{5} \\ 2c_i x_{i,2}^4 \end{bmatrix} \mathrm{d}x_{i,2} = -\frac{m_i}{4}\begin{bmatrix} \frac{2h_i x_{i,2}}{5} \\ \frac{2c_i x_{i,2}}{5} \end{bmatrix}_{x_{i,2}=-1}^{x_{i,2}=1} = -\frac{m_i}{5}\begin{bmatrix} h_i \\ c_i \end{bmatrix} \tag{6.169}$$

and defining

$$G = \sum_{i=1}^{N} G_i = I_2 \sum_{i=1}^{N} \frac{m_i^2}{3}, \tag{6.170}$$

$$\beta = \sum_{i=1}^{N} \beta_i = -\frac{1}{5}\sum_{i=1}^{N} \begin{bmatrix} m_i h_i \\ m_i c_i \end{bmatrix}, \tag{6.171}$$

the least-square solution yields

$$\underline{a}^* = -G^{-1}\beta = \frac{3}{5}\begin{bmatrix} \frac{\sum_{i=1}^{N} m_i h_i}{\sum_{i=1}^{N} m_i^2} \\ \frac{\sum_{i=1}^{N} m_i c_i}{\sum_{i=1}^{N} m_i^2} \end{bmatrix}. \tag{6.172}$$

Finally, applying

$$u_i = \psi_i' \underline{a}^* + \omega_i + \frac{1}{s_i}\hat{v}_i,\ i = 1,\ldots,N, \tag{6.173}$$

with $\hat{v}_i \in \mathbb{R}$, $i = 1,\ldots,N$, the nonlinear equations (6.143) are transformed to the linear differential equations

$$\dot{x}_i = A_t x_i + b_t \hat{v}_i,\ i = 1,\ldots,N. \tag{6.174}$$

The pair $(A_t,\ b_t)$ represents the target dynamics, with

$$A_t = \begin{bmatrix} 0 & 1 \\ -a_0^* & -a_1^* \end{bmatrix},\ b_t = \begin{bmatrix} 0 \\ 1 \end{bmatrix}, \tag{6.175}$$

where a_0^*, a_1^* are given in

$$\underline{a}^* = \begin{bmatrix} a_0^* \\ a_1^* \end{bmatrix}. \tag{6.176}$$

□

The following section attempts to extend the model-matching problem studied here to multi-input nonlinear systems.

6.4.3 Model-matching of multi-input nonlinear systems

We consider a set of N nonlinear systems of the form

$$\dot{x}_i = \mathbf{f}_i(x_i) + \sum_{j=1}^{m} u_{i,j}\mathbf{g}_{i,j}(x_i),\ x_i(0) = x_{i,0},\ i = 1,\ldots,N, \tag{6.177}$$

where $\mathbf{f}_i, \mathbf{g}_{i,1},\ldots,\mathbf{g}_{i,m}$ are smooth vector fields on some neighborhood $X_i \subseteq \mathbb{R}^n$ near the origin containing $x_{i,0}$, with $\mathbf{f}_i(\mathbf{0}) = \mathbf{0}$. We assume that vector fields $\mathbf{g}_{i,1},\ldots,\mathbf{g}_{i,m}$, $i = 1,\ldots,N$, are linearly independent for all $x_i \in X_i$. In the following, we denote the input vectors as

$$u_i = \begin{bmatrix} u_{i,1} & \cdots & u_{i,m} \end{bmatrix}',\ i = 1,\ldots,N. \tag{6.178}$$

In order to proceed with the formulation of the matching problem, we require that systems described in (6.177) be feedback linearizable in the sense that conditions (i) and (ii) of Theorem 6.3.4 are satisfied for $i = 1,\ldots,N$. A linear system, referred to as target system, is defined by the following linear differential equation of the form

$$\dot{\xi} = A\xi + Bv, \tag{6.179}$$

where $(A,\ B)$ is a controllable pair with $A \in \mathbb{R}^{n\times n}$, $B \in \mathbb{R}^{n\times m}$. Without loss of generality, let $(A,\ B)$ be in controllable canonical form with

$$A = \bar{A}_c + \bar{B}_c A_m, \tag{6.180a}$$

$$B = \bar{B}_c B_m, \tag{6.180b}$$

where pair $(\bar{A}_c,\ \bar{B}_c)$ denotes the Brunonvsky canonical form associated with the set of controllability indices: $\mu_1,\ldots,\mu_m$, with $\sum_{j=1}^{m}\mu_j = n$ (cf. Chapter 5, eq. (5.13)) and $A_m \in \mathbb{R}^{m\times n}$, $B_m = \mathbb{R}^{m\times m}$ with $\det(B_m) \neq 0$. We now summarize the model-matching task of N multi-input feedback linearizable systems as follows.

Problem 6.4.3 (Model-matching problem (multi-input case))**.** Consider N multi-input nonlinear systems as in (6.177), and a target system defined by a controllable pair $(A,\ B)$ as in (6.180). Letting $U_i \subseteq X_i$ denote a neighborhood nearby the origin with $x_{i,0} \in U_i$, $i = 1,\ldots,N$, we wish to compute:

(a) a smooth function $\mathbf{q}_i : U_i \to \mathbb{R}^m$ for each $i = 1,\ldots,N$,

(b) a smooth function $\mathbf{S}_i : U_i \to \mathbb{R}^{m\times m}$ such that $\det(\mathbf{S}_i(x_i)) \neq 0\ \forall x_i \in U_i$, for each $i = 1,\ldots,N$,

(c) a local smooth diffeomorphism $T_i : U_i \to \mathbb{R}^n$, with $T_i(\mathbf{0}) = \mathbf{0}$, for each $i = 1,\ldots,N$,

(d) a state-feedback gain matrix $F_i \in \mathbb{R}^{m\times n}$, for each $i = 1,\ldots,N$,

satisfying the following conditions: if we define feedback control

$$u_i = -\mathbf{S}_i^{-1}(x_i)\mathbf{q}_i(x_i) + \mathbf{S}_i^{-1}(x_i)F_i T_i(x_i) + \mathbf{S}_i^{-1}(x_i)B_m\hat{v}_i, \tag{6.181}$$

with $\hat{v}_i \in \mathbb{R}^m$ and perform a change of coordinates as

$$z_i = T_i(x_i), \tag{6.182}$$

then,

$$\dot{z}_i = Az_i + B\hat{v}_i, \tag{6.183}$$

for $i = 1,\ldots,N$, with $(A,\ B)$ denoting the target model. □

Necessary and sufficient conditions for Problem 6.4.3 to have a solution are given in the following theorem.

Theorem 6.4.4. *Given N feedback linearizable systems (in the sense that conditions of Theorem 6.3.4 are in force) of the form* (6.177)*, each associated with a set of integers* $\kappa_1^i, \ldots, \kappa_m^i$ *constructed as in Procedure 6.3.1 and a linear target system as defined in* (6.179) *associated with a Brunovsky form* $(\bar{A}_c,\ \bar{B}_c)$ *defined by controllability indices* $\mu_1, \ldots, \mu_m$*, Problem 6.4.3 has a solution if and only if the following condition is satisfied:*

(i) the sets $\{\kappa_1^i, \ldots, \kappa_m^i\}$ *and* $\{\mu_1, \ldots, \mu_m\}$ *coincide for all* $i = 1, \ldots, N$.

Proof. First, we prove the "if" part of the theorem for the i-th system. Suppose Condition (i) holds. Suppose also that feedback functions $\mathbf{q}_i(x_i)$, $\mathbf{S}_i(x_i)$ and a local diffeomorphism $T_i(x_i)$ exist and are known. Then, from Theorem 6.3.4, variables z_i and v_i defined as

$$z_i = T_i, \tag{6.184}$$

$$v_i = \mathbf{q}_i + \mathbf{S}_i u_i, \tag{6.185}$$

satisfy the following linear differential equation,

$$\dot{z}_i = \bar{A}_c z_i + \bar{B}_c v_i, \tag{6.186}$$

where $(\bar{A}_c,\ \bar{B}_c)$ is the Brunovsky form associated with controllability indices $\kappa_1^i, \ldots, \kappa_m^i$. Now, since target pair $(A,\ B)$ is in canonical form, (6.179) can be written as

$$\dot{\xi} = (\bar{A}_c + \bar{B}_c A_m)\xi + \bar{B}_c B_m v, \tag{6.187}$$

or,

$$\dot{\xi} = \bar{A}_c \xi + \bar{B}_c (A_m \xi + B_m v). \tag{6.188}$$

Since by assumption the sets $\kappa_1^i, \ldots, \kappa_m^i$ and $\mu_1^i, \ldots, \mu_m^i$ coincide, pairs $(\bar{A}_c,\ \bar{B}_c)$ appearing in (6.186) and (6.188) correspond to the same Brunovsky form, thereby being identical. Setting now

$$v_i = A_m z_i + B_m \hat{v}_i, \tag{6.189}$$

in (6.186), yields

$$\dot{z}_i = \bar{A}_c z_i + \bar{B}_c (A_m z_i + B_m \hat{v}_i), \tag{6.190}$$

which is written as

$$\dot{z}_i = (\bar{A}_c + \bar{B}_c A_m) z_i + \bar{B}_c B_m \hat{v}_i), \tag{6.191}$$

or

$$\dot{z}_i = A z_i + B \hat{v}_i, \tag{6.192}$$

due to (6.180), where $(A,\ B)$ denotes the target pair. Now, combining (6.185) and (6.189) leads to

$$A_m z_i + B_m \hat{v}_i = \mathbf{q}_i(x_i) + \mathbf{S}_i(x_i) u_i, \tag{6.193}$$

or

$$u_i = -S_i^{-1}\mathbf{q}_i(x_i) + S_i^{-1} A_m z_i + S_i^{-1} B_m \hat{v}_i, \tag{6.194}$$

which becomes identical to (6.181) if we set $F_i = A_m$. This proves the "if" part of the theorem.

We now prove the "only if" part of the theorem by contradiction. Suppose that Problem 6.4.3 has a solution and that $\{\kappa_1^i, \ldots, \kappa_m^i\}$ and $\{\mu_1, \ldots, \mu_m\}$ represent non-identical sets of controllability indices. Let

$$\dot{\xi} = A\xi + Bv, \tag{6.195}$$

denote the target state-space form. Then, setting $v = B_m^{-1}(\bar{v} - A_m \xi)$ in (6.195) results in

$$\dot{\xi} = \bar{A}_c \xi + \bar{B}_c \bar{v}, \tag{6.196}$$

while setting $\hat{v}_i = B_m^{-1}(\bar{v}_i - A_m z_i)$ in (6.183) with $\bar{v}_i \equiv \bar{v} \in \mathbb{R}^m$ leads to

$$\dot{z}_i = \bar{A}_c z_i + \bar{B}_c \bar{v}_i. \tag{6.197}$$

Pair $(\bar{A}_c,\ \bar{B}_c)$ above denotes the Brunovsky form characterized only by identical sets of controllability indices. However, this contradicts our initial assumption of non-identical sets of controllability indices, thereby proving the "only if" part of the theorem. □

So far, it has been shown that if a set of N feedback linearizable systems with equal state and input dimensions, n and m, respectively, are associated with identical sets of controllability indices $\kappa_1, \ldots, \kappa_m$ defined as in Procedure 6.3.1, then, there are nonlinear feedback controls u_i, and changes of coordinates $z_i = T_i(x_i)$, $i = 1, \ldots, N$, as defined in (6.181), and (6.182), respectively, that transform their nonlinear state-space forms into a linear (target) model represented in canonical form with controllability indices $\mu_1, \ldots, \mu_m$, provided that the sets $\{\kappa_1, \ldots, \kappa_m\}$ and $\{\mu_1, \ldots, \mu_m\}$ coincide. In the following section, we show how to identify optimal target dynamics the selection of which guarantees a minimum performance index defined to penalize joint model-matching control action.

6.4.4 Target selection (multi-input case)

We consider a set of N feedback linearizable systems defined as in (6.177), rewritten below as

$$\dot{x}_i = \mathbf{f}_i(x_i) + \sum_{j=1}^{m} u_{i,j}\mathbf{g}_{i,j}(x_i),\ x_i(0) = x_{i,0},\ i = 1,\ldots,N, \tag{6.198}$$

where vectors $x_i \in \mathbb{R}^n$, $u_i \in \mathbb{R}^m$ and vector fields $\mathbf{f}_i$, $\mathbf{g}_{i,1},\ldots,\mathbf{g}_{i,m}$ are as defined in the previous section. Let $\kappa_1^i,\ldots,\kappa_m^i$ denote the set of controllability indices (see Procedure 6.3.1) associated with the i-th system in (6.198). Suppose that $\kappa_j^i = \kappa_j$ with $j = 1,\ldots,m\ \forall i = 1,\ldots,N$. Assume also that there exist smooth functions $\mathbf{q}_i$, $\mathbf{S}_i$ and a diffeomorphism T_i as defined in Problem 6.4.3 for $i = 1,\ldots,N$. For each $i = 1,\ldots,N$, let also $\mathbf{q}_i$, $\mathbf{S}_i$ and T_i be known and well-defined in an open set $U \subseteq \mathbb{R}^n$ containing all $x_{i,0}$, $i = 1,\ldots,N$.

Picking now a target system represented by a controllable pair $(A,\ B)$ where

$$A = \bar{A}_c + \bar{B}_c A_m, \tag{6.199a}$$

$$B = \bar{B}_c B_m, \tag{6.199b}$$

with $(\bar{A}_c,\ \bar{B}_c)$ denoting the Brunovsky form associated with controllability indices $\mu_1 = \kappa_1,\ldots,\mu_m = \kappa_m$ and $A_m \in \mathbb{R}^{m\times n}$, $B_m \in \mathbb{R}^{m\times m}$ then, the i-th model-matching feedback control law can be constructed as

$$u_i = -\mathbf{S}_i^{-1}(x_i)\mathbf{q}_i(x_i) + \mathbf{S}_i^{-1}(x_i)A_m T_i(x_i) + \mathbf{S}_i^{-1}(x_i)B_m\hat{v}_i, \tag{6.200}$$

where $\hat{v}_i \in \mathbb{R}^m$, and $T_i(x_i)$ denotes a change of coordinates: $z_i = T_i(x_i)$.

Since the Brunovsky form $(\bar{A}_c,\ \bar{B}_c)$ associated with a particular set of controllability indices is unique, it follows that the canonical form of target pair $(A,\ B)$ with known controllability indices can precisely be identified by matrices A_m, B_m shown in (6.199). This becomes pronounced by viewing matrices A_m, B_m appearing in model-matching feedback control u_i as constructed in (6.200).

Setting matrix $B_m = I_m$ for simplicity, a systematic procedure for choosing target matrix A_m is suggested next. In particular, our objective is to identify matrix A_m such that a specific measure of joint model-matching control effort, expressed as a function of $\hat{u}_1,\ldots,\hat{u}_N$, is minimized. Let the model-matching part of control u_i, namely, $u_i - \mathbf{S}_i^{-1}(x_i)B_m\hat{v}_i$, be denoted as $\hat{u}_i$. Clearly, control law

$$\hat{u}_i = -\mathbf{S}_i^{-1}(x_i)\mathbf{q}_i(x_i) + \mathbf{S}_i^{-1}(x_i)A_m T_i(x_i),\ i = 1,\ldots,N, \tag{6.201}$$

is nonlinear in x_i and affine in A_m. Then, for the i-th system, we consider a measure of local model-matching energy loss expressed as

$$\|\hat{u}_i\|^2 = \| - \mathbf{S}_i^{-1}(x_i)\mathbf{q}_i(x_i) + \mathbf{S}_i^{-1}(x_i)A_m T_i(x_i)\|^2, \tag{6.202}$$

which can equivalently be written as

$$\|\hat{u}_i\|^2 = \|(T_i'(x_i) \otimes \mathbf{S}_i^{-1}(x_i))\mathrm{vec}(A_m) - \mathbf{S}_i^{-1}(x_i)\mathbf{q}_i(x_i)\|^2, \tag{6.203}$$

where we have used the identity:

$$\mathbf{S}_i^{-1}(x_i)A_m T_i(x_i) = (T_i'(x_i) \otimes \mathbf{S}_i^{-1}(x_i))\mathrm{vec}(A_m), \tag{6.204}$$

$\mathrm{vec}(\cdot)$ denoting the vectorization operator. Using now the following notation

$$\Psi_i(x_i) = T_i'(x_i) \otimes \mathbf{S}_i^{-1}(x_i), \tag{6.205}$$

$$\underline{a}_m = \mathrm{vec}(A_m), \tag{6.206}$$

$$\sigma_i(x_i) = -\mathbf{S}_i^{-1}(x_i)\mathbf{q}_i(x_i), \tag{6.207}$$

we may write

$$\|\hat{u}_i\|^2 = (\Psi_i(x_i)\underline{a}_m - \sigma_i(x_i))'(\Psi_i(x_i)\underline{a}_m - \sigma_i(x_i)), \tag{6.208}$$

or

$$\|\hat{u}_i\|^2 = \underline{a}_m'\Psi_i'(x_i)\Psi_i(x_i)\underline{a}_m - 2\sigma_i'(x_i)\Psi_i(x_i)\underline{a}_m + \sigma_i'(x_i)\sigma_i(x_i), \tag{6.209}$$

for $i = 1,\ldots,N$. In order to define a local model-matching cost function dependent explicitly on vector $\underline{a}_m = \mathrm{vec}(A_m)$, we proceed with the following simplification as suggested in the single-input case earlier. Let $f_{x_i}(x_{i,1},\ldots,,x_{i,n})$ denote the joint probability density function of (random) variables $x_{i,1},\ldots,x_{i,n}$ corresponding to states of the i-th system. We highlight here that this technical manipulation of state vectors x_i, $i = 1,\ldots,N$, only aims to forestall the dependence of function $\|\hat{u}_i\|^2$ on state variables. Specifically, function $f_{x_i}(x_{i,1},\ldots,,x_{i,n})$ can be considered as a weight function utilized to emphasize/de-emphasize a particular range of variables $x_{i,1},\ldots,x_{i,n}$. Note that f_{x_i} can be designed without any knowledge of statistics of variables $(x_{i,1},\ldots,x_{i,n})$. In this setting, quantity $\|\hat{u}_i\|^2$ is a random variable whose expected

value can be seen as a local model-matching cost function evaluated as

$$\mathbb{E}\|\hat{u}_i\|^2 = -\int_{-\infty}^{\infty}\cdots\int_{-\infty}^{\infty}\Big(\underline{a}_m'\Psi_i'(x_i)\Psi_i(x_i)\underline{a}_m - 2\sigma_i'(x_i)\Psi_i(x_i)\underline{a}_m + \sigma_i'(x_i)\sigma_i(x_i)\Big)f_{x_i}(x_{i,1},\ldots,x_{i,n})\,\mathrm{d}x_{i,1}\cdots\mathrm{d}x_{i,n}, \quad (6.210)$$

for $i = 1,\ldots,N$. Defining now

$$G_i = \int_{-\infty}^{\infty}\cdots\int_{-\infty}^{\infty}\Psi_i'(x_i)\Psi_i(x_i)f_{x_i}(x_{i,1},\ldots,x_{i,n})\,\mathrm{d}x_{i,1}\cdots\mathrm{d}x_{i,n}, \quad (6.211)$$

$$\beta_i = \int_{-\infty}^{\infty}\cdots\int_{-\infty}^{\infty}\sigma_i'(x_i)\Psi_i(x_i)f_{x_i}(x_{i,1},\ldots,x_{i,n})\,\mathrm{d}x_{i,1}\cdots\mathrm{d}x_{i,n}, \quad (6.212)$$

and

$$\gamma_i = \int_{-\infty}^{\infty}\cdots\int_{-\infty}^{\infty}\sigma_i'\sigma_i(x_i)f_{x_i}(x_{i,1},\ldots,x_{i,n})\,\mathrm{d}x_{i,1}\cdots\mathrm{d}x_{i,n}, \quad (6.213)$$

a local model-matching control effort can be expressed as

$$J_i(\underline{a}_m) = \underline{a}_m'G_i\underline{a}_m - 2\beta_i\underline{a}_m + \gamma_i, \quad (6.214)$$

for $i = 1,\ldots,N$, which clearly is a quadratic function of $\underline{a}_m$. Two performance indexes representing specific measures of joint model-matching control effort are suggested next.

6.4.4.1 Minimum worst-case control

We express the joint worst-case model-matching control action by the maximum function:

$$\phi(\underline{a}_m) = \max_{i=[1:N]} J_i, \text{ with } J_i = \mathbb{E}\|\hat{u}_i\|^2, \quad (6.215)$$

and we wish to find vector $\underline{a}_m \in \mathbb{R}^{nm}$ for which $\phi(\underline{a}_m)$ attains its minimum. This is a discrete minimax problem formulated as

$$\min_{\underline{a}_m\in\mathbb{R}^{nm}}\phi(\underline{a}_m) = \min_{\underline{a}_m\in\mathbb{R}^{nm}}\max_{i\in[1:N]}\mathbb{E}\|\hat{u}_i\|^2. \quad (6.216)$$

The maximum function $\phi(\underline{a}_m)$ is continuous and convex by the continuity and convexity of J_i, $i = 1,\ldots,N$, and its sub-level sets are bounded. Thus, a minimizing solution $\underline{a}_m^*$ exists and

is unique. The ε-steepest decent algorithm presented in Chapter 5 can be employed here to approximate the optimal solution $\underline{a}_m^*$. The corresponding model-matching feedback control u_i is constructed by substituting $A_m^* = \text{vec}^{-1}(\underline{a}_m^*)$ into (6.200).

6.4.4.2 Least-squares control

Summing up J_i in (6.214) for $i = 1, \ldots, N$, a joint model-matching control effort is defined as

$$J(\underline{a}_m) = \sum_{i=1}^{N} J_i(\underline{a}_m), \tag{6.217}$$

which is a quadratic function in vector $\underline{a}_m$. Here, we are interested in finding vector $\underline{a}_m$ for which J in (6.217) attains its minimum. This can simply be achieved by requiring

$$\frac{\partial J}{\partial \underline{a}_m} = 0. \tag{6.218}$$

Then, the least-squares solution yields

$$\underline{a}_m^* = -G^{-1}\beta', \tag{6.219}$$

where

$$G = \sum_{i=1}^{N} G_i, \tag{6.220}$$

and

$$\beta = \sum_{i=1}^{N} \beta_i, \tag{6.221}$$

with G_i, β_i as defined in (6.211), (6.212), respectively. Substituting $A_m^* = \text{vec}^{-1}(\underline{a}_m^*)$ into (6.200) yields model-matching feedback laws u_i, $i = 1, \ldots, N$.

Having concluded the model-matching control design of multi-input nonlinear systems, attention is now focused on the familiar stabilization problem of networks composed of heterogeneous nonlinear agents. This is the topic of the next section.

6.5 Regulation problem of networks formed of heterogeneous nonlinear agents

In this section, the model-matching technique suggested earlier along with results on distributed LQR-based feedback control design presented in previous chapters are combined

into a control strategy for tackling regulation problems over networks of nonlinear systems that are feedback linearizable. We recall that this multiple-stage-control approach was also considered in Chapter 5 for stabilizing networks of linear agents. It can also be adopted here, essentially due to the highly useful feedback linearization technique for solving model-matching problems of multiple heterogeneous nonlinear systems. We emphasize that the aforementioned advantage of the feedback linearization method, as shown in the multi-input case, was mainly the results of the following two conjectures: 1) systems are described by differential equations linear in control, and 2) systems have identical sets of controllability indices as defined in Procedure 6.3.1. These simplifying assumptions are also in force in the present section. The regulation problem is formulated next.

We consider a set of N non-identical feedback linearizable systems whose dynamics are described by nonlinear differential equations of the form:

$$\dot{x}_i = \mathbf{f}_i(x_i) + \sum_{j=1}^{m} u_{i,j}\mathbf{g}_{i,j}(x_i),\ x_i(0) = x_{i,0},\ i = 1,\ldots,N, \tag{6.222}$$

where $x_i \in \mathbb{R}^n$, $u_i \in \mathbb{R}^m$, and $\mathbf{f}_i, \mathbf{g}_{i,1}, \ldots, \mathbf{g}_{i,m} \in V(X_i)$, with X_i denoting an open set of R^n. In the sequel, $u_i = \begin{bmatrix} u_{i,1} & \cdots & u_{i,m} \end{bmatrix}'$ denotes the input vector of i-th system. It is also assumed that $\mathbf{f}_i(\mathbf{0}) = \mathbf{0}$, $i = 1,\ldots,N$, which implies that the origin $\mathbf{0}$ is an equilibrium point in the sense that i-th system starting from $x_i(0) = \mathbf{0}$ remains in this state if no input is applied. In the sequel, we also require the following be in force:

Assumption 6.5.1. *Initial conditions $x_i(0) = x_{i,0}$ in* (6.222) *are sufficiently close to the origin $\forall i$.*

Assumption 6.5.2. *Systems in* (6.222) *satisfy conditions of Theorem 6.3.4.*

Assumption 6.5.3. *Systems in* (6.222) *have identical sets of controllability indices denoted as $\kappa_1, \ldots, \kappa_m$.*

Assumption 6.5.4. *For each $i = 1,\ldots,N$ in* (6.222)*, there exist smooth functions $\boldsymbol{q}_i : X_i \to \mathbb{R}^n$, $\boldsymbol{S}_i : X_i \to \mathbb{R}^{m\times m}$, with $\boldsymbol{q}_i(\boldsymbol{0}) = \boldsymbol{0}$ and $\det \boldsymbol{S}_i(\boldsymbol{0}) \neq 0$, such that a local diffeomorphism $z_i = T_i(x_i)$ around $\boldsymbol{0}$, with $T_i(\boldsymbol{0}) = \boldsymbol{0}$, is related to*

$$v_i = q_i(x_i) + S_i(x_i)u_i \tag{6.223}$$

by

$$\dot{z}_i = \bar{A}_c z_i + \bar{B}_c v_i, \tag{6.224}$$

where pair $(\bar{A}_c,\ \bar{B}_c)$ is in Brunovsky canonical form associated with controllability indices $\kappa_1, \ldots, \kappa_m$.

We also introduce the following familiar notation. Let $\hat{x} \in \mathbb{R}^{Nn}$, $\hat{z} \in \mathbb{R}^{Nn}$ and $\hat{u} \in \mathbb{R}^{Nm}$, $\hat{v} \in \mathbb{R}^{Nm}$ be vectors which collect states and inputs of the N systems. Then,

$$\dot{\hat{x}} = \mathrm{Col}(\mathbf{f}_1, \ldots, \mathbf{f}_N) + \mathrm{diag}(\mathbf{g}_1, \ldots, \mathbf{g}_N)\hat{u},\ \hat{x}(0) = \hat{x}_0, \tag{6.225}$$

where $\mathbf{g}_i = \begin{bmatrix} \mathbf{g}_{i,1} & \cdots & \mathbf{g}_{i,m} \end{bmatrix}$, $i = 1, \ldots, N$, $\hat{x}_0 = \begin{bmatrix} \hat{x}_{1,0} & \cdots & \hat{x}_{N,0} \end{bmatrix}$, and

$$\dot{\hat{z}} = \hat{A}_c \hat{z} + \hat{B}_c \hat{v}, \tag{6.226}$$

where

$$\hat{A}_c = I_N \otimes \bar{A}_c, \tag{6.227}$$

$$\hat{B}_c = I_N \otimes \bar{B}_c. \tag{6.228}$$

Let now the i-th system in (6.222) be associated with the i-th node of a graph $\mathscr{G} = (\mathscr{V}, \mathscr{E})$ on N vertices. For simplicity, we presently assume that $\mathscr{G}$ denotes an undirected graph. Let also $\mathscr{L}$ be the Laplacian matrix of $\mathscr{G}$. We use a graph representation in the following manner. If an edge (i, j) with $i, j = 1, \ldots, N$ and $i \neq j$, is present then, 1) system-i has full access to the states of system-j and vice versa, and 2) v_i in (6.223) is a feedback control law constructed as a function of local states z_i and neighboring states z_j with $j \in \mathscr{N}_i$. We recall that $\mathscr{N}_i$ denotes the set of all adjacent nodes of vertex i. Before defining the network regulation problem as a distributed optimal control problem, we introduce the following class of structured feedback functions.

Definition 6.5.1. Let $\hat{x} = \begin{bmatrix} x_1' & \cdots & x_N' \end{bmatrix}' \in \mathbb{R}^{Nn}$. Let also $\mathscr{G} = (\mathscr{V}, \mathscr{E})$ and $d_i = \sum_{(i,j) \in \mathscr{E}} 1$. Then,

$$\mathscr{K}^N_{m,n}(\hat{x}, \mathscr{G}) = \{\Xi : \mathbb{R}^{Nn} \to \mathbb{R}^{Nm} \mid \Xi_i = \Xi[(i-1)m+1 : im] = \phi_i(x_i, \ldots, x_j, \ldots), \\ \text{with } (i, j) \in \mathscr{E}, \text{ and } i = 1, \ldots, N\}, \tag{6.229}$$

where $\phi_i : \mathbb{R}^{(d_i+1)n} \to \mathbb{R}^m$ represents a smooth map.

The network regulation problem is now formulated as an optimal control problem as follows:

$$\min_{\hat{u}} J(\hat{u},\hat{x}_0) = \int_0^\infty (\hat{x}'\hat{Q}\hat{x} + \hat{u}'\hat{R}\hat{u})\,\mathrm{dt} \text{ subject to:} \tag{6.230a}$$

$$\dot{\hat{x}} = \mathrm{Col}(\mathbf{f}_1,\ldots,\mathbf{f}_N) + \mathrm{diag}(\mathbf{g}_1,\ldots,\mathbf{g}_N)\hat{u},\ \hat{x}(0) = \hat{x}_0, \tag{6.230b}$$

$$\hat{u}(t) = \hat{K}(\hat{x}(t)) \tag{6.230c}$$

$$\hat{K}(\hat{x}(t)) \in \mathscr{K}_{m,n}^N(\hat{x},\mathscr{G}) \tag{6.230d}$$

$$\hat{Q} = I_N \otimes Q_1 + \mathscr{L} \otimes Q_2,\ \hat{R} = I_N \otimes R \tag{6.230e}$$

where $\hat{Q} = \hat{Q}' \geq 0$ and $\hat{R} = \hat{R}' > 0$. Next, following a model-matching approach combined with the top-down distributed LQR method described in Chapter 3, we present a suboptimal solution to problem (6.230). This results in a distributed feedback controller $\hat{K}(\hat{x}(t))$ with the following two properties:

(i) $\hat{K}(\hat{x}(t)) \in \mathscr{K}_{m,n}^N(\hat{x},\mathscr{G})$.

(ii) If we apply $\hat{u}(t) = \hat{K}(\hat{x}(t))$, then $\hat{\mathbf{0}} = \begin{bmatrix}\mathbf{0}' & \cdots & \mathbf{0}'\end{bmatrix}'$ is an asymptotically stable equilibrium point of (6.230b).

Overall, the distributed control scheme at node level can be depicted as in Fig. 6.1. The control design procedure is summarized in the following theorem.

Theorem 6.5.5. *Consider N nonlinear systems as defined in* (6.222) *and suppose assumptions 6.5.1, 6.5.2, 6.5.3 and 6.5.4 are in force. Consider also LQR problem* (3.65) *with weighting matrices $(Q_1,\ Q_2,\ R)$ for $N_L = d_{\max} + 1$ systems with dynamics represented by the Brunovsky form $(\bar{A}_c,\ \bar{B}_c)$ associated with controllability indices $\kappa_1,\ldots,\kappa_m$. Define also matrices $K_1 = -R^{-1}\bar{B}_c'P$ and $K_2 = R^{-1}\bar{B}_c'\tilde{P}_2$ where P and $\tilde{P}_2$ are associated with ARE* (3.71) *and* (3.72)*, respectively. Letting $M \in \mathbb{R}^{N\times N}$ be a symmetric matrix with the following property:*

$$\lambda_i(M) > \frac{N_L}{2},\ \forall \lambda_i(M) \in S(M)\backslash\{0\}, \tag{6.231}$$

construct feedback controller as

$$\hat{u} = \mathrm{diag}(\boldsymbol{S}_1^{-1},\ldots,\boldsymbol{S}_N^{-1})(I_N \otimes K_1 + M \otimes K_2)\hat{z} - \mathrm{Col}(\boldsymbol{S}_1^{-1}\boldsymbol{q}_1,\ldots,\boldsymbol{S}_N^{-1}\boldsymbol{q}_N), \tag{6.232}$$

where $\hat{z} = \begin{bmatrix} T_1'(x_1) & \cdots & T_N'(x_N) \end{bmatrix}'$, *with* T_i *as defined in Assumption 6.5.4. Then, the point* $\hat{\mathbf{0}} = \begin{bmatrix} \mathbf{0}' & \cdots & \mathbf{0}' \end{bmatrix}'$ *is an asymptotically stable equilibrium of* (6.230b) *for all initial conditions*

$$\hat{x}_0 = \begin{bmatrix} x_{1,0}' & \cdots & x_{N,0}' \end{bmatrix}', \tag{6.233}$$

sufficiently close to $\hat{\mathbf{0}}$.

Proof. Letting

$$\hat{v} = (I_N \otimes K_1 + M \otimes K_2)\hat{z}, \tag{6.234}$$

we may write the feedback control law in (6.232) as

$$\hat{u} = \text{diag}(\mathbf{S}_1^{-1}, \ldots, \mathbf{S}_N^{-1})\hat{v} - \text{Col}(\mathbf{S}_1^{-1}\mathbf{q}_1, \ldots, \mathbf{S}_N^{-1}\mathbf{q}_N), \tag{6.235}$$

which implies that

$$\hat{v} = \text{Col}(\mathbf{g}_1, \ldots, \mathbf{g}_N) + \text{diag}(\mathbf{S}_1, \ldots, \mathbf{S}_N)\hat{u}. \tag{6.236}$$

In view of Assumption 6.5.4, variables $\hat{z}$ and $\hat{v}$ are related by

$$\dot{\hat{z}} = \hat{A}_c\hat{x} + \hat{B}_c\hat{v}. \tag{6.237}$$

Substituting now $\hat{A}_c$ and $\hat{B}_c$ above for $I_N \otimes \bar{A}_c$ and $I_N \otimes \bar{B}_c$, respectively, and using the feedback control law in (6.234) results in the closed-loop system

$$\dot{\hat{z}} = (I_N \otimes (\bar{A}_c + \bar{B}_c K_1) + M \otimes (\bar{B}_c K_2))\hat{z}, \tag{6.238}$$

where the closed-loop matrix

$$A_{cl} = I_N \otimes (\bar{A}_c + \bar{B}_c K_1) + M \otimes (\bar{B}_c K_2), \tag{6.239}$$

is Hurwitz from Theorem 3.3.14. This proves the theorem. □

Some interesting consequences of Theorem 6.5.5 are listed below.

(i) If matrix $M \in \mathscr{K}_{m,n}^N(\mathscr{G})$, then $\hat{u}$ is a distributed nonlinear state-feedback controller.

(ii) Feedback controller $\hat{v}$ in (6.234) can also be design as

$$\hat{v} = (I_N \otimes K_1 + \mathscr{L} \otimes \Phi K_1)\hat{z}, \tag{6.240}$$

where $\mathscr{L}$ denotes the Laplacian matrix of graph $\mathscr{G}$ and design matrix Φ can be found as suggested in the bottom-up method presented in Chapter 3.

(iii) The control design procedure summarized in Theorem 6.5.5 can immediately be adapted to a directed graph setting by altering condition (6.231) and instead requiring matrix M satisfy the following property:

$$\mathbf{Re}(\lambda_i) > \frac{N_L}{2}, \ \forall \ \lambda_i \in S(M)\backslash\{0\}. \tag{6.241}$$

(iv) The result is irrespective of the LQR tuning. Thus, selecting a target model (A, B) by minimizing a specific measure of joint model-matching control effort may be beneficial for effectively controlling network performance by simply tuning the LQR cost function.

(v) If feedback functions $\mathbf{q}_i$ and $\mathbf{S}_i$ as well as smooth diffeomorphism T_i are well-defined $\forall x_i \in \mathbb{R}^n$ for all $i = 1, \ldots, N$, then feedback control $\hat{u} = \hat{K}(\hat{x}(t))$ as defined in (6.232), is a stabilizing distributed controller in the global sense, i.e., the origin is an asymptotically stable equilibrium for all initial conditions $x_{i,0} \in \mathbb{R}^n$.

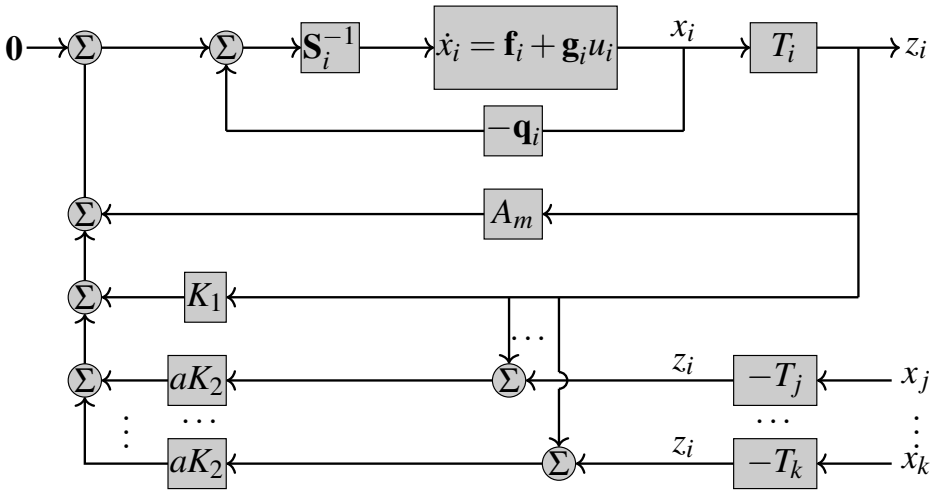

Fig. 6.1 Nonlinear model-matching control with optimal target selection and stabilizing LQR controller with distributed architecture.

The following example attempts to illustrate the effectiveness of the control design method proposed in this section.

6.5.1 Numerical example: stabilization of network of planar two-link robot arms

We consider a directed network of eleven agents modelled as a connected digraph $\mathscr{D}_{11}$ shown in Fig. 6.2. The digraph representation indicates: 1) if an edge (i, j), $i, j = 1, \ldots, 11$, $i \neq j$ is present then j-th agent has full information about the state of i-th agent and 2) the j-th system control law minimizes (among other terms) a weighted norm of the difference $x_i - x_j$. We also denote by $\mathscr{L}_{D,11}$ the in-degree Laplacian matrix of $\mathscr{D}_{11}$. We recall this has been defined in (4.198).

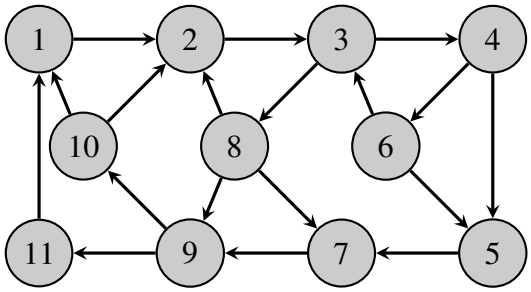

Fig. 6.2 Interconnection scheme of eleven robot arms.

Each node in Fig. 6.2 represents a planar two-link robot arm. The i-th robot is depicted in Fig. 6.3 where $\theta_{i,1}$, $m_{i,1}$, $l_{i,1}$ and $\theta_{i,2}$, $m_{i,2}$, $l_{i,2}$ denote the joint angle, the mass and the length of the first and second link, respectively.

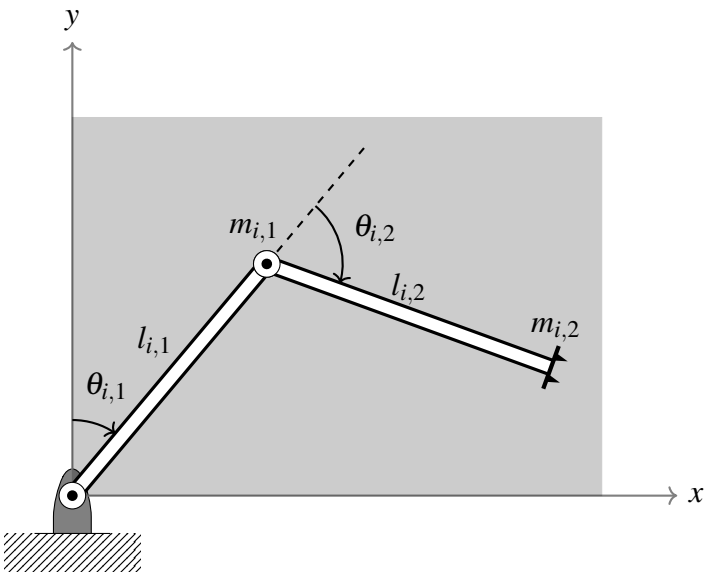

Fig. 6.3 Planar two-link robot arm.

The dynamic model of the i-th robot arm with two degrees of freedom is written as follows [72]:

$$M_i(\theta_i)\ddot{\theta}_i + C_i(\theta_i, \dot{\theta}_i) + G_i(\theta_i) = \tau_i, \tag{6.242}$$

where

$\theta_i = \begin{bmatrix} \theta_{i,1} & \theta_{i,2} \end{bmatrix}'$ is the vector of joint angles,

$\tau_i = \begin{bmatrix} \tau_{i,1} & \tau_{i,2} \end{bmatrix}'$ denotes the vector of applied torques (control input),

$G_i(\theta_i) = \begin{bmatrix} -(m_{i,1}+m_{i,2})gl_{i,1}\sin(\theta_{i,1}) - m_{i,2}gl_{i,2}\sin(\theta_{i,1}+\theta_{i,2}) \\ -m_{i,2}gl_{i,2}\sin(\theta_{i,1}+\theta_{i,2}) \end{bmatrix}$ is the vector of gravitational torques where g denotes gravitational acceleration,

$C_i(\theta_i,\ \dot{\theta}_i) = \begin{bmatrix} -m_{i,2}l_{i,1}l_{i,2}(2\dot{\theta}_{i,1}\dot{\theta}_{i,2} + \dot{\theta}_{i,1}^2)\sin(\theta_{i,2}) \\ -m_{i,2}l_{i,1}l_{i,2}\dot{\theta}_{i,1}\dot{\theta}_{i,2}\sin(\theta_{i,2}) \end{bmatrix}$ denotes the vector of Coriolis and centrifugal forces,

$M(\theta_i) = \begin{bmatrix} D_{i,1} & D_{i,2} \\ D_{i,3} & D_{i,4} \end{bmatrix}$ represents the inertia matrix with

$$D_{i,1} = (m_{i,1}+m_{i,2})l_{i,1}^2 + m_{i,2}l_{i,2}^2 + 2m_{i,2}l_{i,1}l_{i,2}\cos(\theta_{i,2}), \tag{6.243a}$$
$$D_{i,2} = m_{i,2}l_{i,2}^2 + m_{i,2}l_{i,1}l_{i,2}\cos(\theta_{i,2}), \tag{6.243b}$$
$$D_{i,3} = D_{i,2}, \tag{6.243c}$$
$$D_{i,4} = m_{i,2}l_{i,2}^2. \tag{6.243d}$$

Planar coordinates $(x_i,\ y_i)$ of the tip of the i-th robot arm are computed as follows:

$$x_i = l_{i,1}\sin(\theta_{i,1}) + l_{i,2}\sin(\theta_{i,1}+\theta_{i,2}), \tag{6.244a}$$
$$y_i = l_{i,1}\cos(\theta_{i,1}) + l_{i,2}\cos(\theta_{i,1}+\theta_{i,2}). \tag{6.244b}$$

Detailed description of the model can be found in [72]. Length and mass parameters of all robot arms considered in this simulation study, are summarized in Table 6.1.

Choosing the natural set of variables:

$$\xi_i = \begin{bmatrix} \theta_{i,1} & \dot{\theta}_{i,1} & \theta_{i,2} & \dot{\theta}_{i,2} \end{bmatrix}', \tag{6.245}$$

Table 6.1 Length and mass parameters of eleven robot arms.

System	$l_{i,1}$	$l_{i,2}$	$m_{i,1}$	$m_{i,2}$
robot 1	1.50 m	1.00 m	1.10 kg	0.90 kg
robot 2	3.10 m	2.00 m	2.10 kg	1.50 kg
robot 3	0.50 m	1.10 m	1.50 kg	3.20 kg
robot 4	2.00 m	1.30 m	3.10 kg	2.10 kg
robot 5	1.70 m	3.10 m	4.10 kg	2.50 kg
robot 6	2.20 m	4.20 m	5.10 kg	4.20 kg
robot 7	4.10 m	2.50 m	1.20 kg	5.10 kg
robot 8	2.50 m	1.80 m	5.10 kg	2.30 kg
robot 9	1.50 m	3.30 m	1.30 kg	1.20 kg
robot 10	2.70 m	0.80 m	1.40 kg	5.20 kg
robot 11	5.20 m	2.20 m	3.50 kg	2.40 kg

and denoting the i-th input vector as

$$u_i = \begin{bmatrix} u_{i,1} & u_{i,2} \end{bmatrix}' = \begin{bmatrix} \tau_{i,1} & \tau_{i,2} \end{bmatrix}', \tag{6.246}$$

the state-space form of the dynamic model (6.242) is written as:

$$\dot{\xi}_i = \underbrace{\begin{bmatrix} \xi_{i,2} \\ \frac{D_{i,4}}{D_{i,2}^2 - D_{i,1}D_{i,4}}\Phi_i - \frac{D_{i,2}}{D_{i,2}^2 - D_{i,1}D_{i,4}}\Omega_i \\ \xi_{i,4} \\ -\frac{D_{i,2}}{D_{i,2}^2 - D_{i,1}D_{i,4}}\Phi_i + \frac{D_{i,1}}{D_{i,2}^2 - D_{i,1}D_{i,4}}\Omega_i \end{bmatrix}}_{\mathbf{f}_i} + \underbrace{\begin{bmatrix} 0 & 0 \\ \frac{-D_{i,4}}{D_{i,2}^2 - D_{i,1}D_{i,4}} & \frac{D_{i,2}}{D_{i,2}^2 - D_{i,1}D_{i,4}} \\ 0 & 0 \\ \frac{D_{i,2}}{D_{i,2}^2 - D_{i,1}D_{i,4}} & \frac{-D_{i,1}}{D_{i,2}^2 - D_{i,1}D_{i,4}} \end{bmatrix}}_{\mathbf{g}_i} u_i, \ \xi_i(0) = \xi_{i,0}, \tag{6.247}$$

where $D_{i,1}$, $D_{i,2}$ and $D_{i,4}$ are given as in (6.243), and

$$\Phi_i = -m_{i,2}l_{i,1}l_{i,2}(2\xi_{i,2}\xi_{i,4} + \xi_{i,2}^2)\sin(\xi_{i,3}) - (m_{i,1} + m_{i,2})gl_{i,1}\sin(\xi_{i,1}) - m_{i,2}gl_{i,2}\sin(\xi_{i,1} + \xi_{i,3}) \tag{6.248}$$

$$\Omega_i = -m_{i,2}l_{i,1}l_{i,2}\xi_{i,2}\xi_{i,4}\sin(\xi_{i,3}) - m_{i,2}gl_{i,2}\sin(\xi_{i,1} + \xi_{i,3}). \tag{6.249}$$

The control objective is to move the tip of the second link of each robot arm at the highest position which corresponds to planar coordinates $x_i = 0$ and $y_i = l_{i,1} + l_{i,2}$, respectively. Viewing Fig. 6.3, since this position corresponds to zero joint angles $(\theta_{i,1},\ \theta_{i,2})$, we formulate this control task as a regulation problem. A stabilizing distributed controller is designed following a two-step procedure as shown earlier in the chapter. First, we construct a local

model-matching feedback controller mapping the nonlinear dynamics of each robot arm to a linear system (target) and then a distributed stabilizing controller is designed on the target dynamics via a top-down distributed LQR control method. The model-matching task is outlined next.

It is easy to verify that the conditions of Theorem 6.3.4 are satisfied implying that system in (6.247) is feedback linearizable. Note also that the origin is an equilibrium point of (6.247) since $\mathbf{f}_i(\mathbf{0}) = \mathbf{0}$. In the following, we wish to identify smooth functions $\mathbf{q}_i$ and $\mathbf{S}_i$ and a local diffeomorphism T_i well-defined nearby the origin, such that new variables v_i and z_i defined as

$$v_i = \mathbf{q}_i + \mathbf{S}_i u_i, \tag{6.250}$$

$$z_i = T_i, \tag{6.251}$$

are related by

$$\dot{z}_i = \bar{A}_c z_i + \bar{B}_c v_i, \tag{6.252}$$

where pair $(\bar{A}_c,\ \bar{B}_c)$ denotes the Brunovsky canonical form associated with controllability indices $\kappa_1,\ \kappa_2$. These are identified next.

Selecting

$$\mathbf{q}_i = -\begin{bmatrix} D_{i,1} & D_{i,2} \\ D_{i,2} & D_{i,4} \end{bmatrix}^{-1} \begin{bmatrix} \Phi_i \\ \Omega_i \end{bmatrix}, \tag{6.253}$$

$$\mathbf{S}_i = \begin{bmatrix} D_{i,1} & D_{i,2} \\ D_{i,2} & D_{i,4} \end{bmatrix}^{-1}, \tag{6.254}$$

and applying

$$u_i = -\mathbf{S}_i^{-1}\mathbf{q}_i + \mathbf{S}_i^{-1} v_i, \tag{6.255}$$

into (6.247) yields

$$\dot{\xi}_i = \begin{bmatrix} \xi_{i,2} \\ 0 \\ \xi_{i,4} \\ 0 \end{bmatrix} + \begin{bmatrix} 0 & 0 \\ 1 & 0 \\ 0 & 0 \\ 0 & 1 \end{bmatrix} v_i, \tag{6.256}$$

with $v_i \in \mathbb{R}^2$. State-space form (6.256) can be written in standard form as:

$$\dot{\xi}_i = \begin{bmatrix} 0 & 1 & 0 & 0 \\ 0 & 0 & 0 & 0 \\ 0 & 0 & 0 & 1 \\ 0 & 0 & 0 & 0 \end{bmatrix} \begin{bmatrix} \xi_{i,1} \\ \xi_{i,2} \\ \xi_{i,3} \\ \xi_{i,4} \end{bmatrix} + \begin{bmatrix} 0 & 0 \\ 1 & 0 \\ 0 & 0 \\ 0 & 1 \end{bmatrix} v_i, \tag{6.257}$$

which is clearly a linear model. Also, (6.257) is in Brunovsky canonical form associated with controllability indices $\kappa_1 = 2$ and $\kappa_2 = 2$. Interestingly enough, feedback control law u_i in (6.255) immediately maps the nonlinear system (6.247) into the linear model (6.257) without the need of altering coordinates. Thus, in the present instance, local diffeomorphism is the (trivial) linear map $T_i = I_4 \xi_i$. Further, we observe that inertia matrix $M_i(\theta_i)$, defined by functions $D_{i,1}$, $D_{i,2}$, $D_{i,3}$ and $D_{i,4}$ shown in (6.243), is nonsingular and functions $\Phi_i(\xi_i)$, $\Omega_i(\xi_i)$ defined in (6.248), (6.249), respectively, are smooth $\forall \xi_i \in \mathbb{R}^4$. This allows us to guarantee that also feedback functions $\mathbf{q}_i(\xi_i)$ and $\mathbf{S}_i(\xi_i)$ as chosen in (6.253) and (6.254), respectively, are smooth and well-defined $\forall \xi_i \in \mathbb{R}^4$. Thus, we conclude that feedback control law $u_i(\xi_i(t))$ as designed in (6.255) is also well-defined $\forall \xi_i \in \mathbb{R}^4$, i.e., systems in (6.247) are feedback linearizable in the global sense. This highly desirable property appearing in the present study, allows for designing a stabilizing feedback controller v_i in (6.255) $\forall \xi_{i,0} \in \mathbb{R}^4$.

Clearly, feedback law u_i in (6.255) can be seen as a model-matching feedback controller that maps systems' dynamics (6.247) to a linear target model (6.257) represented in the Brunovsky canonical form $(\bar{A}_c,\ \bar{B}_c)$. We are now interested in identifying a new target system with dynamics given by $(\bar{A}_c + \bar{B}_c A_m,\ \bar{B}_c)$. In essence, we wish to compute a matrix $A_m \in \mathbb{R}^{2\times 4}$ such that a measure of the control effort generated by the joint model-matching feedback action is minimimal. For this reason, a further model-matching feedback law is designed as

$$v_i = \mathbf{S}_i^{-1} A_m \xi_i, \tag{6.258}$$

which is substituted in (6.255) yielding

$$u_i = -\mathbf{S}_i^{-1}\mathbf{q}_i + \mathbf{S}_i^{-1} A_m \xi_i. \tag{6.259}$$

To formulate a minimization problem of joint model-matching control effort we proceed with the following conjectures. We consider states $\xi_{i,1}$, $\xi_{i,2}$, $\xi_{i,3}$ and $\xi_{i,4}$ as random variables uniformly distributed in the ranges

$$-\frac{\pi}{2} \leq \xi_{i,1} \leq \frac{\pi}{2},\ -1 \leq \xi_{i,2} \leq 1,\ -\frac{\pi}{2} \leq \xi_{i,3} \leq \frac{\pi}{2},\ -1 \leq \xi_{i,4} \leq 1, \tag{6.260}$$

respectively, and we define the following:

$$\Psi_i = \xi_i' \otimes \mathbf{S}_i^{-1} \tag{6.261}$$

$$\underline{a}_m = \text{vec}(A_m) \tag{6.262}$$

$$\sigma_i = -\mathbf{S}_i^{-1}\mathbf{q}_i. \tag{6.263}$$

Then, a local model-matching control effort is expressed as

$$J_i(\underline{a}_m) = \underline{a}_m' G_i \underline{a}_m - 2\beta_i \underline{a}_m + \gamma_i, \tag{6.264}$$

where G_i, β_i and γ_i above are as defined in (6.211), (6.212) and (6.213), respectively. We evaluate $G = \sum_{i=1}^{11} G_i$ and $\beta = \sum_{i=1}^{11} \beta_i$ and we compute

$$\underline{a}_m^* = -G^{-1}\beta', \tag{6.265}$$

which is the least-squares solution of $\min \sum_{i=1}^{11} J_i(\underline{a}_m)$. Finally, calculating the various integrals in MatLab using symbolic variables, the inverse vectorization operator $\text{vec}^{-1}(\cdot)$, yields $A_m^* = \text{vec}^{-1}(\underline{a}_m^*)$ where

$$A_m^* = \begin{bmatrix} 1.5047 & 0 & 0.0917 & 0 \\ -0.3793 & 0 & 1.0939 & 0 \end{bmatrix}. \tag{6.266}$$

Optimal target system is then defined as $(A,\ \bar{B}_c)$ with

$$A = \bar{A}_c + \bar{B}_c A_m^* = \begin{bmatrix} 0 & 1 & 0 & 0 \\ 51.5047 & 0 & 0.0917 & 0 \\ 0 & 0 & 0 & 1 \\ -0.3793 & 0 & 1.0939 & 0 \end{bmatrix}. \tag{6.267}$$

The i-th system feedback control law u_i is now written as

$$u_i = -\mathbf{S}_i^{-1}\mathbf{q}_i + \mathbf{S}_i^{-1} A_m^* \xi_i + \mathbf{S}_i^{-1}\hat{v}_i. \tag{6.268}$$

Adopting a top-down design procedure, a distributed stabilizing controller $\hat{v}_i$ is designed in the following manner. We solve LQR problem (3.65) with tuning parameters $(Q_1,\ Q_2,\ R)$, for $N_L = 5$ systems with dynamics represented by the target pair $(A,\ \bar{B}_c)$. This choice of N_L systems corresponds to $N_L = d_{\max} + 2$, $d_{\max}$ here denoting the maximum vertex in-degree of

$\mathscr{D}_{11}$. For a particular choice of $(Q_1,\ Q_2,\ R)$ matrices K_1, K_2 are defined as

$$K_1 = -R^{-1}\bar{B}_c' P, \tag{6.269}$$

$$K_2 = R^{-1}\bar{B}_c' \tilde{P}_2, \tag{6.270}$$

where P, $\tilde{P}_2$ are associated with ARE (3.71), (3.72), respectively. Considering the closed-loop matrix

$$A_{cl,11} = I_{11} \otimes A + (I_{11} \otimes \bar{B}_c)(I_{11} \otimes K_1 + M \otimes K_2), \tag{6.271}$$

we wish to select matrix M such that $A_{cl,11}$ above is Hurwitz. Defining $M = \alpha \mathscr{L}_{D,11}$, then, from Theorem 4.3.4, closed-loop matrix $A_{cl,11}$ is guaranteed to be Hurwitz for all $\alpha > 2.5$. Here, we choose $\alpha = 2.6$, which is identical to our decision made in the numerical example studied in Section 5.5 of Chapter 5.

Two different choices of tuning parameters $(Q_1,\ Q_2,\ R)$ are considered in the simulations. The first choice penalizes more heavily the local joint angles $\xi_{i,1}$, $\xi_{i,3}$ than the second and uses $Q_1 = \text{diag}(1,0,1,0)$, $Q_2 = Q_1$, $R = I_2$. Angular velocities are not weighted in this simulation study. In the second choice, LQR cost function is tuned to place more emphasis on the relative state information $(x_i - x_j)$, by selecting $Q_1 = \text{diag}(0.01,0,0.01,0)$, $Q_2 = \text{diag}(100,0,100,0)$, $R = I_2$. Identical initial conditions are considered for both simulation cases.

Simulation results are presented in Fig. 6.4-6.9. Clearly, network stability is maintained for both tuning selections of the LQR performance index. In particular, the proposed distributed control scheme regulates state variables of each subsystem and the control objective of driving each robot arm to a vertical position is achieved. This is illustrated in Fig. 6.6 and Fig. 6.9, where coordinates of the tip of the second link of each robot arm are plotted against time. Note that in these figures, y-coordinate has been normalized by total length $l_{i,1} + l_{i,2}$ so that agents' interactive behavior is depicted clearly.

Network behavior with respect to each LQR tuning decision appears more pronounced in the state-variables graphs. In particular, Fig. 6.7 and Fig. 6.8 demonstrate a simulation scenario in which control action of each robot arm is tuned to penalize heavily weighted norms $\|\theta_{i,1} - \theta_{i,2}\|_{Q_2}$ and $\|\theta_{i,2} - \theta_{j,2}\|_{Q_2}$. This results in a highly coupled distributed control scheme which force robot arms to reach initially an agreement on the joint-angles variables which are subsequently converge to zero. Fig. 6.4 and Fig. 6.5 illustrate a reversed situation where the much loosely coupled distributed control system regulates the angle-variables of each robot arm which then reach an agreement as converging to the origin. We emphasize that this capacity to adjust agents behavior and control performance specifications in networks of non-identical systems highlights a powerful feature of our model-matching control approach.

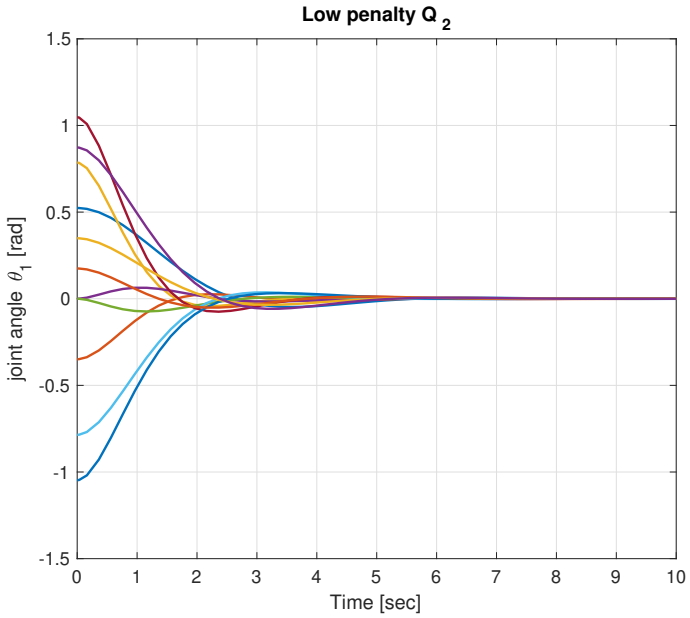

Fig. 6.4 Joint-angle θ_1 response of eleven robot arms under model-matching and top-down control tuned with low penalty Q_2.

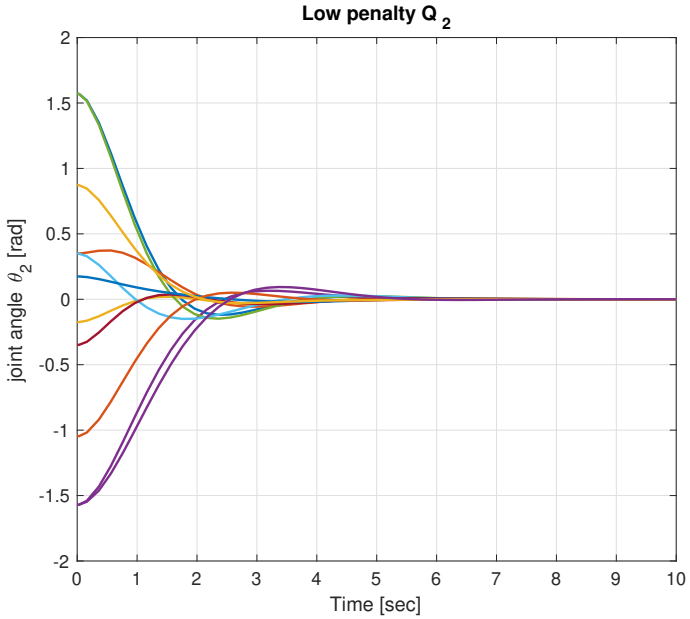

Fig. 6.5 Joint-angle θ_2 response of eleven robot arms under model-matching and top-down control tuned with low penalty Q_2.

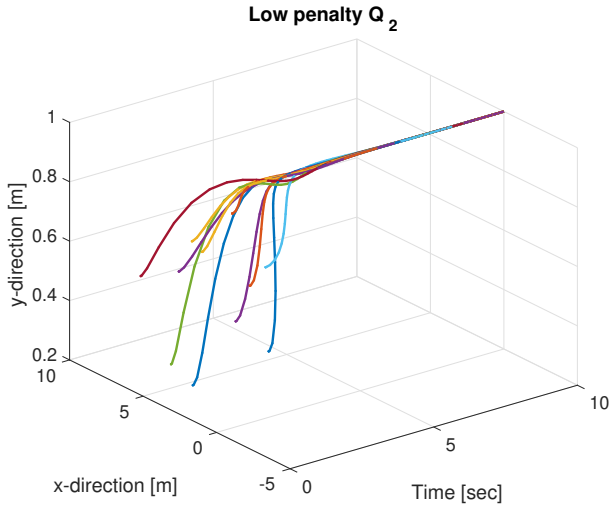

Fig. 6.6 Motion of the tip of eleven robot arms under model-matching and top-down control tuned with low penalty Q_2.

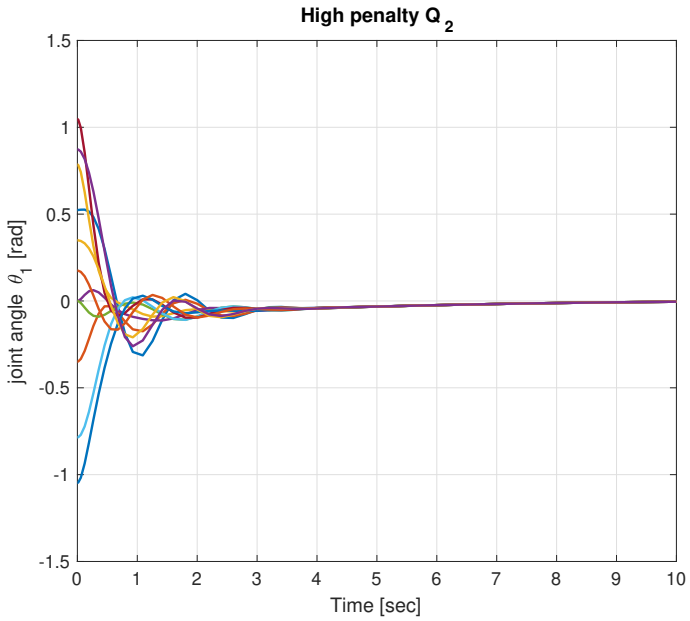

Fig. 6.7 Joint-angle θ_1 response of eleven robot arms under model-matching and top-down control tuned with high penalty Q_2.

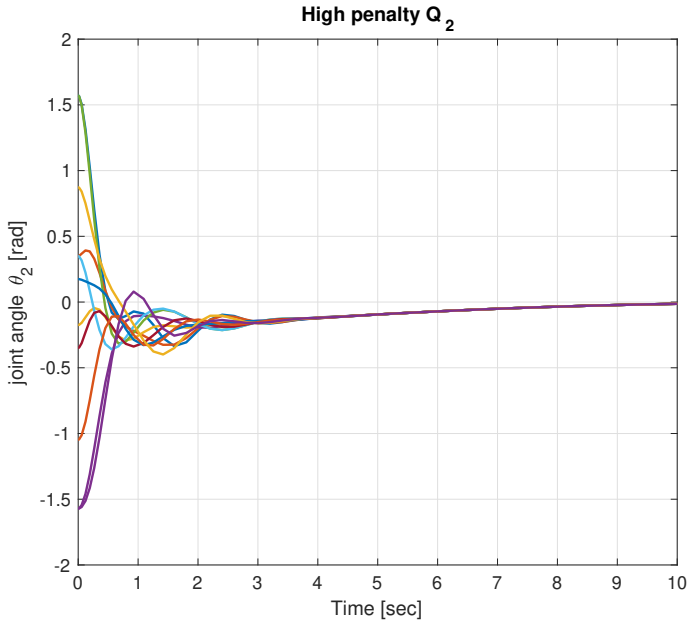

Fig. 6.8 Joint-angle θ_2 response of eleven robot arms under model-matching and top-down control tuned with high penalty Q_2.

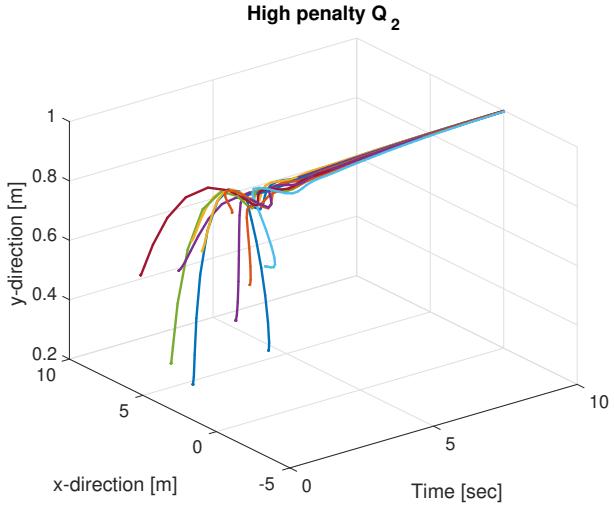

Fig. 6.9 Motion of the tip of eleven robot arms under model-matching and top-down control tuned with high penalty Q_2.

6.6 Conclusion

We have extended the model-matching approach studied in Chapter 5 for linear systems, to a special class of nonlinear systems. In the present setting, the method relies on local nonlinear feedback control and a change of coordinates obtained by solving a feedback linearization task of multiple nonlinear systems. In effect, via feedback control and a coordinate alteration, local dynamics are mapped to a linear model referred to as target system. Since this is identical to all systems, the linearization task here is cast as a model-matching control problem. Similarly to the previous chapter the target system is specified either a priori or obtained by minimizing joint model-matching energy loss. Establishing the notion of controllability indices for nonlinear systems, the proposed model-matching scheme is adapted to a network setup in which heterogeneous nonlinear self-linearizable agents are stabilized by a distributed LQR-based controller designed on target dynamics. Here, the top-down control method is suggested for constructing the distributed scheme. This combined setting leads to a large-scale distributed control scheme which can further be enhanced via an optimal target selection allowing for network performance to be effectively controlled by the LQR tuning parameters. We believe that any distributed state-feedback control design method for dynamically decoupled, identical linear systems can be adopted in this matching approach for regulating networks of multiple heterogeneous nonlinear systems. This represents a highly desirable feature in multi-agent network control and highlights the adaptability of the proposed model-matching control scheme.

Chapter 7

Distributed LQR for coupled LTI systems

In this chapter, we focus on multi-agent networks composed of identical dynamically coupled linear time-invariant systems. We assume that dynamical couplings among agents can be expressed in a state-space form of a certain structure and each system representing an agent can produce actuation signals independently. Effectively, we consider that the topology of physical couplings and the topology of information exchange among agents coincide and are described by the same undirected graph.

We follow a top-down method to approximate a centralized LQR optimal controller by a distributed scheme. Overall network stability is guaranteed via a stability test applied to a convex combination of two Hurwitz matrices. The validity of this condition is consistent with the stability of a class of network topologies which is identified. Sufficient condition for stability of convex combination of Hurwitz matrices can be found in [14]. Our approach builds upon the distributed LQR design proposed in [17] and is motivated by the structure of a large-scale LQR optimal problem.

Our definition of a multi-agent network in the present setting has also been inspired by the structure of a multi-area power system. In the following chapter, to illustrate the applicability of our control algorithm, we address the load frequency control problem of a large-scale power network formed of identical control areas by the distributed LQR-based state-feedback controller proposed in this chapter.

7.1 LQR for dynamically coupled systems

Let

$$\dot{x}_i = A_1 x_i + A_2 \sum_{j=1, j\neq i}^{N_L} (x_i - x_j) + B u_i,\ x_i(0) = x_{i,0},\ i = 1, \ldots, N_L, \tag{7.1}$$

be the state-space forms of N_L dynamically coupled LTI systems representing the individual level dynamics of N_L agents forming a network. Vectors $x_i \in \mathbb{R}^n$, and $u_i \in \mathbb{R}^m$ denote states and inputs of the i-th system, respectively. A complete graph (with all possible edges) $\mathscr{G} = (\mathscr{V}, \mathscr{E})$ with Laplacian matrix $\mathscr{L}_c$ is utilized to model the topology of the physical links between agents. Node $i \in \mathscr{V}$ of $\mathscr{G}$ corresponds to local state x_i while edge $(i, j) \in \mathscr{E}$ is associated with the $x_i - x_j$ term in (7.1). Now construct the aggregate state and input vectors $\tilde{x} \in \mathbb{R}^{nN_L}$, $\tilde{u} \in \mathbb{R}^{mN_L}$, respectively by stacking all state and input vectors, respectively, of all N_L systems taken in ascending order depending on their label in the graph $\mathscr{G}$. The aggregate state-space form of the network becomes

$$\dot{\tilde{x}} = \tilde{A}\tilde{x} + \tilde{B}\tilde{u},\ \tilde{x}(0) = \tilde{x}_0, \tag{7.2}$$

with

$$\tilde{A} = I_{N_L} \otimes A_1 + \mathscr{L}_c \otimes A_2,\ \tilde{B} = I_{N_L} \otimes B. \tag{7.3}$$

Consider now LQR control problem associated with N_L coupled systems:

$$\min_{\tilde{u}}\ J(\tilde{u}, \tilde{x}_0) \text{ s.t. } \dot{\tilde{x}} = \tilde{A}\tilde{x} + \tilde{B}\tilde{u},\ \tilde{x}(0) = \tilde{x}_0, \tag{7.4}$$

where the cost function

$$J(\tilde{u}, \tilde{x}_0) = \int_0^\infty (\tilde{x}'\tilde{Q}\tilde{x} + \tilde{u}'\tilde{R}\tilde{u})\ \mathrm{dt}, \tag{7.5}$$

with

$$\tilde{Q} = I_{N_L} \otimes Q_1 + \mathscr{L}_c \otimes Q_2,\ \tilde{R} = I_{N_L} \otimes R. \tag{7.6}$$

Here the weighting matrices $Q_1 = Q_1' \geq 0$ and $R = R' > 0$ penalize local states and inputs of each node, respectively, while the matrix $Q_2 = Q_2' \geq 0$ is chosen to weigh relative state differences between subsystems. The following stabilizability and observability assumptions guarantee solution to LQR problem (7.4).

Assumption 7.1.1. *Let $C_1'C_1 = Q_1$. The pair $(A_1,\ B)$ is stabilizable and $(A_1,\ C_1)$ is observable.*

Assumption 7.1.2. *Let $C_{12}'C_{12} = Q_1 + N_L Q_2$. The pair $(A_1 + N_L A_2,\ B)$ is stabilizable and $(A_1 + N_L A_2,\ C_{12})$ is observable.*

Under Assumptions 7.1.1 and 7.1.2 problem (7.4) has unique stabilizing solution $\tilde{u} = \tilde{K}\tilde{x}$ which gives an optimum performance index (7.5) equal to $\tilde{x}_0'\tilde{P}\tilde{x}_0$. The optimal state-feedback gain $\tilde{K} = -\tilde{R}^{-1}\tilde{B}'\tilde{P}$ where $\tilde{P}$ is the symmetric positive definite (s.p.d.) solution to the large-scale ARE:

$$\tilde{A}'\tilde{P} + \tilde{P}\tilde{A} - \tilde{P}\tilde{B}\tilde{R}^{-1}\tilde{B}'\tilde{P} + \tilde{Q} = 0. \tag{7.7}$$

Due to special formulation of (7.4), $\tilde{K}$ and $\tilde{P}$ have a specific structure which will prove useful for designing stabilizing distributed controllers in the next section. The special structure of these matrices is proved in Theorem 7.1.3. In the following we set $X = BR^{-1}B'$ for simplicity.

Theorem 7.1.3. *Assume $\tilde{P}$ is the s.p.d solution to* (7.7) *associated with the optimal solution to* (7.4). *Let $\tilde{P} \in \mathbb{R}^{nN_L \times nN_L}$ be decomposed into N_L^2 blocks of dimension $n \times n$, each denoted by $\tilde{P}_{ij}$ and referred to as the (i,j)-block of $\tilde{P}$. Then the following statements hold.*

I. $\sum_{j=1}^{N_L} \tilde{P}_{ij} = P$ *where $P = P' \geq 0$ is the stabilizing solution to the single-node ARE:*

$$A_1'P + PA_1 - PXP + Q_1 = 0. \tag{7.8}$$

II. $\tilde{P}_{ij} = \tilde{P}_{kl} = \tilde{P}_2$ *for all $j \neq i$, $l \neq k$ where $\tilde{P}_2$ is a symmetric matrix associated with the node-level ARE:*

$$\begin{aligned}(A_1 + N_L A_2)'(P - N_L\tilde{P}_2) + (P - N_L\tilde{P}_2)(A_1 + N_L A_2) - (P - N_L\tilde{P}_2)X(P - N_L\tilde{P}_2)\\ + Q_1 + N_L Q_2 = 0.\end{aligned} \tag{7.9}$$

Proof. First we prove part I of the Theorem. The equations corresponding to the diagonal blocks of (7.7) are:

$$\begin{aligned}(A_1 + (N_L-1)A_2)'\tilde{P}_{ii} - A_2'\sum_{\substack{j=1\\ j\neq i}}^{N_L}\tilde{P}_{ij} + \tilde{P}_{ii}(A_1 + (N_L-1)A_2) - \sum_{\substack{j=1\\ j\neq i}}^{N_L}\tilde{P}_{ij}A_2 - \sum_{k=1}^{N_L}\tilde{P}_{ik}X\tilde{P}_{ik}\\ + Q_1 + (N_L-1)Q_2 = 0,\end{aligned} \tag{7.10}$$

for $i = 1, \ldots, N_L$. Note that $\tilde{P}_{ij} = \tilde{P}_{ji}$ due to symmetry of $\tilde{P}$ in (7.7). Now let

$$F_{ii} = \tilde{P}_{ii} + \sum_{\substack{j=1\\ j\neq i}}^{N_L}\tilde{P}_{ij}. \tag{7.11}$$

Substituting (7.11) to (7.10) gives:

$$(N_L-1)(A_2'F_{ii}+F_{ii}A_2)-N_LA_2'\sum_{\substack{j=1\\j\neq i}}^{N_L}\tilde{P}_{ij}-\sum_{\substack{j=1\\j\neq i}}^{N_L}\tilde{P}_{ij}N_LA_2 \tag{7.12a}$$

$$+A_1'(F_{ii}-\sum_{\substack{j=1\\j\neq i}}^{N_L}\tilde{P}_{ij})+(F_{ii}-\sum_{\substack{j=1\\j\neq i}}^{N_L}\tilde{P}_{ij})A_1-\sum_{k=1}^{N_L}\tilde{P}_{ik}X\tilde{P}_{ik}+Q_1+(N_L-1)Q_2=0. \tag{7.12b}$$

Using (7.11) the equations corresponding to the off-diagonal blocks of (7.7) can be written as:

$$(N_L-1)(A_2'\tilde{P}_{ij}+\tilde{P}_{ij}A_2)-A_2'(F_{ii}-\sum_{\substack{k=1\\k\neq i}}^{N_L}\tilde{P}_{ik})-(F_{ii}-\sum_{\substack{k=1\\k\neq i}}^{N_L}\tilde{P}_{ik})A_2-A_2'\sum_{\substack{l=1\\l\neq i\\l\neq j}}^{N_L}\tilde{P}_{il}-\sum_{\substack{l=1\\l\neq i\\l\neq j}}^{N_L}\tilde{P}_{il}A_2 \tag{7.13a}$$

$$+A_1'\tilde{P}_{ij}+\tilde{P}_{ij}A_1-\sum_{k=1}^{N_L}\tilde{P}_{ik}X\tilde{P}_{kj}-Q_2=0. \tag{7.13b}$$

Summing up (7.13a) for all $j\neq i$ block-wise and adding this summation to (7.12a) gives

$$\begin{aligned}&(N_L-1)A_2'F_{ii}+F_{ii}(N_L-1)A_2-(N_L-1)A_2'F_{ii}-F_{ii}(N_L-1)A_2-N_LA_2'\sum_{\substack{j=1\\j\neq i}}^{N_L}\tilde{P}_{ij}\\&-\sum_{\substack{j=1\\j\neq i}}^{N_L}\tilde{P}_{ij}N_LA_2+(N_L-1)A_2'\sum_{\substack{j=1\\j\neq i}}^{N_L}\tilde{P}_{ij}+\sum_{\substack{j=1\\j\neq i}}^{N_L}\tilde{P}_{ij}(N_L-1)A_2+(N_L-1)A_2'\sum_{\substack{k=1\\k\neq i}}^{N_L}\tilde{P}_{ik}\\&+\sum_{\substack{k=1\\k\neq i}}^{N_L}\tilde{P}_{ik}(N_L-1)A_2-(N_L-1)A_2'\sum_{\substack{l=1\\l\neq i\\l\neq j}}^{N_L}\tilde{P}_{il}-\sum_{\substack{l=1\\l\neq i\\l\neq j}}^{N_L}\tilde{P}_{il}(N_L-1)A_2=0,\end{aligned} \tag{7.14}$$

where all the terms associated with A_2 cancel out. By summing up (7.13) over all $j\neq i$ block-wise and adding this summation to (7.12) gives

$$A_1'F_{ii}+F_{ii}A_1-F_{ii}XF_{ii}+\sum_{\substack{k=1\\k\neq i}}^{N_L}\left(\tilde{P}_{ik}X\left(F_{ii}-F_{kk}\right)\right)+Q_1=0. \tag{7.15}$$

Eq. (7.15) has been established in Theorem 7.1.3 of [17]. It is also true here due to (7.14). Adding up (7.15) over all $i = 1, \ldots, N_L$ we get

$$\sum_{i=1}^{N_L} \left(A_1' F_{ii} + F_{ii} A_1 - F_{ii} X F_{ii} + Q_1 \right) = 0, \tag{7.16}$$

which is a sum of N_L identical ARE's, i.e.,

$$N_L (A_1' F_{ii} + F_{ii} A_1 - F_{ii} X F_{ii} + Q_1) = 0. \tag{7.17}$$

Eq. (7.11) implies $F_{ii} = \sum_{i=1}^{N_L} \tilde{P}_{ij}$ which along with (7.17) proves part I.

Since $\tilde{B}$, $\tilde{R}$ are block diagonal and $\tilde{A}$, $\tilde{Q}$ have a repetitive structure, the ARE (7.7) can essentially be decomposed into N_L identical equations. This implies that all $\tilde{P}_{ij}$ with $i, j = 1, \ldots, N_L$ and $j \neq i$ are identically equal. Let $\tilde{P}_2$ be a symmetric matrix representing the off-diagonal blocks $\tilde{P}_{ij}$ of $\tilde{P}$. Setting $P = F_{ii}$ for $i = 1, \ldots, N_L$, and $\tilde{P}_2 = \tilde{P}_{ij}$ for $i, j = 1, \ldots, N_L$ and $j \neq i$, and substituting these matrices into (7.13) gives:

$$\begin{aligned} &(N_L - 1) A_2' \tilde{P}_2 + (N_L - 1) \tilde{P}_2 A_2 - A_2' P - P A_2 + (N_L - 1) A_2' \tilde{P}_2 + (N_L - 1) \tilde{P}_2 A_2 \\ &\quad - (N_L - 2) A_2' \tilde{P}_2 - (N_L - 2) \tilde{P}_2 A_2 + A_1' \tilde{P}_2 + \tilde{P}_2 A_1 - \tilde{P}_2 X (P - (N_L - 1) \tilde{P}_2) \\ &\quad - (P - (N_L - 1) \tilde{P}_2) X \tilde{P}_2 - (N_L - 2) \tilde{P}_2 X \tilde{P}_2 - Q_2 = 0, \end{aligned} \tag{7.18}$$

which after rearranging some terms and multiplying both sides by $-N_L$ becomes:

$$\begin{aligned} &(A_1 + N_L A_2)' (-N_L \tilde{P}_2) + (-N_L \tilde{P}_2)(A_1 + N_L A_2) + N_L A_2' P + P N_L A_2 - (-N_L \tilde{P}_2) X P \\ &\quad - P X (-N_L \tilde{P}_2) - (-N_L \tilde{P}_2) X (-N_L \tilde{P}_2) + N_L Q_2 = 0, \end{aligned} \tag{7.19}$$

or

$$\begin{aligned} &(A_1 + N_L A_2)' (-N_L \tilde{P}_2) + (-N_L \tilde{P}_2)(A_1 + N_L A_2) + N_L A_2' P + P N_L A_2 + P X P \\ &\quad - (P - N_L \tilde{P}_2) X (P - N_L \tilde{P}_2) + N_L Q_2 = 0. \end{aligned} \tag{7.20}$$

Adding now (7.8) to (7.20) results in:

$$\begin{aligned} &(A_1 + N_L A_2)' (-N_L \tilde{P}_2) + (-N_L \tilde{P}_2)(A_1 + N_L A_2) + (A_1 + N_L A_2)' P + P (A_1 + N_L A_2) \\ &\quad - P X P + P X P - (P - N_L \tilde{P}_2) X (P - N_L \tilde{P}_2) + Q_1 + N_L Q_2 = 0, \end{aligned} \tag{7.21}$$

or

$$(A_1+N_LA_2)'(P-N_L\tilde{P}_2)+(P-N_L\tilde{P}_2)(A_1+N_LA_2)-(P-N_L\tilde{P}_2)X(P-N_L\tilde{P}_2) \\ +Q_1+N_LQ_2=0, \quad (7.22)$$

which proves part II. □

By assumption matrices $\tilde{R}$,$\tilde{B}$ are selected block diagonal. Consequently, the state-feedback gain $\tilde{K}=-\tilde{R}^{-1}\tilde{B}'\tilde{P}$ associated with the optimal solution to (7.4) retains the same structure with $\tilde{P}$. This leads to the following Corollary.

Corollary 7.1.1. *Assume $\tilde{K}=-\tilde{R}^{-1}\tilde{B}'\tilde{P}$ is the optimal state-feedback gain obtained from the solution to* (7.4) *which gives minimum performance index $\tilde{x}_0'\tilde{P}\tilde{x}_0$ with $\tilde{P}$ being the s.p.d solution to* (7.7). *Let $\tilde{K}\in\mathbb{R}^{mN_L\times nN_L}$ and $\tilde{P}\in\mathbb{R}^{nN_L\times nN_L}$ be decomposed into N_L^2 blocks of dimension $m\times n$ and $n\times n$ denoted by $\tilde{K}_{ij}$ and $\tilde{P}_{ij}$, respectively each referred to as (i,j)-block of matrix $\tilde{K}$ and $\tilde{P}$, respectively. Then the following are true;*

I. $\tilde{P}=I_{N_L}\otimes P-\mathscr{L}_c\otimes\tilde{P}_2$.

II. $\sum_{j=1}^{N_L}\tilde{K}_{ij}=-R^{-1}B'P$ *for* $i=1,\ldots,N_L$.

III. $\tilde{K}_{ii}=-R^{-1}B'P+(N_L-1)R^{-1}B'\tilde{P}_2$ *for* $i=1,\ldots,N_L$.

IV. $\tilde{K}_{ij}=-R^{-1}B'\tilde{P}_2$ *for* $i,j=1,\ldots,N_L$ *and* $j\neq i$.

V. $\tilde{K}=-I_{N_L}\otimes R^{-1}B'P+\mathscr{L}_c\otimes R^{-1}B'\tilde{P}_2$.

Theorem 7.1.3 states that due to special formulation of the cost function (7.5) and the structure of the aggregate state-space form (7.2), the large-scale LQR problem (7.4), under Assumptions 7.1.1 and 7.1.2, can effectively be reduced to two simpler (low-dimensional) LQR problems associated with node-level ARE's. This feature may be highly beneficial for problems involving graphs with excessively large number of vertices (N_L).

Applying the stabilizing optimal state-feedback control $\tilde{u}=\tilde{K}\tilde{x}$ to (7.2) results in a closed-loop matrix which is Hurwitz and is written as

$$A_{cl}=I_{N_L}\otimes(A_1-XP)+\mathscr{L}_c\otimes(A_2+X\tilde{P}_2). \quad (7.23)$$

Due to Proposition 3.3.2 the spectrum of A_{cl} can be decomposed into:

$$S(A_{cl})=\bigcup_{i=1}^{N_L}S\big(A_1-XP+\lambda_{c,i}(A_2+X\tilde{P}_2)\big) \quad (7.24)$$

where $\lambda_{c,i} \in \{0, N_L, \ldots, N_L\}$.

Remark 7.1.4. Matrix $A_1 - XP + \alpha N_L(A_2 + X\tilde{P}_2)$ is Hurwitz for $\alpha = 0$ and $\alpha = 1$.

In the sequel we require that:

Condition 7.1.5. *Matrix* $A_1 - XP + \alpha N_L(A_2 + X\tilde{P}_2)$ *is Hurwitz for all* $\alpha \in [0,1]$.

Condition 7.1.5 states that all convex combinations of two Hurwitz matrices

$$\mu\bar{A}_1 + (1-\mu)\bar{A}_2 \text{ with } \mu \in [0,1], \tag{7.25}$$

are Hurwitz, where $\bar{A}_1 = A_1 - XP + N_L(A_2 + X\tilde{P}_2)$ and $\bar{A}_2 = A_1 - XP$. Sufficient conditions for Hurwitz stability of convex combination of Hurwitz matrices can be found in Theorem 2.2 in [14]. In essence, Condition 7.1.5 characterizes a class of LQR problems (7.4) which admit of solutions for which the Condition 7.1.5 holds. This will be used later for the design of distributed stabilizing controllers. For a given selection of weighting matrices $(Q_1,\ Q_2,\ R)$ of the LQR problem (7.4), the validity of Condition 7.1.5 can be verified by searching for a symmetric positive definite matrix $\bar{P}$ for which the following LMI

$$\begin{bmatrix} -(\bar{A}_1'\bar{P} + \bar{P}\bar{A}_1) & 0_{n\times n} & 0_{n\times n} \\ 0_{n\times n} & -(\bar{A}_2'\bar{P} + \bar{P}\bar{A}_2) & 0_{n\times n} \\ 0_{n\times n} & 0_{n\times n} & \bar{P} \end{bmatrix} > 0, \tag{7.26}$$

is feasible. Obviously if matrix $\bar{P}$ exists then premultiplying and postmultiplying (7.26) by $[\sqrt{\mu}I_n\ \sqrt{1-\mu}I_n\ 0_{n\times n}]$ and $[\sqrt{\mu}I_n\ \sqrt{1-\mu}I_n\ 0_{n\times n}]'$, respectively, for $\mu \in [0,1]$ leads to Lyapunov inequality

$$(\mu\bar{A}_1 + (1-\mu)\bar{A}_2)'\bar{P} + \bar{P}(\mu\bar{A}_1 + (1-\mu)\bar{A}_2) < 0, \tag{7.27}$$

which admits of a solution $\bar{P} = \bar{P}' > 0$. This demonstrates that $\mu\bar{A}_1 + (1-\mu)\bar{A}_2$ is a Hurwitz matrix for all $\mu \in [0,1]$. Alternatively, the stability of $\mu\bar{A}_1 + (1-\mu)\bar{A}_2$ can be examined via a simple graphical test by plotting the eigenvalue with the maximum real part of the matrix $\mu\bar{A}_1 + (1-\mu)\bar{A}_2$ for $\mu \in [0,1]$.

7.2 Distributed LQR design for dynamically coupled systems

Let a sparse network be formed of N identical dynamically coupled LTI systems. We note here that the index N differs from index N_L utilized earlier for complete-graph topologies.

In the sequel, we use index N pertaining to schemes with sparse structure. Let now the couplings between systems be modelled by a graph $\mathscr{G}_N = (\mathscr{V}, \mathscr{E})$ with Laplacian matrix $\mathscr{L}_N$. The neighborhood of the i-th system is denoted by $\mathscr{N}_i \subset \mathscr{V}$ and comprises all $j \in \mathscr{V}$ with $j \neq i$ for which $(i, j) \in \mathscr{E}$. Let

$$\dot{x}_i = A_1 x_i + A_2 \sum_{j \in \mathscr{N}_i} (x_i - x_j) + B u_i,\ x_i(0) = x_{i,0},\ i = 1, \ldots, N, \tag{7.28}$$

be the dynamics of all systems as described at local level. Vectors $x_i \in \mathbb{R}^n$, $u_i \in \mathbb{R}^m$ denote local state and input variables. Consider now the aggregate state-space form of the network written as

$$\dot{\hat{x}} = \hat{A}\hat{x} + \hat{B}\hat{u},\ \hat{x}(0) = \hat{x}_0, \tag{7.29}$$

where $\hat{x} \in \mathbb{R}^{nN}$, $\hat{u} \in \mathbb{R}^{mN}$ and

$$\hat{A} = I_N \otimes A_1 + \mathscr{L}_N \otimes A_2,\ \hat{B} = I_N \otimes B. \tag{7.30}$$

Note that the Laplacian matrix $\mathscr{L}_N$ in (7.30) does not necessarily correspond to a complete graph in contrast to (7.3) and generically matrix $\tilde{A}$ in (7.30) is sparse. A stabilizing distributed controller for (7.29) is constructed in the following Theorem. For convenience we set $X = BR^{-1}B'$.

Theorem 7.2.1. *Consider a network of N coupled systems with dynamics described in* (7.28)*, and let $\mathscr{G}_N$ be an undirected graph of N vertices with a Laplacian matrix $\mathscr{L}_N$. Let also λ_N be the maximum eigenvalue of $\mathscr{L}_N$, and denote by $d_{\max} = \lceil \lambda_N \rceil$ the smallest integer which is greater than or equal to λ_N. Consider LQR problem* (7.4) *for $N_L = d_{\max}$, define P and $\tilde{P}_2$ via* (7.8) *and* (7.7)*, respectively, and assume Condition 7.1.5 is true. Define also the distributed state-feedback gain:*

$$\hat{K} = -I_N \otimes R^{-1}B'P + \mathscr{L}_N \otimes R^{-1}B'\tilde{P}_2. \tag{7.31}$$

Then, the closed-loop matrix

$$A_{cl} = I_N \otimes (A_1 - XP) + \mathscr{L}_N \otimes (A_2 + X\tilde{P}_2) \tag{7.32}$$

is Hurwitz.

Proof. Consider the spectrum $S(A_{cl}) = S(I_N \otimes (A_1 - XP) + \mathscr{L}_N \otimes (A_2 + X\tilde{P}_2))$. Let $V_N \otimes I_n$ be state-space transformation where $V_N \in \mathbb{R}^{N \times N}$ is an orthogonal matrix whose columns consist of the eigenvectors of $\mathscr{L}_N$. In the transformed coordinates, $\bar{A}_{cl} = I_N \otimes (A_1 - XP) +$

$\Lambda_N \otimes (A_2 + X\tilde{P}_2)$ where $\Lambda_N = \text{diag}(0, \lambda_2, \ldots, \lambda_N)$ with $\lambda_N \leq d_{\max}$. The spectrum of $\bar{A}_{cl}$ is

$$S(\bar{A}_{cl}) = \bigcup_{i=1}^{N} (A_1 - XP + \lambda_i (A_2 + X\tilde{P}_2)), \tag{7.33}$$

where λ_i, $i = 1, \ldots, N$ are the eigenvalues of $\mathscr{L}_N$. Condition 7.1.5 holds, hence $(A_1 - XP) + \alpha d_{\max}(A_2 + X\tilde{P}_2)$ is Hurwitz for all $\alpha \in [0,1]$. Consequently $\bar{A}_{cl}$ is also Hurwitz since $\lambda_i \in [0, d_{\max}]$ for all $i = 1, \ldots, N$. This proves the theorem. □

Remark 7.2.2. For a time-varying graph $\mathscr{G}(t) = (\mathscr{V}, \mathscr{E}(t))$ with fixed number of vertices N and time-varying edges the maximum eigenvalue of the time-varying Laplacian matrix $\mathscr{L}(t)$ is bounded by $2N$. Consequently, solving problem (7.4) for $N_L = 2N$ and assuming Condition 7.1.5 holds, leads to a distributed controller $\hat{K}$ that stabilizes the network for all possible couplings among the N systems. Naturally, this does not imply stability of switching between stable network interconnections.

7.3 Conclusion

A distributed LQR-based controller for stabilizing networks of identical dynamically coupled agents is proposed based on a large-scale LQR optimal control problem. The proposed method considers that dynamical couplings between interconnected systems are expressed in a state-space form of a certain structure, while builds upon and extends the results on distributed LQR control of dynamically decoupled systems proposed in [17]. The control scheme is obtained by optimizing an LQR performance index with a tuning parameter utilized to emphasize/de-emphasize relative state difference between interconnected systems. The proposed approach enhances the multi-agent system modularity and leads to a simple and verifiable stabilizability condition that is valid for a class of network topologies.

Chapter 8

Distributed LQR-based load frequency control of multi-area power networks

8.1 Introduction

Power systems are important in engineering, and their stable and continuous operation is inherently connected to social welfare and economic prosperity. Power system networks can be characterized as large-scale complex systems which encompass a broad array of subsystems and tasks. This intrinsic complexity is constantly evolving and growing in alignment with state-of-the-art technologies, facilitating a more efficient power generation, transmission, and distribution. Recently, the increasing penetration of sustainable energy sources into the energy map and the digitalization of power control systems have resulted in sophisticated concepts, such as intelligent power networks and smart grids. The stochasticity and intermittency of renewable energy sources, along with the decentralization of power generation and the integration of vulnerable communication layers across the physical structure of the power network, are just a few of the vital reasons that render the control of the modern power systems highly challenging.

In this chapter, we consider power system networks formed of distinct control areas which are interconnected via weak transmission lines referred to as tie-lines. Each area maintains a single nominal frequency across its geographical region and comprises either a single or a group of generators. In order for an area composed of multiple generators to maintain its nominal frequency under load variations, a local load frequency controller is used, distributed to the corresponding turbine-governing systems of each generating unit. The design of load frequency control (LFC) is based on a single-plant model which represents the sum of generating units [90]. An area is responsible for meeting power demand 1) of

its own consumers, and 2) of certain adjacent areas with which is interconnected through tie-lines exchanging power normally scheduled for a contracted value. However, due to power load differentiation, the frequency of each area, along with the scheduled power exchange between interconnected areas, may vary from their nominal value.

The rate of change of frequency (RoCoF) is related to the power system inertia and the active power mismatch. The relationship between inertia of a distinct area, RoCoF, and change in active power can be found in [106, 208]. Virtually, synchronous machines have been the main source of system inertia, with the area frequency being directly coupled to the rotational speed of the aggregated synchronous generators [157, 106]. Traditionally, the prime mover of conventional thermal power stations and hydroelectric plants, along with the synchronous generators (typically of large inertia), act as smoothing (low-pass) filters on variations of electric loads and participate primarily in the frequency regulation of the area. In contrast, renewable energy generation units behave differently from conventional synchronous generators, mostly because they are connected through power electronic interfaces. In effect, these devices fully or partly can electrically decouple the generator from the grid [208], hence the coupling between the rotational speed of the generator and the system frequency almost vanishes [131]. For this reason, unlike synchronous generators, inverter-connected generation units do not inherently contribute to the total system inertia [207]. Although control strategies for participation in frequency regulation by inverter-connected sources have been proposed in literature [241, 204, 158], such functions are rarely enabled in reality. Thus, the development of inverter-connected renewable energy sources introduces new challenges in the design of LFC, which is primarily performed by synchronous generating units due to their inherent capability to affect the RoCoF caused by active-power-imbalance events. Here, we focus on the design of distributed LFC schemes for multi-area power systems. In our model, we intentionally consider only synchronous generating units (thermal power stations, hydroelectric power plants) for the reasons outlined above. The violation of steady-state operation caused by active power imbalance is formulated as a feedback disturbance rejection problem of a large scale interconnected system.

LFC is one of the most challenging problems in multi-area power systems. An introduction to power systems design and LFC can be found in textbooks [13, 106, 123], while an overview of control strategies in the field of LFC problems has been discussed in [191, 162]. Comprehensive literature surveys on the topic of LFC for diverse configurations of conventional and future smart power systems can be found in [159, 190, 76, 47]. In typical situations, the geographical expanse and the mere complexity of the system, resulting from dynamical couplings among areas, make centralized control schemes either impossible or undesirable [182, 110, 153]. Hence, decentralized and distributed control is typically needed

to ensure stable network operation. Analytical methods for designing decentralized and distributed LFC strategies have been presented in [4, 2, 15]. Robust decentralized control design methodologies have been proposed in [172], where the authors propose two control schemes for LFC based on robust optimal control techniques and linear matrix inequalities (LMI). A rigorous and computationally efficient method, also based on the versatile formulation of LMI's for robust decentralized control of multi-machine power systems, has been studied in [194].

A systematic methodology based on reachability for identifying the impact of potential cyber attacks in the Automatic Generation Control (AGC) of a two-area power system has been presented in [60]. Set-theoretic methods for LFC design in the context of cyber-physical power systems can be found in [105], while in [54], the authors propose LFC design based on an anti-windup compensator, assuring stability of the closed-loop system even in cases of large load disturbance. Model predictive control has also attracted attention from the power system community in recent years due to its convenience in managing online disturbance rejection problems in the presence of state and input constraints, which is a highly desired feature in a multi-area power system control. Model predictive control with decentralized and distributed architecture for LFC design in interconnected power systems has been proposed in [214, 49, 224, 125, 124].

In this chapter, we formulate the LFC of multi-area power systems as a large-scale optimal control problem in the absence of state and input constraints. An arbitrary number of identical areas is considered. The multi-area power system is represented as a multi-agent network composed of identical dynamically coupled linear time-invariant systems. These dynamical couplings are expressed in a state-space form of a certain structure and represent interconnections between areas through tie-lines. In the present setting, each agent representing an area can produce LFC signals independently and is dynamically coupled with a certain number of its peers referred to as neighboring agents (areas) with whom it can exchange state information. Typically, we assume that the topology of physical couplings (tie-lines) and the topology of information exchange between neighboring agents (areas) coincide and are described by the same graph.

Linear quadratic regulator (LQR) control design has been successfully utilized in frequency regulation problems, mostly due to large stability margins of its stabilizing solution, with the fundamental work of [66] being a benchmark approach to LQR-based LFC of multi-area power systems. Ever since, considerable research has been carried out on this topic; [160, 189, 48, 188] represent some recent work. Over the past few years, there has been a renewal of interest in control of networks composed of a large number of interacting systems. The fundamental work of [17, 46] in this field discusses distributed LQR design

for a set of identical decoupled dynamical systems. There is no documented distributed LQR-based approach to networked systems with dynamical couplings and, consequently, no distributed LQR-based LFC has been reported in literature so far. The research of this chapter motivated by the structure of a multi-area power system with dynamical couplings between interconnected areas, attempts to address this particular gap in literature. The description of our approach is outlined in the following paragraph.

We follow a top-down method to approximate a centralized LQR optimal controller by a distributed control scheme. It is shown that overall network stability is guaranteed via a stability test applied to a convex combination of Hurwitz matrices. The validity of this condition is consistent with the stability of a class of network interconnection structures which is identified. A major assumption of our work is that the dynamical models of each area are identical. Although this assumption may be unrealistic in practice, it simplifies the design problem considerably, which is especially hard due to the coupling terms appearing in the model. Future work will attempt to eliminate or relax this assumption based on results presented in earlier chapters. The simulation study presented in Section 8.4.2 is carried out under considerable perturbations and suggests that this hypothesis is valid and that our results can be extended to the non-identical case with minor modifications.

In this chapter, our interest in distributed LFC arises from the necessity to avoid centralized schemes when these become computationally prohibitive. We wish to tackle the LFC problem of geographically sparse power grids following a distributed control approach, the main advantage of which is that it can replace the conventional centralized controller, which has high communication and processing costs and suffers from a single-point-of-failure drawback [15]. Faults caused by interconnection losses might give rise to an unacceptable frequency deviation and may accelerate a cascading failure event. The proposed distributed LFC controller is stabilizing even if tie-line interconnections and communication links are added to or removed from the overall system, as long as the stability condition given in Section 8.3 (and Section 7.1) is not violated. This powerful feature gives integrity to the control unit of each area and enhances the resilience of the power system as a whole in the presence of interconnection variations. The main contributions of the chapter are listed below.

a. We propose a novel distributed-LQR algorithm for networked systems with dynamical couplings applied to LFC of large-scale multi-area power systems.

b. The control scheme is obtained by optimizing an LQR performance index with a tuning parameter which can be used to emphasize/de-emphasize relative state differences between interconnected areas. In effect, this parameter controls the magnitude of tie-line power exchange and frequency synchronization between interconnected areas.

c. Our approach enhances power system modularity and leads to a simple and verifiable stabilizability condition valid for a class of network topologies. Extensive simulations presented in this work support our conjecture that this stabilization criterion can be extended to more general LFC control network problems.

8.2 Multi-area power system design

Power system networks can be decomposed into multiple distinct dynamical subsystems, referred to as control areas, each area having two primary characteristics; 1) it comprises either a single generator or a group of generators, and 2) it maintains a single frequency across its geographical expanse. The areas are responsible for meeting the demand of their own consumers and are interconnected with each other through transmission lines, referred to as tie-lines, over which they exchange certain amount of power normally scheduled for a contracted value for each tie-line interconnection. In this chapter, we consider a multi-agent representation of power systems where each agent/area has autonomous actuation capacity and is dynamically coupled with certain neighboring agents/areas with which it exchanges state-information. We assume that the topology of the physical links (tie-lines) and the communication scheme coincide. This multi-agent approach to multi-area power systems is illustrated in Fig. 8.1, where physical structure of the network (solid lines) and communication links (dotted lines) are incorporated into one unified entity, representing a modern large-scale power system. The consistency between the structures of the communication network and the physical grid, as shown in Fig. 8.1, facilitates information exchange between control subsystems enabling the development of control schemes with distributed architecture. As mentioned earlier, each distinct area consists of a group of generating units, the aggregate power generation of which should match the demand of the consumers spanned across the geographical expanse covered by the corresponding area. The aggregate generation may comprise thermal power stations, hydroelectric plants, wind turbine farms, photovoltaic and battery storage power stations, and, in general, any type of conventional and renewable energy sources. In this work, to avoid further complications in designing distributed control schemes, the power generation of each area is limited to thermal and hydroelectric power stations.

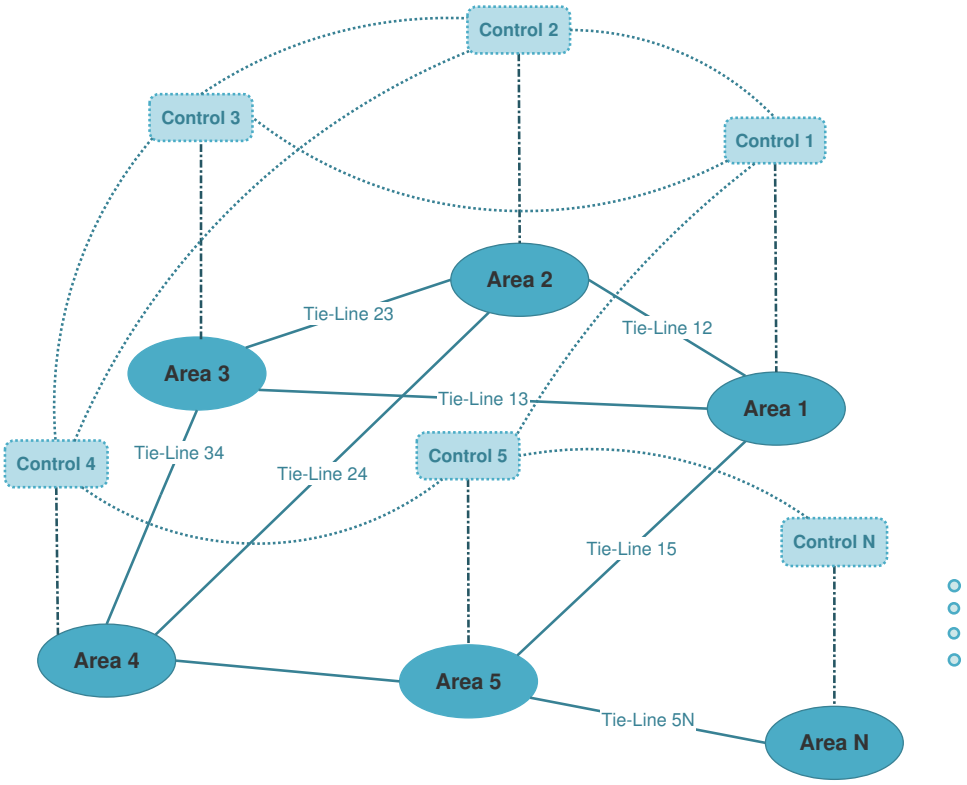

Fig. 8.1 Tie-line interconnections (solid lines) and communication scheme (dotted lines) in large-scale multi-area power system.

8.2.1 Modeling

Let a power system be composed of N areas the topology of which is modeled by an undirected graph $\mathscr{G} = (\mathscr{V}, \mathscr{E})$. Each node $i \in \mathscr{V}$ represents an area and an edge $(i, j) \in \mathscr{E}$ between two nodes denotes interaction between the two nodes/areas. We note that the edge (i, j) of the graph determines coupling terms in the dynamics of area i and j and also indicates information exchange between node i and j. Let also all $j \in \mathscr{V}$ with $j \neq i$ such that $(i, j) \in \mathscr{E}$ be denoted by $\mathscr{N}_i$. In the sequel, all $j \in \mathscr{N}_i$ are referred to as adjacent or neighboring nodes/areas to i. At steady-state operation the power sharing via tie-line interconnection between two areas i and j is denoted by $P_{tie,i,j}$ and is given by:

$$P_{tie,i,j} = \frac{V_i V_j}{X_{ij}} \sin(\delta_i - \delta_j). \tag{8.1}$$

Here, X_{ij} is the reactance of the tie-line which connects the two areas, δ_i, δ_j represent the power angles of equivalent machines of area i and j, respectively, and V_i, V_j are the voltages

at equivalent terminals of area i and j, respectively. A tie-line interconnection in a two-area system is depicted in Fig. 8.2.

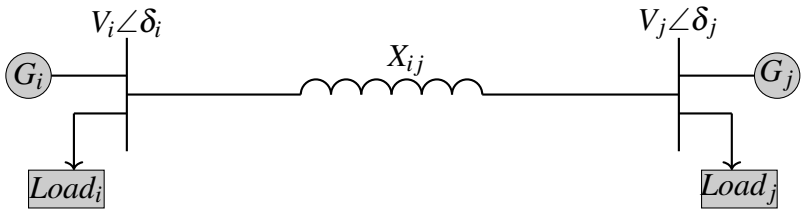

Fig. 8.2 Tie-line interconnection of two-area system.

For small deviations of $(\delta_i,\ \delta_j)$ from equilibrium $(\delta_i^o,\ \delta_j^o)$, the power flow deviation over (i,j)-tie-line from the nominal value is given by the linear equation:

$$\Delta P_{tie,i,j} = T_{ij}(\Delta\delta_i - \Delta\delta_j), \tag{8.2}$$

where the synchronizing torque coefficient $T_{ij} = \frac{|V_i||V_j|}{X_{ij}}\cos(\delta_i^o - \delta_j^o)$, [13]. Notation Δ indicates deviation from steady-state operation conditions. Differentiating (8.2) with respect to time results in:

$$\Delta\dot{P}_{tie,i,j} = K_{tie,i,j}\big(\Delta f_i - \Delta f_j\big), \tag{8.3}$$

where $K_{tie,i,j} = 2\pi T_{ij}$ is referred to as synchronization coefficient between area i and j, while Δf_i and Δf_j represent the frequency deviation of each area from their common nominal value, denoted here by f^o. According to (8.3), the linearized dynamics of the total power inflow to the i-th area from all interconnected areas $j \in \mathcal{N}_i$, is given by:

$$\Delta\dot{P}_{tie,i} = \sum_{j\in\mathcal{N}_i} K_{tie,i,j}(\Delta f_i - \Delta f_j). \tag{8.4}$$

The open-loop linearized dynamics of the i-th interconnected area is represented by a model widely used in literature [13, 106], the block diagram of which is shown in Fig. 8.3.

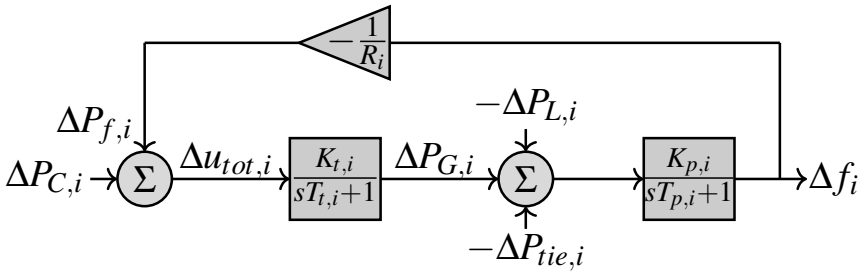

Fig. 8.3 Single block representation of the i-th interconnected area.

The total control signal of the i-th area is the sum of two components: $\Delta u_{tot,i} = \Delta P_{f,i} + \Delta P_{C,i}$, namely the primary frequency control action, defined as $\Delta P_{f,i} = -\frac{1}{R_i}\Delta f_i$ and the AGC signal $\Delta P_{C,i}$ to be designed. The first is a fixed static linear control law performed by the speed governor which is a regulating unit attached on the prime mover. Detailed description of this topic can be found in [106]. The static gain R_i is referred to as speed droop or speed regulation and expresses the ratio of the frequency deviation Δf_i to a change in output generated power by $\Delta P_{G,i}$ assuming the AGC signal $\Delta P_{C,i} = 0$. A typical droop characteristic of a single generator actuated by primary frequency control is shown in Fig. 8.4.

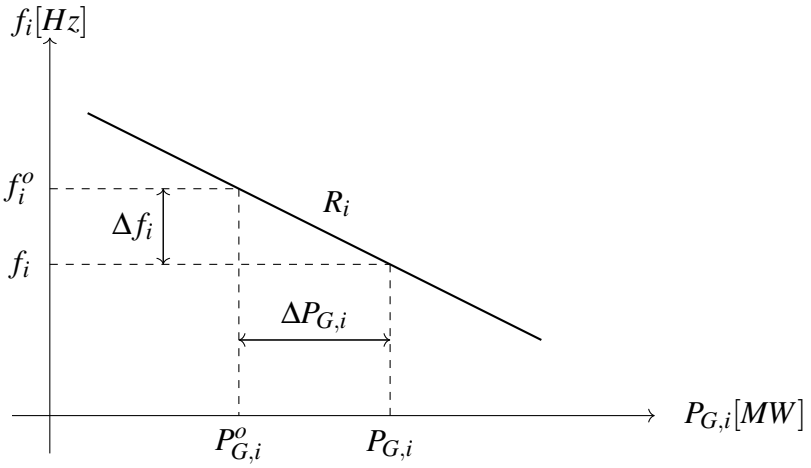

Fig. 8.4 Droop characteristic.

The signal $\Delta u_{tot,i}$ is assumed to be subjected to a component-wise saturation hard constraint of the form:

$$\Delta u_{tot,i,\min} \leq \Delta u_{tot,i} \leq \Delta u_{tot,i,\max}, \tag{8.5}$$

where $\Delta u_{tot,i,\max}$ is taken greater than the maximum expected load deviation $\Delta P_{L,i,\max}$; otherwise, zero frequency deviation error is not guaranteed. Negative values of $\Delta u_{tot,i}$ allow for handling of negative values of $\Delta P_{L,i}$ in case of load reduction. The rate of change of power generation due to the limit of the thermal and mechanical movements in the generating unit of each area, as well as the speed governor dead band, are important issues in power system modeling. For simplicity, these constraints will be ignored in the linear stability analysis carried out in Section 8.3, and they will only be considered in simulation results in Section 8.4.

The corresponding state-space form of each area can be written as:

$$\begin{bmatrix} \Delta\dot{f}_i \\ \Delta\dot{P}_{G,i} \\ \Delta\dot{P}_{tie,i} \end{bmatrix} = \underbrace{\begin{bmatrix} -\frac{1}{T_{p,i}} & \frac{K_{p,i}}{T_{p,i}} & -\frac{K_{p,i}}{T_{p,i}} \\ -\frac{K_{t,i}}{R_i T_{t,i}} & -\frac{1}{T_{t,i}} & 0 \\ 0 & 0 & 0 \end{bmatrix}}_{A_{1,i}} \underbrace{\begin{bmatrix} \Delta f_i \\ \Delta P_{G,i} \\ \Delta P_{tie,i} \end{bmatrix}}_{x_i} + \underbrace{\sum_{j\in\mathcal{N}_i} \begin{bmatrix} 0 \\ 0 \\ K_{tie,i,j}(\Delta f_i - \Delta f_j) \end{bmatrix}}_{E_i} + \underbrace{\begin{bmatrix} 0 \\ \frac{K_{t,i}}{T_{t,i}} \\ 0 \end{bmatrix}}_{B_{u,i}} \underbrace{\Delta P_{C,i}}_{u_i} + \underbrace{\begin{bmatrix} -\frac{K_{p,i}}{T_{p,i}} \\ 0 \\ 0 \end{bmatrix}}_{B_{w,i}} \underbrace{\Delta P_{L,i}}_{w_i}, \tag{8.6}$$

for $i = 1,\ldots,N$, where we have used the state-space differential equations with respect to block diagram Fig. 8.3, along with (8.4). Note that E_i corresponds to the dynamic coupling between the i-th area and its adjacent peers and gives rise to a state-space model of non-standard form. A standard state-space model for the complete network will be derived in the sequel. The variables Δf_i and $\Delta P_{tie,i}$ in the state-vector have been already defined; variable $\Delta P_{G,i}$ in (8.6) is the deviation from equilibrium value of the electrical power generated by the aggregate generating units of each area and is taken equal to the mechanical power produced in the output of the turbines. All parameters involved in (8.6), along with basic power system terminology, are summarized in Table 8.1. The disturbance signal $\Delta P_{L,i}$ denotes a time-varying demand of the consumers of the i-th area which is assumed to be unknown, piece-wise constant with known upper and lower bounds. Here, we study the case where $\Delta P_{L,i,\min} \leq \Delta P_{L,i} \leq \Delta P_{L,i,\max}$, $i = 1,\ldots,N$.

Table 8.1 Parameters and power system terminology.

Parameter, Symbol	**Value**	**Units**
Nominal Frequency, f^o	50	Hz
Power Base, $P_{B,i}$	2000	MW
Load Dependency Factor, D_i	16.66	MW/Hz
Speed Droop, R_i	1.2×10^{-3}	Hz/MW
Generator Inertia Gain, H_i	5	s
Turbine Static Gain, $K_{t,i}$	1	MW/MW
Turbine Time Constant, $T_{t,i}$	0.3	s
Area Static Gain, $K_{p,i}$	0.06	Hz/MW
Area Time Constant, $T_{p,i}$	24	s
Tie-line Coefficient, $K_{tie,i}$	1090	MW/Hz

8.2.2 State-augmentation for integral action

A well-established technique for tackling step-disturbances with zero steady-state error is to include integral action into the state-space model. For the i-th area, let a performance variable be expressed as the summation of the frequency deviation Δf_i multiplied by a bias factor β_i and the total tie-line power inflow $\Delta P_{tie,i}$, i.e., $z_i = \beta_i \Delta f_i + \Delta P_{tie,i}$. This quantity is referred to as "Area Control Error" (ACE) and a usual choice for β_i is $D_i + \frac{1}{R_i}$, [13]. Parameters D_i and R_i are defined in Table 8.1. Take now $z_i = C_{z,i} x_i$ with x_i given in (8.6) and $C_{z,i} = [\beta_i \; 0 \; 1]$ and consider the augmented state-vector:

$$x_{a,i} = \begin{bmatrix} x_i' & \int z_i \end{bmatrix}'. \tag{8.7}$$

The augmented state-space form of the i-th area can then be written as:

$$\dot{x}_{a,i} = \begin{bmatrix} A_{1,i} & 0_{3\times 1} \\ C_{z,i} & 0 \end{bmatrix} x_{a,i} + \begin{bmatrix} B_{u,i} \\ 0 \end{bmatrix} u_i + \begin{bmatrix} E_i \\ 0 \end{bmatrix} + \begin{bmatrix} B_{w,i} \\ 0 \end{bmatrix} w_i, \tag{8.8}$$

where $A_{1,i}$, $B_{u,i}$, E_i and $B_{w,i}$ are as given in Equation (8.6). If the coupling term E_i in Equation (8.8) is neglected, due to state-augmentation by the integral of the ACE signal of each area, a stabilizing control signal u_i would lead automatically to zero steady-state frequency and tie-line power inflow deviations provided these are driven by step disturbances $w_i = \Delta P_{L,i}$. However the term $[E_i' \; 0]'$ involving state-coupling between the i-th area and its neighbors cannot be neglected, and therefore the disturbance rejection task for the complete network becomes more challenging.

8.2.3 Problem statement

Possible power load change in the i-th area of an interconnected power system causes the electrical frequency f_i to deviate from its nominal value. Due to interconnections among the areas through power transmission tie-lines and the dependence of the power exchange between the i-th and j-th area upon the associated difference $\Delta f_i - \Delta f_j$, any power load deviation occurring in the i-th area will also affect the linked j-th area, causing a transient alteration in its frequency f_j. Here, we formulate the LFC of multi-area power systems as a large-scale optimal control problem in the absence of state and input constraints. The special case of N identical areas is considered. The aggregate dynamics in this case can be represented by a state-space model of the form:

$$\dot{\hat{x}} = (I_N \otimes A_1 + \mathscr{L} \otimes A_2)\hat{x} + (I_N \otimes B_u)\hat{u} + (I_N \otimes B_w)\hat{w}. \tag{8.9}$$

Here, $\hat{x} = [x'_{a,1} \ \cdots \ x'_{a,N}]'$, $\hat{u} = [u'_1 \ \cdots \ u'_N]'$, $\hat{w} = [w'_1 \ \cdots \ w'_N]'$ and:

$$A_1 = \begin{bmatrix} -\frac{1}{T_p} & \frac{K_p}{T_p} & -\frac{K_p}{T_p} & 0 \\ -\frac{K_t}{RT_t} & -\frac{1}{T_t} & 0 & 0 \\ 0 & 0 & 0 & 0 \\ \beta & 0 & 1 & 0 \end{bmatrix}, \ A_2 = \begin{bmatrix} 0 & 0 & 0 & 0 \\ 0 & 0 & 0 & 0 \\ K_{tie} & 0 & 0 & 0 \\ 0 & 0 & 0 & 0 \end{bmatrix}, \ B_u = \begin{bmatrix} 0 \\ \frac{K_t}{T_t} \\ 0 \\ 0 \end{bmatrix}, \ B_w = \begin{bmatrix} -\frac{K_p}{T_p} \\ 0 \\ 0 \\ 0 \end{bmatrix}, \tag{8.10}$$

where the subscript i has been neglected from all entries of A_1, A_2, B_u, and B_w since areas are assumed to have identical dynamics. A distributed LQR-based load frequency control design is outlined in the following section.

8.3 Large-scale LQR for load frequency control

In this section, we consider LQR problem (7.4) for a multi-area power system. Recall that we denote by N_L the number of areas of a power network, the topology of which is modeled by a complete graph and by N the number of areas associated with sparse networks. Let the aggregate state-space model of N_L-area power system be written as:

$$\dot{\tilde{x}} = (I_{N_L} \otimes A_1 + \mathscr{L}_c \otimes A_2)\tilde{x} + (I_{N_L} \otimes B_u)\tilde{u} + (I_{N_L} \otimes B_w)\tilde{w}, \tag{8.11}$$

where $\tilde{x} = [x'_{a,1} \ \cdots \ x'_{a,N_L}]'$, $\tilde{u} = [u'_1 \ \cdots \ u'_{N_L}]'$, $\tilde{w} = [w'_1 \ \cdots \ w'_{N_L}]'$, $x_{a,i}$, u_i, w_i, $i = 1, \ldots, N_L$, are defined in (8.8) and:

$$A_1 = \begin{bmatrix} -\frac{1}{T_p} & \frac{K_p}{T_p} & -\frac{K_p}{T_p} & 0 \\ -\frac{K_t}{RT_t} & -\frac{1}{T_t} & 0 & 0 \\ 0 & 0 & 0 & 0 \\ \beta & 0 & 1 & 0 \end{bmatrix}, \ A_2 = \begin{bmatrix} 0 & 0 & 0 & 0 \\ 0 & 0 & 0 & 0 \\ K_{tie} & 0 & 0 & 0 \\ 0 & 0 & 0 & 0 \end{bmatrix}, \ B_u = \begin{bmatrix} 0 \\ \frac{K_t}{T_t} \\ 0 \\ 0 \end{bmatrix}, \ B_w = \begin{bmatrix} -\frac{K_p}{T_p} \\ 0 \\ 0 \\ 0 \end{bmatrix}. \tag{8.12}$$

Parameters in $(A_1, \ A_2, \ B_u, \ B_w)$ can be found in Table 8.1. In view of Assumption 7.1.1, LQR problem (7.4) for $\tilde{A} = I_{N_L} \otimes A_1 + \mathscr{L}_c \otimes A_2$ and $\tilde{B} = I_{N_L} \otimes B_u$ with $(A_1, \ A_2, \ B_u)$ given in (8.12) initially fails to admit a solution since (7.8) cannot be solved. This stems from the fact that the pair $(A_1, \ B_u)$ has an uncontrollable mode at the origin, and the realization (8.11) is non-minimal. The non-minimality is due to a redundant equation related to the sum of the total power inflow $\Delta P_{tie,i}$ to each area, which is identically zero, namely, $\sum_{i=1}^{N_L} \Delta P_{tie,i} = 0$. Next, we show how to address this peculiarity in order to derive a stabilizing controller for the network under study.

Let a permutation matrix:

$$T = \begin{bmatrix} 1 & 0 & 0 & 0 \\ 0 & 1 & 0 & 0 \\ 0 & 0 & 0 & 1 \\ 0 & 0 & 1 & 0 \end{bmatrix}, \tag{8.13}$$

where $T = T' = T^{-1}$, and consider a Kalman decomposition of the pair $(A_1,\ B_u)$ carried out via state-space transformations $Tx_{a,i}$, $i = 1,\ldots,N_L$. Let system matrices $(\bar{A}_1,\ \bar{A}_2,\ \bar{B}_u,\ \bar{B}_w) = (TA_1T',\ TA_2T',\ TB_u,\ TB_w)$ in the new coordinates be written as:

$$\bar{A}_1 = \begin{bmatrix} -\frac{1}{T_p} & \frac{K_p}{T_p} & 0 & -\frac{K_p}{T_p} \\ -\frac{K_t}{RT_t} & -\frac{1}{T_t} & 0 & 0 \\ \beta & 0 & 0 & 1 \\ 0 & 0 & 0 & 0 \end{bmatrix},\ \bar{A}_2 = \begin{bmatrix} 0 & 0 & 0 & 0 \\ 0 & 0 & 0 & 0 \\ 0 & 0 & 0 & 0 \\ K_{tie} & 0 & 0 & 0 \end{bmatrix},\ \bar{B}_u = \begin{bmatrix} 0 \\ \frac{K_t}{T_t} \\ 0 \\ 0 \end{bmatrix},\ \bar{B}_w = \begin{bmatrix} -\frac{K_p}{T_p} \\ 0 \\ 0 \\ 0 \end{bmatrix}, \tag{8.14}$$

where $\bar{B}_u = B_u, \bar{B}_w = B_w$. Let the controllable part of $(\bar{A}_1,\ \bar{B}_u)$ be denoted as $(A_c,\ B_c)$ where

$$A_c = \begin{bmatrix} -\frac{1}{T_p} & \frac{K_p}{T_p} & 0 \\ -\frac{K_t}{RT_t} & -\frac{1}{T_t} & 0 \\ \beta & 0 & 0 \end{bmatrix},\ B_c = \begin{bmatrix} 0 \\ \frac{K_t}{T_t} \\ 0 \end{bmatrix}. \tag{8.15}$$

The zero in the $(4,4)$-entry of $\bar{A}_1$ stands for the uncontrollable mode (at the origin) of $(A_1,\ B_u)$. Now, construct a perturbation matrix as

$$E = \begin{bmatrix} 0_{3\times 3} & 0_3 \\ 0_3' & e \end{bmatrix}, \tag{8.16}$$

where $e < 0$, with $|e|$ sufficiently small, and define:

$$A_{1e} = \bar{A}_1 + E = \begin{bmatrix} A_c & A_{12} \\ 0_3' & e \end{bmatrix},\ A_{2e} = \bar{A}_2 - \frac{1}{N_L}E = \begin{bmatrix} 0_{3\times 3} & 0_3 \\ a_{21} & -\frac{1}{N_L}e \end{bmatrix}, \tag{8.17}$$

where $A_{12} = [-\frac{K_t}{RT_t}\ 0\ 1]'$ and $a_{21} = [K_{tie}\ 0\ 0]$. Since $e < 0$, the pair $(A_{1e},\ B_u)$ is stabilizable. According to Theorem 7.1.3, LQR problem (7.4) with parameters $(A_{1e},\ A_{2e},\ B_u,\ Q_1,\ Q_2,\ R)$

is reduced to two node-level ARE, namely,

$$A_{1e}'P_e + P_eA_{1e} - P_eXP_e + Q_1 = 0, \tag{8.18}$$

$$(A_{1e}+N_LA_{2e})'(P_e - N_L\tilde{P}_{2e}) + (P_e - N_L\tilde{P}_{2e})(A_{1e}+N_LA_{2e}) - (P_e - N_L\tilde{P}_{2e})X(P_e - N_L\tilde{P}_{2e}) + Q_1 + N_LQ_2 = 0, \tag{8.19}$$

where P_e, $\tilde{P}_{2e}$ are e-dependent, and $X = B_uR^{-1}B_u'$. Note that the solution $P_e - N_L\tilde{P}_{2e}$ to ARE (8.19) remains invariant under e-perturbation. Theorem 8.3.1, next, summarizes the method of solving large-scale LQR problem (7.4) with one uncontrollable mode at the origin. For simplicity, we have set $X = B_uR^{-1}B_u'$.

Theorem 8.3.1. *Consider a N_L-area power system with an aggregate state-space form given as in* (8.11)*. Consider a Kalman decomposition of $(A_1,\ B_u)$, and define $(\bar{A}_1,\ \bar{A}_2,\ \bar{B}_u,\ \bar{B}_w)$ as given in* (8.14)*. Choose $e < 0$, with $|e|$ sufficiently small, and define perturbed matrices A_{1e}, A_{2e} as in* (8.17)*. Solving LQR problem* (7.4) *with parameters $(A_{1e},\ A_{2e},\ B_u,\ Q_1,\ Q_2,\ R)$ and defining P_e and $\tilde{P}_{2e}$ from* (8.18) *and* (8.19)*, respectively, leads to the following argument: the matrix,*

$$\bar{A}_1 - XP_e + \alpha(N_L\bar{A}_2 + X\tilde{P}_{2e}), \tag{8.20}$$

I. is Hurwitz for $\alpha = 1$.

II. has $n-1$ eigenvalues in the left-half-plane and one at the origin for $\alpha = 0$.

Proof. In view of the special structure of A_{1e} and A_{2e}, it can easily be seen that:

$$\bar{A}_1 + N_L\bar{A}_2 = A_{1e} + N_LA_{2e}. \tag{8.21}$$

Due to (8.19), matrix $A_{1e} + N_LA_{2e} - XP_e + N_LX\tilde{P}_{2e}$ is Hurwitz and because of (8.21) matrix $\bar{A}_1 + N_L\bar{A}_2 - XP_e + N_LX\tilde{P}_{2e}$ is also Hurwitz. This proves part I.

Now, let matrix P_e in (8.18) be decomposed into blocks of appropriate dimensions according to the Kalman decomposition (8.15). Then, ARE (8.18) can be written as:

$$\begin{bmatrix} A_c & A_{12} \\ 0_3' & e \end{bmatrix}' \begin{bmatrix} P_{11e} & P_{12e} \\ P_{12e}' & P_{22e} \end{bmatrix} + \begin{bmatrix} P_{11e} & P_{12e} \\ P_{12e}' & P_{22e} \end{bmatrix} \begin{bmatrix} A_c & A_{12} \\ 0_3' & e \end{bmatrix} - \begin{bmatrix} P_{11e} & P_{12e} \\ P_{12e}' & P_{22e} \end{bmatrix} \begin{bmatrix} B_c \\ 0 \end{bmatrix} R^{-1} \begin{bmatrix} B_c' & 0 \end{bmatrix} \begin{bmatrix} P_{11e} & P_{12e} \\ P_{12e}' & P_{22e} \end{bmatrix} + \begin{bmatrix} Q_{11} & Q_{12} \\ Q_{12}' & Q_{22} \end{bmatrix} = 0. \tag{8.22}$$

The first diagonal block of (8.22) gives:

$$A_c' P_{11e} + P_{11e} A_c - P_{11e} B_c R^{-1} B_c' P_{11e} + Q_{11} = 0, \tag{8.23}$$

and implies that the matrix $A_c - B_c R^{-1} B_c' P_{11e}$ is Hurwitz where the symmetric positive definite matrix P_{11e} does not depend on parameter e. The two remaining blocks P_{12e} and P_{22e} of P_e are e-dependent and given by:

$$P_{12e} = -(A_c' - P_{11e} B_c R^{-1} B_c' + e I_{n-1})^{-1} (P_{11e} A_{12} + Q_{12}), \tag{8.24}$$

$$P_{22e} = \frac{1}{2e} (P_{12e}' B_c R^{-1} B_c' - 2A_{12}') P_{12e} - \frac{1}{2e} Q_{22}. \tag{8.25}$$

Matrix $A_c' - P_{11e} B_c R^{-1} B_c' + e I_{n-1}$ in (8.24) is invertible since $A_c - B_c R^{-1} B_c' P_{11e}$ is Hurwitz and $e < 0$. Now, the closed-loop matrix $A_{1e} - B_u R^{-1} B_u' P_e$ is Hurwitz and can be written as:

$$A_{1e} - B_u R^{-1} B_u' P_e = \begin{bmatrix} A_c - B_c R^{-1} B_c' P_{11e} & A_{12} - B_c R^{-1} B_c' P_{12e} \\ 0_3' & e \end{bmatrix}. \tag{8.26}$$

Since (8.26) is in canonical form, its spectrum can be decomposed in:

$$S(A_{1e} - B_u R^{-1} B_u' P_e) = S(A_c - B_c R^{-1} B_c' P_{11e}) \cup e. \tag{8.27}$$

Setting $e = 0$ in (8.27) proves the theorem. □

Similarly to Condition 7.1.5, we impose the following stability requirement.

Condition 8.3.2. *Matrix* $\bar{A}_1 - X P_e + \alpha(N_L \bar{A}_2 + X \tilde{P}_{2e})$ *is Hurwitz for all* $\alpha \in (0, 1]$.

In the next paragraph, based on Condition 8.3.2, we propose a stabilizing distributed LQR-based LFC design for multi-area power systems with sparse topology.

8.3.1 Distributed LQR-based LFC

Let an undirected graph $\mathscr{G}_N = (\mathscr{V}, \mathscr{E})$ with Laplacian matrix $\mathscr{L}_N(\mathscr{G}_N)$ describe the interconnection topology of a multi-area power system formed of N identical areas with aggregate state-space form written as:

$$\dot{\hat{x}} = (I_N \otimes A_1 + \mathscr{L}_N \otimes A_2)\hat{x} + (I_N \otimes B_u)\hat{u} + (I_N \otimes B_w)\hat{w}. \tag{8.28}$$

Matrices A_1, A_2, B_u, and B_w are given as in (8.12), while aggregate vectors $\hat{x}$, $\hat{u}$, and $\hat{w}$ are constructed as earlier by stacking vectors $x_{a,i}$, u_i, w_i, respectively, of each area, with

ascending order depending on their label in the graph $\mathscr{G}_N$. Consider a perturbation matrix:

$$E = \begin{bmatrix} 0 & 0 & 0 & 0 \\ 0 & 0 & 0 & 0 \\ 0 & 0 & e & 0 \\ 0 & 0 & 0 & 0 \end{bmatrix}, \tag{8.29}$$

where $e < 0$, with $|e|$ sufficiently small, and define also perturbed matrices A_{1e}, A_{2e} as:

$$A_{1e} = A_1 + E,\ A_{2e} = A_2 - \frac{1}{N_L}E, \tag{8.30}$$

where N_L is as defined in Theorem 7.2.1. A distributed LFC controller for (8.28) is constructed next, in Theorem 8.3.3.

Theorem 8.3.3. *Consider a power system of N identical areas with network topology modeled by a graph $\mathscr{G}_N$ with Laplacian matrix $\mathscr{L}_N$. Let the aggregate state-space form of the entire system be given by* (8.28)*. Let also λ_N be the maximum eigenvalue of $\mathscr{L}_N$ and denote by $d_{\max}$ the smallest integer which is greater than or equal to λ_N, i.e., $d_{\max} = \lceil \lambda_N \rceil$. Set $N_L = d_{\max}$, specify $e < 0$, with $|e|$ sufficiently small, and define perturbed matrices A_{1e}, A_{2e} as in* (8.30)*. Consider an LQR problem* (7.4) *for $N_L = d_{\max}$ perturbed systems (A_{1e}, A_{2e}, B_u), and define P_e and $\tilde{P}_{2e}$ via* (8.18) *and* (8.19)*, respectively, assuming that Condition 8.3.2 holds. Construct a distributed state-feedback controller*

$$\hat{K} = -I_N \otimes R^{-1}B_u'P_e + \mathscr{L}_N \otimes R^{-1}B_u'\tilde{P}_{2e}. \tag{8.31}$$

Then, the closed-loop matrix of the overall system,

$$A_{cl} = I_N \otimes (A_1 - XP_e) + \mathscr{L}_N \otimes (A_2 + X\tilde{P}_{2e}), \tag{8.32}$$

has $3N-1$ eigenvalues in the left-hand-plane and one at the origin.

The proof follows similar arguments stated for proving Theorem 7.2.1 and is omitted. We remark here that under the application of the state-feedback controller (8.31) the network maintains stability even if the controllability Assumption 7.1.1 is not strictly in force. As it will become evident in the following simulation studies, although a single eigenvalue of the closed-loop matrix lying at the origin cannot be shifted, the proposed distributed control scheme guarantees network stability while compensates for unknown, piece-wise constant disturbances. In particular, the uncontrollable mode at the origin pertains to a trivial differential equation $\sum_{i=1}^{N_L} \Delta\dot{P}_{tie,i} = 0$, implying that $\dot{0} = 0$. The latter can easily be removed

via an appropriate state-space transformation leading to a minimal state-space realization of the system. However, this is beyond the scope of the present analysis.

In the following section, the distributed LQR controller constructed above is employed to drive the LFC of a six-area power system. We show that network stability is guaranteed for a class of tie-line interconnection schemes via a single tuning of the LFC controller. In the simulations, we consider three different interconnection examples. We also consider various input and state constraints in the linear model of each area in order to assess the stability margins of the proposed controller. A robust stability analysis has also been carried out as a separate case study involving parametric uncertainties in each area. We stress here that a thorough robust stability and nonlinear analysis are beyond the scope of this chapter. Nonlinearities and parameter perturbations considered in the next section are only used for simulation purposes whereby the performance of the proposed controller is also verified under more intense conditions.

8.4 Simulation case studies

We consider a power system of six identical areas, the parameters of which are summarized in Table 8.1. Three interconnection schemes are considered; each graph shown in Fig. 8.5a–c, with corresponding Laplacian matrix given in (8.33), models the network topology of each interconnection scheme (S_1, S_2, S_3), respectively.

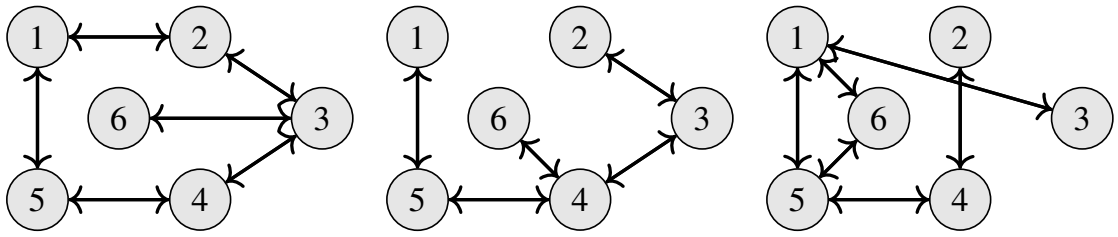

(a) Interconnection scheme S_1 with Laplacian matrix $\mathscr{L}_1$.

(b) Interconnection scheme S_2 with Laplacian matrix $\mathscr{L}_2$.

(c) Interconnection scheme S_3 with Laplacian matrix $\mathscr{L}_3$.

Fig. 8.5 Three different tie-line interconnection schemes of six control areas.

$$\mathscr{L}_1 = \begin{bmatrix} 2 & -1 & 0 & 0 & -1 & 0 \\ -1 & 2 & -1 & 0 & 0 & 0 \\ 0 & -1 & 3 & -1 & 0 & -1 \\ 0 & 0 & -1 & 2 & -1 & 0 \\ -1 & 0 & 0 & -1 & 2 & 0 \\ 0 & 0 & -1 & 0 & 0 & 1 \end{bmatrix}, \mathscr{L}_2 = \begin{bmatrix} 1 & 0 & 0 & 0 & -1 & 0 \\ 0 & 1 & -1 & 0 & 0 & 0 \\ 0 & -1 & 2 & -1 & 0 & 0 \\ 0 & 0 & -1 & 3 & -1 & -1 \\ -1 & 0 & 0 & -1 & 2 & 0 \\ 0 & 0 & 0 & -1 & 0 & 1 \end{bmatrix}, \mathscr{L}_3 = \begin{bmatrix} 3 & 0 & -1 & 0 & -1 & -1 \\ 0 & 1 & 0 & -1 & 0 & 0 \\ -1 & 0 & 1 & 0 & 0 & 0 \\ 0 & -1 & 0 & 2 & -1 & 0 \\ -1 & 0 & 0 & -1 & 3 & -1 \\ -1 & 0 & 0 & 0 & -1 & 2 \end{bmatrix}. \tag{8.33}$$

In the simulations, one scenario of power demand is considered. Specifically, areas are subject to step disturbances which represent power load deviations from a nominal value. Power load profiles of the six areas are depicted in Fig. 8.6. For the control design, we also assume that there is a communication cyber-layer, the topology of which is identical with the tie-line interconnection scheme considered. The performance of the distributed LFC controller designed in Theorem 8.3.3 is verified in three case studies. These are summarized below:

1. We test closed-loop stability of topology S_1, S_2, and S_3, respectively, applying LFC controller derived from the solution of a single LQR problem. This stability test is performed for two different tunings of the LQR performance index. The transients in frequency and total power inflow of the linear model of each area is compared to the responses of a nonlinear model containing saturation hard constraints on the total magnitude of the input signal of each area.

2. We consider parametric uncertainty in the linear model of each area, and we show that closed loop stability of topology S_2 for two different tunings of the LFC controller is maintained. Perturbations have been carried out on the following parameters: turbine time constant $(T_{t,i})$, area time constant $(T_{p,i})$ of each area, respectively, and tie-line coefficient $(K_{tie,i,j})$ of each tie-line interconnection.

3. Tuning the LQR controller via the Bryson's rule, we demonstrate frequency regulation for all interconnection schemes S_1, S_2, and S_3. In this simulation study, the model of each area is subject to a generation rate constraint (GRC) and a saturation hard constraint on the total input signal.

8.4.1 Case study 1

Block representation of the linear dynamics of each control area at local level is given in Fig. 8.3. The corresponding augmented state-space form of each area is shown in (8.8), where the integral of the ACE signal has also been included in the state-vector. We construct the collective state-space of the network as in (8.28), where matrices A_1, A_2, B_u, and B_w are given in (8.12). The Laplacian matrix $\mathscr{L}$ of each topology considered is given in (8.33). Parameter values are given in Table 8.1. The distributed LQR controller presented in Section 8.3.1 is proposed here to drive the AGC signal $\Delta P_{C,i}$ of each area. The control objective is to meet the load demand at each area shown in Fig. 8.6 and recover the nominal operating conditions of each area for three possible interconnections. Stabilizing distributed state-feedback controller is constructed as follows.

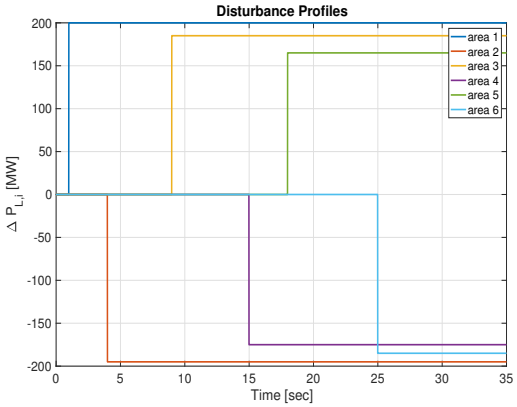

Fig. 8.6 Power demand deviation $\Delta P_{L,i}$ for $i = 1, \ldots, 6$.

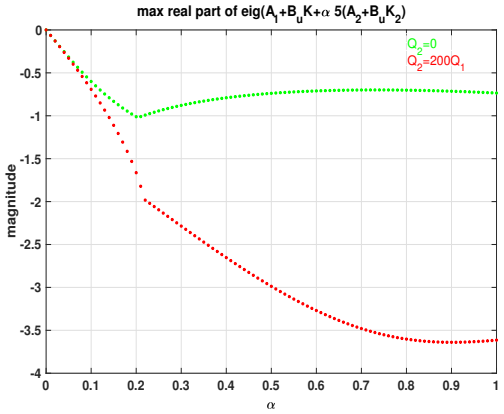

Fig. 8.7 Stability test and validity of Condition 8.3.2.

The maximum eigenvalue of each matrix $(\mathscr{L}_1,\ \mathscr{L}_2,\ \mathscr{L}_3)$ in (8.33) is 4.3028, 4.3028, and 4.3928, respectively. We take the smallest integer denoted by $d_{\max}$ which is greater or equal to the maximum of these (4.3928), i.e., $d_{\max} = 5$. We select perturbation parameter $e = -0.01$, and we alter matrices A_1 and A_2 to A_{1e} and A_{2e}, respectively, according to (8.30). We solve an LQR problem (7.4) for $N_L = d_{\max} = 5$ systems with matrices $(A_{1e},\ A_{2e},\ B_u)$ for two different selections of the weights $\tilde{Q},\ \tilde{R}$. In the first, $\tilde{Q} = I_5 \otimes Q_1$, with $Q_1 = \mathrm{diag}(100, 10, 10, 5000)$ and $\tilde{R} = I_5 \otimes 100$, while in the second, $\tilde{R}$ is kept the same and $\tilde{Q} = I_5 \otimes Q_1 + \mathscr{L}_5 \otimes Q_2$, where $Q_2 = 200Q_1$, $\mathscr{L}_5$ denotes the Laplacian matrix associated with a complete graph (all possible edges) of 5 nodes. Terms in (7.5) pertinent to matrix Q_2 penalize the relative state-difference $(x_i - x_j)$ between neighboring areas. We calculate P_e and $\tilde{P}_{2e}$ from (8.18), (8.19), and define the respective state feedback gains $K = -R^{-1}B_u'P_e$ and $K_2 = R^{-1}B_u'\tilde{P}_{2e}$ for each tuning.

These are:

$$\begin{aligned} K &= \begin{bmatrix} -2502.857 & -1.203 & -1.757 & -7.071 \end{bmatrix}, \\ K_2 &= \begin{bmatrix} -342.491 & -0.104 & 0.225 & 0.000 \end{bmatrix}, \end{aligned} \tag{8.34}$$

for the first tuning where $Q_2 = 0$ and:

$$\begin{aligned} K &= \begin{bmatrix} -2502.857 & -1.203 & -1.757 & -7.071 \end{bmatrix}, \\ K_2 &= \begin{bmatrix} -12084.071 & -2.356 & -6.374 & -43.329 \end{bmatrix}, \end{aligned} \tag{8.35}$$

for the case where $Q_2 = 200Q_1$. Note that $K = -R^{-1}B_u'P_e$ is identically equal for both cases, since P_e is the solution to a single node-level ARE with parameters $(A_{1e},\, B_u,\, Q_1,\, R)$. We also verify Condition 8.3.2, which can be seen to hold. Fig. 8.7 displays the real part of the eigenvalue of the matrix $(A_1 - B_uR^{-1}B_u'P_e) + \alpha d_{\max}(A_2 + B_uR^{-1}B_u'\tilde{P}_{2e})$ with the maximum real part with $\alpha \in [0,1]$ for both tuning choices. In essence, this implies stable network operation under both control schemes for all possible interconnections associated with Laplacian matrices with maximum eigenvalue bounded by $d_{\max}$.

At network level, the distributed stabilizing controller $\hat{K}$ takes the form:

$$\hat{K} = I_6 \otimes K + \mathscr{L}_s \otimes K_2, \tag{8.36}$$

where $\mathscr{L}_s$, $s = 1,2,3$, is given in (8.33) according to each topology. Node-wise, the AGC signal at each area is derived from:

$$\Delta P_{C,i} = Kx_i + K_2 \sum_{j \in \mathscr{N}_i} (x_i - x_j), \tag{8.37}$$

with $i = 1,\ldots,6,\ j \neq i$ and $j \in \mathscr{N}_i$. In effect, each area requires local and neighboring state-information be accessible in order to construct its control signal. In the following simulations, we show the transients in frequency and total power inflow of each area resulting from power demand deviations $\Delta P_{L,i},\ i = 1,\ldots,6$. Comparison with the response of a nonlinear model containing saturation hard constraints on the total input signal of each area is also illustrated in the simulation results. Block representation of each area with saturating input constraint is shown in Fig. 8.8, where the symmetric saturator models the lower and upper bound of the magnitude of the total control signal of each area. Here, we consider -220 [MW] $\leq \Delta u_{tot,i} \leq 220$ [MW], $i = 1,\ldots,6$.

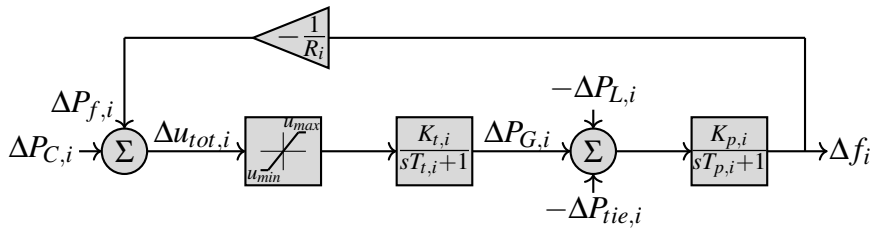

Fig. 8.8 Single block representation of the i-th interconnected area with saturation hard constraint on the total input signal.

Fig. 8.9–8.12 show the transient response of frequency and total power inflow deviations, respectively, of each area from the equilibrium operation for two control schemes given in (8.34), (8.35). Stable operation is guaranteed and the nominal working conditions for all three interconnection schemes are recovered via both LFC control choices. For the given choices of weighting matrices $(Q_1,\ Q_2,\ R)$, stability can also be guaranteed from the validity of Condition 8.3.2, which is verified graphically in Fig. 8.7. Note also that, the magnitude of the total power flow over the tie-lines is significantly limited in the case where the controller is designed as in (8.35). This stems from the large weighting matrix Q_2 selection in the performance index (7.5). In this case, since the relative state-difference between neighboring areas is highly penalized, the areas tend to acquire similar frequencies deviations during the transients (see Fig. 8.11), thus the total power flow over the tie-lines given in (8.4) is kept low. Comparing Fig. 8.10, 8.12, the same behavior is observed for the case in which saturating input constraint is included in the model of each area. Despite the strong nonlinearity introduced by the saturator, total power inflow of each area is significantly reduced when the relative state-difference $(x_i - x_j)$ is penalized heavily in the LQR performance index. This powerful feature to control the magnitude of tie-line power exchange enhances the applicability of the proposed controller and may prove highly beneficial for networks composed of weak tie-line interconnections. Simulations of a fully centralized control scheme carried out with identical tuning parameters, suggest that the proposed distributed control scheme not only respects system constraints but also guarantees a performance almost indistinguishable from the optimal (centralized) one. This becomes evident if one compares Fig. 8.9–8.12 with Fig. 8.13–8.16.

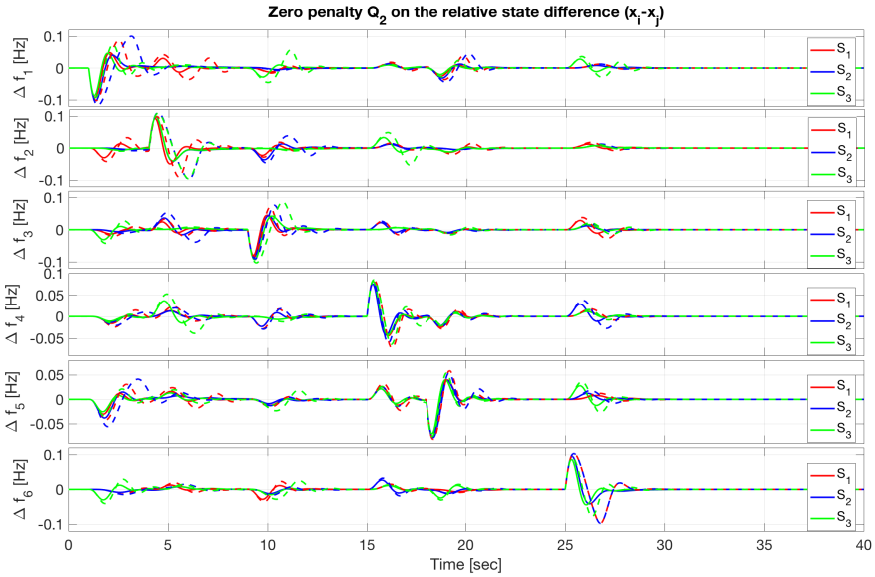

Fig. 8.9 Frequency transients of the six-area power system for three tie-line interconnection schemes (S_1, S_2, S_3). Zero penalty on the relative state-difference between interconnected areas. Solid lines depict transients of the linear model; dashed lines depict transients of the model with saturator (Fig. 8.8).

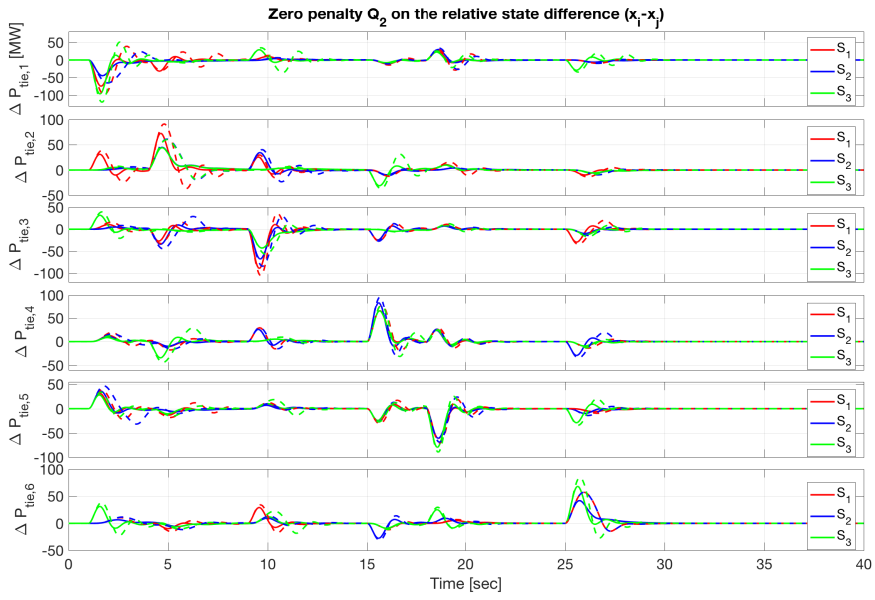

Fig. 8.10 Total power inflow response of the six-area power system for three tie-line interconnection schemes (S_1, S_2, S_3). Zero penalty on the relative state-difference between interconnected areas. Solid lines depict transients of the linear model; dashed lines depict transients of the model with saturator (Fig. 8.8).

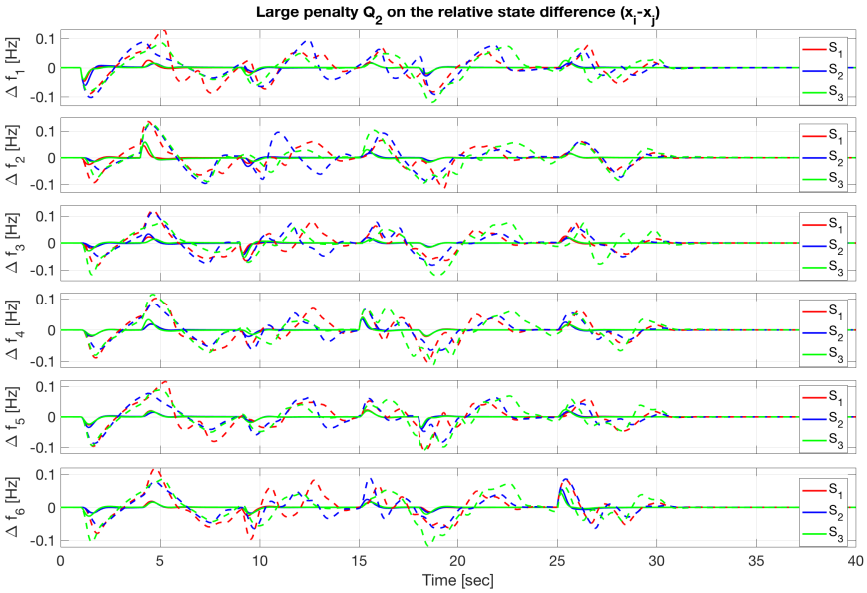

Fig. 8.11 Frequency transients of the six-area power system for three tie-line interconnection schemes (S_1, S_2, S_3). Large penalty on relative state-difference between interconnected areas. Solid lines depict transients of the linear model; dashed lines depict transients of the model with saturator (Fig. 8.8).

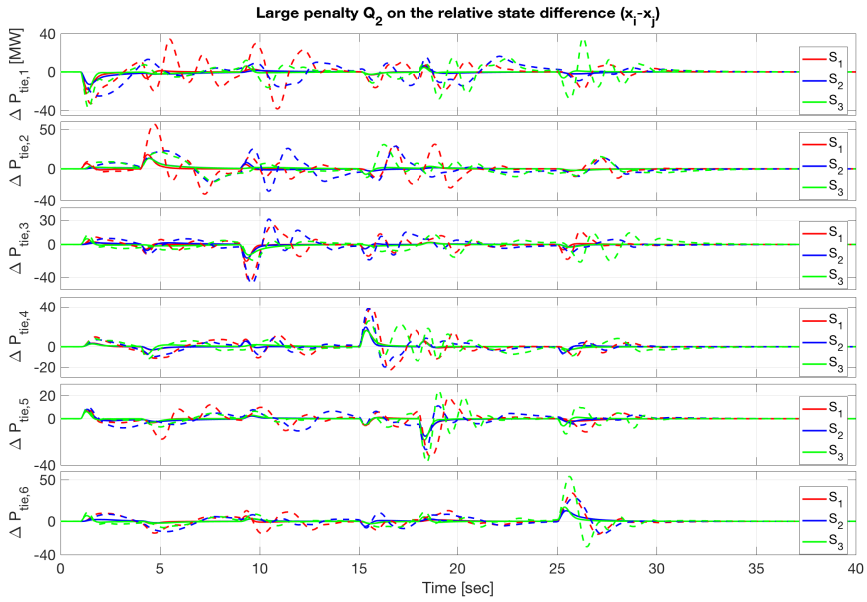

Fig. 8.12 Total power inflow response of the six-area power system for three tie-line interconnection schemes (S_1, S_2, S_3). Large penalty on relative state-difference between interconnected areas. Solid lines depict transients of the linear model; dashed lines depict transients of the model with saturator (Fig. 8.8).

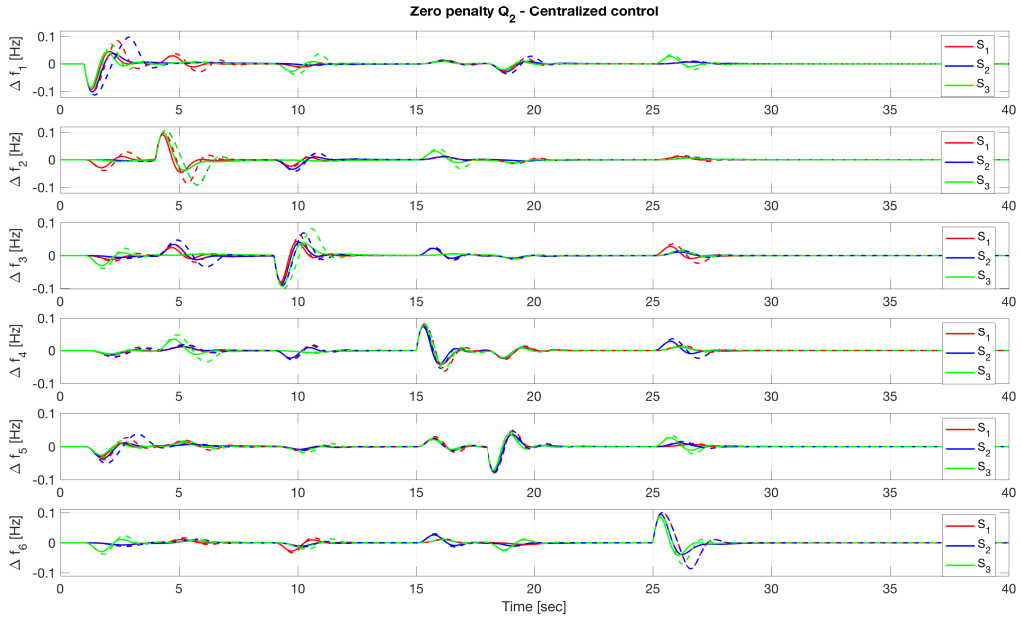

Fig. 8.13 Frequency transients for three interconnection schemes (S_1, S_2, S_3) with centralized control and zero penalty on relative state-difference. Solid lines: transients of the linear model, dashed lines: transients of the model with saturator (Fig. 8.8).

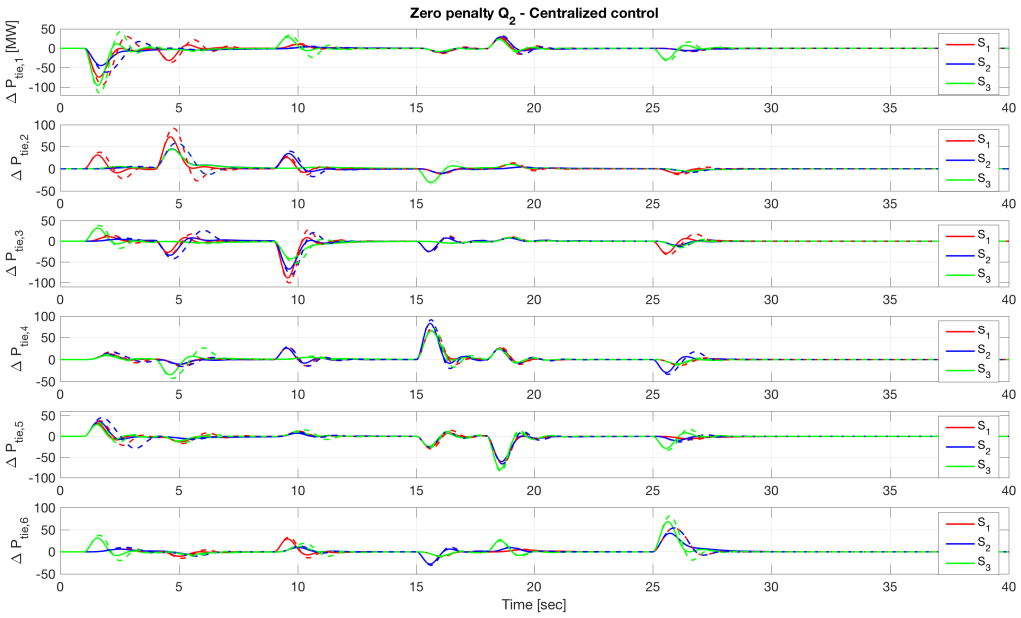

Fig. 8.14 Total power inflow response for three interconnection schemes (S_1, S_2, S_3) with centralized control and zero penalty on relative state-difference. Solid lines: transients of the linear model, dashed lines: transients of the model with saturator (Fig. 8.8).

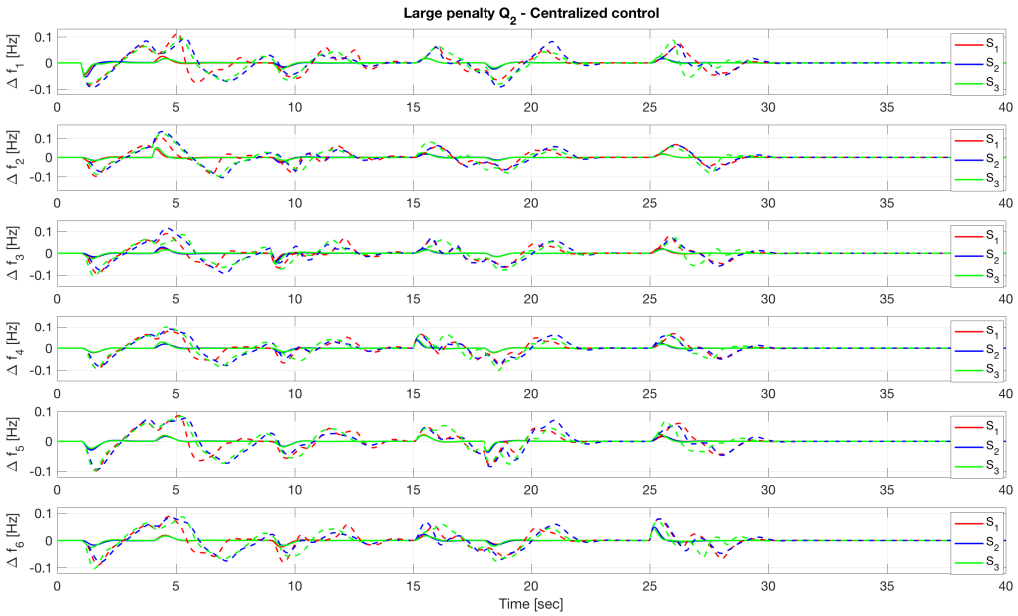

Fig. 8.15 Frequency transients for three interconnection schemes (S_1, S_2, S_3) with centralized control and large penalty on relative state-difference. Solid lines: transients of the linear model, dashed lines: transients of the model with saturator (Fig. 8.8).

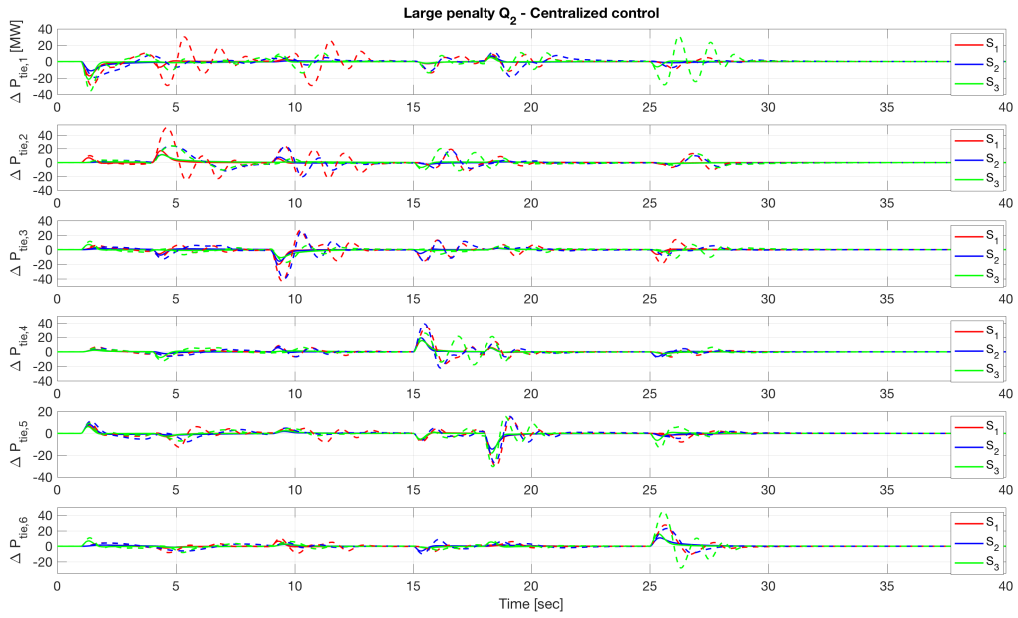

Fig. 8.16 Total power inflow response for three interconnection schemes (S_1, S_2, S_3) with centralized control and large penalty on relative state-difference. Solid lines: transients of the linear model, dashed lines: transients of the model with saturator (Fig. 8.8).

8.4.2 Case study 2

To assess the stability margins of the LFC controller constructed in the previous case study, we introduce uncertain parameters in the model of each area, and we carry out simulations for the interconnection topology S_2 shown in Fig. 8.5b. Both tunings of the LQR performance index considered in the previous section are also employed here. We consider parametric uncertainties in: turbine time constant $T_{t,i}$, area time constant $T_{p,i}$, and tie-line coefficient $K_{tie,i,j}$ for $i, j = 1, \ldots, 6$ and $j \in \mathcal{N}_i$. The perturbation magnitude of each parameter is shown in Table 8.2.

Table 8.2 Parametric uncertainties in $T_{t,i}$, $T_{p,i}$, and $K_{tie,i,j}$, $i = 1, \ldots, 6$, $j \in \mathcal{N}_i$.

Parameter	**Area 1**	**Area 2**	**Area 3**	**Area 4**	**Area 5**	**Area 6**
Turbine Time Constant, $T_{t,i}$	$+20\%$	-20%	-30%	$+30\%$	$+25\%$	-25%
Area Time Constant, $T_{p,i}$	-25%	$+30\%$	$+25\%$	$+20\%$	-20%	$+30\%$

Parameter	**Line 15**	**Line 23**	**Line 34**	**Line 45**	**Line 46**
Tie-line coefficient, $K_{tie,i,j}$	$+20\%$	-20%	-25%	$+30\%$	-25%

The frequency and total power inflow deviation of each subject to step disturbances (Fig. 8.6) are depicted in Fig. 8.17–8.20. The robustness of the proposed distributed LQR-based LFC scheme is validated, and it can be seen that stable operation is maintained even for magnitude of parametric uncertainties taken equal to 30%.

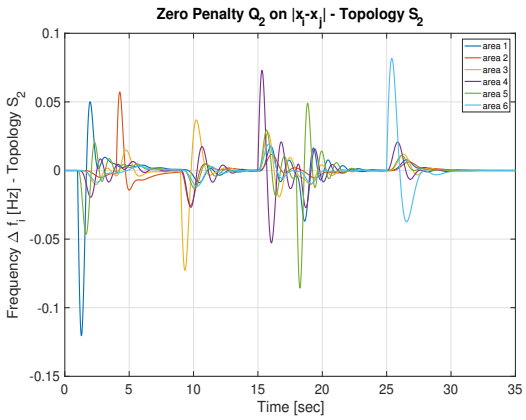

Fig. 8.17 Frequency deviation Δf_i response for $i = 1, \ldots, 6$, topology S_2, control tuning with $Q_2 = 0$, uncertain parameters.

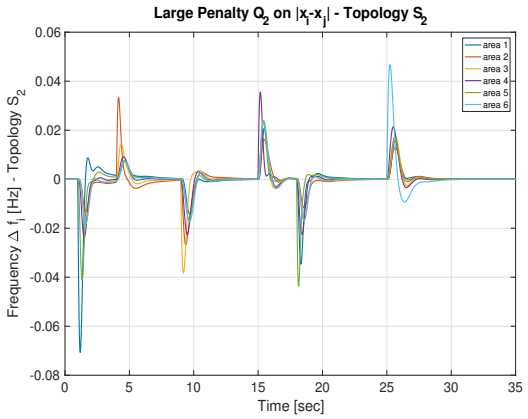

Fig. 8.18 Frequency deviation Δf_i response for $i = 1,\ldots,6$, topology S_2, control tuning with $Q_2 = 200Q_1$, uncertain parameters.

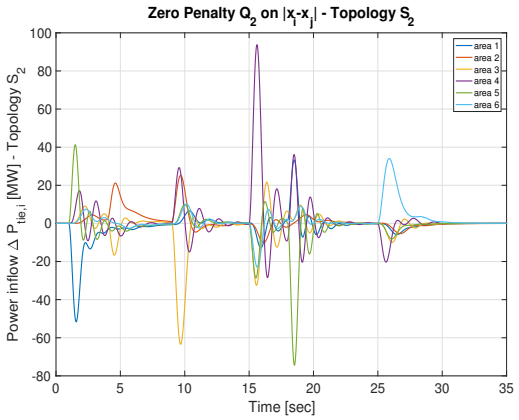

Fig. 8.19 Total power inflow deviation $\Delta P_{tie,i}$ response for $i = 1,\ldots,6$, topology S_2, control tuning with $Q_2 = 0$, uncertain parameters.

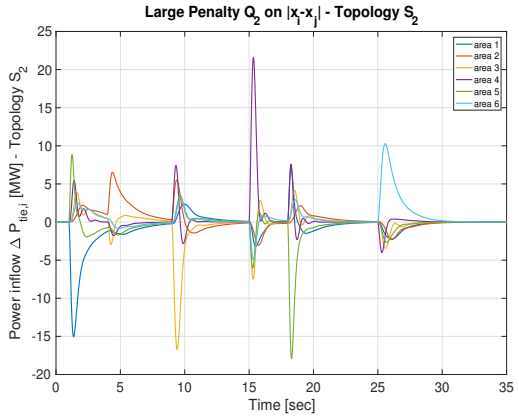

Fig. 8.20 Total power inflow deviation $\Delta P_{tie,i}$ response for $i = 1,\ldots,6$, topology S_2, control tuning with $Q_2 = 200Q_1$, uncertain parameters.

8.4.3 Case study 3

In this simulation study, the linear model of each area is augmented with a saturation hard constraint on the total control signal as well as a generation rate constraint (GRC). The first is formulated as hard input constraint and is taken equal to this considered in the first case study, -220 [MW] $\leq \Delta u_{tot,i} \leq 220$ [MW], $i = 1,\ldots,6$. The second constraint (GRC) can be cast as state constraint imposed on the state variable $\Delta P_{G,i}$, $= 1,\ldots,6$. Here, we consider GRC equal to 10% of the power base of each area per minute (i.e., 3.4 [MW/s]). The augmented block diagram of each area is depicted in Fig. 8.21.

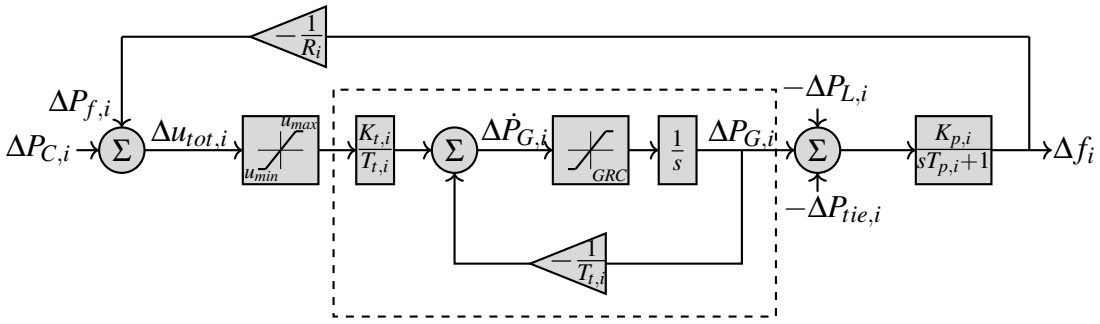

Fig. 8.21 Single block representation of the i-th interconnected area with saturation hard constraint on the total input signal and nonlinear turbine model with GRC.

Areas' power load profiles are modeled as step disturbances as shown in Fig. 8.6. The three tie-line interconnection schemes depicted in Fig. 8.5 are also considered in the present example. In this case study, in order to construct the proposed LFC controller, the weighting matrices of the LQR performance index have been chosen according to Bryson's rule [79]. For a standard LQR problem with weights $(Q,\ R)$, this rule specifies that Q and R are taken diagonal with diagonal entries defined as:

$$Q_{ii} = \frac{1}{(x_{i,max})^2} \text{ and } R_{ii} = \frac{1}{(u_{i,max})^2}, \tag{8.38}$$

where $|x_{i,max}|$ and $|u_{i,max}|$ represent the maximum required values of the state and control variables, respectively. Here, the matrices $(Q_1,\ Q_2,\ R)$ are selected as:

$$Q_1 = \text{diag}(\frac{1}{0.001^2}, \frac{1}{450^2}, \frac{1}{200^2}, \frac{1}{100^2}), \tag{8.39}$$

$$Q_2 = \text{diag}(\frac{1}{0.1^2}, \frac{1}{50^2}, \frac{1}{400^2}, \frac{1}{5000^2}), \tag{8.40}$$

$$R = \frac{10000}{350^2}. \tag{8.41}$$

The frequency transient of the closed-loop system of each area is illustrated in Fig. 8.22.

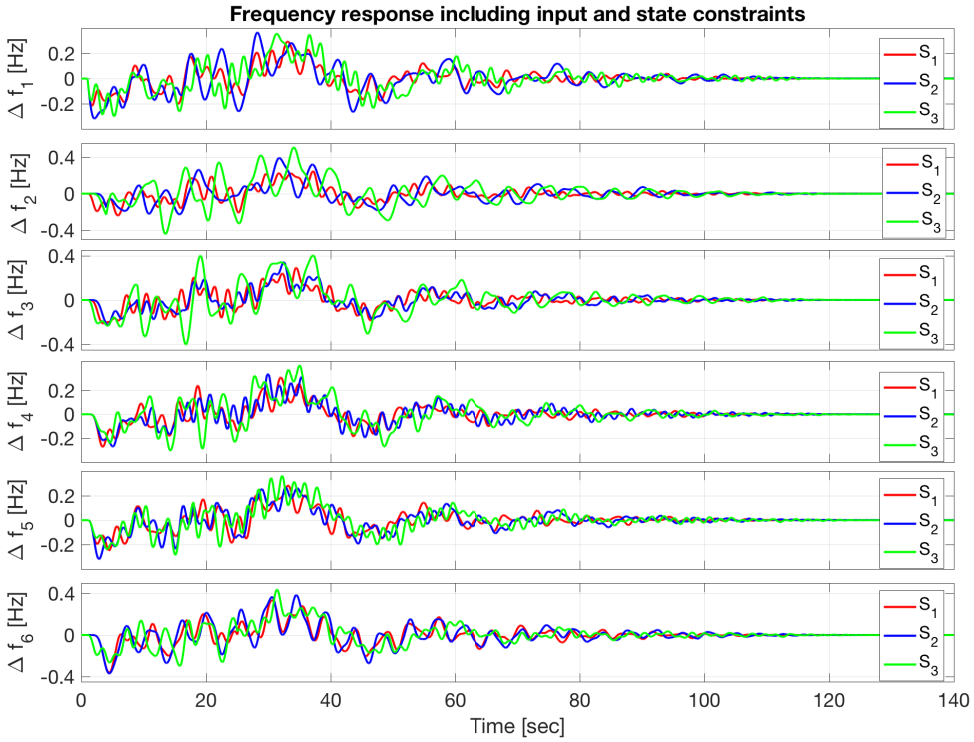

Fig. 8.22 Frequency transients of the six-area power system for three tie-line interconnection schemes (S_1, S_2, S_3). Input and state constraints are included in the model of each area (Fig. 8.21). Selection of weighting matrices according to Bryson's rule.

As it can be seen, the same LFC controller stabilizes the network for topology S_1, S_2, S_3, while the nominal frequency is recovered for all areas. The frequency transient in this case has become considerably slower than in previous studies due to the state constraint GRC, which significantly limits the rate of power generation (3.4 [MW/s]). Despite the strong nonlinearities introduced by the input and state constraints, the closed-loop stability is maintained via the proposed LFC controller.

8.5 Conclusions

A stabilizing distributed LQR-based controller for LFC problems of multi-area power systems is proposed based on the solution of a large-scale LQR optimal problem under the assumption that areas have identical dynamics. The proposed distributed LFC method relies on the results of Chapter 7 illustrating the applicability of the proposed distributed control scheme via various simulation studies. Motivated by the work of [17], we follow a top-down technique

to define a fully centralized controller which is subsequently substituted by a distributed state-feedback configuration with sparse structure. The control scheme is obtained by optimizing an LQR performance index with a tuning parameter utilized to emphasize/de-emphasize relative state difference between interconnected areas. We show that this parameter controls the magnitude of tie-line power exchange and frequency synchronization between interconnected areas. Extensive simulations presented in this chapter support our conjecture that this stabilization criterion can be extended to more general power systems LFC problems. The assumption of identical dynamics is clearly restrictive but simplifies the design problem considerably and leads to the derivation of a stability condition which can easily be verified. Effort to eliminate or relax this assumption will be the topic of future work attempting to adapt the model-matching methods presented in previous chapters to the present setup. The simulation results in Section 8.4.2 carried out under considerable perturbations suggest that this hypothesis is valid and that our results can be extended to the non-identical case.

Chapter 9

Distributed model predictive control design

9.1 Introduction

In this chapter, we investigate receding horizon control (RHC) problems and present distributed model predictive control (DMPC) methods for stabilizing networks of multiple dynamic agents. The basic idea of model predictive control (MPC) is to predict a number of finite forward movements of a system based on a concrete model and a sequence of future control inputs. At each instant t of a discrete-time domain, a receding horizon performance index is optimized over the set of sequences of future control actions subject to a set of constraints. The first component of such an optimal sequence is used as control input at time t. The next instant $t+1$, a new optimization is carried out for a receding horizon shifted by one step ahead yielding a new control input applied at $t+1$.

Large-scale regulation problems associated with networks of multiple dynamic agents are considered in the presence of local state and input constraints as well as coupling constraints. We use a graph representation to denote the topology of a network. In this regard, a labeled node is assigned to a distinct dynamic agent and an oriented arc between two nodes indicates information exchange, a specific control objective involving the two nodes, as well as a potential dynamical coupling between the neighboring agents.

We first focus on stabilization problems of networks composed of dynamically decoupled systems. We propose a distributed network control scheme whereby each local MPC controller optimizes a local performance index which couples the dynamic behavior of neighboring agents. Sufficient conditions for local stability are explicitly derived using local value functions as Lyapunov functions. It is shown that in the presence of nonidentical agents,

the implementation of a distributed MPC scheme requires that a local control unit, in order to predict the future evolution of neighboring agents, have knowledge of model parameters of its neighbors. This requirement is made in many methods proposed for DMPC design (see for example the work in [99–101]).

Our objective is to relax this stringent condition which obliges agents to share private information across a possibly vulnerable communication scheme. We propose a model-matching feedback technique whereby agents are mapped to a target system recursively only by sharing their estimates of a global decision vector. The model-matching controller is performed in a distributed fashion and is in concert with the MPC implementation.

In the second part of the chapter, we address the problem of distributed model predictive control of dynamically coupled systems from an application point of view. In particular, we consider the load frequency control (LFC) problem examined in Chapter 8, and propose a distributed MPC method for distributed LFC design. Finally, a simulation study of a three-area power system illustrates the applicability of the proposed method.

9.2 Model predictive control for networks of dynamically decoupled systems

We investigate a receding horizon optimal control problem of a network of interconnected dynamically decoupled systems. We consider dynamic systems evolving over a discrete-time domain. We note that, although the methods proposed in the section, are compatible with a continuous-time setting, the discretization of the time interval and the system equations makes the subsequent analysis simpler and more meaningful.

9.2.1 Notation and network setup

We consider a set of M dynamically decoupled agents, their future evolution being described by the following linear difference equations:

$$x_{t+1}^i = A_i x_t^i + B_i u_t^i,\ i = 1,\dots,M, \tag{9.1}$$

where $x_t^i \in \mathbb{R}^n$, $u_t^i \in \mathbb{R}^m$ denote the state and input vectors of the i-th agent, respectively, and $A_i \in \mathbb{R}^{n\times n}$, $B_i \in \mathbb{R}^{n\times m}$. Let $\mathscr{X}^i \subseteq \mathbb{R}^n$ and $\mathscr{U}^i \subseteq \mathbb{R}^m$ be known polytopes denoting the set of feasible states and inputs of the i-th agent, respectively, i.e.,

$$x_t^i \in \mathscr{X}^i,\ u_t^i \in \mathscr{U}^i,\ \forall t \geq 0. \tag{9.2}$$

We use the following notation. Letting

$$\hat{x}_t = \mathrm{Col}(x_t^1, \ldots, x_t^M), \tag{9.3}$$

$$\hat{u}_t = \mathrm{Col}(u_t^1, \ldots, u_t^M), \tag{9.4}$$

denote aggregate state and input vectors of the overall system at instant t, respectively, we represent the set of M agents as an aggregate system as follows:

$$\hat{x}_{t+1} = \hat{A}\hat{x}_t + \hat{B}\hat{u}_t, \tag{9.5}$$

where

$$\hat{A} = \mathrm{diag}(A_1, \ldots, A_M), \tag{9.6}$$

$$\hat{B} = \mathrm{diag}(B_1, \ldots, B_M), \tag{9.7}$$

$\hat{x}_t \in \mathscr{X}$, $\hat{u}_t \in \mathscr{U}$, and $\mathscr{X}$, $\mathscr{U}$ represent the Cartesian products $\bigtimes_{i=1}^{M} \mathscr{X}^i$, $\bigtimes_{i=1}^{M} \mathscr{U}^i$, respectively.

In order to formulate an optimal control problem with a cost function which couples the dynamic behavior of the individual agents, we consider the overall system as a multi-agent network the topology of which is modeled by a graph. In particular, we define a connected graph $\mathscr{G} = (\mathscr{V}, \mathscr{E})$, where $\mathscr{V} = \{1, \ldots, M\}$ is the set of nodes and $\mathscr{E} \subseteq \mathscr{V} \times \mathscr{V}$ is the set of edges (i, j) with $i, j \in \mathscr{V}$ and $i \neq j$. Matrix $\mathscr{L}$ represents the in-degree Laplacian of $\mathscr{G}$. We assign the i-th node of $\mathscr{G}$ to the i-th labeled equation in (9.1) and consider the following interaction scheme. If edge (i, j) is present then agent-i is aware of the state x_t^j of agent-j at time t. Analogously, if $(j, i) \in \mathscr{E}$, then agent-j receives state information of agent-i. Obviously, if an edge is undirected then the associated nodes are assumed to exchange their state information at each time instant. We call $\mathscr{N}^i \subseteq \mathscr{V}$ the set of all neighboring nodes to vertex i, i.e., $j \in \mathscr{N}^i$ if $(i, j) \in \mathscr{E}$, and denote as

$$\tilde{x}_t^i = \mathrm{Col}(\ldots, x_t^p, \ldots, x_t^r, \ldots) \in \mathbb{R}^{M^i n}, \tag{9.8}$$

$$\tilde{u}_t^i = \mathrm{Col}(\ldots, u_t^p, \ldots, u_t^r, \ldots) \in \mathbb{R}^{M^i m}, \tag{9.9}$$

aggregate vectors stacking the states and the inputs, respectively, of all neighbors of agent-i, with $p, r \in \mathscr{N}^i$, $M^i = \sum_{j \in \mathscr{N}^i} 1$.

In summary, *hat* notation $(\hat{x}_t,\ \hat{u}_t)$ pertains to aggregate variables of the overall system while *tilde* notation $(\tilde{x}_t^i,\ \tilde{u}_t^i)$ refers to local variables known to an individual agent.

In the following section we formulate a large-scale receding horizon optimal control problem with a cost function which couples the agents' dynamics. We show that the stability of a centralized scheme is subject to the existence of a feasible centralized solution. A distributed version of this problem is treated later in Section 9.2.4.

9.2.2 Centralized model predictive control

Consider a discrete-time domain compatible with the aggregate system

$$\hat{x}_{t+1} = \hat{A}\hat{x}_t + \hat{B}\hat{u}_t. \tag{9.10}$$

Assume that system (9.10) is actuated over a finite future horizon of N steps ahead of instant t by an open-loop control sequence given by

$$\hat{U}_t \triangleq [\hat{u}_{0,t}, \hat{u}_{1,t}, \ldots, \hat{u}_{N-1,t}], \tag{9.11}$$

with $\hat{u}_{k,t} \in \mathscr{U}$ for $k = 0, \ldots, N-1$. In the following, we denote by $\hat{u}_{k,t}$ the computed control input at time t to be applied to system (9.10) at time $t+k$. Similarly, we denote by

$$\hat{X}_t \triangleq [\hat{x}_{0,t}, \hat{x}_{1,t}, \ldots, \hat{x}_{N,t}], \tag{9.12}$$

where $\hat{x}_{k,t} \in \mathscr{X}$ for $k = 0, \ldots, N$, the predicted state trajectory of system (9.10) initialized from $\hat{x}_t$ and actuated by the control sequence $\hat{U}_t$ in (9.11).

Let

$$l_t(\hat{x}_t, \hat{u}_t) : \mathbb{R}^{Nn} \times \mathbb{R}^{Nn} \to \mathbb{R}, \tag{9.13}$$

be a positive function, with $l_t(\mathbf{0}, \mathbf{0}) = 0$, assigning a cost to the control action $\hat{u}_t$ given the aggregate state $\hat{x}_t$ at time t. l_t is a function of the state and input vectors of all agents and may contain terms which couples the dynamic behavior of individual agents.

Given a specific cost function l_t, we consider that a central control unit (CCU) solves the following optimal control problem associated with an optimal value function $J_t^*(\hat{x}_t)$:

$$\mathscr{P}: \underset{\hat{U}_t}{\text{minimize}} \quad \sum_{k=0}^{N-1} l_t(\hat{x}_{k,t}, \hat{u}_{k,t}) + l_N(\hat{x}_{N,t}) \tag{9.14a}$$

$$\text{subject to} \quad \hat{x}_{k+1,t} = \hat{A}\hat{x}_{k,t} + \hat{B}\hat{u}_{k,t}, \quad k = 0, \ldots, N-1, \tag{9.14b}$$

$$\hat{x}_{k,t} \in \mathscr{X},\ \hat{u}_{k,t} \in \mathscr{U}, \quad k = 0, \ldots, N-1, \tag{9.14c}$$

$$\hat{x}_{N,t} \in \mathscr{X}_f, \tag{9.14d}$$

$$\hat{x}_{0,t} = \hat{x}_t, \tag{9.14e}$$

where N is the prediction horizon, l_t and l_N are positive functions representing the running and terminal costs, respectively, associated with the predicted variables $(\hat{x}_{k,t},\ \hat{u}_{k,t})$, and $(\hat{x}_{N,t})$. $\mathscr{X}_f \subseteq \mathbb{R}^{Nn}$ denotes a terminal set in the sense that the last component $\hat{x}_{N,t}$ of the predicted trajectory $\hat{X}_t$ needs to belong to $\mathscr{X}_f$. We denote by

$$\hat{U}_t^* = [\hat{u}_{0,t}, \hat{u}_{1,t}, \ldots, \hat{u}_{N-1,t}], \tag{9.15}$$

the minimizer of problem $\mathscr{P}$. $\mathscr{P}$ as formulated in (9.14) is an optimal control problem of system (9.5) which is solved in a centralized manner. In other words, we assume that there is CCU that collects global information from all individual subsystems (9.1), and solves problem $\mathscr{P}$ at each time-instant t. Once the optimal control sequence $\hat{U}_t^*$ is obtained, the CCU maintains the first component $\hat{u}_{0,t}$ which is decomposed into:

$$\hat{u}_{0,t} = \text{Col}(u_{0,t}^1, u_{0,t}^2, \ldots, u_{0,t}^M), \tag{9.16}$$

while discarding the remaining components of $\hat{U}_t^*$. Then, $u_{0,t}^i$ represents a feasible optimal control input assigned to system-i at time t. The next time step $t+1$, the CCU iterates the above procedure, collecting states from all individual agents and predicting a new state trajectory and optimal control sequence of each individual system. We say that the control policy (9.16) is a centralized model predictive control (CMPC) law. In the next section, we show that the CMPC policy (9.16) results in a stable centralized scheme subject to the existence of a feasible solution to problem (9.14) at each time t. We summarize the CMPC scheme in the following procedure:

Procedure 9.2.1. At time t:

(C1) A central control unit collects measurements of states of all subsystems and computes the minimizer $\hat{U}_t^*$ of problem $\mathscr{P}$.

(C2) The last $N-1$ components of $\hat{U}_t^*$ are discarded and the first one is decomposed into the control inputs of each individual system. The i-th system implements

$$u_t^i = u_{0,t}^i. \tag{9.17}$$

(C3) At time $t+1$, the central unit recollects the new state information $\hat{x}_{t+1}$ and repeats steps (C1), (C2).

Procedure 9.2.1 yields an optimal control law calculated in a centralized fashion using the aggregate state vector $\hat{x}_t$. Thus, the local control law u_t^i obtained in (9.17) is a feedback function

$$u_t^i = \mathscr{K}^i(\hat{x}_t), \tag{9.18}$$

of the aggregate state vector $\hat{x}_t$, implicitly defined by solving the receding horizon optimal control problem (9.14). Analogously, the global control law

$$\hat{u}_t = \mathscr{K}(\hat{x}_t), \tag{9.19}$$

is an implicit state-feedback function. We denote by

$$\hat{x}_{t+1} = f(\hat{x}_t, \hat{u}_t), \tag{9.20}$$

the closed-loop dynamics of the overall system, with $f(\hat{x}_t, \hat{u}_t) = \hat{A}\hat{x}_t + \hat{B}\mathscr{K}(\hat{x}_t)$.

9.2.3 Stability analysis of CMPC

In order to proceed with the stability analysis of (9.20), we assume the following.

Assumption 9.2.1. *The cost term in* (9.14a) *is*

$$l_t(\hat{x}_t, \hat{u}_t) = \|(I_M \otimes Q)\hat{x}_t\|_2 + \gamma\|(\mathscr{L}_c \otimes Q)\hat{x}_t\|_2 + \|(I_M \otimes R)\hat{u}_t\|_2, \tag{9.21}$$

where $Q = Q' > 0$, $R = R' > 0$, $\gamma > 0$, and $\mathscr{L}_c$ is the symmetric version of the Laplacian matrix of graph $\mathscr{G}$ (cf. (4.71)-(4.72)*).*

Assumption 9.2.2. *The terminal set $\mathscr{X}_f$ in* (9.14d) *coincides with the origin, i.e., $\hat{x}_{N,t} = \mathbf{0}$.*

Assumption 9.2.3. *The feasible sets $\mathscr{X} \subseteq \mathbb{R}^{Mn}$ and $\mathscr{U} \subseteq \mathbb{R}^{Mm}$ contain the origin in their interior.*

Remark 9.2.4. The cost function (9.21) is positive and convex with $l_t(\mathbf{0},\mathbf{0}) = 0$. With Assumption 9.2.1 in force, problem $\mathscr{P}$ admits a solution for some finite receding horizon of N steps given that $\mathscr{X}$, $\mathscr{U}$ and $\mathscr{X}_f$ represent convex compact sets.

Under Assumption 9.2.1 and 9.2.2 above, we wish to show that the Procedure 9.2.1 results in a stable centralized control scheme in the sense that

$$\lim_{t\to\infty} \hat{x}_t = \mathbf{0}, \tag{9.22}$$

$$\lim_{t\to\infty} \hat{u}_t = \mathbf{0}. \tag{9.23}$$

We prove stability of the CMPC scheme by using the value function of problem $\mathscr{P}$ as a Lyapunov function. Specifically, let

$$\hat{U}_0^* = [\hat{u}_{0,0}, \hat{u}_{1,0}, \ldots, \hat{u}_{N-1,0}], \tag{9.24}$$

be a minimizer of problem $\mathscr{P}$ for $t = 0$, initial state $\hat{x}_0$, and let also

$$\hat{X}_0 = [\hat{x}_{0,0}, \hat{x}_{1,0}, \ldots, \hat{x}_{N,0}], \tag{9.25}$$

be the predicted state trajectory of the overall system, associated with control sequence $\hat{U}_0^*$. Note that $\hat{x}_{0,0} = \hat{x}_0$ above. Let also $J^*(\hat{x}_0)$ be the optimal value function of $\mathscr{P}$ at $t = 0$, evaluated as follows

$$J^*(\hat{x}_0) = \sum_{k=0}^{N-1} \|(I_M \otimes Q)\hat{x}_{k,0}\|_2 + \gamma \sum_{k=0}^{N-1} \|(\mathscr{L}_c \otimes Q)\hat{x}_{k,0}\|_2 + \sum_{k=0}^{N-1} \|(I_M \otimes R)\hat{u}_{k,0}\|_2. \tag{9.26}$$

Consider now that the shifted control sequence

$$\hat{U}_1 = [\hat{u}_{1,0}, \ldots, \hat{u}_{N-1,0}, \mathbf{0}], \tag{9.27}$$

is implemented at $t = 1$. Since the predicted state $\hat{x}_{1,0}$ is identical to the actual state of the system at $t = 1$, $\hat{U}_1$ is a feasible control sequence in the sense that $\hat{x}_{N-1,1} = \hat{x}_{N,0} = \mathbf{0}$. The value function associated with $\hat{U}_1$ is

$$J(\hat{x}_1) = \sum_{k=0}^{N-1} \|(I_M \otimes Q)\hat{x}_{k,1}\|_2 + \gamma \sum_{k=0}^{N-1} \|(\mathscr{L}_c \otimes Q)\hat{x}_{k,1}\|_2 + \sum_{k=0}^{N-1} \|(I_M \otimes R)\hat{u}_{k,1}\|_2. \tag{9.28}$$

Since

$$\hat{x}_{k,1} = \hat{x}_{k+1,0},\ k = 0,\ldots,N-1, \tag{9.29}$$

$$\hat{u}_{k,1} = \hat{u}_{k+1,0},\ k = 0,\ldots,N-2, \tag{9.30}$$

and $\hat{u}_{N-1,1} = 0$, we may write

$$J(\hat{x}_1) = \sum_{k=1}^{N-1} \|(I_M \otimes Q)\hat{x}_{k,0}\|_2 + \gamma \sum_{k=1}^{N-1} \|(\mathscr{L}_c \otimes Q)\hat{x}_{k,0}\|_2 + \sum_{k=1}^{N-1} \|(I_M \otimes R)\hat{u}_{k,0}\|_2. \tag{9.31}$$

An upper bound of the optimal value function $J^*(\hat{x}_1)$ can be defined as follows. In view of (9.26) and (9.31), we have

$$J(\hat{x}_1) = J^*(\hat{x}_0) - \|(I_M \otimes Q)\hat{x}_0\|_2 - \gamma\|(\mathscr{L}_c \otimes Q)\hat{x}_0\|_2 - \|(I_M \otimes R)\hat{u}_0\|_2, \tag{9.32}$$

which implies that

$$J(\hat{x}_1) \leq J^*(\hat{x}_0). \tag{9.33}$$

Also, by definition of an optimal value function,

$$J^*(\hat{x}_1) \leq J(\hat{x}_1). \tag{9.34}$$

Then, from (9.32)-(9.34),

$$J^*(\hat{x}_1) \leq J^*(\hat{x}_0), \tag{9.35}$$

which implies that $J^*(\hat{x}_1)$ is a non-increasing function along the closed-loop trajectories and can be used as a Lyapunov function. In a similar fashion we can prove that $J^*(\hat{x}_t)$ is a Lyapunov function for $t \geq 2$.

In summary, Assumptions 9.2.1, 9.2.2 are sufficient conditions for the state trajectories of the closed-loop system (9.20) to converge to zero as $t \to \infty$, i.e.,

$$\lim_{t\to\infty} \hat{x}_t = 0,\ \lim_{t\to\infty} \hat{u}_t = 0. \tag{9.36}$$

9.2.4 Distributed model predictive control

In the previous two sections, we assumed that the dynamic models of all agents as well as their state information at each time instant, are known to a central control unit which implements a CMPC policy optimizing a receding horizon performance index. Proving that the optimal value function at each iteration of the MPC controller is an upper-bounded

non-increasing function, we showed that the closed-loop trajectory $\hat{x}_t$ of the overall system converges to the origin as $t \to \infty$.

In the present section, we wish to design a distributed MPC (DMPC) policy which approximates the CMPC scheme in the absence of a central control unit. In particular, we assume that the i-th individual agent representing a dynamic system with state equation as in (9.1), i) has a local control unit, ii) is aware of its own state at each time t, and iii) is aware of the model of its neighbors as well as their state information at each time instant.

Let

$$l_t^i(x_t^i, \tilde{x}_t^i, u_t, \tilde{u}_t^i) : \mathbb{R}^n \times \mathbb{R}^{M^i n} \times \mathbb{R}^m \times \mathbb{R}^{M^i m} \to \mathbb{R}, \tag{9.37}$$

be a positive local cost function with $l_t^i(\mathbf{0},\mathbf{0},\mathbf{0},\mathbf{0}) = 0$ assigning a cost to control actions u_t^i, $\tilde{u}_t^i$ given the local state vectors x_t^i, $\tilde{x}_t^i$ at time t. l_t^i is a function of state and input vectors of agent-i and its neighbors. We recall vectors $\tilde{x}_t^i$, $\tilde{u}_t^i$ are defined in (9.8) and (9.9), respectively.

Given a specific cost function l_t^i, the i-th control unit solves the following optimal control problem associated with an optimal value function $J_t^{i*}(x_t^i, \tilde{x}_t^i)$:

$$\begin{aligned}
\mathscr{P}^i: \underset{\tilde{U}_t^i}{\text{minimize}} \quad & \sum_{k=0}^{N-1} l_t^i(x_{k,t}^i, \tilde{x}_{k,t}^i, u_{k,t}^i, \tilde{u}_{k,t}^i) + l_N(x_{k,t}, \tilde{x}_{N,t}^i) && && \text{(9.38a)}\\
\text{subject to} \quad & x_{k+1,t}^i = A_i x_{k,t}^i + B_i u_{k,t}^i, && k = 0,\dots,N-1, && \text{(9.38b)}\\
& x_{k,t}^i \in \mathscr{X}^i,\ u_{k,t}^i \in \mathscr{U}^i, && k = 0,\dots,N-1, && \text{(9.38c)}\\
& x_{N,t}^i \in \mathscr{X}_f^i, && && \text{(9.38d)}\\
& x_{0,t}^i = x_t^i,, && && \text{(9.38e)}\\
& x_{k+1,t}^j = A_j x_{k,t}^j + B_j u_{k,t}^j,\ j \in \mathscr{N}^i && k = 0,\dots,N-1, && \text{(9.38f)}\\
& x_{k,t}^j \in \mathscr{X}^j,\ u_{k,t}^j \in \mathscr{U}^j,\ j \in \mathscr{N}^i && k = 0,\dots,N-1, && \text{(9.38g)}\\
& x_{N,t}^j \in \mathscr{X}_f^j, && && \text{(9.38h)}\\
& x_{0,t}^j = x_t^j, && && \text{(9.38i)}
\end{aligned}$$

where

$$\tilde{U}_t^i \triangleq [u_{0,t}^i, \tilde{u}_{0,t}^i, \dots, u_{N-1,t}^i, \tilde{u}_{N-1,t}^i] \in \mathbb{R}^{N(M^i+1)m}, \tag{9.39}$$

is the decision vector, $x_{k,t}^i$ represents the prediction made by agent-i at time t about its own state vector at time $t+k$ by assuming that system (9.1) is driven by a control sequence $u_{0,t}^i, \dots, u_{N-1,t}^i$ starting from initial condition x_t^i. Similarly, vectors $\tilde{x}_{k,t}^i$, $\tilde{u}_{k,t}^i$ in (9.38a) denote predictions made by agent-i about its neighbors. We denote by

$$\tilde{U}_t^{i*} = [u_{0,t}^i, \tilde{u}_{0,t}^i, \dots, u_{N-1,t}^i, \tilde{u}_{N-1,t}^i], \tag{9.40}$$

a minimizer of problem $\mathscr{P}^i$.

Problem $\mathscr{P}^i$ is solved locally by the control unit of agent-i. The following procedure defines the iterative implementation of a distributed MPC scheme based on the solution of problem $\mathscr{P}^i$.

Procedure 9.2.2. At time t:

(D1) The i-th control unit measures the state of agent-i and collects measurements of states of all neighboring subsystems. Based on this local information, it computes the minimizer $\tilde{U}_t^{i*}$ of $\mathscr{P}^i$.

(D2) The local control unit maintains the first component of $\tilde{U}_t^{i*}$ and implements:

$$u_t^i = u_{0,t}^i. \tag{9.41}$$

(D3) At time $t+1$, the i-th control unit recollects the new state information x_{t+1}^i, $\tilde{x}_{t+1}^i$ and repeats steps (D1), (D2).

Since problem $\mathscr{P}^i$ as formulated in (9.38) is time-invariant, minimizer $\tilde{U}_t^{i*}$ is a time-invariant function of the local state and the state of neighboring agents. Thus, the control policy u_t^i as defined in (9.41) is a time-invariant feedback control law implicitly derived from the solution of $\mathscr{P}^i$. In this regard, we may write

$$u_t^i = \mathscr{K}^i(x_t^i, \tilde{x}_t^i), \tag{9.42}$$

where $\mathscr{K}^i : \mathbb{R}^n \times \mathbb{R}^{M^i n} \to \mathbb{R}^m$.

In contrast to Procedure 9.2.1 (C1-C2-C3), Procedure 9.2.2 (D1-D2-D3) above is based on local information exchange between neighboring agents. It is clear that different control units being neighboring to each other or not, solve generically different problems. This is also evident since the structure of problem $\mathscr{P}^i$ directly depends on the topology of the associated interaction graph. Thus, it is reasonable to expect that the distributed MPC scheme described in Procedure 9.2.2, does not necessarily guarantee global feasibility and stability. Stability analysis of the DMPC scheme defined by (9.38)-(9.41) is investigated in the next section using value functions of problem $\mathscr{P}^i$ as Lyapunov functions.

9.2.5 Stability analysis of DMPC

Similarly to the stability analysis of the CMPC shown in Section 9.2.3, we assume the following.

Assumption 9.2.5. *The cost term in* (9.38a) *is*

$$l_t^i(x_t^i,\tilde{x}_t^i,u_t^i,\tilde{u}_t^i) = \|Qx_t^i\|_2 + \sum_{j\in\mathscr{N}^i}\|Qx_t^j\|_2 + \gamma\sum_{j\in\mathscr{N}^i}\|Q(x_t^i-x_t^j)\|_2 + \|Ru_t^i\|_2 + \sum_{j\in\mathscr{N}^i}\|Ru_t^j\|_2, \tag{9.43}$$

with $Q=Q'>0$, $R=R'>0$ and $\gamma>0$. Note that $\tilde{x}_t^i$, $\tilde{u}_t^i$ appearing in the left-hand side of (9.43) *denote the aggregate vectors stacking state and input vectors, respectively, of neighboring agents, appearing in the right-hand side of* (9.43) *as x_t^j, u_t^j, $j\in\mathscr{N}^i$.*

Assumption 9.2.6. *The terminal sets $\mathscr{X}_f^i$ and $\mathscr{X}_f^j$, $j\in\mathscr{N}^i$, in* (9.38d) *and* (9.38h)*, respectively, coincide with the origin, i.e., $x_{N,t}^i = x_{N,t}^j = \mathbf{0}$, $j\in\mathscr{N}^i$.*

Assumption 9.2.7. *The feasible sets $\mathscr{X}^i,\mathscr{X}^j\subseteq\mathbb{R}^n$ and $\mathscr{U}^i,\mathscr{U}^j\subseteq\mathbb{R}^m$ contain the origin in their interior, with $j\in\mathscr{N}^i$.*

To simplify the subsequent analysis, we introduce the following notation: a particular variable denoted as $\phi_{k,t}^{j,i}$ will represent a k-step ahead prediction on variable ϕ_{t+k}^j made by agent-i at time t. For instance, $x_{k,t}^{j,i}$ ($u_{k,t}^{j,i}$) denotes the state (input) of agent-j at time $t+k$ as predicted by agent-i at time t via the solution of problem $\mathscr{P}^i$. In view of this notation, cost function (9.43) can be written as

$$\begin{aligned} l_t^i(x_t^{i,i},\tilde{x}_t^{i,i},u_t^{i,i},\tilde{u}_t^{i,i}) = \|Qx_t^{i,i}\|_2 + \sum_{j\in\mathscr{N}^i}\|Qx_t^{j,i}\|_2 + \gamma\sum_{j\in\mathscr{N}^i}\|Q(x_t^{i,i}-x_t^{j,i})\|_2 \\ + \|Ru_t^{i,i}\|_2 + \sum_{j\in\mathscr{N}^i}\|Ru_t^{j,i}\|_2. \end{aligned} \tag{9.44}$$

According to Procedure 9.2.2 and under the assumptions mentioned above, suppose that agent-i solves problem $\mathscr{P}^i$, $i=1,\ldots,M$ at each time instant yielding the feedback law (9.42) denoted here as $u_{0,t}^{i,i}$. Collecting now the control policies of all agents in an aggregate input vector as

$$\hat{u}_{\hat{x}_t} = \mathrm{Col}(u_{0,t}^{1,1},\ldots,u_{0,t}^{M,M}), \tag{9.45}$$

we define the closed-loop dynamics of the overall system as

$$\hat{x}_{t+1} = f(\hat{x}_t,\hat{u}_{\hat{x}_t}), \tag{9.46}$$

where $f(\hat{x}_t,\hat{u}_{\hat{x}_t}) = \hat{A}\hat{x}_t + \hat{B}\hat{u}_{\hat{x}_t}$. In the following theorem, for a particular choice of the cost term l_t^i in (9.43), we derive sufficient conditions for local stability leading to stability of the overall system (9.46). A similar result can be found in [100].

Theorem 9.2.8. *Let M agents with dynamics defined as in* (9.1) *communicate with each other exchanging their state-information according to a connected-graph topology. Suppose that each agent represented by a node $i = \{1,\dots,M\}$ implements control policy* (9.38)-(9.41) *following Procedure 9.2.2 at each time instant t. Suppose that the cost term l_t^i in* (9.43) *is given by* (9.44) *and assume the following:*

(A1) $Q = Q' > 0$, $R = R' > 0$ *and* $\gamma > 0$.

(A2) The terminal sets $\mathscr{X}_f^i$ and $\mathscr{X}_f^j$, $j \in \mathscr{N}^i$, in (9.38d) *and* (9.38h)*, respectively, coincide with the origin, i.e., $x_{N,t}^i = x_{N,t}^j = \mathbf{0}$, $j \in \mathscr{N}^i$.*

(A3) The feasible sets $\mathscr{X}^i, \mathscr{X}^j \subseteq \mathbb{R}^n$ and $\mathscr{U}^i, \mathscr{U}^j \subseteq \mathbb{R}^m$ contain the origin in their interior, with $j \in \mathscr{N}^i$.

(A4) The following inequality:

$$\varepsilon^i - \bar{J}^i \leq 0, \tag{9.47}$$

is satisfied $\forall i = \{1,\dots,M\}$ and for all $x_t^i \in \mathscr{X}^i$, where

$$\varepsilon^i = (1+\gamma) \sum_{j \in \mathscr{N}^i} \sum_{k=1}^{N-1} (\|Q(x_{k,t}^{j,j} - x_{k,t}^{j,i})\|_2 + \|R(u_{k,t}^{j,j} - u_{k,t}^{j,i})\|_2), \tag{9.48}$$

$$\bar{J}^i = \|Qx_t^i\|_2 + \|Ru_t^i\|_2 + \sum_{j \in \mathscr{N}^i} \|Qx_t^j\|_2 + \gamma \sum_{j \in \mathscr{N}^i} \|Q(x_t^i - x_t^j)\|_2 + \sum_{j \in \mathscr{N}^i} \|Ru_{0,t}^{j,i}\|_2. \tag{9.49}$$

Then, the origin of the closed-loop system (9.46) *is asymptotically stable.*

Proof. We prove the theorem for the i-th agent using the value function of problem $\mathscr{P}^i$. Let

$$\tilde{U}_t^{i*} = [u_{0,t}^{i,i}, \tilde{u}_{0,t}^{i,i}, \dots, u_{N-1,t}^{i,i}, \tilde{u}_{N-1,t}^{i,i}], \tag{9.50}$$

be the minimizer of problem $\mathscr{P}^i$ at time t and

$$J_t^{i*}(x_t^i, \tilde{x}_t^i) = \sum_{k=0}^{N-1} \|Qx_{k,t}^{i,i}\|_2 + \sum_{j \in \mathscr{N}^i} \sum_{k=0}^{N-1} \|Qx_{k,t}^{j,i}\|_2 + \gamma \sum_{j \in \mathscr{N}^i} \sum_{k=0}^{N-1} \|Q(x_{k,t}^{i,i} - x_{k,t}^{j,i})\|_2 + \sum_{k=0}^{N-1} \|Ru_{k,t}^{i,i}\|_2 + \sum_{j \in \mathscr{N}^i} \sum_{k=0}^{N-1} \|Ru_{k,t}^{j,i}\|_2, \tag{9.51}$$

be the associated optimal value function. We denote by

$$U_t^{i,i*} = [u_{0,t}^{i,i}, \ldots, u_{N-1,t}^{i,i}], \tag{9.52}$$

$$U_t^{j,i*} = [u_{0,t}^{j,i}, \ldots, u_{N-1,t}^{j,i}], \tag{9.53}$$

the optimal control sequence of agent-i and agent-j as predicted by agent-i at time t, with $i, j = 1, \ldots, M$, $j \neq i$ and $j \in \mathscr{N}^i$. The shifted control sequences

$$U_{t+1}^{i,i} = [u_{1,t}^{i,i}, \ldots, u_{N-1,t}^{i,i}, \mathbf{0}], \tag{9.54}$$

$$U_{t+1}^{j,i} = [u_{1,t}^{j,i}, \ldots, u_{N-1,t}^{j,i}, \mathbf{0}], \tag{9.55}$$

with $j \in \mathscr{N}^i$, are not necessarily feasible at the next time-step $t+1$ since there is a possible mismatch between the predicted state $x_{0,t+1}^{j,i}$ and the actual state x_{t+1}^j. Clearly, $x_{0,t+1}^{j,j} = x_{t+1}^j$ which implies that the following shifted control sequences are feasible at time $t+1$ for agent-i:

$$U_{t+1}^{i,i} = [u_{1,t}^{i,i}, \ldots, u_{N-1,t}^{i,i}, \mathbf{0}], \tag{9.56}$$

$$U_{t+1}^{j,j} = [u_{1,t}^{j,j}, \ldots, u_{N-1,t}^{j,j}, \mathbf{0}], \tag{9.57}$$

with $j \in \mathscr{N}^i$. Let now

$$\begin{aligned} J_{t+1}^i(x_{t+1}^i, \tilde{x}_{t+1}^i) = \sum_{k=0}^{N-1} \|Qx_{k,t+1}^{i,i}\|_2 + \sum_{j\in\mathscr{N}^i} \sum_{k=0}^{N-1} \|Qx_{k,t+1}^{j,i}\|_2 + \gamma \sum_{j\in\mathscr{N}^i} \sum_{k=0}^{N-1} \|Q(x_{k,t+1}^{i,i} - x_{k,t+1}^{j,i})\|_2 \\ + \sum_{k=0}^{N-1} \|Ru_{k,t+1}^{i,i}\|_2 + \sum_{j\in\mathscr{N}^i} \sum_{k=0}^{N-1} \|Ru_{k,t+1}^{j,i}\|_2, \end{aligned} \tag{9.58}$$

be the value function of $\mathscr{P}^i$ associated with control sequences $U_{t+1}^{i,i}$, $U_{t+1}^{j,j}$, $j \in \mathscr{N}^i$ as defined in (9.56), (9.57), respectively. Substituting

$$x_{k,t+1}^{i,i} = x_{k+1,t}^{i,i},\ 0 \leq k \leq N-1, \tag{9.59}$$

$$x_{k,t+1}^{j,i} = x_{k+1,t}^{j,j},\ 0 \leq k \leq N-1, \tag{9.60}$$

and

$$u_{k,t+1}^{i,i} = u_{k+1,t}^{i,i},\ 0 \leq k \leq N-2, \tag{9.61}$$

$$u_{k,t+1}^{j,i} = u_{k+1,t}^{j,j},\ 0 \leq k \leq N-2, \tag{9.62}$$

in (9.58), yields

$$J_{t+1}^i(x_{t+1}^i,\tilde{x}_{t+1}^i) = \sum_{k=1}^{N-1}\|Qx_{k,t}^{i,i}\|_2 + \sum_{j\in\mathcal{N}^i}\sum_{k=1}^{N-1}\|Qx_{k,t}^{j,j}\|_2 + \gamma\sum_{j\in\mathcal{N}^i}\sum_{k=1}^{N-1}\|Q(x_{k,t}^{i,i}-x_{k,t}^{j,j})\|_2 + \sum_{k=1}^{N-1}\|Ru_{k,t}^{i,i}\|_2 + \sum_{j\in\mathcal{N}^i}\sum_{k=1}^{N-1}\|Ru_{k,t}^{j,j}\|_2, \tag{9.63}$$

which is also consistent with $x_{N,t}^{i,i}=0$, $x_{N,t}^{j,j}=0$ due to feasibility of control sequences (9.56), (9.57). In view of (9.51) and (9.63), we may write

$$\begin{aligned} J_{t+1}^i(x_{t+1}^i,\tilde{x}_{t+1}^i) &= J_t^{i*}(x_t^i,\tilde{x}_t^i) \\ &- \|Qx_t^i\|_2 - \|Ru_t^i\|_2 - \sum_{j\in\mathcal{N}^i}\|Qx_t^j\|_2 - \gamma\sum_{j\in\mathcal{N}^i}\|Q(x_t^i-x_t^j)\|_2 - \sum_{j\in\mathcal{N}^i}\|Ru_t^{j,i}\|_2 \\ &+ \sum_{j\in\mathcal{N}^i}\sum_{k=1}^{N-1}(\|Qx_{k,t}^{j,j}\|_2 - \|Qx_{k,t}^{j,i}\|_2) + \sum_{j\in\mathcal{N}^i}\sum_{k=1}^{N-1}(\|R(u_{k,t}^{j,j}\|_2 - \|Ru_{k,t}^{j,i})\|_2) \\ &+ \gamma\sum_{j\in\mathcal{N}^i}\sum_{k=1}^{N-1}(\|Q(x_{k,t}^{i,i}-x_{k,t}^{j,j})\|_2 - \gamma\sum_{j\in\mathcal{N}^i}\sum_{k=1}^{N-1}(\|Q(x_{k,t}^{i,i}-x_{k,t}^{j,i})\|_2. \end{aligned} \tag{9.64}$$

Using a variation of the *triangle inequality axiom* of norms:

$$\|a-b\| \geq \|a\| - \|b\|, \tag{9.65}$$

we have

$$\sum_{j\in\mathcal{N}^i}\sum_{k=1}^{N-1}(\|Qx_{k,t}^{j,j}\|_2 - \|Qx_{k,t}^{j,i}\|_2) \leq \sum_{j\in\mathcal{N}^i}\sum_{k=1}^{N-1}(\|Qx_{k,t}^{j,j} - Qx_{k,t}^{j,i}\|_2), \tag{9.66}$$

$$\sum_{j\in\mathcal{N}^i}\sum_{k=1}^{N-1}(\|R(u_{k,t}^{j,j}\|_2 - \|Ru_{k,t}^{j,i})\|_2) \leq \sum_{j\in\mathcal{N}^i}\sum_{k=1}^{N-1}(\|R(u_{k,t}^{j,j} - Ru_{k,t}^{j,i})\|_2) \tag{9.67}$$

$$+\gamma\sum_{j\in\mathcal{N}^i}(\sum_{k=1}^{N-1}\|Q(x_{k,t}^{i,i}-x_{k,t}^{j,j})\|_2 - \sum_{k=1}^{N-1}\|Q(x_{k,t}^{i,i}-x_{k,t}^{j,i})\|_2) \leq \gamma\sum_{j\in\mathcal{N}^i}\sum_{k=1}^{N-1}(\|Q(x_{k,t}^{j,j}-x_{k,t}^{j,i})\|_2, \tag{9.68}$$

where the sum of the right side of the inequalities above equals ε^i as given in (9.48). Then, from (9.64), (9.66)-(9.68), we have

$$J_{t+1}^i(x_{t+1}^i,\tilde{x}_{t+1}^i) \leq J_t^{i*}(x_t^i,\tilde{x}_t^i) - \bar{J}^i + \varepsilon^i, \tag{9.69}$$

where ε^i, $\bar{J}^i$, are given in (9.48), (9.49), respectively. Letting $J^{i*}_{t+1}(x^i_{t+1}, \tilde{x}^i_{t+1})$ be the optimal value function of problem $\mathscr{P}^i$ at time $t+1$, we have

$$J^{i*}_{t+1}(x^i_{t+1}, \tilde{x}^i_{t+1}) \leq J^i_{t+1}(x^i_{t+1}, \tilde{x}^i_{t+1}), \tag{9.70}$$

while due to Assumption (A4), we may write

$$J^i_{t+1}(x^i_{t+1}, \tilde{x}^i_{t+1}) \leq J^{i*}_t(x^i_t, \tilde{x}^i_t). \tag{9.71}$$

From (9.70) and (9.71), we have

$$J^{i*}_{t+1}(x^i_{t+1}, \tilde{x}^i_{t+1}) \leq J^{i*}_t(x^i_t, \tilde{x}^i_t), \tag{9.72}$$

which further implies that the optimal value function of $\mathscr{P}^i$ is positive and non-increasing along the closed-loop trajectories and thus, can be used as Lyapunov function for agent-i. In view of the positive definiteness of weighting matrices Q, R, inequality (9.47) is sufficient to guarantee that

$$\lim_{t\to\infty} x^i_t = 0, \ \lim_{t\to\infty} u^i_t = 0. \tag{9.73}$$

Overall stability for the aggregate system is established by proving the same arguments for $i = 1, \ldots, M$. □

The main implications of Theorem 9.2.8 are listed below.

(i) The term ε^i appearing in (9.47) and defined in (9.48), can be cast as a mismatch measure between predictions of state trajectories obtained by different (neighboring) nodes. Theorem 9.2.8 emphasizes that this prediction error is crucial for the stability of the DMPC scheme (9.38)-(9.41) which may lead to instability phenomena if the error is excessive. The larger the error, the smaller the set of state trajectories along which the value function of problem $\mathscr{P}^i$ decreases.

(ii) Since the mismatch between predicted and actual system variables are fundamental for the stability of a distributed MPC policy, it is sensible to expect that enabling further information exchange between neighboring agents may lead to more restrictive conditions for stability. More specifically, allowing the exchange of optimal solutions between interconnected subsystems may reduce the mismatch size ε^i thereby relaxing condition (9.47).

(iii) Viewing (9.49), the term $\bar{J}^i$ in (9.47) starts to diminish as state trajectories approach the origin, leading to more tight restrictions on the admissible prediction mismatch indicated by ε^i in (9.47).

(iv) The effect of prediction horizon length on the performance and stability of the DMPC scheme (9.38)-(9.41) is especially hard to identify analytically and in general may differ from typical centralized model predictive control results. For instance, based on the stability condition (9.47), it is readily observed that the terms in ε^i grow redundant by extending the prediction horizon. Therefore, if the prediction horizon length is too long, ε^i may increase excessively thereby leading to violation of inequality (9.47).

DMPC policy (9.38)-(9.41) in order to be implementable, requires each individual agent be aware of the model parameters of its neighbors. Although this information can either be shared offline or in one go, sharing fundamental parameters across a possibly vulnerable communication scheme may be unacceptable or undesirable in some circumstances. In the following section, in order to bypass the peculiarity of transmitting confidential information between agents, we consider the class of linear systems with identical sets of controllability indices and propose a hybrid method which incorporates the model-matching concept studied in Chapter 5, into a distributed model predictive control setting. Next, we briefly review some basic results of Chapter 5 which will help us extend the model-matching method to the discrete-time case.

9.2.6 Model-matching control for discrete-time linear systems

We define the following class of linear systems corresponding to families of systems with identical sets of controllability indices.

Definition 9.2.1. Let $(\bar{A}_d,\, \bar{B}_d) \in \mathbb{R}^{n\times n} \times \mathbb{R}^{n\times m}$, with $\operatorname{rank}(\bar{B}_d) = m$. Define the set:

$$\begin{aligned} S(\bar{A}_d,\, \bar{B}_d) = \{P(\bar{A}_d + \bar{B}_d Z)P^{-1},\, P\bar{B}_d G^{-1}) :\ & P \in \mathbb{R}^{n\times n} \text{ with } \det(P) \neq 0, \\ & Z \in \mathbb{R}^{m\times n}, \\ & G \in \mathbb{R}^{m\times m} \text{ with } \det(G) \neq 0\}. \end{aligned} \tag{9.74}$$

Let $(A_i,\, B_i) \in S(\bar{A}_d,\, \bar{B}_d)$ with $i = 1, \ldots, M$. By Definition 9.2.1, there exist a state-space transformation P_i, a state-feedback gain F_i, and an input scaling matrix G_i such that

$$\begin{aligned} P_i(A_i + B_i F_i)P_i^{-1} &= \bar{A}_d, \\ P_i B_i G_i &= \bar{B}_d, \end{aligned} \tag{9.75}$$

for all $i = 1, \ldots, M$. We say that systems $(A_i,\ B_i)$, $i = 1, \ldots, M$, are feedback equivalent and can match their dynamics via the model-matching operations (9.75). We recall that for the family of controllable continuous-time systems with identical sets of controllability indices, the existence of $(P_i,\ F_i,\ G_i)$ is guaranteed as proved in Theorem 5.2.3, Chapter 5. Since the set of controllability indices of a controllable discrete-time system, say $(A,\ B)$, can be obtained by constructing matrices $\mathscr{C}$, $\bar{\mathscr{C}}$ in a similar manner as in (5.8), (5.9), respectively, Theorem 5.2.3 as well as Definition 9.2.1 are compatible with controllable discrete-time systems.

We now focus on sets of controllable discrete-time models that are derived from continuous time systems with identical sets of controllability indices, via a discretization method with identical sampling periods.

Consider M continuous-time LTI systems with dynamics described by the following state-space equations:

$$\dot{x}^i = A_i x^i + B_i u^i,\ x^i(0) = x_0^i,\ i = 1, \ldots, M, \tag{9.76}$$

where $x^i \in \mathscr{X}^i$, $u^i \in \mathscr{U}^i$ represent the state and input vectors of the i-th system, respectively, and pairs $(A_i,\ B_i)$, $i = 1, \ldots, M$, have identical sets of controllability indices denoted by $\mu_1, \ldots, \mu_m$. For simplicity, assume that $\mathscr{X}^i \equiv \mathbb{R}^n$, $\mathscr{U}^i \equiv \mathbb{R}^m$, and that the state variables of (9.76) are selected such that all systems $(A_i,\ B_i)$, $i = 1, \ldots, M$, are in controllable canonical form. Under these assumptions, as shown in Chapter 5, we may express matrices A_i, B_i as:

$$A_i = \bar{A}_c + \bar{B}_c A_{m,i}, \tag{9.77}$$

$$B_i = \bar{B}_c B_{m,i}, \tag{9.78}$$

where $(\bar{A}_c,\ \bar{B}_c)$ denotes the Brunovsky canonical form associated with controllability indices $\mu_1, \ldots, \mu_m$, and $A_{m,i} \in \mathbb{R}^{m \times n}$, $B_{m,i} \in \mathbb{R}^{m \times m}$ for $i = 1, \ldots, M$.

Let now t_s be an appropriate sampling period such that the following equations

$$\frac{x^i(t + t_s) - x^i(t)}{t_s} = A_i x^i(t) + B_i u^i(t),\ i = 1, \ldots, M, \tag{9.79}$$

are good approximations to (9.76), and define matrices

$$A_{d,i} = t_s \underbrace{(\bar{A}_c + \bar{B}_c A_{m,i})}_{A_i} + I_n, \tag{9.80}$$

$$B_{d,i} = t_s \underbrace{\bar{B}_c B_{m,i}}_{B_i}, \tag{9.81}$$

for $i = 1, \ldots, M$. The discrete-time approximate models to continuous-time systems (9.76) can then be written as:

$$x_{t+1}^i = A_{d,i} x_t^i + B_{d,i} u_t^i, \tag{9.82}$$

where $x_t^i = x^i(t)$, $u_t^i = u^i(t)$ and the distance between time instants $t+1$ and t is selected as t_s. Defining

$$\bar{A}_d = t_s \bar{A}_c + I_n, \tag{9.83}$$

$$\bar{B}_d = t_s \bar{B}_c, \tag{9.84}$$

matrices $A_{d,i}$, $B_{d,i}$ above, are expressed as

$$A_{d,i} = \bar{A}_d + \bar{B}_d A_{m,i}, \tag{9.85}$$

$$B_{d,i} = \bar{B}_d B_{m,i}. \tag{9.86}$$

Clearly, the pair $(\bar{A}_d,\ \bar{B}_d)$ only depends on the set of controllability indices $\mu_1, \ldots, \mu_m$ and the sampling interval t_s. We write systems (9.82) as:

$$x_{t+1}^i = (\bar{A}_d + \bar{B}_d A_{m,i}) x_t^i + \bar{B}_d B_{m,i} u_t^i, \tag{9.87}$$

with $i = 1, \ldots, M$. Setting now

$$u_t^i = B_{m,i}^{-1}(-A_{m,i} x_t^i + v_t^i), \tag{9.88}$$

with $v_t^i \in \mathbb{R}^m$, systems (9.82) are written as

$$x_{t+1}^i = (\bar{A}_d + \bar{B}_d A_{m,i}) x_t^i + \bar{B}_d B_{m,i} [B_{m,i}^{-1}(-A_{m,i} x_t^i + v_t^i)], \tag{9.89}$$

or

$$x_{t+1}^i = \bar{A}_d x_t^i + \bar{B}_d v_t^i, \tag{9.90}$$

with $i = 1, \ldots, M$. We note that under control law (9.88), systems (9.82) acquire identical dynamics denoted by the pair $(\bar{A}_d,\ \bar{B}_d)$. We refer to $(\bar{A}_d,\ \bar{B}_d)$ as a target system and to (9.88) as the associated model-matching controller. Similarly, setting

$$u_t^i = F^i x_t^i + B_{m,i}^{-1} w_t^i, \tag{9.91}$$

in (9.88), with $w_t^i \in \mathbb{R}^m$,

$$F^i = B_{m,i}^{-1}(\Xi - A_{m,i}), \tag{9.92}$$

and $\Xi \in \mathbb{R}^{m\times n}$, for $i = 1, \ldots, M$, yields a new target system described by $(\bar{A}_d + \bar{B}_d\Xi,\ \bar{B}_d)$. In the following, we adopt the zero-order-hold method for discretizing continuous-time systems. We firstly describe the discretization method for a single system and then, we consider the zero-order-hold method for discretizing continuous-time systems with identical sets of controllability indices.

Let the controllable continuous-time system

$$\dot{x} = Ax + Bu, \tag{9.93}$$

with $A \in \mathbb{R}^{n\times n}$, $B \in \mathbb{R}^{n\times m}$, be in controllable canonical form, i.e.,

$$A = \bar{A}_c + \bar{B}_c A_m,\ B = \bar{B}_c B_m, \tag{9.94}$$

where $(\bar{A}_c,\ \bar{B}_c)$ represents the Brunovsky form associated with the set of controllability indices of $(A,\ B)$. Using (9.94), we may write system (9.93) as

$$\dot{x} = (\bar{A}_c + \bar{B}_c A_m)x + \bar{B}_c B_m u, \tag{9.95}$$

or

$$\dot{x} = \bar{A}_c x + \begin{bmatrix} \bar{B}_c A_m & \bar{B}_c B_m \end{bmatrix} \begin{bmatrix} x \\ u \end{bmatrix}. \tag{9.96}$$

A discrete-time (zero-order-hold) equivalent to system (9.96) can be written as

$$x_{t+1} = \bar{A}_d x_t + \begin{bmatrix} \bar{B}_d A_m & \bar{B}_d B_m \end{bmatrix} \begin{bmatrix} x_t \\ u_t \end{bmatrix}, \tag{9.97}$$

where

$$\bar{A}_d = \mathrm{e}^{\bar{A}_c t_s}, \tag{9.98}$$

$$\bar{B}_d = \left(\int_0^{t_s} \mathrm{e}^{\bar{A}_c t} \mathrm{dt} \right) \bar{B}_c, \tag{9.99}$$

with t_s denoting the sampling period. Writing now system (9.97) in a compact form, yields

$$x_{t+1} = (\bar{A}_d + \bar{B}_d A_m) x_t + \bar{B}_d B_m u_t. \tag{9.100}$$

Note that allowing $A_m \in \mathbb{R}^{m \times n}$, $B_m \in \mathbb{R}^{m \times m}$ to be any real $m \times n$, $m \times m$ matrix, respectively, system (9.100) defines a parametric family of discrete-time models derived from the canonical form of continuous-time systems with identical sets of controllability indices via the zero-order-hold method with identical sampling periods t_s. This is highlighted in the following definition.

Definition 9.2.2. Let $(\bar{A}_c,\ \bar{B}_c) \in \mathbb{R}^{n \times n} \times \mathbb{R}^{n \times m}$ be the Brunovsky form associated with the set of controllability indices: $\{\mu_1, \ldots, \mu_m\}$. Let also

$$\bar{A}_d = \mathrm{e}^{\bar{A}_c t_s},\ \bar{B}_d = \left(\int_0^{t_s} \mathrm{e}^{\bar{A}_c t} \mathrm{dt} \right) \bar{B}_c, \tag{9.101}$$

with $t_s > 0$, and define the set:

$$S(\bar{A}_c,\ \bar{B}_c) = \{(\bar{A}_d + \bar{B}_d A_m,\ \bar{B}_d B_m) :\ A_m \in \mathbb{R}^{m \times n},\ B_m \in \mathbb{R}^{m \times m} \text{ with } \det(B_m) \neq 0\}. \tag{9.102}$$

The model-matching procedure is summarized as follows. Consider the following set of controllable continuous-time systems:

$$\dot{x}^i = A_i x^i + B_i u^i,\ i = 1, \ldots, M, \tag{9.103}$$

where $x^i \in \mathbb{R}^n$, $u^i \in \mathbb{R}^m$ represent the state and input vectors of the i-th system. Assume that the sets of controllability indices of $(A_i,\ B_i)$, $i = 1, \ldots, M$, coincide, and that pairs $(A_i,\ B_i)$, $i = 1, \ldots, M$, are in controllable canonical form, i.e.,

$$A_i = \bar{A}_c + \bar{B}_c A_{m,i},\ B_i = \bar{B}_c B_{m,i}, \tag{9.104}$$

where $(\bar{A}_c,\ \bar{B}_c)$ is the Brunovsky form associated with the controllability indices of the pairs $(A_i,\ B_i)$, $i = 1,\ldots,M$, and $A_{m,i} \in \mathbb{R}^{m\times n}$, $B_{m,i} \in \mathbb{R}^{m\times m}$, $\det(B_{m,i}) \neq 0$. Let

$$x_{t+1}^i = (\bar{A}_d + \bar{B}_d A_{m,i})x_t^i + \bar{B}_d B_{m,i} u_t^i,\ i = 1,\ldots,M, \tag{9.105}$$

with $\bar{A}_d$, $\bar{B}_d$ given in (9.101), be the zero-order-hold equivalent models to systems (9.103) with sampling period t_s. Then,

$$u_t^i = F^i x_t^i + B_{m,i}^{-1} w_t^i, \tag{9.106}$$

with

$$F^i = B_{m,i}^{-1}(\Xi - A_{m,i}), \tag{9.107}$$

$\Xi \in \mathbb{R}^{m\times n}$, $v_t^i \in \mathbb{R}^m$, for $i = 1,\ldots,M$, is a model-matching control law whereby dynamics of (9.105) become identical:

$$x_{t+1}^i = (\bar{A}_d + \bar{B}_d \Xi)x_t^i + \bar{B}_d w_t^i. \tag{9.108}$$

In other words, the model-matching control protocol (9.106)-(9.107) yields a zero-order-hold target model denoted by the pair $(\bar{A}_d + \bar{B}_d\Xi,\ \bar{B}_d)$. In the following, we recall how to select an optimal target model.

Let the joint model-matching control effort produced by the application of control protocol (9.106)-(9.107) be expressed as a function of the individual state-feedback gains F^i given in (9.107). In this regard, an optimal target system can be defined by solving the following least-squares problem:

$$\underset{\Xi\ \in\ \mathbb{R}^{m\times n}}{\text{minimize}} \quad \sum_{i=1}^{M} \|F^i\|_F^2 = \|B_{m,i}^{-1}(\Xi - A_{m,i})\|_F^2. \tag{9.109}$$

As shown in Chapter 5, problem (9.109) can be transformed to

$$\underset{\xi\ \in\ \mathbb{R}^{nm}}{\text{minimize}} \quad \sum_{i=1}^{M} \|H_i\xi - c_i\|_2^2, \tag{9.110}$$

using the isometric embedding of the Frobenius norm of $B_{m,i}^{-1}(\Xi - A_{m,i})$ into the Euclidean norm of vector $H_i\xi - c_i$, where $H_i = I_n' \otimes B_{m,i}^{-1}$, $\xi = \text{vec}(\Xi)$, $c_i = \text{vec}(C_i)$ with $C_i = B_{m,i}^{-1}A_{m,i}$. Due to convexity of $\|H_i\xi - c_i\|_2^2$, the unique minimizer of (9.110), denoted here as ξ^*, can be found analytically. Then, the unique minimizer Ξ^* of (9.109) is obtained from

$$\Xi^* = \text{vec}^{-1}(\xi^*). \tag{9.111}$$

We emphasize that problem (9.110) is a centralized least-squares task which is solved analytically using global information. In the following, we wish to address problem (9.110) by a cooperative process which is carried out locally. Specifically, we show that using a distributed optimization algorithm performed at individual-system level, an optimal target system can be attained recursively. In the following paragraph, we describe a distributed gradient descent algorithm.

9.2.6.1 Distributed gradient descent algorithm

Let the least-squares problem

$$\underset{\xi \in \mathbb{R}^p}{\text{minimize}} \quad \sum_{i=1}^{M} f^i(\xi), \tag{9.112}$$

defined on a connected graph $\mathscr{G} = (\mathscr{V}, \mathscr{E})$, be solved cooperatively by M agents, over a common decision variable $\xi \in \mathbb{R}^p$. We assume that $f_i : \mathbb{R}^p \to \mathbb{R}$ is a continuously differentiable convex function privately known by agent-i only. We present the following distributed gradient descent (DGD) algorithm which solves (9.112) locally. DGD carries out the following iteration:

$$\xi_{t+1}^i = w_{ii}\xi_t^i + \sum_{j \in \mathscr{N}^i} w_{ij}\xi_t^j - \alpha_t \nabla f^i(\xi_t^i), \text{ for } i = 1, \ldots, M, \tag{9.113}$$

where $\xi_t \in \mathbb{R}^p$ represents a local copy (estimate) of the global decision vector ξ, held by agent-i at iteration t. Values w_{ij}, with $i, j \in \mathscr{V}$, represent the entries of a symmetric *mixing* matrix $W = [w_{ij}] \in \mathbb{R}^{M \times M}$ which satisfies the following:

$$\text{null}(I - W) = \text{span}\{\mathbf{1}\}, \tag{9.114}$$

$$\sigma_{\max}(W - \frac{1}{M}\mathbf{1}\mathbf{1}') < 1. \tag{9.115}$$

Parameter $\alpha_t > 0$ is the step size for the t-th iteration, and $\nabla f^i(\xi_t^i)$ denotes the gradient of f^i at ξ_t^i. Methods for how to select a step-size α_t as well as variations of the DGD method can be found in [239, 92] and [151, 192], respectively. Detailed description of the algorithm along with convergence results are beyond the scope of this section. A list of important results on (sub)gradient methods for distributed optimization can be found in Section 2.4. Next, we adopt DGD algorithm (9.113) for solving the centralized least-squares problem (9.110) in a distributed fashion.

9.2.6.2 Cooperative model-matching

Problem (9.110) is in the form of problem (9.112) and thus is compatible with the DGD algorithm (9.113). In particular, we may write

$$f^i(\xi^i) = \|H_i\xi^i - c_i\|_2^2 = (\xi^{i\prime}H_i' - c_i')(H_i\xi^i - c_i) = \xi^{i\prime}(H_i'H_i)\xi^i - 2\xi^{i\prime}(H_i'c_i) + c_i'c_i, \tag{9.116}$$

which is a quadratic function of ξ^i and thus

$$\nabla f^i(\xi^i) = 2H_i'H_i\xi^i - 2H_i'c_i, \tag{9.117}$$

is an affine function of ξ^i. In view of (9.117), a distributed optimization algorithm performed by agent-i for solving problem (9.110) locally, is written as

$$\xi_{t+1}^i = w_{ii}\xi_t^i + \sum_{j\in\mathscr{N}^i} w_{ij}\xi_t^j - \alpha_t \underbrace{(2H_i'H_i\xi_t^i - 2H_i'c_i)}_{\nabla f^i(\xi_t^i)}, \tag{9.118}$$

with $i = 1,\ldots,M$. Assuming undirected communication between neighboring agents and denoting by $\mathscr{L}$ the Laplacian matrix of graph $\mathscr{G}$, a Laplacian-based mixing matrix W can be selected as $W = I - \frac{1}{\rho}\mathscr{L}$ where ρ is a scaling parameter with $\rho > \frac{1}{2}\lambda_{\max}(\mathscr{L})$, $\lambda_{\max} \in S(\mathscr{L})$, [192]. Also, the update rule

$$\alpha_t = \frac{1}{(t)^{\frac{1}{2}}}, \tag{9.119}$$

allows for diminishing step size selection ensuring exact convergence with a maximum convergence rate of $O(\frac{\ln t}{\sqrt{t}})$, [192].

Suppose now that ξ_t^i is an estimate of the unique minimizer ξ^* of problem (9.110) computed by agent-i at time t and let

$$\Xi_t^i = \mathrm{vec}^{-1}(\xi_t^i), \tag{9.120}$$

represent an estimate of the unique minimizer Ξ^* of problem (9.109) maintained by agent-i. Then, adopting the feedback policy (9.106)-(9.107) in the present setting, the i-th model-matching controller can be defined as

$$u_t^i = F_t^i x_t^i + B_{m,i}^{-1} w_t^i, \tag{9.121}$$

where $w_t^i \in \mathbb{R}^m$ and

$$F_t^i = B_{m,i}^{-1}(\Xi_t^i - A_{m,i}), \tag{9.122}$$

is an estimate of the optimal model-matching state-feedback gain $F^{i*} = B_{m,i}^{-1}(\Xi^* - A_{m,i})$ obtained at time t. Since F_t^i is completely computed using local information only, the model-matching policy (9.121)-(9.122) is a distributed control protocol. We summarize the distributed model-matching task in the following procedure.

Procedure 9.2.3. At time t, agent-i

(M1) collects estimates ξ_{t-1}^j, $j \in \mathscr{N}^i$, received from neighboring agents at time $t-1$ and obtains an updated estimate ξ_t^i by performing (9.118),

(M2) sends the new estimate ξ_t^i to neighbors and receives their updates,

(M3) computes $\Xi_t^i = \text{vec}^{-1}(\xi_t^i)$,

(M4) constructs state feedback gain F_t^i by (9.122).

We also emphasize the following remarks.

Remark 9.2.9. In view of step (M2) of Procedure 9.2.3, agent-i receives neighboring updates ξ_t^j, $j \in \mathscr{N}^i$ thereby being able to construct matrix Ξ_t^j by

$$\Xi_t^j = \text{vec}^{-1}(\xi_t^j). \tag{9.123}$$

This allows agent-i to predict the state evolution of neighboring agent-j using the state-space equation

$$x_{t+1}^{j,i} = (\bar{A}_d + \bar{B}_d \Xi_t^j) x_t^{j,i} + \bar{B}_d w_t^{j,i}, \tag{9.124}$$

in a model-predictive setup. Note also that system $(\bar{A}_d + \bar{B}_d \Xi_t^j,\ \bar{B}_d)$ represents an estimate of the optimal target system maintained by agent-j at time t.

Remark 9.2.10. The model-matching control protocol (9.121)-(9.122) combined with DGD algorithm (9.118) enables agents to match their dynamics with an optimal target system without any requirement of sharing their model parameters. This absence of transmitting systems' significant information across a possibly vulnerable communication network may be beneficial for multi-agent cyber-physical control schemes prone to malicious cyber activities.

In the following section, we adapt the model-matching control protocol (9.121)-(9.122) to a model predictive control setting.

9.2.7 Distributed model-matching based MPC protocols

Throughout the thesis, it has been highlighted that the information exchange between agents enables multi-agent distributed control problems to be addressed at individual level. Further, in Section 9.2.4, it is shown that receding horizon optimal control problems over networks of multiple systems can be solved locally provided that each individual system is aware of the model parameters of its neighbors. In the present section, we focus on a particular class of linear systems with identical sets of controllability indices, and propose a distributed network control protocol which allows individual systems to 1) exchange state-information locally, 2) map their dynamics to a target system using local information, 3) keep their model parameters private, 4) predict the state evolution of their neighbors, and 5) solve a receding horizon control problem. The solution of the latter yields an implicit stabilizing feedback controller that couples the dynamic behavior of interconnected systems.

In particular, we wish to develop a distributed model-matching based MPC protocol for networks composed of multiple agents whose dynamics are described by linear systems with identical sets of controllability indices. For control design purposes, we focus on discretized models obtained as the zero-order-hold equivalent to continuous-time systems characterized by identical sets of controllability indices. We represent a network of M agents as a connected graph $\mathscr{G} = (\mathscr{V}, \mathscr{E})$ of M nodes as described in Section 9.2.1. In this regard, node-i, $i \in \mathscr{V}$, is assigned to agent-i and the presence of an edge $(i, j) \in \mathscr{E}$ indicates that agent-j is a neighbor of agent-i. In other words, agent-i is able to receive information from agent-j with $j \in \mathscr{N}^i$. The dynamics of agent-i in the continuous-time domain are described by the following continuous-time state-space equation:

$$\dot{z}^i = A_i z^i + B_i u^i, \tag{9.125}$$

with $z^i \in \mathscr{Z}^i$, $u^i \in \mathscr{U}^i$ representing the state and input vectors of agent-i, respectively. We assume that each agent is aware of a state-space transformation $z^i \to x^i = P_i z^i$ under which

$$P_i A_i P_i^{-1} = \bar{A}_c + \bar{B}_c A_{m,i}, \tag{9.126}$$

$$P_i B_i = \bar{B}_c B_{m,i}, \tag{9.127}$$

where $A_{m,i} \in \mathbb{R}^{m \times n}$, $B_{m,i} \in \mathbb{R}^{m \times m}$, and $\bar{A}_c \in \mathbb{R}^{n \times n}$, $\bar{B}_c \in \mathbb{R}^{n \times m}$ are in concert with Definition 9.2.2. Then, the discretized state-space form of the i-th agent in the transformed coordinates is written as

$$x^i_{t+1} = (\bar{A}_d + \bar{B}_d A_{m,i}) x^i_t + \bar{B}_d B_{m,i} u^i_t, \tag{9.128}$$

where $x_t^i \in \mathscr{X}^i$, for $i = 1,\ldots,M$. In the following, we require that the control function u_t^i is designed on the coordinate system $x^i = P_i z^i$. Note that, systems (9.128) are compatible with the model-matching control protocol (9.121)-(9.122) whereby each individual system is mapped to a local target model. The matching protocol is rewritten as follows:

$$\begin{aligned} u_t^i &= F_t^i x_t^i + B_{m,i}^{-1} w_t^i, \\ F_t^i &= B_{m,i}^{-1}(\Xi_t^i - A_{m,i}), \end{aligned} \tag{MP}$$

where Ξ_t^i is defined in (9.120), for $i = 1,\ldots,M$. We define the following sets associated with feasible control input w_t^i shown in (MP) as follows:

$$\mathscr{W}_t^i = \{w_t^i = B_{m,i} u_t^i - (\Xi_t^i - A_{m,i}) x_t^i : \ u_t^i \in \mathscr{U}^i \text{ and } x_t^i \in \mathscr{X}^i\}. \tag{9.129}$$

In order to formulate a receding horizon optimal control problem for deriving the control input w_t^i with respect to (MP), we define the following function. Let

$$l_t^i(x_t^i, \tilde{x}_t^i, w_t, \tilde{w}_t^i) : \mathbb{R}^n \times \mathbb{R}^{M^i n} \times \mathbb{R}^m \times \mathbb{R}^{M^i m} \to \mathbb{R}, \tag{9.130}$$

be a positive local cost function with $l_t^i(\mathbf{0},\mathbf{0},\mathbf{0},\mathbf{0}) = 0$ assigning a cost to control actions w_t^i, $\tilde{w}_t^i$, respectively, given the local state vectors x_t^i, $\tilde{x}_t^i$ at time instant t, for $i = 1,\ldots,M$. Recall that the aggregate vector $\tilde{x}_t^i$ is defined in (9.8) while the aggregate vector $\tilde{w}_t^i$ is in agreement with (9.9).

Given now a specific cost function (9.130), the control input w_t^i in (MP) is derived from the solution of the following receding horizon optimal control problem associated with an optimal value function $J_t^{i*}(x_t^i, \tilde{x}_t^i)$:

$$\mathscr{P}_t^i: \underset{\tilde{W}_t^i}{\text{minimize}} \quad \sum_{k=0}^{N-1} l_t^i(x_{k,t}, \tilde{x}_{k,t}, u_{k,t}^i, \tilde{u}_{k,t}^i) + l_N(x_{k,t}, \tilde{x}_{N,t}^i) \tag{9.131a}$$

$$\text{subject to} \quad x_{k+1,t}^i = (\bar{A}_d + \bar{B}_d \Xi_t^i) x_t^i + \bar{B}_d w_t^i, \qquad k = 0, \dots, N-1, \tag{9.131b}$$

$$x_{k,t}^i \in \mathscr{X}^i,\ w_{k,t}^i \in \mathscr{W}_t^i, \qquad k = 0, \dots, N-1, \tag{9.131c}$$

$$x_{N,t}^i \in \mathscr{X}_f^i, \tag{9.131d}$$

$$x_{0,t}^i = x_t^i, \tag{9.131e}$$

$$x_{k+1,t}^j = (\bar{A}_d + \bar{B}_d \Xi_t^j) x_t^j + \bar{B}_d w_t^j,\ j \in \mathscr{N}^i \qquad k = 0, \dots, N-1, \tag{9.131f}$$

$$x_{k,t}^j \in \mathscr{X}^j,\ w_{k,t}^j \in \mathscr{W}_t^j,\ j \in \mathscr{N}^i \qquad k = 0, \dots, N-1, \tag{9.131g}$$

$$x_{N,t}^j \in \mathscr{X}_f^j, \tag{9.131h}$$

$$x_{0,t}^j = x_t^j, \tag{9.131i}$$

where

$$\tilde{W}_t^i \triangleq [w_{0,t}^i, \tilde{w}_{0,t}^i, \dots, w_{N-1,t}^i, \tilde{w}_{N-1,t}^i] \in \mathbb{R}^{N(M^i+1)m}, \tag{9.132}$$

is the decision vector. We denote by

$$W_t^{i*} = [w_{0,t}^i, \tilde{w}_{0,t}^i, \dots, w_{N-1,t}^i, \tilde{w}_{N-1,t}^i,], \tag{9.133}$$

a minimizer of problem $\mathscr{P}_t^i$. Then, the control input w_t^i in (MP) is defined as

$$w_t^i = w_{0,t}^i. \tag{9.134}$$

The following procedure describes the iterative implementation of a distributed network control policy based on the matching protocol (MP) and the solution of problem $\mathscr{P}_t^i$.

Procedure 9.2.4. At time t:

(N1) The control unit of agent-i maintains an estimate of an optimal target system via Procedure 9.2.3 and receives target estimates from its neighbors.

(N2) It measures the local state and collects measurements of states of all neighboring subsystems.

(N3) Based on the local states, as well as the local and neighboring estimates of the optimal target system, it computes the minimizer $\tilde{W}_t^{i*}$ of $\mathscr{P}_t^i$.

(N4) The local control unit maintains the first component of $\tilde{W}_t^{i*}$ and implements:

$$u_t^i = B_{m,i}^{-1}(\Xi_t^i - A_{m,i})x_t^i + B_{m,1}^{-1} w_{0,t}^i. \tag{9.135}$$

(N5) At time $t+1$, the i-th control unit updates the local and neighboring estimates of the optimal target systems, recollects the new state information x_{t+1}^i, $\tilde{x}_{t+1}^i$ and repeats steps (N3), (N4).

Problem $\mathscr{P}_t^i$ as formulated in (9.131) is time-varying and as a result, minimizer $\tilde{W}_t^{i*}$ is a time-varying function of the local and neighboring states. In this respect, the distributed model-matching based control policy u_t^i as defined in (9.135) represents a time-varying feedback control law implicitly derived from the solution of $\mathscr{P}_t^i$. In this regard, we may write

$$u_t^i = \mathscr{K}_t^i(x_t^i, \tilde{x}_t^i; t), \tag{9.136}$$

where $\mathscr{K}_t^i : \mathbb{R}^n \times \mathbb{R}^{M^i n} \times \mathbb{R} \to \mathbb{R}^m$. Stability properties of the distributed controller u_t^i defined in (9.135) are discussed in the following section.

9.2.8 Stability analysis of model-matching based MPC

In order to derive sufficient conditions for stability of the network control policy (MP)-(9.131)-(9.135) we assume the following.

Assumption 9.2.11. *The cost term in* (9.131a) *is*

$$l_t^i(x_t^i, \tilde{x}_t^i, w_t^i, \tilde{w}_t^i) = \|Qx_t^i\|_2 + \sum_{j\in\mathscr{N}^i} \|Qx_t^j\|_2 + \gamma \sum_{j\in\mathscr{N}^i} \|Q(x_t^i - x_t^j)\|_2 + \|Rw_t^i\|_2 + \sum_{j\in\mathscr{N}^i} \|Rw_t^j\|_2, \tag{9.137}$$

with $Q = Q' > 0$, $R = R' > 0$ and $\gamma > 0$.

Assumption 9.2.12. *The terminal sets $\mathscr{X}_f^i$ and $\mathscr{X}_f^j$, $j \in \mathscr{N}^i$, in* (9.131d) *and* (9.131h)*, respectively, coincide with the origin, i.e., $x_{N,t}^i = x_{N,t}^j = \mathbf{0}$, $j \in \mathscr{N}^i$.*

Assumption 9.2.13. *The feasible sets $\mathscr{X}^i, \mathscr{X}^j \subseteq \mathbb{R}^n$ and $\mathscr{W}^i, \mathscr{W}^j \subseteq \mathbb{R}^m$ contain the origin in their interior, with $j \in \mathscr{N}^i$.*

Letting

$$\hat{x}_{t+1} = f_t(\hat{x}_t, \hat{u}_{\hat{x}_t}), \tag{9.138}$$

denote the closed-loop dynamics of the entire system, where

$$f_t(\hat{x}_t, \hat{u}_{\hat{x}_t}) = \hat{A}\hat{x}_t + \hat{B}\hat{u}_{\hat{x}_t}, \tag{9.139}$$

$$\hat{x}_t = \mathrm{Col}(x_t^1, \ldots, x_t^M), \tag{9.140}$$

$$\hat{u}_t = \mathrm{Col}(u_t^1, \ldots, u_t^M), \tag{9.141}$$

with

$$\hat{A} = \mathrm{diag}(\bar{A}_d + \bar{B}_d A_{m,1}, \ldots, \bar{A}_d + \bar{B}_d A_{m,M}), \tag{9.142}$$

$$\hat{B} = \mathrm{diag}(\bar{B}_d B_{m,1}, \ldots, \bar{B}_d B_{m,M}), \tag{9.143}$$

and u_t^i, $i = 1, \ldots, M$, as given in (9.135). Sufficient conditions for asymptotic stability of the closed-loop system (9.138) are given in the following theorem.

Theorem 9.2.14. *Let M agents with dynamics described by the discrete-time equations* (9.128) *exchange information with each other over a communication scheme modeled as a connected graph. Suppose that each agent is assigned to a node $i = \{1, \ldots, M\}$, and implements network control policy* (MP)-(9.131)-(9.135) *summarized in Procedure 9.2.4 at each time instant t. Suppose that the cost term l_t^i in* (9.131a) *is given by* (9.137) *and assume the following:*

(A1) $Q = Q' > 0$, $R = R' > 0$ *and* $\gamma > 0$.

(A2) The terminal sets $\mathscr{X}_f^i$ and $\mathscr{X}_f^j$, $j \in \mathscr{N}^i$, in (9.131d) *and* (9.131h)*, respectively, coincide with the origin, i.e., $x_{N,t}^i = x_{N,t}^j = \mathbf{0}$, $j \in \mathscr{N}^i$.*

(A3) The feasible sets $\mathscr{X}^i, \mathscr{X}^j \subseteq \mathbb{R}^n$ and $\mathscr{W}^i, \mathscr{W}^j \subseteq \mathbb{R}^m$ contain the origin in their interior, with $j \in \mathscr{N}^i$.

(A4) The following inequality:

$$\boldsymbol{\varepsilon}^i - \bar{J}^i \leq 0, \tag{9.144}$$

is satisfied $\forall i = \{1,\dots,M\}$ *and for all* $x_t^i \in \mathscr{X}^i$*, where*

$$\varepsilon^i = \sum_{k=1}^{N-1} \|R(\Xi_{t+1}^i - \Xi_t^i)x_{k,t}^{i,i}\|_2 + (1+\gamma) \sum_{j\in\mathscr{N}^i} \sum_{k=1}^{N-1} \|Q(x_{k,t}^{j,j} - x_{k,t}^{j,i})\|_2 + \sum_{j\in\mathscr{N}^i} \sum_{k=1}^{N-1} \|R(w_{k,t}^{j,j} - w_{k,t}^{j,i}) - R(\Xi_{t+1}^j - \Xi_t^j)x_{k,t}^{j,j}\|_2, \tag{9.145}$$

$$\bar{J}^i = \|Qx_t^i\|_2 + \|Rw_t^i\|_2 + \sum_{j\in\mathscr{N}^i} \|Qx_t^j\|_2 + \gamma \sum_{j\in\mathscr{N}^i} \|Q(x_t^i - x_t^j)\|_2 + \sum_{j\in\mathscr{N}^i} \|Rw_{0,t}^{j,i}\|_2. \tag{9.146}$$

Then, the origin of the closed-loop system (9.138) *is asymptotically stable.*

Proof. We prove the theorem for the i-th agent using the value function of problem $\mathscr{P}_t^i$. Let

$$\tilde{W}_t^{i*} = [w_{0,t}^{i,i}, \tilde{w}_{0,t}^{i,i}, \dots, w_{N-1,t}^{i,i}, \tilde{w}_{N-1,t}^{i,i}], \tag{9.147}$$

be the minimizer of problem $\mathscr{P}_t^i$ at time t and

$$J_t^{i*}(x_t^i, \tilde{x}_t^i) = \sum_{k=0}^{N-1} \|Qx_{k,t}^{i,i}\|_2 + \sum_{j\in\mathscr{N}^i} \sum_{k=0}^{N-1} \|Qx_{k,t}^{j,i}\|_2 + \gamma \sum_{j\in\mathscr{N}^i} \sum_{k=0}^{N-1} \|Q(x_{k,t}^{i,i} - x_{k,t}^{j,i})\|_2 + \sum_{k=0}^{N-1} \|Rw_{k,t}^{i,i}\|_2 + \sum_{j\in\mathscr{N}^i} \sum_{k=0}^{N-1} \|Rw_{k,t}^{j,i}\|_2, \tag{9.148}$$

be the associated optimal value function. We denote by

$$W_t^{i,i*} = [w_{0,t}^{i,i}, \dots, w_{N-1,t}^{i,i}], \tag{9.149}$$

$$W_t^{j,i*} = [w_{0,t}^{j,i}, \dots, w_{N-1,t}^{j,i}], \tag{9.150}$$

the optimal control sequence of agent-i and agent-j as predicted by agent-i at time t, with $i, j = 1,\dots,M$, $j \neq i$ and $j \in \mathscr{N}^i$. However, the shifted control sequences

$$W_{t+1}^{i,i} = [w_{1,t}^{i,i}, \dots, w_{N-1,t}^{i,i}, \mathbf{0}], \tag{9.151}$$

$$W_{t+1}^{j,i} = [w_{1,t}^{j,i}, \dots, w_{N-1,t}^{j,i}, \mathbf{0}], \tag{9.152}$$

with $j \in \mathscr{N}^i$, are not necessarily feasible at the next time-step $t+1$ since problem $\mathscr{P}_t^i$ is not time-invariant. The shifted control sequences above also fail to be feasible due to a possible mismatch between the predicted state $x_{0,t+1}^{j,i}$ and the actual state x_{t+1}^j. In contrast, since $x_{0,t+1}^{j,j} = x_{t+1}^j$ we may consider the following shifted control sequences which are feasible at

time $t+1$ for agent-i:

$$W^{i,i}_{t+1} = [w^{i,i}_{1,t} - \Xi^i_{t+1}x^i_{0,t+1} + \Xi^i_t x^i_{1,t}, \ldots, w^{i,i}_{N-1,t} - \Xi^i_{t+1}x^i_{N-2,t+1} + \Xi^i_t x^i_{N-1,t}, \mathbf{0}], \tag{9.153}$$

$$W^{j,j}_{t+1} = [w^{j,j}_{1,t} - \Xi^j_{t+1}x^j_{0,t+1} + \Xi^j_t x^j_{1,t}, \ldots, w^{j,j}_{N-1,t} - \Xi^j_{t+1}x^j_{N-2,t+1} + \Xi^j_t x^j_{N-1,t}, \mathbf{0}], \tag{9.154}$$

with $j \in \mathscr{N}^i$. Note that letting (9.153), (9.154) be in force, we have

$$x^i_{k,t+1} = x^i_{k+1,t},\ 0 \le k \le N-1, \tag{9.155}$$

$$x^j_{k,t+1} = x^j_{k+1,t},\ 0 \le k \le N-1, \tag{9.156}$$

which implies that

$$W^{i,i}_{t+1} = [w^{i,i}_{1,t} - (\Xi^i_{t+1} - \Xi^i_t)x^i_{1,t}, \ldots, w^{i,i}_{N-1,t} - (\Xi^i_{t+1} - \Xi^i_t)x^i_{N-1,t}, \mathbf{0}], \tag{9.157}$$

$$W^{j,j}_{t+1} = [w^{j,j}_{1,t} - (\Xi^j_{t+1} - \Xi^j_t)x^j_{1,t}, \ldots, w^{j,j}_{N-1,t} - (\Xi^j_{t+1} - \Xi^j_t)x^j_{N-1,t}, \mathbf{0}]. \tag{9.158}$$

Let now

$$\begin{aligned} J^i_{t+1}(x^i_{t+1}, \tilde{x}^i_{t+1}) = \sum_{k=0}^{N-1} \|Qx^{i,i}_{k,t+1}\|_2 + \sum_{j\in\mathscr{N}^i}\sum_{k=0}^{N-1} \|Qx^{j,i}_{k,t+1}\|_2 + \gamma \sum_{j\in\mathscr{N}^i}\sum_{k=0}^{N-1} \|Q(x^{i,i}_{k,t+1} - x^{j,i}_{k,t+1})\|_2 \\ + \sum_{k=0}^{N-1} \|Rw^{i,i}_{k,t+1}\|_2 + \sum_{j\in\mathscr{N}^i}\sum_{k=0}^{N-1} \|Rw^{j,i}_{k,t+1}\|_2, \end{aligned} \tag{9.159}$$

be the value function of $\mathscr{P}^i_{t+1}$ associated with control sequences $W^{i,i}_{t+1}$, $W^{j,j}_{t+1}$, $j \in \mathscr{N}^i$ as defined in (9.157), (9.158), respectively. Substituting

$$x^{i,i}_{k,t+1} = x^{i,i}_{k+1,t},\ 0 \le k \le N-1, \tag{9.160}$$

$$x^{j,i}_{k,t+1} = x^{j,j}_{k+1,t},\ 0 \le k \le N-1, \tag{9.161}$$

and

$$w^{i,i}_{k,t+1} = w^{i,i}_{k+1,t} - (\Xi^i_{t+1} - \Xi^i_t)x^i_{k+1,t},\ 0 \le k \le N-2, \tag{9.162}$$

$$w^{j,i}_{k,t+1} = w^{j,j}_{k+1,t} - (\Xi^j_{t+1} - \Xi^j_t)x^j_{k+1,t},\ 0 \le k \le N-2, \tag{9.163}$$

in (9.159), yields

$$J_{t+1}^i(x_{t+1}^i,\tilde{x}_{t+1}^i) = \sum_{k=1}^{N-1}\|Qx_{k,t}^{i,i}\|_2 + \sum_{j\in\mathcal{N}^i}\sum_{k=1}^{N-1}\|Qx_{k,t}^{j,j}\|_2 + \gamma\sum_{j\in\mathcal{N}^i}\sum_{k=1}^{N-1}\|Q(x_{k,t}^{i,i}-x_{k,t}^{j,j})\|_2$$
$$+\sum_{k=1}^{N-1}\|Rw_{k,t}^{i,i}-R(\Xi_{t+1}^i-\Xi_t^i)x_{k,t}^i\|_2 + \sum_{j\in\mathcal{N}^i}\sum_{k=1}^{N-1}\|Rw_{k,t}^{j,j}-R(\Xi_{t+1}^j-\Xi_t^j)x_{k,t}^j\|_2, \tag{9.164}$$

which is also consistent with $x_{N,t}^{i,i}=0$, $x_{N,t}^{j,j}=0$ due to feasibility of control sequences (9.157), (9.158). In view of (9.148) and (9.164), we may write

$$J_{t+1}^i(x_{t+1}^i,\tilde{x}_{t+1}^i) = J_t^{i*}(x_t^i,\tilde{x}_t^i)$$
$$\underbrace{-\|Qx_t^i\|_2-\|Rw_t^i\|_2-\sum_{j\in\mathcal{N}^i}\|Qx_t^j\|_2-\gamma\sum_{j\in\mathcal{N}^i}\|Q(x_t^i-x_t^j)\|_2-\sum_{j\in\mathcal{N}^i}\|Rw_t^{j,i}\|_2}_{-\bar{J}^i} \tag{9.165}$$
$$+\underbrace{\sum_{k=1}^{N-1}(\|Rw_{k,t}^{i,i}-R(\Xi_{t+1}^i-\Xi_t^i)x_{k,t}^{i,i}\|_2-\|Rw_{k,t}^{i,i}\|_2)}_{\rho_1^i} \tag{9.166}$$
$$+\underbrace{\sum_{k=1}^{N-1}(\|Qx_{k,t}^{j,j}\|_2-\|Qx_{k,t}^{j,i}\|_2)}_{\rho_2^i} \tag{9.167}$$
$$+\underbrace{\gamma\sum_{k=1}^{N-1}(\|Q(x_{k,t}^{i,i}-x_{k,t}^{j,i}\|_2-\|Q(x_{k,t}^{i,i}-x_{k,t}^{j,j}\|_2)}_{\rho_3^i} \tag{9.168}$$
$$+\underbrace{\sum_{k=1}^{N-1}(\|Rw_{k,t}^{j,j}-R(\Xi_{t+1}^j-\Xi_t^j)x_{k,t}^{j,j}\|_2-\|Rw_{k,t}^{j,i}\|_2)}_{\rho_4^i}, \tag{9.169}$$

or

$$J_{t+1}^i(x_{t+1}^i,\tilde{x}_{t+1}^i) = J_t^{i*}(x_t^i,\tilde{x}_t^i)-\bar{J}^i+\rho^i, \tag{9.170}$$

where $\rho^i=\rho_1^i+\rho_2^i+\rho_3^i+\rho_4^i$. Using now a variation of the *triangle inequality axiom* of norms:

$$\|a-b\|\geq\|a\|-\|b\|, \tag{9.171}$$

and letting

$$\varepsilon^i = \varepsilon_1^i + \varepsilon_2^i + \varepsilon_3^i + \varepsilon_4^i, \tag{9.172}$$

with

$$\varepsilon_1^i = \sum_{k=1}^{N-1} \|R(\Xi_{t+1}^i - \Xi_t^i)x_{k,t}^{i,i}\|_2 \geq \rho_1^i, \tag{9.173}$$

$$\varepsilon_2^i = \sum_{k=1}^{N-1} \|Q(x_{k,t}^{j,j} - x_{k,t}^{j,i})\|_2 \geq \rho_2^i, \tag{9.174}$$

$$\varepsilon_3^i = \gamma \sum_{k=1}^{N-1} \|Q(x_{k,t}^{j,j} - x_{k,t}^{j,i})\|_2 \geq \rho_3^i, \tag{9.175}$$

$$\varepsilon_4^i = \sum_{k=1}^{N-1} \|R(w_{k,t}^{j,j} - w_{k,t}^{j,i}) - R(\Xi_{t+1}^j - \Xi_t^j)x_{k,t}^{j,j}\|_2 \geq \rho_1^i, \tag{9.176}$$

yields

$$\varepsilon^i \geq \rho^i. \tag{9.177}$$

From (9.170) and (9.177), we have

$$J_{t+1}^i(x_{t+1}^i, \tilde{x}_{t+1}^i) \leq J_t^{i*}(x_t^i, \tilde{x}_t^i) - \bar{J}^i + \varepsilon^i, \tag{9.178}$$

where ε^i is given in (9.172) and is consistent with (9.145). From Assumption (A4), (9.178) implies that

$$J_{t+1}^i(x_{t+1}^i, \tilde{x}_{t+1}^i) \leq J_t^{i*}(x_t^i, \tilde{x}_t^i). \tag{9.179}$$

Also, by definition of an optimal value function, we have

$$J_{t+1}^{i*}(x_{t+1}^i, \tilde{x}_{t+1}^i) \leq J_{t+1}^i(x_{t+1}^i, \tilde{x}_{t+1}^i). \tag{9.180}$$

Then, from (9.179), (9.180), we conclude that

$$J_{t+1}^{i*}(x_{t+1}^i, \tilde{x}_{t+1}^i) \leq J_t^{i*}(x_t^i, \tilde{x}_t^i), \tag{9.181}$$

which further implies that the optimal value function of $\mathscr{P}_t^i$ is positive and non-increasing along the closed-loop trajectories and thus, can be used as Lyapunov function for agent-i. In view of the positive definiteness of weighting matrices Q, R, inequality (9.144) is sufficient to guarantee that

$$\lim_{t\to\infty} x_t^i = 0, \ \lim_{t\to\infty} w_t^i = 0. \tag{9.182}$$

Overall stability for the entire system is established by proving (9.181) for $i = 1, \ldots, M$. □

We note that inequality (9.144) coincides with (9.47) when $\Xi^i_{t+1} = \Xi^i_t$ and $\Xi^j_{t+1} = \Xi^j_t$, $j \in \mathscr{N}^i$. This means that as soon as the matching protocol (MP) has achieved consensus, problem $\mathscr{P}^i_t$ becomes time-invariant and sufficient conditions for closed-loop stability can be derived from Theorem 9.2.8.

9.3 Distributed MPC for dynamically coupled systems

In this section, we address the problem of distributed model predictive control of dynamically coupled systems from an application point of view. In particular, we consider the load frequency control (LFC) problem examined in Chapter 8, and propose a distributed MPC method for LFC design. Our method depends on a decoupling technique which allows for a control solution with a distributed architecture. Treating the total power inflows of each area as input variables, we derive a decoupled linearized model for each area of a multi-area network. This allows for the solution of a model predictive control problem with a quadratic performance index and input saturating constraints on the individual tie-line power flows, along with an overall equality constraint to address the energy balance of the network. We present the problem in a descriptive way and as a result certain lines involving the model description as well as the problem formulation may overlap with lines in Chapter 8. In the end of the chapter, we illustrate the effectiveness of the method via a simulation study of a three-area power network.

9.3.1 Two-area power system modelling

We consider a standard linearized model [13] of a two area power system the block diagram of which is depicted in Fig. 9.1. The analysis provided next is extended to the multi-area power system design later in the chapter. Neglecting saturator dynamics appearing in Fig. 9.1, we write the linear state-space model of a two-area system as follows:

$$\dot{x} = Ax + B_u u + B_w w,\ x(0) = x_0, \tag{9.183}$$

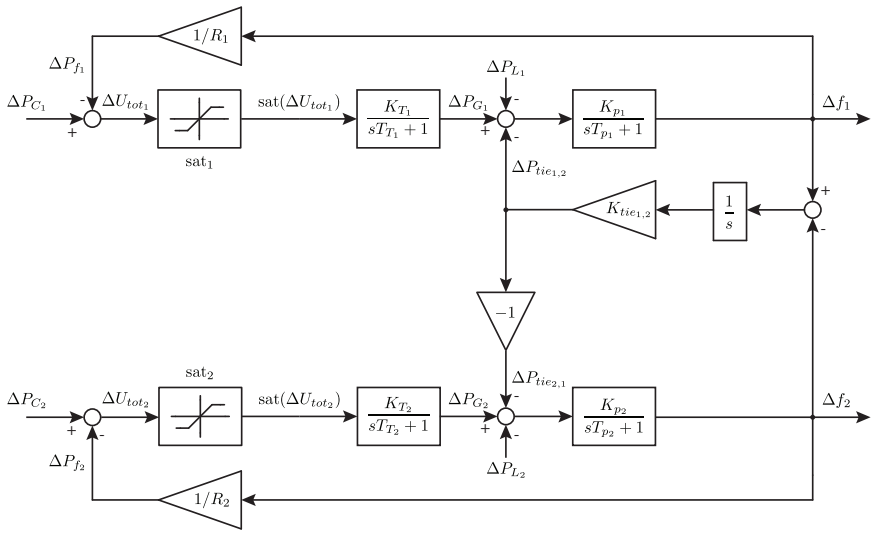

Fig. 9.1 Block-diagram of two-area power system.

where

$$x = \begin{bmatrix} \Delta f_1 & \Delta f_2 & \Delta P_{G1} & \Delta P_{G2} & \Delta P_{tie,1} \end{bmatrix}', \tag{9.184}$$

$$u = \begin{bmatrix} \Delta P_{C,1} & \Delta P_{C,2} \end{bmatrix}', \tag{9.185}$$

$$w = \begin{bmatrix} \Delta P_{L,1} & \Delta P_{L,2} \end{bmatrix}' \tag{9.186}$$

denote the state, input and disturbance vectors, respectively and

$$A = \begin{bmatrix} -\frac{1}{T_{p1}} & 0 & \frac{K_{p1}}{T_{p1}} & 0 & -\frac{K_{p1}}{T_{p1}} \\ 0 & -\frac{1}{T_{p2}} & 0 & \frac{K_{p2}}{T_{p2}} & +\frac{K_{p2}}{T_{p2}} \\ -\frac{K_{t1}}{R_1 T_{t1}} & 0 & -\frac{1}{T_{t1}} & 0 & 0 \\ 0 & -\frac{K_{t2}}{R_2 T_{t2}} & 0 & -\frac{1}{T_{t2}} & 0 \\ K_{tie}1,2 & -K_{tie}1,2 & 0 & 0 & 0 \end{bmatrix}, \tag{9.187}$$

$$B_u = \begin{bmatrix} 0 & 0 & \frac{K_{t,1}}{T_{t,1}} & 0 & 0 \\ 0 & 0 & 0 & \frac{K_{t,2}}{T_{t,2}} & 0 \end{bmatrix}', \tag{9.188}$$

$$B_w = \begin{bmatrix} -\frac{K_{p,1}}{T_{p,1}} & 0 & 0 & 0 & 0 \\ 0 & -\frac{K_{p,1}}{T_{p,2}} & 0 & 0 & 0 \end{bmatrix}'. \tag{9.189}$$

The notation Δ in x, u, w above, indicates deviation from steady-state operation conditions; Δf_i is the frequency deviation from the common nominal value and $\Delta P_{G,i}$ is the deviation from the equilibrium value of the electrical power generated by the lumped alternators of

each area. Here, the electrical power is taken equal to the mechanical power produced in the output of the turbines. $\Delta P_{tie,1}$ denotes the total power inflow of the area-1 with dynamics described by

$$\Delta P_{tie,1} = K_{tie,1,2} \int_0^t (\Delta f_1(\tau) - \Delta f_2(\tau)) \mathrm{d}\tau, \tag{9.190}$$

where $K_{tie,1,2} = 2\pi T_{1,2}$ is the synchronization coefficient between areas 1 and 2. Since power inflow to the area-1 corresponds to equal power outflow from area-2, i.e., $\Delta P_{tie,2} = -\Delta P_{tie,1}$, $\Delta P_{tie,2}$ is a redundant variable and is neglected from eq. (9.183). All parameters involved in (9.183) are summarized in Table 9.1. The disturbance signal $\Delta P_{L,i}$ is associated with a time-varying demand of the consumers of the i-th area which is assumed to be unknown, piece-wise constant and bounded with known upper and lower values. We study the case where

$$\Delta P_{L,i,\min} \leq \Delta P_{L,i} \leq \Delta P_{L,i,\max}, \ i = 1,2. \tag{9.191}$$

Table 9.1 Parameters and power system terminology.

Parameter,Symbol	**Area 2 / Area 1,3**	**Units**
Nominal Frequency, f^o	50/50	Hz
Power Base, $P_{B,i}$	2000/1500	MW
Load Dependency Factor, D_i	16.66/10.50	MW/Hz
Speed Droop, R_i	$1.2 \times 10^{-3}/1.3 \times 10^{-3}$	Hz/MW
Generator Inertia Gain, H_i	5 /4	s
Turbine Static Gain, $K_{t,i}$	1 /1	MW/MW
Turbine Time Constant, $T_{t,i}$	0.3 /0.25	s
Area Static Gain, $K_{p,i}$	0.06 /0.0952	Hz/MW
Area Time Constant, $T_{p,i}$	24 /22.8571	s
Tie-Line Coefficient, $K_{tie,i}$	1090/1090	MW/Hz

The total control signal of the i-th control area is the sum of two components: $\Delta u_{tot,i} = \Delta P_{f,i} + \Delta P_{C,i}$, namely, the primary frequency control action, defined as $\Delta P_{f,i} = -\frac{1}{R_i}\Delta f_i$, and the automatic generation control (AGC) $\Delta P_{C,i}$ to be designed. The first is a fixed static linear control law performed by the speed governor which is a regulating unit attached on the prime mover. Detailed description of this topic can be found in [106]. The static gain R_i is commonly referred to as speed droop or speed regulation. Signal $\Delta u_{tot,i}$ is subject to component-wise saturation hard constraints of the form

$$\Delta u_{tot,i,\min} \leq \Delta u_{tot,i} \leq \Delta u_{tot,i,\max}, \ i = 1,2, \tag{9.192}$$

where saturation limits are assumed to be symmetric in the sense that $\Delta u_{tot,i,\max} = -\Delta u_{tot,i,\min}$. Also, $\Delta u_{tot,i,\max}$ is assumed to be greater than the maximum expected load deviation $\Delta P_{L,i,\max}$, otherwise, zero frequency deviation error is not guaranteed. Negative values of $\Delta u_{tot,i,\min}$ allow for handling negative values of $\Delta P_{L,i}$, that is, in case of load reduction.

Since hard constraints apply to the total input signal of each area it makes sense to formulate the state-space (9.183) such that $\Delta u_{tot,i}$ appears in the input vector u. We have

$$\begin{bmatrix} \Delta P_{C,1} \\ \Delta P_{C,2} \end{bmatrix} = \begin{bmatrix} \Delta u_{tot,1} \\ \Delta u_{tot,2} \end{bmatrix} - \begin{bmatrix} \Delta P_{f,1} \\ \Delta P_{f,2} \end{bmatrix}, \tag{9.193}$$

which can equivalently be written as

$$\begin{bmatrix} \Delta P_{C,1} \\ \Delta P_{C,2} \end{bmatrix} = \begin{bmatrix} \Delta u_{tot,1} \\ \Delta u_{tot,2} \end{bmatrix} + \underbrace{\begin{bmatrix} 1/R_1 & 0 & 0 & 0 & 0 \\ 0 & 1/R_2 & 0 & 0 & 0 \end{bmatrix}}_{B_f} \underbrace{\begin{bmatrix} \Delta f_1 \\ \Delta f_2 \\ \Delta P_{G,1} \\ \Delta P_{G,2} \\ \Delta P_{tie,1} \end{bmatrix}}_{x}. \tag{9.194}$$

Then, adding $B_u B_f x$ to (9.187) with B_f given in (9.194) changes the input vector u in (9.183) to $u = \begin{bmatrix} \Delta u_{tot,1} & \Delta u_{tot,2} \end{bmatrix}'$ and eliminates the primary frequency control from the dynamical equation. The matrix (9.187) is now altered to:

$$A = \begin{bmatrix} -1/T_{p,1} & 0 & K_{p,1}/T_{p,1} & 0 & -K_{p,1}/T_{p,1} \\ 0 & -1/T_{p,2} & 0 & K_{p,2}/T_{p,2} & +K_{p,2}/T_{p,2} \\ 0 & 0 & -1/T_{t,1} & 0 & 0 \\ 0 & 0 & 0 & -1/T_{t,2} & 0 \\ K_{tie,1,2} & -K_{tie,1,2} & 0 & 0 & 0 \end{bmatrix}, \tag{9.195}$$

while matrices B_u and B_w in (9.188) and (9.189), respectively, are unaffected. Essentially, once $\Delta u_{tot,i}$ has been designed, the AGC signal of each area can be generated by:

$$\Delta P_{C,i} = \Delta u_{tot,i} + \frac{1}{R_i} \Delta f_i, \; i = 1,2, \tag{9.196}$$

since the primary frequency control law $\Delta P_{f,i}$ is pre-specified.

9.3.2 State-augmentation for integral action

A well-established technique for tackling step-disturbances with zero steady-state error is to include integral action into the state-space model. For the i-th area, we consider a performance variable expressed as a summation of the frequency deviation Δf_i multiplied by a bias factor B_i and the tie-line power exchange $\Delta P_{tie,i}$, i.e., $z_i = B_i \Delta f_i + \Delta P_{tie,i}$. This quantity is referred to as "Area Control Error" (ACE) and a usual choice for B_i is $D_i + \frac{1}{R_i}$, [13]. Parameters D_i and R_i are defined in Table 9.1. Specifically, constant D_i represents the rate at which system load changes with frequency evaluated at nominal frequency [66]. Let now $z = \begin{bmatrix} z_1 & z_2 \end{bmatrix}' = C_z x$ with x given in (9.184) and

$$C_z = \begin{bmatrix} B_1 & 0 & 0 & 0 & 1 \\ 0 & B_2 & 0 & 0 & -1 \end{bmatrix}, \tag{9.197}$$

and consider the augmented state-vector

$$x_a(t) = \begin{bmatrix} x(t)' & \int_0^t z_1(\tau)\mathrm{d}\tau & \int_0^t z_2(\tau)\mathrm{d}\tau \end{bmatrix}'. \tag{9.198}$$

Then the augmented state-space form of the two-area power system is written as:

$$\dot{x}_a = A_a x_a + B_{u,a} u + B_{w,a} w, \tag{9.199}$$

with

$$A_a = \begin{bmatrix} A & 0_{5\times 2} \\ C_z & 0_{2\times 2} \end{bmatrix}, \; B_{u,a} = \begin{bmatrix} B_u \\ 0_{2\times 2} \end{bmatrix}, \; B_{w,a} = \begin{bmatrix} B_w \\ 0_{2\times 2} \end{bmatrix}, \tag{9.200}$$

where A, C_z, B_u and B_w are given in (9.195), (9.197), (9.188) and (9.189), respectively. Due to state-augmentation with the integral of the ACE signal of each area, designing a stabilizing controller u for (9.199) leads to zero steady-state frequency and tie-line power exchange deviations, Δf_i, $\Delta P_{tie,i}$, respectively, provided that disturbances $\Delta P_{L,i}$, $i = 1,2$ are piece-wise constant.

We now propose an equivalent representation of the state-space form of the two-area system which leads to a pseudo-decoupled model for each area thereby facilitating the multi-area power system design. This becomes evident in the distributed control design studied later. In the sequel, all state-space representations are given in the augmented form.

9.3.3 Decoupled state-space model and multi-area design

By viewing eq. (9.183) we remark that the two areas are governed by differential equations of the same structure differing only in parameters. Also the coupling between the dynamics is due to $\Delta P_{tie,1}$ variable pertaining to the power exchange deviation between the two areas. By introducing the variable $\Delta P_{tie,2} = -\Delta P_{tie,1}$ defined as

$$\Delta P_{tie,2} = K_{tie,2,1} \int_0^t (\Delta f_2(\tau) - \Delta f_1(\tau)) \mathrm{d}\tau, \tag{9.201}$$

where $K_{tie,2,1} = K_{tie,1,2}$ the state-space form of each area in a two-area system can be written as:

$$\begin{bmatrix} \Delta \dot{f}_i \\ \Delta \dot{P}_{G,i} \\ \Delta \dot{P}_{tie,i} \\ z_i \end{bmatrix} = \begin{bmatrix} -\frac{1}{T_{p,i}} & \frac{K_{p,i}}{T_{p,i}} & -\frac{K_{p,i}}{T_{p,i}} & 0 \\ 0 & -\frac{1}{T_{t,i}} & 0 & 0 \\ K_{tie} & 0 & 0 & 0 \\ B_i & 0 & 1 & 0 \end{bmatrix} \begin{bmatrix} \Delta f_i \\ \Delta P_{G,i} \\ \Delta P_{tie,i} \\ \int z_i \mathrm{d}\tau \end{bmatrix} + \begin{bmatrix} 0 \\ 0 \\ -K_{tie} \\ 0 \end{bmatrix} \Delta f_j + \begin{bmatrix} 0 & -\frac{K_{p,i}}{T_{p,i}} \\ \frac{K_{t,i}}{T_{t,i}} & 0 \\ 0 & 0 \\ 0 & 0 \end{bmatrix} \begin{bmatrix} \Delta u_{tot,i} \\ \Delta P_{L,i} \end{bmatrix}, \tag{9.202}$$

where $K_{tie} = K_{tie,1,2} = K_{tie,2,1}$, and $i = 1,2$.

Consider now a multi-area power grid composed of M areas (generically non-identical) interconnected through tie-lines the topology of which is modelled by an undirected graph $\mathscr{G} = (\mathscr{V}, \mathscr{E})$. Node $i \in \mathscr{V}$ represents the i-th interconnected area while $(i,j) \in \mathscr{E}$ stands for the corresponding link between area i and j. We assume that the graph is not necessarily complete which implies that the topology of tie-lines is sparse. The set of areas connected to the i-th node through tie-lines is denoted by $\mathscr{N}_i \subseteq \mathscr{V}$. Let now $\Delta P_{tie,i}$ represent the total power inflow to the i-th area with dynamics described by

$$\Delta P_{tie,i} = \sum_{j \in \mathscr{N}_i} K_{tie,i,j} \int_0^t (\Delta f_i(\tau) - \Delta f_j(\tau)) \mathrm{d}\tau, \tag{9.203}$$

with $i = 1, \cdots, M$. A decoupled state-space equation of the i-th interconnected area can take the following form:

$$\begin{bmatrix} \Delta \dot{f}_i \\ \Delta \dot{P}_{G,i} \\ z_i \end{bmatrix} = \underbrace{\begin{bmatrix} -\frac{1}{T_{p,i}} & \frac{K_{p,i}}{T_{p,i}} & 0 \\ 0 & -\frac{1}{T_{t,i}} & 0 \\ B_i & 0 & 0 \end{bmatrix}}_{A_i} \underbrace{\begin{bmatrix} \Delta f_i \\ \Delta P_{G,i} \\ \int z_i \mathrm{d}\tau \end{bmatrix}}_{x_i} + \underbrace{\begin{bmatrix} 0 & -\frac{K_{p,i}}{T_{p,i}} \\ \frac{K_{t,i}}{T_{t,i}} & 0 \\ 0 & 1 \end{bmatrix}}_{B_{u,i}} \underbrace{\begin{bmatrix} \Delta u_{tot,i} \\ \Delta P_{tie,i} \end{bmatrix}}_{u_i} + \underbrace{\begin{bmatrix} -\frac{K_{p,i}}{T_{p,i}} \\ 0 \\ 0 \end{bmatrix}}_{B_{w,i}} \underbrace{\Delta P_{L,i}}_{w_i}, \tag{9.204}$$

where $\Delta u_{tot,i} = \Delta P_{C,i} + \Delta P_{f,i}$, $i = 1, \cdots, M$. Note that $\Delta P_{tie,i}$ has been eliminated from the state-vector and instead is included in the input vector of the i-th area. This technical manipulation results in a decoupled state-space form thereby facilitating the design of LFC controllers with distributed structure. A schematic representation of (9.204) is shown in Fig. 9.2. Since $\Delta P_{tie,i}$ is defined by (9.203), to avoid any dynamical discrepancy in the model of the i-th area, the exact value of this pseudo control variable will be fixed by including hard equality constraints in the control design.

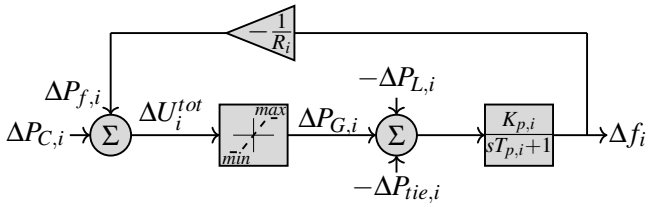

Fig. 9.2 Single block representation of the i-th interconnected area.

In a multi-area power system, the power generation rate of each area should not exceed a specified upper bound. This can be considered as a state constraint by the control of each area with typical maximum value for thermal units being 0.0017 p.u.MW/s. Comprehensive treatment of this topic can be found in [124]. To avoid unnecessary complications, in this study, we only consider saturation input constraints. The load frequency control problem of a distributed multi-area power system is described in the following paragraph.

9.3.3.1 Problem statement

Possible power load change in the i-th area of a power system of multiple interconnected control areas causes the electrical frequency f_i to deviate from its nominal value. Due to interconnections among the areas through power transmission tie-lines and the dependence of the power exchange between the i-th and j-th area upon the associated difference $\Delta f_i - \Delta f_j$, any power load deviation occurring in the i-th area will affect also the linked j-th area causing transients in its frequency f_j. We formulate the LFC problem of a multi-area power system as a disturbance rejection problem in the presence of input constraints. We assume that each area can produce LFC signals independently and can exchange state information with its neighboring areas. Typically, we consider that the topology of physical links (tie-lines) and the topology of information exchange among areas coincide and are described by the same graph. A distributed model-predictive based LFC controller is proposed in the following section.

9.3.4 Model predictive control formulation

Consider a multi-area power system formed of M areas interconnected by tie-lines, and let the dynamics of each area be described by (9.204) written here in a compact form as

$$\dot{x}^i = A_i x^i + \begin{bmatrix} B_{u,i} & B_{w,i} \end{bmatrix} \begin{bmatrix} u^i \\ w^i \end{bmatrix}, x^i(0) = x_0^i, \tag{9.205}$$

with $i = 1, \cdots, M$. To formulate a model predictive control problem we assume the following. The actual power system evolves in real time while the control subsystem of each area predicts local states within a finite future horizon utilizing the system model. All variables involved in (9.205) are discretized using the zero-order-hold method. Representation of predicted variables is in agreement with the notation utilized earlier in the chapter. We assume that the local state can be measured while an estimate of the disturbance signal w_i is obtained by an appropriate observer.

We select a predicted horizon of N time-steps. The discrete-time model of the i-th area obtained as the zero-order-hold equivalent to (9.205), is written as:

$$x_{t+1}^i = A_{d,i} x_t^i + \begin{bmatrix} B_{d,u,i} & B_{d,w,i} \end{bmatrix} \begin{bmatrix} u_t^i \\ w_t^i \end{bmatrix}, x^i(0) = x_0^i. \tag{9.206}$$

In the following, we denote by $x_{k,t}^i$ the predicted state of the i-th area after k sampling intervals starting from t and driven by a sequence of input functions $u_{0,t}^i, \ldots, u_{N-1,t}^i$. For the i-th area let

$$X_t^i = \Phi_i x_t^i + \Psi_{i,1} U_t^i + \Psi_{i,2} W_t^i, \tag{9.207}$$

be an aggregate vector which stacks N consecutive predicted states from time instant t, where

$$X_t^i = \begin{bmatrix} x_{1,t}^{i\prime} & x_{2,t}^{i\prime} & \cdots & x_{N,t}^{i\prime} \end{bmatrix}', \tag{9.208}$$

$$U_t^i = \begin{bmatrix} u_{0,t}^{i\prime} & u_{1,t}^{i\prime} & \cdots & u_{N-1,t}^{i\prime} \end{bmatrix}', \tag{9.209}$$

$$W_t^i = \begin{bmatrix} w_{0,t}^{i\prime} & w_{1,t}^{i\prime} & \cdots & w_{N-1,t}^{i\prime} \end{bmatrix}', \tag{9.210}$$

$$\Phi_i = \begin{bmatrix} A_{d,i}^{\prime} & A_{d,i}^{2\prime} & \cdots & A_{d,i}^{N\prime} \end{bmatrix}' \tag{9.211}$$

$$\Psi_{i,1} = \begin{bmatrix} B_{d,u,i} & 0 & \dots & 0 \\ A_{d,i}B_{d,u,i} & B_{d,u,i} & \dots & 0 \\ \vdots & \vdots & \ddots & \vdots \\ A_{d,i}^{N-1}B_{d,u,i} & A_{d,i}^{N-2}B_{d,u,i} & \dots & B_{d,u,i} \end{bmatrix}, \tag{9.212}$$

$$\Psi_{i,2} = \begin{bmatrix} B_{d,w,i} & 0 & \dots & 0 \\ A_{d,i}B_{d,w,i} & B_{d,w,i} & \dots & 0 \\ \vdots & \vdots & \ddots & \vdots \\ A_{d,i}^{N-1}B_{d,w,i} & A_{d,i}^{N-2}B_{d,w,i} & \dots & B_{d,w,i} \end{bmatrix}. \tag{9.213}$$

Typically, vector X_t^i contains all the local state predictions over a future horizon of N steps. These are computed by the controller which employs the actual state x_t^i to initialize the prediction. In the extreme case where the actual value x_t^i is not available at the t-th instant the controller may perform the prediction starting from the last available state, e.g. x_{t-1}^i, adjusting the prediction horizon accordingly.

The receding horizon optimal control problem of area-i at time t is formulated as follows:

$$\mathscr{P}^i: \underset{U_t^i}{\text{minimize}} \quad X_t^{i\prime}\tilde{Q}_i X_t^i + U_t^{i\prime}\tilde{R}_i U_t^i \tag{9.214a}$$

$$\text{subject to} \quad X_t^i = \Phi_i x_t^i + \Psi_{i,1}U_t^i + \Psi_{i,2}W_t^i, \tag{9.214b}$$

$$H_1 U_t^i = \Omega_i, \tag{9.214c}$$

$$H_2 U_t^i \leq \Gamma_i, \tag{9.214d}$$

$$x_{N,t}^i = 0, \tag{9.214e}$$

where

$$H_1 = \left[I_N \otimes \begin{bmatrix} 0 & 1 \end{bmatrix} \right], \tag{9.215a}$$

$$\Omega_i = \begin{bmatrix} \Delta P_t^{tie,i} \\ \Delta P_{t+1}^{tie,i} \\ \Delta P_{3,t-1}^{tie,i} \\ \vdots \\ \Delta P_{N,t-1}^{tie,i} \end{bmatrix}, \tag{9.215b}$$

$$H_2 = \begin{bmatrix} I_N \otimes \begin{bmatrix} 1 & 0 \end{bmatrix} \\ -I_N \otimes \begin{bmatrix} 1 & 0 \end{bmatrix} \end{bmatrix}, \tag{9.215c}$$

$$\Gamma_i = \begin{bmatrix} I_N \otimes \gamma_i \\ I_N \otimes \gamma_i \end{bmatrix}, \tag{9.215d}$$

$$\tilde{Q}_i = I_N \otimes Q_i, \text{ with } Q_i = Q_i' > 0, \tag{9.215e}$$

$$\tilde{R}_i = I_N \otimes R_i, \text{ with } R_i = R_i' > 0, \tag{9.215f}$$

$$\gamma_i = |\Delta u_{tot,i,max}| = |\Delta u_{tot,i,min}|. \tag{9.215g}$$

Matrices Q_i, R_i weigh predicted states and inputs, respectively, at each iteration of the predicted horizon. They are tuning parameters of the MPC controller the choice of which can be guided by simulations. The parameter γ_i in (9.214d) represents saturation hard constraint of each area. We denote by

$$U_t^{i*} = [u_{0,t}^i, u_{1,t}^i, \ldots, u_{N-1,t}^i], \tag{9.216}$$

the minimizer of problem (9.214). If problem (9.214) is feasible, the control unit of the i-th area generates the AGC signal by the following control law:

$$\Delta P_t^{C,i} = \begin{bmatrix} 1 & 0 \end{bmatrix} u_{0,t}^i + \Delta P_{f,i}, \tag{9.217}$$

where $u_{0,t}^i$ is the first component of minimizer U_t^{i*} and $\Delta P_{f,i}$ is the fixed droop controller.

We note that the first two equality constraints (pertaining to the first two instants of the prediction horizon) in (9.214c) is given by the actual values of $\Delta P_t^{tie,i}$ and $\Delta P_{t+1}^{tie,i}$ which are known signals at time t. Specifically, at time t, the value of $\Delta P_t^{tie,i}$ can be measured by the

i-th control unit, while the actual value of $\Delta P_{t+1}^{tie,i}$ can be computed at time t by

$$\Delta P_{t+1}^{tie,i} = \Delta P_t^{tie,i} + t_s \sum_{j \in \mathcal{N}_i} K_{tie,i,j}(\Delta f_t^i - \Delta f_t^j), \tag{9.218}$$

with t_s representing the sampling period of the discretization. Note that $\Delta P_t^{tie,i}$, Δf_t^i and Δf_t^j in (9.218) are actual and known signals to the controller at time instant t. The difference equation (9.218) can be considered as the zero-order-hold equivalent to the continuous model (9.203). This implies that the proposed MPC controller does not violate the dynamics of the actual model at real time while performs state predictions depending on actual values at t and $t+1$ instants. The remaining equality constraints in (9.214c) pertaining to the following $N-2$ time-steps of the prediction, are computed by the predictions of the previous step as follows:

$$\Delta \hat{P}_{\mu+1,t-1}^{tie,i,i} = \Delta P_{\mu,t-1}^{tie,i,i} + t_s \sum_{j \in \mathcal{N}_i} K_{tie,i,j}(\Delta f_{\mu,t-1}^{i,i} - \Delta f_{\mu,t-1}^{j,j}), \tag{9.219}$$

where $\mu = 2, \ldots, N-1$.

At each iteration, the control unit of the i-th area measures the local state x_t^i and estimates the disturbance signal w_t^i which is taken constant along the prediction horizon. At the same time, the control unit receives the current and the predicted states from its neighboring areas and transmits its own information to them. The distributed MPC scheme (9.214)-(9.217) is summarized in the following procedure.

Procedure 9.3.1. At time t, the control unit of area-i

(1) measures x_t^i and estimates w_t^i,

(2) sends x_t^i and X_{t-1}^i to neighboring controllers and receives x_t^j, X_{t-1}^j, $j \in \mathcal{N}_i$,

(3) initializes the state prediction starting from x_t^i,

(4) solves quadratic program (9.214),

(5) if (9.214) is feasible, generates the AGC signal by (9.217), otherwise from

$$\Delta P_t^{C,i} = \begin{bmatrix} 1 & 0 \end{bmatrix} u_{1,t-1}^{i,i} + \Delta P_{f,i}, \tag{9.220}$$

(6) constructs X_t^i,

(7) iterates starting form (1).

Remark 9.3.1. The optimal control problem (9.214) requires data transmission among coupled areas. This implies that the communication topology should coincide with the physical topology of the power network in order for the model predictive control policy (9.214)-(9.217) to be implemented. However, interconnected areas only need to exchange their frequency information (actual and future predictions) while variables associated with the remaining state-vector are not communicated. Hence, in sparse networks with limited interconnections the communication will not be excessive.

9.3.5 Case study: MPC design for multi-area power system

We consider a power system of three nonidentical control areas interconnected via tie-lines. The physical links (solid lines) and the communication topology (dashed lines) are depicted in Fig. 9.3.

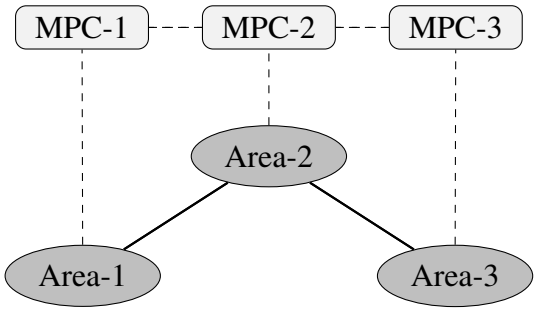

Fig. 9.3 Topology of physical links (tie-lines) and communication scheme.

The dynamics of each area are given by (9.204). Table 9.1 summarizes the parameters considered in the three areas. We consider the following simulation scenario. Power demand deviations from the equilibrium operation of each area appear as unknown piece-wise constant disturbances in the model of each subsystem. We consider three disturbances one for each area. The disturbance in area-1 is taken as $\Delta P_{L,1} = 150\ [MW]$ and occurs at the first second of the simulation while the disturbances in area-2 and area-3 are taken as $\Delta P_{L,2} = 200\ [MW]$ and $\Delta P_{L,3} = 150\ [MW]$ and occur at the 11-th and 21-th second, respectively. The control unit of each area implements the distributed MPC scheme (9.214)-(9.217) to generate the AGC signal. The predictive controller iterates every $t_s = 0.1\ [sec]$ and predicts control sequences over a prediction horizon of $N = 15$ steps. In the simulation, we tune the MPC controllers of the three areas identically. We choose weighting matrices: $Q_i = \text{diag}(500, 0, 500)$ penalizing local states and $R_i = 100 I_2$ penalizing inputs. The hard constraint γ_i has been taken 10% greater than the magnitude of the respective disturbances of each area.

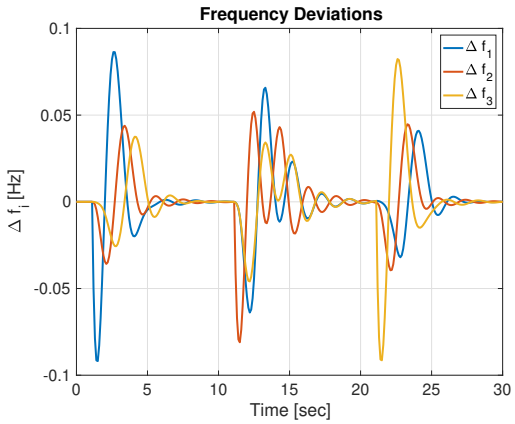

Fig. 9.4 Frequency deviations of each area driven by step disturbances.

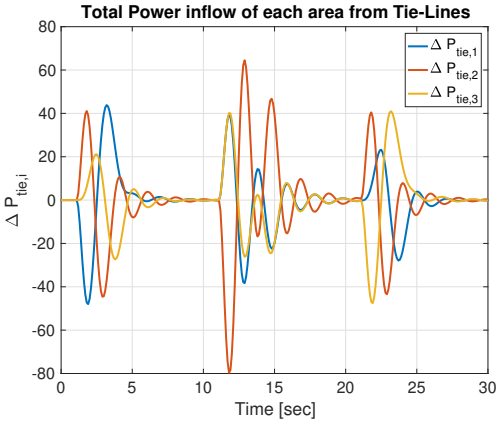

Fig. 9.5 Power flow via tie-lines.

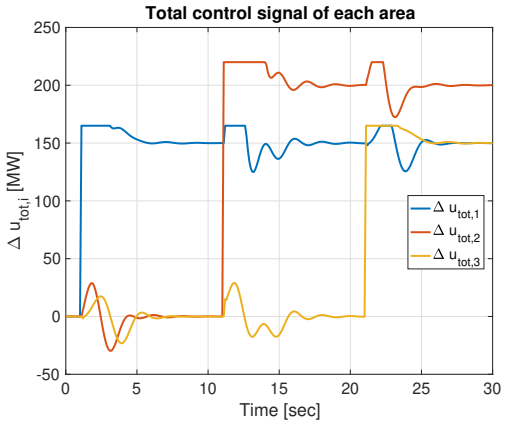

Fig. 9.6 Total optimal control signal of each area.

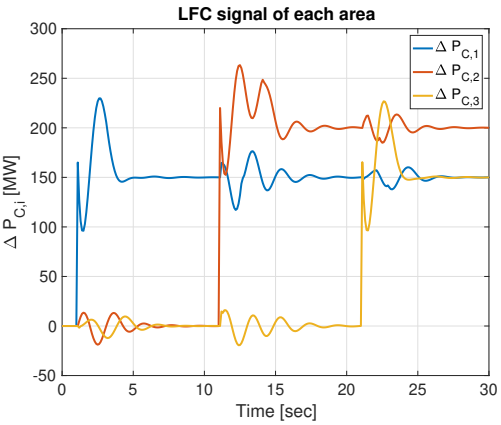

Fig. 9.7 AGC signal of each area.

Fig. 9.4 and 9.5 show the deviations of the frequency and the total power-flow of each area, respectively, from their equilibrium values. The generated AGC signal is shown in Fig. 9.7. This is derived from the control law (9.217). The total control signal as computed by the solution of problem (9.214) is depicted in Fig. 9.6. Clearly, the proposed distributed MPC scheme respects the hard saturation limits and maintains the stability of the power network.

9.4 Conclusions

In this chapter, we focus on large-scale receding horizon control problems and address the stabilization problem of multi-agent networks from a model predictive control perspective. We first present a distributed network control scheme whereby each local MPC controller

optimizes a local performance index that couples the dynamic behavior of neighboring agents. Sufficient conditions for local stability are explicitly derived using local value functions as Lyapunov functions. It is shown that in the presence of nonidentical agents, the implementation of a distributed MPC scheme requires that a local control unit, in order to predict the future evolution of neighboring agents, have access to model parameters of its neighbors. In an attempt to relax this stringent requirement, we propose a distributed model-matching time-varying feedback technique whereby agents are mapped to an optimal target system recursively only by sharing their estimates of a global decision vector that minimizes a least-squares optimization problem. The proposed model-matching control protocol is then combined with a distributed MPC scheme which couples the dynamic behavior of interconnected agents and stabilizes the entire system. Sufficient conditions for stability of the combined control scheme are derived using Lyapunov functions.

In the second part of the chapter, we study the problem of distributed model predictive control of dynamically coupled systems from an application point of view. In particular, we consider the load frequency control (LFC) problem examined in Chapter 8, and propose a distributed MPC method for distributed LFC design based on a decoupling technique which allows for control design with distributed architecture. Manipulating the total power inflows to each area as input variables, a decoupled linearized model for each area is derived. This design strategy allows for the formulation and solution of a model predictive control problem with a quadratic performance index, input saturating constraints on the individual tie-line power flows and an overall equality constraint to address the energy balance of the network.

Chapter 10

Conclusions and future work

This thesis deals with regulation problems of large-scale networked systems and focuses on the stabilization of networks of multiple interconnected agents. Our interpretation of multi-agent systems emerges from the abundance of applications involving networks of multiple independently actuated systems demanding network control design with distributed architecture.

In a descriptive way, the problem of distributed control of multi-agent networks is formulated as follows. A network is composed of (or decomposed into) distinct dynamical subsystems that can independently generate their decision variables. The subsystems are represented as dynamic agents with joint objectives, which typically couple their dynamic behavior as well as are in concert with certain dynamic interconnections. Local interactions are represented by a connected graph (digraph), where the vertices denote subsystems-agents, and the edges between vertices represent dynamical couplings or coupling terms in control objectives corresponding to the associated vertices. It is assumed that the interaction graph (digraph) also represents a communication scheme according to which subsystems exchange state-information with their neighboring peers. In the presence of dynamical couplings between agents, we assume that the entire system is expressed in a state-space form, which is consistent with the associated communication topology. Overall, a network is represented as a large-scale distributed control scheme composed of multiple local controllers, each defined using local information only.

Several results on distributed control over networks of dynamic agents rely on specific assumptions, such as undirected information exchange, identical agent dynamics, linear dynamics, open-loop decoupled dynamics. Our main objective is to relax a number of simplifying factors appearing in the relevant literature and propose systematic methods for tackling stabilization problems over multi-agent networks of various settings. We briefly review the main results of the thesis as follows.

Chapter 3 concisely reviews the regulation problem and LQR control theory and introduces the concept of regulation over networks of multiple dynamic agents. In this introductory chapter, two results of distributed LQR control established for networks with undirected topology are also reviewed. Focusing on undirected connected graphs, in the first part of Chapter 4, we follow a two-step design procedure and propose an LQR-based distributed control scheme which combines the main features of the top-down and bottom-up methods reviewed in Chapter 3. In the second part of Chapter 4, emphasis is placed on multi-agent networks with directed topology. We show that the strict limitation of bidirectional communication between interconnected agents, postulated in [17, 46], can be removed. Specifically, we show that this useful relaxation relies on two independent results: 1) the gain-margin property of the LQR control holds for complex multiplicative perturbations (see Theorem 3.2.8), and 2) the potentially non-simple structure of the Laplacian matrix can be neglected for stability analysis and control design. A top-down distributed LQR control method extending the results of [17] to directed graphs, is summarized in Theorem 4.3.4.

In Chapter 5, we adapt the two distributed LQR-based techniques [17, 46] to a more general agent-model setup. Specifically, rather than assuming identical system dynamics, we consider that agent models belong to a class of systems that share a minimal set of structural properties. In particular, we define the class of systems with identical sets of controllability indices and propose a model-matching feedback protocol that allows the stabilization problem of networks of heterogeneous dynamically decoupled agents to be tackled via distributed LQR-based techniques initially proposed for network of identical systems. Typically, agents are mapped to a common target model via a local state-feedback control scheme combined with a change of coordinates and an input-scaling matrix transformation. Under this setup, network stability is guaranteed by a distributed state-feedback controller designed on the target dynamics. Further, to enhance the optimality of the overall distributed feedback scheme, we propose an optimal target system the selection of which minimizes a certain measure of the joint model-matching control effort.

In Chapter 6, we extend the proposed model-matching control scheme to the nonlinear dynamics case thereby allowing regulation problems over networks of heterogeneous nonlinear agents to be solved via distributed LQR control. Particularly, using Lie algebra and differential geometry tools, we present an analytic procedure for how to derive a set of controllability indices (c.i.) from the state-space of a nonlinear system. Typically, a set of c.i. defines a specific class of nonlinear systems that can match the model of all target systems with identical sets of c.i., via the input-to-state linearization method. Existence conditions for the proposed nonlinear model-matching feedback scheme are identified. Similarly to the linear case, we show that the target dynamics can either selected without any optimality

criterion or by minimizing a certain cost function defined as the energy loss produced by the nonlinear model-matching feedback scheme.

Chapter 7 is devoted to the stabilization problem of networks of dynamically coupled agents. Focusing on linear dynamical agents, we assume that coupling terms between interconnected agents are expressed in a state-space form of a certain structure. We follow a top-down approach, which results in a distributed scheme whose stability is verified via a stability test involving a convex combination of two Hurwitz matrices. In Chapter 8, a case study of load frequency control (LFC) problem over a six-area power network illustrates the applicability of the results proposed in Chapter 7. We propose a novel LQR-based distributed LFC algorithm for large-scale multi-area power networks. The control scheme is obtained by optimizing an LQR performance index with a tuning parameter which can be used to emphasize/de-emphasize relative state differences between interconnected areas. We show that this parameter can be used to control the magnitude of tie-line power exchange and frequency synchronization between interconnected areas. Our approach enhances power system modularity and leads to a simple and verifiable stabilizability condition for a class of network topologies. Extensive simulations presented in the chapter support our conjecture that this stabilization criterion can be extended to more general multi-area power systems LFC problems.

Finally, in Chapter 9, we examine receding horizon control problems over networks of multiple dynamic agents. For a network setup composed of non-identical dynamically decoupled systems, we propose a distributed model predictive control scheme and derive sufficient conditions for convergence and stability of the overall distributed control system. It is shown that the proposed distributed network control protocol requires that each individual system be aware of the model parameters of its neighbors. Subsequently, we focus on a particular class of discrete-time linear systems and propose a distributed model-matching-based MPC protocol which let individual systems map their dynamics to a common target model using local information only, keep their model parameters private, and construct an implicit stabilizing feedback controller that couples their dynamic behavior with their neighboring systems. In the second part of the chapter, we address the problem of distributed model predictive control of dynamically coupled systems from an application point of view. In particular, we consider the load frequency control (LFC) problem examined in Chapter 8, and propose a distributed MPC method for distributed LFC design. Our method depends on a novel decoupling technique which enables the design of an MPC-based LFC controller with a distributed architecture.

10.1 Future work

The research of this thesis has attempted to address important problems arising in multi-agent systems and begets new directions for future work on distributed network control. We list a number of open problems and propose important topics for further study.

1) The distributed LQR-based techniques proposed in the thesis rely on the assumption that the system state is perfectly measured by the control unit. An important topic for research is the extension of the methods to the output-feedback case.

2) The model-matching method proposed for tackling regulation problems of networks of nonidentical dynamics proves powerful for a certain class of heterogeneous systems. Approximate model-matching and extension of the method to a more general framework represent topics for future work. In particular, the approximate model-matching can be expressed as follows. Assume that the dynamics of agents are uncertain and are described by parametric families. Is it possible to apply local state-feedback control and input scaling transformations so that the uncertainty radius of the resulting target system is minimized facilitating the network stabilization task?

3) The stabilization problem of dynamically coupled systems is a hard problem to solve due to the presence of coupling terms. For the case of identical dynamics, we have proposed a distributed LQR-based feedback controller which is stabilizing subject to sufficient conditions. Future work will attempt to relax this condition based on the optimality and robust stability margins of LQR control.

4) The optimality criterion that has been employed throughout the thesis is based on quadratic optimal control. It would be interesting to investigate the applicability of robust control methods such as H_∞ control which is insensitive to model parameter variations.

5) We have proposed a cooperative model-matching method carried out over a network of linear systems in a fully distributed manner. The method has been adapted to an MPC setting enhancing the privacy of local agents. Extension of the method to the nonlinear dynamics case as well as derivation of sufficient conditions for convergence and stability of the overall distributed nonlinear control scheme is a definite challenge for further research.

6) Network control lies in the intersection of control and communication theories. Problems associated with the communication scheme of a multi-agent network, such as

delays, quantized information exchange and varying interaction topologies are very important issues and represent directions for future research.

References

[1] Altafini, C. (2013). Consensus problems on networks with antagonistic interactions. *IEEE Trans. Automat. Contr.*, 58(4):935–946.

[2] Andreasson, M., Dimarogonas, D. V., Johansson, K. H., and Sandberg, H. (2013). Distributed vs. centralized power systems frequency control. In *2013 Eur. Control Conf. ECC 2013*, pages 3524–3529.

[3] Andreasson, M., Dimarogonas, D. V., Sandberg, H., and Johansson, K. H. (2014a). Distributed control of networked dynamical systems: Static feedback, integral action and consensus. *IEEE Trans. Automat. Contr.*, 59(7):1750–1764.

[4] Andreasson, M., Dimarogonas, D. V., Sandberg, H., and Johansson, K. H. (2014b). Distributed PI-control with applications to power systems frequency control. In *Proc. Am. Control Conf.*, pages 3183–3188.

[5] Antsaklis, P. J. and Michel, A. N. (2006). *Linear systems*. Birkhäuser.

[6] Aoki, M. (1972). On feedback stabilizability of decentralized dynamic systems. *Automatica*, 8(2):163–173.

[7] Atinc, G. M., Stipanovic, D. M., Voulgaris, P. G., and Karkoub, M. (2013). Collision-free trajectory tracking while preserving connectivity in unicycle multi-agent systems. In *Proc. Am. Control Conf.*, pages 5392–5397.

[8] Bamieh, B., Paganini, F., and Dahleh, M. A. (2002). Distributed control of spatially invariant systems. *IEEE Trans. Automat. Contr.*, 47(7):1091–1107.

[9] Bamieh, B. and Voulgaris, P. G. (2005). A convex characterization of distributed control problems in spatially invariant systems with communication constraints. *Syst. Control Lett.*, 54(6):575–583.

[10] Bauso, D., Giarré, L., and Pesenti, R. (2006). Non-linear protocols for optimal distributed consensus in networks of dynamic agents. *Syst. Control Lett.*, 55(11):918–928.

[11] Beard, R. W. and Ren, W. (2007). *Distributed Consensus in Multi-vehicle Cooperative Control*. Springer.

[12] Bertsekas, D. P. and Tsitsiklis, J. N. (1989). *Parallel and Distributed Computation: Numerical Methods*. Prentice-Hall, Inc.

[13] Bevrani, H. (2009). *Robust Power System Frequency Control*. Springer.

[14] Białas, S. (2004). A sufficient condition for Hurwitz stability of the convex combination of two matrices. *Control Cybern.*, 33(1):109–112.

[15] Bidram, A., Lewis, F. L., and Davoudi, A. (2014). Distributed control systems for small-scale power networks: Using multiagent cooperative control theory. *IEEE Control Syst.*, 34(6):56–77.

[16] Bin, M., Notarnicola, I., Marconi, L., and Notarstefano, G. (2019). A System Theoretical Perspective to Gradient-Tracking Algorithms for Distributed Quadratic Optimization. In *2019 IEEE Conf. Decis. Control*, pages 2994–2999.

[17] Borrelli, F. and Keviczky, T. (2008). Distributed LQR design for identical dynamically decoupled systems. *IEEE Trans. Automat. Contr.*, 53(8):1901–1912.

[18] Borrelli, F., Keviczky, T., Balas, G. J., Stewart, G., Fregene, K., and Godbole, D. (2005a). Hybrid decentralized control of large scale systems. In *Lect. Notes Comput. Sci.*, volume 3414, pages 168–183.

[19] Borrelli, F., Keviczky, T., Fregene, K., and Balas, G. J. (2005b). Decentralized receding horizon control of cooperative vehicle formations. In *Proc. 44th IEEE Conf. Decis. Control. Eur. Control Conf. CDC-ECC '05*, volume 2005, pages 3955–3960.

[20] Boyd, S., El Ghaoui, L., Feron, E., and Balakrishnan, V. (1994). *Linear Matrix Inequalities in System and Control Theory*. Society for Industrial and Applied Mathematics.

[21] Boyd, S., Ghosh, A., Prabhakar, B., and Shah, D. (2005). Gossip algorithms: Design, analysis and applications. In *Proc. - IEEE INFOCOM*, volume 3, pages 1653–1664.

[22] Boyd, S., Parikh, N., Chu, E., Peleato, B., and Eckstein, J. (2010). Distributed optimization and statistical learning via the alternating direction method of multipliers. *Found. Trends Mach. Learn.*, 3(1):1–122.

[23] Camacho, A. (1970). Externalities, Optimality and Informationally Decentralized Resource Allocation Processes. *Int. Econ. Rev. (Philadelphia).*, 11(2):318–327.

[24] Camponogara, E., Jia, D., Krogh, B. H., and Talukdar, S. (2002). Distributed Model Predictive Control. *IEEE Control Syst.*, 22(1):44–52.

[25] Cao, M., Spielman, D. A., and Morse, A. S. (2005). A lower bound on convergence of a distributed network consensus algorithm. In *Proc. 44th IEEE Conf. Decis. Control. Eur. Control Conf. CDC-ECC '05*, volume 2005, pages 2356–2361.

[26] Cao, Y. and Ren, W. (2009). Lqr-based optimal linear consensus algorithms. In *Proc. Am. Control Conf.*, pages 5204–5209.

[27] Cao, Y. and Ren, W. (2014). Finite-time consensus for multi-agent networks with unknown inherent nonlinear dynamics. *Automatica*, 50(10):2648–2656.

[28] Cao, Y., Yu, W., Ren, W., and Chen, G. (2013). An overview of recent progress in the study of distributed multi-agent coordination. *IEEE Trans. Ind. Informatics*, 9(1):427–438.

[29] Chang, D. E., Shadden, S. C., Marsden, J. E., and Olfati-Saber, R. (2003). Collision Avoidance for Multiple Agent Systems. In *Proc. IEEE Conf. Decis. Control*, volume 1, pages 539–543.

[30] Chang, T. H., Hong, M., Liao, W. C., and Wang, X. (2016a). Asynchronous Distributed ADMM for Large-Scale Optimization - Part I: Algorithm and Convergence Analysis. *IEEE Trans. Signal Process.*, 64(12):3118–3130.

[31] Chang, T. H., Liao, W. C., Hong, M., and Wang, X. (2016b). Asynchronous Distributed ADMM for Large-Scale Optimization - Part II: Linear Convergence Analysis and Numerical Performance. *IEEE Trans. Signal Process.*, 64(12):3131–3144.

[32] Chen, C. T. (1984). *Linear System Theory and Design*. OXFORD UNIVERSITY PRESS, third edition.

[33] Chen, F. and Dimarogonas, D. V. (2019). Consensus Control for Leader-follower Multi-agent Systems under Prescribed Performance Guarantees. In *2019 IEEE Conf. Decis. Control*, pages 4785–4790.

[34] Chilali, M. and Gahinet, P. (1996). H_∞ design with pole placement constraints: An LMI approach. *IEEE Trans. Automat. Contr.*, 41(3):358–367.

[35] Christofides, P. D., Scattolini, R., Muñoz de la Peña, D., and Liu, J. (2013). Distributed model predictive control: A tutorial review and future research directions. *Comput. Chem. Eng.*, 51:21–41.

[36] Christopher Edwards, S. K. S. (1998). *Sliding Mode Control Theory And Applications*. Taylor & Francis Group, LLC.

[37] Chu, K. (1974). Decentralized Control of High-Speed Vehicular Strings. *Transp. Sci.*, 8(4):361–384.

[38] Cloosterman, M. B., van de Wouw, N., Heemels, W. P., and Nijmeijer, H. (2009). Stability of networked control systems with uncertain time-varying delays. *IEEE Trans. Automat. Contr.*, 54(7):1575–1580.

[39] Cui, G., Xu, S., Ma, Q., Li, Y., and Zhang, Z. (2018). Prescribed performance distributed consensus control for nonlinear multi-agent systems with unknown dead-zone input. *Int. J. Control*, 91(5):1053–1065.

[40] Dai, X., Bourdais, R., Guéguen, H., and Statement, A. C. P. (2019). Dynamic Reduction of The Iterations Requirement in A Distributed Model Predictive Control. In *2019 IEEE Conf. Decis. Control*, pages 6392–6397.

[41] D'Andrea, R. and Dullerud, G. E. (2003). Distributed Control Design for Spatially Interconnected Systems. *IEEE Trans. Automat. Contr.*, 48(9):1478–1495.

[42] de Galland, C. M. and Hendrickx, J. M. (2019). Lower bound performances for average consensus in open multi-agent systems (extended version). In *2019 IEEE Conf. Decis. Control*, pages 7429–7434.

[43] Delvenne, J. C., Carli, R., and Zampieri, S. (2009). Optimal strategies in the average consensus problem. *Syst. Control Lett.*, 58(10-11):759–765.

[44] Demyano, V. F. and Malozemo, V. N. (1974). *Introduction to minimax*. Dover Publications, Inc., New York.

[45] Desai, J. P., Ostrowski, J. P., and Kumar, V. (2001). Modeling and control of formations of nonholonomic mobile robots. *IEEE Trans. Robot. Autom.*, 17(6):905–908.

[46] Deshpande, P., Menon, P. P., Edwards, C., and Postlethwaite, I. (2012). Sub-optimal distributed control law with H_2 performance for identical dynamically coupled linear systems. *IET Control Theory Appl.*, 6(16):2509–2517.

[47] Deva Brinda, M., Suresh, A., and Rashmi, M. R. (2018). A literature survey on LFC in a deregulated electricity environment. *World Rev. Sci. Technol. Sustain. Dev.*, 14(1):1–10.

[48] Devi, P. S., Santhi, R. V., and Pushpalatha, D. V. (2016). Introducing LQR-fuzzy technique with dynamic demand response control loop to load frequency control model. *IFAC-PapersOnLine*, 49(1):567–572.

[49] Diab, A. A. and El-Sattar, M. A. (2018). Adaptive model predictive based load frequency control in an interconnected power system. *Proc. 2018 IEEE Conf. Russ. Young Res. Electr. Electron. Eng.*, pages 604–610.

[50] Doan, T. T., Bose, S., Nguyen, D. H., and Beck, C. L. (2019a). Convergence of the Iterates in Mirror Descent Methods. *IEEE Control Syst. Lett.*, 3(1):114–119.

[51] Doan, T. T., Maguluri, S. T., and Romberg, J. (2019b). Convergence Rates of Distributed Two-Time-Scale Gradient Methods under Random Quantization. In *IFAC-PapersOnLine*, volume 52, pages 267–272.

[52] Dong, W. and Farrell, J. A. (2008a). Consensus of multiple nonholonomic systems. In *Proc. IEEE Conf. Decis. Control*, pages 2270–2275.

[53] Dong, W. and Farrell, J. A. (2008b). Cooperative control of multiple nonholonomic mobile agents. *IEEE Trans. Automat. Contr.*, 53(6):1434–1448.

[54] Dritsas, L., Kontouras, E., Kitsios, I., and Tzes, A. (2018). Aggressive Control Design for Electric Power Generation Plants. In *MED 2018 - 26th Mediterr. Conf. Control Autom.*, pages 667–672.

[55] Duchi, J. C., Agarwal, A., and Wainwright, M. J. (2012). Dual averaging for distributed optimization: Convergence analysis and network scaling. *IEEE Trans. Automat. Contr.*, 57(3):592–606.

[56] Dullerud, G. E. and D'Andrea, R. (2004). Distributed control of heterogeneous systems. *IEEE Trans. Automat. Contr.*, 49(12):2113–2128.

[57] Dunbar, W. B. and Murray, R. M. (2004). Receding horizon control of multi-vehicle formations: A distributed implementation. In *Proc. IEEE Conf. Decis. Control*, volume 2, pages 1995–2002.

[58] Dunbar, W. B. and Murray, R. M. (2006). Distributed receding horizon control for multi-vehicle formation stabilization. *Automatica*, 42(4):549–558.

[59] Egerstedt, M., Hu, X., and Stotsky, A. (2001). Control of mobile platforms using a virtual vehicle approach. *IEEE Trans. Automat. Contr.*, 46(11):1777–1782.

[60] Esfahani, P. M., Vrakopoulou, M., Margellos, K., Lygeros, J., and Andersson, G. (2010). Cyber attack in a two-area power system: Impact identification using reachability. In *Proc. 2010 Am. Control Conf. ACC 2010*, pages 962–967.

[61] Fahimi, F. (2007). Non-linear model predictive formation control for groups of autonomous surface vessels. *Int. J. Control*, 80(8):1248–1259.

[62] Fax, J. A. and Murray, R. M. (2002). Information flow and cooperative control of vehicle formations. *IFAC Proc. Vol.*, 15(1):115–120.

[63] Fax, J. A. and Murray, R. M. (2004). Information flow and cooperative control of vehicle formations. *IEEE Trans. Automat. Contr.*, 49(9):1465–1476.

[64] Ferraz, H. and Hespanha, P. (2019). Iterative algorithms for distributed leader-follower model predictive control. In *2019 IEEE Conf. Decis. Control*, pages 3533–3539.

[65] Fidan, B. and Hendrickx, J. M. (2008). Rigid Graph Control Architectures for Autonomous Formations. *IEEE Control Syst.*, 28(6):48–63.

[66] Fosha, C. E. and Elgerd, O. I. (1970). The Megawatt-Frequency Control Problem: A New Approach Via Optimal Control Theory. *IEEE Trans. Power Appar. Syst.*, PAS-89(4):563–577.

[67] Franceschelli, M., Pisano, A., Giua, A., and Usai, E. (2015). Finite-Time Consensus with Disturbance Rejection by Discontinuous Local Interactions in Directed Graphs. *IEEE Trans. Automat. Contr.*, 60(4):1133–1138.

[68] Franco, E., Magni, L., Parisini, T., Polycarpou, M. M., and Raimondo, D. M. (2008). Cooperative constrained control of distributed agents with nonlinear dynamics and delayed information exchange: A stabilizing receding-horizon approach. *IEEE Trans. Automat. Contr.*, 53(1):324–338.

[69] Freeman, R. A., Yang, P., and Lynch, K. M. (2006). Stability and convergence properties of dynamic average consensus estimators. In *Proc. IEEE Conf. Decis. Control*, pages 398–403.

[70] Gielen, R. H., Olaru, S., Lazar, M., Heemels, W. P., van de Wouw, N., and Niculescu, S. I. (2010). On polytopic inclusions as a modeling framework for systems with time-varying delays. *Automatica*, 46(3):615–619.

[71] Gu, G., Marinovici, L., and Lewis, F. L. (2012). Consensusability of discrete-time dynamic multiagent systems. *IEEE Trans. Automat. Contr.*, 57(8):2085–2089.

[72] Guechi, E. H., Bouzoualegh, S., Zennir, Y., and Blažič, S. (2018). MPC control and LQ optimal control of a two-link robot arm: A comparative study. *Machines*, 6(3).

[73] Guo, W., Lü, J., Chen, S., and Yu, X. (2011). Second-order tracking control for leader-follower multi-agent flocking in directed graphs with switching topology. *Syst. Control Lett.*, 60(12):1051–1058.

[74] Gupta, V., Hassibi, B., and Murray, R. M. (2004). On the synthesis of control laws for a network of autonomous agents. In *Proc. Am. Control Conf.*, volume 6, pages 4927–4932.

[75] Gupta, V., Hassibi, B., and Murray, R. M. (2005). A sub-optimal algorithm to synthesize control laws for a network of dynamic agents. *Int. J. Control*, 78(16):1302–1313.

[76] Haes Alhelou, H., Hamedani-Golshan, M. E., Zamani, R., Heydarian-Forushani, E., and Siano, P. (2018). Challenges and opportunities of load frequency control in conventional, modern and future smart power systems: A comprehensive review. *Energies*, 11(10).

[77] Haghighi, R., Wang, D., and Low, C. (2014). Real-time distributed optimal trajectory generation for nonholonomic vehicles in formations. In *Proc. - IEEE Int. Conf. Robot. Autom.*, pages 3589–3594.

[78] Heemels, W. P. H., Teel, A. R., Van De Wouw, N., and Nešić, D. (2010). Networked control systems with communication constraints: Tradeoffs between transmission intervals, delays and performance. *IEEE Trans. Automat. Contr.*, 55(8):1781–1796.

[79] Hespanha, J. P. (2005). Undergraduate lecture notes on LQG/LQR Controller Design.

[80] Hespanha, J. P., Naghshtabrizi, P., and Xu, Y. (2007). A survey of recent results in networked control systems. *Proc. IEEE*, 95(1):138–172.

[81] Hinrichsen, D. and Pritchard, A. J. (1988). On the robustness of root locations of polynomials under complex and real perturbations. In *Proc. IEEE Conf. Decis. Control*, pages 1410–1414.

[82] Ho, Y. C. and Chu, K. C. (1971). Team Decision Theory and Information Structures in Optimal Control Problems-Part I. *IEEE Trans. Automat. Contr.*, 17(1):15–22.

[83] Hong, Y., Gao, L., Cheng, D., and Hu, J. (2007). Lyapunov-based approach to multi-agent systems with switching jointly connected interconnection. *IEEE Trans. Automat. Contr.*, 52(5):943–948.

[84] Horn, R. A. and Johnson, C. R. (1991). *Topics in matrix analysis*. Cambridge University Press.

[85] Horton, J. (2008). *Digital communications by satellite*, volume 67. Prentice-Hall International, Inc.

[86] Hu, J. and Lin, Y. S. (2010). Consensus control for multi-agent systems with double-integrator dynamics and time delays. *IET Control Theory Appl.*, 4(1):109–118.

[87] Huang, H., Yu, C., and Wu, Q. (2010). Distributed LQR design for multi-agent formations. In *Proc. IEEE Conf. Decis. Control*, pages 4535–4540.

[88] Hurwicz, L. (2011). Optimality and informational efficiency in resource allocation processes. *Stud. Resour. Alloc. Process.*, pages 393–460.

[89] Inalhan, G., Stipanović, D. M., and Tomlin, C. J. (2002). Decentralized optimization, with application to multiple aircraft coordination. In *Proc. IEEE Conf. Decis. Control*, volume 1, pages 1147–1155.

[90] Iracleous, D. P. and Alexandridis, A. T. (2005). A multi-task automatic generation control for power regulation. *Electr. Power Syst. Res.*, 73(3):275–285.

[91] Jadbabaie, A., Lin, J., and Morse, A. S. (2003). Coordination of groups of mobile autonomous agents using nearest neighbor rules. *IEEE Trans. Automat. Contr.*, 48(6):988–1001.

[92] Jakovetic, D., Xavier, J., and Moura, J. M. (2014). Fast distributed gradient methods. *IEEE Trans. Automat. Contr.*, 59(5):1131–1146.

[93] Jovanovic, M. R. (2005). On the optimality of localized distributed controllers. In *Proc. Am. Control Conf.*, volume 7, pages 4583–4588.

[94] Jovanović, M. R. and Bamieh, B. (2005). On the ill-posedness of certain vehicular platoon control problems. *IEEE Trans. Automat. Contr.*, 50(9):1307–1321.

[95] Jovanović, M. R., Fowler, J. M., Bamieh, B., and D'Andrea, R. (2008). On the peaking phenomenon in the control of vehicular platoons. *Syst. Control Lett.*, 57(7):528–537.

[96] Kao, C. Y. and Lincoln, B. (2004). Simple stability criteria for systems with time-varying delays. *Automatica*, 40(8):1429–1434.

[97] Karayiannidis, Y., Dimarogonas, D. V., and Kragic, D. (2012). Multi-agent average consensus control with prescribed performance guarantees. In *Proc. IEEE Conf. Decis. Control*, pages 2219–2225.

[98] Katsoukis, I. and Rovithakis, G. A. (2015). Leader-follower tracking with prescribed transient and steady state performance guarantees for a class of unknown nonlinear multi-agent systems. In *23rd Mediterr. Conf. Control (MED) 2015*, pages 1027–1032.

[99] Keviczky, T., Borrelli, F., and Balas, G. J. (2004). A study on decentralized receding horizon control for decoupled systems. In *Proc. Am. Control Conf.*, volume 6, pages 4921–4926.

[100] Keviczky, T., Borrelli, F., and Balas, G. J. (2006a). Decentralized receding horizon control for large scale dynamically decoupled systems. *Automatica*, 42(12):2105–2115.

[101] Keviczky, T., Borrelli, F., Fregene, K., Godbole, D., and Balas, G. J. (2008). Decentralized receding horizon control and coordination of autonomous vehicle formations. *IEEE Trans. Control Syst. Technol.*, 16(1):19–33.

[102] Keviczky, T., Vanek, B., Borrelli, F., and Balas, G. J. (2006b). Hybrid decentralized receding horizon control of vehicle formations. In *Proc. Am. Control Conf.*, volume 2006, pages 3358–3363.

[103] Khalil, H. K. (1996). *Nonlinear systems*. Prentice Hall, Inc., third edition.

[104] Kim, S., Oh, H., and Tsourdos, A. (2013). Nonlinear model predictive coordinated standoff tracking of a moving ground vehicle. *J. Guid. Control. Dyn.*, 36(2):557–566.

[105] Kontouras, E., Tzes, A., and Dritsas, L. (2018). Set-theoretic detection of data corruption attacks on cyber physical power systems. *J. Mod. Power Syst. Clean Energy*, 6(5):872–886.

[106] Kundur, P. (1993). *Power System Stability And Control*. McGraw-Hill, Inc.

[107] Kuramoto, Y. (1984). *Chemical Oscillations, Waves, and Turbulence*, volume 19 of *Springer Series in Synergetics*. Springer.

[108] Kuwata, Y. and How, J. P. (2011). Cooperative distributed robust trajectory optimization using receding horizon MILP. *IEEE Trans. Control Syst. Technol.*, 19(2):423–431.

[109] Lan, G., Lee, S., and Zhou, Y. (2020). Communication-efficient algorithms for decentralized and stochastic optimization. *Math. Program.*, 180(1-2):237–284.

[110] Langbort, C., Chandra, R. S., and D'Andrea, R. (2004). Distributed control design for systems interconnected over an arbitrary graph. *IEEE Trans. Automat. Contr.*, 49(9):1502–1519.

[111] Lau, R., Persiano, R. C., and Varaiya, P. P. (1972). Decentralized Information and Control: a Network Flow Example. *IEEE Trans. Automat. Contr.*, AC-17(4):466–473.

[112] Levine, W. S. and Athans, M. (1966). On the Optimal Error Regulation of a String of Moving Vehicles. *IEEE Trans. Automat. Contr.*, 11(3):355–361.

[113] Li, Z., Liu, X., Ren, W., and Xie, L. (2013). Distributed tracking control for linear multiagent systems with a leader of bounded unknown input. *IEEE Trans. Automat. Contr.*, 58(2):518–523.

[114] Li, Z., Wen, G., Duan, Z., and Ren, W. (2015). Designing Fully Distributed Consensus Protocols for Linear Multi-Agent Systems with Directed Graphs. *IEEE Trans. Automat. Contr.*, 60(4):1152–1157.

[115] Lin, F., Fardad, M., and Jovanovic, M. R. (2013). Design of optimal sparse feedback gains via the alternating direction method of multipliers. *IEEE Trans. Automat. Contr.*, 58(9):2426–2431.

[116] Liu, J., Chen, X., De La Peña, D. M., and Christofides, P. D. (2010a). Sequential and iterative architectures for distributed model predictive control of nonlinear process systems. Part I: Theory. In *Proc. 2010 Am. Control Conf. ACC 2010*, pages 3148–3155.

[117] Liu, J., Chen, X., De La Peña, D. M., and Christofides, P. D. (2010b). Sequential and iterative architectures for distributed model predictive control of nonlinear process systems. Part II: Application to a catalytic alkylation of benzene process. In *Proc. 2010 Am. Control Conf. ACC 2010*, pages 3156–3161.

[118] Liu, J., Chen, X., de la Peña, D. M., and Christofides, P. D. (2010c). Sequential and iterative architectures for distributed model predictive control of nonlinear process systems. *AIChE J.*, 56(8):2137–2149.

[119] Liu, J., De La Peña, D. M., and Christofides, P. D. (2009). Distributed model predictive control of nonlinear process systems. *AIChE J.*, 55(5):1171–1184.

[120] Liu, J., Muñoz de la Peña, D., and Christofides, P. D. (2010d). Distributed model predictive control of nonlinear systems subject to asynchronous and delayed measurements. *Automatica*, 46(1):52–61.

[121] Liu, Y., Passino, K. M., and Polycarpou, M. M. (2003). Stability analysis of M-dimensional asynchronous swarms with a fixed communication topology. *IEEE Trans. Automat. Contr.*, 48(1):76–95.

[122] Ma, C. Q. and Zhang, J. F. (2010). Necessary and sufficient conditions for consensusability of linear multi-agent systems. *IEEE Trans. Automat. Contr.*, 55(5):1263–1268.

[123] Ma, J. (2018). *Power System Wide-Area Stability Analysis and Control*. Wiley.

[124] Ma, M., Chen, H., Liu, X., and Allgöwer, F. (2014). Distributed model predictive load frequency control of multi-area interconnected power system. *Int. J. Electr. Power Energy Syst.*, 62:289–298.

[125] Ma, M., Zhang, C., Liu, X., and Chen, H. (2017). Distributed Model Predictive Load Frequency Control of the Multi-Area Power System after Deregulation. *IEEE Trans. Ind. Electron.*, 64(6):5129–5139.

[126] Macellari, L., Karayiannidis, Y., and Dimarogonas, D. V. (2017). Multi-Agent Second Order Average Consensus with Prescribed Transient Behavior. *IEEE Trans. Automat. Contr.*, 62(10):5282–5288.

[127] Maestre, J. M., Muñoz De La Peña, D., and Camacho, E. F. (2011). Distributed model predictive control based on a cooperative game. *Optim. Control Appl. Methods*, 32(2):153–176.

[128] Maestre, J. M. and Negenborn, R. R. (2014). *Distributed Model Predictive Control Made Easy*, volume 69. Springer.

[129] Mansoori, F. and Wei, E. (2019). A General Framework of Exact Primal-Dual First Order Algorithms for Distributed Optimization. In *2019 IEEE Conf. Decis. Control*, pages 6386–6391.

[130] Marschak, T. A. (1968). Centralized Versus Decentralized Resource Allocation: The Yugoslav "Laboratory". *Q. J. Econ.*, 82(4):561.

[131] Masood, N. A., Modi, N., and Yan, R. (2016). Low inertia power systems: Frequency response challenges and a possible solution. In *Proc. 2016 Australas. Univ. Power Eng. Conf. AUPEC 2016*.

[132] Massioni, P. and Verhaegen, M. (2009). Distributed control for identical dynamically coupled systems: A decomposition approach. *IEEE Trans. Automat. Contr.*, 54(1):124–135.

[133] Mastellone, S., Stipanović, D. M., Graunke, C. R., Intlekofer, K. A., and Spong, M. W. (2008). Formation control and collision avoidance for multi-agent non-holonomic systems: Theory and experiments. *Int. J. Rob. Res.*, 27(1):107–126.

[134] Matei, I. and Baras, J. S. (2011). Performance evaluation of the consensus-based distributed subgradient method under random communication topologies. *IEEE J. Sel. Top. Signal Process.*, 5(4):754–771.

[135] Mayne, D. Q. (2014). Model predictive control: Recent developments and future promise. *Automatica*, 50(12):2967–2986.

[136] McFadden, D. (1969). On the Controllability of Decentralized Macroeconomic Systems: The Assignment Problem. In Kuhn, H. and Szegö, G., editors, *Math. Syst. Theory Econ. I / II*, pages 221–239. Springer.

[137] Melzer, S. M. and Kuo, B. C. (1971). Optimal regulation of systems described by a countably infinite number of objects. *Automatica*, 7(3):359–366.

[138] Menon, P. P. and Edwards, C. (2010). Static output feedback stabilisation and synchronisation of complex networks with H2 performance. *Int. J. Robust Nonlinear Control*, 20(6):703–718.

[139] Mesbahi, M. and Egerstedt, M. (2010). *Graph theoretic methods in multiagent networks*. Princeton University Press.

[140] Mirkin, B. M. and Gutman, P. O. (2005). Output-feedback co-ordinated decentralized adaptive tracking: The case of MIMO subsystems with delayed interconnections. *Int. J. Adapt. Control Signal Process.*, 19(8):639–660.

[141] Mohar, B. (1991). The Laplacian Spectrum of Graphs. *Graph Theory, Comb. Appl.*, 2:871–898.

[142] Motee, N. and Jadbabaie, A. (2009). Approximation methods and spatial interpolation in distributed control systems. In *Proc. Am. Control Conf.*, pages 860–865.

[143] Muñoz de la Peña, D. and Christofides, P. D. (2008). Lyapunov-based model predictive control of nonlinear systems subject to data losses. *IEEE Trans. Automat. Contr.*, 53(9):2076–2089.

[144] Munsing, E., Mather, J., and Moura, S. (2017). Blockchains for decentralized optimization of energy resources in microgrid networks. In *1st Annu. IEEE Conf. Control Technol. Appl. CCTA 2017*, pages 2164–2171.

[145] Münz, U., Papachristodoulou, A., and Allgöwer, F. (2010). Delay robustness in consensus problems. *Automatica*, 46(8):1252–1265.

[146] Naghshtabrizi, P., Hespanha, J. P., and Teel, A. R. (2010). Stability of delay impulsive systems with application to networked control systems. *Trans. Inst. Meas. Control*, 32(5):511–528.

[147] Nedić, A. and Olshevsky, A. (2015). Distributed optimization over time-varying directed graphs. *IEEE Trans. Automat. Contr.*, 60(3):601–615.

[148] Nedic, A. and Olshevsky, A. (2016). Stochastic Gradient-Push for Strongly Convex Functions on Time-Varying Directed Graphs. *IEEE Trans. Automat. Contr.*, 61(12):3936–3947.

[149] Nedic, A., Olshevsky, A., and Rabbat, M. G. (2018). Network Topology and Communication-Computation Tradeoffs in Decentralized Optimization. *Proc. IEEE*, 106(5):953–976.

[150] Nedić, A., Olshevsky, A., Shi, and Wei (2017). Achieving geometric convergence for distributed optimization over time-varying graphs. *SIAM J. Optim.*, 27(4):2597–2633.

[151] Nedić, A. and Ozdaglar, A. (2009). Distributed subgradient methods for multi-agent optimization. *IEEE Trans. Automat. Contr.*, 54(1):48–61.

[152] Negenborn, R. R. and Maestre, J. M. (2014). Distributed model predictive control: An overview and roadmap of future research opportunities. *IEEE Control Syst.*, 34(4):87–97.

[153] Olfati-Saber, R. (2006). Flocking for multi-agent dynamic systems: Algorithms and theory. *IEEE Trans. Automat. Contr.*, 51(3):401–420.

[154] Olfati-Saber, R., Fax, J. A., and Murray, R. M. (2007). Consensus and cooperation in networked multi-agent systems. *Proc. IEEE*, 95(1):215–233.

[155] Olfati-Saber, R. and Murray, R. M. (2004). Consensus problems in networks of agents with switching topology and time-delays. *IEEE Trans. Automat. Contr.*, 49(9):1520–1533.

[156] Olshevsky, A. and Tsitsiklis, J. N. (2006). Convergence rates in distributed consensus and averaging. In *Proc. IEEE Conf. Decis. Control*, pages 3387–3392.

[157] Osbouei, B. A., Taylor, G. A., Bronckart, O., Maricq, J., and Bradley, M. (2019). Impact of inertia distribution on power system stability and operation. In *2019 IEEE Milan PowerTech, PowerTech 2019*.

[158] Oshnoei, A., Khezri, R., Muyeen, S. M., and Blaabjerg, F. (2018). On the contribution of wind farms in automatic generation control: Review and new control approach. *Appl. Sci.*, 8(10):1848.

[159] Pandey, S. K., Mohanty, S. R., and Kishor, N. (2013a). A literature survey on load-frequency control for conventional and distribution generation power systems. *Renew. Sustain. Energy Rev.*, 25:318–334.

[160] Pandey, S. K., Mohanty, S. R., Kishor, N., and Catalão, J. P. (2013b). An advanced LMI-based-LQR design for load frequency control of an autonomous hybrid generation system. *IFIP Adv. Inf. Commun. Technol.*, 394:371–381.

[161] Papachristodoulou, A., Jadbabaie, A., and Munz, U. (2010). Effects of delay in multi-agent consensus and oscillator synchronization. *IEEE Trans. Automat. Contr.*, 55(6):1471–1477.

[162] Pappachen, A. and Peer Fathima, A. (2017). Critical research areas on load frequency control issues in a deregulated power system: A state-of-the-art-of-review. *Renew. Sustain. Energy Rev.*, 72:163–177.

[163] Pasqualetti, F., Bicchi, A., and Bullo, F. (2007). Distributed intrusion detection for secure consensus computations. In *Proc. IEEE Conf. Decis. Control*, pages 5594–5599.

[164] Pasqualetti, F., Bicchi, A., and Bullo, F. (2012). Consensus computation in unreliable networks: A system theoretic approach. *IEEE Trans. Automat. Contr.*, 57(1):90–104.

[165] Pavel, L. (2007). An extension of duality to a game-theoretic framework. *Automatica*, 43(2):226–237.

[166] Pin, G. and Parisini, T. (2011). Networked predictive control of uncertain constrained nonlinear systems: Recursive feasibility and input-to-state stability analysis. *IEEE Trans. Automat. Contr.*, 56(1):72–87.

[167] Qu, G. and Li, N. (2018). Harnessing smoothness to accelerate distributed optimization. *IEEE Trans. Control Netw. Syst.*, 5(3):1245–1260.

[168] Raffard, R. L., Tomlin, C. J., and Boyd, S. P. (2004). Distributed optimization for cooperative agents: Application to formation flight. In *Proc. IEEE Conf. Decis. Control*, volume 3, pages 2453–2459.

[169] Ren, W. (2007). Consensus seeking in multi-vehicle systems with a time-varying reference state. In *Proc. Am. Control Conf.*, pages 717–722.

[170] Ren, W. and Atkins, E. (2007). Distributed multi-vehicle coordinated control via local information exchange. *Int. J. Robust Nonlinear Control*, 17(10-11):1002–1033.

[171] Ren, W. and Beard, R. W. (2005). Consensus seeking in multiagent systems under dynamically changing interaction topologies. *IEEE Trans. Automat. Contr.*, 50(5):655–661.

[172] Rerkpreedapong, D., Hasanović, A., and Feliachi, A. (2003). Robust load frequency control using genetic algorithms and linear matrix inequalities. *IEEE Trans. Power Syst.*, 18(2):855–861.

[173] Richards, A. and How, J. (2004). A decentralized algorithm for robust constrained model predictive control. In *Proc. Am. Control Conf.*, volume 5, pages 4261–4266.

[174] Richards, A. and How, J. P. (2007). Robust distributed model predictive control. *Int. J. Control*, 80(9):1517–1531.

[175] Rodríguez-Seda, E. J., Tang, C., Spong, M. W., and Stipanović, D. M. (2014). Trajectory tracking with collision avoidance for nonholonomic vehicles with acceleration constraints and limited sensing. *Int. J. Rob. Res.*, 33(12):1569–1592.

[176] Romao, L., Margellos, K., Notarstefano, G., and Papachristodoulou, A. (2019). Subgradient averaging for multi-agent optimisation with different constraint sets. In *2019 IEEE Conf. Decis. Control*, pages 7448–7453.

[177] Rotkowitz, M. and Lall, S. (2005). A characterization of convex problems in decentralized control. *IEEE Trans. Automat. Contr.*, 50(12):1984–1996.

[178] Saber, R. O. and Murray, R. M. (2003). Flocking with Obstacle Avoidance: Cooperation with Limited Communication in Mobile Networks. In *Proc. IEEE Conf. Decis. Control*, volume 2, pages 2022–2028.

[179] Sadowska, A., Van Den Broek, T., Huijberts, H., Van De Wouw, N., Kostić, D., and Nijmeijer, H. (2011). A virtual structure approach to formation control of unicycle mobile robots using mutual coupling. *Int. J. Control*, 84(11):1886–1902.

[180] Sakurama, K. (2019). Formation-oriented Motion Coordination of Multi-agent Systems over Relative Measurements. In *2019 IEEE Conf. Decis. Control*, pages 2782–2787.

[181] Santini, S., Salvi, A., Valente, A. S., Pescape, A., Segata, M., and Lo Cigno, R. (2017). A Consensus-Based Approach for Platooning with Intervehicular Communications and Its Validation in Realistic Scenarios. *IEEE Trans. Veh. Technol.*, 66(3):1985–1999.

[182] Scattolini, R. (2009). Architectures for distributed and hierarchical Model Predictive Control - A review. *J. Process Control*, 19(5):723–731.

[183] Scoy, B. V. and Lessard, L. (2019). A Distributed Optimization Algorithm over Time-Varying Graphs with Efficient Gradient Evaluations. In *IFAC-PapersOnLine*, volume 52, pages 357–362.

[184] Segovia, P., Rajaoarisoa, L., Nejjari, F., Duviella, E., and Puig, V. (2019). A communication-based distributed model predictive control approach for large-scale systems. In *2019 IEEE Conf. Decis. Control*, pages 8366–8371.

[185] Seiler, P., Pant, A., and Hedrick, K. (2004). Disturbance propagation in vehicle strings. *IEEE Trans. Automat. Contr.*, 49(10):1835–1841.

[186] Seuret, A., Dimarogonas, D. V., and Johansson, K. H. (2008). Consensus under communication delays. In *Proc. IEEE Conf. Decis. Control*, pages 4922–4927.

[187] Seuret, A., Dimarogonas, D. V., and Johansson, K. H. (2009). Consensus of double integrator multi-agents under communication delay. *IFAC Proc. Vol.*, 8(PART 1):376–381.

[188] Shahalami, S. H. and Farsi, D. (2018). Analysis of Load Frequency Control in a restructured multi-area power system with the Kalman filter and the LQR controller. *AEU - Int. J. Electron. Commun.*, 86:25–46.

[189] Shankar, G., Lakshmi, S., and Nagarjuna, N. (2015). Optimal load frequency control of hybrid renewable energy system using PSO and LQR. In *Proc. 2015 IEEE Int. Conf. Power Adv. Control Eng. ICPACE 2015*, pages 195–199.

[190] Shankar, R., Pradhan, S. R., Chatterjee, K., and Mandal, R. (2017). A comprehensive state of the art literature survey on LFC mechanism for power system. *Renew. Sustain. Energy Rev.*, 76:1185–1207.

[191] Shayeghi, H., Shayanfar, H. A., and Jalili, A. (2009). Load frequency control strategies: A state-of-the-art survey for the researcher. *Energy Convers. Manag.*, 50(2):344–353.

[192] Shi, W., Ling, Q., Wu, G., and Yin, W. (2015). Extra: An exact first-order a lgorithm for decentralized consensus optimization. *SIAM J. Optim.*, 25(2):944–966.

[193] Shin, J. and Kim, H. J. (2009). Nonlinear model predictive formation flight. *IEEE Trans on Sys, Man, and Cybern - Part A: Systems and Humans*, 39(5):1116–1125.

[194] Siljak, D. D., Stipanovic, D. M., and Zecevic, A. I. (2002). Robust decentralized turbine/governor control using linear matrix inequalities. *IEEE Trans. Power Syst.*, 17(3):715–722.

[195] Smith, T. R., Hanssmann, H., and Leonard, N. E. (2001). Orientation control of multiple underwater vehicles with symmetry-breaking potentials. In *Proc. IEEE Conf. Decis. Control*, volume 5, pages 4598–4603. IEEE.

[196] Stewart, B. T., Venkat, A. N., Rawlings, J. B., Wright, S. J., and Pannocchia, G. (2010). Cooperative distributed model predictive control. *Syst. Control Lett.*, 59(8):460–469.

[197] Stipanović, D. M., Hokayem, P. F., Spong, M. W., and Šiljak, D. D. (2007). Cooperative avoidance control for multiagent systems. *J. Dyn. Syst. Meas. Control. Trans. ASME*, 129(5):699–707.

[198] Stipanović, D. M., Inalhan, G., Teo, R., and Tomlin, C. J. (2004). Decentralized overlapping control of a formation of unmanned aerial vehicles. *Automatica*, 40(8):1285–1296.

[199] Strogatz, S. H. (2001). Exploring complex networks. *Nature*, 410(6825):268–276.

[200] Sundaram, S. and Hadjicostis, C. N. (2008a). Distributed function calculation via linear iterations in the presence of malicious agents - Part I: Attacking the network. In *Proc. Am. Control Conf.*, pages 1350–1355.

[201] Sundaram, S. and Hadjicostis, C. N. (2008b). Distributed function calculation via linear iterations in the presence of malicious agents - Part II: Overcoming malicious behavior. In *Proc. Am. Control Conf.*, pages 1356–1361.

[202] Sundhar Ram, S., Nedić, A., and Veeravalli, V. V. (2010). Distributed Stochastic Subgradient Projection Algorithms for Convex Optimization. *J. Optim. Theory Appl.*, 147(3):516–545.

[203] Swaroop, D. and Hedrick, J. K. (1996). String stability of interconnected systems. *IEEE Trans. Automat. Contr.*, 41(3):349–357.

[204] Taha Attya, A. B. and Hartkopf, T. (2013). Control and quantification of kinetic energy released by wind farms during power system frequency drops. *IET Renew. Power Gener.*, 7(3):210–224.

[205] Tang, W. and Daoutidis, P. (2019). Distributed control and optimization of process system networks: A review and perspective. *Chinese J. Chem. Eng.*, 27(7):1461–1473.

[206] Tanner, H. G., Jadbabaie, A., and Pappas, G. J. (2003). Stable Flocking of Mobile Agents Part II: Dynamic Topology. In *Proc. IEEE Conf. Decis. Control*, volume 2, pages 2016–2021.

[207] Tielens, P. and Hertem, D. V. (2012). Grid Inertia and Frequency Control in Power Systems with High Penetration of Renewables. In *Young Res. Symp. Electr. Power Eng.*, number 2, pages 1–6.

[208] Tielens, P. and Van Hertem, D. (2016). The relevance of inertia in power systems. *Renew. Sustain. Energy Rev.*, 55:999–1009.

[209] Tjell, K. and Wisniewski, R. (2019). Privacy Preservation in Distributed Optimization via Dual Decomposition and ADMM. In *2019 IEEE Conf. Decis. Control*, pages 7203–7208.

[210] Tsitsiklis, J. N. (1984). *Problems in decentralized decision making and computation*. PhD thesis, Massachusetts Institute of Technology.

[211] Tsitsiklis, J. N., Bertsekas, D. P., and Athans, M. (1986). Distributed Asynchronous Deterministic and Stochastic Gradient Optimization Algorithms. *IEEE Trans. Automat. Contr.*, 31(9):803–812.

[212] Ursino, B., Gambuzza, L. V., Latora, V., and Frasca, M. (2019). Control of synchronization of a group of nodes in directed networks. In *2019 18th Eur. Control Conf. ECC 2019*, pages 2820–2825.

[213] Valbuena Reyes, L. A. and Tanner, H. G. (2015). Flocking, Formation Control, and Path Following for a Group of Mobile Robots. *IEEE Trans. Control Syst. Technol.*, 23(4):1268–1282.

[214] Venkat, A. N., Hiskens, I. A., Rawlings, J. B., and Wright, S. J. (2008). Distributed MPC strategies with application to power system automatic generation control. *IEEE Trans. Control Syst. Technol.*, 16(6):1192–1206.

[215] Venkat, A. N., Rawlings, J. B., and Wright, S. J. (2005). Stability and optimality of distributed model predictive control. In *Proc. 44th IEEE Conf. Decis. Control. Eur. Control Conf. CDC-ECC '05*, volume 2005, pages 6680–6685.

[216] Vidyasagar, M. (2002). *Nonlinear systems analysis*, volume 42. Society for Industrial and Applied Mathematics, Philadelphia, 2nd edition.

[217] Vlahakis, E., Dritsas, L., and Halikias, G. (2019a). Distributed LQR design for a class of large-scale multi-area power systems. *Energies*, 12(14).

[218] Vlahakis, E. E., Dritsas, L. D., and Halikias, G. D. (2019b). Distributed LQR based Suboptimal Control for Coupled Linear Systems. In *8th IFAC Work. Distrib. Estim. Control Networked Syst.*, volume 52, pages 109–114. Elsevier Ltd.

[219] Vlahakis, E. E., Dritsas, L. D., and Halikias, G. D. (2019c). Distributed LQR design for identical dynamically coupled systems : Application to Load Frequency Control of multi-area Power Grid . In *2019 IEEE Conf. Decis. Control*, pages 4471–4476.

[220] Vlahakis, E. E., Dritsas, L. D., and Halikias, G. D. (2019d). Distributed Model Predictive Load Frequency Control of multi-area Power Grid: A Decoupling Approach. In *8th IFAC Work. Distrib. Estim. Control Networked Syst.*, volume 52, pages 205–210. Elsevier Ltd.

[221] Vlahakis, E. E. and Halikias, G. D. (2018). Model-Matching type-methods and Stability of Networks consisting of non-Identical Dynamic Agents. In *IFAC-PapersOnLine*, volume 51, pages 426–431. Elsevier B.V.

[222] Vlahakis, E. E. and Halikias, G. D. (2019). Distributed LQR Methods for Networks of Non-Identical Plants. In *Proc. IEEE Conf. Decis. Control*, volume 2018, pages 6145–6150. IEEE.

[223] Vlahakis, E. E., Milonidis, E., and Halikias, G. D. (2018). Cooperative Distributed LQR Control for Longitudinal Flight of a Formation of Non-Identical Low-Speed Experimental UAV's. In *2018 UKACC 12th International Conference on Control (CONTROL)*, pages 295–300.

[224] Wang, D., Glavic, M., and Wehenkel, L. (2014a). Comparison of centralized, distributed and hierarchical model predictive control schemes for electromechanical oscillations damping in large-scale power systems. *Int. J. Electr. Power Energy Syst.*, 58:32–41.

[225] Wang, L. and Xiao, F. (2010). Finite-time consensus problems for networks of dynamic agents. *IEEE Trans. Automat. Contr.*, 55(4):950–955.

[226] Wang, L. Y., Syed, A., Yin, G., Pandya, A., and Zhang, H. (2012). Coordinated vehicle platoon control: Weighted and constrained consensus and communication network topologies. In *Proc. IEEE Conf. Decis. Control*, pages 4057–4062.

[227] Wang, S. H. and Davison, E. J. (1973). On the Stabilization of Decentralized Control Systems. *IEEE Trans. Automat. Contr.*, 18(5):473–478.

[228] Wang, W., Wang, D., Peng, Z., and Li, T. (2016). Prescribed Performance Consensus of Uncertain Nonlinear Strict-Feedback Systems with Unknown Control Directions. *IEEE Trans. Syst. Man, Cybern. Syst.*, 46(9):1279–1286.

[229] Wang, Y., Wang, D., and Zhu, S. (2017). Formation tracking of multi-vehicle systems in unknown environments using a multi-region control scheme. *Int. J. Control*, 90(12):2760–2771.

[230] Wang, Z., Xu, J., and Zhang, H. (2014b). Consensusability of multi-agent systems with time-varying communication delay. *Syst. Control Lett.*, 65(1):37–42.

[231] Wei, E. and Ozdaglar, A. (2012). Distributed alternating direction method of multipliers. In *Proc. IEEE Conf. Decis. Control*, pages 5445–5450.

[232] Wen, G., Li, Z., Duan, Z., and Chen, G. (2013). Distributed consensus control for linear multi-agent systems with discontinuous observations. *Int. J. Control*, 86(1):95–106.

[233] Wu, M. and Amin, S. (2019). Learning an Unknown Network State in Routing Games. In *8th IFAC Work. Distrib. Estim. Control Networked Syst.*, volume 52, pages 345–350. Elsevier Ltd.

[234] Xie, G. and Wang, L. (2007). Consensus control for a class of networks of dynamic agents. *Int. J. Robust Nonlinear Control*, 17(10-11):941–959.

[235] Xu, J., Zhang, H., and Xie, L. (2013). Input delay margin for consensusability of multi-agent systems. *Automatica*, 49(6):1816–1820.

[236] You, K. and Xie, L. (2011). Network topology and communication data rate for consensusability of discrete-time multi-agent systems. *IEEE Trans. Automat. Contr.*, 56(10):2262–2275.

[237] Yu, W., Chen, G., and Cao, M. (2010a). Distributed leader-follower flocking control for multi-agent dynamical systems with time-varying velocities. *Syst. Control Lett.*, 59(9):543–552.

[238] Yu, W., Chen, G., and Cao, M. (2010b). Some necessary and sufficient conditions for second-order consensus in multi-agent dynamical systems. *Automatica*, 46(6):1089–1095.

[239] Yuan, K., Ling, Q., and Yin, W. (2016). On the convergence of decentralized gradient descent. *SIAM J. Optim.*, 26(3):1835–1854.

[240] Yucelen, T. and Egerstedt, M. (2012). Control of multiagent systems under persistent disturbances. In *Proc. Am. Control Conf.*, pages 5264–5269.

[241] Žertek, A., Verbič, G., and Pantoš, M. (2012). A novel strategy for variable-speed wind turbines' participation in primary frequency control. *IEEE Trans. Sustain. Energy*, 3(4):791–799.

[242] Zhan, J. and Li, X. (2013). Flocking of multi-agent systems via model predictive control based on position-only measurements. *IEEE Trans. Ind. Informatics*, 9(1):377–385.

[243] Zhang, L., Shi, Y., Chen, T., and Huang, B. (2005). A new method for stabilization of networked control systems with random delays. *IEEE Trans. Automat. Contr.*, 50(8):1177–1181.

[244] Zhang, Y., Ravier, R. J., Zavlanos, M. M., and Tarokh, V. (2019). A Distributed Online Convex Optimization Algorithm with Improved Dynamic Regret. In *2019 IEEE Conf. Decis. Control*, number 1, pages 2449–2454.

[245] Zhongkui Li, Zhisheng Duan, Guanrong Chen, and Lin Huang (2009). Consensus of Multiagent Systems and Synchronization of Complex Networks: A Unified Viewpoint. *IEEE Trans on Circuits Syst. I: Regular Papers*, 57(1):213–224.

[246] Zhu, M. and Martinez, S. (2012). On distributed convex optimization under inequality and equality constraints. *IEEE Trans. Automat. Contr.*, 57(1):151–164.